

UNCLASSIFIED

AD NUMBER

AD819317

LIMITATION CHANGES

TO:

Approved for public release; distribution is unlimited.

FROM:

Distribution authorized to U.S. Gov't. agencies and their contractors; Critical Technology; JUN 1967. Other requests shall be referred to Air Force Flight Dynamics Laboratory, Attn: FDM, Wright-Patterson AFB, OH 45433. This document contains export-controlled technical data.

AUTHORITY

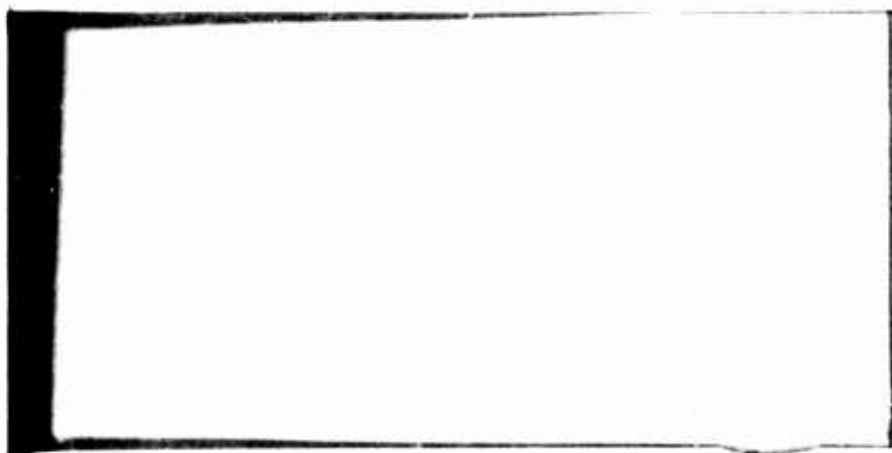
AFWAL ltr, 18 Jan 1983

THIS PAGE IS UNCLASSIFIED

FILE COPY

AD819317

17



STATEMENT OF UNCLASSIFIED

This document is subject to special export controls and each transmittal to foreign governments or foreign nationals may be made only with prior approval of *Air Force Flight Dynamics Laboratory, Attn: FDM, Wright-Patterson Air Force Base, Ohio 45433.*

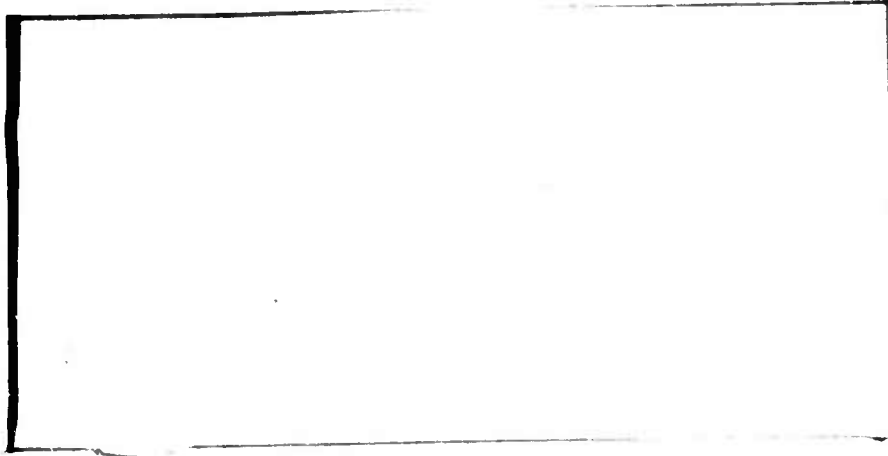
NORTHROP NORAIR

DDC
RECEIVED
SEP 5 1967
A

**Best
Available
Copy**

Statement 2. Monitor: Air Force Flight Dynamics Laboratory
Attn: FDM
Wright-Patterson AFB, Ohio 45433.

Abhealy
5 September 67



ACQUISITION	
REPORT	WRITE SECTION <input type="checkbox"/>
DISC	DIFF. SECTION <input checked="" type="checkbox"/>
UNCLASSIFIED	<input type="checkbox"/>
JUSTIFICATION	
BY	
DISTRIBUTION/AVAILABILITY CODES	
DECL.	AVAIL. CODE
2	

In reply refer to:

1900-67-223

LRF:jts

3901 West Broadway, Hawthorne, California 90250

Telephone (213) 675-4611

NORTHROP NORAIR A Division of Northrop Corporation

31 August 1967

Subject: Contract AF33(657)-13930
X-21A Laminar Flow Control Program

To: Air Force Flight Dynamics Laboratory
Air Force Systems Command
Wright-Patterson Air Force Base, Ohio 45433

Attn: Mr. P. P. Antonatos, FDM x 52614

Reference: Contract AF33(657)-13930, SA-3
Exhibit A (DD Form 1423)

Enclosure: Northrop Report NOR 67-136, Final Report on
LFC Aircraft Design Data--Laminar Flow Control
Demonstration Program, dtd June 1967 (10 copies)

1. The enclosed report is submitted in accordance with the referenced supplemental agreement and exhibit to the subject contract. This report supersedes Northrop Report NOR 61-141, dated April 1964, having the same title.

AD-439815

2. The submission of this report completes all contractual requirements.

Northrop Corporation
Norair Division



L. R. Fowell, Director
X-21A Project

cc: Defense Documentation Center
Defense Supply Agency
Cameron Station
Alexandria, Virginia 22314 w/enc. (1 cy)
AFPR (CMRHK & CMRPI) (1 cy)
AFPR (CMRHE) w/enc. (1 cy)
AFCMD (CMCA) (2 cys)

31 August 1967

Subject: Contract AF33(657)-13930
X-21A Laminar Flow Control Program

To: Air Force Flight Dynamics Laboratory
Air Force Systems Command
Wright-Patterson Air Force Base, Ohio 45433

Attn: Mr. P. P. Antonatos, FDM

Reference: Contract AF33(657)-13930, SA-3
Exhibit A (DD Form 1423)

Enclosure: Northrop Report NOR 67-136, Final Report on
LFC Aircraft Design Data--Laminar Flow Control
Demonstration Program, dtd June 1967 (10 copies)

1. The enclosed report is submitted in accordance with the referenced supplemental agreement and exhibit to the subject contract. This report supersedes Northrop Report NOR 61-141, dated April 1964, having the same title.

2. The submission of this report completes all contractual requirements.

Northrop Corporation
Norair Division



L. R. Fowell, Director
X-21A Project

cc: Defense Documentation Center
Defense Supply Agency
Cameron Station
Alexandria, Virginia 22314 w/enc. (1 cy)
AFPR (CMRKA & CMRPI) (1 cy)
AFPR (CMRHE) w/enc. (1 cy)
AFCMO (CMCA) (2 cys)

(258470)

**NORTHROP CORPORATION
NORAIR DIVISION**

14
NOR-67-136
9 FINAL REPORT LFC AIRCRAFT DESIGN DATA
LAMINAR FLOW CONTROL DEMONSTRATION PROGRAM.
15 Contract AF 33(657)-13930
11 June 1967
12 415p.

PREPARED BY

X-21A Engineering Section

APPROVED BY

George L. Gluyas
G. L. Gluyas, Chief
X-21A Engineering Group

L. R. Powell
L. R. Powell, Director
X-21A Project

REVISIONS

CHANGE	DATE	ENGINEER	PAGES AFFECTED OR REMARKS

ENGINEER	NORTHROP CORPORATION NORAIR DIVISION	PAGE 1
CHECKER		REPORT NO. NOR-67-136
DATE June 1967		MODEL X-21A

FOREWORD

The final report on the LFC Design Data for the X-21A demonstration airplane, Contract AF 33(657)-13930, is a revision of Report NOR 61-141, "Laminar Flow Control Demonstration Program, Final Report - LFC Design Data," Contract AF 33(600)-42052, April 1964. The revision is the addition of new technical information that resulted from the continuation of the program beyond the April 1964 date, and retains all pertinent data from the earlier report.

The report embraces several different technologies or disciplines: external aerodynamics, boundary layer theory, internal aerodynamics, propulsion, miscellaneous LFC design criteria, aircraft performance, and structural design and analysis. The report summarizes the present state-of-the-art in LFC aircraft design and serves as a basis for future effort in this field of development.

ENGINEER	NORTHROP CORPORATION NORAIR DIVISION	PAGE 11
CHECKER		REPORT NO. NOR 67-136
DATE June 1967		MODEL X-21A

TABLE OF CONTENTS

	<u>Page</u>
FOREWORD	1
TABLE OF CONTENTS	11
INTRODUCTION	111
Section 1 - "Concept of LFC by Suction and Theoretical Background, Including Boundary Layer Stability Criteria"	1.00
Section 2 - "Calculation of Boundary Layer Development and Suction Requirements on a Laminar Flow Control Wing Using Digital Computer Programs"	2.00
Section 3 - "Suction Slot Design"	3.00
Section 4 - "Design of Flow Passages Between the Slots and Main Ducts"	4.00
Section 5 - "Main Duct and Mixing Chamber Design Analysis"	5.00
Section 6 - "External Pressure Distribution Criteria and Wing Design to Meet These Criteria"	6.00
Section 7 - "Effects of Nacelles, Pods and Fuselage on the Wing Pressure Field and Adaptation of Wing Contours"	7.00
Section 8 - "Pumping System"	8.00
Section 9 - "Main Propulsion System"	9.00
Section 10 - "Waviness and Surface Smoothness Criteria"	10.00
Section 11 - "Effect of Acoustical and Vibration Environment on the Maintenance of Laminar Flow"	11.00
Section 12 - "Performance Prediction and Effect of LFC on Performance Parameters"	12.00
Section 13 - "Designing for Satisfactory Flying Qualities on an LFC Aircraft"	13.00
Section 14 - "Ice Protection Systems"	14.00
Section 15 - "Structural and Stress Design Considerations"	15.00

ENGINEER	NORTHROP CORPORATION NORAIR DIVISION	PAGE
CHECKER		111
DATE		REPORT NO.
June 1967		NOR-67-136
		MODEL
		X-21A

INTRODUCTION

In August 1960, Northrop Norair was awarded a United States Air Force contract to modify two WB-66 aircraft to a configuration subsequently designated X-21A, incorporating laminar flow control (LFC) on the wings. The primary objectives were to demonstrate the technical feasibility and practicality of the design, manufacture, operation and maintenance of a laminar flow control aircraft system; and to provide data for direct application to the design of future LFC aircraft, using technologies developed by Northrop Norair in previous Air Force research contracts. The modification of the WB-66 involved removal of the wings and replacing them with laminar flow control wings, replacement of the propulsion engines with pylon-mounted YJ79-GE-13 engines on the aft fuselage, the installation of LFC suction compressors in pods mounted under the wing, and the modification of the fuselage required by the wing and engine replacement.

The engineering development of the X-21A required the integration of the technologies used in the design of high subsonic aircraft with laminar flow control technologies. This required the aerodynamic development of airfoil sections so as to establish favorable chordwise and spanwise distributions of pressure, the development of a suction system throughout the wing, and the development of efficient structure to accommodate the passage of air from the boundary layer to the suction compressors.

This report presents a description of the engineering methods and procedures used to make the LFC modification (the X-21A airplane); and it includes improvements, such as wing nose modifications, that were developed in the X-21A flight test programs. The LFC suction surface design, as modified for the second (SN 55-4104) airplane, provided almost total laminarization of the wing upper suction surface in the cruise flight condition.

The engineering methods and procedures described are recommended as the basis for design of future laminar flow control aircraft. It is probable that additional research investigations could be helpful in further improving LFC performance, with the subject of most interest being the reduction of boundary layer disturbances generated in the wing nose region of aircraft as large as, or larger than, the X-21A.

The report is divided into 15 sections, each of which covers a specific design consideration for the X-21A airplane. Each section has its own list of symbols, to minimize the confusion of duplication of symbols among the various technologies represented in the report.

To aid in introducing the X-21A airplane and its LFC performance, the following figures, summarizing data through 1965, are included in the introduction:

- I.1 General Arrangement - X-21A
- I.2 Flight Envelope - LFC Investigation
- I.3 Step-by-Step Growth in Laminar Area Throughout Program
- I.4 Laminar Flow Area - 1965

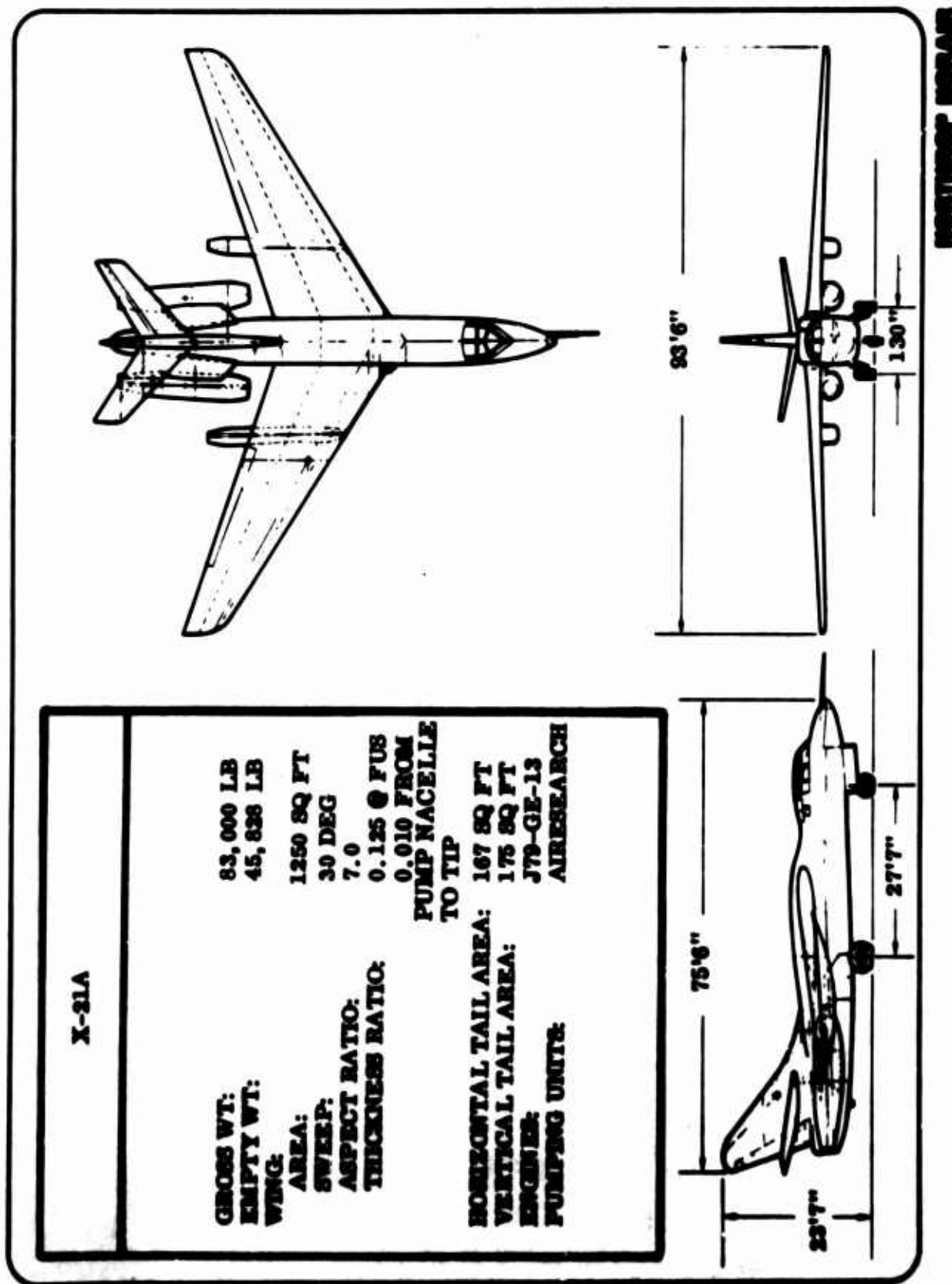


FIGURE 1.1. GENERAL ARRANGEMENT - X-21A AIRPLANE

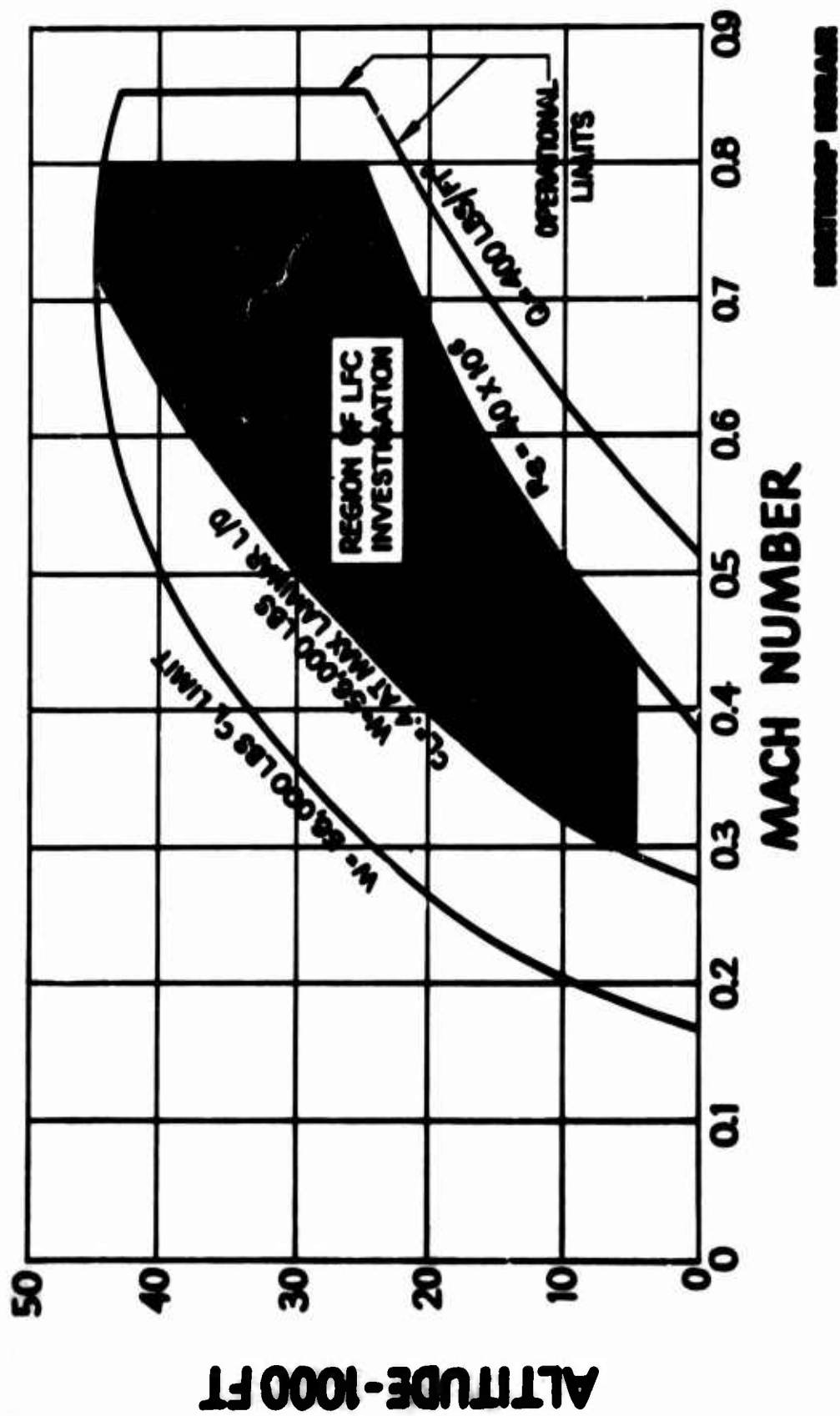
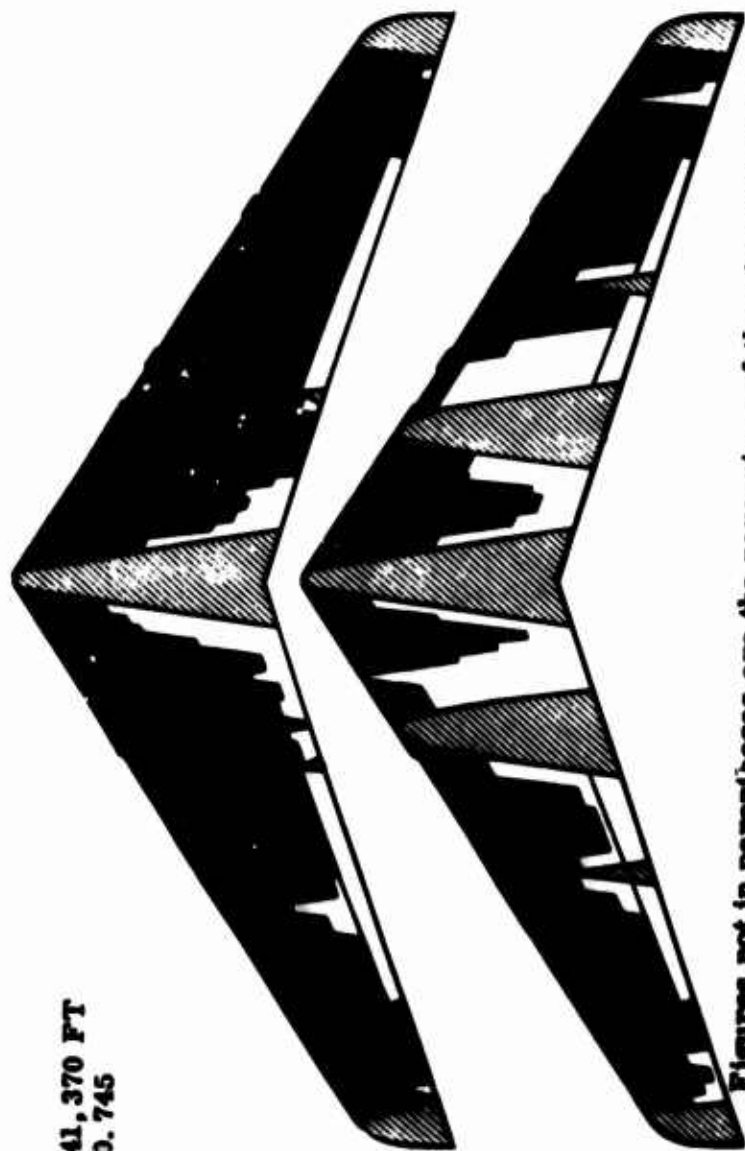


FIGURE 1.2 FLIGHT ENVELOPE - LFC INVESTIGATION

ALTITUDE = 41,370 FT
MACH NO. = 0.745



76%
(90)

57%
(73)

81%
(96)

57%
(73)

Figures not in parentheses are the percentage of the wing wetted area that was laminarized. The figures in parentheses are the percentages laminarized of the wing area available for laminarization.

WESTINGHOUSE

FIGURE 1.4. LAMINAR FLOW AREA - JULY 1965

ENGINEER	NORTHROP CORPORATION NORAIR DIVISION	PAGE 1.00
CHECKER		REPORT NO. NOR 67-136
DATE June 1967		MODEL X-21A

SECTION 1

CONCEPT OF LFC BY SUCTION AND THEORETICAL
BACKGROUND, INCLUDING BOUNDARY LAYER
STABILITY CRITERIA

BY:

W. G. Wheldon

March 1964

Revised May 1967

ENGINEER	NORTHROP CORPORATION NORAIR DIVISION	PAGE 1.01
CHECKER		REPORT NO. NOR 67-136
DATE June 1967		MODEL X-21A

1.1 INTRODUCTION

Laminar flow control (LFC) is the reduction in wake drag of an aerodynamic surface by laminarization of the boundary layer through withdrawal of small quantities of boundary layer air by suction. It is found that the force equivalent of the energy expended in pumping the boundary layer air to free stream velocity, when added to the wake drag of the now laminar boundary layer, is a much smaller quantity than the drag of the same wing without LFC. This section of the report discusses the principles of maintaining the boundary layer in a condition of laminar flow from the leading to the trailing edges of a wing at large Reynolds numbers. The individual problems with cross-flow and tangential flow will be considered together with the special problem of stability within the stagnation zone on a swept wing. The criteria used for establishing the optimum suction distribution are discussed together with factors which will minimize the required suction.

This section discusses only the problems of laminar flow on wings and empennage. It is considered that the laminarization of fuselages and nacelles is not yet at a stage of development sufficiently advanced to recommend that it be used on current aircraft.

1.2 CONCEPT OF STABILITY IN THE LAMINAR BOUNDARY LAYER

The determination of whether a given boundary layer will remain laminar as it proceeds across the wing surface is dependent upon the shape of the boundary layer velocity profiles. If conditions are such that a flow disturbance will amplify, then instability exists. Typical disturbances are surface roughness, pressure fluctuations through the slots, surface vibration and sound. Even though there is an unstable profile at a given point in the stream, disturbances which are small relative to the boundary layer thickness may amplify only slowly. That is, transition may not occur for some distance behind the instability. However, in the general case, if critical conditions are exceeded it must be assumed that transition will occur.

It has been an impression among aerodynamicists that a chordwise gradient of decreasing pressure will exert a stabilizing influence on the boundary layer of a wing and delay transition. However, considering the case of the swept wing, one discovers that this criterion alone no longer governs. In fact, transition occurs at high Reynolds numbers very far forward on the leading edge in spite of the existence of a so-called "favorable" pressure gradient. Crossflow develops in the boundary layer quite far forward on the wing and the shape of the boundary layer crossflow profile leads to instability.

ENGINEER	NORTHROP CORPORATION NORAIR DIVISION	PAGE 1.02
CHECKER		REPORT NO. NOR-67-136
DATE June 1967		MODEL X-21A

The crossflow velocity at any point within the boundary layer is the component of the local velocity vector which is normal to the potential flow vector just outside the boundary layer. The potential flow vector changes in direction continuously as it leaves the leading edge and passes across the wing.

Figure 1.1 shows the three-dimensional boundary layer profile of a swept wing. One sees the familiar tangential profile at right angles to the crossflow profile, and the vector sum of these two.

There is little tendency of the boundary layer flow on a straight wing to be deflected either inboard or outboard, and hence little crossflow exists. By use of airfoil sections which exhibit the "favorable" pressure gradient forward of mid-chord it is possible to maintain a laminar boundary layer over considerable portions of its chord by careful smoothing. On a swept wing smoothing alone cannot prevent transition near the leading edge.

Figure 1.2 shows the path of a potential flow streamline as it passes across a swept wing. As it reaches the leading edge it is immediately deflected outward and depending upon the sharpness of the leading edge it turns rapidly through almost 90° and moves inboard. This is because it now sees a cross-streamwise pressure gradient with lower pressure inboard. As it moves aft it encounters an opposite pressure gradient and is thus moved outboard. The paths of the streamlines inside of the boundary layer follow the same general excursions, but because of their relatively slower velocities and reduced centrifugal forces their angular deflections (under the influence of the cross-streamwise pressure gradients) are greater.

Figure 1.3 shows the chordwise distribution of pressure for two types of airfoils, one in which the forward and aft pressure gradients are steep, and one in which the gradients are shallow. The former is preferred for a high subsonic LFC wing for two reasons. It provides more lift for a given maximum negative pressure and it provides a shorter region of crossflow. Furthermore, the chordwise distribution of pressure should be nearly constant along the span to provide straight isobars along the wing element lines. Figure 1.4 shows an isobar diagram for a conventional subsonic transport swept wing. Isobars not parallel to the wing element lines indicate varying spanwise conditions of pressure and crossflow. Local increases in isobar sweep such as those which usually occur near the leading edge of the wing tip and wing root are accompanied by significantly increased crossflow.

Examples of crossflow profiles for various positions along the chord of a 33° swept laminar flow control wing are shown in Figure 1.5. These curves are calculated from a knowledge of pressure distribution, geometrical characteristics and freestream conditions. Experimental determination of crossflow profiles would be extremely tedious and is found unnecessary because of the high degree of accuracy of their prediction by analysis. In this figure the crossflow velocity (v) is ratioed to the flow velocity at infinity (U_∞). The height of the boundary layer above the surface is represented

ENGINEER	NORTHROP CORPORATION NORAIR DIVISION	PAGE 1.03
CHECKER		REPORT NO. NOR-67-136
DATE June 1967		MODEL X-21A

by the ratio y/c multiplied by the square root of the chord Reynolds number. One sees that at the leading edge the boundary layer is quite thin but the crossflow velocity in the negative direction (that is, toward the fuselage) is quite high. In the mid-chord region the crossflow velocity is small but further aft in the region of the rear pressure rise it again builds up to large magnitudes. This is coupled with large boundary layer thickness. The crossflow Reynolds number, defined as the product of the maximum crossflow velocity and the height of the boundary layer (to the point at which crossflow returns to 1/10 of its maximum value) divided by local kinematic viscosity, is a large number at positions very close to the leading edge and over a substantial portion of the rear part of the wing.

The influence of suction in preventing transition on a wing at high chord Reynolds numbers is to reduce the boundary layer thickness and the maximum crossflow Reynolds number in the boundary layer. At first thought one might consider the simplest LFC system to be one in which the suction distribution was maintained constant across the chord. However, there are two reasons for not following this system. The first is, of course, that efficiency is of prime concern to an LFC system, and in order to attain the necessary boundary layer stability at critical positions along the chord, more suction than necessary would have to be applied over the remainder. The second reason is that this very oversuction can be troublesome from the standpoint of required wing smoothness. That is, the greater the suction, the thinner the boundary layer becomes and with excessive suction the wing smoothness must be near-perfect.

This, then, brings up the problem of determining for all points along the chord the proper amount of suction assuming a continuous suction surface. In practice, the correct suction distribution is determined on the basis of local boundary layer stability. Reference 1 contains an excellent discussion of the concept of boundary layer stability and of the critical crossflow velocities tolerable on a swept wing. Reference 1 shows that the critical crossflow Reynolds numbers obtained experimentally usually exceed the minimum values predicted by theory. (The term "minimum" is used because the theory computes the neutral crossflow stability limits for a range of disturbance frequencies. The "minimum" limit pertains to the frequency giving the lowest critical crossflow Reynolds number.) In general, the experimentally tolerable crossflow Reynolds numbers are of the order of eighty percent higher than the theoretical minimum limiting values. The eighty percent factor is not precise and is itself somewhat related to the chordwise pressure distribution. For the practical design of the LFC wing, the limiting crossflow Reynolds numbers are based on theoretical calculations which then are scaled up by a factor based on experimental results. The use of the eighty percent factor as a constant has been found to give accurate estimates of the total suction requirement for an airfoil, but usually some minor adjustments of the chordwise suction distribution are required.

ENGINEER	NORTHROP CORPORATION NORAIR DIVISION	PAGE
CHECKER		1.04
DATE	June 1967	REPORT NO. NOR-67-136
		MODEL X-21A

The theory shows that the minimum crossflow stability limit Reynolds number becomes greater in direct proportion to negative increases in the second derivative of the crossflow profile at the wall. Calculations of the crossflow stability limit Reynolds number on swept laminar suction wings have shown considerably higher stability limit Reynolds numbers for the crossflow in the region of the rear pressure rise where the maximum crossflow velocity occurs relatively close to the wing surface, i.e., where the second derivative of crossflow velocity at the wall has larger negative values than in the leading edge regions. Figure 1.6 shows this relationship. This plot shows that the theoretical minimum stability limit crossflow Reynolds number has a value of about 60 when the shape of the non-dimensionalized crossflow profile at the wall is flat. As the curvature of the profile increases so does the stability limit.

This, then, is the primary criterion which is used for evaluating the suction quantity and distribution which must be generated by the suction system on swept LFC wings. The specific procedures involved in computing the suction are discussed in another portion of this report. However, the general process is to calculate the boundary layer characteristics with an assumed suction distribution and to compare the actual crossflow Reynolds numbers with the stability limit values. In this way, the need for increasing or decreasing the suction can be seen. This is done numerically by using suitable programs on high speed digital computers.

1.3 STRAIGHT WINGS VERSUS SWEPT WINGS - LEADING EDGE FLOW AND CROSSFLOW

Another factor making it more difficult to maintain a laminar boundary layer on a swept wing than on a straight wing at the same chord Reynolds number is associated with the attachment line* flow at the leading edge. Research in the early 1950's disclosed that flow disturbances at the leading edge of a swept wing could propagate spanwise over major portions of the wing. This would cause turbulence everywhere downstream of the contaminated leading edge area.

To gain an understanding of the phenomenon, consider a point-disturbance located at some position aft of the leading edge in a laminar boundary layer. Turbulence will be generated in a wedge approximately 14° wide which is centered on the potential flow streamlines passing through the point of origin. The effect of a disturbance in the region of the attachment line is much more serious than the same disturbance further aft unless

* Following the practice of Reference 3, the "attachment line" in the sense used here is the "stagnation" line for the swept wing leading edge, being the locus of those points along the wing leading edge at which the potential flow velocity has no component on the plane perpendicular to the wing leading edge sweep angle at those points. Fluid elements impacting on this line move in a spanwise direction only. Fluid elements impacting just above or below this line describe a path such that they eventually traverse the upper or lower surface of the wing, respectively.

ENGINEER	NORTHROP CORPORATION NORAIR DIVISION	PAGE 1.05
CHECKER		REPORT NO. NOR-67-136
DATE June 1967		MODEL X-21A

special measures have been taken. It is found that a point disturbance so located on a wing with large leading edge radius may travel long distances along the leading edge, with turbulent streaming aft for the entire length of the contaminated leading edge area.

This phenomenon was found to explain the inability to obtain laminar boundary layers over the inboard wing of the X-21A during early flight tests of that aircraft. Laminar flow was experienced in the outer third of the wing semispan and occasionally over the middle third, but never over the inboard third, that is, inboard of the pumping pod.

The inner region is, of course, one with much larger leading edge radius than elsewhere. Figure 1.7 shows the pattern formed on the surface of an otherwise laminar wing behind a point-disturbance which is located off the attachment line. Figure 1.8 is a view looking aft at the leading edge of a swept wing showing the effect of the spanwise propagation of a disturbance located directly on the attachment line. In this case a turbulent wedge is formed as before, but its apex straddles the stagnation line, and so the disturbance spreads spanwise. Depending upon the leading edge radius, the unit Reynolds number and the location of the disturbance, the turbulence spreads outboard along the span in an increasingly wide pattern with increasing unit Reynolds number, as indicated in Figure 1.9.

A stagnation zone may be defined such that a point disturbance within it will cause spanwise contamination of the wing. Consider traversing the wing surface in a direction normal to the attachment line until a point is reached at which the streamline direction is 10° divergent from the attachment line. Twice the distance of that traverse may be taken to define the width of such a stagnation zone.

Preliminary indications from wind tunnel tests of a 33° swept two-dimensional large scale model are that the boundary of the turbulent wedge nearest to the attachment line may be less than 10° from its streamline of origin. It was found possible in this test to locate a disturbance on one side of the attachment line such that spanwise contamination would occur only on that side of the wing, with no influence on the opposite surface. Thus, it is possible to cause spanwise contamination on only the upper surface or only on the lower surface, depending upon the position of the disturbance above or below the attachment line.

Prior to the aforementioned wind tunnel tests in late 1963 at Northrop Norair, little was known about the characteristics of the spanwise growth of the turbulence along the span of a swept wing. These tests showed that instead of an abrupt spanwise contamination at a critical Reynolds number, the spanwise growth was gradual.

ENGINEER	NORTHROP CORPORATION NORAIR DIVISION	PAGE
CHECKER		1.06
DATE		REPORT NO.
June 1967		NGR-67-136
		MODEL
		X-21A

Northrop Norair's wind tunnel tests, as well as X-21A flight tests, have verified that rather extensive laminar flow up to high length Reynolds number can be established when an undisturbed laminar stagnation line boundary layer has been obtained.

Reference 3 points out that in order to establish an undisturbed laminar attachment line boundary layer on swept wings, it is essential to minimize disturbances which may cause turbulent bursts at the front attachment line, and to reduce the boundary layer momentum thickness Reynolds number R_θ at the front attachment line to sufficiently low values. ($R_\theta \leq 150$ for very small disturbances and $R_\theta \leq 100$ for large disturbances.)

Increasingly higher values of the attachment momentum thickness Reynolds numbers, upwards of 200 as stated in References 4 and 5, might be possible under absence of freestream microscale turbulence, provided other finite disturbances have been eliminated.

These values of R_θ (100 - 150) can be considered typical for the maximum allowable momentum thickness Reynolds number on the attachment line of a swept wing having no suction in the stagnation zone. It is indicated that a leading edge flow which is otherwise supercritical can be stabilized by a reduction of its leading edge radius, application of suction in the stagnation zone, or a combination of both. It is clear that in order to be effective the position of the reduced leading edge radius must coincide geometrically with the location of the stagnation point at the design flight condition. The beneficial influence of reduced leading edge radius is to impart an increased chordwise acceleration to the potential flow streamline starting from the attachment line. In this way, the streamline is turned more quickly and the stagnation zone is narrowed, thus reducing the crossflow region.

There are several sources of contamination and destabilization leading to spanwise spread of turbulence on current subsonic swept wing aircraft. Foremost is turbulence generated on the fuselage forward of the wing leading edge and passing down the wing. The larger the wing leading edge, the farther outboard the turbulence spreads. In the region immediately outboard of the turbulent zone, laminar flow will be reinstated, at least at the leading edge. Nevertheless, weak vortices within the laminar region will continue to propagate down the leading edge and will be shed continuously from the leading edge. The suction system may be unable to introduce the necessary stabilization and transition may occur at varying distances aft of the leading edge. The outboard boundary of transition may then sweep gradually aft as in Figure 1.10 instead of forming

ENGINEER	NORTHROP CORPORATION NORAIR DIVISION	PAGE 1.07
CHECKER		REPORT NO. NOR 67-136
DATE June 1967		MODEL X-21A

a distinct edge aligned 7 degrees to the direction of flight.

Other sources of disturbances are insects impinging on the leading edge at take-off, uneven wing panel splices which cross the stagnation zone, non-uniformity in suction distribution along the slots (particularly as they cross the splices), fasteners in the stagnation zone which are not smooth, and inadequate devices for elimination of fuselage-generated disturbance which themselves generate disturbances.

Solutions to the problems of spanwise contamination on swept LFC wings are in three general categories. First of these is the arrest of disturbances coming down the leading edge from the fuselage. The most obvious method is a fence parallel to the aircraft plane of symmetry at the leading edge and extending forward, such as shown in Figure 1.11. Slots are provided at the fence leading-edge intersection to remove the turbulent boundary layer generated by the fence itself. In addition, the fence should be contoured with its leading edge sloping inboard to avoid separation on its outboard surface. Another solution, perhaps preferable, is the use of vertical slots across the stagnation zone for removal of large disturbances from the fuselage. A third method of avoiding disturbance from the fuselage turbulent boundary layer is to provide a gutter or cut-back section of the wing nose at the wing-body intersection such that the turbulent air from the fuselage passes through the gutter region, and only uncontaminated air meets the wing leading edge.

A second major solution is the reduction in wing leading edge radius. As an example of this, boundaries of spanwise contamination are shown for two leading edge radii at the same unit Reynolds number in Figure 1.12.

Finally, recent research shows that vertical slots across the stagnation zone improved stabilization of the stagnation zone boundary layer flow. It is obvious that the slot spacing should be sufficiently close to prevent any disturbance from escaping from the stagnation zone before encountering a slot. Special attention must be given to the end of the vertical slot, for a vortex may be created at this point which, if the slot extends out of the stagnation zone, creates a turbulent wedge, and if it does not, may itself cause spanwise contamination. Obviously a succession of turbulent wedges would negate the benefits from suction further aft.

All of the devices described have been tried on the inboard wing of the X-21A airplane and have been found effective in improving the wing laminarization.

ENGINEER	NORTHROP CORPORATION NORAIR DIVISION	PAGE 1.08
CHECKER		REPORT NO. NOR-67-136
DATE June 1967		MODEL X-21A

1.4 PREVENTION OF TRANSITION BY SUCTION THROUGH DISCRETE SLOTS

In the boundary layer computations the quantity of suction is calculated as a function of distance along the chord and is a continuous area suction calculation rather than a calculation for discrete slots. Norair's laminar flow control system employs many closely-spaced thin slots running spanwise along the wing from the leading edge to the trailing edge for the removal of the boundary layer air. One of the criteria used for the design of the suction system applies to the height of the individual layer of air removed by each slot, which must be approximately equal to the slot width. Observance of this sucked-height to slot-width ratio criterion and of a maximum slot Reynolds number criterion provides a sufficient number of slots for an approximation to distributed suction, even though in practice the boundary layer air is removed in individual steps.

The stabilization of the tangential flow profiles is all that is required on a straight wing for attainment of laminar flow, but on a swept wing tangential flow is of secondary interest. Only in the midchord region of a swept wing where the chordwise pressure distribution may be nearly constant, and in the stagnation zone as previously discussed, is it likely that cross flow will be sufficiently small that the tangential profiles will require attention, particularly when high level acoustic disturbances are present at high Reynolds number. In the calculation of suction requirements for a swept wing the analyst concerns himself primarily with assurance of adequate crossflow stability across the chord, but in the midchord region stabilization of the tangential flow profiles may determine the suction requirements.

1.5 LIMITING REYNOLDS NUMBERS ASSOCIATED WITH STAGNATION ZONE FLOW, CROSS-FLOW AND TANGENTIAL FLOW

The Reynolds numbers listed here are recommended as maximum values to be used in the design of suction LFC wings.

1.5.1 STAGNATION ZONE FLOW

The maximum stagnation zone momentum thickness Reynolds number on a swept wing in the stagnation zone is recommended to be 100. This Reynolds number is defined as the product of the component of free stream velocity parallel to the leading edge of the wing and the momentum thickness of the stagnation zone boundary layer divided by local potential kinematic viscosity. The local momentum thickness Reynolds number will rise to magnitudes much greater than 100 at positions further aft on the chord of the wing. However, it is considered adequate that this criterion be satisfied only at the attachment line or stagnation zone. The equations governing calculation of this Reynolds number for a swept leading edge are:

ENGINEER	NORTHROP CORPORATION NORAIR DIVISION	PAGE 1.09
CHECKER		REPORT NO. NOR-67-136
DATE June 1967		MODEL X-21A

$$R_\theta = U_\infty (\sin \Lambda) (\theta / \nu) = \text{Momentum thickness Reynolds number}$$

where $U_\infty = Q_0' = \text{free stream velocity}$

$\Lambda = \text{Wing element line sweep angle}$

$\nu = \frac{\mu}{\rho} \text{ local potential kinematic viscosity}$

$\theta = \text{Momentum thickness of the boundary layer}$

$$\theta = K_\theta \sqrt{\nu / (dU/dS)}$$

where

$dU/dS = \text{Potential flow velocity gradient in the plane normal to the attachment line}$

$K_\theta = \text{Is a coefficient function of the suction coefficient } F_0^* \text{ in the stagnation zone and is given in Section 3}$

$K_\theta = .407 \text{ for a swept wing having no suction at the attachment line}$

1.5.2 LIMITING CROSSFLOW REYNOLDS NUMBERS

Limiting crossflow Reynolds numbers are based on the shape and size of the crossflow profiles across the chord of the wing. The recommended limitations on crossflow Reynolds number are 1.8 times the values shown in Figure 1.6.

1.5.3 TANGENTIAL FLOW

Results from investigations in an attempt to find a tangential design criterion have led to the formulation of a relationship between the momentum thickness Reynolds number and the second derivative at the wall of the tangential velocity profile.

Figure 1.14 shows the tangential stability criteria. These curves were obtained by examination of the stability of laminar velocity profiles, as given in Reference 7.

The curve labeled (a) corresponds to data shown in Reference 6. Figure 79 of this reference defines the critical momentum thickness Reynolds number as a function of the second derivative of the

ENGINEER	NORTHROP CORPORATION NORAIR DIVISION	PAGE 1.10
CHECKER		REPORT NO. NOR-67-136
DATE June 1967		MODEL X-21A

velocity profile at the wall. Data from this report were taken from theoretical stability analysis performed by Ulrich and shown in Reference 7. A curve faired through the data points gave an expression for the critical momentum thickness Reynolds number, as follows:

$$R_{\theta \text{ crit}}^{1/3} \cong 6 - 127 \frac{\partial^2 (u/U_m)}{\partial (y/\theta)^2 \text{ wall}}$$

where

$R_{\theta \text{ crit}}$ = critical momentum thickness Reynolds number

$U_m = Q' =$ potential flow velocity

y = height above surface

$$\frac{\partial^2 (u/U_m)}{\partial (y/\theta)^2 \text{ wall}} = \text{non-dimensional expression of the second derivative of the velocity at the wall}$$

The curve labeled (b) corresponds to results obtained by analysis of a 33° swept 10-foot chord suction wing test performed at Northrop Norair and Ames.

Northrop Norair performed an empirical study to establish design criteria for suction requirements in the region of a swept wing with flat pressure and negligible boundary layer crossflow. The region of validity for this study is limited in the upper surface of the airfoils analyzed from .15 x/c to .50 x/c and on the lower surface from .25 x/c to .50 x/c and for a range of momentum thickness Reynolds number that varies from 600 to 2600. The amount by which $R_{\theta \text{ tr}}$ exceeded $R_{\theta \text{ crit}}$ was usually 200 with an upper limit of 800 for very low turbulence intensities, where the subscript "tr" refers to transition value.

Based on these results a conservative stability limit for tangential flow can be obtained in the form

$$R_{\theta \text{ tr}} \cong R_{\theta \text{ crit}} + 200$$

where $R_{\theta \text{ crit}}$ has the expression seen above or

$$R_{\theta \text{ tr}}^{1/3} = 7.6 - 106 \frac{\partial^2 (u/U_m)}{\partial (y/\theta)^2 \text{ wall, or}}$$

ENGINEER	NORTHROP CORPORATION NORAIR DIVISION	PAGE 1.11
CHECKER		REPORT NO. NOR-67-136
DATE June 1967		MODEL X-21A

$$R_{\theta_{tr}} = 200 + \left[6 - 127 \frac{\partial^2 \left(\frac{u}{U_m} \right)}{\partial (y/\theta)^2 \text{ wall}} \right]^3$$

Both expressions are valid only for $R_{\theta_{tr}}$ ranging between 600 and 2600, which corresponds approximately to a value of the second derivative between -.02 and -.06. Tangential flow Reynolds number is defined as the product of boundary layer momentum thickness times local potential flow velocity divided by local potential flow kinematic viscosity.

1.6 MINIMIZATION OF SUCTION REQUIREMENTS

Fuel expenditure for driving the pumping machinery and the weight and space of the machinery itself is the price that is paid for the drag reduction in an LFC system. Careful attention is required to assure that minimum practical suction quantity and pressure drag is specified.

1.6.1 WING PRESSURE DISTRIBUTIONS

In the design of a Laminar Flow Control wing, among other requirements, proper wing surface pressure distribution and suction distributions should be satisfied in order to meet the required minimum suction specifications. Wing surface pressure distribution for this purpose can be analyzed considering two principal directions of the wing surface, in the chord direction and along the wing span.

1.6.1.1 CHORDWISE PRESSURE DISTRIBUTION

The optimum chordwise pressure distribution for an LFC wing is one in which the pressure coefficient versus x/c diagram shows an appreciable chordwise extent of constant pressure for both the upper and lower surfaces. Such a pressure distribution is shown in Figure 1.13. This was measured on the X-21A wing at 24% of semi-span. Design of airfoil sections requires considerable testing in a wind tunnel of adequate Mach number capability because the influence of compressibility cannot properly be predicted in the leading edge regions by any of the presently existing theories, and stabilization of the stagnation zone flow may impose additional leading edge constraints. At any rate, in the region of constant pressure, the crossflow velocities are minimized, thus greatly reducing the amount of suction needed for that reason. It has been found that the position of the rear

ENGINEER	NORTHROP CORPORATION NORAIR DIVISION	PAGE 1.12
CHECKER		REPORT NO. NOR 67-136
DATE June 1967		MODEL X-21A

pressure rise can be moved quite far aft on the chord without separation over the rear of the wing.

1.6.1.2 SPANWISE PRESSURE DISTRIBUTION UNIFORMITY

It is necessary to design LFC surfaces with a high degree of spanwise pressure distribution uniformity. There are two reasons, the first of which is the prevention of excessive isobar sweep. Any non-uniformity in the spanwise pressures is accompanied by some areas where the sweep is reduced and other areas where the sweep of the isobars is increased. This means higher suction requirements in the area of greater sweep. The other reason is the inefficiency in the total suction quantities which must be removed in any one duct if the external pressure at the middle of the duct is, for example, much lower than the pressures at the ends of the duct. Then, the duct pressure level must be adequate to remove air at the middle and this results in over-throttling at the ends where such a low duct pressure is not necessary.

It is recommended that the wing design be optimized as soon as possible in the wind tunnel program and that this be done with the wing attached to the fuselage. In this manner, the proper wing twist can be selected together with local changes in airfoil section parameters near the wing root and wing tip in order to maintain constant pressures along the wing element line. The wing root and the wing tip are special problems and some penalties must obviously be sustained in these areas.

Having selected the distribution of airfoil parameters such as thickness, twist and camber, the nacelles can then be installed on the wing. Various measures are available for minimizing this influence on the pressure distributions. In the X-21A program, the propulsion nacelles were located aft on the fuselage and pumping nacelles were placed on the wings. The shape of the pumping nacelles in the planview was chosen to approximate the paths of the streamlines which would have existed were the nacelles not in place. However, on the inboard side of the wing near the leading edge a region of locally higher pressures was found which could not be eliminated by changes in nacelle contours. This was compensated by a local thickening of the wing itself in the affected area.

ENGINEER	NORTHROP CORPORATION NORAIR DIVISION	PAGE 1.13
CHECKER		REPORT NO. NOR-67-136
DATE June 1967		MODEL X-21A

1.6.2 PRESSURE DROP AND SUCTION QUANTITY

Boundary layer stability analysis provides the necessary information for the determination of the adequate suction flow rates in the spanwise and chordwise directions. The inflow rate distribution should be adequately obtained by setting a nominal pressure drop through the skin which must be sufficient to ensure a fairly uniform inflow and small degree of distortion on the nominal inflow rate distribution when the surface pressure conditions are varied. As a representative value for this minimum pressure drop that will give good condition for suction distribution, one-half the value of the variation in pressure drop along the surface can be used. For a duct in which ΔC_{ps} is the variation of spanwise surface pressure and ΔC_{pc} is the chordwise variation of surface pressure, the design duct pressure should be about $1/2 (\Delta C_{ps} + \Delta C_{pc})$ below the most negative surface pressure. With the ideal condition of a suction wing with straight isobars and with suction duct length to diameter ratios of less than 300, the suction requirements will be minimized and less pumping power is required to provide laminar flow.

Suction quantities and suction quantity distribution are also important in complying with the minimum suction specification. These are related to the suction inflow velocity distribution and how efficiently the distribution is realized in order to provide suction flow that closely approaches area suction. When suction is obtained through slots cut in the skin of the wing, the slots should be designed so that slot Reynolds number remains low; a typical value for slot Reynolds numbers is 100. Reference 5 shows measurements of slot flow Reynolds numbers over the adverse pressure gradient of a swept suction wing at various chord Reynolds numbers and the influence on laminar flow on that region of the wing when high Reynolds numbers and consequently increasing slot Reynolds number were reached. Recent suction duct experiments have shown that slot flow velocity fluctuations increase as the slot Reynolds number increases above 120.

Since boundary layer stability conditions establish the amount of suction required and this suction is realized on a swept suction wing through the slots, the slot velocity is inversely proportional to the slot widths and spacing. The flow quantity through the slot is determined by the product of the equivalent suction inflow velocity v , and the spacing between slots. Typical values for the suction quantity coefficients (v/U_∞) are approximately 5×10^{-4} per surface with a value of 10^{-4} in regions of the wing with a relatively flat pressure distribution and small crossflow. This value increases up to 10×10^{-4} near the leading edge for moderately swept back wings.

ENGINEER	NORTHROP CORPORATION NORAIR DIVISION	PAGE 1.14
CHECKER		REPORT NO. NOR 67-136
DATE June 1967		MODEL X-21A

1.6.3 SOUND

As indicated in Reference 2, sound of a high pressure level is a detriment to laminar flow. In general, the influence is felt in regions where otherwise the suction levels are low, that is, over the mid-chord region of a wing with a flat mid-chord pressure distribution. Depending upon the amplitude of the sound, it can be compensated by addition of small amounts of suction in these areas. Section 11 of this report contains a more complete discussion of the influence of sound on the maintenance of laminar flow in the boundary layer of a swept wing. It is indicated therein (as based on wind tunnel tests) that a moderate increase in total suction, concentrated as indicated, is sufficient to compensate the destabilization of a strong sound environment.

1.6.4 MULTIPLE FLIGHT CONDITIONS

If the suction system must be designed to accommodate the attainment of laminar flow at multiple flight conditions, some penalties must be taken in the suction requirements. Since the required suction differs as the pressure distribution and Reynolds number differ, a suction distribution optimized for one flight condition may not be adequate in other cases. Consequently, it is desirable to minimize the number of flight conditions for which LFC must be operational.

1.6.5 MAXIMUM SLOTTED AREA

The laminarization of the maximum possible surface of the wing is necessary in order to gain the greatest benefit from LFC. There may be some penalties because of non-uniform pressures in the regions of the nacelles, wing root and wing tip; however, these should be minimized.

1.6.6 OPTIMIZING SUCTION QUANTITIES

In the calculation of suction quantities for an LFC wing it is advisable to reduce the suction quantities at all points along the chord to the minimum necessary values. The actual suction output of the final duct design should be considered. (In practice, it is found that the slot and duct design cannot yield the exact suction distribution called for in the earlier suction calculations for more than a single flight condition.)

1.6.7 SMOOTHNESS AND SLOT TOLERANCES

Close observation of smoothness and slot-quality tolerances must be followed to minimize the disturbances which may affect the

ENGINEER	NORTHROP CORPORATION NORAIR DIVISION	PAGE 1.15
CHECKER		REPORT NO. NOR 67-136
DATE June 1967		MODEL X-21A

suction requirements. Non-uniformities often call for local changes in suction. Since the pressure in the entire duct must be varied to compensate for a local boundary layer disturbance this may represent a considerable change in suction quantity and distribution.

1.7 REFERENCES

1. Pfenninger, W. and Bacon, J. W., Jr., "About the Development of Swept Laminar Suction Wings with Full Chord Laminar Flow," Northrop Corporation, Norair Division Report NOR 60-299 (BLC-130), September 1960. Presented to the Tenth International Congress of Applied Mechanics, Stressa, Italy, September 1960.
2. Bacon, J. W., Jr., Pfenninger, W. and Moore, C. Roger, "Influence of Acoustical Disturbances on the Behaviour of a Swept Laminar Suction Wing," Northrop Norair Report NOR 61-10, April 1961.
3. Carlson, J. C., "Low Drag Boundary Layer Suction Experiments using a 33° Swept 15% Thick Laminar Suction Wing with Suction Slots Normal to the Leading Edge," Norair Report NOR 64-281, November 1964.
4. Pfenninger, W., "Some Results from the X-21 Program, Part I, Flow Phenomena at the Leading Edge of Swept Wings," AGARDograph 97, Part IV, "Recent Developments in Boundary Layer Research," May 1965.
5. Carlson, J. C., "Investigation of the Laminar Flow Control Characteristics of a 33° Swept Suction Wing at High Reynolds Numbers in the NASA Ames 12-Foot Pressure Wind Tunnel in August 1965," Norair Report NOR 66-58, January 1966.
6. Carlson, J. C., Bacon, J. W., Jr., "Influence of Acoustical Disturbances in the Suction Ducting System on the Laminar Flow Control Characteristics of a 33° Swept Suction Wing," Norair Report NOR 65-232, August 1965.
7. Ulrich, A., "Theoretical Investigation of Drag Reduction by Maintaining the Laminar Boundary Layer by Suction," NACA TM No. 1121, June 1947.

JUNE 1967

PAGE 1.16
REPORT NO. NOR 67-136
MODEL X-21A

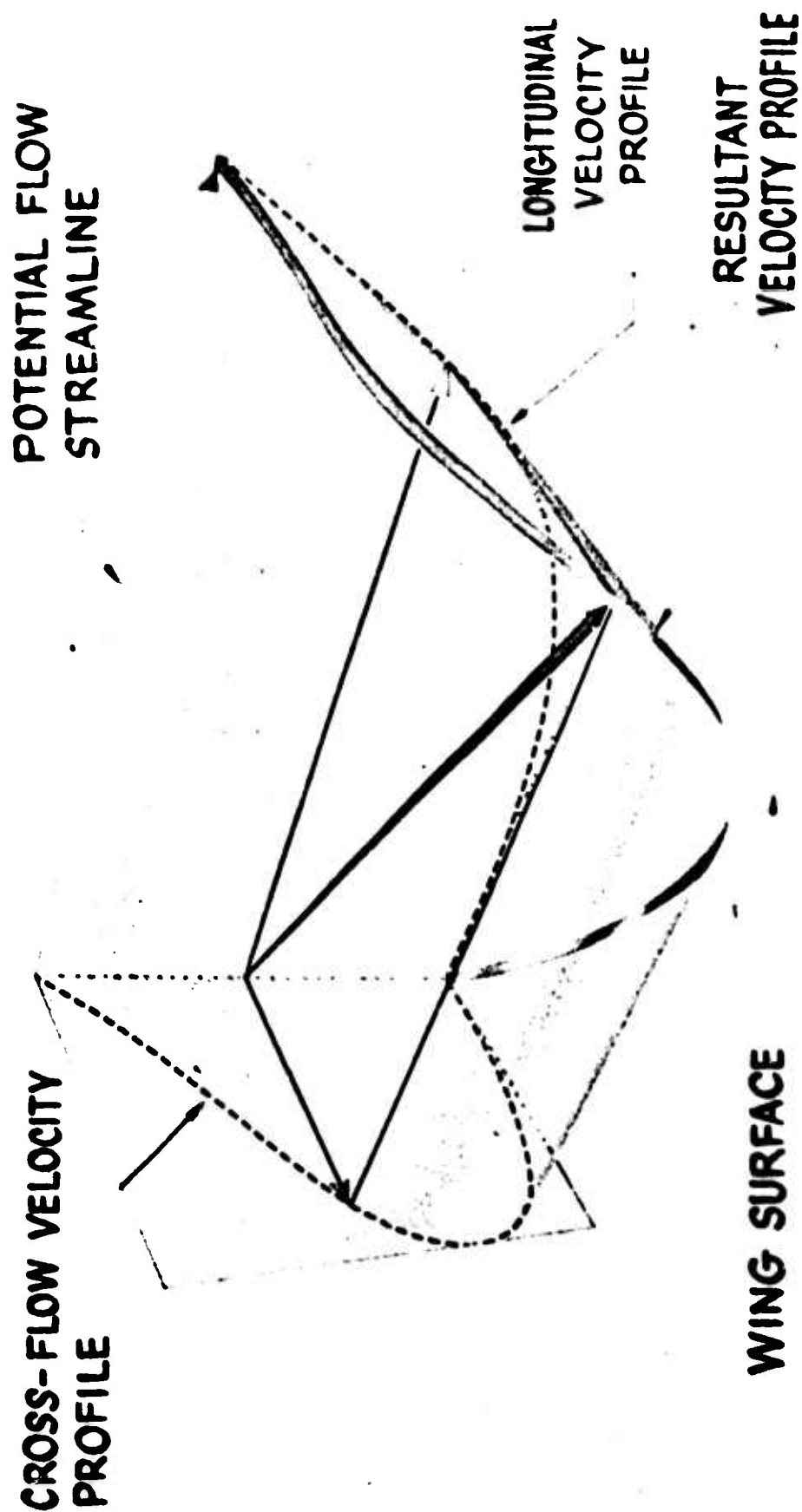


FIGURE 1.1 DIAGRAM OF BOUNDARY LAYER VELOCITY PROFILE

ENGINEER	NORTHROP CORPORATION NORAIR DIVISION	PAGE 1.17
CHECKER		REPORT NO. NOR 67-136
DATE June 1967		MODEL X-21A

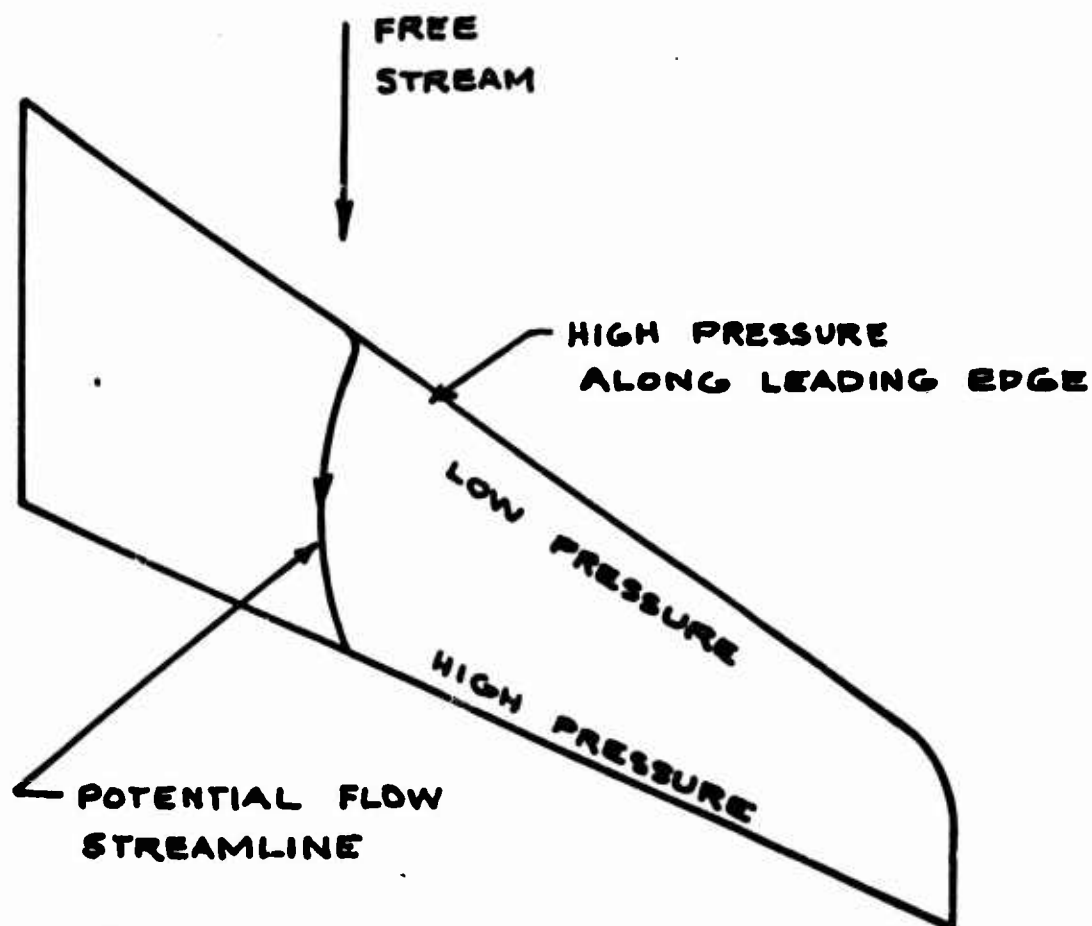


FIGURE 1.2
POTENTIAL FLOW STREAMLINE PATH
ACROSS A SWEPT WING

ENGINEER	NORTHROP CORPORATION NORAIR DIVISION	PAGE 1.18
CHECKER		REPORT NO. NOR 67-136
DATE June 1967		MODEL X-21A

PRESSURE
COEFFICIENT

C_p

- .8

- .4

0

.4

.8

STEEPER
GRADIENTS
PREFERRED
FOR LFC
SWEEP WING

CHORD
STA

x/c

SAMPLE DIAGRAMS
FOR UPPER SURFACE

FIG. 1.0 COMPARISON OF CHORDWISE
DISTRIBUTIONS OF PRESSURE

JUNE 1967

PAGE 1.19
REPORT NO. NOR 67-136
MODEL X-21A

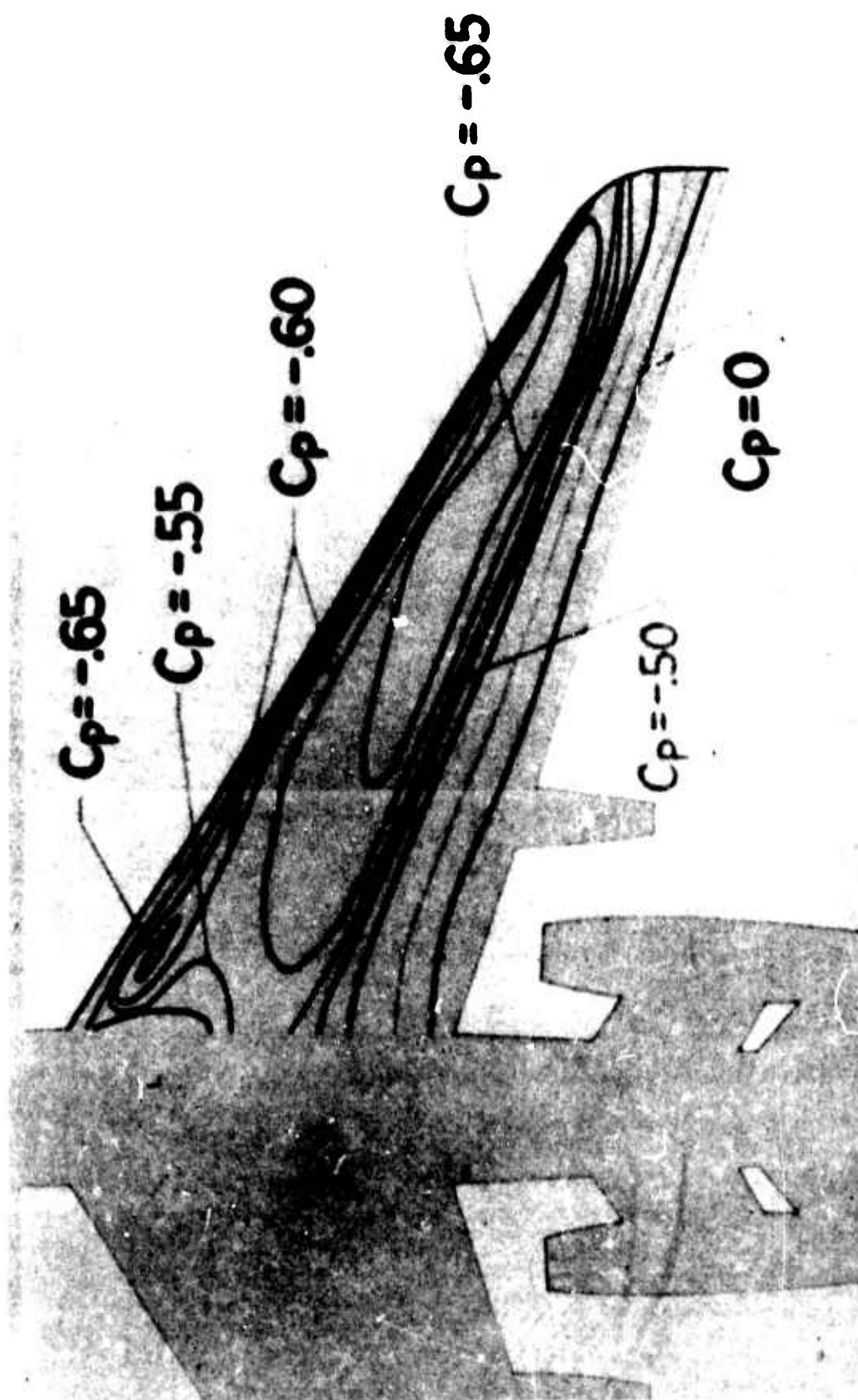


FIGURE 1.4 ISOBAR DIAGRAM - X-21A WING

ENGINEER	NORTHROP CORPORATION NORAIR DIVISION	PAGE 1.20
CHECKER		REPORT NO. NOR 67-136
DATE June 1967		MODEL X-21A

$$R_C = 30 \times 10^6$$

x chordwise distance from wing leading edge in flight direction *
 y normal distance from the wall
 C wing chord in flight direction
 n crossflow velocity in the boundary layer at the distance y from the wall
 U_∞ free stream velocity
 R_C wing chord Reynolds number
 $R_C = U_\infty C / \nu$

* wall = wing surface

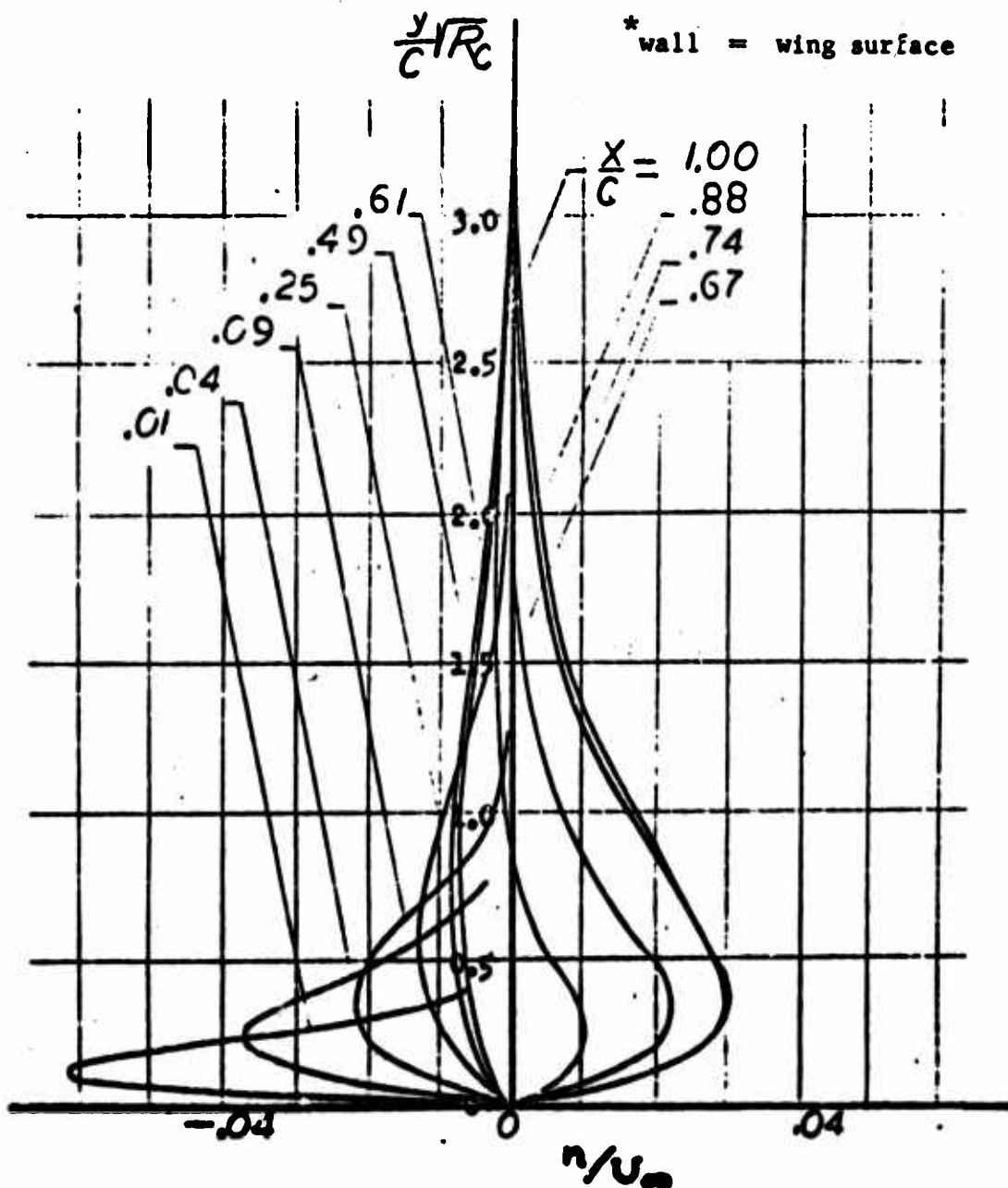


FIG. 1.5 CROSSFLOW BOUNDARY LAYER PROFILES ON A 30-DEGREE SWEEP SUCTION WING

ENGINEER	NORTHROP CORPORATION NORAIR DIVISION	PAGE 1.21
CHECKER		REPORT NO. NOR 67-136
DATE June 1967		MODEL X-21A

SYMBOLS : R_{n_s} = CROSSFLOW STABILITY LIMIT REYNOLDS NO,
BASED ON u_{MAX} AND $\delta_{.1u_{MAX}}$
 u = CROSSFLOW VELOCITY IN BOUNDARY LAYER.
 y = DISTANCE NORMAL TO WALL.
 δ = BOUNDARY LAYER THICKNESS

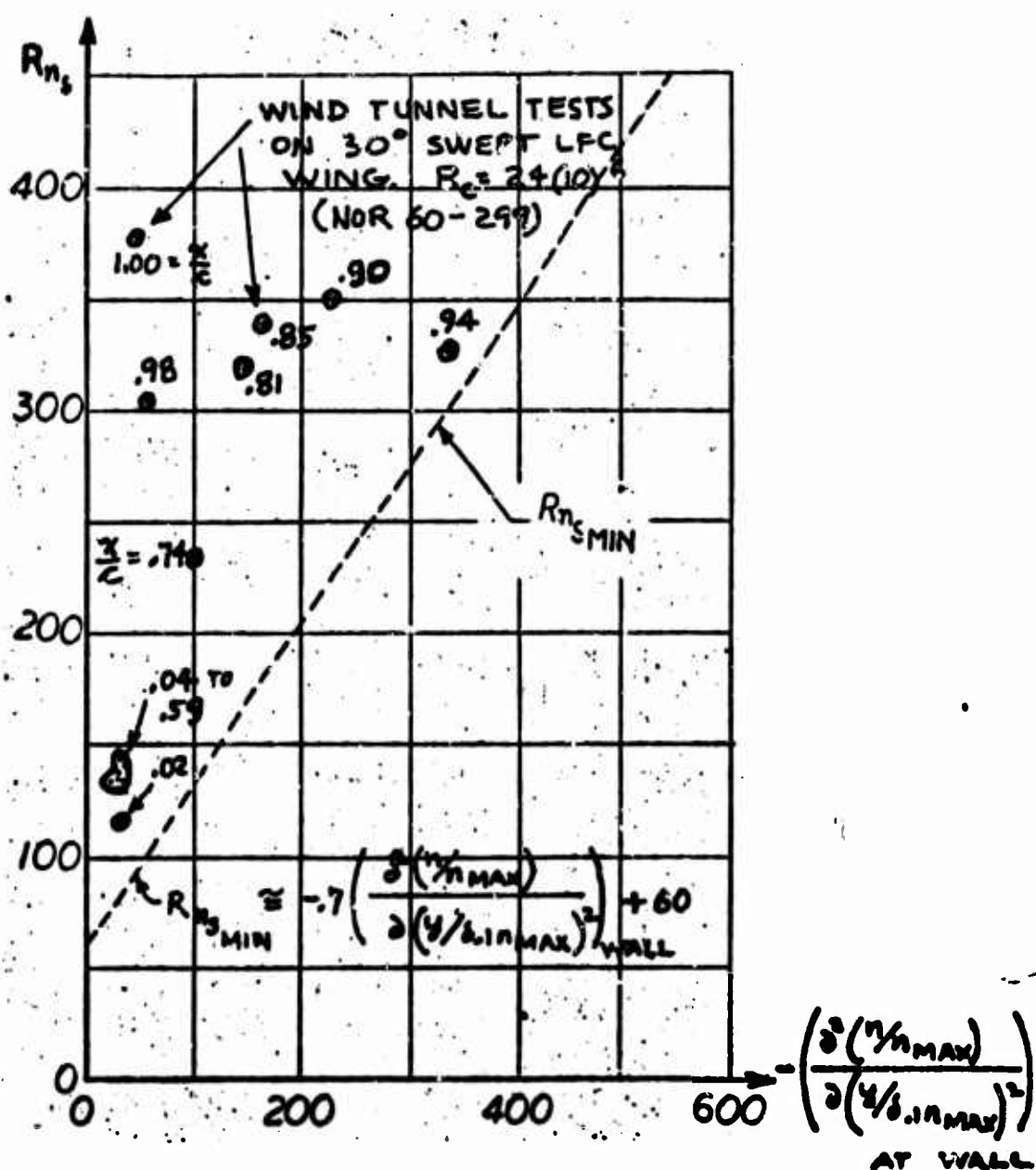
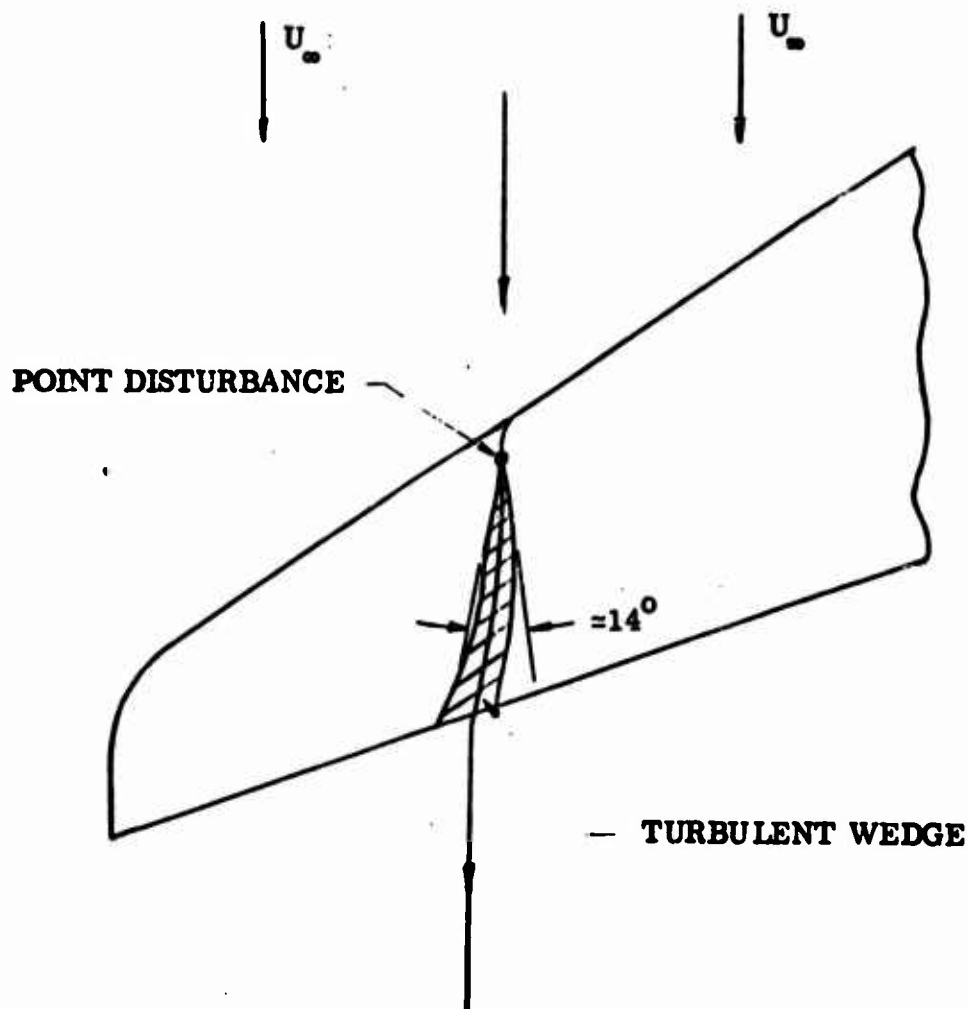


FIG. 1.6 MINIMUM CROSSFLOW STABILITY REYNOLDS NUMBER

ENGINEER	NORTHROP CORPORATION NORAIR DIVISION	PAGE 1.22
CHECKER		REPORT NO. NOR 67-136
DATE June 1967		MODEL X-21A



**FIGURE 1.7. TURBULENT WEDGE INDUCED BY A DISTURBANCE
LOCATED IN A LAMINAR BOUNDARY LAYER DOWNSTREAM
FROM LEADING EDGE OF A SWEEP WING**

ENGINEER	NORTHROP CORPORATION NORAIR DIVISION	PAGE 1.23
CHECKER		REPORT NO. NOR 67-136
DATE June 1967		MODEL X-21A

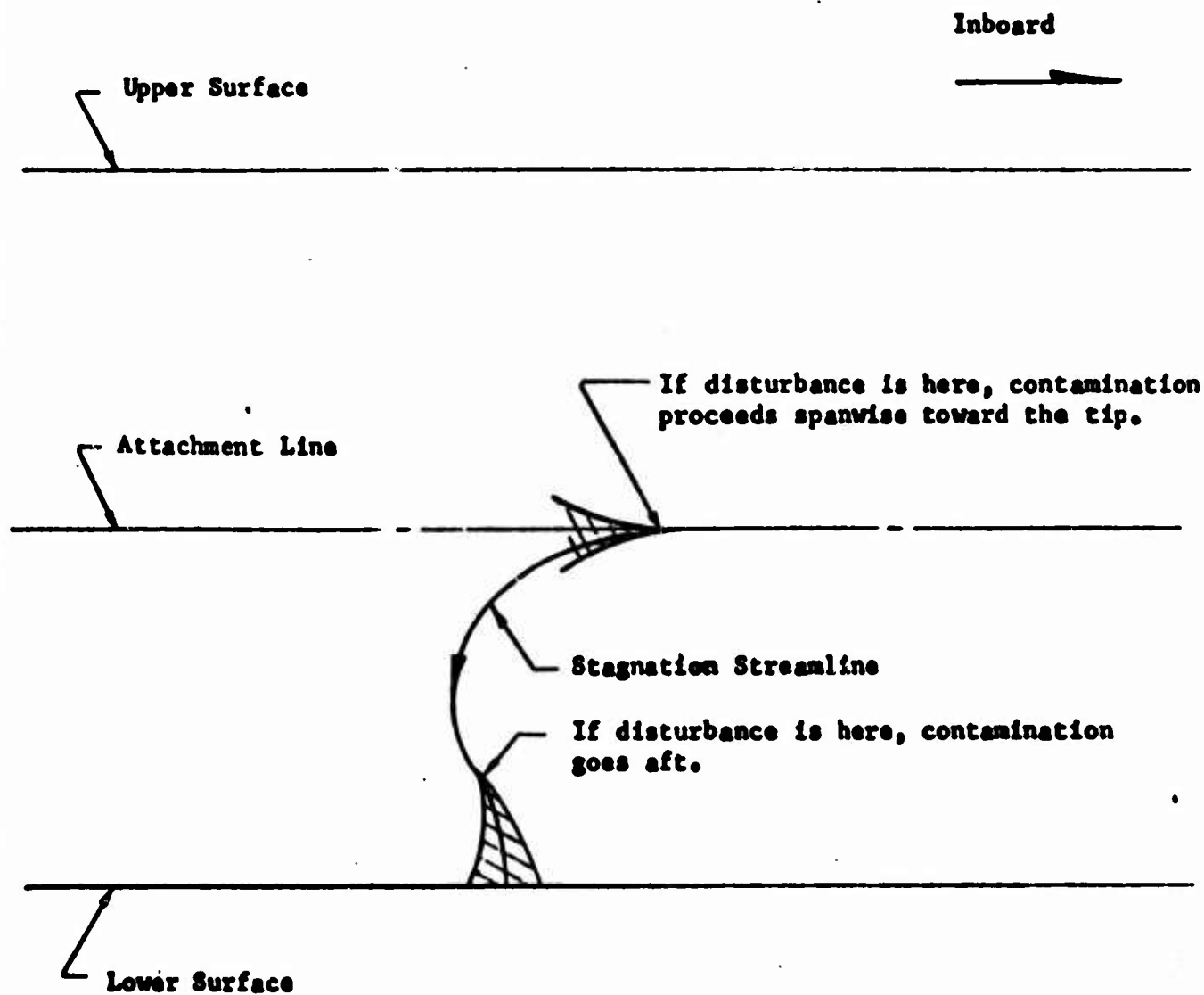


FIGURE 1.8

VIEW LOOKING AFT AT LEADING EDGE OF A SWEEP WING
ILLUSTRATING EFFECT OF SPANWISE FLOW AND OF DISTURBANCE
LOCATION ON THE PATTERN OF TURBULENCE

ENGINEER	NORTHROP CORPORATION NORAIR DIVISION	PAGE 1.24
CHECKER		REPORT NO. NOR 67-136
DATE June 1967		MODEL X-21A

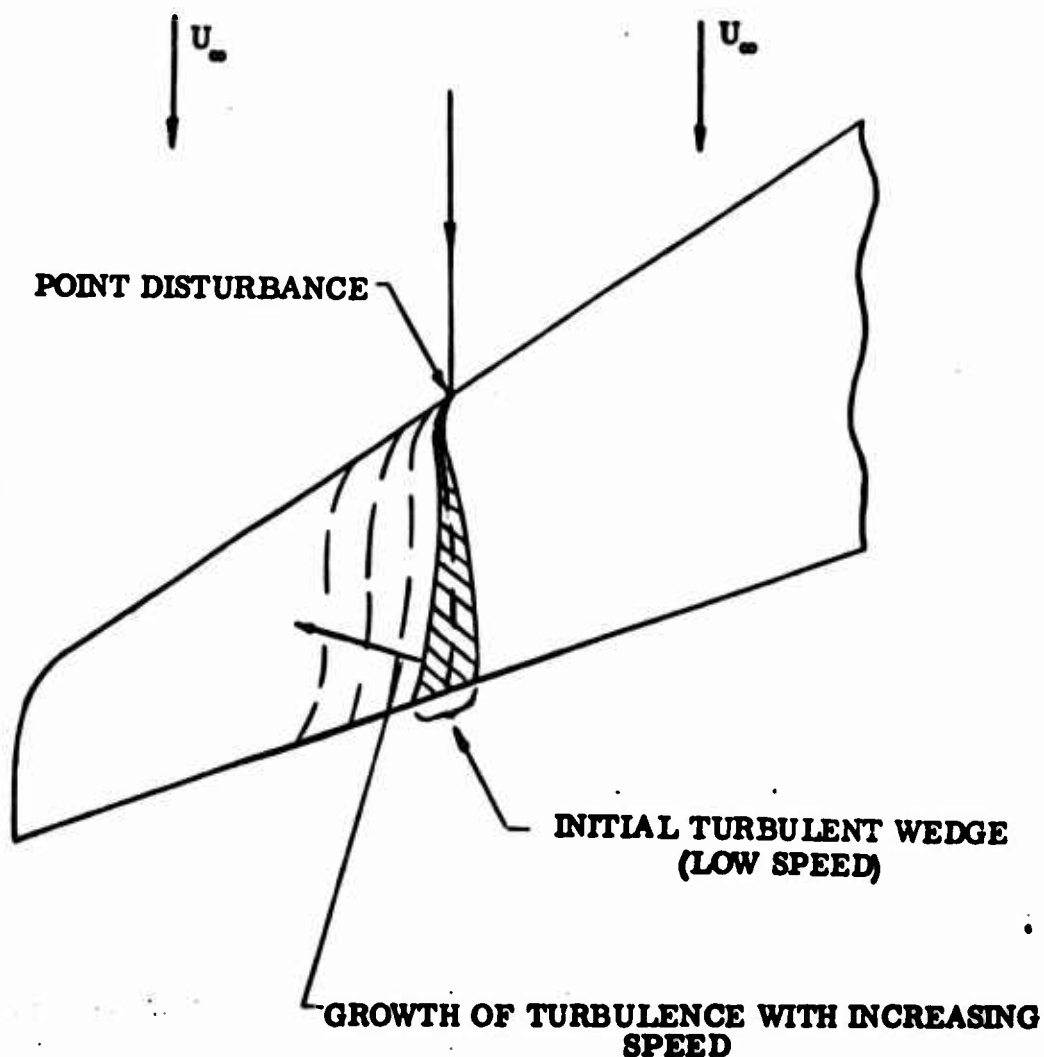


FIGURE 1.9 SPANWISE GROWTH OF TURBULENCE FROM A DISTURBANCE LOCATED AT THE LEADING EDGE OF A SWEEPED WING IN AN OTHERWISE LAMINAR BOUNDARY LAYER FLOW

ENGINEER	NORTHROP CORPORATION NORAIR DIVISION	PAGE 1.25
CHECKER		REPORT NO. NOR 67-136
DATE June 1967		MODEL X-21A

DATA Airplane No. AF 55-408
Flight 54, Run 20
Altitude $h = 39,600$ ft
Mach No. $M = .71$
Gross Weight = 58,050
Lift Coefficient $C_L = .31$

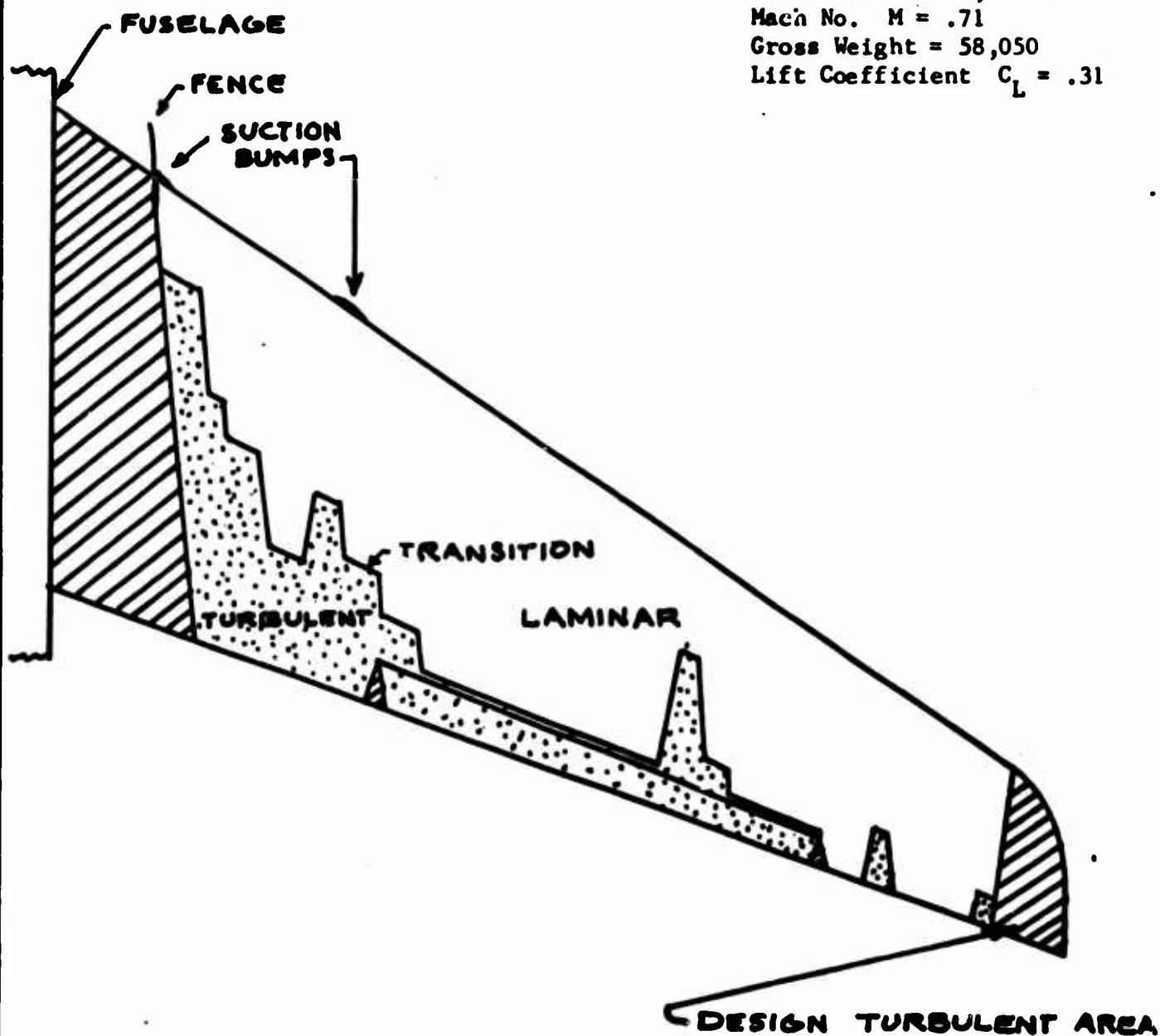


FIGURE 1.10 LAMINARIZATION PATTERN ON X-21A WING
WITH LOCAL SUCTION "BUMPS" ON LEADING EDGE

JUNE 1967

PAGE 1.26
REPORT NO. NOR 67-136
MODEL X-21A



FIGURE 1.11 LEADING EDGE FENCE FOR ARREST OF FUSELAGE DISTURBANCE
PROPAGATION ALONG LEADING EDGE OF X-21A WING

269-123 Norair
E. Wing Modification #17

2.00
NOR 67-136
X-21A

SECTION 2

CALCULATION OF BOUNDARY LAYER DEVELOPMENT
AND SUCTION REQUIREMENTS ON A LAMINAR FLOW
CONTROL WING USING DIGITAL COMPUTER PROGRAMS

by

E. A. Gloyn

March 1964

Revised May 1967

SECTION 2

TABLE OF CONTENTS

Calculation of Boundary Layer Development and Suction Requirements
on a Laminar Flow Control Wing Using Digital Computer Programs

APPENDIX A:	Suction Distribution Calculation Steps
APPENDIX B:	Derivation of the Irrotationality Condition for Swept Tapered Wings
APPENDIX C:	Rules for Selecting Points for Curve Fitting Subroutines
APPENDIX D:	Deck Set-Up for 919K (U* and V* Iteration Program)
APPENDIX E:	Deck Set-Up for Boundary Layer Input Program BB62-A and Integration Program BB65-A
APPENDIX F:	Definition of Parameters Printed by Boundary Layer Input and Integration Program (BB62-A/ BB65-A)
APPENDIX G:	Outline of Program Mode of Operation for Suction Optimization
APPENDIX H:	Wake Drag Computing Form
APPENDIX I:	Incremental Equivalent Drag Computing Form

ENGINEER	NORTHROP CORPORATION NORAIR DIVISION	PAGE 2.02
CHECKER		REPORT NO. NOR 67-136
DATE June 1967		MODEL X-21A

2.1 SUMMARY

The suction requirements of a laminar flow control wing are determined through use of Northrop Norair's general digital computer boundary layer calculation method. This section describes the use of the digital computer programs for the specific case of a swept tapered wing in subsonic flow with straight isobars and no heat transfer through the surface. The swept wing coordinate system and the components of the potential flow velocities and boundary layer velocities are defined. A method is presented for accomplishing the conversion from measured wind tunnel pressure data to the velocity components used by the program.

To determine the stability of the laminar boundary layer with a given suction distribution, one must consider stability at the leading edge, crossflow stability and tangential stability. Criteria for determining these types of stability have been derived from theory and from wind tunnel and flight test investigations. Comparison of parameters calculated by the program with the stability limit parameters determines the required suction distribution.

The primary use of the boundary layer computer programs in the design of an LFC wing will be the calculation of suction requirements. Other applications include determination of boundary layer development with and without suction, prediction of the boundary layer thickness and the profile drag of a laminar wing, and correlation of predicted boundary layer stability with flight test and wind tunnel results.

Throughout the report, it is assumed that the reader has some familiarity with digital computers but is not a professional programmer. Hence the emphasis is on the use of the programs in the design and flight test of a subsonic laminar swept tapered wing. For the modifications necessary to deal with other geometric configurations, three-dimensional flow fields, incompressible or supersonic flow, or surfaces with heat transfer, the reader should consult Ref. 1 on the general three-dimensional boundary layer program.

ENGINEER	NORTHROP CORPORATION NORAIR DIVISION	PAGE 2.03
CHECKER		REPORT NO. NOR 67-136
DATE June 1967		MODEL X-21A

2.2 INTRODUCTION

The development of the laminar boundary layer on a swept wing with known distributions of surface static pressure and suction inflow can be calculated by the finite-difference method developed by G. S. Raetz (Reference 1). This method has been programmed for use on the IBM 7090 computer. During the design of the X-21A airplane, three IBM decks were required: a Fortran deck to convert surface static pressures to potential flow velocities, an "input" deck and an "integration" deck in Fortran language. The input program calculates the flow parameters of the boundary layer differential equation at each chordwise step from the distribution of the component of potential flow velocity normal to the wing element lines, the suction velocity distribution, the leading edge and trailing edge sweep angles, the Mach number, temperature, and the spanwise velocity at the leading edge. The flow parameters are stored on a magnetic tape. The integration program performs a numerical integration of the boundary layer equations and calculates the boundary layer profiles of velocity, temperature and shear. From these profiles, parameters can be calculated which permit a determination of the boundary layer stability. It should be emphasized that the equations of the input program to determine the coefficients depend on the geometry of the body and the type of flow (compressible or incompressible) but that the equations for the finite difference integration are perfectly general.

2.3 SYMBOLS

- b' Wing span
- c' Surface length from stagnation point in streamwise direction
- c_s' Surface arc length from stagnation point
- cd_s Section suction drag coefficient
- cd_w Section wake drag coefficient
- C_p Pressure coefficient, $C_p = (p_s' - p_o') / (\frac{1}{2} \rho_o' Q_o'^2)$
- F^* Non-dimensional suction parameter. $F^* = w' / \sqrt{R_c / Q_o'}$

ENGINEER	NORTHROP CORPORATION NORAIR DIVISION	PAGE 2.04
CHECKER		REPORT NO. NOR-67-136
DATE June 1967		MODEL X-21A

2.3 SYMBOLS (Continued)

F_o^*	Non-dimensional suction parameter. $F_o^* = w/\sqrt{R_c} \lambda'_{wall}/(Q_o' \Lambda_o')$
H	Boundary layer shape factor. $H = \delta_s'/\delta_{ss}' = \frac{\delta^*'}{\theta'}$
L'	Distance from vertex along radial line
L_o'	A reference length taken as the maximum length from the vertex along the radial lines
M_o	Free stream Mach number
n'	Component of boundary layer velocity normal to potential velocity, Q' , i.e., crossflow velocity
N'	Absolute viscosity, external
N'_o	Absolute viscosity, free stream, $= \mu_o$
N	N'/TN'_o
P	Non-dimensional static pressure $P = \frac{p'}{p_o^*}$
p'	Static pressure
p_o'	Free stream static pressure
p_o^*	Static pressure parameter $p_o^* = \frac{\sigma}{\sigma-1} M_o^2 p_o', \frac{\sigma}{\sigma-1} = \gamma$
p_d'	Duct static pressure
$PHI = \varphi$	Shear coefficient defined in Reference 1, print-out notation
p_s'	Surface static pressure
q'	Boundary layer velocity
Q'	Local potential flow velocity
Q_o'	Free stream velocity
Q	$Q'/Q_o' = (U^{*2} + V^{*2})^{1/2}$
r'	Gas constant (1716 ft ² /sec ² °R)
R	Reynolds number $= L_o' U' \Lambda' / N'$
R_c	Chord Reynolds number. $R_c = Q_o' c' \Lambda_o' / \mu_o'$

ENGINEER	NORTHROP CORPORATION NORAIR DIVISION	PAGE 2.05
CHECKER		REPORT NO. NOR-67-136
DATE June 1967		MODEL X-21A

2.3 SYMBOLS (Continued)

$R_{\delta_{ss}} = R_{\theta}$ Momentum thickness Reynolds number. $R_{\delta_{ss}} = Q'\delta'_{ss}\Lambda'/\mu'_e$

R_n Boundary layer crossflow Reynolds number

$R_{n\delta}$ Boundary layer crossflow Reynolds number, based on total height δ' of boundary layer

$R_{n\delta} = n'_{\max} \delta'\Lambda'/\mu'_e$, where $\delta' = z'$ at $K = 2$. $K = 2$ corresponds to $\frac{u'}{U'} = .9975$, for 20 calculation steps through the boundary layer.

RN $R_{n\delta}/R_c$, in print out

$R_{0.1}$ Actual boundary layer crossflow Reynolds number, based on height z' somewhat less than δ' , where $n' = 0.1 n'_{\max}$

$$R_{0.1} = n'_{\max} z' 0.1 n'_{\max} \Lambda'/\mu'_e$$

$RO.1$ $R_{0.1}/R_c$, in print out

R_{ns} Critical crossflow stability Reynolds number, based on second derivative of velocity at wall

RNS R_{ns}/R_c , in print out

$R_{ns_{\min}}$ Minimum or neutral crossflow stability Reynolds number, less than R_{ns} .

NOTE: $RQ1 < RNS$ for crossflow stability.

R_o' Unit Reynolds number based on reference conditions (free stream). $R_o' = \frac{Q_o' \Lambda_o'}{\mu_o'}$

s' Component of boundary layer velocity in direction of potential velocity, Q'

t' Internal or boundary layer temperature

t_w' Wall temperature ($^{\circ}K$)

T' External or potential flow temperature = $t'_{K=1}$

$K = 1$ corresponds to $\frac{u'}{U'} = 1$

ENGINEER	NORTHROP CORPORATION NORAIR DIVISION	PAGE 2.06
CHECKER		REPORT NO. NOR-67-136
DATE June 1967		MODEL X-21A

2.3 SYMBOLS (Continued)

T_o'	Free stream temperature
t	$r't'/(Q_o')^2$
T	$r'T'/(Q_o')^2$, also $T = t$ in print out notation
u'	Component of q' normal to radial lines (velocity in ξ^2 direction).
U'	Component of Q' normal to radial lines (velocity in ξ^2 direction).
U	U'/Q'
U^*	U'/Q_o'
v'	Component of q' along radial lines (velocity in η direction).
v	v'/Q'
V'	Component of Q' along radial lines (velocity in η direction). For flow toward tip, V' is negative.
V	v'/Q' , also $V = v$ in print out notation.
V^*	V'/Q_o'
$w'=f'$	Suction velocity normal to wing surface (for suction, w' is negative).
\dot{w}	Suction flow rate
x'	Surface length in streamwise direction
x_s'	Length along surface arc from stagnation point
y'	Normal distance from center line of airplane to point on wing
z'	Height in boundary layer from wing surface
ZR	$z' \sqrt{R_c}/c'$
α'	$\partial x_s'/\partial \xi$ (equal to $2 L_o' \eta \xi Y_o'$ for tapered wing)
β'	$\partial L'/\partial \eta$ (equal to L_o' for tapered wing)

ENGINEER	NORTHROP CORPORATION NORAIR DIVISION	PAGE 2.07
CHECKER		REPORT NO. NOR-67-136
DATE June 1967		MODEL X-21A

2.3 SYMBOLS (Continued)

- $\gamma_s \left(\frac{\sigma-1}{\sigma} \right)$ Ratio of specific heat at constant pressure to specific heat at constant volume (equal to 1.4 for air).
- δ' Boundary layer thickness (complete list is given in App. F).
- $\delta'_s = \delta'_x$ Streamwise displacement thickness. $\delta'_s = \int (1-s'\lambda'/(Q'\Lambda')) dz'$
- $\delta'_{ss} = \theta_x$ Streamwise momentum thickness
- $\delta'_{ss} = \int (1-s'/Q') (s'/Q') (\lambda'/\Lambda') dz'$
- δ'_{uu} $\int (1-u'/U') (u'/U') (\lambda'/\Lambda') dz'$
- δ'_{uv} $\int (1-u'/U') (v'/V') (\lambda'/\Lambda') dz'$
- δ'_{vu} $\int (1-v'/V') (u'/U') (\lambda'/\Lambda') dz'$
- ϵ Gross error index defined in Reference 1.
- ζ Curvilinear coordinate normal to wing surface.
 $\zeta = (1-u'/U')^{1/2}$
- η Curvilinear coordinate along radial lines
- θ Local sweep angle (radians); momentum thickness
- θ_1 Leading edge sweep angle
- θ_2 Trailing edge sweep angle
- κ Thermal conductivity
- λ' Internal density (within boundary layer)
- Λ' External density (local density in potential flow)
- Λ'_0 Free stream density
- σ Non-dimensional constant-pressure specific heat coefficient
 $\sigma = \frac{\sigma'}{p}$
- σ' Constant-pressure specific heat coefficient
- μ'_1 Boundary layer internal viscosity
- μ'_e Local external viscosity
- μ'_0 Reference viscosity (usually free stream)

ENGINEER	NORTHROP CORPORATION NORAIR DIVISION	PAGE 2.08
CHECKER		REPORT NO. NOR-67-136
DATE June 1967		MODEL X-21A

2.3 SYMBOLS (Continued)

- ξ^2 Curvilinear coordinate along arc struck from point of intersection of leading and trailing edges
- ξ^* Singularity factor (equal to ξ for calculations where coordinate system starts from partial stagnation line or from front attachment line in swept wings).
- φ Shear coefficient defined in Reference 1, labelled PHI in print out.
- γ Angle from leading edge to radial line
- γ_0 Included angle between leading and trailing edges = $\theta_1 - \theta_2$
- Ω External vorticity

ENGINEER	NORTHROP CORPORATION NORAIR DIVISION	PAGE 2.09
CHECKER		REPORT NO. NOR-67-136
DATE June 1967		MODEL X-21A

2.3 SYMBOLS (Continued)

Superscript

' Denotes dimensioned quantity

Subscripts

x Streamwise direction

a Along arc

e External, in potential flow

i Internal, within boundary layer

LE At wing leading edge

max Maximum value

o Reference value or free stream

TE At wing trailing edge

wall At wing surface

For the symbols denoting velocities, temperatures, and densities, the lower case letters denote values within the boundary layer (n , q , s , t , u , v , λ) and capital letters denote values in the potential flow (Q , T , U , V , Λ).

2.4 SWEPT WING COORDINATE SYSTEM

The general three-dimensional boundary layer calculation uses the coordinates ξ^2 , η , ζ where ξ^2 and η are orthogonal curvilinear coordinates fixed on the body surface and the ζ coordinate is normal to the surface. The boundary layer development is calculated as a function of distance from the stagnation point for each surface, upper or lower. If the wing surface of a swept tapered wing is considered to be cut at the stagnation line and at the trailing edge and then flattened out holding the leading edge sweep angle fixed, geometric relationships between the streamwise surface distances, arc surface distances and angles can be defined as in Figure 2.1. The constant ξ^2 and η lines are the radial and circumferential lines generated from the point of intersection of the flattened surface. This system of flattening the wing surface results in an error in angle of sweep except at the leading edge or flow attachment line. The maximum error occurs at the trailing edge, where the X-21A sweep is 18.7° flattened and 18.8° projected. The error in sweep is not considered significant to the calculations of the boundary layer on the X-21A wing or on any other wing of similar sweep and thickness ratio.

ENGINEER	NORTHROP CORPORATION NORAIR DIVISION	PAGE 2.10
CHECKER		REPORT NO. NOR 67-136
DATE June 1967		MODEL X-21A

2.4 SWEPT WING COORDINATE SYSTEM (Continued)

The definition of the coordinates are:

$$\xi = \sqrt{Y/Y_0}$$

$$\eta = L'/L_0'$$

Y = Angle from leading edge to a radial line

Y_0 = Included angle between wing leading edge and trailing edge of flattened wing surface = $\theta_1 - \theta_2$

L' = Distance along a radial line from vertex

L_0' = A reference length taken as the maximum length along the radial lines

Defining the ξ function as a square root provides for closely spaced points in the leading edge region where the velocity is changing rapidly, and for wider spacing further aft.

Figure 2.1 shows this coordinate system. Other coordinates which will be used in the discussion are also shown.

θ_1 = Leading edge sweep angle

θ_2 = Trailing edge angle of flattened surface

θ = Local sweep angle on flattened surface

c' = Surface chord length from stagnation point in stream-wise direction

x' = Streamwise surface distance from stagnation point

c_a' = Surface arc length from stagnation point to trailing edge

x_a' = Distance along surface arc from stagnation point

y' = Normal distance from centerline of airplane to point on wing

b' = Wing span

ENGINEER	NORTHROP CORPORATION NORAIR DIVISION	PAGE 2.11
CHECKER		REPORT NO. NOR 67-136
DATE June 1967		MODEL X-21A

2.4 SWEPT WING COORDINATE SYSTEM (Continued)

The following relationships exist between the coordinates:

$$x_a' = L'Y$$

$$\xi^2 = Y/Y_0 = x_a'/c_a'$$

$$\xi^2 = \theta_1 - \arctan [\tan \theta_1 - (x'/c') (\tan \theta_1 - \tan \theta_2)] / (\theta_1 - \theta_2)$$

If the airfoil sections are not similar at all spanwise stations or if there is a spanwise variation of stagnation point location, the flattened surface will not have a straight trailing edge. Furthermore, unless the airfoil section is symmetric, θ_2 will differ for the upper and lower surfaces. These discrepancies will usually be quite small, as shown in 2.4, page 2.09.

If the flow parameters are independent of the spanwise coordinate η and thus depend only on ξ , the boundary layer becomes a function of only the two variables ξ and ζ . This will occur on a swept tapered wing if the isobars coincide with the radial lines (lines of constant ξ). Wind tunnel tests of the X-21A wing indicated that the isobars were sufficiently straight except in the regions near the fuselage and the pumping nacelles and at the wing tip. For these special regions, a three-dimensional form of the boundary layer program was used which solved the boundary layer differential equations considering both spanwise and chordwise variation of pressure coefficient and suction quantity. For all other regions, boundary layer calculations were made assuming that the flow parameters were invariant with η . This corresponds to setting η equal to 1 and setting the derivatives of the flow parameters with respect to η equal to zero. With these simplified equations, a dimensionless "similar solution" is obtained which is assumed to be valid for all η stations within the region of straight isobars. Note that this "similar solution" does not imply two-dimensional flow, for the potential velocity has components normal to and along the wing element line.

The three-dimensional boundary layer program requires more machine time for its calculations and more man hours to assure that the input curves of U^* and F_0^* are smooth in both the ξ^2 and η directions, and that these U^* and F_0^* curves have derivatives equal to zero at the side boundaries of the calculation region. Having completed the machine calculation, the region for which the solution is valid must be determined. This region of validity may be considerably smaller than the calculation region due to cumulative errors. Reprogramming will probably eliminate these difficulties in the use of this method, but it is preferable to

ENGINEER	NORTHROP CORPORATION NORAIR DIVISION	PAGE 2.12
CHECKER		REPORT NO. NOR 67-136
DATE June 1967		MODEL X-21A

2.4 SWEPT WING COORDINATE SYSTEM (Continued)

design the wing for straight isobars and thus reduce both these calculation difficulties and the difficulties encountered in designing slots and ducts for rapidly varying suction distributions. Detailed use of the three-dimensional program will not be discussed here. Results of three-dimensional calculations for the X-21A wing differed from previous "similar solution" results in requiring more suction near the wing root and the pumping pod and less suction in the tip region.

The components of the potential flow velocity vectors are defined by Figure 2.2

Q_0' = Free stream velocity

Q' = Local potential flow velocity

U' = Component of Q' normal to radial line

V' = Component of Q' along radial line (for flow toward tip, V' is negative)

Non-dimensional velocity ratios can then be defined.

$U^* = U'/Q_0'$

$V^* = V'/Q_0'$

$Q = Q'/Q_0' = \sqrt{U^{*2} + V^{*2}}$

Figure 2.2 also defines the components of the velocity vectors within the boundary layer.

s' = Component of boundary layer velocity in direction of potential velocity, Q' .

n' = Component of boundary layer velocity normal to potential velocity, Q' .

v' = Component of boundary layer velocity along radial lines (η direction).

u' = Component of boundary layer velocity normal to radial lines (ξ^2 direction).

$q' = \text{Boundary layer velocity} = \sqrt{(s')^2 + (n')^2} = \sqrt{(u')^2 + (v')^2}$

ENGINEER	NORTHROP CORPORATION NORAIR DIVISION	PAGE
CHECKER		2.13
DATE	June 1967	REPORT NO. NOR 67-136
		MODEL X-21A

2.5 CONVERSION FROM C_p to U^* , V^* DATA

The boundary layer input program requires that the velocity ratios U^* and V^* be known as functions of the surface arc coordinate ξ^2 . Wind tunnel data are usually presented as C_p versus chordwise station, where

$$C_p = (p_s' - p_o') / (\frac{1}{2} \Lambda_o' \eta_o' Q_o'^2)$$

p_s' = Local static pressure on airfoil surface

p_o' = Free stream static pressure

Λ_o' = Free stream density

Q_o' = Free stream velocity

First, the relation between surface distances and chord distances must be determined from equations of the wing surface, from drawings of airfoils on arc, or from measurements. Second, accurately determine the true stagnation point at the given flight condition from wind tunnel tests conducted specifically for this purpose. If, as is usually the case, the true stagnation point does not coincide with the most forward point on the airfoil, the coordinates should be transferred. The pressure and suction distributions can then be plotted as functions of the coordinate ξ^2 , which varies between zero and unity. Once the distribution of C_p on a surface arc is determined, these data can be converted to U^* , V^* data using a short IBM program. (For keypunch forms and deck set up see Appendix D.) The conversion depends upon the compressible energy equation, the condition of irrotationality of the external flow, and the assumption that flow parameters are invariant with η .

The compressible energy equation can be written in terms of pressure coefficient, C_p , and velocity ratio, Q . (See Reference 2, p. 55.)

$$C_p = 2 \left\{ \left[1 + (\gamma - 1) M^2 (1 - Q^2) / 2 \right]^{\frac{\gamma}{\gamma - 1}} - 1 \right\} / \gamma M^2$$

where γ is the ratio of the specific heat at constant pressure to the specific heat at constant volume and M is the free stream Mach number. Solving for Q^2 ,

ENGINEER	NORTHROP CORPORATION NORAIR DIVISION	PAGE 2,14
CHECKER		REPORT NO. NOR 67-136
DATE June 1967		MODEL X-21A

2.5 CONVERSION FROM C_p DATA TO U*, V* DATA, (Continued)

$$Q^2 = 1 - 2[(1 + \frac{\gamma}{2} M^2 C_p) \frac{\gamma-1}{\gamma} - 1] / [(\gamma-1) M^2]$$

For air, $\gamma = 1.4$, so the equation becomes

$$Q^2 = 1 - 5 [(1 + 0.7 M^2 C_p)^{2/7} - 1] / M^2 \quad (2a)$$

For a "similar" solution, the requirement of irrotational potential flow leads to the equation (See Appendix B)

$$\partial V^* / \partial (\xi)^2 = \gamma_0 U^*$$

$$V^* = \int_0^{\xi^2} \gamma_0 U^* d\xi^2 + \text{const.} = \gamma_0 \int_0^{\xi^2} \frac{\xi^2}{\sqrt{Q^2 - V^{*2}}} d\xi^2 + V^*_{LE} \quad (3)$$

The velocity ratio, V^* , is calculated by solving first for Q at a point on the arc from the known value of C_p at that point. V^* on the right hand side of the equation is then assumed to equal $\sin \theta$ and the integration is performed yielding a new approximation of V^* . The process is continued until two consecutive approximations of V^* are sufficiently close.

The constant of integration is the value of V^* at the stagnation line.

If the stagnation C_p is known, the value of V^* at the stagnation line may be calculated.

$$V^{*2} = Q^2_{LE} = 1 - 5 [(\frac{\gamma}{2} M^2 C_p + 1)^{2/7} - 1] / M^2$$

$$V^*_{LE} = -\sqrt{(V^*_{LE})^2}$$

The iteration is then performed with V^* at the stagnation line fixed. If the stagnation C_p is not known, it can be calculated from compressible flow equations, stagnating only the component normal to the leading edge.

ENGINEER	NORTHROP CORPORATION NORAIR DIVISION	PAGE	2.15
CHECKER		REPORT NO.	NOR 67-136
DATE June 1967		MODEL	X-21A

2.5 CONVERSION FROM C_p DATA TO U^* , V^* DATA (Continued)

This U^* , V^* iteration program, 919K¹, punches the final values of U^* versus ξ^2 in the proper format for use in the boundary layer input program, BB62A.

2.6 THE F_o^* PARAMETER

The optimum suction can be determined by a process of successive approximations or by direct calculation from the program. The program contains an option statement that determines the required suction distribution to satisfy the boundary layer stability criteria for given input conditions. Otherwise, for an initial suction distribution, the boundary layer development is calculated and the stability determined. (Appendix A outlines the calculation step for each version.)

The suction is specified by the suction parameter, F_o^* , where F_o^* is a continuous function of arc chord. Although the LFC system provides for suction through discrete slots, the boundary layer stability is calculated assuming a continuous suction distribution, such as might be obtained through a hypothetical porous wing surface. The suction parameter F_o^* is defined:

$$F_o^* = (w' \lambda'_{wall} \sqrt{Rc}) / Q_o' \Lambda_o'$$

where

- w' = suction inflow velocity (for inflow, w' is negative, but for outflow, w' is positive)
- Rc = Chord Reynolds number
- Q_o' = Free stream velocity
- λ'_{wall} = Density within boundary layer at wing surface
- Λ_o' = Free stream density

¹Footnote

919K, BB62A, and BB65A are deck numbers assigned by Norair to the digital computer programs. 919K denotes the U^* , V^* iteration deck, BB62 denotes the boundary layer input deck, and BB65A denotes the boundary layer integration and summary deck.

ENGINEER	NORTHROP CORPORATION NOR AIR DIVISION	PAGE
CHECKER		2.16
DATE	June 1967	REPORT NO. NOR-67-136
		MODEL X-21A

2.6 THE F_o^* PARAMETER (Continued)

Thus, F_o^* is always negative for suction. Figures 2.3 and 2.4 present typical distributions of F_o^* .

2.7 DIGITAL COMPUTER PROGRAMS

All data required for the boundary layer programs have now been determined. The program RB62A/5A requires inputs of two different types. General inputs referring to physical quantities and control-type indicators referring to the internal structure of the computing method are used in the program.

General input information required: (1) freestream Mach number, temperature and static pressure; (2) geometric information as Q_1 and θ_2 (leading edge and trailing edge sweep angles), reference chord C' , and when the computation starts at the leading edge, V^* , the non-dimensional velocity component along the leading edge at the front attachment line for swept wings; (3) when the calculation starting point is not at the front attachment line, the initial profiles are required; and (4) the U^* and F_o^* distributions when the latter is an input to the program. Control-type indicators are required that state integration step inputs, flow parameters to be used by the integration phase of the program, printed or punched output, initial profile iteration steps and direct suction input data.

Usually the boundary layer computations for a wing begin at the flow attachment line at the leading edge, and no starting boundary layer profiles are required. The program automatically computes the starting profiles in this case. However, if the computation is begun at some chordwise station downstream of the flow attachment line, starting profiles for the spanwise velocity parameter ($v = v'/Q'$), the temperature parameter ($t = r't'/Q_o'^2$), and the shear coefficient ϕ as defined in Reference 1 are required. The boundary layer profiles of the forward derivatives of these parameters also are required.¹ These starting profiles normally are taken from a previous computation wherein print out of the profiles has been requested. In the print-out, the FORTRAN

¹

See footnote on next page.

ENGINEER	NORTHROP CORPORATION NORAIR DIVISION	PAGE 2.17
CHECKER		REPORT NO. NOR-67-136
DATE June 1967		MODEL X-21A

2.7 DIGITAL COMPUTER PROGRAMS (Continued)

language for the parameters v , t , and ϕ are V , T , and Φ , respectively; and the print out of the forward derivatives are designated VA , TA , and SA , respectively. The starting profiles need not be exact, because the program iterates on the starting profiles until they are compatible with the continued development of the boundary layer. Appendix E includes a sample of a key punch form for starting profiles to be used if required.

It is wise to check the distribution of C_p versus ξ^2 and F_o^* versus ξ^2 to identify any errors in tabulating or key punching the data, and to determine if an adequate number of points has been used for a correct interpolation. The curve fitting sub-routines of BB62A/5A and 919K fit the input data points with cubic equations. If the input curve of U^* or F_o^* is not similar to a cubic curve, the points must be spaced carefully to obtain a satisfactory curve fit. Rules for selecting input data points and key punch forms for BB62A/5A are given in Appendices C and E.

¹Footnote

In the difference method of solution of the boundary layer equations, associated with each point is a parallelepiped domain which is replaced by a lattice of points with constant spacings a , b , c and integer indices i , j , k in the coordinate directions.

In this lattice the dependent variables v , t , and ϕ and the derivatives are replaced by their set of values at the lattice points, each such value being identified by the subscript i , j , k as necessary. Forward derivative is interpreted as the values of the first derivative of the dependent variables in the i or chordwise direction.

ENGINEER	NORTHROP CORPORATION NORAIR DIVISION	PAGE 2.18
CHECKER		REPORT NO. NOR-67-136
DATE June 1967		MODEL X-21A

2.7 DIGITAL COMPUTER PROGRAMS (Continued)

The parameters calculated by the Raetz boundary layer integration method are in a non-dimensional form. Additional calculations are required to reduce the data to conventional quantities. The boundary layer program thus consists of two distinct sets of calculations: (1) the numerical integration of the boundary layer equations for V , T , and Φ and the calculation of certain non-dimensional parameters, and (2) the summary phase in which the integration results are converted to conventional boundary layer parameters. A magnetic tape is used to connect the two sets of calculations. Subroutines have been added to calculate R_{ns} and to print dimensional velocity profiles.

Appendix E presents keypunch forms and Appendix F presents definitions of the parameters printed by the summary part of the program.

2.8 LAMINAR BOUNDARY LAYER STABILITY

Because low energy boundary layer air on a swept wing tends to be deflected toward regions of lower static pressure, both the direction and the magnitude of the boundary layer velocity vectors will vary with height from the wing surface. The locus of the velocity vectors at a given point on the wing will form a three-dimensional surface as in Figure 1.1 of Section 1. This velocity surface can be projected onto planes in the potential flow direction and normal to the potential flow direction, giving tangential (or longitudinal) and crossflow (or transverse) velocity profiles. With this projection, the crossflow velocity vanishes at the outer edge of the boundary layer. Figure 1.5 shows the general shapes of these profiles. The crossflow profile changes direction, being directed inboard for the forward part of the wing (the region of decreasing pressure) and outboard for the aft wing (the region of increasing pressure). Figure 1.5 of Section 1 shows typical crossflow profiles at various chordwise locations.

The subject of boundary layer stability is discussed in more detail in Section 1. However, a review is appropriate at this time, using the notation applicable to this section of the report.

The stability of a laminar boundary layer will depend on both tangential and crossflow profiles. Aft of the stagnation line, the crossflow profile is more critical and, in most cases, a consideration of only crossflow stability is sufficient. At the stagnation line the tangential profile will be in the V' direction, directed toward the tip along the leading edge. There is no crossflow profile at the stagnation line.

Boundary layer stability is determined from two Reynolds numbers, a crossflow Reynolds number and a momentum thickness Reynolds number. The crossflow Reynolds number is defined

ENGINEER	NORTHROP CORPORATION NORAIR DIVISION	PAGE 2.19
CHECKER		REPORT NO. NOR-67-136
DATE June 1967		MODEL X-21A

2.8 LAMINAR BOUNDARY LAYER STABILITY (Continued)

$$R_{0.1} = (n'_{\max} z'_{0.1 n'_{\max}} \Lambda') / \mu_e' \quad (\text{called actual crossflow Reynolds number})$$

where

$$n'_{\max} = \text{Maximum value of crossflow velocity}$$

$$z'_{0.1 n'_{\max}} = \text{Height from surface where } n' \text{ is one tenth its maximum value}$$

(Note: There are two such points for a typical crossflow profile; the one furthest from the wing surface is $z'_{0.1 n'_{\max}}$. See Figure 2.5.)

$$\mu_e' = \text{Viscosity at the outer edge of the boundary layer}$$

$$\Lambda' = \text{Density at outer edge of boundary layer}$$

The tangential momentum thickness Reynolds number is defined

$$R_{\delta_{ss}} = (Q' \delta'_{ss} \Lambda') / \mu_e'$$

where

$$Q' = \text{Local potential flow velocity}$$

$$\Lambda' = \text{Density at the outer edge of the boundary layer}$$

$$\mu_e' = \text{Viscosity at the outer edge of the boundary layer}$$

$$\delta'_{ss} = \int_0^{\delta} (\lambda' / \Lambda') (1 - s' / Q') (s' / Q') ds'$$

From results of numerical integration of the Orr-Sommerfeld equations, Dr. W. B. Brown has found a linear equation relating the minimum crossflow stability Reynolds number, $R_{n_s \min}$ and the second derivative of the crossflow velocity at the wall. Wind tunnel tests on a 7 ft. chord swept wing (Reference 3) demonstrated that laminar flow could be maintained for crossflow Reynolds number 1.8 times the theoretical minimum value. Figure 2.6 shows $R_{n_s \min}$, and $R_{n_s} = 1.8 R_{n_s \min}$.

ENGINEER	NORTHROP CORPORATION NORAIR DIVISION	PAGE 2.20
CHECKER		REPORT NO. NOR-67-136
DATE June 1967		MODEL X-21A

2.8 LAMINAR BOUNDARY LAYER STABILITY (Continued)

To evaluate crossflow stability from results of the IBM programs, the actual and critical magnitudes are compared. The actual value of $R_{0.1}/R_c$ (labelled R0.1 in the IBM print out) is computed in the program from the calculated crossflow velocity profile. The critical value, R_{ns}/R_c (labelled RNS) is evaluated in the program from the second derivative at the wall,

$$N_{ZZ} = (\partial^2(n'/n'_{\max})/\partial(z'/z'_{0.1} n'_{\max})^2$$

and from the linear equation

$$R_{ns} = 102 - 1.29 N_{ZZ}.$$

These two Reynolds numbers can be plotted as a function of the surface arc, ξ^2 . The actual crossflow Reynolds number printed by the integration program will have a plus or minus sign to indicate the direction of crossflow, the positive sign indicating flow toward the fuselage and the negative sign flow toward the wing tip. The sign of the critical crossflow Reynolds number is given, and is the same as that of the actual crossflow Reynolds number at the same ξ^2 . If the absolute value of R_{ns}/R_c exceeds the absolute value of $R_{0.1}/R_c$, suction is adequate for stability.

A criterion for a stable tangential boundary layer profile is shown in Section 1. The allowable tangential momentum thickness Reynolds number is specified by equation and by graph as a function of the second derivative of the tangential velocity profile at the wall. Both the neutral stability value and a somewhat higher value of momentum thickness Reynolds number, determined from tests, are shown. Tangential instability is most likely to occur in the mid-chord region at high values of chord Reynolds number. In the mid-chord region, with a flat chordwise pressure gradient, suction requirements for crossflow stability are quite low because the boundary layer air is deflected only slightly from the potential flow direction. Suction increases may be required in the mid-chord region to reduce $R_{\delta ss}$ to a satisfactory value. The IBM program prints out $R_{\delta ss}$ labelled RDELSS and, if dimensional data is requested, $R_{\delta ss}$ is also printed out and is labelled TANCRT.

During flight tests of the X-21A, it was discovered that the leading edge region of a swept wing is particularly sensitive to disturbances. Disturbances in the stagnation region of a swept wing may cause turbulence which spreads spanwise along the leading edge instead of producing chordwise turbulent wedges.

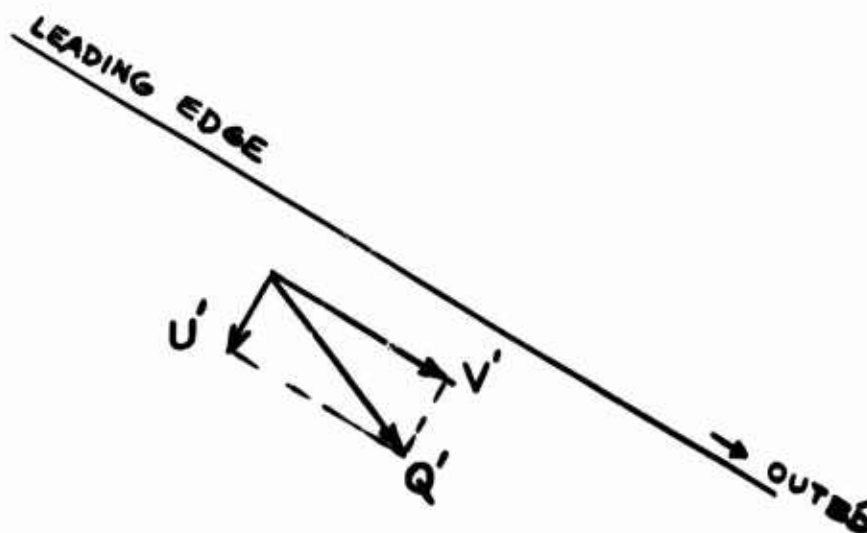
ENGINEER	NORTHROP CORPORATION NORAIR DIVISION	PAGE 2.21
CHECKER		REPORT NO. NOR-67-136
DATE June 1967		MODEL X-21A

2.8 LAMINAR BOUNDARY LAYER STABILITY (Continued)

Wind tunnel tests (Reference 4) indicated that a disturbance would cause complete spanwise contamination when the stagnation line momentum thickness Reynolds number was greater than approximately 100. However, if the disturbance is located aft of the point where the potential flow velocity vector has turned 10.6 degrees from the stagnation line, the turbulence will spread chordwise rather than spanwise (Reference 5).

The stability of the laminar boundary layer in the stagnation zone can be estimated from results of the IBM calculations. The attachment line momentum thickness Reynolds number is based on the attachment line momentum thickness, the spanwise velocity along the leading edge and the external kinematic viscosity. This Reynolds number is identical to $R_{\delta_{ss}}$ at the attachment line along which Q' equals V' .

Therefore, to determine the stability of the leading edge boundary layer, the calculated value of $R_{\delta_{ss}}$ can be compared with its critical value of 100. This stability criterion should be applied from the attachment line to the point where the potential flow velocity vector has turned 10.6 degrees from the leading edge sweep angle. As the following sketch shows, this point can be located by determining where the variable $U = U'/Q'$ attains the value of $\sin 10.6^\circ = 0.184$. U is not printed out by the IBM program, but can be obtained from the equation $U = U^*/Q$. U^* and Q are printed out on the IBM program.



Aft of this point, crossflow again becomes the critical factor in determining stability. At low unit Reynolds numbers or with small leading edge radii, leading edge suction may not be required.

ENGINEER	NORTHROP CORPORATION NORAIR DIVISION	PAGE 2.22
CHECKER		REPORT NO. NOR 67-136
DATE June 1967		MODEL X-21A

2.8 LAMINAR BOUNDARY LAYER STABILITY (Continued)

The two numerical stability limits for $R_{\delta_{ss}}$, the critical turning angle of 10.6 degrees, and the multiplying factor of 1.8 for the minimum crossflow stability limit Reynolds number, R_{δ_s} , have all been determined experimentally. These stability criteria are tentative and representative of mean conditions. In a specific case the criteria may be exceeded or may be smaller depending upon geometric and flow characteristics.

2.9 OPTIMIZATION OF SUCTION DISTRIBUTION

As discussed in Section 2.8, the stability of the laminar boundary layer is determined from the comparison of actual and critical Reynolds numbers. In the design of an LFC wing, it is desirable to find a suction distribution which is just adequate to maintain a stable laminar boundary layer in the presence of small disturbances. Excessive suction is inefficient because it requires more work by the pumping system. It may actually be harmful because a very thin boundary layer is extremely sensitive to surface roughness. Hence if the critical crossflow Reynolds number is much larger than the actual crossflow Reynolds number, the suction should be reduced.

The optimum suction distribution is found by the process of obtaining the adequate velocity profile that satisfies the boundary layer stability criteria. This process is automatically carried out in the program if the option of direct suction is requested. An outline of the program mode of operation for direct suction calculations is shown in Appendix G.

The required F_o^* will depend on the margin between the actual and critical stability Reynolds numbers, on the chordwise location (leading edge, midchord, or aft chord), the C_p distribution, the chord Reynolds number, compressibility effects, and wing geometry. In general, a swept wing will require high suction at the leading edge to control crossflow and leading edge instabilities, low suction in the midchord region, and high suction to control crossflow instability in the region of the rear pressure rise. This shape applies to both the upper and the lower surfaces, but the upper surface will have a higher leading edge suction peak.

2.10 OTHER APPLICATIONS OF THE BOUNDARY LAYER PROGRAM

2.10.1 BOUNDARY LAYER DEVELOPMENT WITH NO SUCTION

The growth of the laminar boundary layer without suction can be obtained by setting F_o^* equal to zero and the option for direct suction equal to zero. A distribution of five points (one card) with all F_o^* 's equal to zero is used. The

ENGINEER	NORTHROP CORPORATION NORAIR DIVISION	PAGE	2.23
CHECKER		REPORT NO.	NOR 67-136
DATE June 1967		MODEL	X-21A

BB62A/5A program will calculate the boundary layer development up to the point where laminar separation begins. At this point the numerical integration diverges and meaningless numbers are calculated. However, the program will continue calculating with these meaningless numbers until it reaches a point where one of the values of the temperature profile ($t = rt'/Q_0'^2$) becomes negative. Then the remark "T IS NEGATIVE" is printed out and execution stops. In this case, summary information is not calculated.

To obtain summary data, it is necessary to stop the integration before t becomes negative. It is usually satisfactory to stop the integration before a positive chordwise pressure gradient (usually, the "rear pressure rise") is encountered. The way to determine how far aft the data are usable is by observing the divergence of the profile shapes from normal profile shapes.

Stability of the laminar boundary layer with no suction can be determined from the tangential and crossflow Reynolds numbers as explained in Section 2.8. This no-suction stability calculation enables one to determine the required location of the first suction slot for a given flight condition.

No-suction calculations can also be performed to determine whether a proposed slot can be eliminated. This has been done in the X-21A program in a region of four slots to determine if the third slot could be eliminated. A continuous suction distribution which dropped to zero was assumed forward of the point midway between the first two slots. The profile at this point was then used as an initial profile for a no-suction run to the second slot. Flow through slot number 2 was determined by calculating the amount of boundary layer air removed based on requirements determined in a previous continuous suction analysis. The boundary layer profiles at the rear of the slot were found using the continuity, energy, and momentum equations for compressible flow. These profiles were then used as initial profiles for a second no-suction run.

2.10.2 BOUNDARY LAYER THICKNESS, WAKE DRAG AND SUCTION DRAG

The thickness of the laminar boundary layer, δ' , can be defined as the height at which the boundary layer velocity is 99.75 percent of the potential flow velocity. This boundary layer thickness can be obtained directly if dimensional print-out is requested. Then δ' (in inches) is printed out at each print-out station as the value of z' corresponding to $K = 2.0$ on the integration phase print-out, where 20 calculation steps are made through the boundary layer.

ENGINEER	NORTHROP CORPORATION NORAIR DIVISION	PAGE 2.24
CHECKER		REPORT NO. NOR 67-136
DATE June 1967		MODEL X-21A

(If dimensional print-out is not requested, δ' can be obtained from ZR_w)

The local wake drag coefficient for an LFC wing can be obtained from the free stream Mach number, the trailing edge angle, and the values of T, P, DELUUR, DELVUR and USTAR printed for the trailing edge by the computer program. By use of the momentum theorem for flow through a streamtube, the wake drag coefficient can be expressed in terms of the trailing edge sweep angle and the values of the momentum thicknesses, δ'_{uu} and δ'_{vu} at a station far downstream. (For proof, see Reference 6).

$$c_{dw} = 2 \cos \theta_2 (\delta'_{uu} \cos^2 \theta_2 + \delta'_{vu} \sin^2 \theta_2) / c'$$

where

$$\delta'_{uu} = \int (1 - u'/U') (u'/U') (\lambda'/\Lambda') dz'$$

$$\delta'_{vu} = \int (1 - v'/V') (u'/U') (\lambda'/\Lambda') dz'$$

and the subscript ∞ denotes downstream values. The downstream values of δ'_{uu} and δ'_{vu} are related to their values at the trailing edge by integrating the wake momentum equations (as derived by Squire and Young in Reference 7) yielding the relations:

$$\delta'_{uu} = \frac{H+5}{2} (U'/U_{o'}) \delta'_{uuTE} (\Lambda'/\Lambda_{o'})$$

$$\delta'_{vu} = (U'/U_{o'}) \delta'_{vuTE}$$

Since the computer program solves the boundary layer equations assuming laminar flow, the value of the calculated shape factor, H, is a laminar value. In the wake behind the wing, the flow becomes turbulent. The Squire and Young relationship between the trailing edge and downstream values of δ'_{uu} applies to turbulent flow. The assumption is made that at the trailing edge, H changes from a laminar value to a turbulent value without changes in the trailing edge momentum thicknesses, δ'_{uu} and δ'_{vu} . For incompressible turbulent flow, H at the trailing edge is approximately equal to 1.4. The compressible value of H is related to its incompressible value by the equation

ENGINEER	NORTHROP CORPORATION AERONAUTICS DIVISION	PAGE 2.25
CHECKER		REPORT NO. NOR-67-136
DATE June 1967		MODEL X-21A

2.10.2 BOUNDARY LAYER THICKNESS, WAKE DRAG AND SUCTION DRAG (Continued)

$$H_{comp} = (H_{incomp} + 1) (1 + 0.2M^2) / (1.4TM^2) - 1$$

and for an incompressible turbulent H of 1.4

$$H_{comp} = 1.2(1 + 0.2M^2) / (.7TM^2) - 1$$

This value of H is used in the equation for δ'_{uu} .

Appendix H presents a calculation for the wake drag coefficient of an LFC wing. In this form the computations have been simplified using the relationship $\Lambda'/\Lambda_0' = P/T$ and $U'/U_0' = U^*/\cos \theta_2$.

The foregoing calculation of wake drag coefficient is used in conjunction with a theoretical calculation of boundary layer development on the wing. The calculation of wake drag coefficient based on flight test measurements of the trailing edge boundary layer pressure measurements is made by Chang's method, referenced in Section 12.

The equation used to compute the incremental value of equivalent suction drag coefficients is

$$dC_{Ds}/R_c = F^* \left\{ 1.0 + \frac{t'_{wall}}{0.2 T_0' M^2} \left[\left(\frac{P_0'}{P_s' - 0.035 M^2} \right)^{2/7} - 1.0 \right] \right\}$$

This equation was derived assuming that the pressure drop through the slots is five percent of the free stream dynamic pressure, $\frac{1}{2}\rho_0'(Q_0')^2$, and that the suction chamber temperature is the same as that at the wing surface. Appendix I presents a calculation form for the incremental value of equivalent suction drag coefficient.

An estimate of the local suction drag for a given distribution of suction parameter and pressure coefficient can be obtained by plotting dC_{Ds} vs. ξ^2 , integrating and multiplying the result by the square root of the chord Reynolds number. Then the total section drag coefficient is equal to the sum of the section wake drag coefficient, c_{dw} , and the section suction drag coefficient c_{ds} . Of course, if the details of the pumping system are known, the suction drag should be calculated by the methods of Section 12 and not by this method.

ENGINEER	NORTHROP CORPORATION NORAIR DIVISION	PAGE 2.26
CHECKER		REPORT NO. NOR-67-136
DATE June 1967		MODEL X-21A

2.10.3 CALCULATION OF THE THEORETICAL STABILITY OF FLIGHT TEST SUCTION REQUIREMENTS

The boundary layer programs can be used to calculate the predicted stability of a tested suction. In the X-21A tests, the actual surface static pressure distributions were measured, using flush static orifices at Wing Station 330 ($y/(2b) = .588$) and strip-a-tube at other wing stations. From these pressures, the C_p and U^* distributions were obtained. Pressures in the ducts were measured by static pressure orifices at the duct ends. The pressure variation along a duct had previously been calculated, hence the duct pressures could be found for the same wing station as the surface static pressures. The flow rate, \dot{w} (lbs/sec), was determined for each duct from known relationships between the non-dimensional duct pressure drop $(p_d - p_s)/p_d$, and the flow rate parameter, $(\dot{w}/T')/p_d$. F_o^* was determined from \dot{w} . The laminar boundary layer development was calculated as usual and compared with the indications of laminar flow in flight.

For examples thus far calculated, when laminar flow has been indicated by the total pressure probes, the suction was adequate or more than adequate. Figures 2.7 and 2.8 show distributions of F_o^* , $R_{0.1}/R_c$, and R_{ns}/R_c for examples of flight test suction distributions from the X-21A program.

2.10.4 DETERMINATION OF "STREAMLINES"

Strictly speaking, a streamline defines the path of a particle of fluid. In regard to streamlines within the boundary layer of a wing laminarized by suction, the fluid particles progress toward the surface and disappear into the wing. Thus a true streamline within the boundary layer might begin at some chordwise station aft of the leading edge, progress downward through the boundary layer, and disappear at a downstream chordwise station. A more meaningful determination of boundary layer flow paths across the chord of a wing can be made by neglecting the component of velocity normal to the wing surface and examining only the u' and v' components of velocity. In this way the flow path at any height within the boundary layer (e.g., at the outer edge or at mid-height) can be determined.

The following equation holds for any "streamline" or flow path parallel to the wing surface:

$$u' dL' - v' dx'_s = 0$$

ENGINEER	NORTHROP CORPORATION NORAIR DIVISION	PAGE 2,27
CHECKER		REPORT NO. NOR-67-136
DATE June 1967		MODEL X-21A

2.10.4 DETERMINATION OF "STREAMLINES" (Continued)

In the swept wing coordinate system

$$dL' = L_o' d\eta$$

$$dx_a' = d(\xi^2) \Psi_o \eta L_o' \xi d\xi$$

so

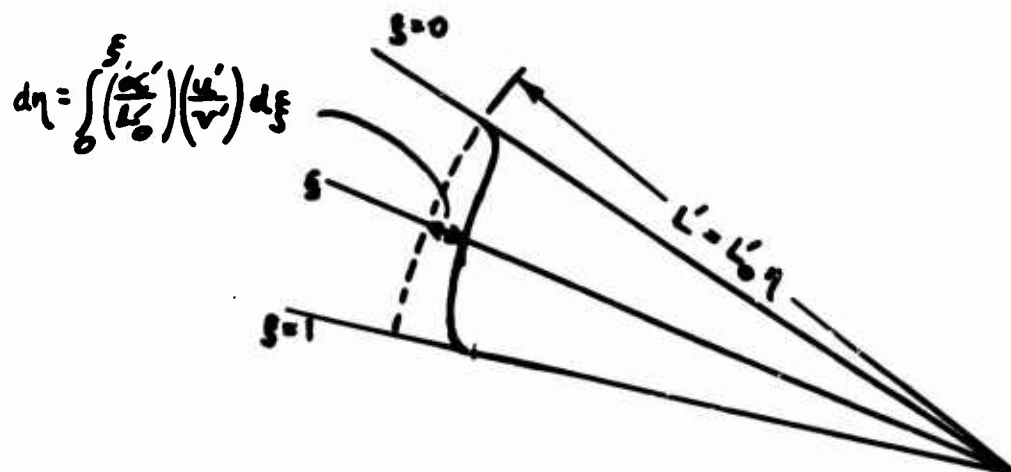
$$u' L_o' d\eta - v' 2 \Psi_o \eta L_o' \xi d\xi = 0$$

$$d\eta/d\xi = (v'/u') 2 \Psi_o \eta \xi$$

and since for a swept wing $\alpha' = 2 L_o' \eta \xi \Psi_o$

$$d\eta/d\xi_{\text{streamline}} = (\alpha'/L_o') (v'/u')$$

The deflection of the "streamlines" from the surface arc at any arc chord station ξ^2 are obtained by integration. The following sketch clarifies the relation:



Actually, the integration cannot be performed explicitly because v'/u' is indeterminate at the leading edge. However, a good approximation to the integral is obtained by plotting $\frac{d\eta}{d\xi}$ versus ξ and integrating graphically.

An example of the potential flow "streamline" path across a swept LFC wing is shown in Figure 1.2.

ENGINEER	NORTHROP CORPORATION NORAIR DIVISION	PAGE	2.28
CHECKER		REPORT NO.	NOR 67-136
DATE		MODEL	X-21A
June 1967			

2.11 REFERENCES

1. Raetz, G. S., "A Method of Calculating Three-Dimensional Laminar Boundary Layers of Steady Compressible Flows," Norair Division, Northrop Corporation Report NAI-58-73 (BLC-114), December, 1957.
2. Liepmann, H. W. and Roshko, A., "Elements of Gasdynamics," John Wiley and Sons, 1957.
3. Pfenninger, W. and Bacon, John, "About the Development of Swept Laminar Suction Wings with Full Chord Laminar Flow," Norair Report NOR-60-299 (BLC-130), January, 1961.
4. Carlson, J. C., "Results of a Low Speed Wind Tunnel Test to Investigate the Influence of Leading Edge Radius and Angle of Attack on the Spanwise Spread of Turbulence along the Leading Edge of a Swept-Back Wing," Norair Report NOR-64-30, March, 1964.
5. Gregory, N., "Transition and the Spread of Turbulence on a 60° Swept-Back Wing," Journal of the Royal Aeronautical Society, September, 1960.
6. Raetz, G. S., "Evaluation of the Profile Drag Coefficient of an Untapered Swept Suction Wing," Appendix I of Northrop Report NAI 57-317 (BLC-93).
7. Squire, H. B. and Young, A. D., "The Calculation of the Profile Drag of Aerofoils," R&M 1838, 1937.
8. Der, J. Jr., and Raetz, G. S., "Solution of General Three-Dimensional Laminar Boundary Layer Problems by an Exact Numerical Method," IAS Paper 62-70, January, 1962.

ENGINEER	NORTHROP CORPORATION NORAIR DIVISION	PAGE 2.29
CHECKER		REPORT NO. NOR 67-136
DATE June 1967		MODEL X-21A

2.12 TABLE OF FIGURES

- 2.1 Swept Wing Coordinate Systems
- 2.2 Velocity Components
- 2.3 Suction and Crossflow Reynolds Number Distributions,
Design Suction X-21A Wing, $\eta = .31$ Lower Surface
- 2.4 Suction and Crossflow Reynolds Number Distributions,
Design Suction X-21A Wing, $\eta = .31$ Upper Surface
- 2.5 Boundary Layer Profiles
- 2.6 R_{n_s} and R_{n_s}
 \min
- 2.7 (a & b) X-21A Flight Test Suction: Correlation of Suction
Distributions
- 2.8 X-21A Flight Test Section: Actual and Critical Crossflow
Reynolds Numbers

ENGINEER	NORTHROP CORPORATION NORAIR DIVISION	PAGE 230
CHECKER		REPORT NO. NOR 67-136
DATE June 1967		MODEL X-21A

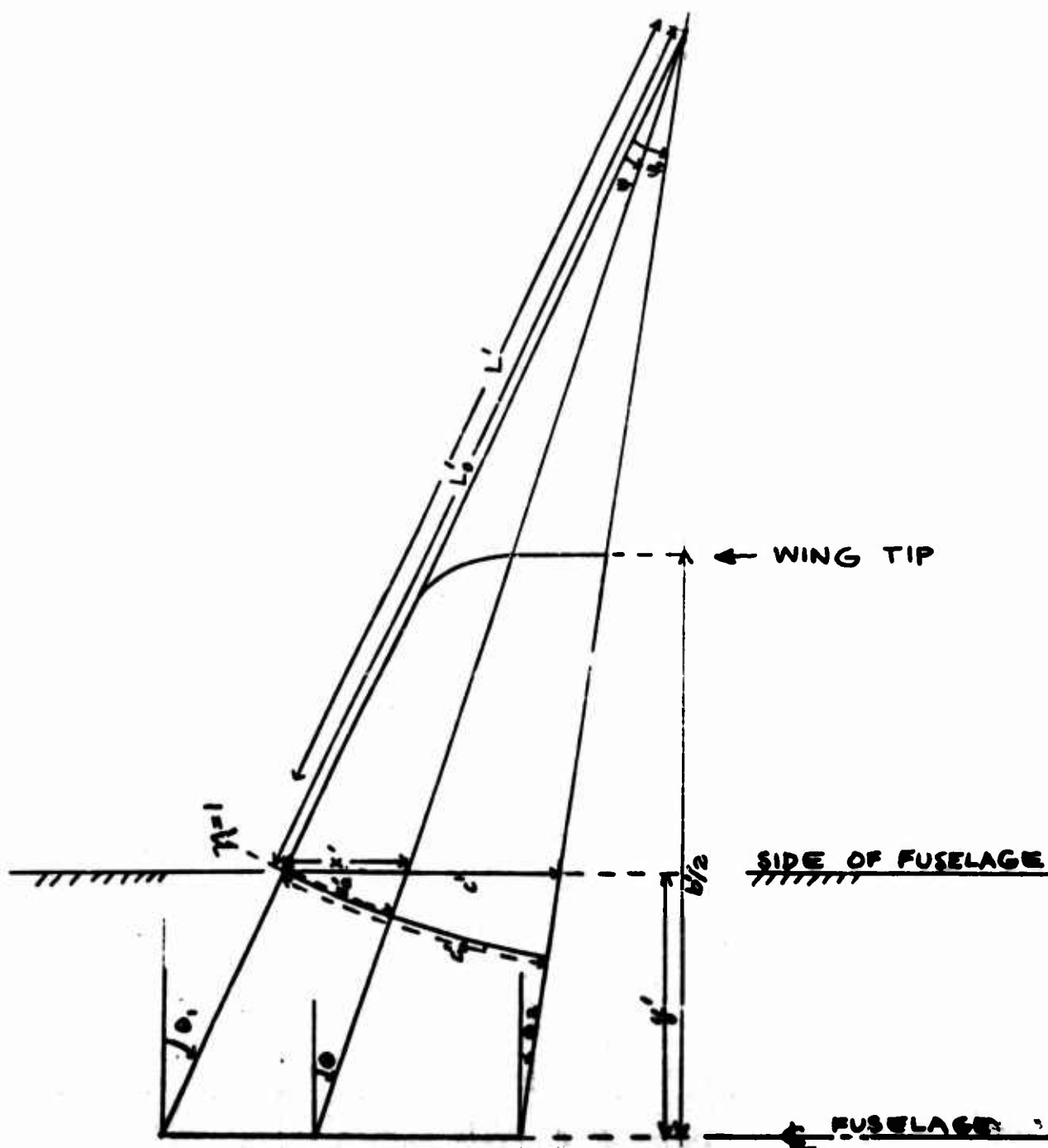
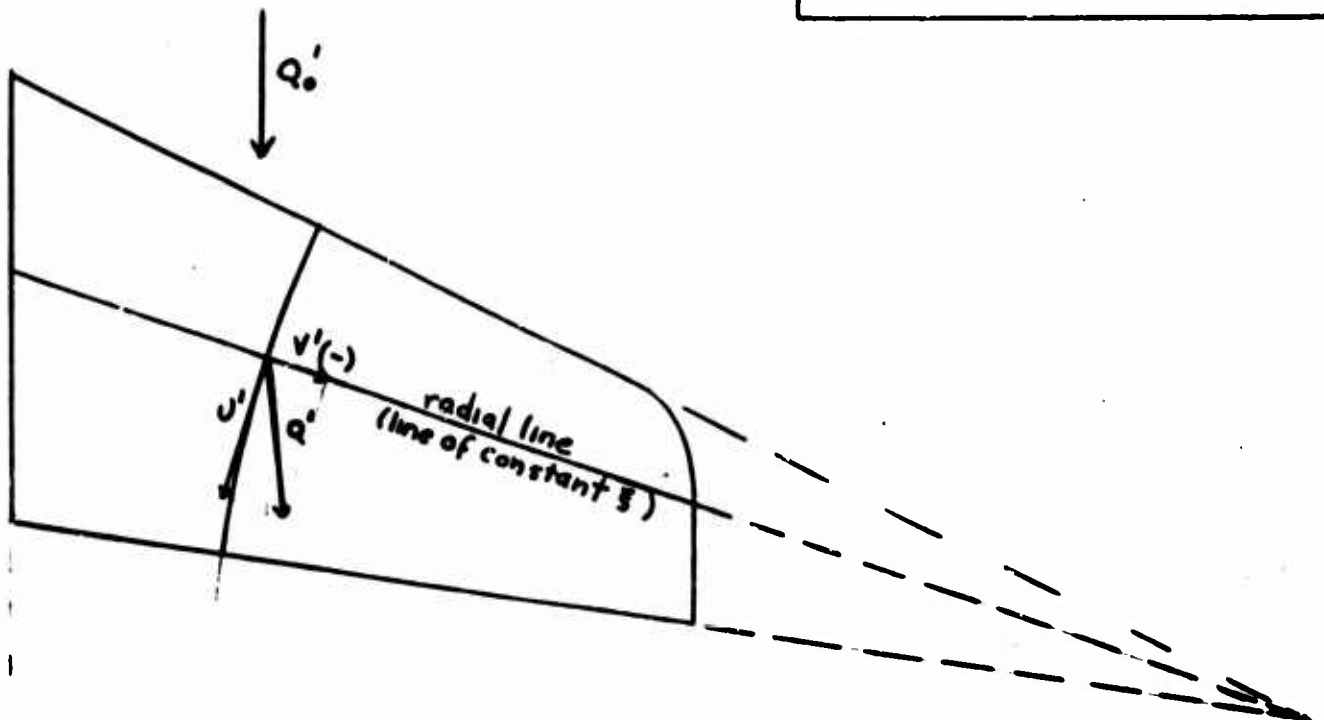


FIGURE 2.1 SWEPT WING COORDINATE SYSTEMS

ENGINEER	NORTHROP CORPORATION NORAIR DIVISION	PAGE 2.31
CHECKER		REPORT NO. NOR-67-136
DATE June 1967		MODEL X-21A

Potential Flow Velocity Components



Boundary Layer and Potential Flow Velocity Components

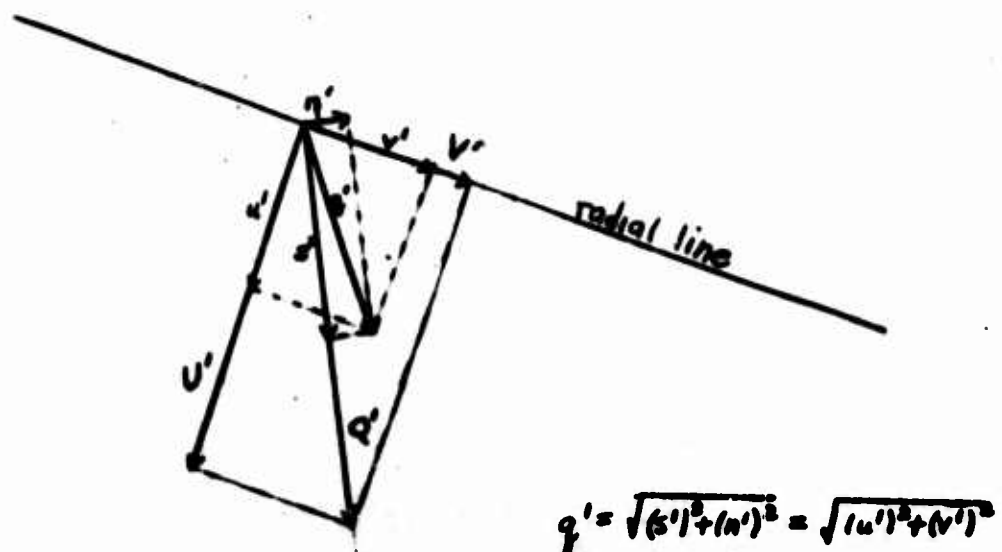


FIGURE 2.2 VELOCITY COMPONENTS

ENGINE
CHECK
DATE

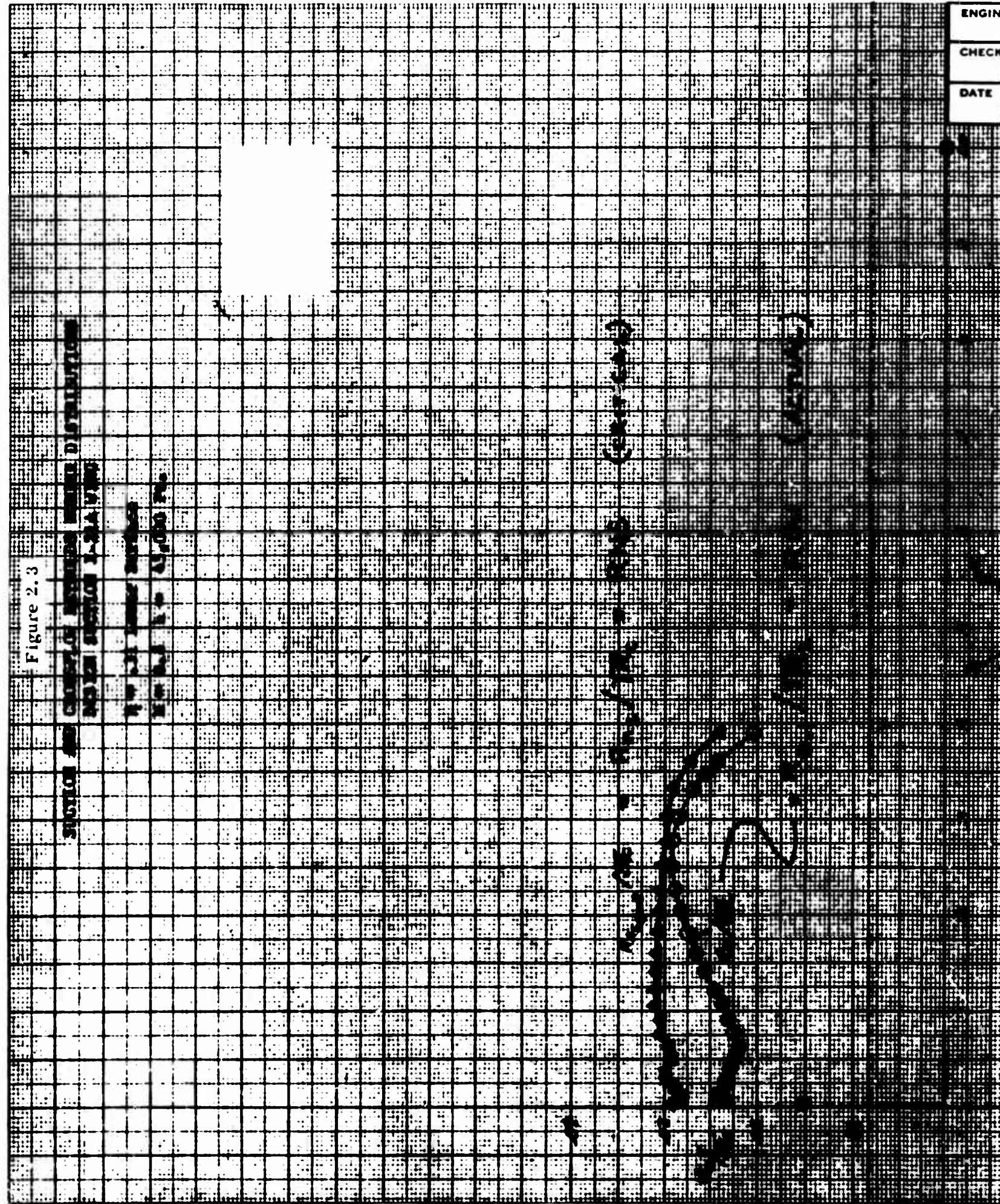
Figure 2.3

STATION AND COUNTRY OF ORIGIN OF DISTRIBUTION

NO. 221 STATION 1-34 1/2

NO. 221 STATION 1-34 1/2

NO. 221 STATION 1-34 1/2



ENGINEER	NORTHROP CORPORATION NORAIR DIVISION	PAGE 2.32
CHECKER		REPORT NO. NOR-67-136
DATE		MODEL X-21A

Figure 2.3

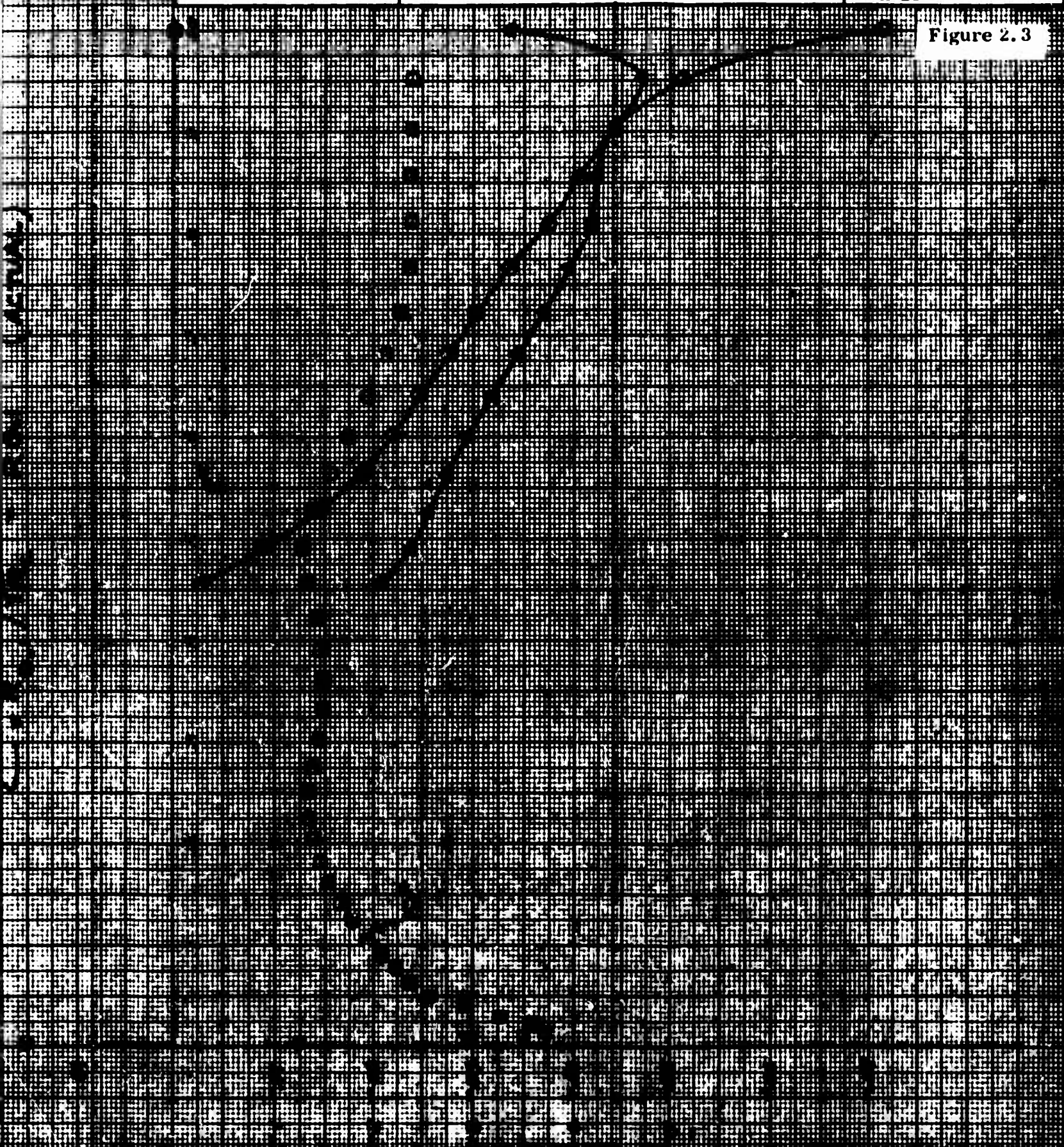


Figure 2.4

Figure 2.4 shows the results of the simulation for the system with the following parameters:

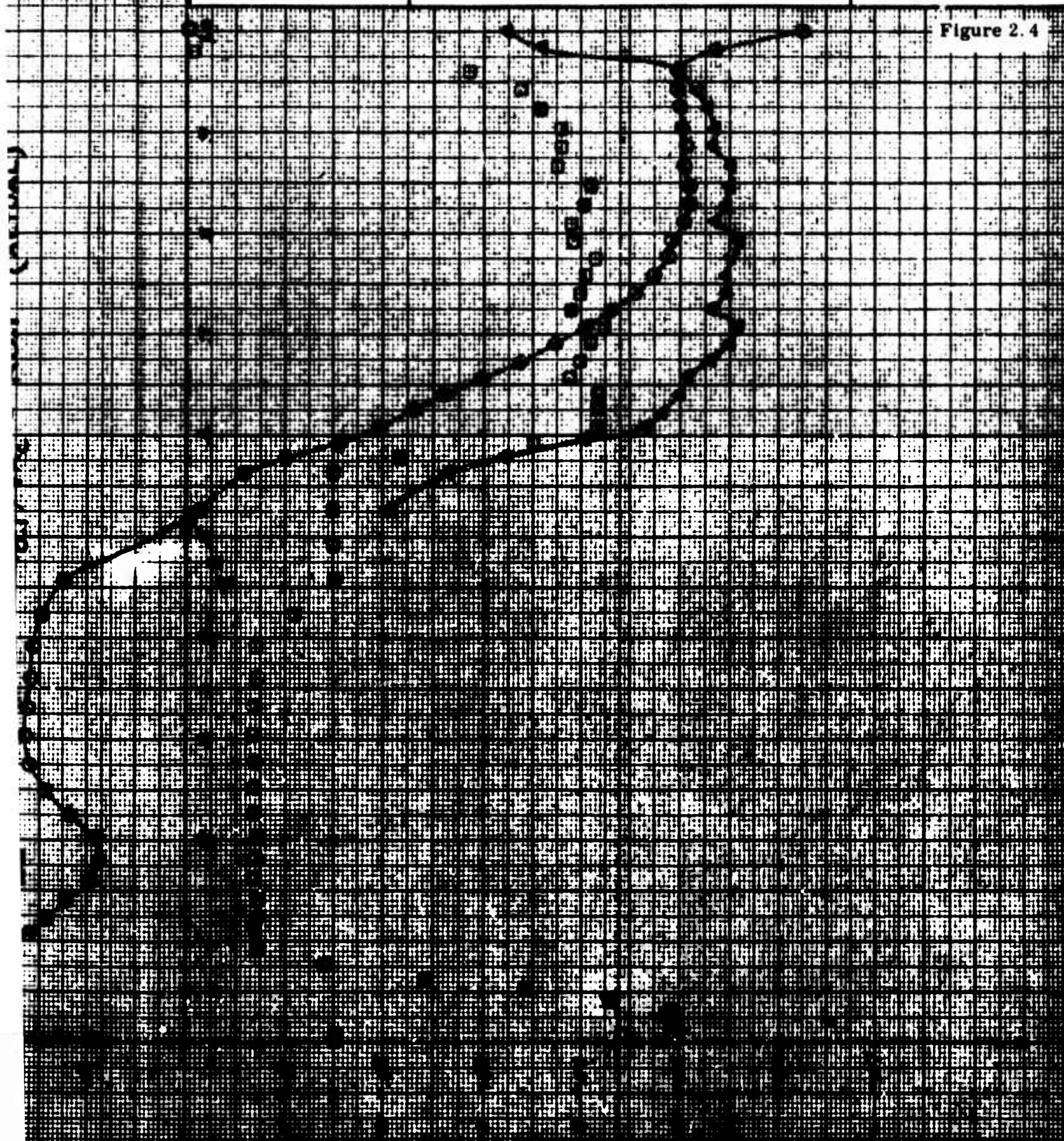
$\lambda = 0.1$ (input rate)
 $\mu = 0.6$ (service rate)
 $N = 45,000$ (N)

$$RMS = \frac{RMS}{N} = RMS \quad (\text{CRITICAL})$$

$$ROI = \frac{ROI}{N} = ROI \quad (\text{ACTUAL})$$

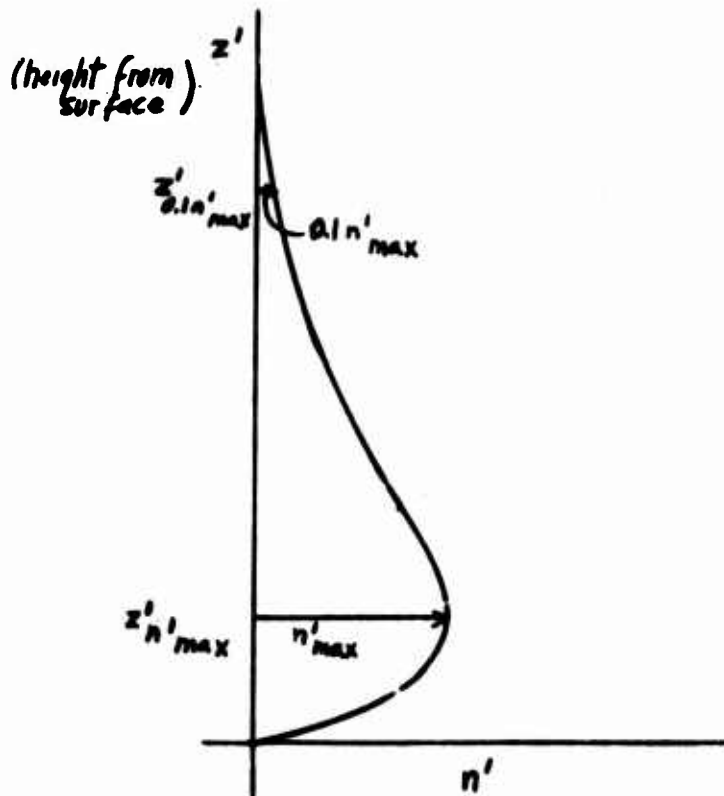
ENGINEER	NORTHROP CORPORATION NORAIR DIVISION	PAGE 2.33
CHECKER		REPORT NO. 67-136
DATE		MODEL X-21A

Figure 2.4



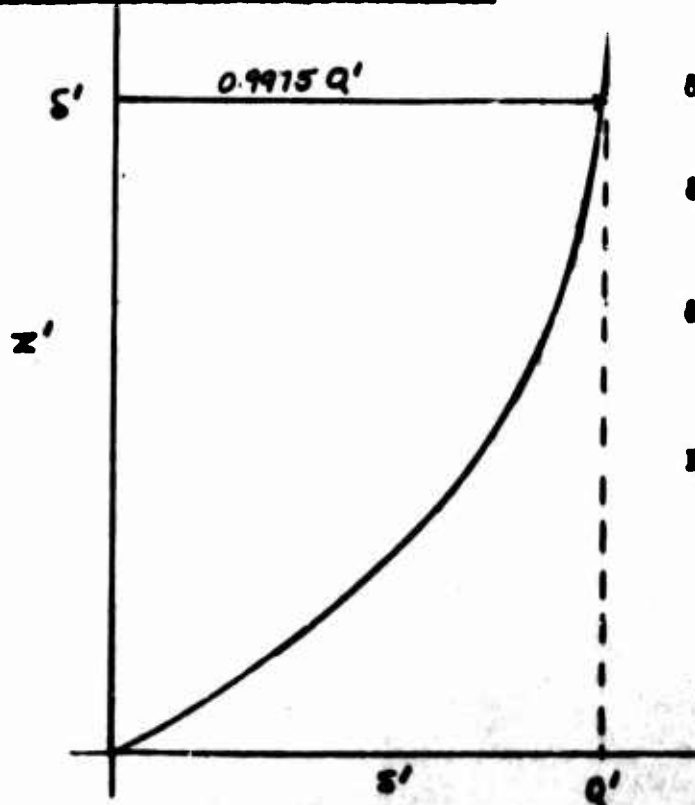
ENGINEER	NORTHROP CORPORATION NORAIR DIVISION	PAGE 2.34
CHECKER		REPORT NO. NOR-67-136
DATE June 1967		MODEL X-21A

Boundary Layer Crossflow Profile



$$R_n = n'_{max} z'_{0.1n'_{max}} \Lambda' / \mu_e'$$

Boundary Layer Tangential Profile



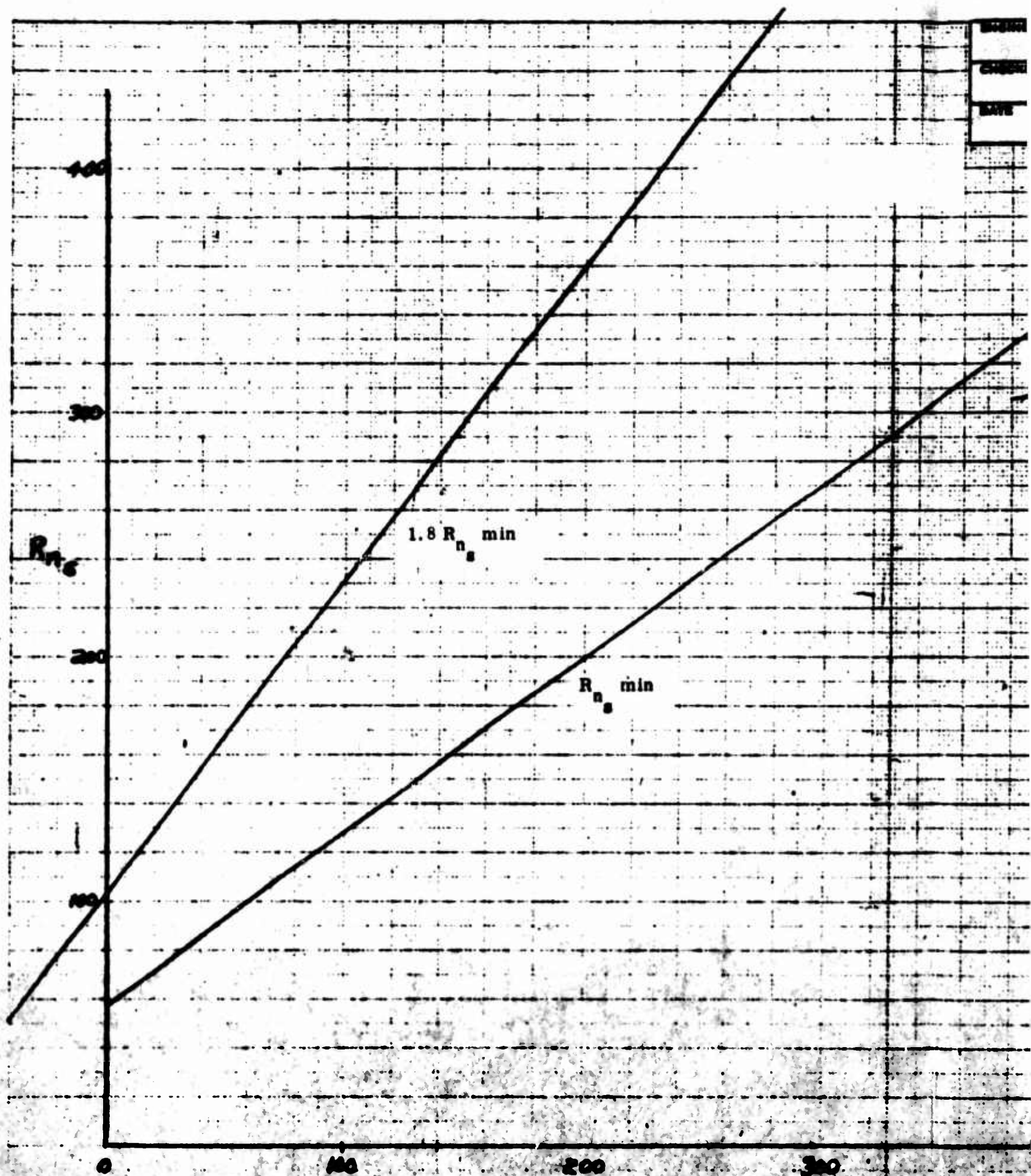
δ' = height at which velocity is $0.9975 Q'$

δ'_θ = tangential displacement thickness = $\int_0^{\delta'} (1 - s'/Q') ds'$

$\delta'_{\theta\theta}$ = tangential momentum thickness = $\int_0^{\delta'} (s'/Q')(1 - s'/Q') ds'$

$$R_{\theta\theta} = Q'^2 \delta'_{\theta\theta} \Lambda' / \mu_e'$$

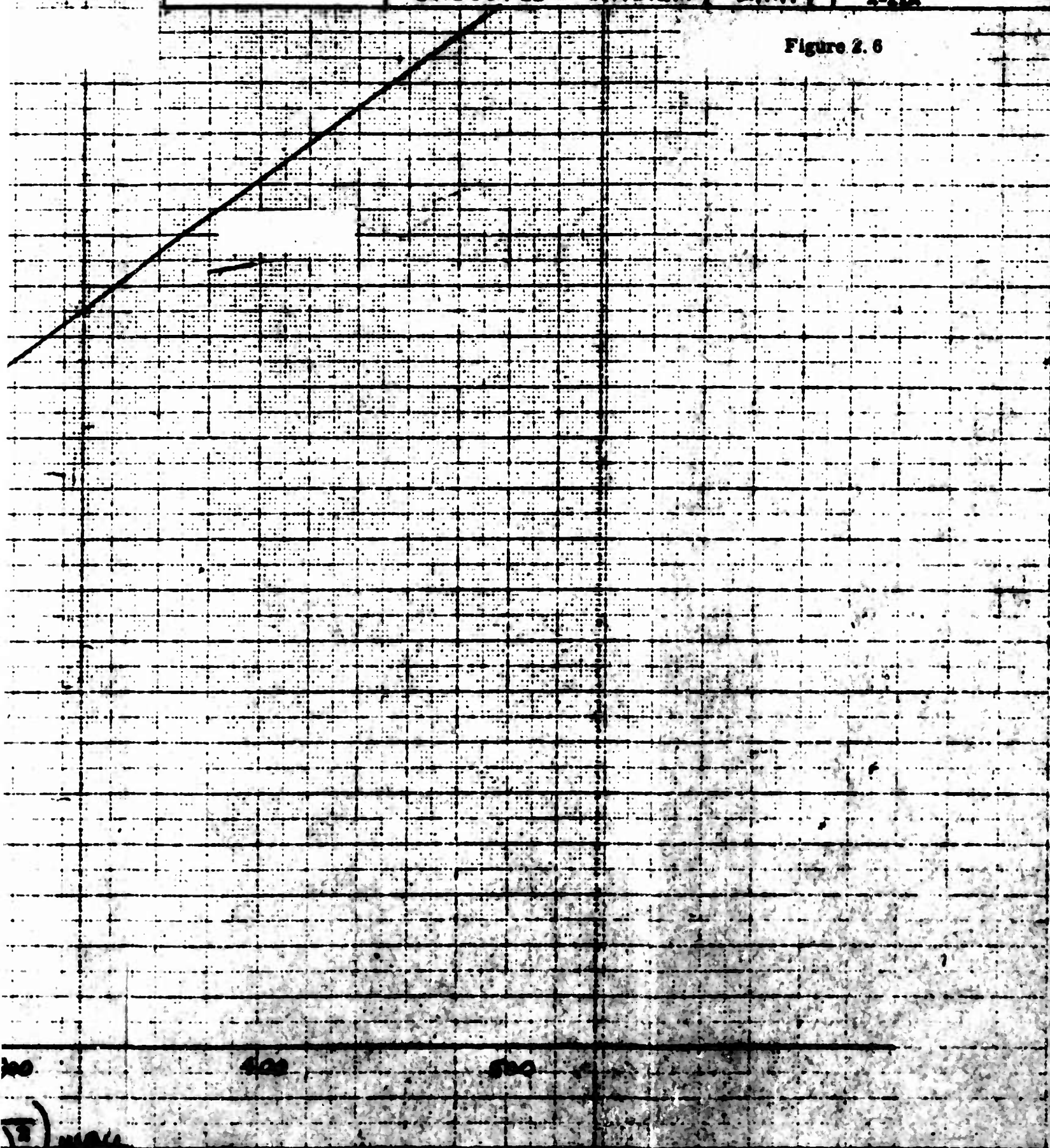
FIGURE 2.5 BOUNDARY LAYER PROFILES



$$N_{32} = - \left(\frac{\sum \eta / \eta_{\max}}{\sum (\eta / \eta_{\max})^2} \right) \eta_{\max}$$

DESIGNER	NORTHROP CORPORATION NORAIR DIVISION	FILE	2.35
CHECKER		REPORT NO.	67-136
DATE	CROSSFLOW STABILITY LIMIT	MODEL	S-21A

Figure 2.6



\sqrt{x} max

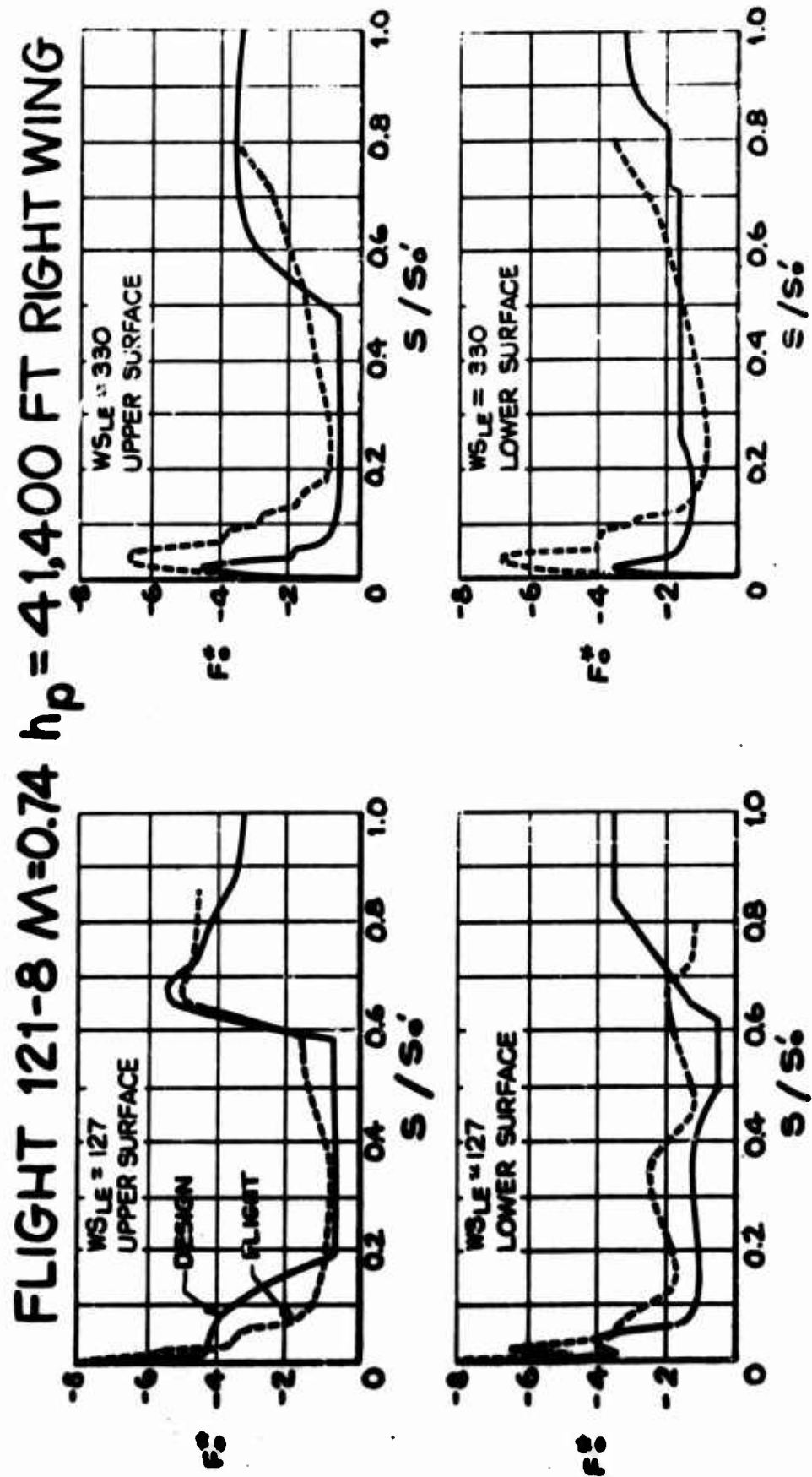


FIGURE 2-7a CORRELATION OF SUCTION DISTRIBUTIONS

RIGHT WING UPPER SURFACE

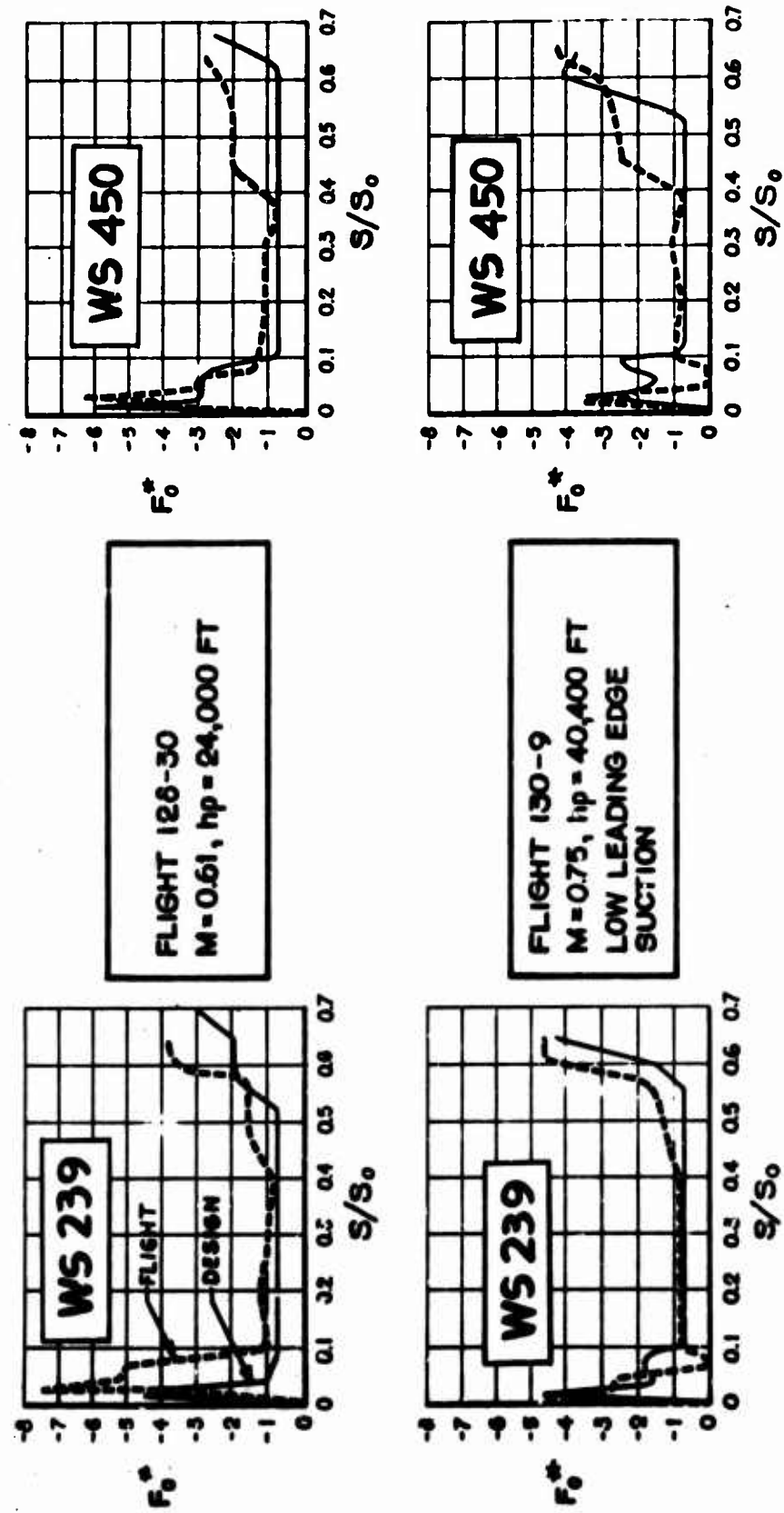


FIGURE 2.7b CORRELATION OF SUCTION DISTRIBUTIONS

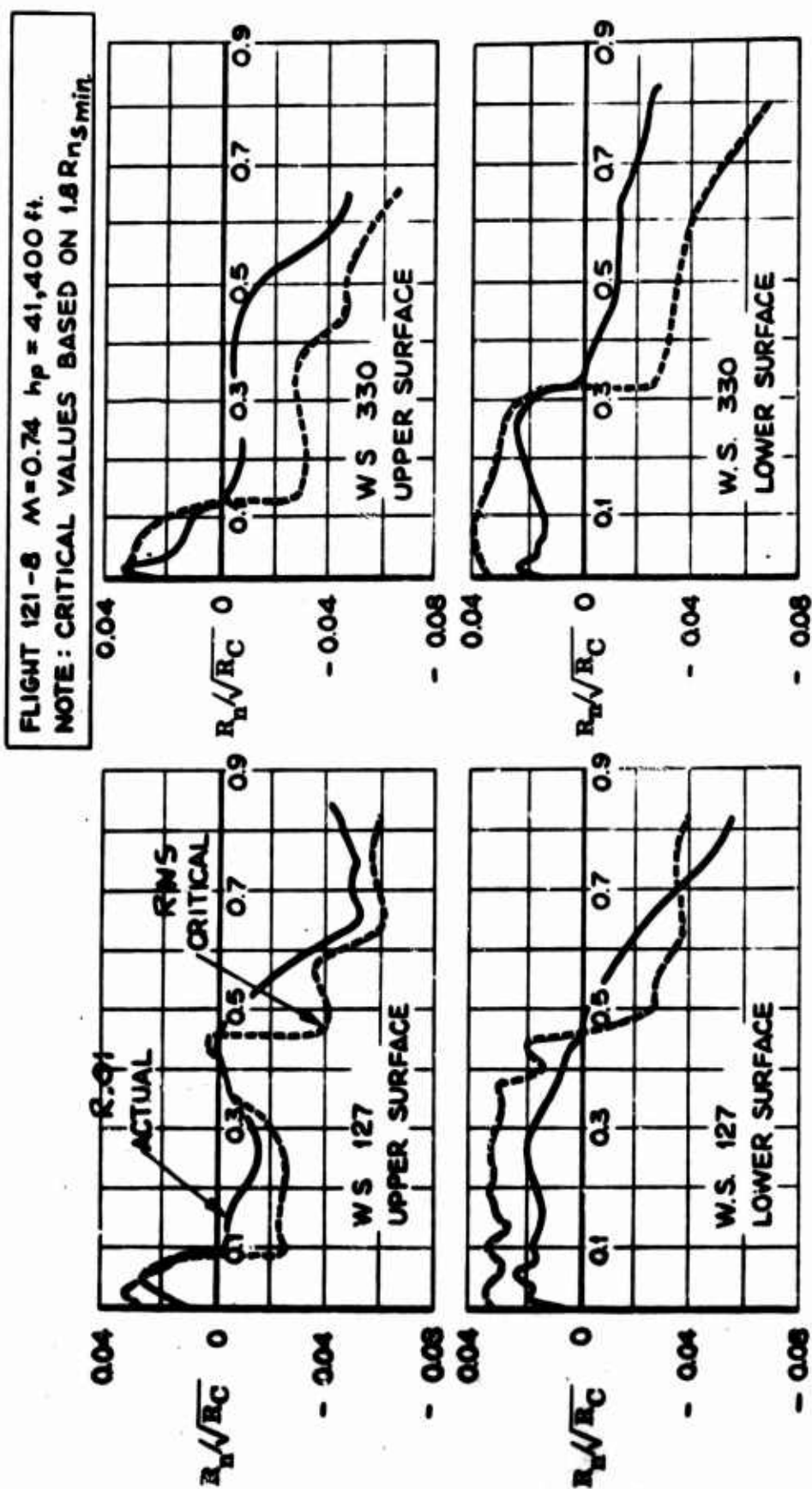


FIGURE 2.8. ACTUAL AND CRITICAL CROSSFLOW REYNOLDS NUMBER

ENGINEER	NORTHROP CORPORATION NORAIR DIVISION	PAGE 2.39
CHECKER		REPORT NO. NOR-67-136
DATE June 1967		MODEL X-21A

2.13 APPENDIX A

SUCTION DISTRIBUTION CALCULATION STEPS

1. Determine geometry, θ_1 , θ_2 , c' , c_a' , x' , x_a' , L_o' .
2. Measure or compute surface static pressure distributions. Plot the pressure coefficient, C_p , versus ξ^2 from the stagnation point along the surface arc. Fill out key punch forms for 919K.
3. Convert C_p data to U^* , V^* data using the computer program, 919K, which punches cards of the U^* versus ξ^2 distribution. Check results.
4. Determine the distribution of the suction parameter, F_o^* , versus ξ^2 , only when direct suction version is not requested.
5. Fill out key punch forms, set up deck, and run input and integration programs BB62-A and BB65-A.
6. Analyze the stability of the laminar boundary layer from parameters calculated by BB65/A.
 - a) Plot $R_{0.1}/R_c$ (labelled $RO.1$), and R_{ns}/R_c (labelled RNS), and F_o^* versus ξ^2 . Compare $RO.1$ and RNS . $RO.1$ must be less than RNS for crossflow stability.
 - b) For tangential boundary layer stability, verify that R_{oss} is compatible with the criteria of Section 1.
 - c) For leading edge stability, check that R_{oss} is less than 100 in the stagnation region.

These steps a, b, and c are required only when suction is an input to the program.

ENGINEER	NORTHROP CORPORATION NORAIR DIVISION	PAGE 2.40
CHECKER		REPORT NO. NOR-67-136
DATE June 1967		MODEL X-21A

2.14 APPENDIX B

DERIVATION OF THE IRROTATIONALITY CONDITION FOR SWEEP TAPERED WINGS

Reference 1 defines the external vorticity, Ω' , by the following equation

$$\Omega' = [\partial(\beta'V')/\partial\xi - \partial(\alpha'U')/\partial\eta]/\alpha'\beta'$$

where the definitions of symbols are

$$\alpha' = \partial x'_a / \partial \xi$$

$$\beta' = \partial L' / \partial \eta$$

U' = Component of local potential flow velocity normal to element line

V' = Component of local potential flow velocity along element line

and x'_a and L' are defined by Figure 2.1.

If the external flow is isentropic, $\Omega' = 0$. Then

$$\partial(\beta'V')/\partial\xi = \partial(\alpha'U')/\partial\eta$$

Dividing by Q_0' ,

$$\partial(\beta'V^*)/\partial\xi = \partial(\alpha'U^*)/\partial\eta$$

$$\beta' \partial V^* / \partial \xi + V^* \partial \beta' / \partial \xi = \alpha' \partial U^* / \partial \eta + U^* \partial \alpha' / \partial \eta$$

From the geometry of a swept tapered wing (Figure 1),

$$L' = L_0' \eta$$

$$x'_a = L' \gamma = L_0' \eta \xi^2 \gamma_0$$

so

$$\alpha' = \partial x'_a / \partial \xi = 2 L_0' \eta \xi \gamma_0$$

$$\partial \alpha' / \partial \eta = 2 L_0' \xi \gamma_0$$

$$\beta' = \partial L' / \partial \eta = L_0'$$

ENGINEER	NORTHROP CORPORATION NORAIR DIVISION	PAGE 2.41
CHECKER		REPORT NO. NOR-67-136
DATE June 1967		MODEL X-21A

2.14 APPENDIX B (Continued)

DERIVATION OF THE IRROTATIONALITY CONDITION FOR SWEEP TAPERED WINGS

$$\partial \beta' / \partial \xi = 0$$

and from the definition of a similar solution, $\partial U^* / \partial \eta = 0$.

Hence

$$L_0 \partial v^* / \partial \xi = U^* L_0 \gamma_0$$

$$\partial v^* / \partial \xi = U^* \gamma_0 \partial(\xi^2) / \partial \xi$$

$$\partial v^* / \partial(\xi^2) = U^* \gamma_0$$

$$v^* = \gamma_0 \int_0^{\xi^2} U^* d(\xi^2) + \text{const.}$$

ENGINEER	NORTHROP CORPORATION NORAIR DIVISION	PAGE 2.42
CHECKER		REPORT NO. NOR-67-136
DATE June 1967		MODEL X-21A

2.15 APPENDIX C RULES FOR SELECTING POINTS FOR CURVE FITTING SUBROUTINES

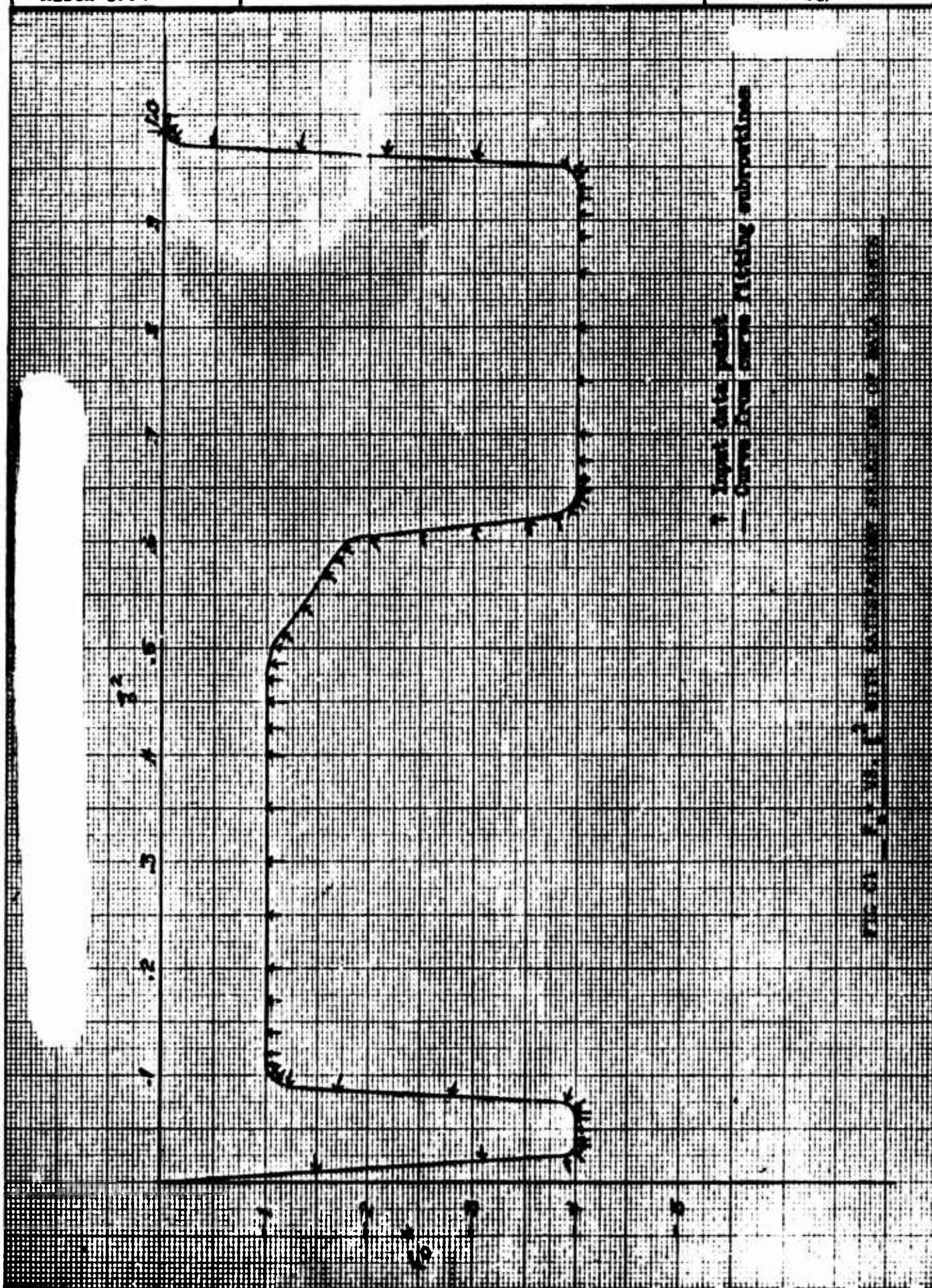
The continuous derivative curve fitting and interpolation subroutines are used in the boundary layer input program, BB62A, and in the U*, V* iteration program, 919K. The curve fitting subroutine fits a cubic equation to each set of two input points, (x_i, y_i) and (x_{i+1}, y_{i+1}) . This is accomplished by writing a cubic equation which passes through the two points of the i th interval with unknown coefficients, a_i and b_i . The coefficients can be determined by setting the first and second derivatives of the interpolation cubics for the i th and the $(i+1)$ th intervals equal at $x = x_{i+1}$. A second subroutine will interpolate for specified values of the independent variable x using the cubic equation with the calculated coefficients.

The subroutines will handle almost any type of input curve if the data points are properly selected according to the following rules:

1. The independent variable x must be sequenced from the minimum value to the maximum value.
2. For each value of x on the input curve, there must be one and only one value of y , i.e. $y = f(x)$ is a single valued function. (Of course, one y may correspond to more than one x .)
3. The interpolation method may be considered analogous to passing a flexible beam through the points x_i, y_i . Therefore, the user should consider whether the curve can "escape" from the desired shape with his proposed selection of input data points. Generally, points should be closely spaced where the curve has sharp corners and rapid changes of derivatives.
4. Rapid changes of the spacing interval are unadvisable. A usable rule of thumb states that an interval should not be more than double nor less than half the preceding interval.

Figures C1 and C2 show a sample Fo* curve with satisfactory and unsatisfactory selection of input data points.

ENGINEER E. A. Gloyd	NORTHROP CORPORATION NORAIR DIVISION	PAGE 2.43
CHECKER		REPORT NO. NOR-67-136
DATE March 1964		MODEL X-21A



ENGINEER E. A. Gloyd	NORTHROP CORPORATION NORAIR DIVISION	PAGE 2.44
CHECKER		REPORT NO. NOR-67-136
DATE March 1964		MODEL X-21A

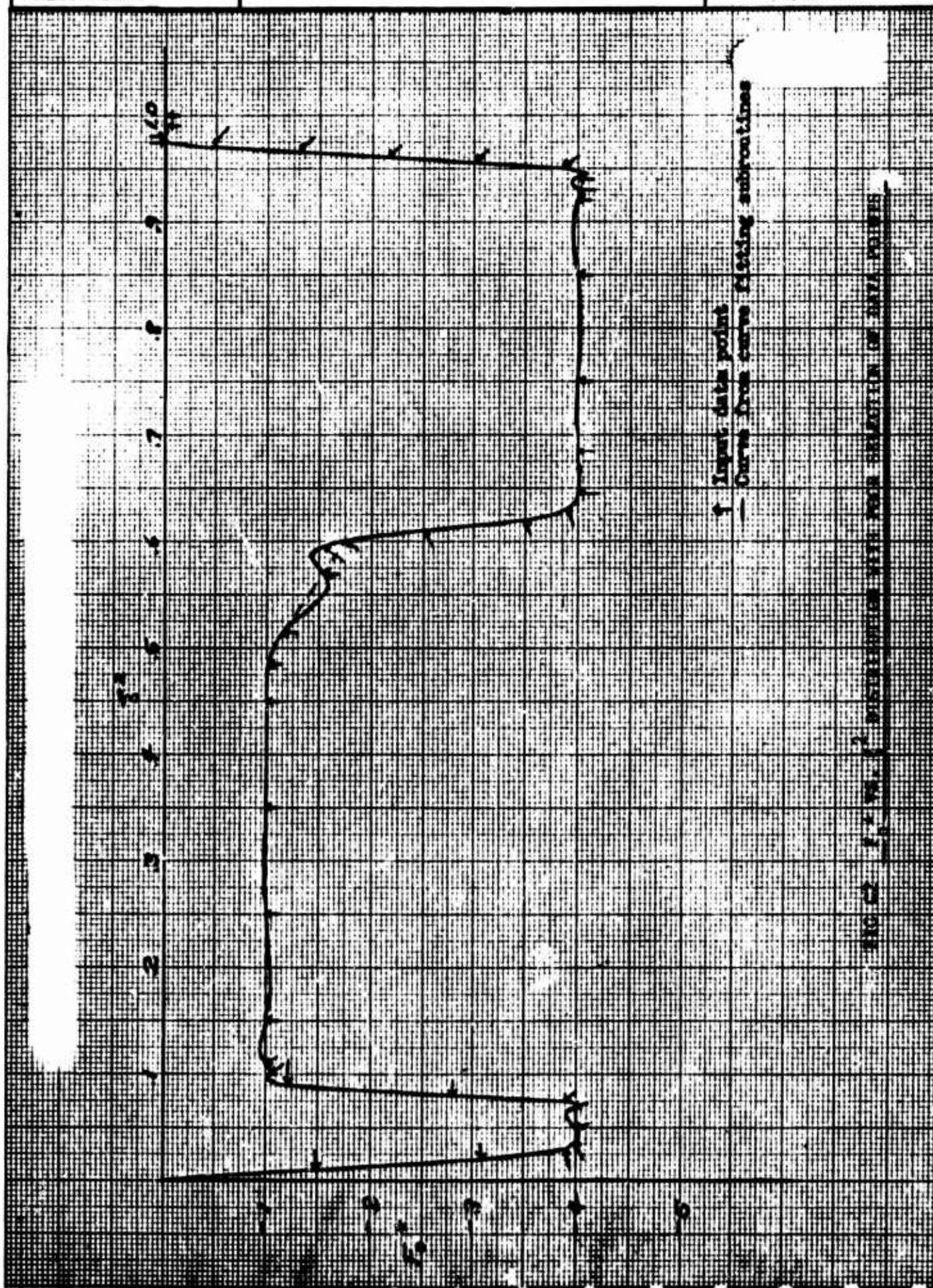


FIG. 12. f, y, x, z^2 DISTRIBUTION WITH FOUR SUBROUTINES OF DATA POINTS

ENGINEER	NORTHROP CORPORATION NORAIR DIVISION	PAGE 2.45
CHECKER		REPORT NO. NOR-67-136
DATE June 1967		MODEL X-21A

2.16 APPENDIX D

DECK SET UP FOR 919K (U* V* ITERATION PROGRAM)

There are two versions of 919K, version A which iterates to find V^* at the leading edge and version B which uses an input value of V^*_{LE} . The deck set up is

1. 919K deck, either version.
2. Subroutines - any order but must include

CCDIS
TDSEQ
SIGMA
SUMI

3. Card #1001: Mach number, θ_1 , θ_2 , accuracy.
4. Card #1002: Number of C_p , case identification.
5. Cards #1003 and subsequent cards: ξ^2 and C_p values listed in order of increasing ξ^2 .
6. For version B, a card giving V^* at the leading edge.
No card for version A.

For additional cases repeat steps 3 through 6.

Control cards may be required by the particular digital computer system. For the Norair 7090 FIB system, three cards are required:

1. \$ EXECUTE FIB first card
2. * XEQ second card, placed before program deck.
3. * DATA placed between program deck and data,
before card #1001 in this instance.

Form 20-700 (R. 7-63)

2.46
67-136
X-21A

ENGINEER	NORTHROP CORPORATION NORAIR DIVISION	PAGE 2.47
CHECKER		REPORT NO. NOR-67-136
DATE June 1967		MODEL X-21A

2.17 APPENDIX E

Deck Set Up for Boundary Layer Input Program BB62-A and Integration Program BB65-A.

1. Control Card: \$ Execute Fib (for Northrop's 7090 IBM System)
2. Control Card: *XEQ (for Northrop's 7090 IBM System)
3. Card: Chain (1, 8)
4. BB62A Program Deck (Main input program and subroutines)
5. Card: Chain (2, 8)
6. BB65-A Program Deck (Main integration program and subroutines)
7. Card: Chain (3, 8)
8. Three cards corresponding to subroutine chain (3, 8)
9. Control Card: *Data (for Northrop's 7090 IBM System)

DATA REQUIRED BY INPUT PROGRAM BB62-A

10. Card 1: Control Card (for Northrop's 7090 IBM System)

PROGRAM IDENTIFICATION

11. Card 2: General Inputs
12. Card 3: Integration Steps Inputs
13. Card 4: Set of Programming Control Indicators
14. Card 5: Symbols Card
15. Card 6: Number of U^* Data Points
16. Card 7 to $(m-1)$: ξ^2 versus U^* Distribution
17. Card m : Number of F_0^* Data Points
18. Cards $(m+1)$ to n : ξ^2 versus F_0^* Distribution

ENGINEER	NORTHROP CORPORATION NORAIR DIVISION	PAGE 2.48
CHECKER		REPORT NO. NOR-67-136
DATE June 1967		MODEL X-21A

19. Card (n+1): Input Data Required for Direct Suction Calculations
DATA REQUIRED BY INTEGRATION PROGRAM BB65-A
20. Card (n+2): Set of Programming Control Indicators
21. Card (n+3): Set of Control Indicators for Printout Purposes
22. Cards (n+4) to (n+40): Set of Optional Initial Profiles

EXPLANATION OF BB62A/5A KEY PUNCH FORM

Card 1: Column 1: write 1

Columns 14-19: write INPUT

Columns 20-72, alpha numeric data to identify case being calculated.

Card 2: General Inputs. Format (7 F10.5, I2)

Columns 1-10, Free stream Mach number

Columns 11-20, Free stream temperature in ($^{\circ}$ K)

Columns 21-30, Free stream static pressure in atmospheres

Columns 31-40, wing leading edge sweep angle in radians, θ_1

Columns 41-50, wing trailing edge sweep angle in radians, θ_2

Columns 51-60, wing leading edge non-dimensional potential flow velocity $V_{L.E.}^*$ (with the current program the selection is $V_{L.E.}^* = \sin \theta_2$)

Columns 61-70, reference chord in feet

Columns 71-72, control indicator "L CODE," write 0 or 1; if "L CODE" = 0, L'_0 is supplied in the output in feet

If "L CODE" = 1, L'_0 is supplied non-dimensionally

NOTE: If "L CODE" = 0, a later used indicator in the integration program called "IND (14)" must also be made zero; if "L CODE" = 1, then IND (14) = 1.

ENGINEER	NORTHROP CORPORATION NORAIR DIVISION	PAGE 2.49
CHECKER		REPORT NO. NOR-67-136
DATE June 1967		MODEL X-21A

Card 3: Integration step inputs. Format (2 F10.5, 10I5)

- Columns 1-10: Step length interval along the ξ direction
FORTRAN name: DELSKI = $\Delta\xi$
- Columns 11-20: Step length interval along the η direction
FORTRAN name: DELETA = $\Delta\eta$
(Use 0.0 when 2-dimensional case is considered)
- Columns 21-25: Maximum number of steps in the ξ direction
FORTRAN name: IMAX = imax
- Columns 26-30: Print out frequency along the chord
FORTRAN name: IFRQ
- Columns 31-35: First chord station at which computation starts
FORTRAN name: IMID = starting value of I
If starting at leading edge IMID = 0
- Columns 36-40: Maximum number of steps in the η direction
FORTRAN name: JMAX = jmax
(use 0.0 when 2-dimensional case is considered)
- Columns 41-45: Print out frequency along the η direction
FORTRAN name: JFRQ (use 0.0)

Card 4: Control Indicators: Format (30I1)

Each indicator called "IND()" is defined by a number 0 or 1.

IND(1) to IND(20): If any of these indicators is zero, the corresponding boundary layer equation coefficient A that has the same indicator subscript is not calculated. If any indicator is 1, the corresponding A coefficient is calculated.

IND(1)	1	A1 is computed
	0	A1 is not computed
IND(2)	1	A2 is computed
	0	A2 is not computed

ENGINEER	NORTHROP CORPORATION NORAIR DIVISION	PAGE 2.50
CHECKER		REPORT NO. NOR-67-136
DATE June 1967		MODEL X-21A

. . .
 . . .
 . . .
 . . .
 IND(20) 1 A20 is computed

A20 is not computed

IND(21) to IND(28) are not used in program; set equal to 0.
IND(29) is used for non-stagnation zero calculation.

If IND(29) = 1, then the starting value of I = 0 is
not the stagnation point.

If IND(29) = 0, then the starting value of I = 0 is
the stagnation point.

IND(30): If zero, integration program (linked to the input
program through a "CHAIN JOB") is executed; if 1, it is not
executed.

For "similar solution" swept tapered wing, A(7)=A(11)=A(12)=
A(14)=A(18)=0.

Card 5: Symbols card. Format (12A6)

As shown, unless program is changed, IT is used to print out
the names of the variables UX(1) to UX(10) which are calcu-
lated in subroutine SUB4. The user may choose to change the
program to calculate different sets of variables. With the
current program the selection is:

$$UX(1); XI-SQ = \xi^2$$

$$UX(6); F_0^* = f_0^*$$

$$UX(2); U^* = U^1/Q_0^1$$

$$UX(7); RN/PT = R_0; Q P/NT^2$$

$$UX(3); V^* = V^1/Q_0^1$$

$$UX(8); XA(PT) = C^1(L^1) (01-02)\xi^2$$

ENGINEER	NORTHROP CORPORATION NORAIR DIVISION	PAGE 2.51
CHECKER		REPORT NO. NOR-67-136
DATE June 1967		MODEL X-21A

UX(4); CP = cp UX(9); THETA = $\theta = (\theta_1 - \theta_2) \xi^2$

UX(5); $Q = (U^{*2} + V^{*2})^{\frac{1}{2}}$ UX(10); X/C =

$$\frac{L^1}{C^1} \cos \theta_1 \left(\frac{\sin \theta_1}{\cos \theta_1} - \frac{\sin \theta}{\cos \theta} \right)$$

Card 6: Number of U* data points. Format (I5)

Columns 1 to 5: Number of points supplied in the given tangential potential flow velocity distribution along the chord (U* vs ξ^2). Maximum = 100).

Columns 6 to 71: Not used in program; available to user to identify case.

Card 7 to (m-1) ξ^2 versus U* distribution. Format (10F7.4)

With 10 spaces of 7 columns each per card, the given U* versus ξ^2 distribution, in order of increasing ξ^2 . (Maximum of 20 cards)

Card m: Number of F_o^* data points. Format I5

Columns 1 to 5: Number of points supplied in the given suction F_o^* coefficient distribution. (Maximum = 100)

Columns 6 to 71: Not used in program, available for identification.

Card (m+1) to n: ξ^2 versus F_o^* distribution. Format (10F7.4)

Suction coefficient distribution inputted as done with the U* distribution. (Maximum of 20 cards)

Card n+1 Direct suction input data. Format (I1, 5F10.5)

Column 1: First column is reserved for IND(15)

If IND(15) = 0 a suction coefficient distribution is inputted as done in cards (m+1) to n.

ENGINEER	NORTHROP CORPORATION NORAIR DIVISION	PAGE 2.52
CHECKER		REPORT NO. NOR-67-136
DATE June 1967		MODEL X-21A

If IND(15) = 1 the program will calculate the suction coefficient distribution to satisfy certain stability criterias and the corresponding boundary layer development.

Columns 2-11: SARG, defines the minimum margin of crossflow stability. $SARG = (RNS) - (R0.1)$. If considerable margin is required, a value of 0.004 is appropriate; if no margin is required a value of $SARG = 0.0$ may be used ($RNS = R0.1$).

Columns 12-21: TARG, defines the maximum momentum thickness Reynolds number Re_{max} (called TANCRT in program) for the tangential flow stability criteria.

Columns 22-31: SLP, defines the maximum rate at which the suction coefficient may vary along the chord. A value of $SLP = 70$ should be used.

Columns 32-41: FOMIN, defines the minimum suction coefficient F_0^* required by the designer all along the chord except the L.E. region.

Columns 42-51: TARG2, defines a convenient maximum momentum thickness Reynolds number in the region of adverse pressure gradient. In general, a value of $TARG\ 2 = k\ TARG$ with k , varying from .95 to 1.0, can be adopted.

Card n+2: Integration program control indicators card. Format (14I5, I2)

Columns 1-5: : Maximum number of steps in the ξ direction, 1 max. Same as IMAX of input program.

Columns 6-10: IND(1): First chord station to be computed; must be zero or an even integer. Same as IMID of input program.

Columns 11-15: IND(2); number of iterations desired on initial profile, must be an even integer; if $IND(1) = 0$, then IND(2) must be zero.

ENGINEER	NORTHROP CORPORATION NORAIR DIVISION	PAGE 2.53
CHECKER		REPORT NO. NOR-67-136
DATE June 1967		MODEL X-21A

- Columns 16-20: IND(3); iteration printout frequency must be an even integer and a factor of IND(2); if IND(1) = 0, then IND(3) must be zero.
- Columns 21-35: IND(4); integration printout frequency, must be an even integer and a factor of imax.
- Columns 26-30: IND(5). Side data control at $j = 0$. If zero, it will proceed with 2-dimensional calculation; if 1, it will proceed with 3-dimensional calculation.
- Columns 31-35: IND(6), side data control at $j = J_{max}$. Same as IND(5).
- Columns 36-40: IND(7). Boundary layer profile punch control.
- 0 - no punch out desired
 - 1 - punch out iterated initial profile only (i.e., u, t, φ , at last iteration station)
 - 2 - Punch out final integration profile only (i.e., $v, t, \varphi, \Delta \xi, L'_{10}, v_a, t_a, a$ at $I = I_0$)
 - 3 - Both the iterated and integrated profiles are punched as described above.

In case IND(3) and IND(4) are not factors of IND(2) and IND(1) respectively, then the punched profiles will be the last calculated profiles and not the last printed profiles.

Columns 41-45: IND(8), Initial profile input indicator.

If IND(1) = 0 {

- IND(8) = 0 Initial profile is calculated by program
- IND(8) = 1 Initial profiles v, t, φ are read into program

ENGINEER	NORTHROP CORPORATION NORAIR DIVISION	PAGE 2.54
CHECKER		REPORT NO. NOR-67-136
DATE June 1967		MODEL X-21A

If IND(1) 0 IND(8) = 0 or IND(8) = 1. The initial profiles V , T , ϕ , $\Delta\xi$, L'_0 and v_a , t_a , ϕ_a from previous run are required.

Columns 46-50: IND(9); Additional printout in input program

0 - No printout

1 - UX functions as calculated in SUB4 are printed

Columns 51-55: IND(10) Gas type

0 - Ideal gas assumption will be used

1 - Real gas assumption will be used

Columns 56-60: IND(11) = n ; Derivative control, 2- or 3-dimensional calculation control

0 - 2-dimensional calculation

1 - 3-dimensional calculation

Columns 61-65: IND(12), subscript K_0 definition (vertical steps)

= 0; $K_0 = 20$

$\neq 0$; then IND(12) = K_0 (K_0 even integer)

Columns 66-70: IND(13) Error computation (ϵ)

0 - Error is not computed

1 - Error is computed

Columns 71-72 IND(14) Output data dimensions control. If "LCODE" = 1, IND(14) = 1 and output data is provided dimensionally; if "LCODE" = 0, IND(14) = 0 and part of the data is provided dimensionally.

ENGINEER	NORTHROP CORPORATION NORAIR DIVISION	PAGE 2-55
CHECKER		REPORT NO. NOR-67-136
DATE June 1967		MODEL X-21A

Card n+3: Boundary layer profile control indicator. Format (9I5)

Set of control indicators used to determine which particular functions must be printed; their order will also determine their printout order. There are 17 built-in profiles (BLP (k, 1)....BLP (k, 17) in internal program nomenclature) and 3 more may be programmed as required. Only 9 indicators may be used. The number defines the BLP (k) profile; their sequence, the printout order.

NOTE: . The subsequent cards are only included if the initial profiles are supplied, avoiding the iteration process. The requirements are different according to the starting point of calculation, i.e., if Istart (IND(1)) is the stagnation line or not. Each profile requires a set of 6 cards.

Cards (n+4) to (n+9): Initial velocity profile. Format (4E15.8)

(V(J,K), K = 1, KMAX+1)

FORTTRAN Symbol: V Definition: v

For similar solutions $J_{max} = 0$

Cards (n+10) to (n+15): Initial temperature profile. Format (4E15.8)

(T(J,K), K = 1, KMAX+1)

FORTTRAN Symbol: T Definition: t

Cards (n+16) to (n+21): Initial shear stress profile. Format (4E15.8)

(S(J,K), K = 1, KMAX+1)

FORTTRAN Symbol: S Definition: τ_0

Card n+22: Step length interval along the ξ direction. Format (4E15.8)

Same as in Card 3.

$$\Delta \xi = \frac{1}{I_{MAX}}$$

L'_0 = reference length

ENGINEER	NORTHROP CORPORATION NORAIR DIVISION	PAGE 2.56
CHECKER		REPORT NO. NOR-67-136
DATE June 1967		MODEL X-21A

NOTE: Value of L'_0 in dimensional or non-dimensional form depending on the value of the LCODE control indicator.

FORTRAN Name	Definition
--------------	------------

DAL, XLOPRL	$\Delta \xi, L'_0$
-------------	--------------------

Values of DAL and XLOPRL used are those obtained from previous calculation.

Cards (n+23) to (n+28): Forward velocity derivative v_a . Format (4E15.8)

(VA(J,K), K = 1, KMAX+1)

FORTRAN Symbol	Definition
----------------	------------

VA	v_a
----	-------

Cards (n+29) to (n+34): Forward temperature derivative. Format (4E15.8)

(TA(J,K), K = 1, KMAX+1)

FORTRAN Symbol	Definition
----------------	------------

TA	t_a
----	-------

Cards (n+35) to (n+40): Forward shear derivative. Format (4E15.8)

(SA(J,K), K = 1, KMAX+1)

FORTRAN Symbol	Definition
----------------	------------

SA	φ_a
----	-------------

NOTE: If IND(8) = 0 and IND(1) = 0 (stagnation starting point) then cards (n+4) to (n+40) (initial profile cards) are not needed.

If IND(8) = 0 or IND(8) \neq 1 and IND(1) \neq 0 (non-stagnation starting point) then cards (n+4) to (n+40) are required.

If IND(8) = 1 and IND(1) = 0 (stagnation starting point with profiles known from previous runs), then cards (n+4) to (n+21) are required.

JOB TITLE		ENGINEER		ANALYST	
FIG E1 B.L. INPUT AND INTEGRATION PROGRAM		DATE 7 OF 3		DATE	
DATA SERIAL NO.	FOR ORG. NO.	DASH			
<p>GENERAL INPUTS</p> <p>INPUT 1</p> <p>INPUT 2</p> <p>INPUT 3</p> <p>INPUT 4</p> <p>INPUT 5</p> <p>INPUT 6</p> <p>INPUT 7</p>					
<p>INTEGRATION STEPS INPUTS</p> <p>INPUT 1</p> <p>INPUT 2</p> <p>INPUT 3</p> <p>INPUT 4</p> <p>INPUT 5</p> <p>INPUT 6</p> <p>INPUT 7</p>					
<p>INPUT PROGRAM CONTROL INDICATORS (I.E. FLOW PARAMETER CONTROL CARD)</p> <p>INPUT 1</p> <p>INPUT 2</p> <p>INPUT 3</p> <p>INPUT 4</p> <p>INPUT 5</p> <p>INPUT 6</p> <p>INPUT 7</p>					
<p>SYMBOLS - CARD</p> <p>INPUT 1</p> <p>INPUT 2</p> <p>INPUT 3</p> <p>INPUT 4</p> <p>INPUT 5</p> <p>INPUT 6</p> <p>INPUT 7</p>					
<p>N° OF U° DATA POINTS (MAX=100)</p> <p>INPUT 1</p> <p>INPUT 2</p> <p>INPUT 3</p> <p>INPUT 4</p> <p>INPUT 5</p> <p>INPUT 6</p> <p>INPUT 7</p>					
<p>U° DISTRIBUTION</p> <p>INPUT 1</p> <p>INPUT 2</p> <p>INPUT 3</p> <p>INPUT 4</p> <p>INPUT 5</p> <p>INPUT 6</p> <p>INPUT 7</p>					

KEY PUNCH FORM - GENERAL PURPOSE
FORM 20-700 (11-7-63)

JOB TITLE		ENGINEER		ANALYST		PAGE E3 OF 3	
FIG E3 INITIAL PROFILE CARD 6 - D.L. INTEGR. PROG.		FOR ORGN. NO.		DATE			
PREP	DPD JOB NO.	DASH					
<p>THESE CARDS ARE USED { IF INDI=0 AND INDI=0: CARDS (N+4) TO (N+40) ARE REQUIRED; CASE (1) IN THE FOLLOWING ORDER { IF INDI=1 AND INDI=1: CARDS (N+4) TO (N+40) ARE REQUIRED; CASE (2) { IF INDI=2 AND INDI=2: CARDS (N+4) TO (N+40) ARE REQUIRED; CASE (3)</p>							
<p>VELOCITY PROFILE [V(J,1) TO V(J, KMAX)] (USED IN CASES (2) & (3))</p>							
XXXXXXE'XX	XXXXXXE'XX	XXXXXXE'XX	XXXXXXE'XX	XXXXXXE'XX	XXXXXXE'XX	XXXXXXE'XX	IPV N+4
							N+9
<p>TEMPERATURE PROFILE [T(J,1) TO T(J, KMAX)] (USED IN CASES (2) & (3))</p>							
XXXXXXE'XX	XXXXXXE'XX	XXXXXXE'XX	XXXXXXE'XX	XXXXXXE'XX	XXXXXXE'XX	XXXXXXE'XX	IPT N+10
							N+15
<p>SHEAR PROFILE [S(J,1) TO S(J, KMAX)] (USED IN CASES (2) & (3))</p>							
XXXXXXE'XX	XXXXXXE'XX	XXXXXXE'XX	XXXXXXE'XX	XXXXXXE'XX	XXXXXXE'XX	XXXXXXE'XX	IPS N+16
							N+21
<p>AS = DAL L₀ = XLAPL [USED IN CASES (2)]</p>							
XXXXXXE'XX	XXXXXXE'XX	XXXXXXE'XX	XXXXXXE'XX	XXXXXXE'XX	XXXXXXE'XX	XXXXXXE'XX	N+22
<p>FORMED VELOCITY DERIVATIVE [W(J,1) TO W(J, KMAX)] (USED IN CASE (2))</p>							
XXXXXXE'XX	XXXXXXE'XX	XXXXXXE'XX	XXXXXXE'XX	XXXXXXE'XX	XXXXXXE'XX	XXXXXXE'XX	IPVA N+23
							N+28
<p>FORWARD TEMPERATURE DERIVATIVE [TA(J,1) TO TA(J, KMAX)] (USED IN CASE (2))</p>							
XXXXXXE'XX	XXXXXXE'XX	XXXXXXE'XX	XXXXXXE'XX	XXXXXXE'XX	XXXXXXE'XX	XXXXXXE'XX	PTA N+29
							N+34
<p>FORWARD SHEAR DERIVATIVE [SA(J,1) TO SA(J, KMAX)] (USED IN CASE (2))</p>							
XXXXXXE'XX	XXXXXXE'XX	XXXXXXE'XX	XXXXXXE'XX	XXXXXXE'XX	XXXXXXE'XX	XXXXXXE'XX	PSA N+35

2.59
67-136
X-21A

ENGINEER	NORTHROP CORPORATION NORAIR DIVISION	PAGE 2.60
CHECKER		REPORT NO. NOR-67-136
DATE June 1967		MODEL X-21A

2.19 APPENDIX F

Definitions of Parameters Printed by Boundary Layer Input and Integration Program (BB6-2A/5A).

PRINT OUT DEFINITION

INPUT PROGRAM

Page 1	L	Number of flow parameters (25)
	Mach No.	M'_0 free stream Mach number
	TO PRIME	T'_0 free stream temperature
	DEL SKI	$\Delta \xi$
	IMAX	$I_{max} = I_0$
	IFRQ	Print out frequency (I)
	IMID	I start
	DEL ETA	$\Delta \eta$
	JMAX	$J_{max} = J_0$
	JFRQ	Print out frequency (J)
	A(I)	Input control IND(I)

Page 2 GIVEN USTR

XI-SQUARE	ξ^2 coordinate direction
USTR	$U^* = \frac{U}{Q'_0}$ non-dimensional velocity component

Page 3 GIVEN SUCTION DISTRIBUTION

XI-SQUARE	ξ^2
FO-STAR	$F_{0*} = f_{0*} = \frac{\lambda'_{wall}}{\lambda'_0} \frac{w'_{wall} \sqrt{K_c'}}{Q'_0}$

ENGINEER	NORTHROP CORPORATION NORAIR DIVISION	PAGE 2.61
CHECKER		REPORT NO. NOR-67-136
DATE June 1967		MODEL X-21A

2.9 APPENDIX F (Continued)

PO'	P'_0 (atm) free stream absolute pressure (static)
QO'	Q'_0 (ft/sec) free stream velocity
LO'	L'_0 (ft) if LCODE = 0
LO'/C'	$\frac{L'_0 R'_0}{C'}$ if LCODE = 1
RE/FT	$R'_0 \frac{U*P}{NT^2}$ unit Reynolds number
C'	Streamwise surface chord length in feet
REO	R'_0 (1/ft) free stream unit Reynolds number $\frac{Q'_0 \Lambda'_0}{\mu_0}$

Page 4	I	i, chordwise step
	J	J, spanwise step (equals 0 for similar solutions)
	V	V, external flow velocity component (non-dimensional)
	T	T, external flow temperature (non-dimensional)
	P	P, external flow pressure (non-dimensional)
	G	g, wall temperature (if specified)
	Q	Q, external flow resultant velocity
	A1,A2.....,A30	Ai flow parameters
	UX1, UX2,...UX10	UX(I) functions (defined in App. E)

INTEGRATION PROGRAM

First two pages contain general information

I

1

ENGINEER	NORTHROP CORPORATION NORAIR DIVISION	PAGE 2.62
CHECKER		REPORT NO. NOR-67-136
DATE June 1967		MODEL X-21A

2.19 APPENDIX F (Continued)

J	j
XI-SQ	ξ^2
P	$P = \frac{P'}{P_o^*}$ non-dimensional pressure coeff.
Q	$Q = \frac{Q'}{Q_o'}$ non-dimensional external flow velocity
GWT	$g = (r'g')/Q_o'^2$ non-dimensional wall temperature
Q'	Q' (ft/sec)
T _o *	$T_o^* (^{\circ}K)$ $T_o^* = Q_o'^2/r'$
P _o *	$P_o^* (atm)$ $P_o^* = P_o' T_o^*/T_o'$

BOUNDARY LAYER PROFILES BLP(1).....BLP(17)

No.	LCODE \neq 0	LCODE = 0	LCODE \neq 0	LCODE = 0
1	V	V	v	v
2	T	T	t	t
3	PHI	PHI	φ	φ
4	S	S	$s = s'/Q'$	$S = s'/Q'$
5	N	N	$n = n'/Q'$	$n = n'/Q'$
6	U'	U'	u' (ft/sec)	u' (ft/sec)
7	V'	V'	v' (ft/sec)	v' (ft/sec)
8	T'(*K)	T'(*K)	t'(^{\circ}K)	t'(^{\circ}K)
9	Z	Z'(ft)	$z = \frac{z'}{c'} \sqrt{R_c'}$	z'(inches)
10	N'/NO'	N'/NO'	μ'/μ_o'	μ'/μ_o'
11	DT/T/Z	DT'/Z'	$\partial(t'/T')/\partial z$	$\partial t'/\partial z' (^{\circ}K/ft)$
12	DU/DZ	DU'/Z'	$\partial u/\partial z$	$\partial u'/\partial z' (1/sec)$

ENGINEER	NORTHROP CORPORATION NORAIR DIVISION	PAGE 2.63
CHECKER		REPORT NO. NOR-67-136
DATE June 1967		MODEL X-21A

2.19 APPENDIX F (Continued)

No.	LCODE $\neq 0$	LCODE = 0	LCODE $\neq 0$	LCODE = 0
13	DV/DZ	DV'/Z'	$\partial u / \partial z$	$\partial u' / \partial z' (1/sec)$
14	DS/DZ	DS'/Z'	$\partial s / \partial z$	$\partial s' / \partial z' (1/sec)$
15	DN/DZ	DN'/Z'	$\partial n / \partial z$	$\partial n' / \partial z' (1/sec)$
16	T/T1	T/T1	t/T	t/T
17	U	U	u	u

The 3 remaining BLP can be programmed by the customer and in the present program are:

18	SQ	-	s' / Q_0'	-
19	NQ	-	n' / Q_0'	-
20	-	-	-	-

PRINT OUT

DEFINITION

DEL S

$$\delta' s = \int \frac{(1 - \lambda' s')}{\lambda' Q'} dz'$$

DEL N

$$\delta' n = \int \frac{n'}{Q'} \frac{\lambda'}{\lambda'} dz'$$

DEL SS

$$\delta' ss = \int (1 - s' / Q') (s' / Q') (\lambda' / \lambda') dz'$$

DEL NS

$$\delta' ns = \int \frac{n'}{Q'} \frac{s'}{Q'} \frac{\lambda'}{\lambda'} dz'$$

DEL NN

$$\delta' nn = \int \frac{(n')^2}{Q'} \frac{\lambda'}{\lambda'} dz'$$

DEL U

$$\delta' u = \int (1 - \frac{u'}{u'} \frac{\lambda'}{\lambda'}) dz'$$

ENGINEER	NORTHROP CORPORATION NORAIR DIVISION	PAGE 2.64
CHECKER		REPORT NO. NOR-67-136
DATE June 1967		MODEL X-21A

2.19 APPENDIX F (Continued)

PRINT OUT

DEFINITION

DEL V

$$\delta'_{\text{v}} = \int (1 - \frac{v'}{V'}) \frac{\lambda'}{\Lambda'} dz'$$

DEL UU

$$\delta'_{\text{uu}} = \int (1 - \frac{u'}{U'}) (\frac{u'}{U'}) (\frac{\lambda'}{\Lambda'}) dz'$$

DEL UV

$$\delta'_{\text{uv}} = \int (1 - \frac{u'}{U'}) \frac{v'}{V'} \frac{\lambda'}{\Lambda'} dz'$$

DEL VV

$$\delta'_{\text{vv}} = \int (1 - \frac{v'}{V'}) \frac{v'}{V'} \frac{\lambda'}{\Lambda'} dz'$$

NOTE; If LCODE = 0, then $\delta' = \delta'$ (ft); if LCODE \neq 0, then
 $\delta' = \frac{\delta'}{C'} R_c$

RO.1

$$RO.1 \begin{cases} \text{If LCODE} = 0, \text{ then } RO.1 = \frac{(\Lambda' Q') N}{N'} \max Z_{0.1} n_{\max} \\ \text{If LCODE} \neq 0, \text{ then } RO.1 = RO.1 / \sqrt{R_c} \end{cases}$$

RN

$$R_n \begin{cases} \text{If LCODE} = 0, \text{ then } R_n = \frac{(\Lambda' Q') Z(K=2) n_{\max}}{N'} \\ \text{If LCODE} \neq 0, \text{ then } R_n = R_n / \sqrt{R_c} \end{cases}$$

RDELS

$$R_{\delta_s} \begin{cases} \text{If LCODE} = 0, \text{ then } R_{\delta_s} = \frac{(\Lambda' Q') \delta'_s}{N'} \\ \text{If LCODE} \neq 0, \text{ then } R_{\delta_s} = R_{\delta_s} / \sqrt{R_c} \end{cases}$$

RDELSS

$$R_{\delta_{ss}} \begin{cases} \text{If LCODE} = 0, \text{ then } R_{\delta_{ss}} = \frac{(\Lambda' Q') \delta'_{ss}}{N'} \\ \text{If LCODE} \neq 0, \text{ then } R_{\delta_{ss}} = R_{\delta_{ss}} / \sqrt{R_c} \end{cases}$$

H

$$H = \delta_s / \delta_{ss} = \delta^* / \theta \text{ form factor}$$

HI

$$H_1 = (H+1.0) * t'_k = 1/t'_w - 1.0$$

ENGINEER	NORTHROP CORPORATION NORAIR DIVISION	PAGE 2.65
CHECKER		REPORT NO. NOR-67-136
DATE June 1967		MODEL X-21A

2.19 APPENDIX F (Continued)

PRINT OUT

DEFINITION

HWPR	$n'_w \text{ (BTU/sec ft}^2\text{)} \quad h'_w = k'_w \left(\frac{\partial t'}{\partial z'} \right)_w$
CFU	$Cfu = \frac{\mu'_{wall}}{\frac{1}{2} \Lambda'_0 Q'_0{}^2} \left(\frac{\partial u'}{\partial z'} \right)_{wall} \quad \text{LCODE} = 0, Z' \text{ (ft)}$
CFV	$Cfv = \frac{\mu'_{wall}}{\frac{1}{2} \Lambda'_0 Q'_0{}^2} \left(\frac{\partial v'}{\partial z'} \right)_{wall} \quad \text{LCODE} \neq 0, z = \frac{z'}{R_c'}$
X1/L	Chordwise coordinate
Y1/L	Spanwise coordinate
U*	U*
NMAX	nmax
ZPEAK	$Z_{peak} \begin{cases} \text{If LCODE} = 0, Z'_{peak} = Z'_{nmax} \text{ (ft)} \\ \text{If LCODE} \neq 0, Z'_{peak} = \frac{Z'_{nmax}}{c'} \sqrt{R_c'} \end{cases}$
Z01	$Z_{0.1n_{max}} \begin{cases} \text{If LCODE} = 0, Z_{0.1n_{max}} = Z'_{0.1n_{max}} \text{ (ft)} \\ \text{If LCODE} \neq 0, Z_{0.1n_{max}} = \frac{Z'_{0.1n_{max}}}{c'} \sqrt{R_c'} \end{cases}$
NZZ	$\frac{(Z_{0.1})^2}{n_{max}^2} \frac{\partial^2 n}{\partial z^2}$
RNS	$R_{ns} \begin{cases} \text{If LCODE} = 0, R_{ns} = 102 - 1.29 \text{ NZZ} \\ \text{If LCODE} \neq 0, R_{ns} = (102 - 1.29 \text{ NZZ}) / \sqrt{R_c'} \end{cases}$
TANCRT	$R_{ns} \sqrt{R_c'}$
CFPO	Crossflow suction coefficient F_{0*}

ENGINEER	NORTHROP CORPORATION NORAIR DIVISION	PAGE 2.66
CHECKER		REPORT NO. NOR-67-136
DATE June 1967		MODEL X-21A

2.19 APPENDIX F (Continued)

A(J,20)	Flow parameter
TFFO	Tangential flow suction coefficient F_o^*
WALL DENSITY RATIO	$\frac{\lambda'_{wall}}{\lambda'_o}$
RHOS	Wall density, λ'_{wall} (slugs/ft ³)
FS	Suction inflow velocity for continuous suction feet/sec) = $w' = f'$
VOLS	Specific volume of air at surface = $(1/32.2 \text{ RHOS})$
W/A	Suction weight flow = $32.2\lambda'_{wall} w'$
FSTARR	$F^* = \frac{F_o^* \lambda'_o}{\lambda'_{wall} Q'_o} = \frac{w'}{Q'_o} \sqrt{R_c'}$
UX1, UX2,.....,UX10	UX(I) functions (defined in App. E)

FLUID PROPERTIES AND OTHER CONSTANTS

$$\begin{aligned}
 \sigma_1 &= 3.5 \\
 \sigma'_2 &= 3.35 \times 10^{-12} (1/^\circ K)^4 \\
 \sigma'_3 &= 2.85 \times 10^{-12} (1/^\circ K)^4 \\
 \sigma_2 &= \sigma'_2 T^{*4} \\
 \sigma_3 &= \sigma'_3 T^{*4} \\
 \gamma' &= 1716.0 (\text{ft/sec}^{20} R) \\
 \frac{\gamma'}{\sigma'} &= (1 + \sigma'_3 T_o'^4) / [\sigma' (1 + \sigma'_2 T_o'^4)] \\
 \kappa'_1 &= .476 \times 10^{-5} \left(\frac{\text{cal}}{\text{cm}_{\text{sec}} (^\circ K)^{3/2}} \right)
 \end{aligned}$$

ENGINEER	NORTHROP CORPORATION NORAIR DIVISION	PAGE 2.67
CHECKER		REPORT NO. NOR-67-136
DATE June 1967		MODEL X-21A

2.19 APPENDIX F (Continued)

$$K'_2 = v'_2$$

a necessary condition for K constant and $K_t = 0.0$

$$K'_3 = v'_3$$

$$v'_1 = 1.422 \times 10^{-5} \left(\frac{\text{gm}}{\text{cm}_{\text{sec}} (\text{OK})^{\frac{1}{2}}} \right)$$

$$v'_2 = 112.0 (\text{OK})$$

$$v'_3 = 0.0 (\text{OK})^2$$

$$K'_1/T'_1 = .92155 \times 10^{-4} \frac{\text{gm}}{\text{cm}_{\text{sec}} (\text{OK})^{\frac{1}{2}}}$$

$$T_o^* = M_o'^2 T'_o / (1 - \frac{r'_1}{\sigma'_o}) (\text{OK})$$

$$T_o = (\sigma' - 1.0) / (\sigma' M'_o)$$

$$P'_o = \text{Free stream pressure (atm)}$$

$$P_o = T_o$$

$$P_o^* = P'_o T^*/T'_o (\text{atm})$$

$$Q'_o = 49.1 (1.8 T'_o)^{\frac{1}{2}} M'_o (\text{ft/sec})$$

$$R_o(1) = 3.2794397 \times 10^2 \frac{P_o Q'_o}{N_o T'_o} (1/\text{ft})$$

$$N'_o = J' \sqrt{T'_o} / (1 + v'_2/T'_o + v'_3/T'_o{}^2) \left(\frac{\text{gm}}{\text{cm}_{\text{sec}}} \right)$$

$$K'_o = K'_1 T'_o / (1 + K'_2/T'_o + K'_3/T'_o{}^2) \left(\frac{\text{cal}}{\text{cm}_{\text{sec}} (\text{OK})} \right)$$

$$\pi = \sigma' v' K' = \sigma/K \text{ Prandtl number}$$

ENGINEER	NORTHROP CORPORATION NORAIR DIVISION	PAGE 2.68
CHECKER		REPORT NO. NOR-67-136
DATE June 1967		MODEL X-21A

APPENDIX G

Outline of Program Model of Operation for Suction Optimization *

An observation of a wing whord boundary layer development with suction shows four types of crossflow velocity profiles.

- a. Stagnation zone velocity profiles
- b. A forward-chord interval with totally positive crossflow velocities along the boundary layer height.
- c. A mid-chord interval with crossflow velocities of both signs with negative velocities close to the wing surface. (Cross-over type profiles.)
- d. A rear-chord interval with totally negative crossflow velocities.

Each of these areas asks for different suction requirements according to the boundary layer stability criteria that have to be satisfied, and the corresponding stability margins required by the customer.

The program respects the following stability criteria:

1. $RNS = (102 - 1.29 NZZ) / \sqrt{R}$ (critical crossflow Reynolds number) with a minimum margin of stability
 $m = RNS - R0.1$
2. $R_{\theta_{ss}} = R_{\theta} < 2000$ or any desired level (critical tangential Reynolds number) (see 2.8).

The crossflow criterion is not used where crossflow velocity profiles of the "cross over" type are present. No criterion is available at present, and in the program it is assumed that the tangential stability is critical. The program will calculate a local minimum suction coefficient at each point, which probably will not render the best practical suction distribution for a given margin of stability, but will define minimum levels to smooth out data conveniently for each application, so from the first run a good theoretical minimum suction distribution is obtained. These levels may be somewhat changed in certain chord stations when sensitivity (variation of stability margin with suction changes) allows it. A minimum suction coefficient

* Direct Suction Option, Ref. 2.9.

ENGINEER	NORTHROP CORPORATION NORAIR DIVISION	PAGE 2.69
CHECKER		REPORT NO. NOR-67-136
DATE June 1967		MODEL X-21A

APPENDIX G (Continued)

magnitude may be specified as an extra requirement along the chord. The stagnation zone stability criterion $R_0 < 100$ is not included presently in the suction calculations. It is indirectly satisfied, however, when a specified amount of leading edge suction is input at the first chord station producing a different set of initial profiles, used as boundary conditions. This suction will not show in the output, except through the effects or variations manifested in the initial profile characteristics. If the leading edge suction is reasonable, the program will accept the corresponding new profiles and will proceed to calculate the minimum suction requirement as well. This is done, for example, when it is required to start with a profile of specified momentum thickness Reynolds number obtained experimentally.

The suction change required when the tangential stability is more critical, is obtained through a combined exponential linear function which assures a continuous and sufficiently rapid variation. In this way, the iteration proceeds along the chord eliminating the time consuming process of stopping and recalculating each step with no sensitive output effectiveness change.

The same methods may be applied to suction calculation determined by the crossflow stability condition, with equally successful results. Nevertheless, the program offers a more direct possibility due to the form in which the critical crossflow Reynolds number definition is supplied. It will be briefly described in the following discussion.

The critical crossflow Reynolds number is available as a function of the second derivative of the crossflow velocity profile at the wall, the so-called crossflow criterion.

$$RNS = f_1 (\partial^2 n / \partial z^2) \quad (1)$$

On the other hand, one of the boundary conditions is a function φ_ζ , depending upon the suction coefficient F_0^* .

$$\varphi_\zeta = f_2 (F_0^*) \quad (2)^1$$

From definitions provided in the study of the applied boundary layer equations, a new equation was derived.

¹ φ_ζ = derivative of φ with respect to ζ . $\zeta = 1.0$ at the wall.

ENGINEER	NORTHROP CORPORATION NORAIR DIVISION	PAGE 2.70
CHECKER		REPORT NO. NOR-67-136
DATE June 1967		MODEL X-21A

APPENDIX G (Continued)

$$\varphi_c = f_3 (\partial^2 n / \partial z^2) \quad (3)$$

At each chord station the solution is calculated from essentially the values of the unknowns at the upstream points, which means that at the point $i + 1, j, k$ the solution of the difference system of equations is obtained using data at the previous step i, j, k with the corresponding boundary condition. The crossflow velocity profile at station $i + 1$ is obtained from the boundary layer velocity component profiles (v, u) at station i according to the analytic properties of the differential system, and no iteration is necessary at a given station since, according to Eq. (3), φ_c is then established for step $i + 1$ from data belonging to step i .

The stability condition requires that $RNS > R0.1$ where $R0.1$ is the actual crossflow Reynolds number and is known. If it is specified that the crossflow stability margin be m , then $R0.1 + m = RNS$.

Once RNS is obtained, equation (1) supplies the required value of $(\partial^2 n / \partial z^2)$ and equation (3) the corresponding φ . Finally, equation (2) determines the required F_0^* . The suction coefficient thus determined will maintain the desired stability margin. In certain areas it may result that RNS is slightly above $(R0.1 + m)$ due to accumulated errors in the computation, but never less than $(R0.1 + m)$. In other areas, to maintain the margin " n " would require positive mass transfer (blowing) since the margin is naturally larger than " M " even without mass transfer (suction). At these points, the program uses the minimum possible suction which is either zero or a specified value if desired (FOMIN input defined in Appendix E).

Region of Positive Crossflow Velocity Profile

At any station, the suction coefficient is first calculated to satisfy the crossflow criterion. Immediately after, the program tests whether or not the tangential criterion is also met. If not, suction is increased over the last suction coefficient value found. The program then proceeds to repeat the same process at the next chord station. The suction change required from one step to the other is determined by the nature of the boundary layer equations and boundary conditions when calculating to satisfy the crossflow stability condition.

ENGINEER	NORTHROP CORPORATION NORAIR DIVISION	PAGE 2.71
CHECKER		REPORT NO. NOR-67-136
DATE June 1967		MODEL X-21A

APPENDIX G (Continued)

In the region of crossover profiles in the mid-chord span there is no satisfactory definition of the critical and actual crossflow Reynolds numbers. Since no crossflow stability criterion is available at present, the suction is calculated under the tangential stability condition only, with the same procedure used previously. The only difference is that in the second region the minimum suction requirement is determined by the crossflow criterion and it is tested or recalculated, if called for, to assure having the $R_{\theta_{ss}}$ below a specified value. Thus, when the $R_{\theta_{ss}}$ approaches the $R_{\theta_{ss}}$ limit the suction is increased, and when it tends to move below the limit the suction is decreased.

As implied above, there is no crossflow stability history along this chord-interval where crossover profiles exist, but at the end of it when the crossflow profile becomes totally negative, crossflow stability must be assured. It is possible that in the last station of this interval the suction is also sufficient to cover the crossflow condition with sufficient margin. If it is not so, that is if the crossflow margin is too small or even negative, it is necessary to introduce suction a little before the profile becomes negative. This occurs very near the point where the adverse pressure gradient becomes strong. Adequate suction may be provided by slightly lowering the maximum allowable $R_{\theta_{ss}}$ requirement at that point. An input TARG2 (defined in Appendix E) takes care of this. On the other hand, if the margin is larger than specified, nothing need be done about it, since the calculated suction is already the minimum needed to satisfy the tangential criterion and cannot be lowered.

The Last Chord-Interval

Suction is determined here by the crossflow stability condition and tested or readjusted, if necessary, to meet the tangential stability criterion also. The calculated suction will try to maintain the specified crossflow margin of stability.

DATA SHEET

Form 20-172 (2-4-53)

APPENDIX H WAVE DRAG COMPUTING FORM

2.72

67-136

X-21A

1	M	
2	θ_2	
3	$\cos \theta_2$	$\cos (2)$
4	$\cos^2 \theta_2$	(3)
5	$\sin^2 \theta_2$	$1.0 - (4)$
6	T	
7	P	
8	DELUUR	
9	DELVUR	
10	USTHR	
11	$0.7T$	$0.7(6)$
12	$\frac{1.2}{2.7T}$	$\frac{1.2}{(11)}$
13	M^2	$(1)^2$
14	$0.2M^2$	$0.2(13)$
15	$1 + 0.2M^2$	$1.0 + (14)$
16	$\frac{1 + 0.2M^2}{0.7T}$	$(15)/(11)$
17	$\frac{1.2}{0.7T M^2}$	$(12) \times (13)$
18	H_{TURB}	$(17) - 1.0$
19	$\frac{H_{TURB}}{0.7T}$	$(18) \div 0.7$
20	U_{T0}/U_0'	$(19)/(6)$
21	$(U_{T0}/U_0')^{0.8}$	$(20)^{0.8}$
22	$P/T \cdot A'/A'$	$(7)/(6)$
23	$\delta u_{\infty} \frac{1}{U_0'}$	$(21)(22)$
24	$\delta w_{\infty} \frac{1}{U_0'}$	$(23)(6)$
25		$(24)(6)$
26		$(25)(6)$
27		$(26) + (24)$
28	$c_{dH} \sqrt{R_0}$	$2.0 (27)(6)$
29	$\sqrt{R_0}$	
30	c_{dH}	$(28)/(29)$

ENGINEER	NORTHROP CORPORATION NORAIR DIVISION	PAGE 2731
CRACKER		REPORT NO. NOR-67-136
DATE June 1967		MODEL X-21A

APPENDIX I

Incremental Equivalent Suction Drag Computing Form

1	M_0	
2	P'_0	
3	T'_0	
4	P	
5	t'_{wall} if GWT = 0; $t'_{wall} = T'_0$	
6	FSTARR	
7	M_0^2	① ²
8	δM_0^2	⑦ x 1.4
9	$\delta M_0^2 P$	④ x ⑧
10	P'_0	② x ⑨
11	$.035 M^2$	⑦ x .035
12	$P'_0 - .035 M^2$	⑩ - ⑪
13	$\frac{P'_0}{P'_0 - .035 M^2}$	② / ⑫
14		⑬ ^{2/7}
15		⑭ - 1
16	$\frac{(\delta-1)M^2}{2}$.2 x ⑦
17	$\left(\frac{\delta-1}{2}\right) M^2 T'_0$	⑮ x ③
18		⑤ / ⑰
19		⑮ x ⑱
20		1 + ⑲

ENGINEER	NORTHROP CORPORATION NORAIR DIVISION	PAGE 2.74
CHECKER		REPORT NO. NOR-67-136
DATE June 1967		MODEL X-21A

APPENDIX I (Continued)

21	$dC_{Dg} \sqrt{R'_c}$	(6) x (20)
22	R'_c	
23	$\sqrt{R'_c}$	(22) .5
24	dC_D	(21) / (23)

ENGINEER	NORTHROP CORPORATION NORAIR DIVISION	PAGE 3.00
CHECKER		REPORT NO. NOR 67-136
DATE June 1967		MODEL X-21A

SECTION 3

SUCTION SLOT DESIGN

BY:

K. H. Rogers

April 1967

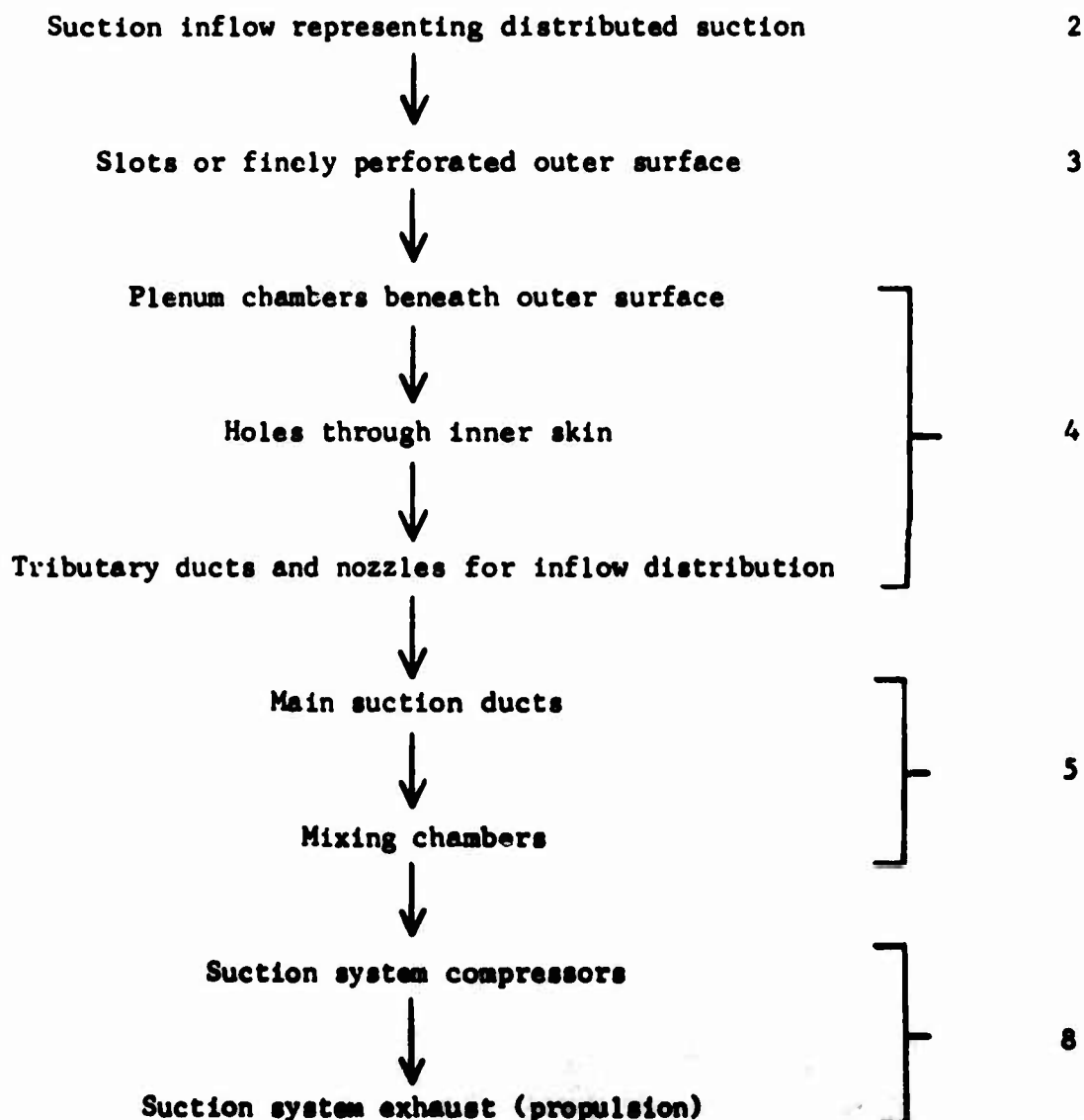
ENGINEER	NORTHROP CORPORATION NORAIR DIVISION	PAGE 3.01
CHECKER		REPORT NO. NOR 67-136
DATE June 1967		MODEL X-21A

3.1 INTRODUCTION

The suction slot design, described in this section, is the first of a series of flow devices through which the suction air passes from the suction surface to the suction pod exhaust. The entire flow sequence of the suction system is shown in the following chart.

Suction System Flow Sequence

Reference Section No.



ENGINEER	NORTHROP CORPORATION NORAIR DIVISION	PAGE 3.02
CHECKER		REPORT NO. NOR-67-136
DATE June 1967		MODEL X-21A

3.1 INTRODUCTION (Continued)

The primary objective of the suction surface design is to provide a suction distribution approximating the calculated requirements for distributed suction. The design must be practical from the standpoint of manufacture and maintenance; and irregularities in either the surface or the inflow must be minimized. In the suction surface design, the wing geometry, LFC flight conditions, suction distribution, and boundary layer average properties already have been determined.

The use of fine slots for the suction surface, rather than porous or finely perforated panels, was considered at Northrop Norair the most practical design. The suction surface design of fine spanwise slots sawed in the outer skin, with spanwise plenum chambers beneath the slots, has been developed at Northrop Norair under the direction of W. Pfenninger. The slot width is made approximately equal to the sucked height of the boundary layer, and the slot width Reynolds number (or flow rate per slot) is made sufficiently small so that rounding of the leading edge of the slot is considered unnecessary. The possibility of using a finely perforated suction surface instead of slots in the wing nose region to improve laminarization is discussed in Section 15.7.2.4.

3.2 NOMENCLATURE

Lower Case Letters

- c = wing chord, ft.
- Δc_p = pressure coefficient, $\Delta p/q_\infty$
- $\Delta c_{p\text{slot}}$ = Δp slot/ q_∞
- Δc_n = slot spacing normal to slot direction, ft.
- h = altitude, ft.
- k_θ = momentum thickness coefficient, see Fig. 3.5.1.
- Δl = incremental length of slot, ft.
- n' = crossflow velocity within B.L., ft./sec.
(orthogonal to s')
- p = static pressure, lb./ft.²
- Δp = increment of pressure, lb./ft.²
- q_∞ = free stream dynamic pressure ($\frac{\rho}{2} u_\infty^2$)
- q_{slot} = dynamic pressure ($\frac{\rho}{2} u_s^2$), lb./ft.²
- q' = resultant velocity vector within boundary layer

ENGINEER	NORTHROP CORPORATION NORAIR DIVISION	PAGE 3.03
CHECKER		REPORT NO. NOR-67-136
DATE June 1967		MODEL X-21A

r = radius of leading edge, ft
 s' = velocity component within B.L., in direction of potential flow Q' , ft/sec (orthogonal to n')
 t = thickness of outer skin = depth of slot, ft
 u' = component of q' normal to element line, ft/sec
 \bar{u}_s = average slot velocity, ft/sec
 u_∞ = velocity of free stream, = Q'_0 , ft/sec
 v' = component of q' parallel to element line, ft/sec
 v_s = distributed suction velocity at surface, ft/sec
 w = slot width, ft
 z = distance from external surface, ft
 z_1 = sucked height of boundary layer, ft

Capital Letters

B.L. = boundary layer
 F^* = $\frac{v_s}{u_\infty} R_c^{.5}$, suction volume flow parameter
 F^*_0 = $\frac{\rho_s v_s}{\rho_\infty u_\infty} R_c^{.5}$, suction mass flow parameter
 LFC = Laminar Flow Control
 M_∞ = Mach number of free stream
 N = $\frac{n'}{Q'}$
 Q' = local velocity outside B.L., ft/sec
 Q'_0 = u_∞ , free stream velocity, ft/sec
 R_c = chordwise Reynolds number = $\rho_\infty u_\infty c / \mu_\infty$
 R_w = slot width Reynolds number = $\rho_s u_s w / \mu_s$
 R'_∞ = unit Reynolds number of free stream = $\rho_\infty u_\infty / \mu_\infty$
 R_{oss} = momentum thickness Reynolds number of spanwise flow at the leading edge attachment line. See Eq. (1).

ENGINEER	NORTHROP CORPORATION NORAIR DIVISION	PAGE 3.04
CHECKER		REPORT NO. NOR 67-136
DATE June 1967		MODEL X-21A

R_θ = equivalent to $R\delta_{ss}$, used in Section 1

S = s'/Q'

S_{ZR}, N_{ZR} = components of non-dimensional slope of boundary layer profile in same directions as S and N ; $(S_{ZR}^2 + N_{ZR}^2)^{.5} = \frac{dq'}{dz} \left(\frac{c}{Q' R_c^{.5}} \right)$

U = U'/Q' ; see Figure 3.3

V = V'/Q' ; see Figure 3.3

U', V' = orthogonal components of Q' outside B.L.; see Fig. 3.3

U^* = U'/Q'_o , see Figure 3.3

$Z\eta$ = z_1/w = sucked height/slot width

Greek Letters

β = slot parameter $2\tau/R_w = 4t/wR_w$

ξ = $(1 - \frac{u'}{U'})^{.5}$

Λ = sweep of wing leading edge

μ = absolute viscosity, lb sec/ft²

ρ = mass density, slug/ft³ or lb sec²/ft⁴

τ = slot parameter $2t/w$

τ_θ = thickness ratio of ellipse containing leading edge shape

Subscripts

∞ = freestream

s = slot

3.3 CHORDWISE SLOTS IN THE LEADING EDGE REGION

Wind tunnel experiments conducted during the X-21A program show that chordwise slots in the leading edge region of a swept wing (in the flow attachment zone) are effective in preventing the spanwise propagation of disturbance from the fuselage or from a roughness particle or the like. Chordwise slots, in conjunction with a smaller leading edge radius, are included in the revised design of the inboard wing nose of the second (AF 55-410A) airplane. The chordwise slots are .0035 wide, spaced .75 inches apart, and extend chordwise somewhat beyond the chordwise limits of travel of the flow attachment line for the various LFC flight conditions. The leading edge radius is about 1.5 inches over most of the inboard wing, increasing to about 1.8 inches at the inboard end of the final installation. The new nose section is added onto the old and is commonly called the "scab-on" nose region.

ENGINEER	NORTHROP CORPORATION NORAIR DIVISION	PAGE 3.05
CHECKER		REPORT NO. NOR-67-136
DATE June 1967		MODEL X-21A

The chordwise slots lead to chordwise plenum chambers with holes connecting to the scab-on duct. The design is similar to that of the spanwise slots except no tributary ducts are used to guide the flow spanwise into the internal, scab-on, duct. Most of the flow from the chordwise slots turns and flows spanwise along the scab-on duct to control-valves at the ends of the scab-on installation; but additional inflow is led into the original nose through numerous holes drilled into the original nose and through the original spanwise slots in that area.

The primary design criterion for the chordwise slots is sufficient suction to reduce the momentum thickness Reynolds number at the attachment line to values below 100. The momentum thickness Reynolds number is designated $R_{\theta_{ss}}$ in Section 2, but often is designated simply R_{θ} .

Due to the chordwise distribution of surface pressure, relatively strong suction, sufficient to meet the requirements stated, always exists along the attachment line when the scab-on internal pressure is low enough to prevent outflow at the ends of the chordwise slots. Best LFC results appear to coincide with strong leading edge suction.

The size and spacing of the chordwise slots are based on wind tunnel tests as well as practical considerations of fabrication. In a typical LFC flight condition, analysis shows that the impinging streamlines cross about eight chordwise slots before reaching the first slot in the region of the spanwise slots. The suction flow rate and the slot width Reynolds numbers along the attachment line are greater than those elsewhere on the wing.

An approximate equation for the momentum thickness Reynolds number $R_{\theta_{ss}}$ at the attachment line, useful in preliminary design studies, is

$$R_{\theta_{ss}} = K_{\theta} \tan \Lambda \left[\frac{R'_{\theta} \tau \cos \Lambda}{(1 + \tau_e)} \right]^{.5} \quad (1)$$

The coefficient K_{θ} is plotted in Figure 3.1 as a function of the suction coefficient F_{θ}^* . The value of the parameter τ_e , the thickness ratio of an ellipse fairing into the nose shape, is about twice the thickness ratio of the airfoil. If the chordwise gradient of potential flow velocity at the stagnation line is known, then the momentum thickness can be calculated more accurately from the equations of 1.5.1.

3.4 SPANWISE SLOTS

3.4.1 Slot Design Process and Criteria

The basis for the slot design is the distribution of surface suction required, the distribution of surface pressure, and the computation of average boundary layer characteristics as described in the preceding Sections 1 and 2.

ENGINEER	NORTHROP CORPORATION NORAIR DIVISION	PAGE	3.06
CHECKER		REPORT NO.	NOR 67-136
DATE		MODEL	X-21A
June 1967			

An allowable value for slot width Reynolds number R_w is assumed (e.g., let $R_w < 100$ for cruise), and the slot spacing Δc_n is calculated. Later the calculated value of Δc_n may be modified because of practical considerations such as avoiding stringer structure or providing a slot drop-out pattern on a tapered wing. The sucked height z_s is calculated, and the slot width w is made approximately equal to the sucked height. The pressure-drop through the slotted surface is calculated, and the result must be compatible with internal pressure requirements for the plenum chamber beneath the slot and with the pressure requirements of the suction duct.

Some adjustments in suction distributions must be made to accommodate various flight conditions. The slot design process and the performance of the design for various flight conditions are iterative and have been adapted to computer solution.

Progressing from root to tip on a tapered LFC wing, some slots will drop-out, and some slots may be reduced in width. The slot velocity should be gradually reduced to zero as the drop-out point is approached in order to minimize vortex formation at the end of the slot. This gradual reduction in suction can be achieved by omitting the last several holes beneath the suction slot.

As a matter of convenience in analysis, the nominal slot spacing used in converting distributed suction to slot flow rates is determined by dividing the duct width by the number of slots in the duct at the particular span station analyzed. The true slot positions are used in determining the external pressure at the slot.

The basic equations that apply to the slot design and to the slot performance are derived in the following subsections.

3.4.2 Derivation of Equation for Slot Spacing Δc_n

In Figure 3.2 assume a suction strip Δl wide normal to the slot length. Equating the average inflow normal to the surface to the flow into the slot,

$$v_s \Delta c_n = w \bar{u}_s, \text{ or}$$

$$\Delta c_n = \frac{w \bar{u}_s}{v_s} \quad (1)$$

ENGINEER	NORTHROP CORPORATION NORAIR DIVISION	PAGE 3.02
CHECKER		REPORT NO. NOR-67-136
DATE June 1967		MODEL X-21A

In equation (1), $w_{\bar{s}}$ is proportional to the slot width Reynolds number R_w which is a measure of the mass flow rate per slot, and v_s is proportional to the distributed suction strength parameter F_o^* . Making the conversions, in order to use the parameters available in the boundary layer computer program, equation (1) becomes,

$$\Delta c_n = \frac{R_w}{F_o^*} \frac{(\mu_s)}{\mu_\infty} \frac{c}{R_\infty^{1.5}} \quad (2)$$

3.4.3 Derivation of Equation for Sucked Height z'

Again in Figure 3.2, assume a suction strip Δl wide normal to the slot width. The lower or cross-section view of Figure 3.2 shows that the sucked height z' is approximately equal to the slot width ω . Equating the average inflow to the surface to the flow in the sucked region of the boundary layer, and assuming a constant velocity gradient du'/dz in the sucked portion near the surface,

$$\Delta c_n v_s = \frac{du'}{dz} \frac{z'^2}{2}, \text{ or}$$

$$z'^2 = \frac{2 \Delta c_n v_s}{\left(\frac{du'}{dz}\right)} \quad (3)$$

The distributed velocity v_s is proportional to the suction parameter F^* through the relation,

$$v_s = \frac{Q_o' F^*}{R_c^{.5}}, \quad (4)$$

and the velocity gradient, in terms of parameters available in the computer program output, is

$$\frac{du'}{dz} = \frac{Q' R_c^{.5}}{c} \left[(S_{ZR}^2 + N_{ZR}^2)^{.5} \frac{u'}{(u'^2 + v'^2)^{.5}} \right]_{\xi=.95} \quad (5)$$

where the values of velocity components u' and v' and velocity gradient components S_{ZR} and N_{ZR} within the sucked layer are assumed applicable to the boundary layer height $\xi=.95$, where $\frac{u'}{U} \approx .10$. See Figure 3.3 for velocity vector diagram.

ENGINEER	NORTHROP CORPORATION NORAIR DIVISION	PAGE 3.08
CHECKER		REPORT NO. NOR 67-136
DATE June 1967		MODEL X-21A

Substituting (4) and (5) into (3), and noting that

$$\frac{Q'_{10}}{Q'} = \frac{U}{U^*}, \text{ then} \quad (6)$$

$$z_1^2 = \frac{2 \Delta c_n F^* U}{R'_{\infty} U^*} \left[\frac{(u'^2 + v'^2)^{.5}}{u'_1 (S_{ZR}^2 + N_{ZR}^2)^{.5}} \right] \xi = .95 \quad (7)$$

Equation (7), although more complex in form than equation (3), is easier to use in the slot design program because of the availability of parameters in the boundary layer computer output program. The sucked height z_1 should be approximately equal to the slot width w .

3.4.4 Pressure-Drop Through the Slot $\Delta c_{P_{slot}}$

The pressure-drop coefficient ($\Delta P_{slot}/q_{slot}$) is shown versus the parameter $\beta = 2\pi/R_w$ in Figure 3.4. The pressure-drop relationship has been derived theoretically and confirmed by experiment. See Norair Report NAI-58-19, for example.

If the value of β becomes less than about .03, the flow will separate from the forward lip of a sharp edged slot and may or may not reattach to the slot wall. It is considered best to keep the value of β well above the value .03 in order to avoid the possibility of unsteady flow due to the separation phenomenon.

The pressure-drop relationship shown in Figure 3.4 is derived for flow between two plenum chambers. The error involved due to external flow across the slot is considered negligible for LFC slot design because of the low energy level of the sucked layer.

For convenience in design and analysis, all of the pressures in the suction system are referred to the flight dynamic pressure $q_{\infty} = \left(\frac{\rho u^2}{2}\right)_{\infty}$. On this basis the pressure-drop coefficient for the suction slot is expressed as follows:

$$\Delta c_{P_{slot}} = \Delta P_{slot}/q_{\infty} = \frac{\Delta P_{slot}}{q_{slot}} \left(\frac{q_{slot}}{q_{\infty}} \right) \quad (8)$$

ENGINEER	NORTHROP CORPORATION NORAIR DIVISION	PAGE 3.09
CHECKER		REPORT NO. NOR-67-136
DATE June 1967		MODEL X-21A

Equation (8), converted to a form containing the parameters appearing in the boundary layer computer program output, becomes

$$\Delta C_{P_{\text{slot}}} = \left(\frac{\Delta P_{\text{slot}}}{q_{\text{slot}}} \right) \left(\frac{R_w}{R'_w} \right)^2 \left(\frac{\mu_s}{\mu_\infty} \right)^2 \frac{F^*}{F_o^*} \quad (9)$$

3.4.5 Typical Values for Slot Dimensions

Typical values of slot spacings and slot widths for the X-21A spanwise slots are shown in the following table:

Design Parameter	Portion of Wing		
	Fwd.	Intermediate	Aft
	1% to 5%	5% to 40%	40% to 100%
Slot Spacing $\Delta C_n \sim \text{in}$	1.1	2.0	1.2
Slot Width $w \sim \text{in}$.003 .004	.006 .007	.005 .005

The values shown in the example are not intended as design guidelines but simply order-of-magnitude data for one particular wing section. The calculated slot dimensions become larger with larger wing chord and with higher altitude operation, and become smaller if the allowable slot width Reynolds number R_w is reduced.

Although not shown in the preceding table, the strong suction rates are in the forward and aft regions of the wing chord. It is interesting to note that the slot widths and the slot spacings tend to be smaller in these regions of strong suction. Regions of strong suction are associated with relatively large velocity gradients near the surface and smaller sucked height (or slot width) for a given mass flow into the slot. The mass flow per slot tends to be equalized by closer slot spacing in the regions of strong suction. The foregoing explanation is oversimplified but provides some insight into the reasons for the chordwise distribution of slot width and slot spacing.

ENGINEER	NORTHROP CORPORATION NORAIR DIVISION	PAGE 3.10
CHECKER		REPORT NO. NOR 67-136
DATE June 1967		MODEL X-21A

MOMENTUM
THICKNESS
COEFFICIENT

Notes: See Figure 2 of AFFDL-TR-67-33
for similar, universal relation
of momentum thickness versus
suction strength.

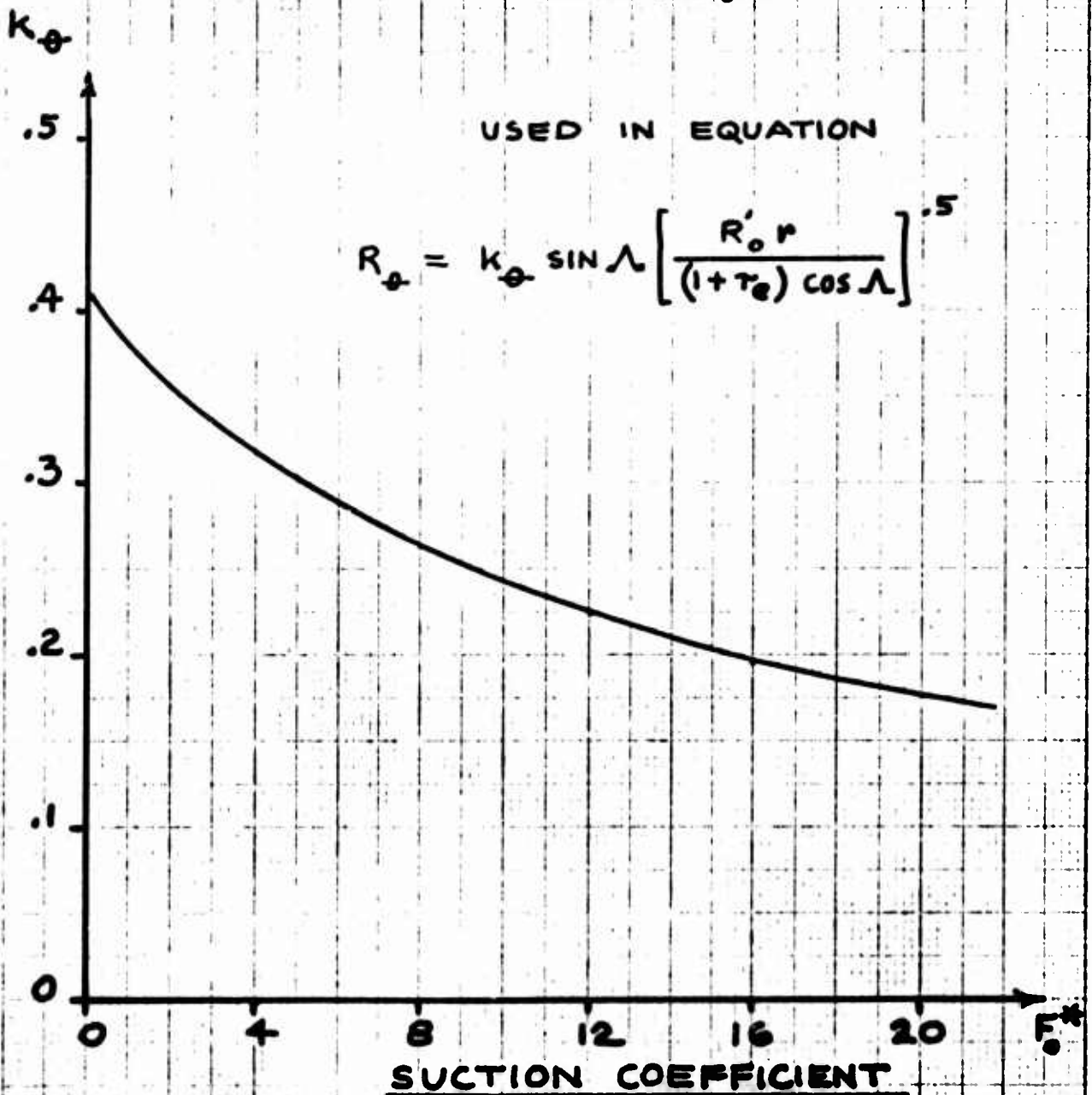


FIG. 3.1 MOMENTUM THICKNESS COEFFICIENT k_{θ}
VS SUCTION COEFFICIENT F_o^*

ENGINEER	NORTHROP CORPORATION NORAIR DIVISION	PAGE 3.11
CHECKER		REPORT NO. NOR 67-136
DATE June 1967		MODEL X-21A

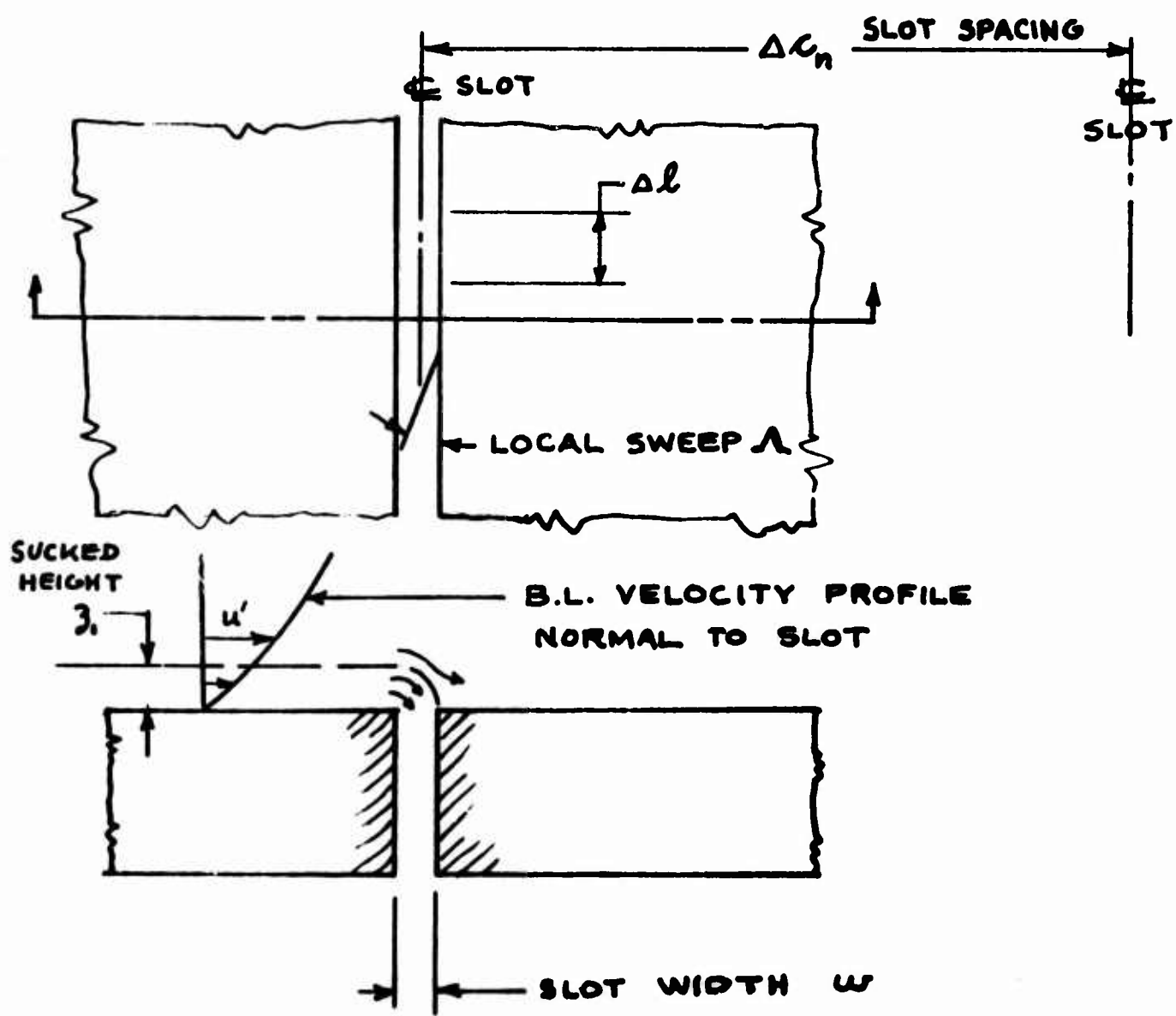


FIG. 3.2 DIAGRAM OF FLOW THROUGH A SLOT

ENGINEER	NORTHROP CORPORATION NORAIR DIVISION	PAGE 3.12
CHECKER		REPORT NO. NOR 67-136
DATE June 1967		MODEL X-21A

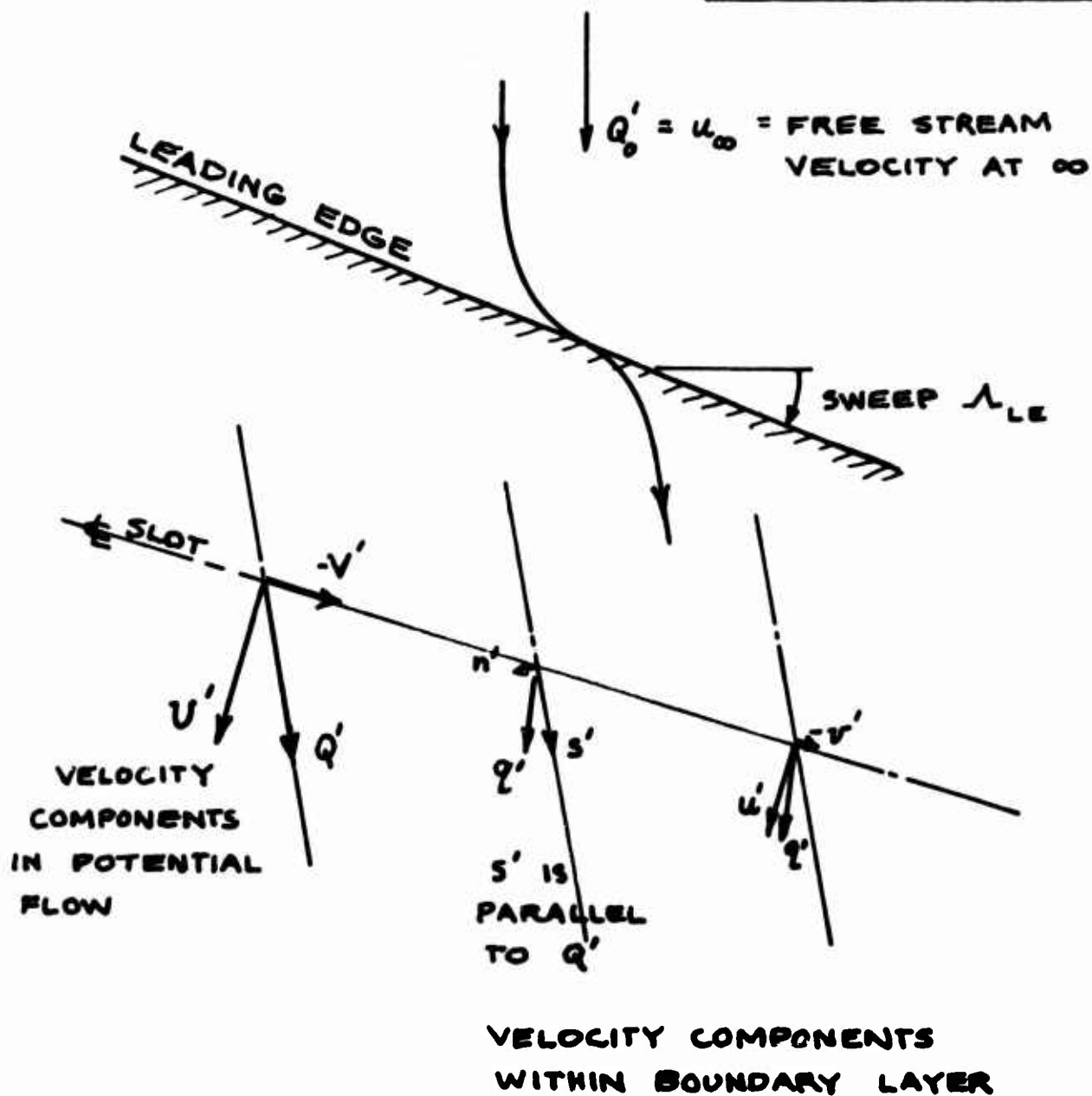


FIG 3.3 VELOCITY VECTOR DIAGRAM FOR FLOW OVER A SWEEP WING

$$\left(\frac{\Delta P}{\rho}\right) = \frac{2.16}{\beta} + \frac{16}{\beta^2}$$

HOLE

$$\frac{\Delta P}{\rho} = 2.16 + 16/\beta$$

BEYOND INLET LENGTH

SLOTS

$$\frac{\Delta P}{\rho} = 1.62 + 6/\beta$$

BEYOND INLET LENGTH

SHARP EDGE INLET

ROUNDED EDGE INLET

FIGURE

ENGINEER	NORTHROP CORPORATION NORAIR DIVISION	PAGE 4.00
CHECKER		REPORT NO. NOR 67-136
DATE June 1967		MODEL X-21A

SECTION 4

DESIGN OF FLOW PASSAGES BETWEEN
SLOTS AND MAIN DUCTS

BY:

K. H. Rogers

April 1967

ENGINEER	NORTHROP CORPORATION NORAIR DIVISION	PAGE 4.01
CHECKER		REPORT NO. NOR-67-136
DATE June 1967		MODEL X-21A

4.1 INTRODUCTION

The flow passages from the suction slot to the suction duct (main duct) are the plenum chamber beneath the slot, the holes through the inner skin, and the plenums (tributary ducts) and flow metering nozzles beneath the inner skin. The slot plenum and holes are designed to provide nearly uniform inflow along the suction slot, and to minimize disturbances within the plenum and at the hole inlet. The nozzles beneath the inner skin provide the design distribution of suction and direct the flow downstream in the suction duct.

4.2 NOMENCLATURE

Lower Case Letters

a	radius of hole, tube, or nozzle, ft
c	velocity of sound, ft/sec
c_p	constant pressure specific heat, .24 btu/lb ^o R
Δc_p	pressure-drop coefficient $\Delta p/q$
d	diameter of hole, ft
d_e	diameter of tributary duct at exit, ft
g	acceleration of gravity, 32.2 ft/sec ²
h	depth of slot plenum chamber, ft
k	ratio of specific heats = 1.40
l	length of tributary duct, ft
\dot{m}	mass flow rate through tributary duct and nozzle, slug/sec
p	pressure, lb/ft ²
Δp	increment of pressure, lb/ft ²
q	dynamic pressure, $\frac{\rho u^2}{2}$
r	pressure ratio p/p_o
s	spacing of holes, ft
t	thickness of skin, ft
u	velocity, ft/sec
\bar{u}	average velocity, ft/sec
w	width of slot, ft
x	effective length of tributary nozzle, hole, or tube, ft
y	chordwise offset of holes from slot, ft
z_1	sucked height, ft

ENGINEER	NORTHROP CORPORATION NORAIR DIVISION	PAGE 4.02
CHECKER		REPORT NO. NOR-67-136
DATE June 1967		MODEL X-21A

Capital Letters

A	effective area of nozzle, ft^2
A_g	gross or actual area of nozzle, ft^2
J	mechanical equivalent of heat, 778 ft lb/btu
M	Mach number
R	gas constant (air) = 53.3 ft lb/lb ^o R
R_d	diameter Reynolds number $\frac{\rho u d}{\mu}$
R_a	radius Reynolds number $\frac{\rho u a}{\mu}$
R_w	slot width Reynolds number $\frac{\rho u w}{\mu}$
R'_∞	unit Reynolds number of free stream, $(\frac{\rho u}{\mu})_\infty$
T	temperature, ^o Rankine
U	velocity ratio, u/u_∞

Greek Letters

β	hole or nozzle design parameter τ/R_a
γ	slot velocity variation $\frac{u_{s \max}}{u_s} - 1$
γ_d	steady state spanwise variation in slot velocity, due to tributary duct,
γ_f	fluctuating slot velocity variation, due to combination of slot width Reynolds number $R_w > 100$ and plenum geometry.
γ_h	steady state spanwise variation in slot velocity, due primarily to hole location and plenum geometry.
μ	viscosity, absolute, lb sec/ft ²
ρ	density, slug/ft ³ = lb sec ² /ft ⁴
τ	ratio t/a or x/a

Subscripts

o	reservoir condition
d	duct or tributary duct
e	tributary duct exit (ahead of nozzle)

ENGINEER	NORTHROP CORPORATION NORAIR DIVISION	PAGE	4.03
CHECKER		REPORT NO.	NOR-67-136
DATE		MODEL	X-21A
June 1967			

f fluctuating
g gross (area)
h hole
max maximum
n nozzle
s slot
 ∞ infinity or free stream condition

4.3 SLOT PLENUM CHAMBER AND HOLE LOCATION

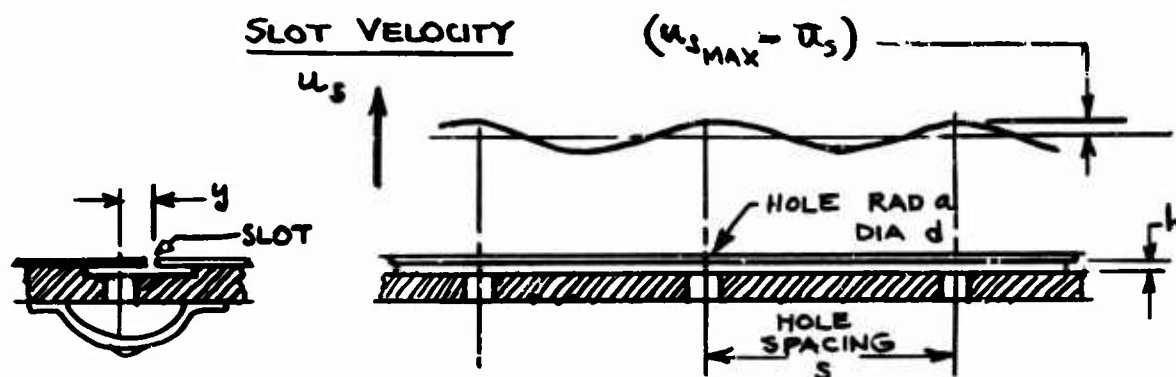
Part 4.3.1 applies to the design criteria for plenum chambers and hole locations for the X-21A airplane. In the latter part of the X-21A program laboratory experiments showed that pressure and velocity fluctuations develop within the plenum chamber and slot at slot width Reynolds numbers $R_w > 100$. The fluctuations appear to begin at $R_w \approx 100$ and grow with increasing R_w , such that the slot velocity variation γ_f may reach values of about $3(10^{-3})$ at $R_w = 200$, for example. Whether or not the fluctuations contribute a significant effect upon LFC test results has not been determined, but the desirability of suppressing all flow disturbances in an LFC design is unquestioned; and further experimentation at Norair has developed plenum chamber and hole location criteria that suppress the fluctuations at the higher values of slot width Reynolds numbers. The new design shows shallower plenum chambers, with staggered holes on each side of the slot.

As a result of these later experiments, the old criterion of Part 4.3.1 is recommended only for slot width Reynolds numbers $R_w < 100$, and the new plenum design criteria of Part 4.3.2 is recommended for $R_w > 100$. Possibly future experiments relating slot plenum design to laminarization performance may modify the foregoing restriction on the plenum design.

4.3.1 Slot Plenum Chamber and Hole Location - $R_w < 100$

The primary consideration in designing the plenum chamber beneath the slot and the location of holes leading from the plenum chamber, when the slot width Reynolds number $R_w < 100$, is to minimize the steady state variation of slot inflow velocity caused by the holes. The plenum chamber, the holes, and the steady state spanwise variation in slot velocity are shown in the accompanying diagram.

ENGINEER	NORTHROP CORPORATION NORAIR DIVISION	PAGE 4.04
CHECKER		REPORT NO. NCR-67-136
DATE June 1967		MODEL X-21A



The steady state spanwise variation in slot velocity is expressed by the parameter $\lambda_h = \left(\frac{u_{s,MAX}}{\bar{u}_s} - 1 \right)$. The most important parameters

affecting the magnitude of the velocity variation γ_h , as determined by experiments, are the chordwise displacement ratio, y/a , of the holes with respect to the slot, and the ratio of hole spacing to plenum depth, (s/h) . Tests show that moving the row of holes from beneath the slot is particularly effective in reducing the value of γ_h and this design feature is recommended. Figure 4.1 shows the parameter λ_h versus the spacing ratio (s/h) , for a chordwise displacement $y = 1.7a$. The chordwise displacement $y = 1.7a$ is considered a suitable or representative value.

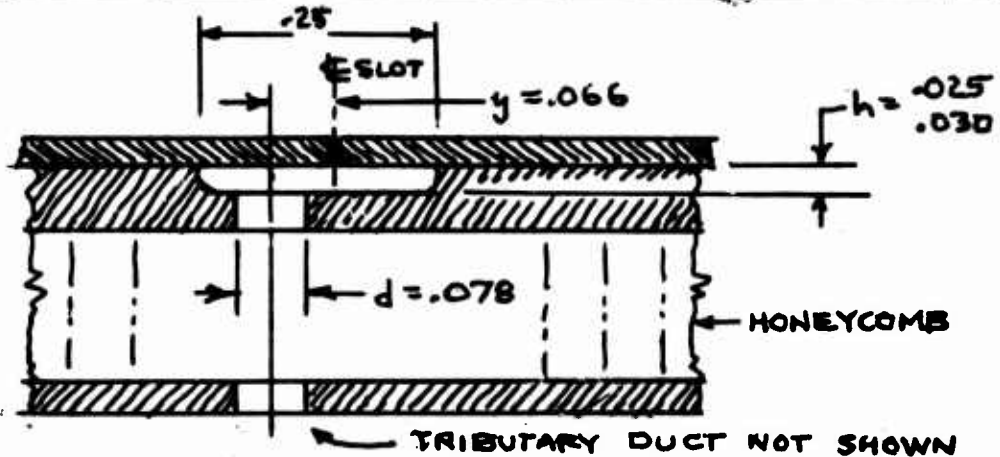
It is recommended that the nominal design criterion for the plenum and holes be $\lambda_h \leq .01$, which corresponds to $(s/h) \leq 15$ for a configuration with the holes offset from the slot by 1.7 times the hole radius. It may be necessary to increase the value of λ_h locally, in the panel splice regions, due to increased hole spacing to allow for fasteners. The width of the plenum must be sufficient to accommodate the offset holes.

A consideration in selecting the hole spacing is the tooling for drilling the holes. If the drilling apparatus travels on a track, and uses a standard bicycle-type chain for registering hole spacing, the hole spacing must be equal to the length of a standard chain link, for example, 1/4 inch or 3/8 inch.

It may be helpful to illustrate the design principles of this section with an example. Assume that the hole spacing is 3/8 inch. Then the plenum depth should be at least $(.375/15) = .025$ inches. Assume that the hole diameter is $5/64 = .078$ inch. The explanation for the assumption of the hole diameter is given in Part 4.4.1. Solve for the chordwise offset $y = \frac{1.7}{2} (.078) = .066$ inches. The plenum and

hole dimensions are shown on the accompanying sketch, five times full size. The plenum width is made .25 inches to provide space for the chordwise offset of the holes, y .

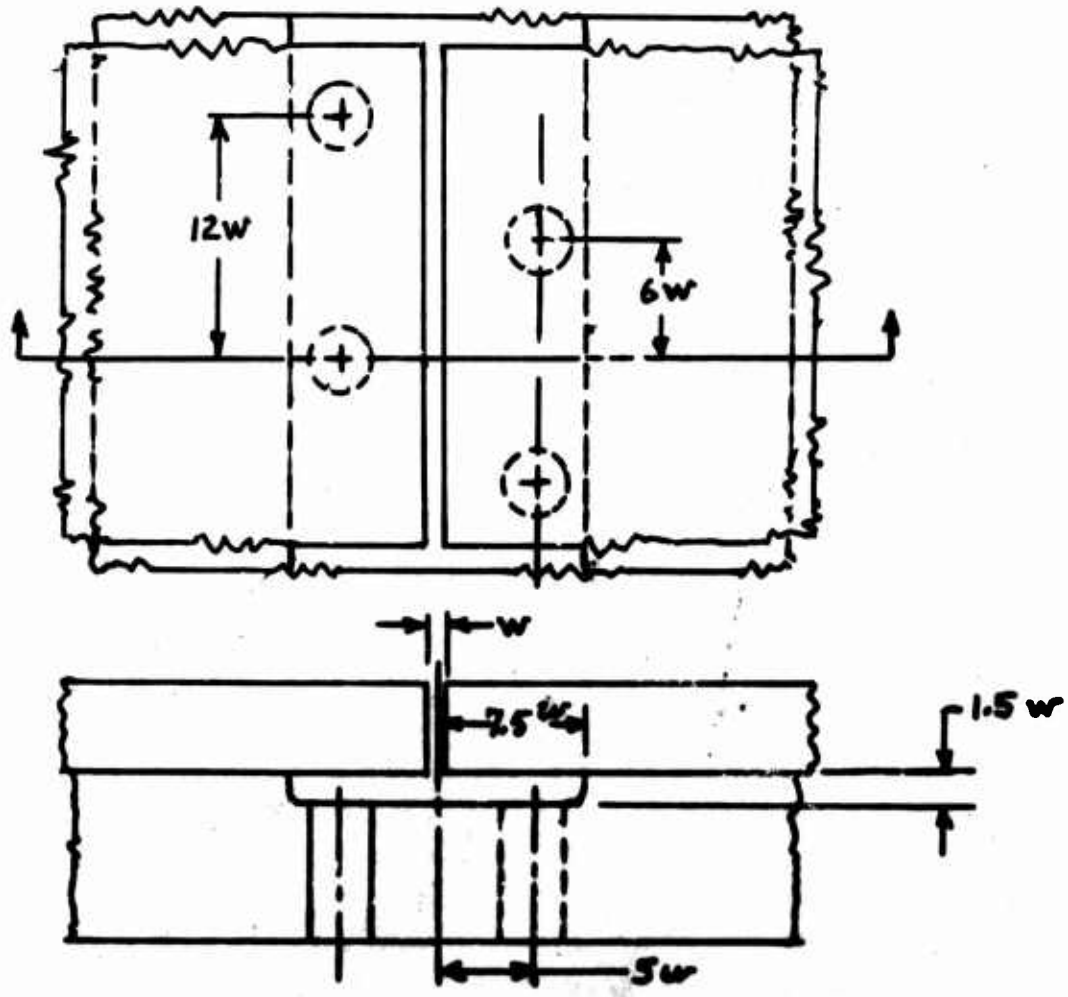
ENGINEER	NORTHROP CORPORATION NORAIR DIVISION	PAGE 4.05
CHECKER		REPORT NO. NOR 67-136
DATE June 1967		MODEL X-21A



At ribs and splices or anywhere that the hole pattern must be interrupted, the plenum depth can be increased locally to accommodate a greater hole spacing.

4.3.2 Recommended Slot Plenum Chamber and Hole Location When $R_w > 100$

In order to suppress slot flow fluctuations at slot width Reynolds numbers $R_w > 100$ a very shallow plenum design with a double row of staggered holes is suggested and shown in the following sketch.



ENGINEER	NORTHROP CORPORATION NORAIR DIVISION	PAGE
CHECKER		4,06
DATE		REPORT NO.
June 1967		NOR 67-136
		MODEL
		X-21A

The suggested plenum design and applicable performance charts of slot flow fluctuations are shown in the following report:

W. Pfenninger; J. Bacon; and J. Goldsmith: About Flow Disturbances Induced by Low Drag Boundary Layer Suction through Slots, Boundary Layer Research Group, Northrop Corporation, Norair Division, Hawthorne, California, September 1966.

(Paper presented at IUGG - IUTAM Symposium on Boundary Layers and Turbulence Including Geophysical Applications, September 19 - 24, 1966, Kyoto, Japan.)

4.4 HOLES THROUGH THE INNER SKIN

4.4.1 General Considerations

An important criterion for the hole design is to minimize the magnitude of flow disturbances that may occur at the hole inlet and propagate through the slot to the external boundary layer. In the design of holes through a honeycomb inner skin it appears impractical to eliminate the possibility of flow disturbances at the hole inlet by either providing a rounded inlet or holding the diameter Reynolds number below the critical value for flow separation within the hole. Consequently, the possibility of a disturbance at the hole inlet is accepted, but the magnitude of the disturbance is minimized by designing for a relatively low velocity through the hole. The velocity through the hole is related to the ratio of hole spacing to hole diameter, $(s/2a)$, as shown in part 4.4.2. It is suggested that ratio $(s/2a)$ be not greater than six, because of considerations of hole velocity, and not less than four, because of structural considerations. A further consideration in the selection of the value of $(s/2a)$ is the beneficial effect of pressure-drop through the holes in minimizing slot velocity variations due to pressure variations along the surface or beneath the holes. From all of these considerations a ratio of $(s/2a) \approx$ five is suggested for a tentative or trial value.

4.4.2 Equations for Hole Design

Equating the flow rate through the slot and one hole:

$$\rho_s \bar{u}_s w s = \rho_h \bar{u}_h \frac{\pi d^2}{4} \quad (1)$$

ENGINEER	NORTHROP CORPORATION NORAIR DIVISION	PAGE 4.07
CHECKER		REPORT NO. NOR-67-136
DATE June 1967		MODEL X-21A

Multiplying both sides of (1) by $\frac{1}{\mu}$:

$$R_d = \frac{4}{\pi} \left(\frac{s}{d}\right) R_w \quad (2)$$

For example, let $(s/d) = (s/2a) = 4.8$, then

$$R_d = 6.1 R_w \quad (3)$$

Equation (2) can be used as a basis for deriving expressions for the velocity, dynamic pressure, and pressure-drop coefficient for the hole:

Extracting the velocity \bar{u}_h from R_d in (2):

$$\bar{u}_h = \left(\frac{\mu}{\rho}\right)_h \frac{4}{\pi} \left(\frac{s}{d}\right) R_w \quad (4)$$

Equation (4) can be rewritten:

$$\frac{\bar{u}_h}{u_\infty} = \left(\frac{\mu}{\rho u}\right)_\infty \frac{\rho_\infty}{\rho_h} \frac{\mu_h}{\mu_\infty} \frac{4}{\pi d} \left(\frac{s}{d}\right) R_w, \text{ and} \quad (5)$$

$$\frac{q_h}{q_\infty} = \frac{\rho_\infty}{\rho_h} \left[\frac{\mu_h}{\mu_\infty} \frac{4}{\pi d} \left(\frac{s}{d}\right) \frac{R_w}{R'_h} \right]^2 \quad (6)$$

The pressure-drop through the hole, in terms of the flight dynamic pressure q_∞ is

$$\Delta C_{ph} = \frac{\Delta p_h}{q_h} \cdot \frac{q_h}{q_\infty} = \frac{\Delta p_h}{q_h} \frac{p_\infty}{p_h} \left[\frac{\mu_h}{\mu_\infty} \frac{4}{\pi d} \left(\frac{s}{d}\right) \frac{R_w}{R'_h} \right]^2 \quad (7)$$

The coefficient $(\Delta q_h/q_h)$ is shown in Figure 3.4 as a function of the parameter τ/R_h . The pressure-drop data of Figure 3.4 have been confirmed by both experiment and theory; see Norair Report NAI-58-19, for example. The pressure-drop coefficient $(\Delta p_h/q_h)$ for both faces of a honeycomb inner skin can be assumed to be 3.0.

Substituting $(\Delta p_h/q_h) = 3.0$ into equation (7) yields

$$\Delta C_{ph} = 3 \frac{\rho_\infty}{\rho_h} \left[\frac{\mu_h}{\mu_\infty} \frac{4}{\pi d} \left(\frac{s}{d}\right) \frac{R_w}{R'_h} \right]^2 \quad (8)$$

for honeycomb skin.

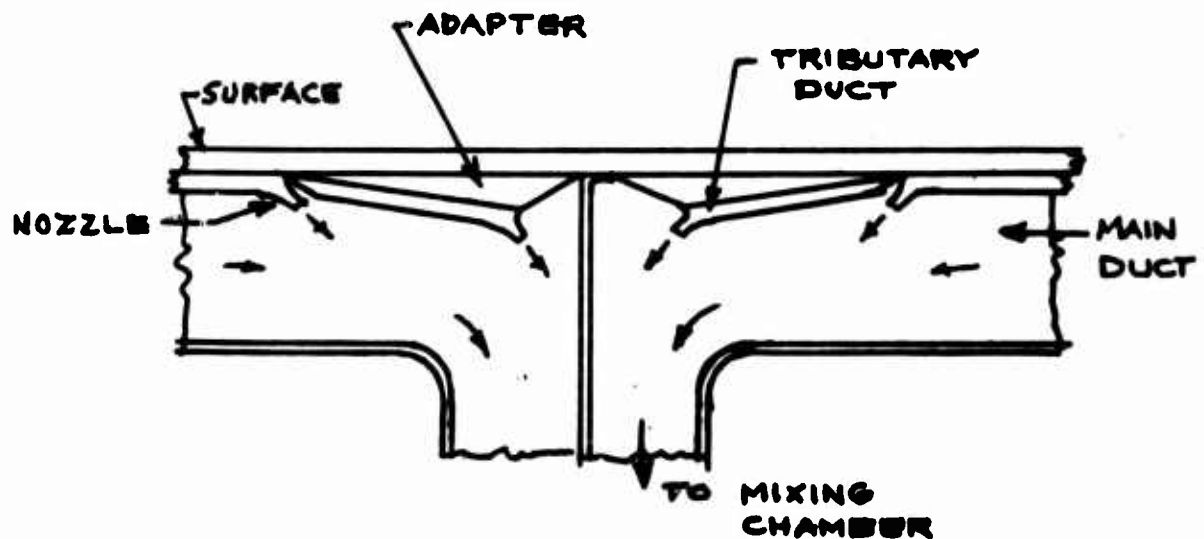
ENGINEER	NORTHROP CORPORATION NORAIR DIVISION	PAGE 4.08
CHECKER		REPORT NO. NOR 67-136
DATE June 1967		MODEL X-21A

Atypical value of ΔC_{p_h} for $Re=100$ at cruise, assuming honeycomb skin, is .02.

4.5 FLOW METERING DEVICES BENEATH THE INNER SKIN

4.5.1 General Description

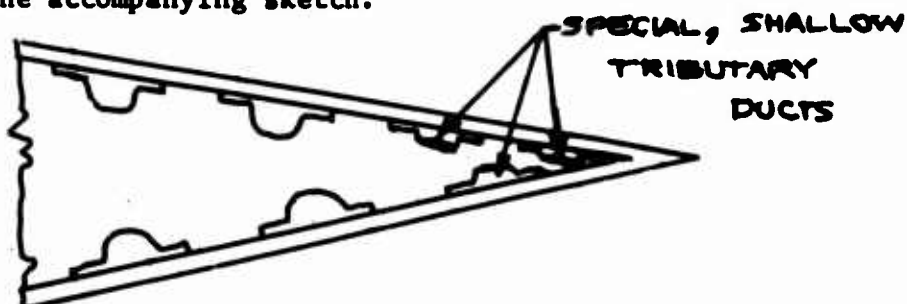
The suction air passes through the holes in the inner skin into a plenum chamber beneath the inner skin and then through a flow metering nozzle into the suction duct (main duct). The plenum chamber beneath the inner skin is analyzed as a small suction duct with inflow normal to the duct flow, and is commonly called a "tributary duct." An example of a tributary duct is shown in Figure 4.2.* The top view in the example shows the nozzles offset from the row of holes, in order to minimize the total height of the tributary duct. The length of the tributary duct can be varied by adding or removing a section in the mid-region of the tributary duct. Adapters can be used at the end of a suction duct to provide clearance between the nozzle and the end wall of the main suction duct, as shown in the accompanying sketch.



* Flow metering devices simpler than the tributary ducts shown (for example, long perforated channel strips) may be feasible for most of the ducts. See report, "Flow Metering Devices for Suction Ducts," by J. H. ...

ENGINEER	NORTHROP CORPORATION NORAIR DIVISION	PAGE 4.09
CHECKER		REPORT NO. NOR 67-136
DATE June 1967		MODEL X-21A

Special, shallow, tributary ducts may be required for the last few slots in the trailing edge region because of the reduced clearance between the upper and lower skins. The upper and lower tributary ducts can be staggered to improve the clearance, as shown in the accompanying sketch.



The size of the tributary duct is a design compromise. A smaller one is lighter in weight per unit length, but requires more nozzles per airplane and smaller dimensional tolerances. The maximum length of tributary duct may be limited by considerations of maximum allowable variations in surface pressure per tributary duct. The maximum depth and width of the tributary duct are limited by space as well as weight considerations. Perhaps the most important design consideration is the variation in slot velocity induced by the pressure-drop in the tributary duct, ~~as~~ reduced by increasing the duct area and/or reducing the duct length. The size shown in Figure 4.2 is not necessarily the optimum size for any LFC aircraft.

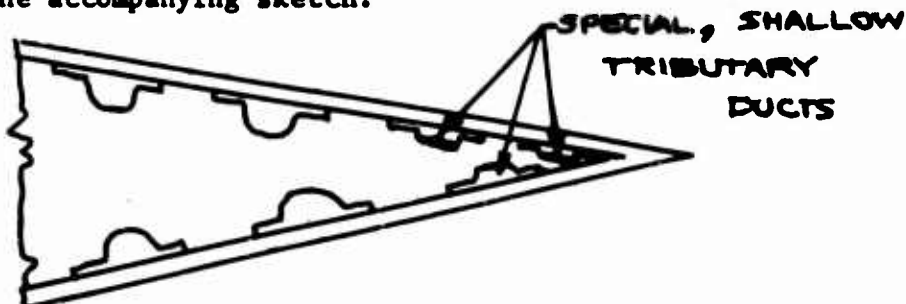
Design equations for tributary ducts are derived in part 4.3.2.

The nozzle has a rounded or trumpet shaped inlet to prevent flow separation. The nozzle directs the air from the tributary duct downstream in the main duct in order to provide smooth duct flow and conserve part of the kinetic energy of the relatively high speed nozzle flow.

In most of the suction ducts the duct velocity and length-diameter ratio are low enough that it is not essential to direct the nozzle flow downstream in the main duct. In such ducts it may be feasible to make a simpler flow metering device than the one shown in Figure 4.2. Sharp edge metering holes are not recommended, however, unless it can be shown that the disturbances at the hole inlet have no effect on the stability of the external boundary layer.

ENGINEER	NORTHROP CORPORATION NORAIR DIVISION	PAGE 4.09
CHECKER		REPORT NO. NOR 67-136
DATE June 1967		MODEL X-21A

Special, shallow, tributary ducts may be required for the last few slots in the trailing edge region because of the reduced clearance between the upper and lower skins. The upper and lower tributary ducts can be staggered to improve the clearance, as shown in the accompanying sketch.



The size of the tributary duct is a design compromise. A smaller one is lighter in weight per unit length, but requires more nozzles per airplane and smaller dimensional tolerances. The maximum length of tributary duct may be limited by considerations of maximum allowable variations in surface pressure per tributary duct. The maximum depth and width of the tributary duct are limited by space as well as weight considerations. Perhaps the most important design consideration is the variation in slot velocity induced by the pressure drop in the tributary duct, ~~as~~ reduced by increasing the duct area and/or reducing the duct length. The size shown in Figure 4.2 is not necessarily the optimum size for any LFC aircraft.

Design equations for tributary ducts are derived in part 4.5.2.

The nozzle has a rounded or trumpet shaped inlet to prevent flow separation. The nozzle directs the air from the tributary duct downstream in the main duct in order to provide smooth duct flow and conserve part of the kinetic energy of the relatively high speed nozzle flow.

In most of the suction ducts the duct velocity and length-diameter ratio are low enough that it is not essential to direct the nozzle flow downstream in the main duct. In such ducts it may be feasible to make a simpler flow metering device than the one shown in Figure 4.2. Sharp edge metering holes are not recommended, however, unless it can be shown that the disturbances at the hole inlet have no effect on the stability of the external boundary layer.

ENGINEER	NORTHROP CORPORATION NORAIR DIVISION	PAGE 4.10
CHECKER		REPORT NO. NOR-67-136
DATE June 1967		MODEL X-21A

Nozzles can be separate inserts or can be part of the tributary duct. Nozzle sizes must be provided in sufficiently small increments to avoid excessive variation in slot inflow distribution from one tributary duct to the next. Increments of no more than 3% diameter are suggested.

Design equations for nozzles are derived in Part 4.5.3.

4.5.2 Equations for Tributary Duct Design

The tributary duct design analysis consists of determining the pressure-drop along the tributary duct and the resulting variation in slot inflow velocity. If the variation in slot inflow velocity appears to be excessive, design changes, from the slots to the end of the tributary duct, may be in order.

Equating the flow rate in the slot and the tributary duct exit section (immediately upstream of the nozzle), assuming a circular duct section:

$$\rho_s \bar{u}_s w_l = \rho_e u_e \frac{\pi}{4} d_e^2 \quad (9)$$

Multiplying both sides of (9) by $\frac{1}{\mu}$:

$$R_{de} = \frac{4}{\pi} \left(\frac{1}{d_e} \right) R_w \quad (10)$$

The relationships among the duct Reynolds number R_{de} , the duct length-to-diameter ratio (l/d_e), and the pressure-drop coefficient ($\Delta p_d/q_e$) for small suction ducts with inflow normal to the duct length can be derived from Norair Report NAI-55-286. These relationships are shown in Figure 4.3.

The pressure-drop coefficient for the tributary duct, based on the free stream dynamic pressure, is

$$\Delta C_{pd} = \left(\frac{\Delta p_d}{q_e} \right) \left(\frac{q_e}{q_w} \right) \quad (11)$$

where $\left(\frac{\Delta p_d}{q_e} \right)$ is determined from Figure 4.3.

ENGINEER	NORTHROP CORPORATION NORAIR DIVISION	PAGE 4.11
CHECKER		REPORT NO. NOR-67-136
DATE June 1967		MODEL X-21A

The steady state spanwise variation in slot velocity due to the pressure-drop in the tributary duct can be determined approximately from the equation

$$\gamma_d \approx .5 (.65) \left(\frac{\Delta C_{p_d}}{\Delta C_{p_s} + \Delta C_{p_h}} \right) \approx .32 \left(\frac{\Delta C_{p_d}}{\Delta C_{p_s} + \Delta C_{p_h}} \right) \quad (12)$$

The value of γ_d normally is somewhat greater than the corresponding value of γ_h . No criterion has been determined for the maximum allowable value of γ_d , but a suggested or tentative criterion is $\gamma_d \leq .03$.

4.5.2 Equations for Nozzle Design

4.5.2.1 Assumptions and Introductory Discussion

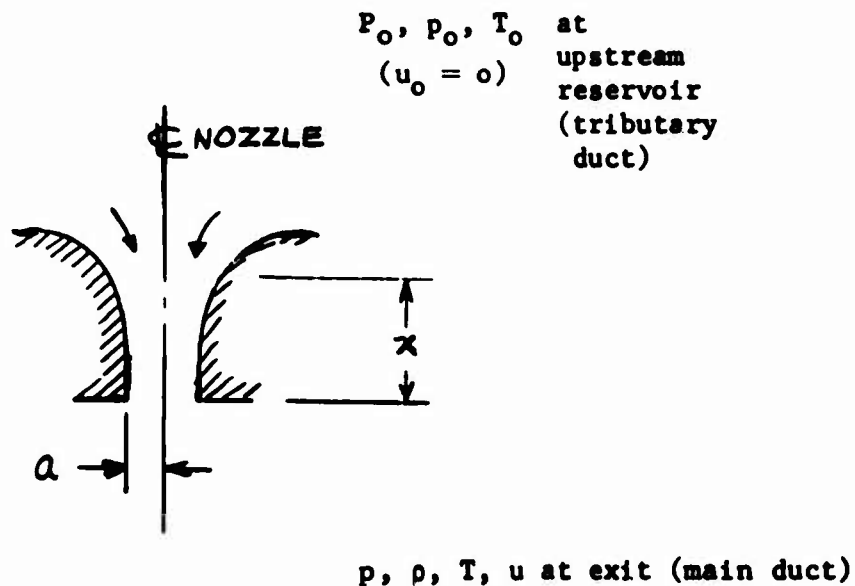
The data presented for calculating the pressure-drop through the slots or through the holes in the inner skin are based on the assumption of incompressible flow. See Figure 3.4, for example. The assumption is valid, within slide rule accuracy, because the pressure-drop through the slot or holes is small compared with the total pressure. The pressure-drop through the nozzle generally is greater than that through the slot or holes and the total pressure is less; thus the pressure ratio r for the nozzle often is small enough to warrant or require the use of compressible flow equations in the design of the nozzle.

The determination of the nozzle size required actually is a part of the main duct analysis, Section 5; but the equations for nozzle design are included in Section 4 because the nozzle is part of the flow passage system between the slots and the main duct. In this respect, the analyses of Sections 4 and 5 are interdependent and overlapping. The state of the air in the tributary duct is determined from the preceding analyses, and the pressure in the main duct is determined from the duct momentum equation, Section 5. The relationship between the pressure ratio r of the main duct to tributary duct, and the nozzle velocity, flow rate, and diameter are developed in the following equations, assuming compressible flow.

ENGINEER	NORTHROP CORPORATION NORAIR DIVISION	PAGE 4.12
CHECKER		REPORT NO. NOR-67-136
DATE June 1967		MODEL X-21A

The basic equations for compressible flow, and the derivation of the mass flow rate of a compressible flow nozzle, are well known and are included in this section as a matter of convenience.

4.5.2.2 Basic Equations - Compressible Flow Nozzle



Equation of state

$$\frac{P_o}{\rho_o T_o} = \frac{p}{\rho T} = g R \quad (13)$$

Isentropic relations

$$\frac{T_o}{T} = 1 + \left(\frac{k-1}{2}\right) M^2 \quad (14)$$

$$\frac{p_o}{p} = \left(\frac{T_o}{T}\right)^{\frac{k}{k-1}} = \left[1 + \left(\frac{k-1}{2}\right) M^2\right]^{\frac{k}{k-1}} \quad (15)$$

$$\frac{\rho_o}{\rho} = \left(\frac{T_o}{T}\right)^{\frac{1}{k-1}} = \left(\frac{p_o}{p}\right)^{\frac{1}{k}} \quad (16)$$

$$u^2 = T_o \cdot 2 g J c_p \left(1 - \frac{T}{T_o}\right) \quad (17)$$

$$J c_p = R \left(\frac{k}{k-1}\right) \quad (18)$$

ENGINEER	NORTHROP CORPORATION NORAIR DIVISION	PAGE 4.13
CHECKER		REPORT NO. NOR 67-136
DATE June 1967		MODEL X-21A

Velocity of sound

$$c = (gk R T)^{.5} \quad (19)$$

Mass flow rate

$$\dot{m} = \rho u A \quad (20)$$

where A is an effective area of the nozzle, less than the gross area A_g . The relation between the effective area A and the gross area A_g is shown in part 4.5.2.4.

The mass flow rate also can be expressed in terms of the slot Reynolds number as

$$\dot{m} = \rho_s \bar{u}_s w l = \mu l R_w \quad (21)$$

Eliminating \dot{m} between (20) and (21)

$$A = \frac{\mu_n l R_w}{(\rho u)_n} \quad (22)$$

where the subscript n has been added to signify "nozzle." An expression for the mass flow parameter $(\rho u)_n$ is derived in the following part 4.5.2.3.

The following units and constants are used in the preceding equations:

$$p = \text{psf} = \text{lb/ft}^2$$

$$\rho = \text{slugs/ft}^3 = \text{lb sec}^2/\text{ft}^4$$

$$T = \text{degrees Rankine, } ^\circ R$$

$$c, u = \text{ft/sec}$$

$$\dot{m} = \text{slug/sec}$$

$$g = 32.2 \text{ ft/sec}^2$$

$$R = 53.3$$

$$k = 1.40$$

$$J = 778 \text{ ft lb/btu}$$

$$c_p = .24 \text{ btu/lb } ^\circ \text{Rankine}$$

ENGINEER	NORTHROP CORPORATION NORAIR DIVISION	PAGE 4.14
CHECKER		REPORT NO. NOR-67-136
DATE June 1967		MODEL X-21A

4.5.2.3 Derivation of Flow Rate Function ρu - Compressible Flow Nozzle

The velocity and flow rate of a compressible flow nozzle, in terms of the pressure ratio r , are derived as follows:

$$\text{Let } r = p/p_o \quad (23)$$

From (13), (16), and (23),

$$\rho = \rho_o r^{\frac{1}{k}} = \frac{p_o}{gRT_o} r^{\frac{1}{k}} \quad (24)$$

Substituting (16) and (23) into (17)

$$u^2 = T_o 2 g J c_p \left(1 - r^{\frac{k-1}{k}}\right), \text{ or}$$

$$u = \left[T_o 2 g J c_p \left(1 - r^{\frac{k-1}{k}}\right)\right]^{.5} \quad (25)$$

Multiplying (24) and (25),

$$\rho u = (\rho u)_n = \frac{p_o}{T_o} \frac{1}{.5 R} \left(\frac{2 J c_p}{g}\right)^{.5} r^{\frac{1}{k}} (1 - r^{\frac{k-1}{k}})^{.5} \quad (26)$$

4.5.2.4 Nozzle Area Correction

The relation between the effective area and gross area of the nozzle is

$$A_g = \left(\frac{\Delta p}{q_n}\right)^{.5}, \quad A = \left(\frac{\Delta p}{c_n}\right)^{.5} \frac{\mu_n^1 R_w}{(\rho u)_n} \quad (27)$$

where the pressure-drop coefficient $\frac{\Delta p}{q_n}$ is determined

from Figure 3.4 as a function of $\beta = \frac{\pi \mu x}{A}$, for a

tube with rounded inlet. Examination of Equation (21) shows that β can also be expressed as

$$\beta = \frac{\pi x}{l R_w}, \quad (28)$$

where the length x is approximately equal to the length of the straight section (if any), plus one-half of the length of the bell-mouth inlet.

ENGINEER	NORTHROP CORPORATION NORAIR DIVISION	PAGE 4.15
CHECKER		REPORT NO. NOR-67-136
DATE June 1967		MODEL X-21A

4.5.2.5 Calculation of Maximum Nozzle Size

The maximum size of nozzle anticipated can be calculated from Equation (27) by selecting a minimum value for ΔC_{p_n} (corresponding to a minimum nozzle velocity) and using the incompressible flow relation

$$u_n = u_\infty \left(\frac{\rho_\infty}{\rho_n} \right)^{.5} \Delta C_{p_n}^{.5} \quad (29)$$

Substituting (29) into (27),

$$A_g = \left(\frac{\Delta p}{q_n} \right)^{.5} \frac{\mu_n}{\mu_\infty} \left(\frac{\rho_\infty}{\rho_n} \right)^{.5} \frac{1}{R'_\infty \Delta C_{p_n}^{.5}} \quad (30)$$

A sample calculation applicable to the example used in the preceding parts, and assuming $\Delta C_{p_n}^{.5} = .25$, shows that the maximum nozzle diameter is about .20 inch. Examination of Figure 4.2 shows that a .20 diameter nozzle need not extend below the lower surface of the tributary duct.

4.6 ADDITIONAL REFERENCES

Some of the analyses of this section and the following section about suction ducts are based on investigations made in the Norair Boundary Layer Research Laboratory prior to the inception of the X-21A program. Applicable preliminary investigations include the following:

- BLC 29 Pfenninger, W.: Some General Considerations of Losses in Boundary Layer Ducting Systems, February 1954.
- BLC 30 Rogers, K. H.: A Method of Calculating the Pressure Distribution in Suction Ducts, February 1954.
- BLC 70 Pfenninger, W.; and Rogers, K. H.: Further Investigations of an Improved Suction Duct, May 1955.

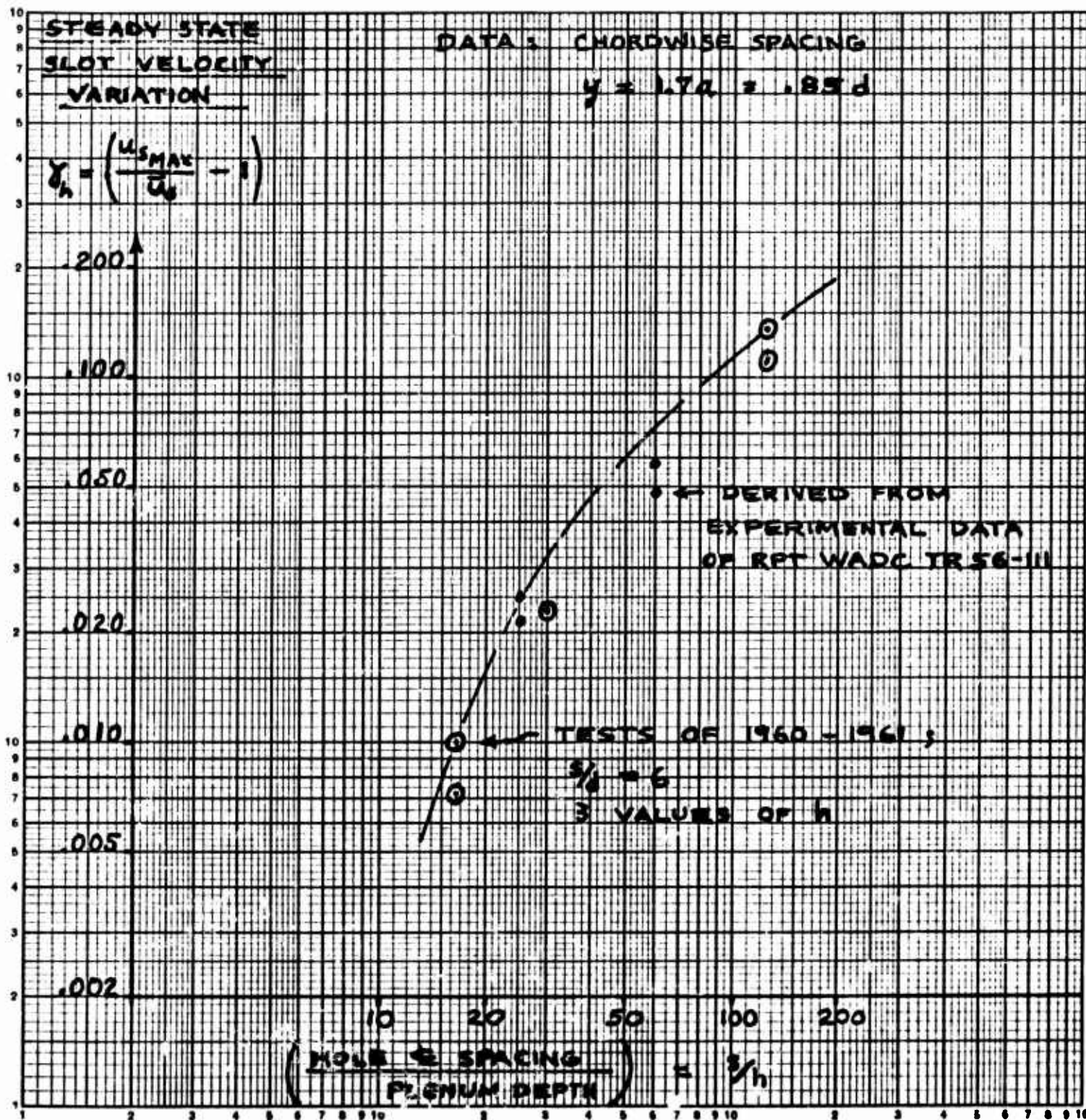


FIG. 4.1 SLOT VELOCITY VARIATION γ_h VS
HOLE SPACING / PLENUM DEPTH s/h



HOLES
INNER

→ FLOW IN SUCTION DUCT
(MAIN DUCT)

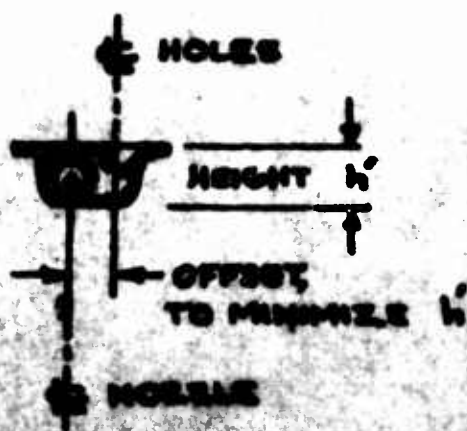
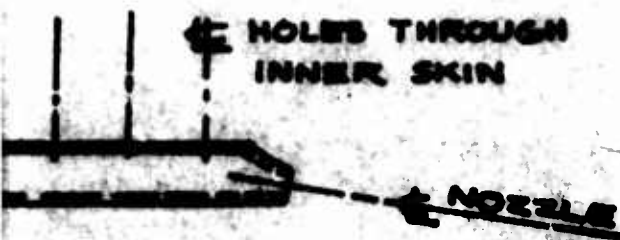
K R
APR 64

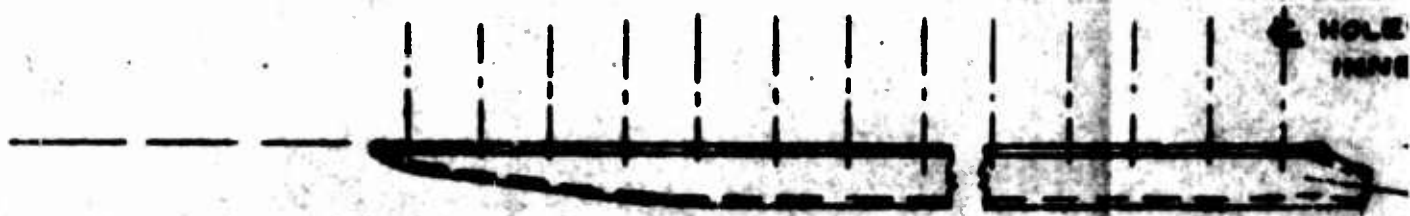
5-17
PAGE 126
X-21A

FIG. 4.2 TRIBUTARY DUCT

FULL SIZE

NOTE: OFFSET NOZZLE DESIGN SHOWN WAS NOT USED ON X-21A AIRPLANE. A SMALLER, SYMMETRICAL, NOZZLE WAS USED.





→ FLOW IN SUCTION DUCT
(MAIN DUCT)

APR 64

A.37

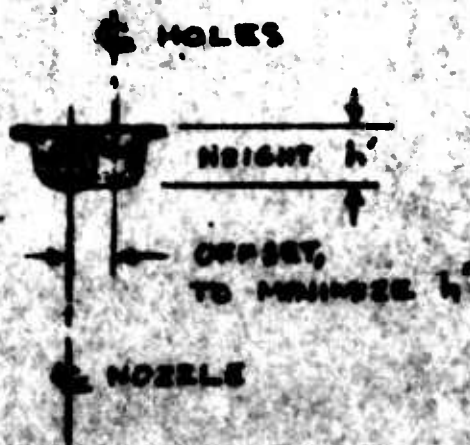
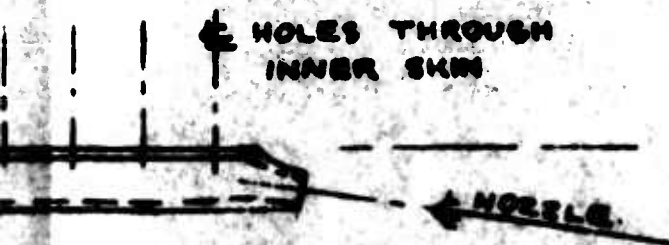
SECRET-196

X-21A

FIG. 4.2 TRIBUTARY DUCT

FULL SIZE

NOTE: OFFSET NOZZLE DESIGN
SHOWN WAS NOT USED
ON X21A AIRPLANE



ENGINEER <i>[Signature]</i>	NORTHROP CORPORATION NORAIR DIVISION	PAGE 4.18
CHECKER		REPORT NO. NOR 67-136
DATE Apr 67		MODEL X-21A

PRESSURE-DROP
COEFFICIENT

DATA DERIVED FROM
REPORT NAI-55-286.

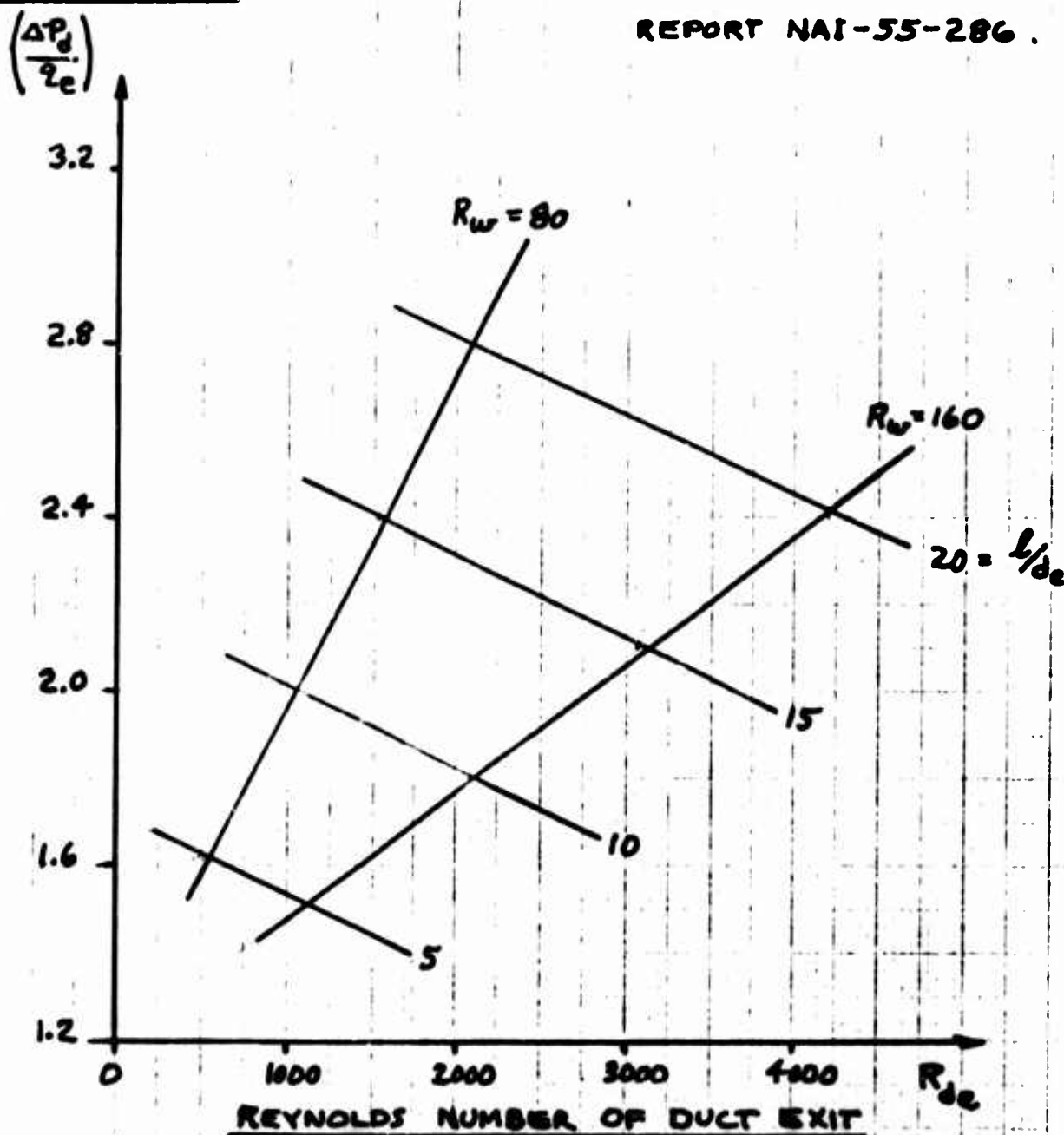


FIG 4.3 PRESSURE-DROP ALONG TRIBUTARY DUCTS

ENGINEER	NORTHROP CORPORATION NORAIR DIVISION	PAGE 5.00
CHECKER		REPORT NO. NOR 67-136
DATE June 1967		MODEL X-21A

SECTION 5

MAIN DUCT AND MIXING CHAMBER

DESIGN ANALYSIS

BY:

K. H. Rogers

April 1967

ENGINEER	NORTHROP CORPORATION NORAIR DIVISION	PAGE	5.01
CHECKER		REPORT NO.	NOR 67-136
DATE		MODEL	X-21A
June 1967			

5.1 INTRODUCTION

The flow from the tributary ducts is directed through nozzles downstream into the main suction duct. The flow from the main suction ducts, in turn, is directed through nozzles downstream into the mixing chamber. If the latter nozzles are adjustable, they are called valves, or flow control valves. The air flows from the mixing chambers to the compressors.

The nozzle or jet inflow is directed downstream into the main duct or mixing chamber to provide smooth duct flow and to conserve part of the kinetic energy of the relatively high velocity jets. The conservation of part of the kinetic energy of the jets appears as static pressure recovery in the duct. The pressure recovery is very efficient if the jet inlet velocity is only slightly greater than the main duct stream velocity, and is inefficient if the duct velocity is small compared with the jet velocity. The pressure recovery from the inlet jets can be used effectively in providing nearly constant static pressure along long suction ducts. The pressure recovery of the inlet jets permits the use of much longer suction ducts, and more efficient suction ducts, than would be possible with inflow normal to the duct length.

The determination of the pressure distribution along the suction duct or the mixing chamber, and the determination of the nozzle sizes required, are made in one analysis by the use of the duct momentum equation, derived in this section. The duct momentum equation includes the effects of the rate of change of momentum of the inlet jets, the rate of change of momentum of the main duct stream, and the wall friction force. The value of the coefficients for pressure recovery of the inlet jets and for wall friction are determined from experiments.

Suction air from the farthest aft regions of the wing, including the aileron, is ducted forward and injected downstream into the deeper ducts through relatively large transfer nozzles. Inflow from the transfer nozzles is treated analytically in the same way as inflow from the tributary nozzles in the suction duct analysis.

The duct momentum equation also can be used for the analysis of suction ducts with inflow normal to the duct length if suitable experiments are made to evaluate the empirical coefficients of wall friction and pressure recovery (or loss) from the inlet jets.

ENGINEER	NORTHROP CORPORATION NORAIR DIVISION	PAGE 5.02
CHECKER		REPORT NO. NOR 67-136
DATE June 1967		MODEL X-21A

5.2 NOMENCLATURE

Lower Case Letters

a	radius of nozzle, ft
Δc_p	pressure-drop coefficient, $\Delta p/q$.
d	hydraulic diameter of main duct, ft
	$d = \frac{4 A}{\text{perimeter}}$
d_n	diameter of nozzle, ft
f	pressure recovery coefficient, applied to rate of change of momentum of nozzle jet
g	acceleration of gravity, 32.2 ft/sec ²
j,k	adjacent stations along duct, marking the beginning and end of the duct length increment Δl .
k	wall friction coefficient. See F, or Eq. (26)
l	length of main duct, ft
Δl	incremental length of main duct, ft
l_j	length of tributary duct, ft
\dot{m}_i	mass flow rate of jet inlet, slug/sec
\dot{m}_j, \dot{m}_k	mass flow rate in main duct, at stations j and k, slug/sec
n	ratio of specific heats, 1.40
p	pressure, lb/ft ²
Δp	pressure-rise from main duct station j to k. ($\Delta p = p_k - p_j$), lb/ft ²
q	dynamic pressure $\frac{\rho}{2} u^2$, lb/ft ²

ENGINEER	NORTHROP CORPORATION NORAIR DIVISION	PAGE 5.03
CHECKER		REPORT NO. NOR 67-136
DATE June 1967		MODEL X-21A

r pressure ratio for nozzle

u velocity, ft/sec

u_1 approximate velocity of inlet jet, ft/sec

w slot width, ft

x effective length of nozzle, ft

Capital Letters

A area of main duct crosssection, ft²

B, C terms in compressible flow equation

$$u_1 \approx B - C \Delta p$$

Ref. Eqs. (12), (13)

B', C' terms in incompressible flow equation

$$u_1 \approx B' - C' \Delta p$$

Ref. Eqs. (17), (18)

C_p specific heat at constant pressure, .24 Btu/lb °Rankine

F friction force over incremental duct length Δl .
Ref. Eq. (26)

J mechanical equivalent of heat, 778 ft lb/Btu

M flight Mach number

R_a radius Reynolds number for nozzle, $\frac{\rho_a u_a}{\mu}$

R_d Reynolds number of main duct, $\frac{\rho_o u d}{\mu}$

R_w slot width Reynolds number, $(\frac{\rho u}{\mu})_s w$

R' unit Reynolds number of free stream, $(\frac{\rho u}{\mu})_\infty$

R gas constant 53.3 ft lb/lb °R

ENGINEER	NORTHROP CORPORATION NORAIR DIVISION	PAGE 5.04
CHECKER		REPORT NO. NOR 67-136
DATE June 1967		MODEL X-21A

T temperature, °Rankine

U velocity ratio u/u_∞

Greek Letters

β nozzle parameter τ/R_a

μ absolute viscosity, lb sec/ft²

ρ density, slug/ft³ = lb sec²/ft⁴

τ nozzle geometry x/a

Subscripts

o upstream end of main duct

d duct

i inlet jet

j, k adjacent duct stations

n nozzle

t reservoir condition upstream of nozzle

Superscripts

A bar above the letter means that it is the average value, for the incremental length Δl . For example:

$$\bar{A} = \frac{A_j + A_k}{2},$$

$$\bar{d} = \frac{d_j + d_k}{2}, \text{ etc.}$$

ENGINEER	NORTHROP CORPORATION NORAIR DIVISION	PAGE 5.05
CHECKER		REPORT NO. NOR 67-136
DATE June 1967		MODEL X-21A

5.3 SUCTION DUCT ANALYSIS

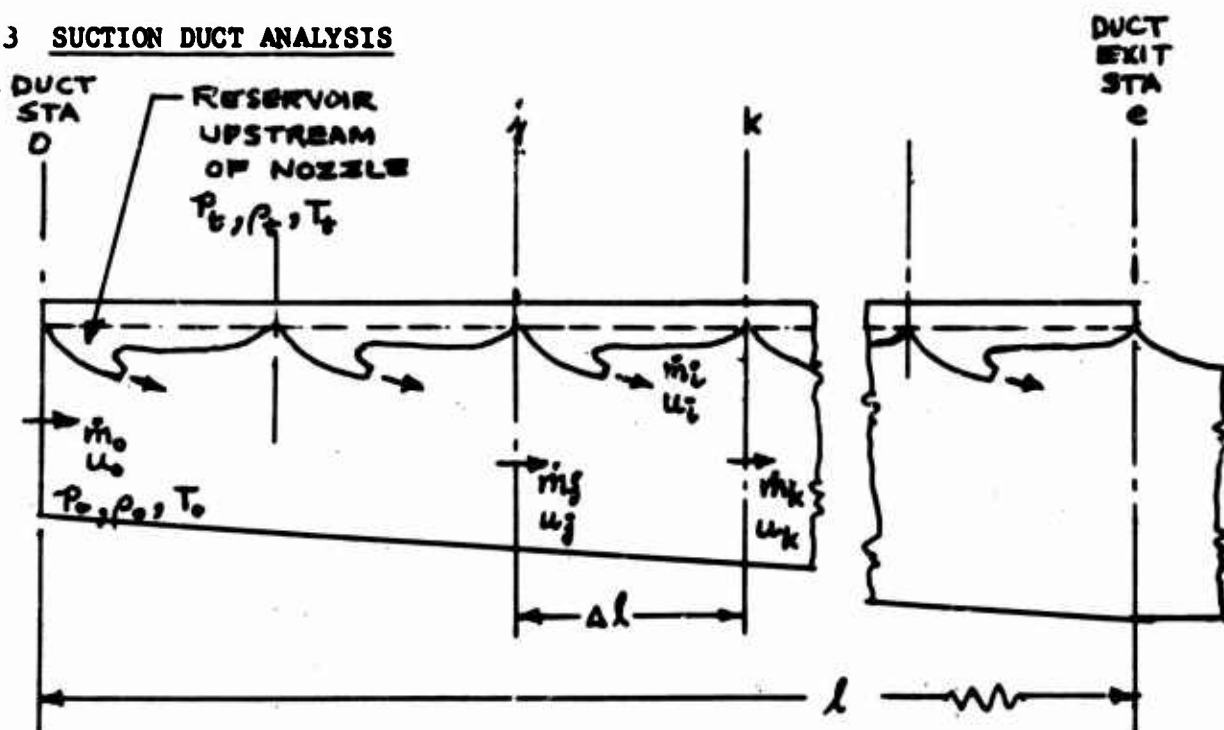


Fig. 5.1 SUCTION DUCT ANALYTICAL MODEL

5.3.1 Description of Analytical Model

The suction duct to be analyzed is shown in the accompanying sketch, Fig. 5.1. The analytical model applies to either a suction duct or a mixing chamber. Each incremental length Δl of the duct has one or more inlet jets of mass flow rate \dot{m}_i directed substantially downstream into the main duct. Jets in the same incremental length Δl , with the same reservoir pressure (same p_0 immediately upstream of the nozzle), can be lumped together in the analysis. The incremental length Δl should be greater than and preferably several times the hydraulic diameter of the main duct in order to allow sufficient length for mixing.

The analysis makes the simplifying assumption that the velocity and pressure are constant across the duct section at the end of each incremental length Δl . The density is assumed constant along the duct length.

ENGINEER	NORTHROP CORPORATION NORAIR DIVISION	PAGE 5.06
CHECKER		REPORT NO. NOR-67-136
DATE June 1967		MODEL X-21A

5.3.2 Derivation of Equations

Mass Flow Rate

The mass flow rate at any duct station j is

$$\dot{m}_j = \dot{m}_0 + \sum_0^j \dot{m}_i \quad (1)$$

The mass flow rate for a single tributary nozzle, from Section 4, is

$$\dot{m}_i = \mu l_i R w_i \quad (2)$$

Duct Velocity

The duct velocity at any duct station j is

$$u_j = \frac{\dot{m}_j}{\rho_0 A_j} \quad (3)$$

where ρ_0 is the duct density, calculated for duct station 0 but applicable everywhere along the duct. That is,

$$\rho_0 = \frac{p_0}{g R T_t} \quad (4)$$

Similarly, the duct velocity at station k is

$$u_k = \frac{\dot{m}_k}{\rho_0 A_k} \quad (5)$$

Nozzle Velocity

The equation for nozzle velocity is taken from Section 4. The nozzle velocity for compressible flow is

$$u_i = \left\{ 2g R T_t \left(\frac{n}{n-1} \right) \left[1 - \left(\frac{p_i + .5 \Delta p}{p_t} \right)^{\frac{n-1}{n}} \right] \right\}^{.5} \quad (6)$$

$$\text{where } \Delta p = p_k - p_j \quad (7)$$

and $n = 1.40$.

ENGINEER	NORTHROP CORPORATION NORAIR DIVISION	PAGE 5.07
CHECKER		REPORT NO. NOR-67-136
DATE June 1967		MODEL X-21A

The term Δp is the variable or unknown to be found in the solution of the duct momentum equation. It is convenient

to expand the term $\left(\frac{p_j + .5\Delta p}{p_t}\right)^{\frac{n-1}{n}}$ as follows, retaining only the first two terms. Δp is always quite small compared with p_j , and the second order term Δp^2 is relatively insignificant.

$$\left(\frac{p_j + .5\Delta p}{p_t}\right)^{\frac{n-1}{n}} \approx \left(\frac{p_j}{p_t}\right)^{\frac{n-1}{n}} + \frac{.5}{p_t} \left(\frac{n-1}{n}\right) \left(\frac{p_j}{p_t}\right)^{\frac{1}{n}} \Delta p \quad (9)$$

Substituting (9) into (6):

$$u_1 = \left\{ 2g RT_t \left(\frac{n}{n-1}\right) \left[1 - \left(\frac{p_j}{p_t}\right)^{\frac{n-1}{n}} \right] - \frac{gRT_t}{p_t} \left(\frac{p_j}{p_t}\right)^{\frac{1}{n}} \Delta p \right\}^{.5} \quad (10)$$

Expanding (10) and retaining only the first two terms:

$$u_1 \approx B - C \Delta p \quad (11)$$

where

$$B = \left\{ 2gRT_t \left(\frac{n}{n-1}\right) \left[1 - \left(\frac{p_j}{p_t}\right)^{\frac{n-1}{n}} \right] \right\}^{.5}, \text{ and} \quad (12)$$

$$C = \frac{.3535 (gRT_t)^{.5}}{p_t \left\{ \left(\frac{n}{n-1}\right) \left[1 - \left(\frac{p_j}{p_t}\right)^{\frac{n-1}{n}} \right] \right\}^{.5} \left(\frac{p_j}{p_t}\right)^{\frac{1}{n}}} \quad (13)$$

the nozzle velocity for incompressible flow is

$$u_1 = \left[\frac{2 (p_t - p_j - .5\Delta p)}{\rho_o} \right]^{.5} \quad (14)$$

Expanding (14) and retaining only the first two terms:

$$u_1 \approx \left[\frac{2 (p_t - p_j)}{\rho_o} \right]^{.5} - \frac{.5}{\rho_o} \left[\frac{2 (p_t - p_j)}{\rho_o} \right]^{-.5} \Delta p \quad (15)$$

or, putting (15) in the same form as (11),

$$u_1 \approx B' - C' \Delta p \quad (16)$$

where

$$B' = \left[\frac{2 (p_t - p_j)}{\rho_o} \right]^{.5} \quad (17)$$

$$C' = \left[\frac{.3535}{\rho_o (p_t - p_j)} \right]^{.5} \quad (18)$$

ENGINEER	NORTHROP CORPORATION NORAIR DIVISION	PAGE 5.08
CHECKER		REPORT NO. NOR 67-136
DATE June 1967		MODEL X-21A

Momentum Equation

The duct momentum equation for an incremental length Δl is derived by equating the rate of change of momentum to the pressure and friction forces. With reference to the increment jk shown in Fig. 5.1, the momentum equation is

$$\Sigma f \dot{m}_i (u_i - u_k) + \dot{m}_j (u_j - u_k) = \bar{A} \Delta p + F \quad (19)$$

where

$$F = \frac{k \Delta l \bar{A} \rho_0 \bar{u}^2}{2 d R_d} \quad (20)$$

f = pressure recovery factor, shown in Figure 5.2

k = friction coefficient ($k = .316$ for smooth pipes, according to the Blasius formula)

and

$$\bar{A} = \frac{A_j + A_k}{2} \quad (21)$$

The three terms F , f and k are discussed in more detail in this section.

Substituting (11) into (19), for compressible flow nozzles,

$$\Sigma f \dot{m}_i (B - u_k - C \Delta p) + \dot{m}_j (u_j - u_k) = \bar{A} \Delta p + F \quad (22)$$

Equation (22) can be written

$$\Delta p = \frac{\Sigma f \dot{m}_i (B - u_k) + \dot{m}_j (u_j - u_k) - F}{\bar{A} + \Sigma f \dot{m}_i C} \quad (23)$$

Equation (23) applies to compressible flow nozzles, with B and C defined in equations (12) and (13). For incompressible flow nozzles, substitute B' and C' for B and C . B' and C' are defined in Equations (17) and (18).

Evaluation of Pressure Recovery Coefficient f (Ref. Fig. 5.2)

In the evaluation of the pressure recovery coefficient f , a negligible error is involved if the velocity ratio for entering Figure 5.2 is calculated based on the duct pressure p_j instead of $p_j + .5\Delta p$. The velocity ratio for entering Figure 5.2 then for compressible flow, from Equation (6):

ENGINEER	NORTHROP CORPORATION NORAIR DIVISION	PAGE 5.09
CHECKER		REPORT NO. NOA-67-136
DATE June 1967		MODEL X-21A

$$\frac{u_1'}{u_k} = \frac{\left\{ \frac{2gRT}{2} \left(\frac{n}{n-1} \right) \left[1 - \left(\frac{p_1}{p_t} \right)^{\frac{n-1}{n}} \right] \right\}^{.5}}{u_k} \quad (24)$$

For incompressible flow, the velocity ratio for entering Figure 5.2 is, from Equation (14):

$$\frac{u_1'}{u_k} = \left[\frac{2 (p_t - p_1) \rho_0}{\rho_0 u_k^2} \right]^{.5} \quad (25)$$

The data shown in Figure 5.2 are based on a limited number of experiments, and are considered tentative, pending a more comprehensive evaluation.

Evaluation of Friction Term F

Substituting $\rho_0 \bar{u} d / \mu_0$ for R_d in Equation (20), and collecting

$$F = \frac{k \Delta l \bar{A} \rho_0^{.75} \mu_0^{.25} \bar{u}^{1.75}}{2 \bar{d}^{-1.25}} \quad (26)$$

The bar above the letter means average value for the increment Δl . For example, $\bar{u} = (u_1 + u_k)/2$, etc. The friction factor k is empirical, evaluated from suction duct experiments. The value varies, depending primarily upon the roughness of the duct walls. A representative value, including the effect of rivet heads and fasteners, is

$$k \approx .50 \quad (27)$$

5.3.3 Method of Calculating Pressure Distribution Along the Suction Duct

A starting pressure p_0 at the upstream end of the main duct, station 0, must be assumed. The duct density ρ_0 is then calculated from Equation (4).

Beginning with the first upstream increment of duct length, the pressure change Δp_1 is calculated from Equation (23), assuming either compressible or incompressible nozzle flow, whichever is applicable. The increment Δp_1 then is added to the starting pressure p_0 to provide the upstream duct pressure p_1 for the second increment. Thus, the pressure distribution along the main duct is determined one step at a time, beginning with the upstream end.

ENGINEER	NORTHROP CORPORATION NORAIR DIVISION	PAGE 5.10
CHECKER		REPORT NO. NOR 67-136
DATE June 1967		MODEL X-21A

For convenience, the duct momentum equation is repeated, followed by a reference table for evaluation of the terms of the equation:

$$\Delta p = p_k - p_j = \frac{\sum f \dot{m}_i (B - u_k) + \dot{m}_j (u_j - u_k) - F}{\bar{A} + \sum \dot{m}_i \theta} \quad (23 \text{ repeated})$$

Term	Reference	
	Compressible Flow Nozzle	Incompressible Flow Nozzle
f	Eq. (24) and Fig. 5.2	Eq. (25) and Fig. 5.2
\dot{m}_i	Eq. (2)	Eq. (2)
B or B'	Eq. (12)	Eq. (17)
C or C'	Eq. (13)	Eq. (18)
\dot{m}_j	Eq. (1)	Eq. (1)
u_j	Eq. (3)	Eq. (3)
u_k	Eq. (5)	Eq. (5)
F	Eq. (26)	Eq. (26)
\bar{A}	Eq. (21)	Eq. (21)

5.4 DETERMINATION OF NOZZLE SIZES

After the pressure distribution along the suction duct has been determined from the duct momentum equation, as shown in part 5.3, the nozzle sizes can be computed. The derivation of the equations for nozzle size determination is presented in Section 4. For compressible flow nozzles the nozzle size is expressed as a function of the nozzle pressure ratio r . For incompressible flow nozzles, the nozzle size is expressed as a function of the nozzle pressure-drop coefficient Δc_p .

ENGINEER	NORTHROP CORPORATION NORAIR DIVISION	PAGE 5.11
CHECKER		REPORT NO. NOR-67-136
DATE June 1967		MODEL X-21A

The equations for nozzle size determination are repeated here, with the notation applicable to this section.

Compressible Flow Nozzle

$$A_g = \left(\frac{\Delta p}{q_n}\right)^{.5} \frac{\dot{m}_n}{(\rho u)_n} = \left(\frac{\Delta p}{q_n}\right)^{.5} \frac{\mu \frac{1}{R_w}}{(\rho u)_n} \quad (28)$$

Where $\left(\frac{\Delta p}{q_n}\right)$ is determined from Figure 4.7.2 as a function of

$$\beta = \frac{\pi x}{l \frac{1}{R_w}}, \text{ and}$$

$$(\rho u)_n = \frac{p_t}{T_t^{.5}} \frac{1}{R} \left(\frac{2 J_1 C_p}{g}\right)^{.5} r^{\frac{1}{n}} \left(1 - r^{\frac{n-1}{n}}\right)^{.5}, \quad (29)$$

$$\text{where } r = \left(\frac{p_1 + p_k}{2 p_t}\right) \quad (30)$$

The nozzle diameter is

$$d_n = \left(\frac{\pi A_g^{.5}}{4}\right) \quad (31)$$

Incompressible Flow Nozzle

$$A_g = \left(\frac{\Delta p}{q_n}\right)^{.5} \frac{\mu_n}{\mu} \left(\frac{\rho}{\rho_n}\right)^{.5} \frac{1}{R'_{\infty} \Delta C_{p_n}} \quad (32)$$

$$\text{where } \Delta C_{p_n} = \Delta p_n / q_{\infty}, \text{ and} \quad (33)$$

$\left(\frac{\Delta p}{q_n}\right)$ is determined from Figure 3.4. The nozzle diameter is determined from Equation (31).

5.5 SOLUTIONS BY AUTOMATIC COMPUTER

The solution of the duct momentum equation and the determination of required nozzle sizes for a given suction surface, suction distribution, and flight condition can be done with an automatic computer program, utilizing the equations of Sections 3, 4, and 5 and the boundary layer computer program described in Section 2. The program also can accommodate the transfer of flow from another suction duct and thereby can determine transfer nozzle sizes as well as tributary nozzle sizes.

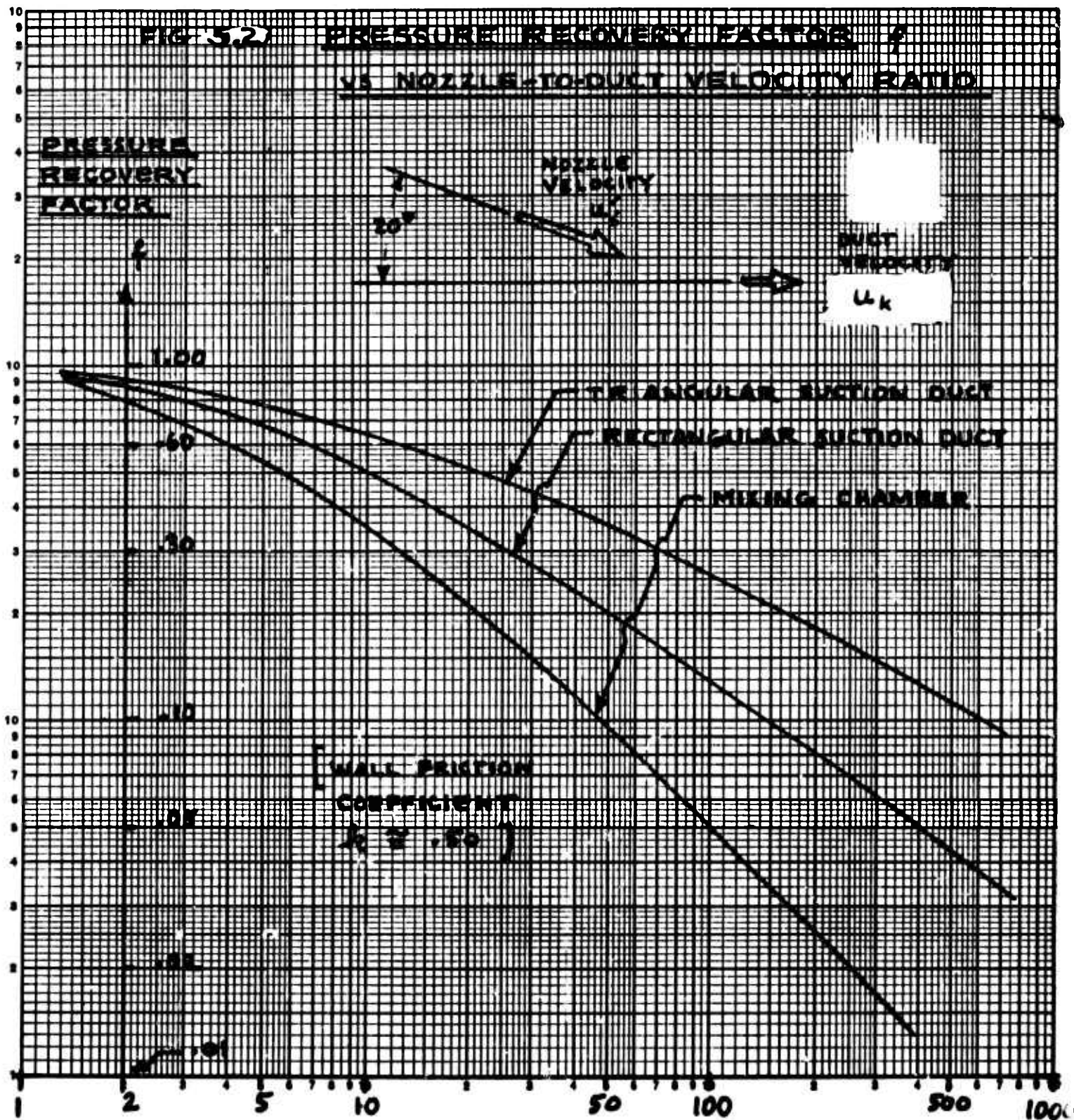
ENGINEER	NORTHROP CORPORATION NORAIR DIVISION	PAGE 5.12
CHECKER		REPORT NO. NOR-67-136
DATE June 1967		MODEL X-21A

Such a nozzle sizing program was used in the X-21A design.

A somewhat simpler but similar program can be used to determine the valve or nozzle sizes leading from the suction ducts to the mixing chamber ahead of the compressor inlet.

5.6 OVERALL DUCTING SYSTEM PRESSURE DIAGRAM

In a bi-level suction system, such as used on the X-21A airplane, the flow from the low-pressure upper-surface ducts is mixed in a chamber ahead of the low-pressure compressor and then pumped up to the approximate pressure level of the remainder of the suction flow and then mixed in a second chamber upstream of the high pressure compressor. A pressure diagram for this X-21A system described is shown in Figure 5.3.



VELOCITY RATIO $\left(\frac{u_i'}{u_k}\right)$

*** SEE EQ (24) & (25)**

ENGINE

CHECKE

DATE

ABSOLUTE
PRESSURE

DATE

P_{ABSOLUTE}
IN WATER

100

80

60

40

20

0

0

2

4

6

8

10

12

14

16

18

20

22

24

26

28

30

32

34

36

38

40

42

44

46

48

50

52

54

56

58

60

62

64

66

68

70

72

74

76

78

80

82

84

86

88

90

92

94

96

98

100

102

104

106

108

110

112

114

116

118

120

122

124

126

128

130

132

134

136

138

140

142

144

146

148

150

152

154

156

158

160

162

164

166

168

170

172

174

176

178

180

182

184

186

188

190

192

194

196

198

200

202

204

206

208

210

212

214

216

218

220

222

224

226

228

230

232

234

236

238

240

242

244

246

248

250

252

254

256

258

260

262

264

266

268

270

272

274

276

278

280

282

284

286

288

290

292

294

296

298

300

302

304

306

308

310

312

314

316

318

320

322

324

326

328

330

332

334

336

338

340

342

344

346

348

350

352

354

356

358

360

362

364

366

368

370

372

374

376

378

380

382

384

386

388

390

392

394

396

398

400

402

404

406

408

410

412

414

416

418

420

422

424

426

428

430

432

434

436

438

440

442

444

446

448

450

452

454

456

458

460

462

464

466

468

470

472

474

476

478

480

482

484

486

488

490

492

494

496

498

500

502

504

506

508

510

512

514

516

518

520

522

524

526

528

530

532

534

536

538

540

542

544

546

548

550

552

554

556

558

560

562

564

566

568

570

572

574

576

578

580

582

584

586

588

590

592

594

596

598

600

602

604

606

608

610

612

614

616

618

620

622

624

626

628

630

632

634

636

638

640

642

644

646

648

650

652

654

656

658

660

662

664

666

668

670

672

674

676

678

680

682

684

686

688

690

692

694

696

698

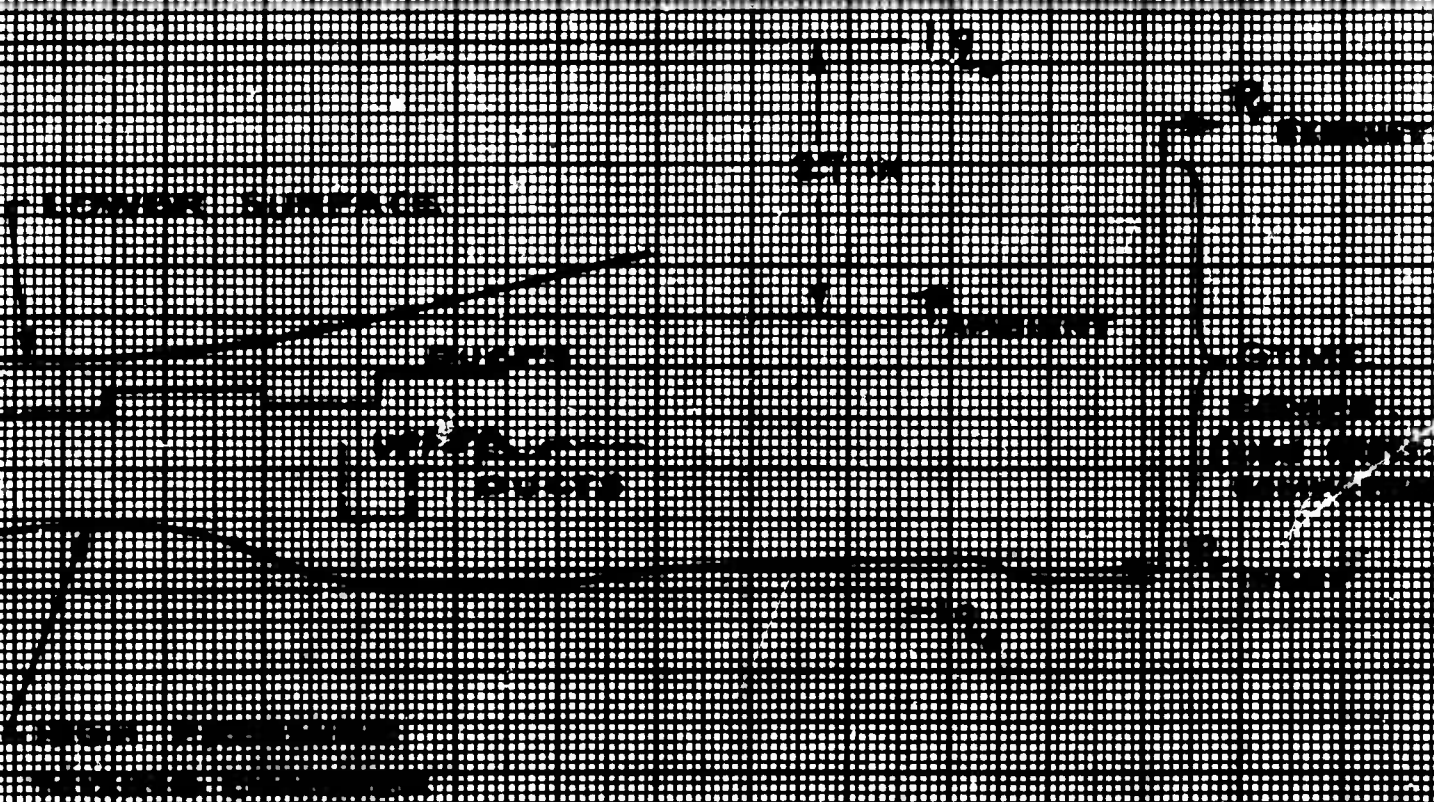
700

702

704

ENGINEER	NORTHROP CORPORATION NORAIR DIVISION	PAGE	5.14
CHECKER		REPORT NO.	NOK 67-136
DATE	JAN 65	MODEL	X-21A

DATA: X-21A AIRPLANE SN 55-400 FIG. 5.3
 FLIGHT 77, RUN NO. 2
 L. W. MOORE, JR. M. S. 174 0.25, 20
 ALTITUDE 10000 FT
 ALTITUDE 10000 FT
 ALTITUDE 10000 FT



ENGINEER	NORTHROP CORPORATION NORAIR DIVISION	PAGE 6.00
CHECKER		REPORT NO. NOR 67-136
DATE June 1967		MODEL X-21A

SECTION 6

EXTERNAL PRESSURE DISTRIBUTION CRITERIA AND
WING DESIGN TO MEET THESE CRITERIA

BY:

C. W. Winter

March 1964

Revised April 1967

ENGINEER	NORTHROP CORPORATION NORAIR DIVISION	PAGE
CHECKER		6.01
DATE		REPORT NO.
June 1967		NOR 67-136
		MODEL
		X-21A

6.1 INTRODUCTION

The design of a Laminar Flow Control wing, in addition to the usual design factors such as an optimum combination of area, aspect ratio, sweep and thickness to chord ratio, is governed by the two additional important factors of proper surface pressure distribution and suction distribution. An iterative procedure, combining analytical and experimental techniques, is applicable to the development of a wing configuration for any aircraft being adapted to Laminar Flow Control. This method was used by Norair in designing the wing for the X-21A airplane. The choice of the optimum pressure distribution is largely governed by the cruising flight condition. The ideal wing is one for which the chordwise pressure distribution is identical at all wing stations. Furthermore, the ideal chordwise pressure distribution is shaped for minimum required suction and for maximum possible lift without exceeding the local sonic velocity by more than a specified amount. Flight tests by Norair on a laminar wing glove on an F-94 aircraft indicated a local Mach number of 1.04 to be conservative, even though exceeded in the F-94 tests under certain conditions. LFC flight tests on the X-21A airplane verified the previous results, showing that a local Mach number of 1.04 can be exceeded somewhat without loss of Laminar Flow.

The foregoing considerations suggest that the upper surface pressure distribution should be relatively flat-topped to approximately mid-chord without the local Mach number exceeding 1.04. The lower surface pressure distribution must be such that the necessary airplane lift is attained.

6.2 NOTATION

C_{L_A}	Airplane lift coefficient, $C_{L_A} = W/qS$
C_p	Pressure coefficient, $C_p = \Delta p/q$
C_m	Pitching moment coefficient
c	Wing chord
c_{av}	Average wing chord, S/b
c_l	Local lift coefficient

ENGINEER	NORTHROP CORPORATION NORAIR DIVISION	PAGE 6.02
CHECKER		REPORT NO. NOR 67-136
DATE June 1967		MODEL X-21A

FRL	Fuselage Reference Line
LFC	Laminar Flow Control
M	Mach number
P_l	Local static pressure, LBS/FT ²
P_∞	Freestream static pressure, LBS/FT ²
q_∞	Freestream dynamic pressure, LBS/FT ²
S_w	Wing planform area, FT ²
W	Airplane gross weight, LBS
x/c	Dimensionless streamwise distance from leading edge
η	Distance normal to airplane plane of symmetry as a ratio of wing semi-span
γ	Ratio of specific heats for air, c_p/c_v
Λ	Sweep angle of a wing element line, DEG
α	Angle of attack, DEG

6.3 WING DESIGN CRITERIA

The success in configuring the airfoil contours of a swept wing to efficiently obtain full-chord laminar flow by suction depends upon the degree of satisfaction of a number of criteria. One of the most important of these is the ability to fly at high subsonic Mach numbers and at lift coefficients for maximum lift/drag ratios without formation of shock waves on the wing surfaces. Elimination of the shock waves can be accomplished by maintaining local flow velocities normal to the wing isobars less than the speed of sound.

The optimum Laminar Flow Control wing may be considered to be one which, at the design flight condition, has a chordwise pressure distribution that is identical at all spanwise stations. This type of pressure distribution is ideal since it has straight isobars everywhere coincident with the wing element lines, and satisfies the two-dimensional boundary conditions of the existing Laminar Flow Control theory used for computing suction quantities (Reference 1).

ENGINEER	NORTHROP CORPORATION NORAIR DIVISION	PAGE 6.03
CHECKER		REPORT NO. NOR 67-136
DATE June 1967		MODEL X-21A

The pressure distribution criteria must apply everywhere within the exposed wing area which is designed for Laminar Flow. This would exclude an area near the wing-fuselage intersection, an area at the tip and any other areas blanketed by pumping pods, pylons or fairings (Reference 1).

Along any element line, within the Laminar Flow Control area, the magnitude of the pressure coefficient should not vary more than 0.1*. The gradient magnitude must not be greater than 0.02* per foot of span (Reference 1).

The local Mach number normal to the element lines within the LFC area must not exceed 1.04. This criterion may be applied to element lines rather than to isobars to avoid the dilemma faced by consideration of flat upper surface pressure distributions, both chordwise and spanwise, where very small pressure coefficient gradients may cause the isobars to be highly swept locally.

6.3.1 Wing Pressure Distributions

6.3.1.1 Chordwise Pressure Distribution

The problem of developing a wing for a Laminar Flow Control airplane is one of contouring it so as to establish favorable chordwise and spanwise pressure distributions. The upper and lower surface velocities should rise rapidly at the front of the airfoil, as indicated in Figure 6.1 by a rapid decrease in pressure coefficient. Large leading edge negative pressure peaks which could cause early transition of the boundary layer must be avoided, but the airfoil section should be designed to load the leading edge rapidly in order to minimize cross-flow in the boundary layer. In the mid-chord region the pressures should be approximately constant, corresponding on the upper surface to a local velocity normal to the element lines which is equal to, or slightly in excess of, the speed of sound. Under these conditions, the aft pressure rise will be fairly steep. This type of chordwise pressure distribution minimizes the suction requirements while providing a maximum amount of lift without shock effects.

* NOTE: Quantities identified with an asterisk * are presented to show order of magnitude only. Critical values are subject to change depending upon the airplane mission.

ENGINEER	NORTHROP CORPORATION NORAIR DIVISION	PAGE 6.04
CHECKER		REPORT NO. NOR 67-136
DATE June 1967		MODEL X-21A

The lower surface pressure coefficient distribution should be similar in shape to that of the upper surface but should be such as to give an adequate local lift coefficient. The pressure coefficient at the trailing edge is about +.20.

The desired chordwise pressure distribution is affected by the geometric distribution of the thickness and camber of the airfoil section together with three-dimensional induced effects due to camber, aspect ratio, twist and taper.

6.3.1.2 Spanwise Pressure Distribution

The laminar flow control wing requirement for a spanwise lift distribution involving straight isobars implies that the local section lift coefficient remains constant across the wing span. Obtaining a constant spanwise lift distribution is the first requirement in obtaining the same aerodynamic characteristics at all wing stations (references 2 and 3).

One of the analysis tools is an induction lift matrix which calculates the angle of attack distribution corresponding to a constant spanwise lift coefficient. The twist distribution is derived by this method.

The lines of constant pressure in a typical LFC wing isobar diagram (Figure 6.2) are almost coincident with the straight element lines of the wing. This isobar pattern represents a considerable improvement over the usual swept wing, which may have much larger losses in aerodynamic sweep at the root and tip. When isobars are swept less than the wing element lines and aerodynamic sweep is reduced, the allowable cruise Mach number must be reduced to avoid local shock waves. Also, a non-uniform isobar pattern leads to a more complex suction system design.

Figure 6.3 illustrates flight test and wind tunnel measurements of the spanwise distribution of pressure coefficient along the 10% chord line for the X-21A wing in cruising flight.

ENGINEER	NORTHROP CORPORATION NORAIR DIVISION	PAGE 6.05
CHECKER		REPORT NO. NOR 67-136
DATE June 1967		MODEL X-21A

6.3.2 Wing Twist Distribution

As already mentioned, the requirement for a spanwise lift distribution that has relatively straight isobars dictates that the wing be twisted. An induction lift matrix may be used to calculate this twist. The theory indicates a large parabolic increase in the local geometric angle of attack at the wing root, and a similar large increase at the tip. Figure 6.4 illustrates a typical wing twist distribution for an LFC wing. The large angle of attack theoretically required to maintain a constant lift coefficient in the wing tip region does not prove to be a satisfactory configuration based on experimental results. (It is impossible to maintain a constant lift coefficient all the way to the wing tip.)

6.3.3 Wing Section Characteristics

6.3.3.1 Wing Thickness Distribution

When the selection of the basic airfoil section has been made, modifications may be made, depending upon the results of analytical and experimental studies, to the basic section to bring its final configuration to that which will achieve the desired results for the airplane mission.

Experimental results indicate that wing thickening is needed near the root because it is not completely possible to maintain the upper surface pressure distribution in this area in spite of the large increase in twist. There is considerable advantage in reduction of weight and stiffening of the wing when the root is thick. Slight thickening near the wing tip may be required resulting from mechanical compromises if the wing is developed from a series of straight element lines. A typical thickness distribution for an LFC wing configuration designed to cruise at Mach 0.80 and 0.30 lift coefficient, is shown on Figure 6.5.

6.3.3.2 Wing Camber Distribution

The camber distribution for the typical swept wing shown in Figure 6.6 indicates that, as a generality, the camber line exhibits a local curvature near the leading edge followed first by a long flat area

ENGINEER	NORTHROP CORPORATION NORAIR DIVISION	PAGE 6.06
CHECKER		REPORT NO. NOR 67-136
DATE June 1967		MODEL X-21A

and next by a considerable amount of rather localized curvature at the start of the aft pressure rise. This condition has been referred to as "aft camber." The spanwise distribution of camber involves a reduction of leading edge camber very near the root. This reduction results from the necessity for increasing the magnitudes of the upper surface pressure coefficients at the inboard leading edge. This is accomplished not only by reducing the camber, but also by local thickening.

Analysis of experimental data indicates that moving the location of maximum chordwise thickness aft will increase the sweep of the isobars in the out-board region of the wing. Increasing the isobar sweep angle allows higher angles of attack and lift coefficients to be obtained before limiting shock strength is encountered.

6.4 ANALYTICAL METHODS

At any spanwise station, the chordwise distribution of lift is determined primarily by the airfoil section. Because an iterative procedure must be used in the design process to establish the correct wing section, the first step is to select a standard low drag section of approximately the proper design lift coefficient for the mission of the airplane. The selected section may be somewhat removed from the optimum section required to satisfy the conditions set for the design, but it does allow the initiation of a wind tunnel program from which experimental data can be obtained for correlation with theory. Theodorsen's method for calculating the incompressible velocity distribution, when programmed for a computer, is a useful analytical tool. The Theodorsen procedure may be used to evaluate incompressible increments in velocity and pressure distributions for changes in airfoil shapes. In the area of compressibility corrections, the generally used first order theories such as the Prandtl-Glauert or Karman-Tsien methods are not sufficiently accurate when dealing with velocities which must rise close to the sonic velocity on the wing. These corrections are only adequate when used for thin wings at low angles of attack. A better approximation is that of John Spreiter of NASA (Reference 4). Excellent correlation is obtained from

ENGINEER	NORTHROP CORPORATION NORAIR DIVISION	PAGE
CHECKER		6.07
DATE		REPORT NO. NOR 67-136
June 1967		MODEL X-21A

Spreiter's theory for the upper portion of the wing aft of the maximum thickness point and for most of the lower surface. For the forward upper portion of the wing, particularly at the inboard stations, predictions by this and all other standard methods are of the incorrect sign. This forward upper portion is the most difficult to match to the sonic pressure line. Spreiter's formula, (Reference 4, Eq. No. 31), as modified for use with swept back wings is:

$$C_p = \frac{-2 (1 - M_\infty^2 \cos^2 \Lambda)}{(\gamma + 1) M_\infty^2} \left(1 - \left[1 + \frac{3}{4} (\gamma + 1) \frac{M_\infty^2 C_{p_{1\infty}}}{(1 - M_\infty^2 \cos^2 \Lambda)^{3/2}} \right]^{2/3} \right)$$

where $C_{p_{1\infty}}$ is the pressure coefficient measured in the conventional manner on the same wing and at the same angle of attack.

A graph illustrating the effects of the formula on incompressible pressure coefficients is shown in Figure 6.7. The theoretical curves indicate increasing values for C_p with increasing Mach number, whereas the test data shows the reverse in the case for the upper forward wing section. Experimentally determined compressibility corrections may be used to cover the wing section where Spreiter's formula is invalid (Reference 2). A method presented in Reference 5 may be of some assistance in this area of the wing, but this method also has limitations in that at the design angle of attack, the stagnation line must be assumed to be at the geometric leading edge of the airfoil.

The aeroelastic effects on a typical LFC wing may be considerable if the wing is highly swept and has a relatively high aspect ratio. Digital computer programs are available for aeroelastic analyses. The aeroelastic problem is to determine the distribution of local aerodynamic angle of attack differences between the model and the airplane.

The change in shape of the airplane wing due to flight loads for a given root-chord angle of attack will differ from that of the model under tunnel test conditions. If no effort is made to account for this change, large errors in estimating full scale pressure distributions will be sustained by direct use of the tunnel data. It is recommended that this be accounted for as accurately as possible by building the pressure distribution model with a twist distribution differing from wings of the airplane, so that under load the model will more closely match the airplane under load.

ENGINEER	NORTHROP CORPORATION NORAIR DIVISION	PAGE 6.08
CHECKER		REPORT NO. NOR 67-136
DATE June 1967		MODEL X-21A

The process follows:

- (1) Previous to specifying final airplane wing lines, develop the model wing to the point that tests demonstrate a uniform span loading at the design Mach number and lift coefficient. When this criterion is satisfied, assume that these tunnel data are the final airplane wing pressures.
- (2) Assume that sum of the span load distributions computed theoretically for the unloaded model plus the changes due to tunnel loads is exactly equal to the corresponding sum for the unloaded airplane wing plus the aeroelastic changes due to inertia and flight loads. Then solve for that no-load twist of the airplane wing which satisfies this equality. Specify this twist distribution for the airplane wing. Of course, the process of equating load distributions really infers that the sum of the local lift coefficients at any point along the span must be equal.

When this procedure was followed in the X-21A program, the unloaded model wing tip was washed out six tenths of a degree more than the specified airplane wing twist.

It may be found that at a point in time after the wing twist decision point has been passed, further modifications affecting the span loading may be made and re-tested in the tunnel. If the tunnel results verify the change, then a modification of the foregoing process is in order, i.e., given an airplane Mach number and lift coefficient, find the model root chord angle of attack at which to measure the chordwise pressure distribution. This value of α will differ from point to point along the span, however, the essence of the matter is to assume that at a given position along the span, a theoretical change in local angle of attack caused by local wing modification will cause the same change in chordwise pressure distribution as would be caused by an equal change in root angle of attack on a model of fixed configuration.

6.5 AERODYNAMIC DESIGN TEST TECHNIQUES

The development of a new wing configuration is initiated by analytical studies and testing of wind tunnel models. Early X-21A model testing experience revealed the necessity for building each of the model wing panels in one piece to avoid the adverse effects of surface discontinuities on surface pressures and also to reduce the complexity of the model aeroelastic analysis.

ENGINEER	NORTHROP CORPORATION NORAIR DIVISION	PAGE 6.09
CHECKER		REPORT NO. NOR-67-136
DATE June 1967		MODEL X-21A

From experimental data from small scale wind tunnel models based on data taken at $M = 0.30$, it is concluded that high Reynolds number tunnel operation is not essential in order to obtain pressure coefficient accuracy, provided that the Reynolds number is sufficiently high to prevent separation. Inspection of the graphs of pressure coefficient versus angle of attack for various positions on the X-21A model wing showed that for angles of attack less than 8 degrees and within a range of mean aerodynamic chord Reynolds number of 1.4 to 4.1 million, the data at a given angle of attack all fell within a band of $\pm .015$. The average transducer accuracy is not better than this.

The design and construction of wind tunnel models for LFC tests requires strict control of the contours of the aerodynamic surfaces. If model tolerances are too lenient, adverse effects on the accuracy of the pressure measurements result. To insure accurate model pressure data, model wing ordinate tolerances of the order of $\pm 0.002"$ to $0.005"$ are recommended with the more stringent tolerances applicable in the 0% to 50% x/c area. As the full scale LFC airplane waviness tolerances are quite small, the model tolerances must also be stringent. To maintain equal waviness tolerances in terms of wave amplitude to wave length, the model absolute tolerances would bear the same relationship as the model to airplane scale factor. For example, a representative tolerance for wave amplitude on the X-21A airplane was .003 inches for repeated 3-inch long waves. The corresponding dimensions on the .06 model are .0002 amplitude on .2 long waves. An amplitude tolerance of .0002 is far less than the model contour tolerance. Thus, the same waviness ratio could not be achieved on the model; but the example shows the extreme importance of model smoothness. A surface waviness of .0030 inches per inch wave length was maintained on the critical models used by Northrop Norair.

Low speed wind tunnel model tests are valuable in investigating configurations leading to constant wing chord line isobars for the simulated design Mach number. Use of low speed models is an inexpensive method to obtain large amounts of preliminary data on wing geometry, tip configuration, wing-mounted nacelles and wing root-body intersections.

Full span pressure models must be tested extensively at high speeds to develop the optimum wing configuration, wing nacelles, and to determine the effects of the wing body intersection under the influence of compressibility. Preliminary high speed wing tunnel tests run with Norair's X-21A model, using a basic NACA low drag airfoil section, revealed that the pressure distributions obtained were unsatisfactory for an LFC airplane. The primary difficulty was that the upper surface leading edge pressures did not drop fast enough. Later tests using modified airfoils achieved the desired pressure distributions.

ENGINEER	NORTHROP CORPORATION NORAIR DIVISION	PAGE 6.10
CHECKER		REPORT NO. NOR 67-136
DATE June 1967		MODEL X-21A

The wing surface static pressure measurements for the model data were obtained with the use of a pressure model which contained approximately three hundred orifices total for the upper and lower surfaces. It required approximately three minutes to read these pressures at a single angle of attack by use of Scanivalves located in the model fuselage. Automatic read-out equipment and data reduction is mandatory when sampling this large a number of pressures. The reduction process must provide a print-out of all data at a single test point arranged in columns and rows according to spanwise station, chordwise station and surface (upper or lower). The pressure data should be integrated to yield local and total lift and pitching moment coefficients. The model testing program for the X-21A involved about one hundred sixty (160) hours of high speed testing and approximately one thousand three hundred (1300) hours in low speed facilities.

Wing surface static pressure distributions also were obtained in the X-21A program from flight testing. The purpose of these tests was to evaluate the degree of accuracy of the method of using wind tunnel measurements, modified by estimates of aeroelasticity, for predicting flight pressure distributions, and further, to evaluate the degree by which the specific LFC criteria applying to pressure distributions are satisfied in an actual wing design. It was found that there was excellent correlation between the flight measurements and the predictions based on wind tunnel tests. The criteria regarding the flat-topped chordwise distribution of pressure in the mid-chord region and the uniform distribution of pressure along the spanwise element lines were shown to have been satisfied (see Figures 6.1 and 6.3).

The flight wing surface static pressure measurements were obtained using two types of instrumentation. The first type, which is preferred because of greater accuracy, employed flush static orifices which were installed when the wing was fabricated. The second type of instrumentation was "Strip-a-tube." This second type may be installed after the wing is built. Strip-a-tube installations offer more flexibility but suffer somewhat in accuracy. It is an external installation and the orifices are spaced above the wing surface a small distance. Extra care is needed when using Strip-a-tube in the leading edge region to fair the tubing in the direction of the local streamlines.

ENGINEER	NORTHROP CORPORATION NORAIR DIVISION	PAGE 6.11
CHECKER		REPORT NO. NOR 67-136
DATE June 1967		MODEL X-21A

6.6 PRESSURE DISTRIBUTION IN THE WING NOSE REGION

Both analytical and experimental determinations of the pressure distribution in the wing nose flow attachment zone and in the adjacent regions of strong chordwise pressure gradients deserve special attention in the design-development of an LFC airplane. The chordwise pressure distribution for the various LFC flight conditions must be known much more accurately in the wing nose region than in any other part of the wing in order to design a satisfactory suction surface and ducting system to accommodate the chordwise changes in pressures and flow directions in this region.

A computer program developed by J. Goldsmith, references 7 and 8, based on the Theodorsen method of determining velocity and pressure distribution on an airfoil, has been found useful for the analytical determinations of chordwise distribution of pressures in the wing nose region. Families of wing nose shapes can be investigated conveniently by this method for the design-analysis. The wing nose shape for a proposed major modification program was determined by the method described, and subsequent flight tests on the first X-21A airplane (-408) with a dummy wing nose duplicating the proposed major modification verified the results of the calculations. The flight tests used about 18 flush pressure taps per spanwise station in the wing nose region to accurately define the chordwise distribution of pressure.

The new leading edge radius for the proposed modification faired into the original wing at front spar station 402 and radius = 1.47 inches. The radius increased linearly to 2.00 inches at front spar station zero, and the forward tangency point increased linearly to 2.40 inches ahead of the original wing at the same front spar station zero. The new leading edge radius was faired into the original wing at about 3% chord by an elliptical shape tangent to the wing nose circle and tangent to the original wing. Only minor corrections to the wing nose fairing, in the outer wing, were required as a result of the flight test data.

6.7 REFERENCES

1. G. L. Gluyas, W. G. Wheldon: Norair Report Number NOR 61-118, "A Method for Development of the Wing Configuration for a Subsonic Logistic Airplane Employing Laminar Flow Control," June 1961.

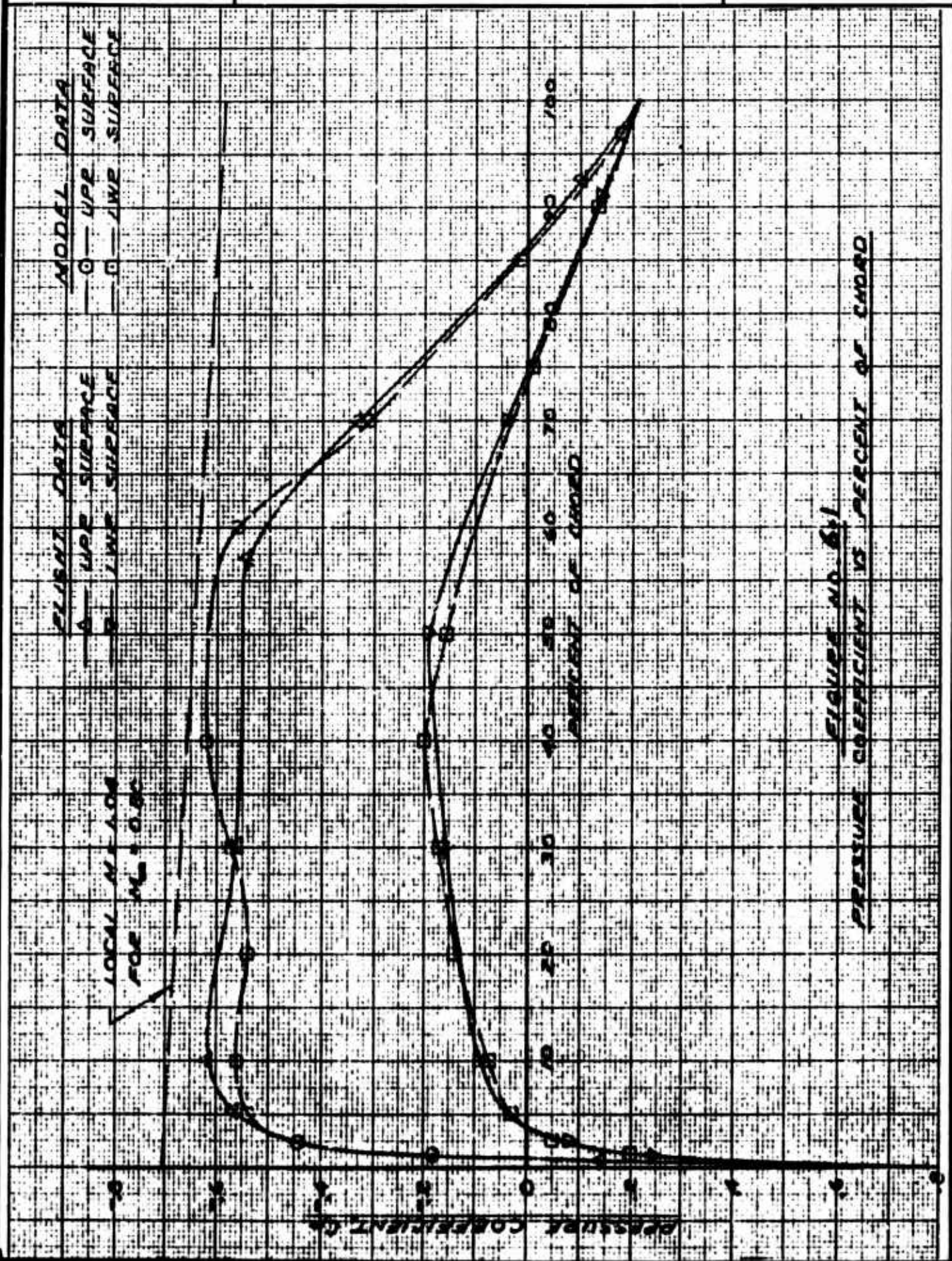
ENGINEER	NORTHROP CORPORATION NORAIR DIVISION	PAGE 6.12
CHECKER		REPORT NO. NOR 67-136
DATE June 1967		MODEL X-21A

2. Norair Report Number NOR 61-133, "Laminar Flow Control Demonstration Airplane System Design Analysis Summary Report," August 1961
3. "The Laminar Flow Control Presentation for the Aeronautical Systems Division," May 3 - 4, 1962
4. John Spreiter, Alberta Y. Alksne: NACA TR 1359, "Thin Airfoil Theory Based on Approximate Solution of the Transonic Flow Equation," 1958
5. Milton VanDyke: NACA TR 1274, "Second-Order Subsonic Airfoil Theory Including Edge Effects," March 1956
6. Norair Report Number NOR 60-136, "Considerations on the Selection of the Size of the BLC Technological Airplane," May 1960
7. J. Goldsmith: "IBM Computer Programs for Calculating the Velocity and Pressure on or near Two-Dimensional Airfoils," Northrop Norair Report NOR 61-214, (or BLC-132), Sept. 1961.
8. J. Goldsmith: "Recent Modifications of the Computer Programs for Calculating Two-Dimensional Airfoil Velocities," Northrop Norair Report NOR 66-119 (or BLC-170), March 1966.

6.8 ILLUSTRATIONS INDEX

- 6.1 Pressure Coefficient versus Percent of Chord
- 6.2 Typical Upper Wing Surface Isobar Configuration
- 6.3 Pressure Coefficient versus Semi-Span Station
- 6.4 Typical Wing Twist Distribution
- 6.5 LFC Wing Thickness Distribution
- 6.6 LFC Wing Camber Distribution
- 6.7 Compressibility Corrections

ENGINEER	NORTHROP CORPORATION NORAIR DIVISION	PAGE 6.13
CHECKER		REPORT NO. NOR 67-136
DATE June 1967		MODEL X-21A



ENGINEER	NORTHROP CORPORATION NORAIR DIVISION	PAGE 6.14
CHECKER		REPORT NO. NOR 67-136
DATE June 1967		MODEL X-21A

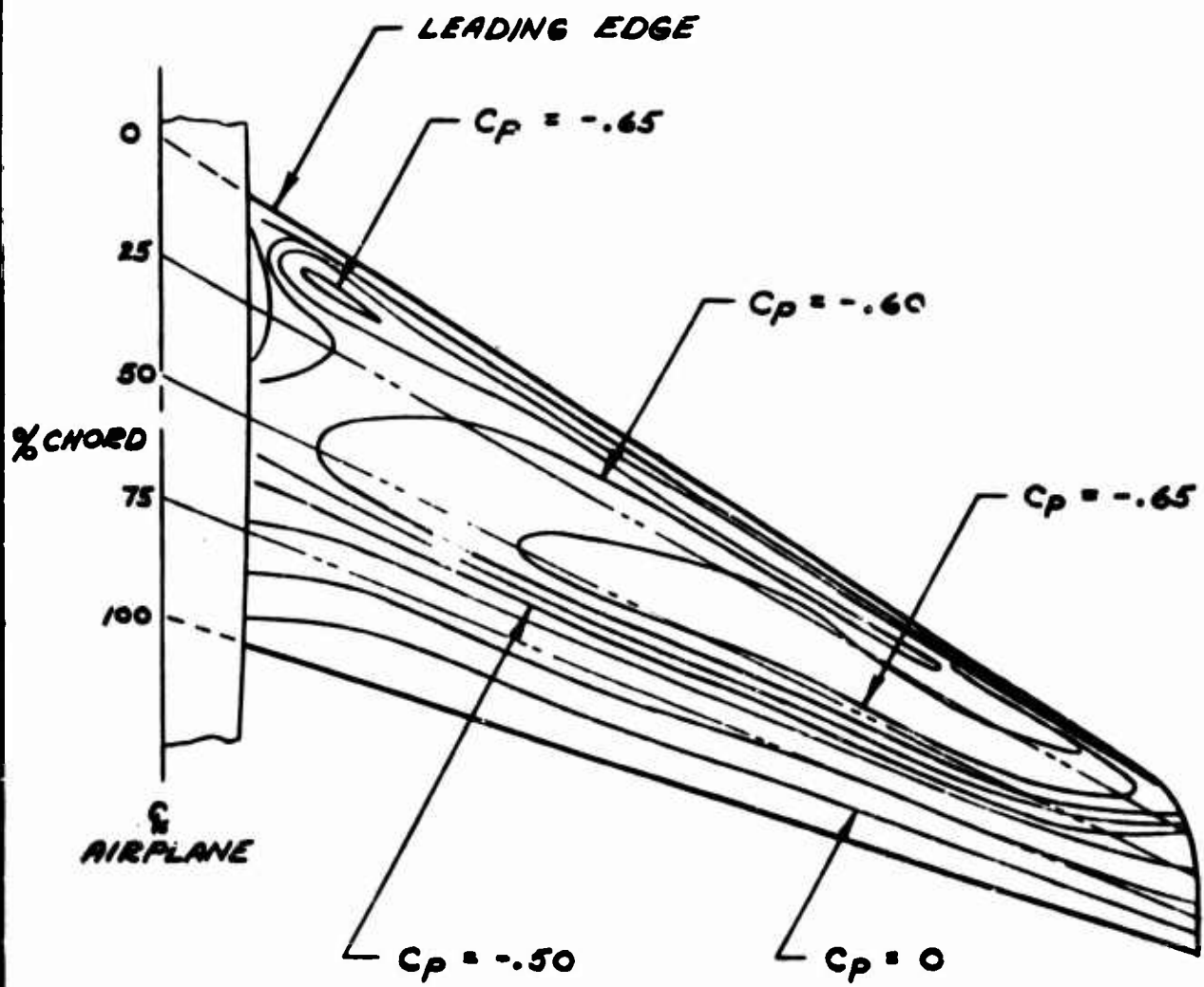
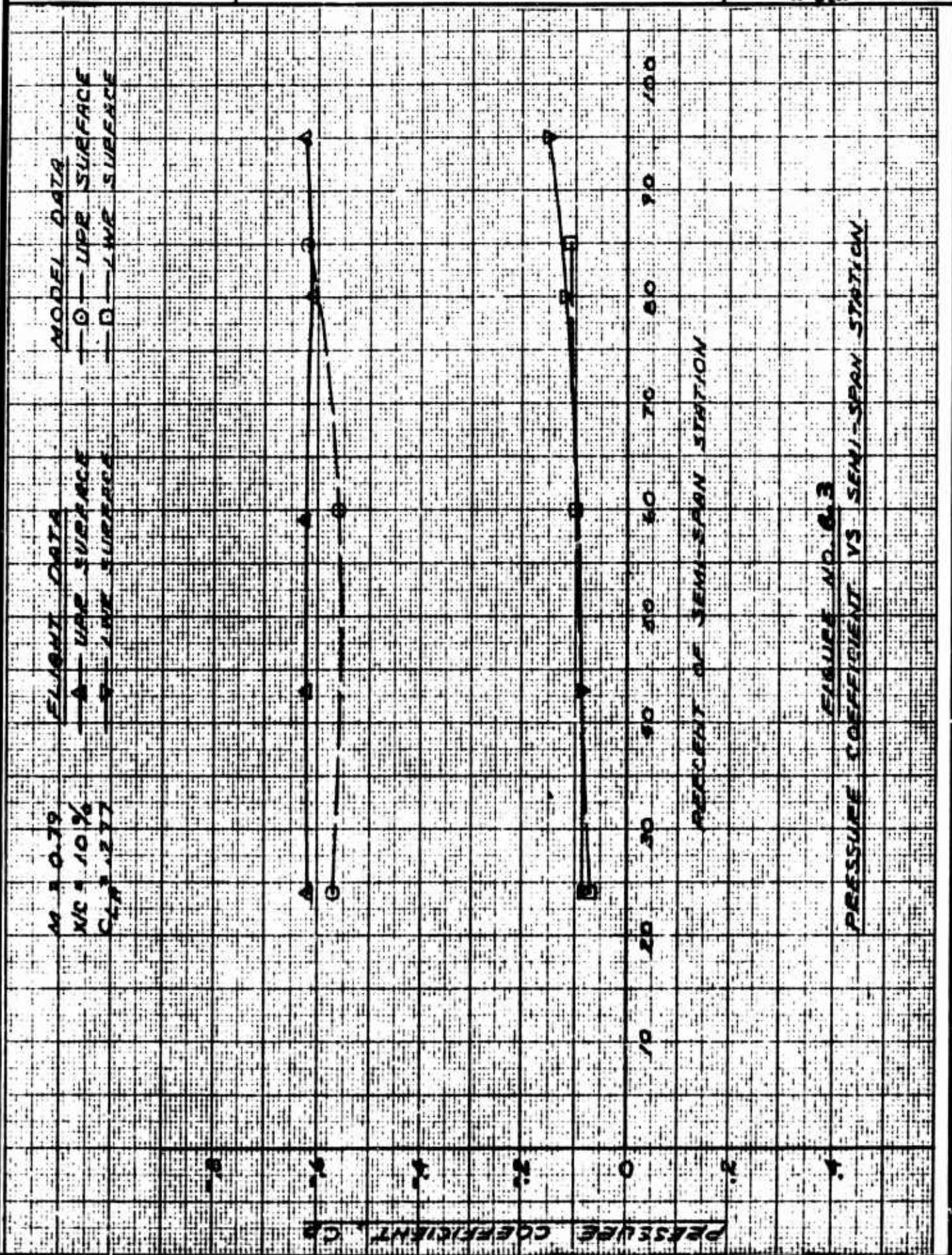
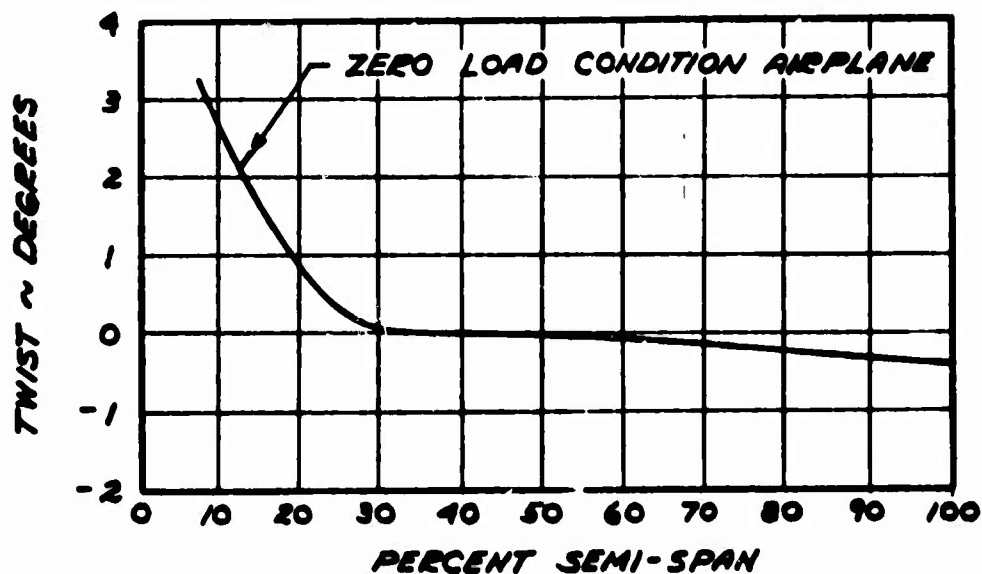


FIGURE NO. 6.2
TYPICAL UPPER WING SURFACE ISOBAR CONFIGURATION

ENGINEER	NORTHROP CORPORATION NORAIR DIVISION	PAGE
CHECKER		6.15
DATE		REPORT NO.
June 1967		NOR 67-136
		MODEL
		X-21A



ENGINEER	NORTHROP CORPORATION NORAIR DIVISION	PAGE 6.16
CHECKER		REPORT NO. NOR 67-136
DATE June 1967		MODEL X-21A



NOTE: TWIST ANGLE MEASURED FROM FUSELAGE
REFERENCE LINE PARALLEL TO THE PLANE
OF SYMMETRY

FIGURE NO. 6.4
WING TWIST DISTRIBUTION

ENGINEER	NORTHROP CORPORATION NORAIR DIVISION	PAGE 6.17
CHECKER		REPORT NO. NOR 67-136
DATE June 1967		MODEL X-21A

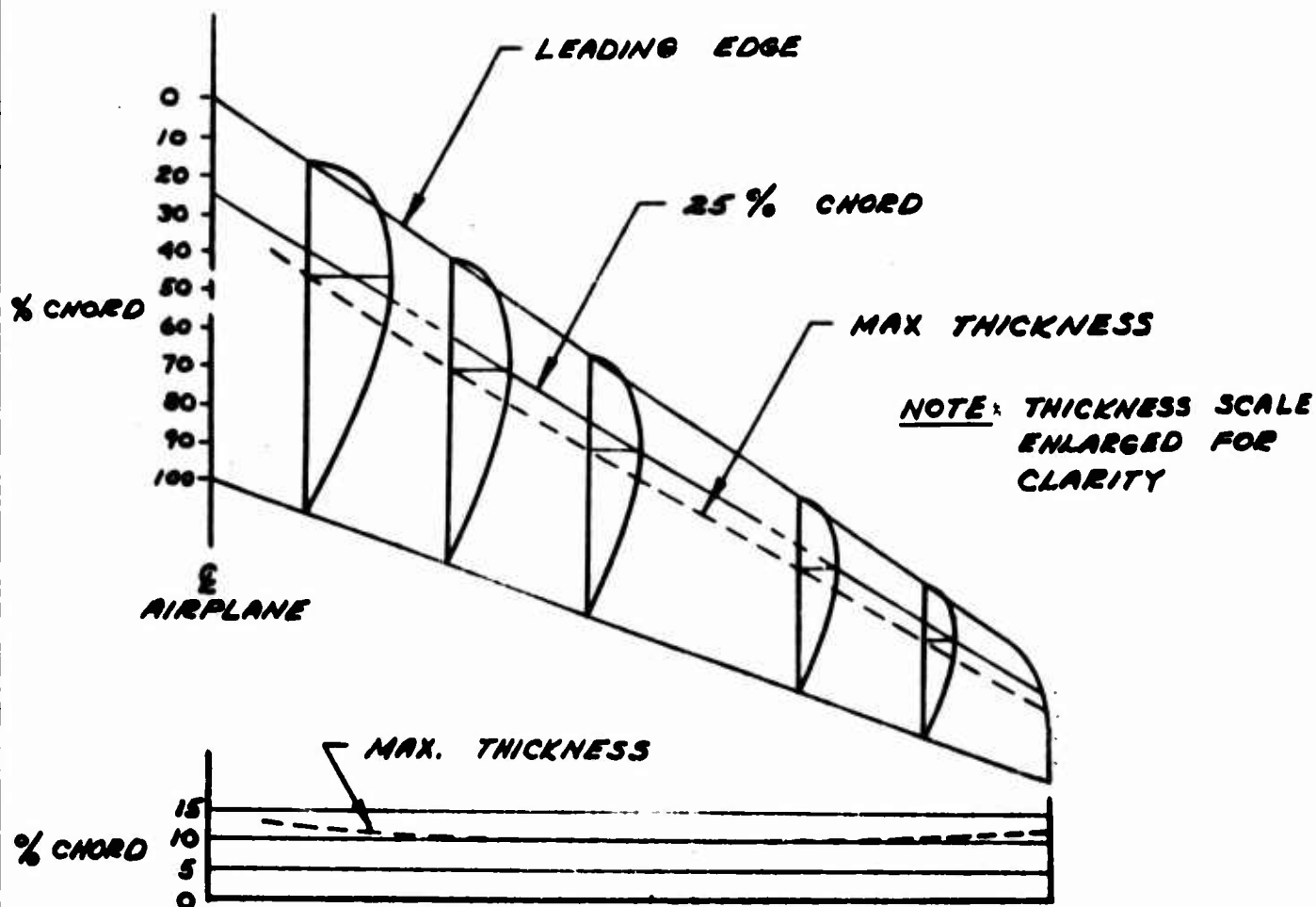


FIGURE NO. 6.5
LFC WING THICKNESS DISTRIBUTION

ENGINEER	NORTHROP CORPORATION NORAIR DIVISION	PAGE 6.18
CHECKER		REPORT NO. NOR 67-136
DATE June 1967		MODEL X-21A

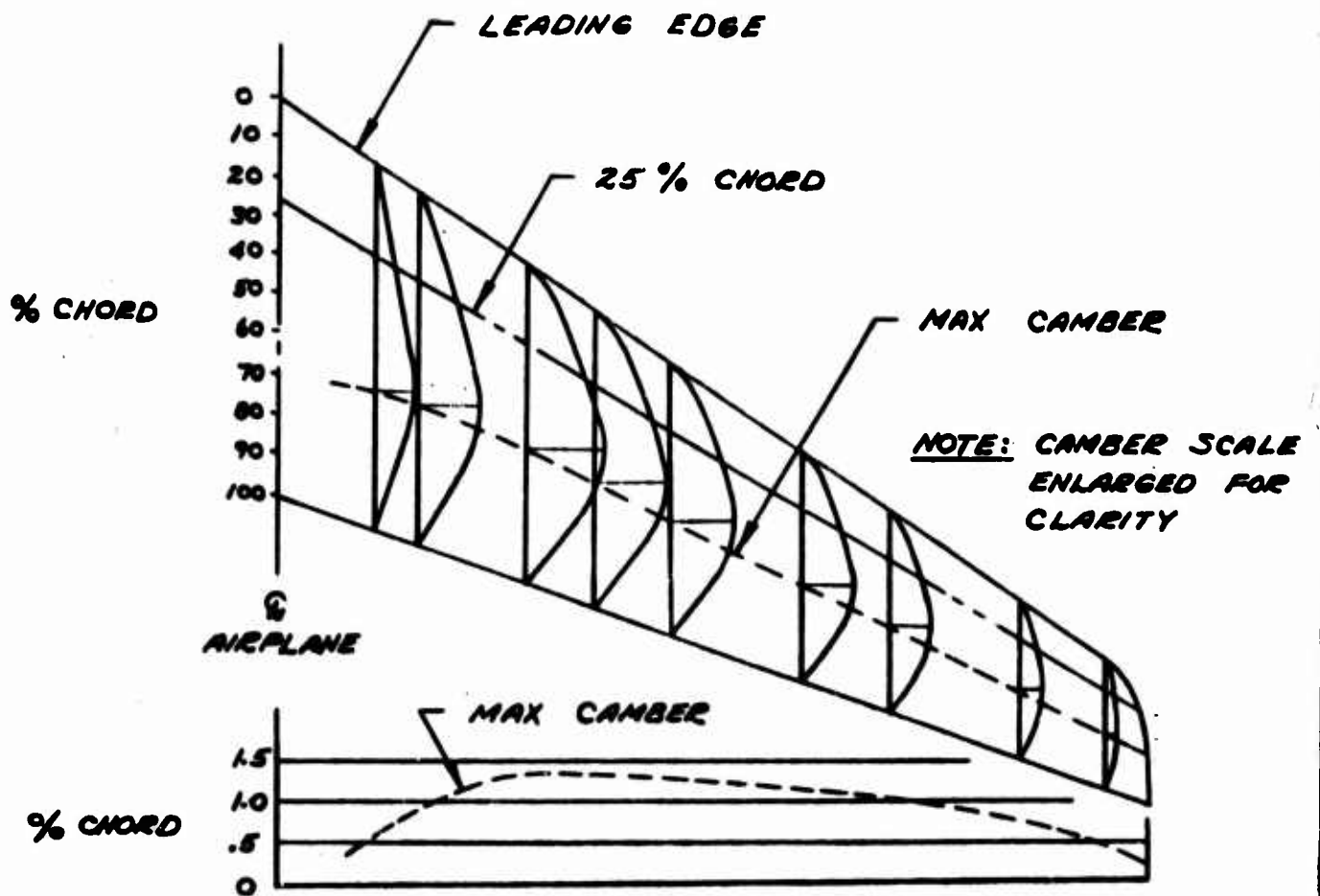


FIGURE NO. 6.6
LFC WING CAMBER DISTRIBUTION

ENGINEER	NORTHROP CORPORATION NORAIR DIVISION	PAGE 6.19
CHECKER		REPORT NO. NOR 67-136
DATE June 1967		MODEL X-21A

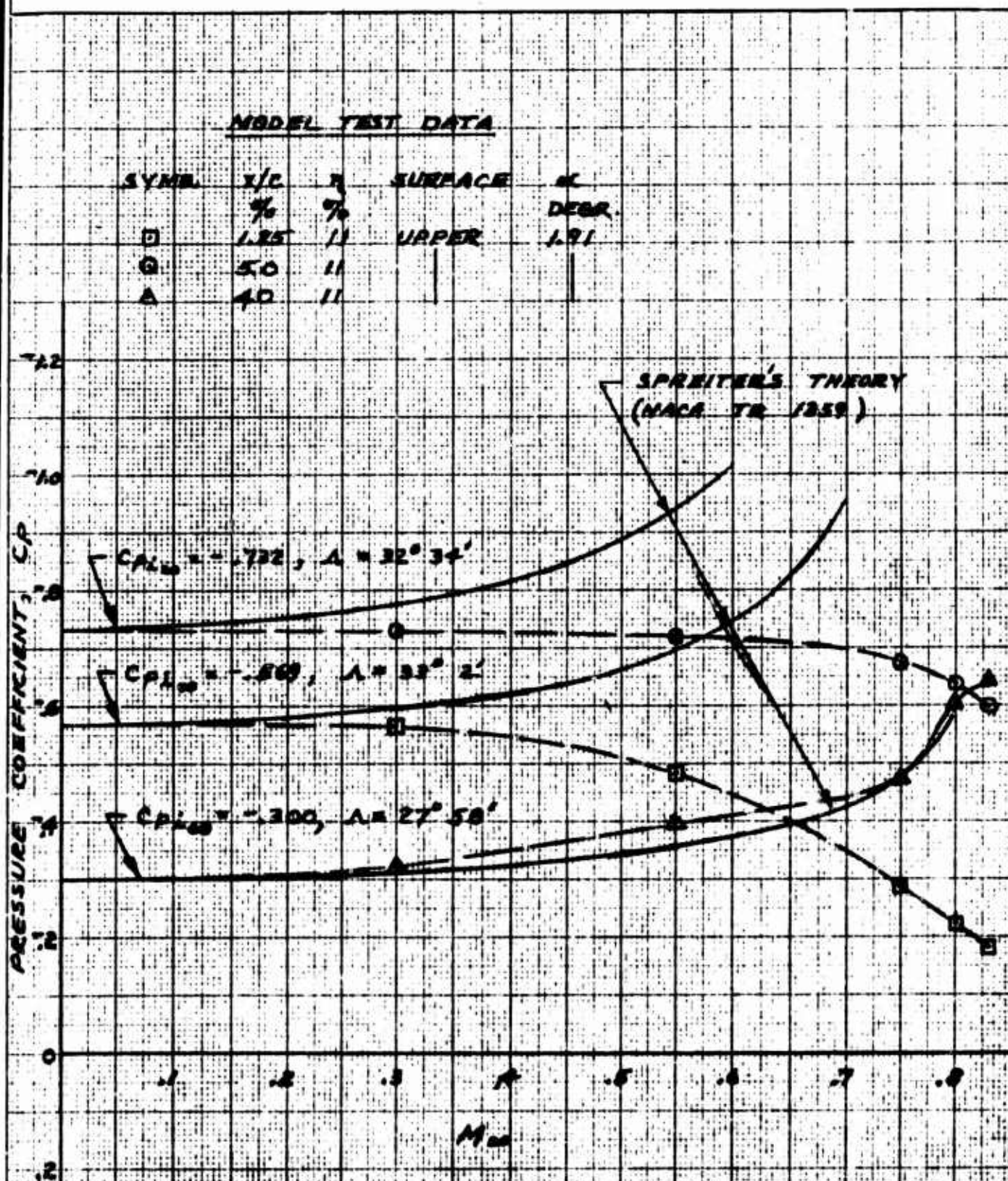


FIGURE NO. 6.7
COMPRESSIBILITY CORRECTIONS

ENGINEER	NORTHROP CORPORATION NORAIR DIVISION	PAGE 7.00
CHECKER		REPORT NO. NOR 67-136
DATE June 1967		MODEL X-21A

Section 7

EFFECTS OF NACELLES, PODS AND FUSELAGE ON THE
WING PRESSURE FIELD AND ADAPTATION OF WING
CONTOURS

By: W. G. Wheldon

March, 1964

Revised April 1967

ENGINEER	NORTHROP CORPORATION NORAIR DIVISION	PAGE
CHECKER		7.01
DATE		REPORT NO. NOR 67-136
June 1967		MODEL X-21A

7.1 INTRODUCTION

Special attention must be given to the task of designing non-suction aerodynamic surfaces in proximity to the LFC wing. Major elements falling in this category are wing mounted nacelles, wing tips and the fuselage area directly abreast of the wing root. In any high speed subsonic wing design problem the effort is always to attain as high a speed and as high a lift coefficient as possible at that speed without encountering shock waves in cruising flight. The only design which satisfies this requirement is one having a two-dimensional airfoil pressure distribution optimized for the design Mach number and lift coefficient, and having this same chordwise distribution at all spanwise stations. The LFC wing design allows no large relaxation of these requirements anywhere on the wing, hence nacelles, wing tips and fuselage must be contoured so as to satisfy this requirement.

The design objective in regard to surface pressure distribution, described in the preceding paragraph, is important on an LFC wing for other reasons. Spanwise variations in surface pressure along the wing element lines cause spanwise variations in crossflow that make the determination of required suction more difficult. Also, spanwise variations in surface pressure along the spanwise suction ducts penalize the duct performance and make the suction ducting design more difficult. A penalty to the suction duct performance, in terms of lower pressures in the ducts, results in increased equivalent drag of the wing.

7.2 GENERAL CONSIDERATIONS

The general problem in which the final pressure distribution over the laminar surfaces of the wing is specified at a given Mach number and lift coefficient is addressed here. It is also possible that the general volume requirements of the nacelles might be specified. The position of the wing tips and wing root is known. An adequate theory is needed which would allow the shape of the nacelles, wing tips and wing root junctions to be defined such that the specified pressure distribution would result. However, no such theory exists. Efforts are in progress to solve this inverse problem for the wing alone, but because of inadequacy of the elementary subsonic compressibility theory near the stagnation zones, this effort cannot attain the desired 100% success. Flow solutions have been obtained for intricate body shapes, wing body intersections, nacelles with spiked inlets and so forth for incompressible flow. All of these have a limitation on the number of control points on the surface of the body being approximated, and none exists as far as is known, which will give an adequate representation of the LFC wing problem, namely the wing-fuselage-nacelles-tip combination.

ENGINEER	NORTHROP CORPORATION NORAIR DIVISION	PAGE
CHECKER		7.02
DATE		REPORT NO.
June 1967		NOR 67-136
		MODEL
		X-21A

Consequently, the design of the LFC wing is largely iterative. A considerable amount of analysis must take place at the initiation of the project followed by as much low speed testing as possible. Finally a high speed test is made to evaluate the influence of compressibility, and depending upon the results the entire procedure must be repeated as many times as required for satisfactory convergence.

The X-21 program proceeded with the objective that the spanwise pressure coefficient along any wing element line at the design flight condition should be nearly constant. Although the final wing design shows variations in surface pressure of several percent of the free stream dynamic pressure as compared with the ideal distribution, the resulting spanwise variation of inflow is considered sufficiently small, and the X-21 flight tests have not indicated any loss of laminar flow area from this cause alone.

Low speed testing is highly recommended because of the large amount of configuration variations which can be investigated for low cost. Though not always 100% correct the general rule can be followed that at a given position on the wing surface, if the nacelle is added such that no change in the pressure there takes place under low speed test conditions, then the pressure at that same point in a compressible flow will also be the same with or without the added protuberance. This allows changes to the fuselage or nacelles or pylons in a low speed tunnel which minimize the pressure disturbances from these sources, with the good expectation that the same desirable effects will also be realized at high Mach number conditions. As a general rule, it also is recommended that as soon as possible in the wind tunnel program the wing configuration should be tested with nacelles, pylons and other appurtenances which can conceivably cause an influence on the wing pressure distribution. For example, the main engine nacelles which are aft-mounted on the fuselage of the X-21 were always tested in conjunction with the wings, since it was discovered early in the program that these nacelles could cause a pressure coefficient change of the order of .05 to the inboard wing upper and lower surface.

The turbulent wedge regions of the wing are available for sizable contour modifications. These are narrow wedges which stream aft on either side of the pylon, nacelle or wing root intersection in which turbulent flow is anticipated in spite of LFC. No slots are cut into the area. No advantage of this was taken on the X-21 program, but it does represent an important area of freedom for consideration in other designs.

ENGINEER	NORTHROP CORPORATION NORAIR DIVISION	PAGE 7.03
CHECKER		REPORT NO. NOR-67-136
DATE June 1967		MODEL X-21A

7.3 CONTOUR AND LOCATION OF WING MOUNTED NACELLES

The design objective of the LFC airplane is that it shall exhibit laminar flow over the greatest possible portion of the exposed wing area. It is important that the placement and configuration of all nacelles, fairings or other protuberances which are to be attached to the wing should be so shaped and located that a minimum of distortion shall be created in the wing pressure distributions. Many mutually dependent considerations must be weighed in locating the nacelles on the wing. These include the diameter of the nacelle, the ground clearance, sonic fatigue problems and a number of others, none of which are unique to the LFC airplane. Some of these considerations are, of course, of more importance to LFC, an example being a decision to locate propulsion nacelles on the wing, whereas purely from the standpoint of pressure distribution uniformity, it would be preferable to mount them on the fuselage. Certain of these considerations will be elaborated upon in the following paragraphs:

7.3.1 Maximum Nacelle Diameter

Obviously the nacelle diameter of wing mounted nacelles should be minimized insofar as possible. This rule is usually followed, of course, from the standpoint of drag reduction. However, the large diameter nacelle has a profound influence on the pressure distribution. One compensating change is to extend the length of the pylon between the nacelle and the wing, but the ground clearance may become a problem. Longitudinally, the maximum diameter of the nacelle should be separated by a large distance from the maximum thickness of the wing. From the standpoint of inlet or compressor noise this may favor moving the maximum nacelle thickness behind the maximum wing thickness.

7.3.2 Length of Pylon Allowable

As stated it may be desirable to increase the pylon length but the distance available may be minimized by negative dihedral of the wing, large nacelle diameter, or by short landing gear struts.

7.3.3 Longitudinal Position of Maximum Thickness

The superposition of regions of accelerated flow from the wing maximum thickness and from the pylon-nacelle combination should be avoided. Otherwise, locally reduced pressures in this area will result in regions of locally high crossflow, and other problems associated with spanwise pressure gradients, and can set the pressure rise requirements of the main suction compressor.

ENGINEER	NORTHROP CORPORATION NORAIR DIVISION	PAGE 7.04
CHECKER		REPORT NO. NOR 67-136
DATE June 1967		MODEL X-21A

7.3.4 Pylon Thickness

If a thin airfoil section is desirable for a pylon supporting a nacelle from the lower wing surface, it must be borne in mind that if the pumping compressors are in the nacelle, all the flow coming from the suction ducts in the wing must pass through this pylon. This may result in thickness greater than originally intended and may lead to a design in which the pylon is discarded in favor of a nacelle flush against the surface of the wing.

7.3.5 Lower Surface Maximum Negative Pressure Coefficients

The compressor system recommended for a swept wing LFC installation consists of a high pressure compressor coupled with a low pressure compressor, although for some other applications other arrangements may prove optimum. The terms "high pressure" and "low pressure" refer to the areas of the wing from which the suction air is drawn by each of these two compressors. Obviously, the lower surface is served by the high pressure compressor since the external pressures over the lower surface are always greater in absolute magnitude than on the upper surface. This compressor arrangement loses its advantages unless the maximum negative pressure coefficient which the high pressure compressor must provide remains sufficiently below the most negative pressure in the system. This imposes on the configuration design a requirement that the pressure coefficient on the wing lower surface never be greater than a specified value. This requirement is in addition to requirements on maximum allowable cross-flow Reynolds number and of spanwise pressure uniformity.

7.3.6 Effects on the Wing Upper Surface

Two undesirable effects can occur on the wing upper surfaces as a result of the lower surface nacelle-pylon installation. First, if the pylon passes above the stagnation line of the wing, a turbulent wedge is created by the intersection streaming aft from the leading edge on the upper surface of the wing, thus eliminating a large portion of laminar area. If the major portion of the volume of the nacelle is not kept aft of the maximum thickness point on the wing there will likely be an appreciable pressure disturbance on

ENGINEER	NORTHROP CORPORATION NORAIR DIVISION	PAGE 7.05
CHECKER		REPORT NO. NOR-67-136
DATE June 1967		MODEL X-21A

the wing upper surface, particularly near the leading edge. Even with the application of these principles in the X-21 pumping nacelle design, the pressure coefficient on the wing upper surface at 1½% of chord was changed by an order of 0.10 between nacelle-on and nacelle-off in tests at high speed. Other proposed X-21A nacelles having a larger proportion of their volume moved closer to the leading edge had a much greater disturbing effect on the upper surface pressures. This was true even of pylons which had their leading edge at 30% chord on the wing lower surface.

7.3.7. Camber of Nacelle and Pylon

In the X-21 program cambering the nacelle in the plan view was a powerful influence in minimizing local regions of distorted flow. It is found that the proper contours in the sides of the pylon or nacelle generally are similar to the paths of the otherwise undisturbed potential flow streamlines on the wing lower surface. The ideal procedure would be to define a stream tube in the vicinity of the wing having the required maximum cross sectional area and to build the pylon and nacelle combination to conform to the surfaces of this stream tube. Presumably, a design would evolve which would have negligible influence on wing pressure distribution. This should be a design goal; however, the accelerations of flow around the forward portion of the nacelle will influence at least the level of the wing pressure.

7.3.8. Local Airfoil Modification

It appears probable that the aerodynamicist's most effective tool for minimizing the influence of nacelles and pylons on the wing pressure is the local modification of the airfoil shapes. One proposed method takes the incremental pressure field caused by the nacelle, and by theoretical means designs a new airfoil section changed from the original in such a way as to produce an equal and opposite pressure disturbance. This was done on the X-21A in the limited region of the inboard forward lower surface adjacent to the pumping nacelle, where the nacelle causes an impediment to the spanwise flow along the leading edge. The wing was thickened slightly for about three feet spanwise in this area and as far aft as 15% chord. This served to accelerate the flow and eliminate the slight stagnation zone created by the nacelle.

ENGINEER	NORTHROP CORPORATION NORAIR DIVISION	PAGE 7.06
CHECKER		REPORT NO. NOR 67-136
DATE June 1967		MODEL X-21A

7.3.9 Proximity to Inboard End of LFC Aileron

If the nacelle installation is laid out so that it is in proximity to the inboard end of an LFC aileron, then it may be possible to design the inboard rib of the aileron to swing inside the pumping nacelle and allow the flow from the aileron surface itself to be ducted inboard into the nacelle rather than forward across the aileron spar.

7.3.10 Number of Nacelles per Wing

To minimize the area of turbulent wing surface, the minimum possible number of nacelles per wing is preferable. The influences of these nacelles can never be completely eliminated and if they are such as to create problems incapable of solution with the suction system, then it is better to concentrate them in one area of the wing so that each one does not cause its own reduction in laminar area. For example, installation of two propulsion engines in a single pod should be considered.

7.3.11 Toe-In and Toe-Out of Nacelles and Pylons

This alignment parameter does not have a powerful influence on pressure distribution but toe-in (toe-out) can be used to equalize peak pressure coefficients on opposite sides of a nacelle.

7.4 CONTOURING THE FUSELAGE FOR OPTIMIZATION OF THE INBOARD WING PRESSURE DISTRIBUTION

A difficult task for the LFC airplane designer is the determination of the proper wing placement and the contouring of the fuselage to obtain a favorable pressure distribution in the region of the wing root. The problem is complicated by the necessity for avoidance of abrupt surface contours which might lead to shock waves on the fuselage when flying at the design flight condition. Just as in the case of wing-mounted nacelles, this problem can more easily be solved by making theoretical studies and a considerable amount of low speed wind tunnel testing followed by high speed testing and repetitions of this cycle.

ENGINEER	NORTHROP CORPORATION NORAIR DIVISION	PAGE 7.07
CHECKER		REPORT NO. NOR 67-136
DATE June 1967		MODEL X-21A

Consider the case of a wing tested without fuselage. If the wing is tapered and/or any of the element lines are swept, the plane of symmetry of the wing imposes the end condition that there be no lateral velocity components. This end condition does not exist elsewhere along the semi-span wing, and therefore the same chordwise pressure distributions cannot be expected to apply even though the airfoil sections are the same. The addition of a fuselage further restrains the streamlines. Thus the ideal pressure distribution of straight isobars along wing element lines cannot be expected in the region of the wing root.

It appears probable that one type of airplane to which LFC will be applied is the cargo transport, a major requirement for which is that the cargo bay be uninterrupted through the region of the wing carry-through. This, then, suggests that the configuration either be high wing or low wing.

The X-21 is a high wing aircraft and the problems of designing the top fuselage fairing for that airplane help to illustrate some of the problems that might be encountered on a new design. The parallel is not perfect because the existing fuselage of the B-66 imposed certain restraints in optimizing the X-21 design.

It is recommended that a maximum effort be expended in the twisting and cambering of the wing near the side of the fuselage, in order to retain a uniform pressure distribution in this area. This should be done with the wing in as near a final position on the fuselage as possible, and with an estimate of the proper fairing. This was done in the X-21 design, but it was found that in spite of this the pressures over the fuselage were less negative than on the adjacent wing sections. It was found that the influence of contouring the fairing in the plan view was very local. The major improvement in wing pressures was obtained with a fairing which had a small radius of curvature directly over the leading edge of the wing in the side view, plus a considerable change in curvature over the latter 50% of chord, where the long sloping fairing raised the top of the fuselage almost one maximum wing thickness above the upper surface. This fairing has a profound effect on wing pressures as far as the mid semi-span at Mach 0.8. Figure 7.1 shows the side view of this fairing and also shows the original fuselage structural top for the original WB66D airplane. Figure 7.2 shows the chordwise pressure distributions at a wing station near the fuselage to illustrate the effect of changing from an earlier fairing to the fairing finally adopted. The improvement is easily seen in this Figure.

ENGINEER	NORTHROP CORPORATION NORAIR DIVISION	PAGE 7.08
CHECKER		REPORT NO. NOR 67-136
DATE June 1967		MODEL X-21A

7.5 CONTOURING THE WING TIPS

Of paramount importance to the design of an aircraft employing LFC is the attainment of laminar flow over the greatest possible surface area. The wing tip region poses a problem because of the difficulty in extending a uniform pressure pattern into the area. At the extreme tip the pressures on the upper and lower surfaces of a lifting wing tend toward a common level. These changes pose problems in the design of internal ducting for the removal of the wing tip boundary layer air, and in proper application of the boundary layer theory for predicting wing tip suction requirements. Compensating features of the wing tip are the low chord Reynolds number for which laminar flow must be designed and also the reduced leading edge radius, if the wing carries appreciable taper.

Inspection of the literature dealing specifically with pressure distributions over the wing tips shows that curving sweep-back of the leading edge, increasing camber and relative thickening of the airfoils will straighten the isobars and delay the drop-off of local lift coefficient along the span. Low speed wind tunnel tests on the X-21 wing verified these principles. It is found that on a swept tapered wing in which the wing tip has merely been squared off the isobars tend to sweep forward toward the leading edge of the tip chord. The rear pressure rise is initiated much further forward on the chord than at wing stations further inboard. These two effects are alleviated by the aft curving of the leading edge and by a thickening of the rear half of the airfoils in the tip region. In the X-21 design, a fairing of the wing tip beginning at 95% of semi-span on the leading edge and fairing out at 50% of chord of the theoretical tip chord was adequate to avoid the forward sweep of the isobars which would otherwise have occurred. In addition, a tendency at cruise conditions toward separated flow over the tip airfoils initiating at the leading edge was avoided by a local increase in leading edge radius over the outer 10% of semi-span.

ENGINEER	NORTHROP CORPORATION NORAIR DIVISION	PAGE 7.09
CHECKER		REPORT NO. NOR 67-136
DATE June 1967		MODEL X-21A

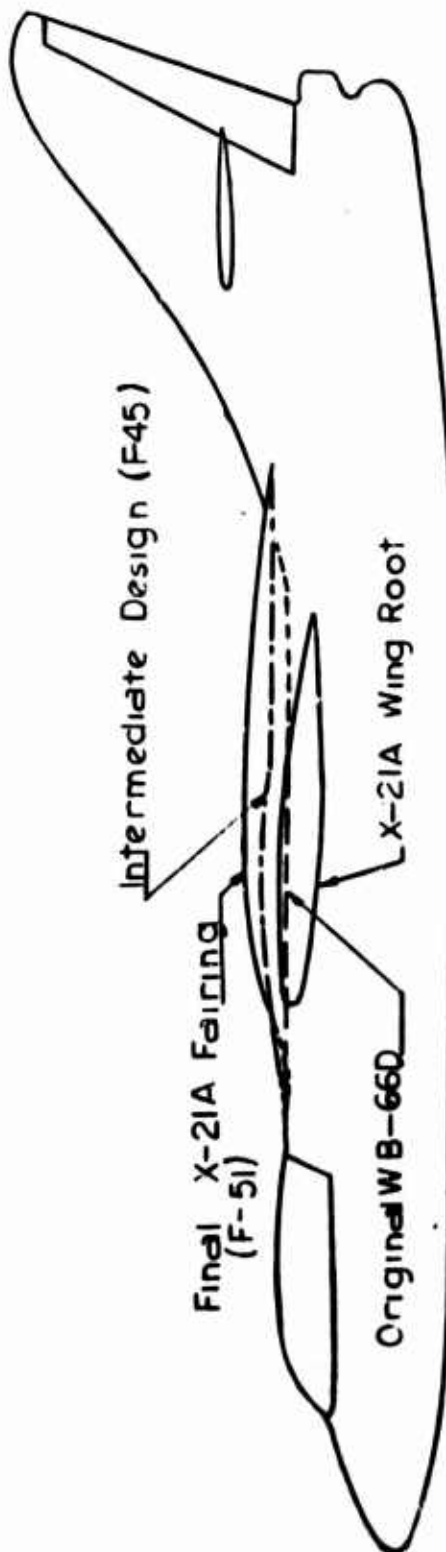
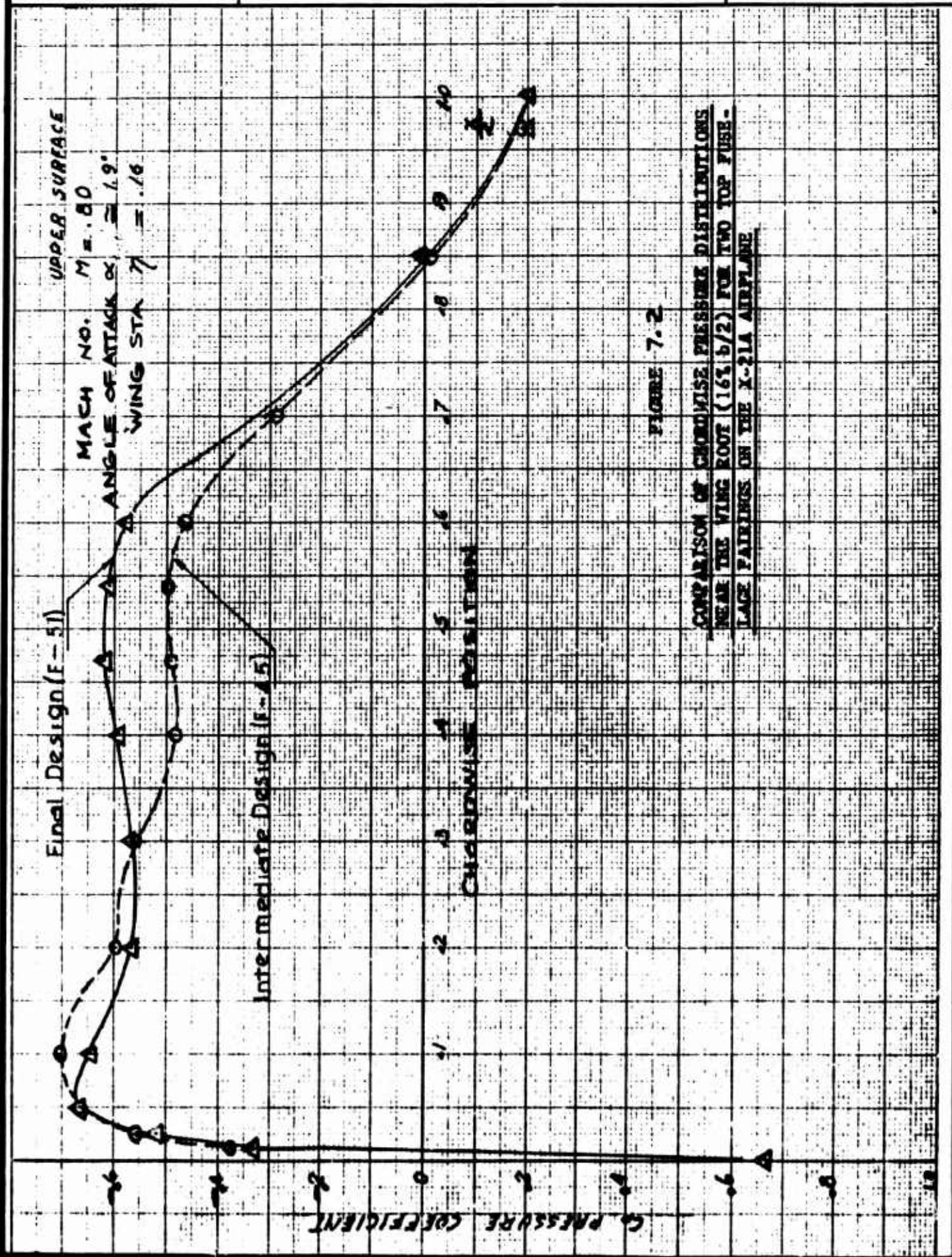


FIGURE 7.1

X-21A TOP FUSELAGE FAIRINGS FOR WING PRESSURE DISTRIBUTION IMPROVEMENT AND ORIGINAL WB-66D CONTOUR

ENGINEER	NORTHROP CORPORATION NORAIR DIVISION	PAGE 7.10
CHECKER		REPORT NO. NOR 67-136
DATE June 1967		MODEL X-21A



ENGINEER	NORTHROP CORPORATION NORAIR DIVISION	PAGE 8.00
CHECKER		REPORT NO. NOR 67-136
DATE June 1967		MODEL X-21A

SECTION 8

PUMPING SYSTEM

BY:

W. A. Monahan, Jr.

March 1964

Revised April 1967

ENGINEER	NORTHROP CORPORATION NORAIR DIVISION	PAGE
CHECKER		8.01
DATE		REPORT NO.
June 1967		NOR 67-136
		MODEL
		X-21A

TABLE OF CONTENTS

		<u>Page No.</u>
8.0	Pumping System	8.02
8.1	Pumping System Requirements	8.02
8.1.1	Problem Statement	8.02
8.1.2	Compressor Arrangement	8.02
8.1.3	LFC Airflow	8.03
8.1.4	Compressor Power Source	8.04
8.1.5	Thrust Specific Fuel Consumption	8.04
8.1.6	Equipment Size and Weight	8.05
8.1.7	Requirement Specification	8.05
8.1.8	Suction Flow Control Valves	8.06
8.1.9	Bleed Air Ducting	8.09
8.1.10	Collapsing Pressures	8.11
8.1.11	Noise Control	8.11
8.1.12	F.O.D. Screens	8.11
8.1.13	Inter-Compressor Duct	8.11
8.2	System Performance Analysis	8.12
8.3	Description of X-21A Pumping System	8.12
8.3.1	Problem Statement	8.12
8.3.2	Compressor Arrangement	8.12
8.3.3	LFC Airflow	8.13
8.3.4	Compressor Power Source	8.14
8.3.5	Thrust Specific Fuel Consumption	8.14
8.3.6	Equipment Size, Weight, and Characteristics	8.15
8.3.7	Requirement Specification	8.16
8.3.8	Suction Flow Control Valves	8.16
8.3.9	Bleed Air Ducting	8.23
8.3.10	Collapsing Pressures	8.24
8.3.11	Noise Control	8.24
8.3.12	F.O.D. Screens	8.25
8.3.13	Inter-Compressor Duct	8.25
8.4	Description of LFC-LTA System	8.25
8.4.1	Problem Statement	8.26
8.4.2	Compressor Arrangement	8.26
8.4.3	LFC Airflow	8.27
8.4.4	Compressor Power Source	8.27
8.4.5	Thrust Specific Fuel Consumption	8.28
8.4.6	Equipment Size and Weight	8.29
8.4.7	Requirement Specification	8.29
8.4.8	Internal Flow System and Flow Control Valves	8.29
Table I	Suction Valve Airflow and Design Data	8.30
Figures 8.1 through 8.16		8.31

ENGINEER	NORTHROP CORPORATION NORAIR DIVISION	PAGE 8.02
CHECKER		REPORT NO. NOR 67-136
DATE June 1967		MODEL X-21A

8.0 PUMPING SYSTEM

This section describes: 1) the general equipment and installation requirements for a pumping system; 2) the analytical development of the recommended system, and a typical performance analysis; 3) a description of the practical application of these precepts in the X-21A LFC Demonstration Airplane Program; and 4) a description of the pumping system in an LFC large logistics transport study.

8.1 PUMPING SYSTEM REQUIREMENTS

8.1.1 Problem Statement

The job of the pumping system is to apply suction to the wing in such a manner that air near the surface will be removed and ultimately discharged aft at or near free-stream conditions. Figure 1.14 shows the pressure coefficients and pressure levels that exist on a typical wing during high altitude cruise. Note the chordwise pressure profile as well as the general difference in levels between the upper and lower surfaces. Other wings will have different coefficients, and with different flight conditions, different pressure levels will exist, but the profiles will have similar shapes. Even for a given wing and flight condition, any one curve such as this can show profiles at one selected wing station only.

LFC is primarily a cruise device, and the shaded portion of Figure 1.2 shows the flight regimes where LFC will most probably be used for subsonic flight. The pumping system may be called on to perform anywhere in the flight regime, but for purposes of specifying a design point for the suction compressors, the high-altitude, low weight, cruise condition should be chosen. Maximum corrected flow will occur at this condition.

8.1.2 Compressor Arrangement

From Figure 1.14 it is apparent that use of a single suction compressor would require that all flow except that from the lowest pressure would need to be throttled to the same low pressure. Dividing the total suction into a number of levels, each serviced by a separate compressor is a more efficient solution in terms of suction power required. For reasons of relative simplicity, it is generally desirable to use only two suction levels, dividing the total suction air into two quantities, arbitrarily called "low pressure" and "high pressure" as shown in Figure 5.3. Two principal schemes for pumping the "low" and

ENGINEER	NORTHROP CORPORATION NORAIR DIVISION	PAGE 8.03
CHECKER		REPORT NO. NOR 67-136
DATE June 1967		MODEL X-21A

"high" pressure levels are shown in Figure 8.1. Figure 8.1A shows the parallel arrangement, wherein each of the compressors operates independently and discharges to atmosphere; Figure 8.1B is a series system wherein the low pressure quantity is pumped up to the pressure level of the high pressure quantity and then the entire amount compressed and discharged to atmosphere. The latter system is the one used in the X-21A airplane.

8.1.3 LFC Airflow

LFC airflow can be computed from the methods given in Section 2. To allow for deviations from the calculated requirements of the suction system, a range of airflows and pressure ratios required should be specified rather than a single-combination point.

The adequacy of an engineering proposal to meet airflow and pressure ratio requirements should be checked by considerations of the fundamentals of compressor design. The map for the compressor selected should be examined to assure that the operational combinations of airflow and pressure ratio have a safe and reasonable stall margin at the high altitude design cruise condition, where the corrected weight flows are greatest. In Figure 8.2 points of interest are the "nominal" airflow, point "A" on the compressor map, which should be in a region of high efficiency for each compressor, and the so-called "minimum-minimum" condition, "min-min" refers to the point on each compressor map representing the flow and pressure ratio at minimum low pressure and minimum high pressure system flows. These are "nominal" flows, minus, for example, the recommended 7%. The "min-min" point on each compressor should have as much stall margin as is compatible with handling the "nominal" flow efficiently. A compressor sized to give about 10% airflow stall margin at "nominal" is recommended, at least as a first approximation. More airflow stall margin can be had at a fixed pressure ratio by decreasing compressor size, while compressor changes such as altering blade shape or the number of stages may be necessary to place the operating point in the highest possible efficiency island.

With a compressor optimized for a single high corrected flow design point, like point "A" on the compressor map, stall may occur at low flow rates. Although it should generally be unnecessary, if operation at a low LFC flow rate such as point "B" on the map is desired, the compressor can be moved out of stall by adding enough auxiliary air to the LFC airflow to move the operating point to a stall free region. See paragraph 8.3.3 for a discussion of this auxiliary air feature on the X-21A.

ENGINEER	NORTHROP CORPORATION NORAIR DIVISION	PAGE 8.04
CHECKER		REPORT NO. NOR 67-136
DATE June 1967		MODEL X-21A

Inlets to most high performance axial flow compressors are carefully designed to minimize pressure distortion, but for an LFC suction compressor, highly distorted compressor face flow patterns are likely to exist. These patterns, in terms of regions of constant Mach number, should be estimated and included in the specification requirements.

Research has indicated that noise may have a deleterious effect on maintaining laminar flow. It may be necessary that suction compressors be designed to minimize blade passage noise. The possibility exists that this noise will propagate upstream through the air ducting to disturb the laminar boundary layer at the slots. Special attention should be given to rotor-to-stator separation, blade spacing, unequal strut locations, and other techniques to minimize noise generation.

8.1.4 Compressor Power Source

Two (2) fundamental methods for supplying power to the compressors are shown in Figure 8.3. Appendix C of IAS Paper 61-52 develops analytically the relative merits of the two schemes, and it is shown that while Class I systems are more efficient, their advantage is small and other considerations could decide in favor of Class II.

Power extraction from the main propulsion engine (Class I system) by "bleed and burn" is the method used in the X-21A airplane.

8.1.5 Thrust Specific Fuel Consumption (TSFC)

Several parameters of compressor-turbine design exert a major influence on performance while others have little effect. For transports or long-range aircraft, overall TSFC and size will be important factors in equipment selection. The required pressure ratio of the high pressure compressor has a greater effect on TSFC than any other cycle parameter. For a bleed-and-burn system other cycle parameters having a major influence on TSFC are turbine pressure ratio and compressor nozzle pressure ratio. In addition to its primary function of removing air from the boundary layer, the pumping system can make an efficient contribution to the total airplane thrust. Where the pumping system power is taken directly from the engine, as in Class I of Figure 8.3, the result is to reduce primary jet velocity, thereby improving primary engine propulsion efficiency. The pumping system jet discharge, being at relatively low velocity, also should have a high propulsion efficiency. This points up the fact that power extracted from the primary engine for pumping purposes also produces thrust efficiently, and the "trade-offs" in relative proportions of thrust, with their respective fuel consumptions, must be rigorously analysed.

ENGINEER	NORTHROP CORPORATION NORAIR DIVISION	PAGE 8.05
CHECKER		REPORT NO. NOR 67-136
DATE June 1967		MODEL X-21A

For a long-endurance aircraft, low TSFC is required with weight and size becoming less important factors. To this end, an exhaust heat regenerator may show an endurance gain in spite of its additional weight.

The performance figures for the pumping equipment are integrated with those of the propulsion system to arrive at an overall TSFC.

The take-off thrust augmentation potential of the pumping system can be appreciable and hence should not be overlooked. In general, for a bleed and burn system, maximum horsepower available limits the thrust potential of the compressor. Horsepower limitations are related to the maximum quantities, temperatures, and pressures of the bleed air available, turbine case pressures, transmission horsepower capabilities, and suction duct pressure-differentials. Any modification to a bleed burn system to improve its take-off thrust will probably result in a decrement to its cruise performance. Where compressor power is derived from a separate turboshaft engine, suction compressor system thrust can be a significant fraction of the total, perhaps to the extent of eliminating a complete engine. Excess power from the separate compressor drive engine can be used as an auxiliary power supply.

The necessity of design-point optimization is pointed out in Paragraph 8.3.5.

8.1.6 Equipment Size and Weight

A lightweight, compact system is desirable not only for the usual reasons of low airplane weight and ease of installation, but wind tunnel and flight tests have shown that aerodynamic disturbances of wing pressure distribution must be minimized. Ideally, surface pressure, for any given percent chord, should remain the same all along the span. In this way, lines of constant pressure, or isobars, will coincide with straight suction slots. Pylons, nacelles, or other additions to the wing will distort the isobar patterns and result in non-uniform slot pressures. (See more complete discussion of this effect in Sections 1 and 7). This makes the job of predicting and applying proper suction more difficult. Minimizing compressor and compressor pod size, particularly width, helps reduce pressure disturbances and hence improves LFC.

8.1.7 Requirement Specification

All of the foregoing considerations and others of importance can be combined into a specification typical of those applying to turbomachinery.

ENGINEER	NORTHROP CORPORATION NORAIR DIVISION	PAGE 8.06
CHECKER		REPORT NO. NOR 67-136
DATE June 1967		MODEL X-21A

8.1.8 Suction Flow Control Valves

8.1.8.1 General Considerations, Number Required

The overall suction rate on the wing surfaces can be raised or lowered by varying the RPM of the suction compressors. However, to vary the suction on certain sections of the wings independently of other sections of the wing, suction control valves are required. The number of valves required depends upon the type of aircraft and its mission. A demonstration aircraft such as the X-21A has a need for varying the suction independently over many wing "strips", as well as varying the suction on the inboard strips independently of the outboard strips. The X-21A uses a total of 96 suction control valves.

The number of suction control valves required for a production long range aircraft would depend on the extent that the suction requirements varied with the minimum and maximum cruise altitudes, and with the range of airspeeds and angle of attacks at these cruise altitudes. Suction control valves would probably be required only for the wing leading edge region. Only 12 suction control valves are required for a laminar flow control large transport airplane described in Section 8.4.

8.1.8.2 Valve Location

Location of the suction control valves is mainly a function of the location and routing of the suction system and mixing chambers. As shown on Figure 8.8, the X-21 valves controlling the forward and mid-wing suction are located in the wing in bays located between the inboard and outboard fuel tanks. The trailing edge valves are located in the suction pod itself. Compressor inlet distortion must be considered if the valves are located just upstream of the compressors. Where valves are located near the compressors, flow tests are recommended to define if suitable compressor inlet conditions exist. Location of the valves must also be such that access to the valves can be provided for servicing. The valves should be given the same maintainability considerations as any functional fuel or hydraulic component.

ENGINEER	NORTHROP CORPORATION NORAIR DIVISION	PAGE 8.07
CHECKER		REPORT NO. NOR 67-136
DATE June 1967		MODEL X-21A

8.1.8.3 Valve Sizing and Flow Characteristics

The valve sizes and mixing chamber pressures can be determined analytically in the same way that the tributary nozzles are sized in the suction duct analysis of Section 4. Because of the unusual shape and arrangement of valves and mixing chambers, it is advisable to make flow tests to determine the pressure distribution in the mixing chambers.

In general, the valves are sized so that they are about 70% open for the design suction flow rate, thereby providing additional flow capabilities in the fully open position.

The choice of butterfly or flapper valves depends on their location in the system. Butterfly valves are very satisfactory in upstream applications, but if valving is used near the point where suction air is discharged into the compressors, flapper valves are desirable. They can be designed both to minimize separation, which can propagate disturbances upstream, and to minimize total pressure losses at the valve discharge. Valves should be designed to fully close, if practicable, even though such a degree of modulation is far beyond that which will be required for laminar flow. The full-closure ability will be found useful for system trouble-shooting.

To prevent unnecessary loss of energy, it is recommended that the flapper type flow control valves exhaust into a mixing chamber, rather than a plenum chamber, so that part of the kinetic energy of the valve exit flow can be recovered. On the X-21A the valves are shaped like rectangular nozzles, discharging in a direction substantially aligned with the flow in the mixing chamber. The side of the "nozzle" nearest the mixing chamber is a movable vane, supplying the valve action. The wall of the nozzle opposite the vane fairs smoothly into the wall of the mixing chamber, thereby minimizing regions of separated flow. In a production design most of the suction ducts would discharge into the mixing chamber through fixed nozzles rather than through flow control valves.

Unstable pressure fluctuations caused by flow separation or valve "flutter" are potentially dangerous in that these fluctuations might propagate upstream through the ducting system and slots and disturb or prevent the development of laminar boundary layer flow over the wing. Flow separation on the flapper type valves can be minimized by limiting the angle of airflow over the flapper.

ENGINEER	NORTHROP CORPORATION NORAIR DIVISION	PAGE 8.08
CHECKER		REPORT NO. NOR 67-136
DATE June 1967		MODEL X-21A

Unstable flow separation at bends in the ducting and valves can be minimized by contracting the flow area through the bend and/or by using turning vanes. Valve flutter can be minimized by eliminating "free-play" in the valves.

8.1.8.4 Valve Bodies

Valve bodies of fiberglass laminates were used successfully on the odd-shaped X-21A valve bodies with their turns, twists, and contractions to meet the flow paths. Where upstream ductwork can incorporate these directional changes, valve bodies can be simpler in design. Welded aluminum valve bodies may prove less costly and easier to maintain, or perhaps thin-wall castings may prove less expensive and lighter in weight especially when dealing with the larger sized valves and larger quantities. The materials to be used to fabricate the valve bodies are, therefore, largely dependent upon system design.

If fiberglass laminates are used, it is recommended that finished valve bodies with all cutouts therein be oven post-cured for a period of from 12 to 16 hours at 275°F to cause a relatively rapid dimensional shrinkage by accelerating "polymer growth" and thereby preventing any later change in shape when installed and operated in the aircraft. For a production contract it is recommended that sectional metal cores of high dimensional stability and capable of re-use, be used on which to form the body shapes, instead of plaster male cores. The long-range tooling cost will surely be less, and, more important, only negligible dimensional variations will exist between parts.

8.1.8.5 Valve Actuators

Actuators for the valve can be electric, hydraulic, pneumatic or possibly mechanical. The actuator selection depends on the many factors such as availability of power, reliability, size, and cost, that have to be considered in the design of any aircraft system. Small D.C. motors were used for actuators on the X-21A. Actuation speed of the valves also enters into the actuator selection. On the X-21 an actuation time of from 10 to 30 seconds was specified for the valves to go from the closed to the open position or vice versa. This operating time was too slow; a faster operating time in the 5 to 10 second range is preferable.

ENGINEER	NORTHROP CORPORATION NORAIR DIVISION	PAGE 8.09
CHECKER		REPORT NO. NOR 67-136
DATE June 1967		MODEL X-21A

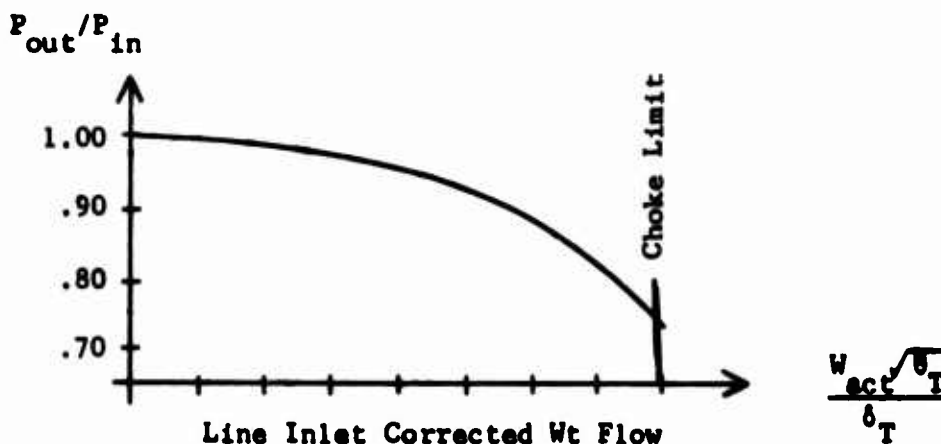
8.1.8.6 Valve Flapper Position Indicators

A valve position indication is very useful in adjusting suction levels. Position of the valves may be indicated directly through a potentiometer linked to the flapper shaft, or an indirect indication can be used such as flow measuring and/or duct pressure measuring instruments.

8.1.9 Bleed Air Ducting

For the case of a bleed-burn LFC pumping system, the configuration may necessitate a long bleed-air run between the engine and the pumping system. For just such a case in the X-21A, unique engine bleed curves were developed based on engine specification bleed data and calculated bleed line pressure drop characteristics. The procedure is as follows:

- 1) From compressible flow analysis and using assumed "k" factors for sections of line, a curve of pressure ratio versus corrected weight flow for the external collector manifold and line is made:



Where W_{act} = actual weight flow rate, lb/sec.

θ_T = temperature ratio ($T_{inlet}/T_{standard\ atmospheric}$) where T is absolute temperature.

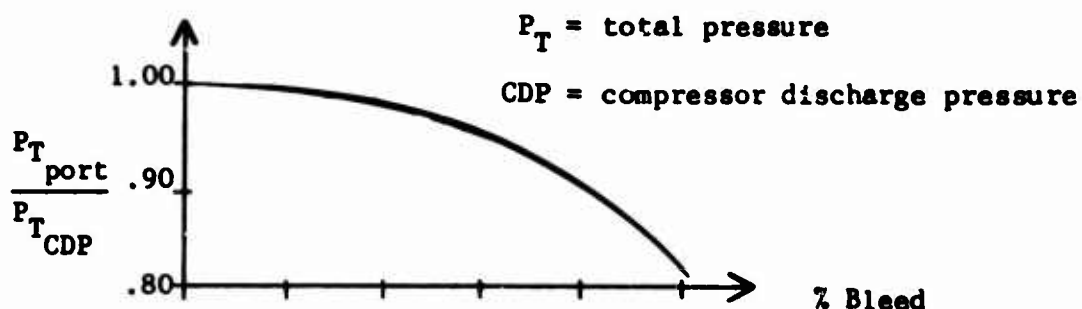
δ_T = pressure ratio ($P_{inlet}/P_{standard\ atmospheric}$) where P is absolute pressure.

The line can be so sized that choking will occur (that is, $\frac{W_{act} \sqrt{\theta_T}}{\delta_T} = .344$, at which value $M_n = 1.00$) at that actual

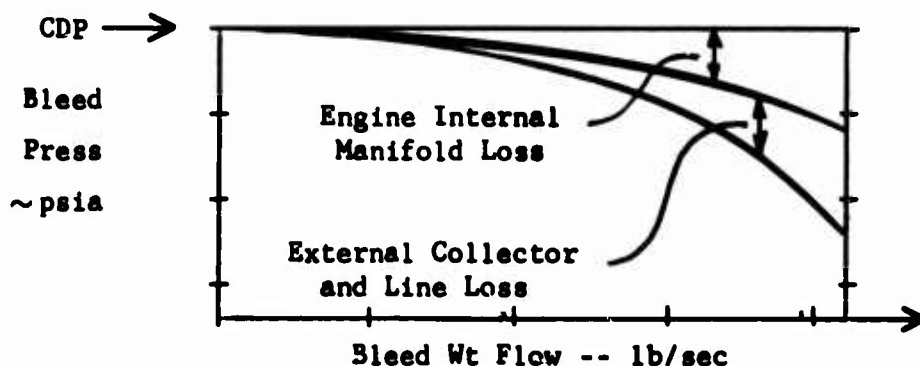
weight flow representing the maximum allowable percentage bleed from the engine. Thus the engine is automatically protected from over-bleeding.

ENGINEER	NORTHROP CORPORATION NORAIR DIVISION	PAGE 8.10
CHECKER		REPORT NO. NOR 67-136
DATE June 1967		MODEL X-21A

- 2) From Engine Model Specification data, engine internal manifold losses are plotted:



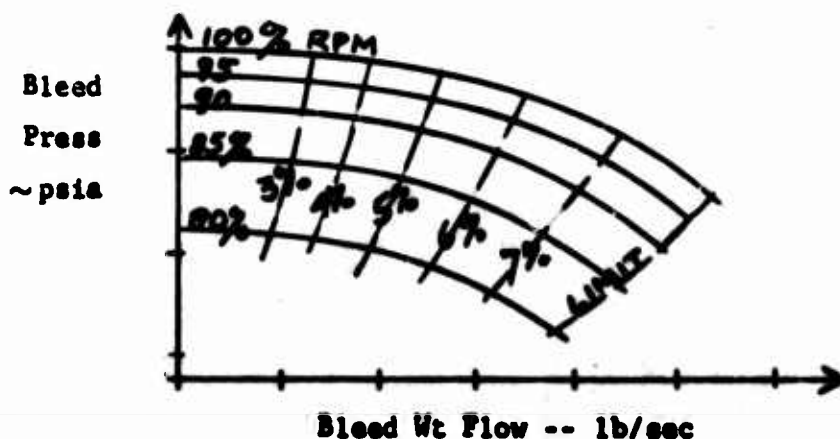
- 3) For the design flight condition (and repeated for other flight conditions, if more than one), this is converted into actual quantities:



$$W_{\text{actual}} = \frac{\% \text{ bleed}}{100} \times W_{\text{inlet}} \quad \delta_T = \frac{P_T \text{ @ external collector inlet}}{14.7 \text{ psia}}$$

$$W_{\text{corr.}} = \frac{W_{\text{act}} \times \sqrt{\theta_T}}{\delta_T} \quad \delta_T = \frac{T_T \text{ @ external collector inlet}}{519^\circ \text{ R}}$$

- 4) The pressure loss is then subtracted from engine compressor discharge pressure for various RPM settings. A separate family of curves is made for each design flight condition.



ENGINEER	NORTHROP CORPORATION NORAIR DIVISION	PAGE 8.11
CHECKER		REPORT NO. NOR 67-136
DATE June 1967		MODEL X-21A

8.1.10 Collapsing Pressures

Maximum normal pressure levels for inlet duct collapsing loads occur at sea level static operation during system check-out. Failure of controls can and does occur, and, if overspeed results, high pressure differentials will be reached. In case of a double failure, such as both speed control and pressure control, damaging differentials can be reached. It is likely that pressure sensitive switches will be needed to limit differentials to tolerable values.

8.1.11 Noise Control

In addition to low noise design of compressors (Paragraph 8.1.3), if it is necessary to attenuate noise propagating upstream in the ducts, acoustical liners can be applied to the interior surface of each major inlet duct to attenuate high frequency noise generated by compressor blade passing intervals. Liner construction may be similar to that used on the X-21A (See paragraph 8.3.11) or of another design to achieve another desired result.

8.1.12 Foreign Object Damage Screens

Even with a rigorous program emphasizing housekeeping and cleanup during construction it may be impossible to achieve complete absence of loose hardware from the wing. Even with some type of in-plant vacuuming, suction compressors may dislodge nuts, bolts, rivets, and other hardware as the wing flexes. The solution is the use of F.O.D. screens until the wing becomes "cleaned out." On the X-21A, F.O.D. screens have returned their cost many times over in blades, compressors, and man-hours saved. They are judged to be necessary, not merely optional, at least until many flights are accomplished.

8.1.13 Inter-Compressor Duct

The duct between the two compressors and into which high pressure and trailing edge valves may discharge must be specially sized. The flow criterion is to present an optimum static pressure as LFC flow progressively enters the duct, but by so doing severe velocity distortions may result.

ENGINEER	NORTHROP CORPORATION NORAIR DIVISION	PAGE 8.12
CHECKER		REPORT NO. NOR 67-136
DATE June 1967		MODEL X-21A

8.2 SYSTEM PERFORMANCE ANALYSIS

As discussed in Section 8.1 the recommended sources of a major portion of the energy for an LFC compressor system are the main propulsion engines. In such a system, operation of the compressors exerts an influence on the performance of the main engines, and vice-versa. Hence, the analysis of both systems should be combined. The techniques of recommended procedure are discussed in connection with the main propulsion engines in Section 9.2.

8.3 DESCRIPTION OF X-21A PUMPING SYSTEM

8.3.1 Problem Statement

The X-21A has explored a flight envelope extending from sea level static to Mach .80 at about 44,000 ft. and attained mean aerodynamic chord Reynolds numbers to 40 million. See Figure 1.2. It was specified that the pumping equipment must provide airflow rates, at all LFC flight conditions, of from 85% to 130% of the nominal calculated airflow. These rather wide limits were necessary because of the unproven status of the airflow estimates.

Detailed design of the pumping system installation was to follow the general practices commonly used for engine installations: the same fuel and oil filtering, mounting, firewalling, fire zoning, and provisions for access were followed as if it were a propulsion engine. This concept led to a practical, reliable, and maintainable installation.

8.3.2 Compressor Arrangement

Both the series and parallel compressor systems were studied. The parallel system eliminated interaction between compressors inherent in a series system and hence reduced manipulation of suction flow control valves, but higher bleed flows were required.

The series system was selected because the components were smallest, pod bulk could be minimized, and wing isobars would remain straighter and near the ideal. It appeared likely that more could be learned about collector duct design and system control problems by using a series system. Additionally, TSFC and weight were low. Finally it was selected because it more closely resembled the arrangement which probably would be used in an operational airplane.

ENGINEER	NORTHROP CORPORATION NORAIR DIVISION	PAGE 8.13
CHECKER		REPORT NO. NOR 67-136
DATE June 1967		MODEL X-21A

8.3.3 LFC Airflow

An example of the compressor airflow and pressure ratio requirements for a typical cruise flight is shown in the following table. The flight condition is 41,300 feet altitude at Mach .75, made in 1965 after an enlarged tailpipe had been installed on the GTMC (gas turbine motor compressor, high pressure).

LFC COMPRESSOR	AIRFLOW W ~ lb/sec	AIRFLOW PARAMETER $\frac{W \sqrt{\theta}}{\delta}$	PRESSURE RATIO
ATMC, air turbine motor compressor (low pressure)	1.94	21	1.40
GTMC, gas turbine motor compressor (high pressure)	7.18	64	1.93

The tabulated data are plotted on compressor performance charts in Figures 8.4 and 8.5. Flow rates and pressure ratios are somewhat greater than had been estimated early in the program, due primarily to greater suction flow requirements in the nose and aft regions of the inboard wing. Because of the greater pressure ratio and also because of inlet flow distortions the GTMC often had operated near the surge line and had required the use of the auxiliary air scoop to avoid the surge line. Installation of a larger tailpipe moved the operating point farther from surge, making the use of the anti-surge air scoop unnecessary for normal operations. As explained in paragraph 8.1.3, the retractable auxiliary air scoop had been designed into the original installation to permit the addition of airflow to avoid compressor stall or surge in conditions wherein the flow rate was too low or the pressure ratio too high. The retractable anti-surge inlet is shown in Figure 8.6.

ENGINEER	NORTHROP CORPORATION NORAIR DIVISION	PAGE 8.14
CHECKER		REPORT NO. NOR 67-136
DATE June 1967		MODEL X-21A

8.3.4 Compressor Power Source

The moderate air pumping horsepower requirements of the low pressure compressor allowed the assumption that it should be driven by its own hydraulic or air turbine motor, and hence its power source was specified to be integral or geared to the common power source. The large horsepower requirements of the high pressure compressor could best be met by a hot-gas turbine, either a complete turbo-shaft engine or a bleed-burn turbine. Either high-pressure power source was acceptable from an efficiency standpoint, but the bleed-burn system was the one used on the X-21A.

Take-off thrust augmentation potential of the pumping system was studied for the X-21A for one bleed-and-burn system and for two turbo-shaft driven systems. Figure 8.7 shows the results of this analysis.

8.3.5 Thrust Specific Fuel Consumption

More importance was placed on functional design and installation considerations than on range performance optimization, hence low TSFC was not the primary consideration. The reasoning for this was that the attainment and evaluation of full-chord laminar flow and the difference in resulting drag could be assessed using a pumping system of virtually any efficiency as long as it had compressors of the proper pressure ratio and air flow characteristics; also, the X-21A was not, in other respects, optimized for range performance and hence there was little reason to do so in this one area. Additionally, the program schedule could only be accomplished by utilizing "off-the-shelf" hardware, and in fact, all proposals received utilized adaptations of turbine systems in current production.

The requirement to operate satisfactorily over a broad range of LFC flows and pressures coupled with the use of "off-the-shelf" turbines prevented the attainment of highest system efficiencies. To see what could be achieved by an optimization study, a narrow-range set of conditions was assigned and all equipment, except the propulsion engines, was re-designed for best efficiency at that point. The study showed that a 12% reduction in combined propulsion system and LFC pumping system TSFC could be realized by such optimization.

ENGINEER	NORTHROP CORPORATION NORAIR DIVISION	PAGE 8.15
CHECKER		REPORT NO. NOR 67-136
DATE June 1967		MODEL X-21A

8.3.6 Equipment Size, Weight, and Characteristics

Manufacturer AiResearch
 Model Specification SC-5402
 Model AiResearch System 386020
 Low Pressure Compressor ATMC 30-4
 High Pressure Compressor GTMC 75-5

	<u>ATMC 30-4</u>	<u>GTMC 75-5</u>
Compressor Diameter	13.3 in.	22.2 in.
Compressor Stages	2	3
Compressor Blades/Stage	15,19	23,27,28
Compressor RPM (at 100% Speed)	15,957	8,750
Compressor Dis. Nozzle Area	67.4 in ²	153 in ²
Turbine-to-Compressor Gear Ratio	3.76	4.80
Turbine Type	Axial Inflow	Radial Inflow
Turbine Basic Parts From	CSDS100-8	GTCP85-104
Turbine Stages	1	1
Turbine RPM (at 100% Speed)	60,000	42,000
Turbine Dis. Nozzle Area	12.56 in ²	26.5 in ²
Length, Overall	36.84 in.	47.50 in.
Length, Tailpipe(s)	none	27.50 in.
Fuel Specification	none	JP-4
Oil Specification	MIL-L-7808	same
Weight, Units Only	165 lbs	540 lbs
Weight, Valves and Regulators	8.7 lbs	20.1 lbs

Installed Performance	Sea Level Static (All Valves Open)		[45,000 Ft., .8 M ₀] *	
	<u>L.P.</u>	<u>H.P.</u>	<u>L.P.</u>	<u>H.P.</u>
Comp. Airflow, Actual	18.0	43.0	1.64	5.84
lbs/sec Corr.	18.5	44.0	16.95	49.1
Turbine Airflow, Each	1.13	4.80	.318	.86
lbs/sec Total		5.93		1.178
Turbine Airflow, Each	345	915	247	968
Fuel Flow, lbs/sec	none	233	none	48.4
Thrust, lbs (gross)	9	815	4.	109.4

*As explained in paragraph 8.3.3, and shown in Figures 8.4 and 8.5, typical suction flow rates used in the flight test program were somewhat greater than the original design values listed here, but well within the capabilities of the pumping units selected.

ENGINEER	NORTHROP CORPORATION NORAIR DIVISION	PAGE 8.16
CHECKER		REPORT NO. NOR 67-136
DATE June 1967		MODEL X-21A

8.3.7 Requirement Specification

The requirements were found to be achievable by a number of different combinations of compressors, control methods, and power sources. A design competition among suppliers was used to find the optimum combination of equipment.

In the proposal analysis, more importance was assigned to functional design and installation considerations than to performance optimization. The bleed-burn system was selected because of its small size, light weight, ease of installation, and excellent efficiency in cruise. Even including the weight of ducts, flexible joints, connections, insulations, etc., the bleed-and-burn system was lightest. The rather substantial amount of compressor bleed air required from the propulsion engine was less than half of that which was allowed by the engine specification.

8.3.8 Suction Flow Control Valves

8.3.8.1 General Description

The X-21A was to explore the full range of LFC from 15% under-suction, through 100% design suction, to 30% over-suction, each with wide variations in flow from adjacent wing ducts. The flow rates in individual ducts were controlled by flow control valves. The design, procurement, and use of these valves are covered in this section.

Figure 8.8 shows how suction air flows out of wing ducts through a collector system of ducts and valves, and then into the compressors. The assemblies of valves and ducting are largely contained within the wing between the front and rear spars as shown in the mock-up photograph, Figure 8.9. Because of integral fuel tankage in the rest of the adjacent wing the valve and duct area is referred to as the wing "dry bay." Photographs of the low pressure and high pressure "dry bay" valves and the trailing edge valves are shown in Figures 8.10, 8.11 and 8.12.

ENGINEER	NORTHROP CORPORATION NORAIR DIVISION	PAGE 8.17
CHECKER		REPORT NO. NOR 67-136
DATE June 1967		MODEL X-21A

8.3.8.2 Sizing and Analysis of Flow Control Valves

The sizing of the valves follows standard analysis techniques and is a function of the flow rate through the valve, the upstream pressure, and the downstream or mixing chamber pressures. The valve sizes and mixing chamber pressures can be determined in the same way that the tributary duct nozzles were sized. See Sections 4 and 5 for this analysis. Table I shows for each valve the section of wing surface that the valve controls, the suction flow rate, and the pressure upstream of the valve. The flight condition tabulated is for 40,000 feet altitude and a speed of $M = 0.7$.

The flow control valves were designed to be about 70% open at the 100% design flow rate, thereby providing additional flow capacity when the valve is fully open.

To prevent unnecessary loss of energy the flow control valves were designed to exhaust into a mixing chamber, rather than a plenum chamber. The valves were shaped like rectangular nozzles, discharging in a direction aligned with the flow in the mixing chamber. The side of the "nozzle" nearest the mixing chamber is a movable vane. The wall of the nozzle opposite the vane fits into the wall of the mixing chamber, thereby minimizing regions of separated flow.

8.3.8.3 Valve Bodies

Valve bodies were made of structural glass cloth laminate because it could be molded or shaped into the unique designs required with a minimum amount of tooling. Standardization of body shapes was not possible because of the individual requirements each valve had to meet in shape, sizing, actuator and motor location, space limitations, and special mounting features.

To meet various structural and stiffness requirements, low pressure valve bodies have .088 inch thick walls and .156 inch thick mounting flanges and vane guards. High pressure valve bodies have .080 inch walls except in outlet areas and flanges where walls are thickened to .150 inch for stiffness. Trailing edge valve bodies have .250 inch fluted core fiberglass with mounting flanges .187 inch thick.

ENGINEER	NORTHROP CORPORATION NORAIR DIVISION	PAGE 8.18
CHECKER		REPORT NO. NOR 67-136
DATE June 1967		MODEL X-21A

Some of the valve bodies and ductwork incorporate sound absorbing material to absorb forward-propagating compressor noise. (See Section 11 for Acoustic Criteria.) A cavity in the valve body contains Johns Mansville Microbar sound absorbing material, .50 inch thick. A 1-mil Mylar sheet was installed loose against the outside (dark side) of the Micro-bar material to prevent fluid or moisture from being absorbed by the material. These were covered and retained in place by an .040 inch thick metal retainer sheet, perforated 51% open with staggered holes, and riveted in place. (Sound-absorbing walls were incorporated into several LFC airflow collector ducts, the mixing duct chamber forward of the high-pressure compressor unit, and the inlet elbow forward of the low-pressure compressor unit. See other parts of this section and section 11.)

The outlet of a butterfly valve is structurally stable, but the flapper-type valve outlet is inherently unstable because it has only 3 fixed walls, the flapper making the fourth side. Such outlets were stabilized by attachment of the adjacent valve and by increasing the corner wall thickness.

Butterfly vanes were foam-filled fiberglass with an imbedded metal torque plate retaining a serrated hub tube near the vane's C.G. For the flapper vanes, all thickness taper was on the outside wall. Some vanes were aluminum and some were foam-filled fiberglass.

Because flapper body outlets would spread apart during the cutout and trimming operation, generous tolerances were allowed on width dimensions. Vane width, individually fit for each valve, would control gaps. The outlet was not stabilized by means of a bar or stiffener because the stiffener might cause an airflow disturbance which could travel upstream and because of vane-to-stiffener interferences.

To further minimize possible LFC airflow disturbances, aft vertical walls of trailing edge valves were tapered, and wherever the valve bodies were pierced to allow shafting, linkages, or pins to actuate the closing vanes, the cutout was sealed.

ENGINEER	NORTHROP CORPORATION NORAIR DIVISION	PAGE 8.19
CHECKER		REPORT NO. NOR 67-136
DATE June 1967		MODEL X-21A

There were no failures to any of the bodies or flanges. This is believed to be due to the use of extra-thick and over-strong wall and flanges. While such a design philosophy may not be "sophisticated," the difficulty of valve replacement dictated this approach in the X-21A program with its many valves. Flange installation with Loctite on bolts has worked out well. While disassembly is more difficult with Loctite applied, vibration has not loosened any screws or bolts treated in this manner.

8.3.8.4 Valve Operating Time

An operating time of 10 to 30 seconds under normal design conditions (2.5 psi bursting to 1.0 psi collapsing) and up to 50 seconds under maximum adverse conditions (3.5 psi bursting to 2.0 psi collapsing) was established. The duration selected is a compromise between too fast an action which would make the setting of valve positions difficult and too slow an action which would consume too much time for adjustment considering the numerous valves.

Flight testing has shown that the control valves located within the wing became sluggish in operation after flying for one or two hours at high altitudes. The trailing edge valves located in the compressor pod are in a warmer environment and their operating time has been satisfactory. The cause of the sluggish operation under cold temperature conditions was found to be: excessive grease in the gearbox, hardening of the grease in some of the bearings, binding between the flapper and the valve body at the flapper hinge. In some instances there was binding between the flapper and the body along the flapper length.

If the fiberglass valve body has not been adequately post-cured, it shrinks over a long period (up to 4 months) from "polymer growth;" that is, the molecular chains continue to get longer and longer by absorption of adjacent atoms. These absorptions reduced the volume occupied by the material. Only after this stage is reached will the material's normal coefficient of linear thermal expansion take over and control a dimensional change during a temperature change.

ENGINEER	NORTHROP CORPORATION NORAIR DIVISION	PAGE 8.20
CHECKER		REPORT NO. NOR 67-136
DATE June 1967		MODEL X-21A

This phenomenon was not given adequate consideration during gapping of the closing vanes to the valve walls: One set of trailing edge valves was checked and 80% of them showed the original gaps had almost fully closed. To lessen possible friction between flapper and side walls, the walls were sprayed with a solid film lubricant.

8.3.8.5 Valve Leakage

Leakage was minimized at valve sidewalls and hinge to minimize flow disturbances that could disturb laminar flow. Leakage flow requirements were originally based on relative cross-sectional area; the greater the main flow, the greater the leakage flow that could be tolerated. Because some tall, narrow valves of high perimeter-to-area ratio could not meet the requirements, the leakage flow requirement was changed and based on the more realistic relative perimeter, since it is the perimeter that leaks, not the area. Finally leakage measurement was simplified to a dimensional check of the vane-to-body clearance when closed, as given in the table below:

Flapper or Butterfly Width (Nominal)	Vane-to-body-gap
5.50 inches or less	.005 to .012 inch
6.00 inches or above	.009 to .020 inch

In addition, the gap between the vane and body was held to the same minimums in the hinge area. This close-fitting gap functions as a single-labyrinth seal across the entire width of the valve flapper; the use of edge grooves to create a multi-labyrinth seal was considered but discarded as unnecessary. To achieve these vane-to-body gaps vanes were widened with epoxy applied to the edges and sanded to fit, or washer-like shims were used to spread the body. Vanes were retained on hinge pins by serrations or by pins driven 90° to the hinge pins.

8.3.8.6 Valve Actuator and Motor Mechanism

Explosion-proof actuators were required since valves were located adjacent to fuel lines and tanks. Actuators required a brake of sufficient torque to insure fast coast-down to prevent overtravel past a selected vane position.

ENGINEER	NORTHROP CORPORATION NORAIR DIVISION	PAGE 8.21
CHECKER		REPORT NO. NOR 67-136
DATE June 1967		MODEL X-21A

Because of the various angles of vane closure, size of flappers, torque required, time to operate, types of drives, and special mounting requirements, 42 versions of actuator mechanisms were required. Three or four stages of planetary gearing give speed reductions of 303 to 1 and 2,560 to 1, and together with worm drives or screw jack drives effect overall reductions up to 166,500 to 1. See Figure 8.13a for a cross-section view of a representative four stage gear reduction mechanism and worm drive segment; see Figure 8.13b for a typical butterfly valve and its drive mechanism; and see Figure 8.13c for a typical "double" valve and its driven mechanism.

Ten motor versions were required to satisfy the requirements of the various valves. The motors turn at about 15000 RPM and operate on 28 Volt DC. Each motor assembly consists of an integral assembly of motor, current and thermal protector, and radio noise filter.

External microswitches at both position extremes interrupt the power and stop the motor on some of the valves. On other valves the actuator housing encases an open and closed signal microswitch arrangement. When the vane reaches full travel and the motor lugs down, torque increases; the torque build-up in the gear mechanism moves a ring gear which in turn moves a bar rack to actuate the microswitch, shutting-off the motor. When power is removed or when power is reversed, the bar rack is centered by means of shimmed springs on each end of the rack and the motor is then ready to accept another electrical signal.

The worm wheel segment in the rotary drive has a set of screw stops which will stop the actuator and prevent flapper damage in case of faulty microswitch action. Two additional shut-off safeguards are provided by a protector sensitive to both current and heat: if the motor stall current exceeds the current setting of the protector the power is interrupted by circuit-breaker action; and if both the microswitch and current-limiter fail, the stalled motor heats up the thermal portion of the protector which opens and interrupts the power.

ENGINEER	NORTHROP CORPORATION NORAIR DIVISION	PAGE 8.22
CHECKER		REPORT NO. NOR 67-136
DATE June 1967		MODEL X-21A

8.3.8.7 Valve Flapper Position Potentiometer

A two watt, 500 ohm, continuous wound, potentiometer was installed on each valve to indicate the vane's position to the flight test engineer. Potentiometer location was largely dependent on available space and thus differed among the various valves. Rotation is continuous without stops and the variable portion occupies 355°. The narrow 5° null angle requires careful rotational positioning at installation.

8.3.8.8 Qualification Testing of Valves

Of the 96 valves total on the X-21A, there were 48 different designs as far as size, actuator type, motor size, etc. To test 48 separate valves was not considered economically feasible. Four valves were chosen as being representative of the different designs and subjected to various environmental and performance tests. Military specifications were used as a basis for specifying the environmental tests to be conducted.

8.3.8.9 Valve Procurement Specification

The remaining minor requirements for design, construction, and test are similar to those of other aircraft airflow systems parts. It was convenient, therefore, to follow the MIL-Spec format for that type of component in the specific Design Specification for these valves, including therein those requirements unique to a suction flow control valve as discussed above and the usual minor requirements.

8.3.8.10 Valve and Ducting Mock-Up

The complex design and installation of valves and related ductwork was simulated by a mock-up. Figure 8.9 shows the low pressure valves and ductwork (that draw from the wing upper forward surface) in the left hand half of the picture and the high pressure valves and ductwork (that draw from the wing lower forward surface) in the right hand half of the picture. The mock-up proved very beneficial for engineering, tooling, manufacturing, compressor vendor, and valve vendor coordination.

ENGINEER	NORTHROP CORPORATION NORAIR DIVISION	PAGE 8.23
CHECKER		REPORT NO. NOR 67-136
DATE June 1967		MODEL X-21A

8.3.8.11 Valve Installation Techniques

Since the "dry bay" (no fuel) is made no larger than necessary (see Section 9.1.1.2), there is little unused room to assist in installation and subsequent service of the valves. Valves and ductwork were first fit in the airplane and attached to one another with temporary fasteners; thus the airplane itself was used as the master jig for locating attachments. The individual parts were removed and holes, fastening devices, secondary bonds and fiberglass bracketry, wiring and instrumentation, and other necessary work that could not be done in the airplane due to space limitations were completed. As a consequence, several bench assemblies of several valves each were made and these clusters are installed in a predetermined sequence. (A full-scale mock-up proved invaluable in working out these techniques.) To expedite assembly, floating nut plates were used as generously as possible. To protect against F.O.D. to the compressors, self-locking fasteners were used on valve flanges and related ductwork, and all screws and bolts were installed with wet Loctite, Grade B (yellow), applied to the threads.

It is difficult to maintain or service the valves in the X-21A. In the design, ease of maintenance was subordinated to functional requirements, and consequently it is necessary to remove secondary structure and equipment to reach a malfunctioning valve.

8.3.9 Bleed Air Ducting

The bleed duct is sized to handle flow requirements up to and including the maximum allowable from the engine. Beyond the maximum allowable engine flow, the duct will choke, thus preventing over-bleed of the engine. The design procedures used were the same as described in paragraph 8.1.9. Figure 8.14 is the developed pressure curve and Figure 8.15 is the schematic diagram of the bleed duct system.

A connection is provided for supplying air to the system from ground equipment, such as an MA-1 compressor, for system checks. Ducting connections are made by means of quick disconnect clamps. In the wing, where leakage must be minimized and the installation is more or less permanent, connections use a metal gasket that deforms under clamp pressure to provide essentially zero leakage. Elsewhere, a gasket-less connection is used. This style allows frequent removals without gasket replacement costs. Insulation is applied to reduce heat loss to less than 50°F.

ENGINEER	NORTHROP CORPORATION NORAIR DIVISION	PAGE 8.24
CHECKER		REPORT NO. NOR 67-136
DATE June 1967		MODEL X-21A

8.3.10 Collapsing Pressures

The maximum differential collapsing pressures that the inlet ducts are subjected to under normal 100% operation are -6.0 psi for the low pressure duct and -3.55 psi for the high pressure duct for the combination of modulating valve settings causing the highest pressure differential. Should the controls of one unit fail (pressure regulator goes wide open and speed governor goes to 110%, just below the emergency overspeed cut-off) but the other operates normally, even higher differentials can exist: -8.25 psi is reached in the low pressure duct with L.P. turbine control failure; and -4.8 psi is reached in the high pressure duct with H.P. turbine control failure. It may be argued that these combinations of double failures need not be designed for; however, the consequences of not doing so are so serious that they must be considered.

Pressure differentials of several psi could be handled by the relatively circular fiberglass inlet ducts, but could not be handled by the flat diagonal spars in the wing trailing edge. Normally, with all valves moderately open, a uniform negative pressure would exist in all ducts; this wing-skin collapsing pressure could be safely sustained. However, if a modulating valve controlling one duct is closed, the full pressure difference exists across the flat diagonal spar. Strengthening to withstand such load was intolerably heavy so a differential pressure sensing switch was installed in each inlet duct. Its setting is just below the pressure level where safe structure loads are exceeded and is $-3.0 \pm .15$ psi; when the pressure is reached, the unit is shut-off. These switches were never actuated during the X-21A program because malfunctions of the pumping controls or off-design value settings causing the overpressure in the ducts did not occur.

8.3.11 Noise Control

Noise output of the compressors was specified to be no more than 106 decibels measured five (5) feet in front of the compressors.

In addition to noise attenuation of some valves discussed in paragraph 8.3.8.2 the inlet ducts were also treated to reduce noise. Acoustical liners were applied to the interior surface of duct. Liner construction consists of a .50 inch thick acoustical batt covered with an .001 inch thick Mylar sheet, in turn covered with perforated aluminum alloy sheet of 51% open area. The liner is designed to attenuate the high frequency noise generated by compressor blade passing intervals.

ENGINEER	NORTHROP CORPORATION NORAIR DIVISION	PAGE 8.25
CHECKER		REPORT NO. NOR 67-136
DATE June 1967		MODEL X-21A

8.3.12 Foreign Object Damage Screens

To prevent F.O.D., screens of .25 mesh x .025 wire were installed in front of each compressor. Screens were formed into a dome-shape and, to allow for material displacement during forming, a mesh without joint connections was used. Damage to the blades has been confined to the first rotor leading edge, to the first stator leading edge to a lesser degree, and to a small degree to the second rotor. All damage has been burnished out within specified maintenance limits and no blades have been replaced. The F.O.D. screens have returned their cost many times over in blades, compressors, and man-hours saved.

8.3.13 Inter-Compressor Duct

The inter-compressor duct acts also as a flow mixing chamber for the trailing edge valves. As can be seen in Figure 8.8, the duct has a "coke-bottle" shape with the flow area contracting in the vicinity of the exits for the trailing edge valves. This duct shape was incorporated to lower the static pressure (by increasing the flow velocity), in the mixing duct so reverse flow would not occur in the trailing edge duct leading to the lowest surface pressure area. The design of the inter-compressor duct and trailing edge valves was such that the static pressures were approximately equal along the duct. The total pressures, however, had large variations at the outlet of each valve. These variations in total pressure, coupled with the short mixing length (about 1½ diameters) ahead of the compressor, resulted in large velocity variations at the compressor inlet. Tests were conducted at the suction compressor supplier's facility with these large velocity variations with no adverse effect on the compressors.

8.4 DESCRIPTION OF LAMINAR FLOW CONTROL-LARGE TRANSPORT AIRPLANE (LFC-LTA)

A design study was conducted for applying laminar flow control to an existing large transport airplane. The C-141 was chosen as a model for this study. The study considered the problem of incorporating LFC as a major change to an in-production turbulent flow airplane. The resulting modified airplane design is illustrated in Figure 8.16.

ENGINEER	NORTHROP CORPORATION NORAIR DIVISION	PAGE 8.26
CHECKER		REPORT NO. NOR 67-136
DATE June 1967		MODEL X-21A

8.4.1 Problem Statement

The flight regime for the LFC-LTA during which LFC is required is tabulated below.

Flight Condition	Mach No. M	Altitude h	Lift Coefficient C_L

Design	0.767	40,000	0.38
Off-Design	0.77	40,000	0.24
	0.72	35,000	0.46

All of the wing surface is to be laminarized except wing tips, upper wing over the fuselage, and the turbulent wedges that exist at pod-to-wing and wing-to-body intersections.

8.4.2 Compressor Arrangement

An analysis compared one, two, and three level suction systems; i.e., one, two or three compressors in series. Several suction levels minimize required throttling of air and its attendant wastefulness of energy. The analysis shows that the two-level system is quite superior to the single-level system, and that the three-level system offers an additional, but small, gain in efficiency. Considering the added complexity of a three-level system, it was ruled out as not worth its cost. This is particularly true when the low pressure compression of the two-level system can be accomplished in one stage.

The low pressure regime starts at 1% chord and extends to 77% as compared to 67% on the X-21. This difference arises for three reasons; (1) the difference in pressure distribution arising from a higher design lift coefficient from the LFC-LTA, (2) the reduction in leading edge suction arising from reduced sweep, (3) the relatively higher efficiency of the low pressure turbine, whose power is derived from the bleed-burn system, allows the split to be located in its optimum position, whereas the lower efficiency of the X-21A turbine which derived its power directly from bleed air, demanded flow be held to as little as practical.

ENGINEER	NORTHROP CORPORATION NORAIR DIVISION	PAGE 8.27
CHECKER		REPORT NO. NOR 67-136
DATE June 1967		MODEL X-21A

8.4.3 LFC Airflow

Methods of designing for optimum suction distribution are described in Sections 1 and 2. Basic suction distribution is modified by: 1) increasing the suction rate in the low-suction region of the lower inboard portion of the wing to counteract the effects of noise from the fuselage turbulent boundary layer; and 2) increasing suction in all other low suction regions to provide adequate capability for off-design flight conditions. Suction slots have spacings of approximately 1.5 inches in the wing forward region, 4.0 inches in the intermediate region, and 3.0 inches in the aft region. Such chordwise slot spacing remains nearly constant when going outboard (in spite of wing taper) by dropping out some 65% of the slots in an irregular pattern from root toward tip. Slot widths are .004", .009" and 0.006" in forward, intermediate, and aft regions respectively.

The flow rates for the design and off-design conditions are shown in the table below for one (of four) pumping unit.

Design Condition	Low Pressure			High Pressure		
	Act. Flow	Corr. Flow	Press. Ratio	Act. Flow	Corr. Flow	Press. Ratio
Basic Design	3.41			9.16		
Basic Design plus Noise	3.41			9.82		
Basic Design plus Noise plus Off-Design	3.57	27.2	1.33	10.18	59.1	= 2.0
	LBS/SEC.	LBS/SEC.	P ₂ /P ₁	LBS/SEC.	LBS/SEC.	P ₄ /P ₃
		CORR.			CORR.	

8.4.4 Compressor Power Source

As discussed in Section 8.1.4 a thermodynamically optimum pumping system should extract its energy from the main propulsion system. This is because the propulsive efficiency, $\eta_p = 2/(1+V_g/V_o)$, of the pumping system is higher than that of the engine system, where V_g is the exhaust velocity of the pumping system at ambient pressure, and V_o is the flight speed.

ENGINEER	NORTHROP CORPORATION NORAIR DIVISION	PAGE 8.28
CHECKER		REPORT NO. NOR 67-136
DATE June 1967		MODEL X-21A

Power may be efficiently extracted from the primary system in at least three ways: (1) by direct power take-off through existing or added accessory drive pads; (2) by adding an additional turbine stage to supply a large power take-off capability; or (3) by bleeding air from the compressor and mechanical power (bleed-burn system). All three methods are thermodynamically identical provided component efficiencies are the same. The first method is not possible since power requirements of the suction system greatly exceed power extraction limits of the engine pads and engine redesign is impractical. The second method offers minimum installation flexibility but requires so large a development program that it also is deemed impractical. The bleed-burn system offers maximum installation flexibility and its development can be independent. There was some feeling that the SFC penalty for the amount of bleed required was so great that component rematch in the basic engine cycle would be desirable and necessary. However, no rematch was required or desirable for bleed rates within specification allowances since component efficiencies are flat up to the bleed limit. In fact, the bleed limit is specified by the engine manufacturer at the value where component efficiencies begin to diminish.

8.4.5 Thrust Specific Fuel Consumption

Performance of the pumping system has been integrated with the propulsion system to arrive at an overall TSFC. However, the TSFC of the propulsion engines is approximately seven (7) times more influential on overall TSFC than is TSFC of the pumping equipment. Therefore, the first consideration, even above that of pumping system proposal comparison, is to choose one or more propulsion engines of low SFC, at appropriate cruise power settings, from which a choice can be made. Then, integrate the pumping systems for an overall TSFC. It is important that pumping equipment be designed specifically for the job, especially turbines; it was indicated in Section 8.3.5 that a 12% saving in TSFC could be obtained by optimization of the X-21A system.

ENGINEER	NORTHROP CORPORATION NORAIR DIVISION	PAGE
CHECKER		8.29
DATE		REPORT NO.
June 1967		NOR 67-136
		MODEL
		X-21A

8.4.6 Equipment Size and Weight
and
8.4.7 Requirement Specification

Two suction system pumping units of equal capacity are mounted on each wing. The criterion of location is that each unit shall handle the same amount of flow. Since suction flow coefficients are similar inboard and outboard, equal flow will occur when approximately equal surface areas are pumped. The inboard unit is nested between and slightly above the engines on the lower wing surface at 28 percent semispan, and the outboard suction pod is at 66 percent of semispan. The locations can be varied somewhat to meet other considerations since location is not sensitive for small changes (see Section 7 for further discussion of the effect of pod location on wing pressure fields).

Norair has been supported in the design and in the analysis of the pumping system by AiResearch Manufacturing Division of Arizona, a Division of the Garrett Corporation, a wholly owned subsidiary of Signal Oil and Gas Company. AiResearch has proposed a design for a two-level system which is comprised of a two-stage low pressure compressor with variable inlet guide vanes, for flow control, exhausting into a three-stage high pressure compressor. Both units are driven through an appropriate shafting and gear box arrangement by a three-stage axial flow turbine with an annular combustor utilizing high pressure bleed air from the propulsion engines. High component efficiencies were possible because the unit is designed for a narrow range of operation. Bleed flow requirements are about 2.7% of engine primary flow, about one-half the engine limit. See Figure 8.17 for a view of the proposed unit.

8.4.8 Internal Flow System and Flow Control Valves

The internal flow system follows the recommended practice of discharging air from the various wing ducts into mixing chambers to conserve energy. Relatively few suction valves are needed, 12 per airplane compared with 96 for the X-21A. Valves are required only for the wing nose region in order to vary the suction in this region for off-design conditions. Valves are not required for the other ducts since the off-design suction requirements for the rest of the wing do not change excessively from the design condition. These changes can be handled by varying the overall wing suction level by suction compressor RPM change.

ENGINEER			NORTHROP CORPORATION						PAGE		
CHECKER			NORAIR DIVISION						8.30		
DATE			TABLE I - Suction Valve Airflow Data						REPORT NO.		
June 1967									NOR 67-136		
									MODEL		
									X-21A		
	Valve No.		Suction Surface Location (% Chord)	Pressure psfa	Flow #/sec (act)	Wing Sect'n	Type Valve	Flow Area		Flapper	
	L.H.	R.H.						In ²	W x D	L	W
Low Pressure Valves	-1	-2	1.0 to 1.75U	323	.07	Inb'd	Fl.	4.6	2.0 x 2.3	6.0	2.0
	-3	-4	1.0 to 1.75U	272	.07	Outb'd	Fl.	5.0	2.0 x 2.5	6.0	2.0
	-5	-6	1.75 to 7.7 U	211	.16	Inb'd	But.	4.5	3.0 x 1.5	7.5	3.0
	-7	-8	1.75 to 7.7 U	217	.14	Outb'd	But.	5.6	3.7 x 1.5	7.5	3.7
	-9	-10	7.7 to 15.0U	248	.06	Inb'd	Fl.	2.8	2.0 x 1.4	5.0	2.0
	-11	-12	7.7 to 15.0U	248	.08	Outb'd	Fl.	4.6	2.0 x 2.3	6.0	2.0
	-13	-14	15 to 25.4U	262	.11	Inb'd	Fl.	2.6	2.0 x 1.3	6.0	2.0
	-15	-16	15 to 25.4U	260	.11	Outb'd	Fl.	6.2	2.0 x 3.1	9.0	2.0
	-17	-18	25.4 to 34.4U	267	.08	Inb'd	Fl.	2.7	1.5 x 1.8	6.0	1.5
	-19	-20	25.4 to 34.4U	268	.08	Outb'd	Fl.(D)	3.6	2.0 x 1.8	4.0	2.0
			U = Upper Surface					3.9	2.3 x 1.9	4.0	2.0
	-21	-22	34.4 to 43.1U	276	.06	Inb'd	Fl.(D)	0.7	6.6 x 1.8	4.0	0.6
			L = Lower Surface					1.0	1.0 x 1.0	4.0	1.0
	-23	-24	34.4 to 43.1U	279	.07	Outb'd	Fl.(D)	2.8	1.2 x 2.3	3.5	1.2
								2.9	2.2 x 1.3	3.0	2.2
High Pressure Valves	-25	-26	43.1 to 51.6U	273	.10	Inb'd	Fl.	4.0	2.0 x 2.0	7.5	2.0
	-27	-28	43.1 to 51.6U	276	.16	Outb'd	Fl.	14.5	5.0 x 2.9	8.0	5.0
	-29	-30	51.6 to 60.0U	288	.11	Inb'd	Fl.	4.8	2.0 x 2.4	8.5	2.0
	-31	-32	51.6 to 60.0U	294	.18	Outb'd	Fl.(D)	9.0	5.0 x 1.8	5.8	5.0
							8.0	5.0 x 1.6	5.0	5.0	
	-33	-34	60.0 to 67.0U	299	.10	Inb'd	But.	4.2	3.8 x 1.1	5.9	3.8
	-35	-36	60.0 to 67.0U	301	.28	Outb'd	But.	12.2	6.8 x 1.8	6.5	0.8
	-37	-38	0 to 1.0 U	337	.02	Inb'd	Fl.	1.3	2.1 x 0.6	4.2	2.1
	-39	-40	0 to 1.0 U	357	.02	Outb'd	Fl.	1.9	2.1 x 0.9	5.3	2.1
	-41	-42	0 to 1.0 L	399	.03	Inb'd	Fl.	1.9	2.1 x 0.9	5.3	2.1
Trailing Edge Valves	-43	-44	0 to 1.0 L	396	.03	Outb'd	Fl.	1.9	2.1 x 0.9	5.3	2.1
	-45	-46	1.0 to 3.0L	381	.09	Inb'd	But.	4.1	4.5 x 0.9	4.5	4.5
	-47	-48	1.0 to 3.0L	387	.09	Outb'd	But.	4.1	4.5 x 0.9	4.5	4.5
	-49	-50	5.0 to 8.5L	345	.06	Inb'd	Fl.	5.0	4.5 x 1.1	4.9	4.5
	-51	-52	5.0 to 8.5L	356	.07	Outb'd	Fl.	6.3	4.5 x 1.4	6.3	4.5
	-53	-54	8.5 to 15.0 L	345	.10	Inb'd	Fl.	5.0	4.5 x 1.1	5.1	4.5
	-55	-56	8.5 to 15.0 L	330	.14	Outb'd	Fl.	7.2	4.5 x 1.6	5.7	4.5
	-57	-58	15.0 to 26.1L	349	.11	Inb'd	Fl.	3.6	4.5 x 0.8	3.6	4.5
	-59	-60	15.0 to 26.1L	380	.18	Outb'd	Fl.	6.3	4.5 x 1.4	6.3	4.5
	-61	-62	26.1 to 44.5L	350	.15	Inb'd	Fl.	5.5	6.5 x 0.9	3.6	6.5
-63	-64	26.1 to 44.5L	331	.11	Outb'd	Fl.	11.6	5.5 x 2.1	7.7	5.5	
-65	-66	44.5 to 60.0L	353	.09	Inb'd	Fl.	4.6	6.5 x 0.7	4.1	6.5	
-67	-68	44.5 to 60.0L	351	.19	Outb'd	Fl.	10.2	5.5 x 2.4	8.0	5.5	
-69	-70	60.0 to 72.2L	363	.08	Inb'd	Fl.	4.1	4.1 x 1.0	7.0	4.1	
-71	-72	60.0 to 72.2L	366	.20	Outb'd	Fl.	12.3	4.1 x 5.0	7.0	4.1	
-73	-74	72.2 to 78.5L	369	.05	Inb'd	Fl.	2.0	0.5 x 3.9	9.0	0.5	
-75	-76	67.0 to 74.0U	312	.13	Inb'd	Fl.	12.5	3.2 x 3.9	9.0	3.2	
-77	-78	67.0 to 74.0U	319	.51	Outb'd	Fl.	44.1	11.3 x 3.9	9.0	11.3	
-79	-80	72.2 to 78.5L	374	.11	Outb'd	Fl.	3.9	1.0 x 3.9	9.0	1.0	
-81	-82	78.5 to 84.5L	367	.05	Inb'd	Fl.	1.7	0.5 x 3.3	8.0	0.5	
-83	-84	74.0 to 81.0U	327	.14	Inb'd	Fl.	5.6	2.6 x 3.3	8.0	2.6	
-85	-86	74.0 to 81.0U	335	.58	Outb'd	Fl.	33.7	10.2 x 3.3	8.0	10.2	

Static duct press. upstream of valve

FL(D) = Double Flapper But. = Butterfly

D = Depth, inches

L = Flapper length, inches

W = Flapper width, inches

W = Width, inches

ENGINEER			NORTHROP CORPORATION NORAIR DIVISION						PAGE 8.31	
CHECKER									REPORT NO. NOR 67-136	
DATE June 1967			TABLE Ia - Suction Valve Airflow Data						MODEL X-21A	
Valve No.		Suction Surface Location (% Chord)	Press- ure psfa	Flow #/sec (act)	Wing Sect'n	Type Valve	Flow Area		Flapper	
L.H.	R.H.						In ²	W x D	L	W
-87	-88	78.5to84.5L	375	.12	Outb'd	Fl.	3.6	1.1 x 3.3	8.0	1.1
-89	-90	84.5to100L	370	.15	Inb'd	Fl.	4.6	1.6 x 2.9	7.0	1.6
-91	-92	81.0to87.2U	348	.12	Inb'd	Fl.	4.1	1.4 x 2.9	7.0	1.4
-93	-94	81.0to100 U	337	.41	Outb'd	Fl.	18.3	6.3 x 2.9	7.0	6.3
-95	-96	87.2tp100U	355	.22	Inb'd	Fl.	6.7	2.3 x 2.9	7.0	2.3

ENGINEER	NORTHROP CORPORATION NORAIR DIVISION	PAGE 8.32
CHECKER		REPORT NO. NOR 67-136
DATE June 1967		MODEL X-21A

Figure 8-1

LFC Compressor Arrangement Alternatives

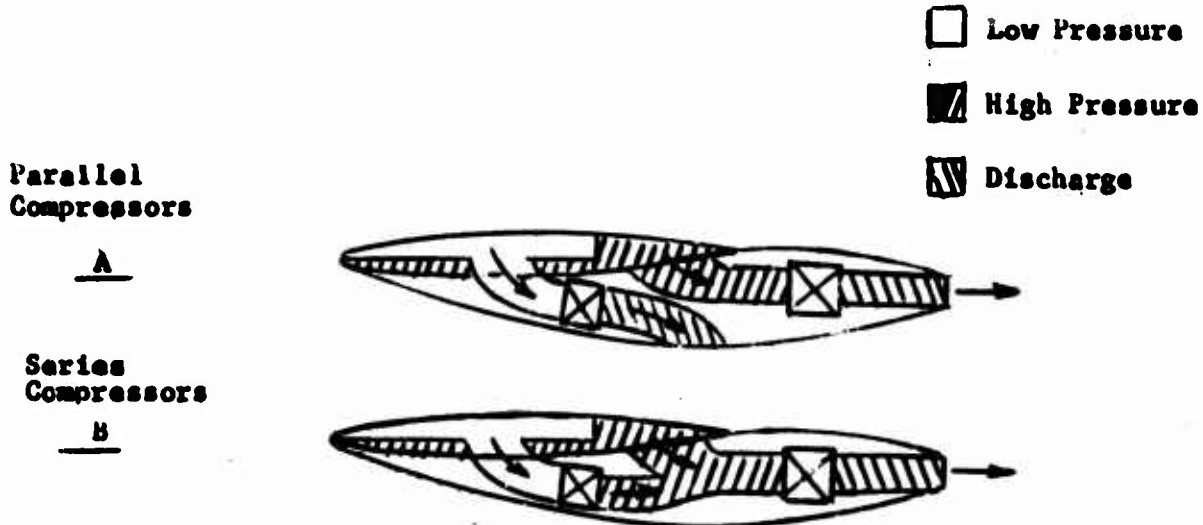
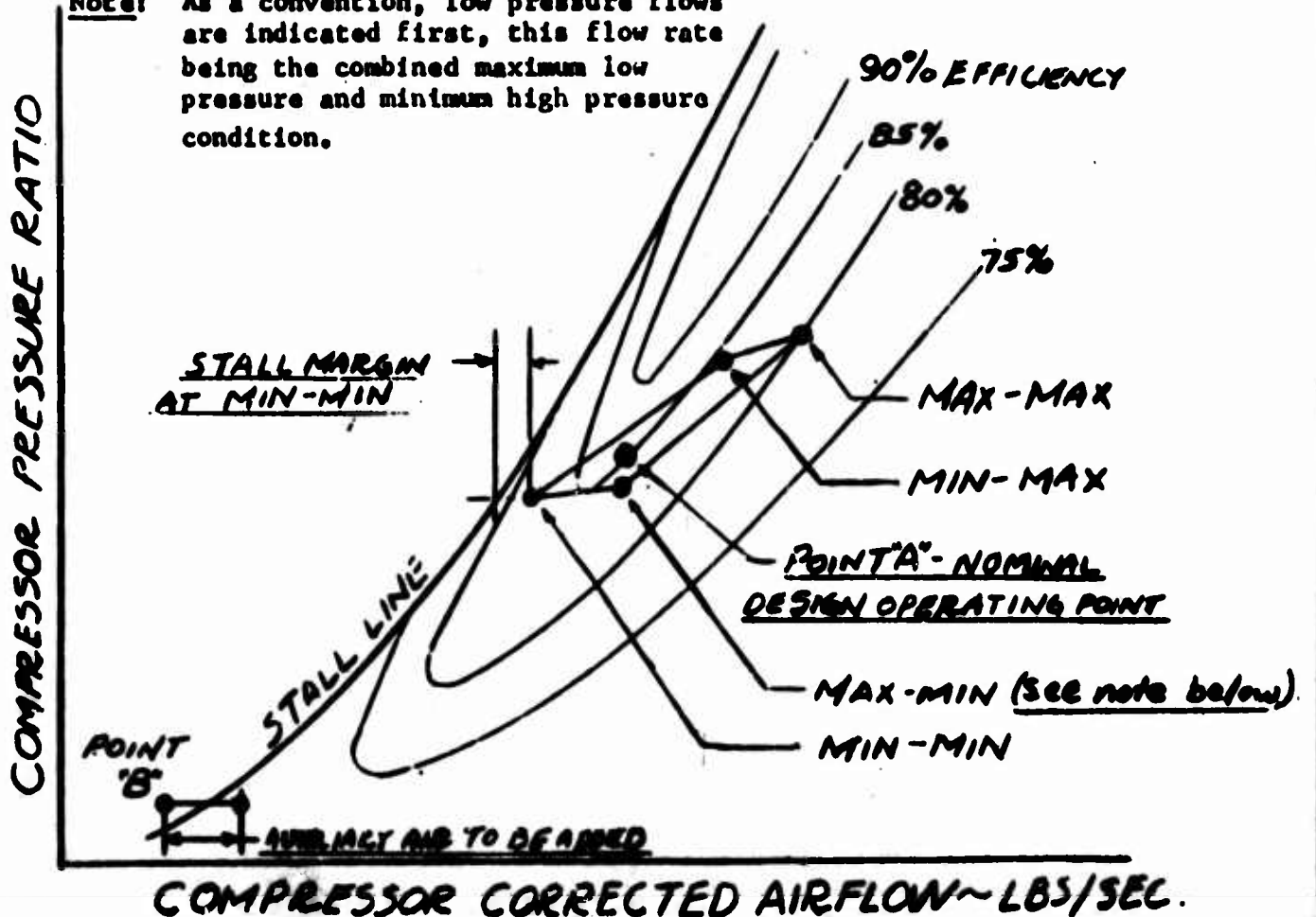


Figure 8.2

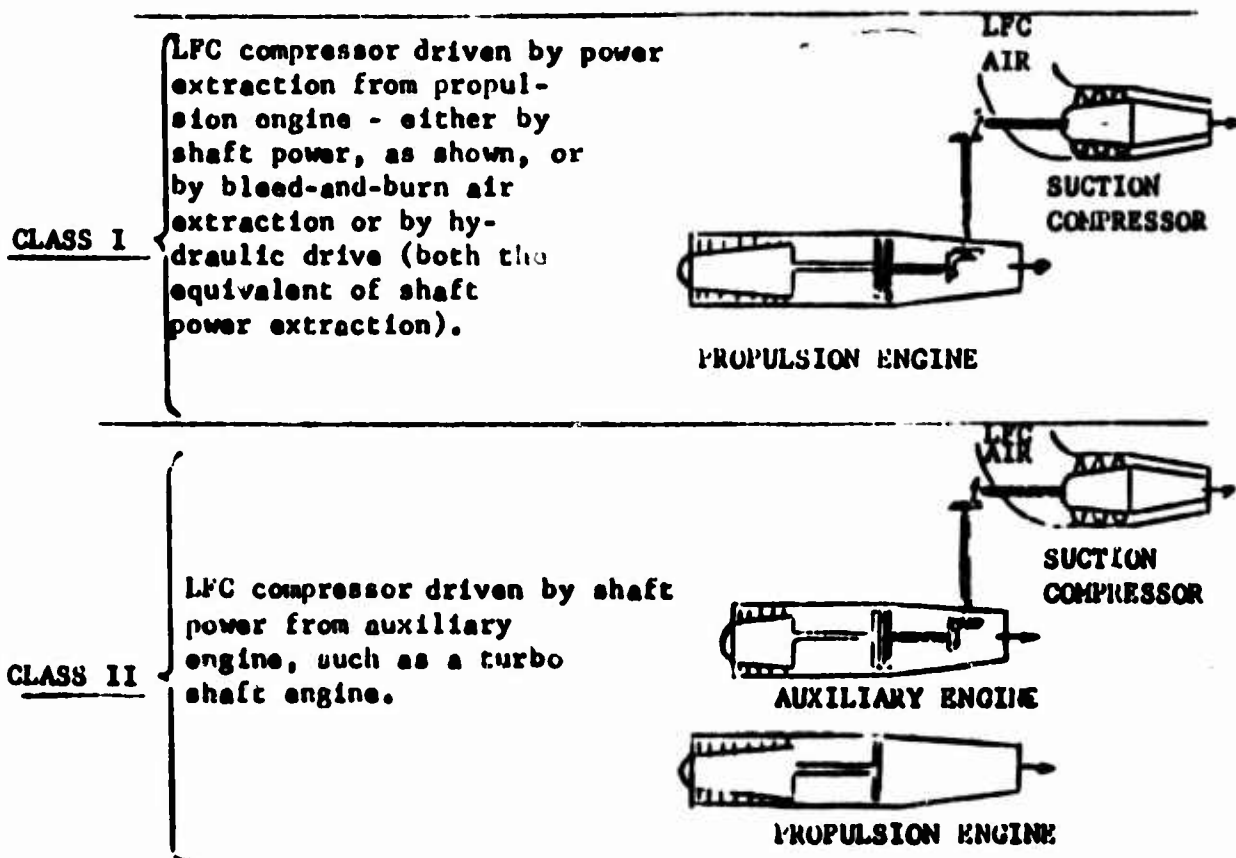
TYPICAL HIGH PRESSURE COMPRESSOR MAP

Note: As a convention, low pressure flows are indicated first, this flow rate being the combined maximum low pressure and minimum high pressure condition.



ENGINEER	NORTHROP CORPORATION NORAIR DIVISION	PAGE
CHECKER		8.33
DATE		REPORT NO NOR 67-136
June 1967		MODEL X-21A

Figure 8.3
SCHEMATIC DIAGRAM OF PRINCIPAL CLASSES
OF PROPULSION SYSTEM CONFIGURATIONS



ENGINEER	NORTHROP CORPORATION NORAIR DIVISION	PAGE 8.34
CHECKER		REPORT NO. NOR 67-136
DATE June 1967		MODEL X-21A

DATA: AIRRESEARCH MODEL ATMC
13.3 IN. DIA TWO STAGE LOW PRESSURE

P_1 = INLET TOTAL PRESSURE, PSIA

P_2 = EXIT STATIC PRESSURE, PSIA

T_1 = INLET TOTAL TEMP, °R

$\delta = P_1 / 14.7$

$\sigma = T_1 / 519$

W = AIR FLOW ~ LB/SEC

N = SPEED ~ RPM

**PRESSURE
RATIO**

$\left(\frac{P_2}{P_1}\right)$

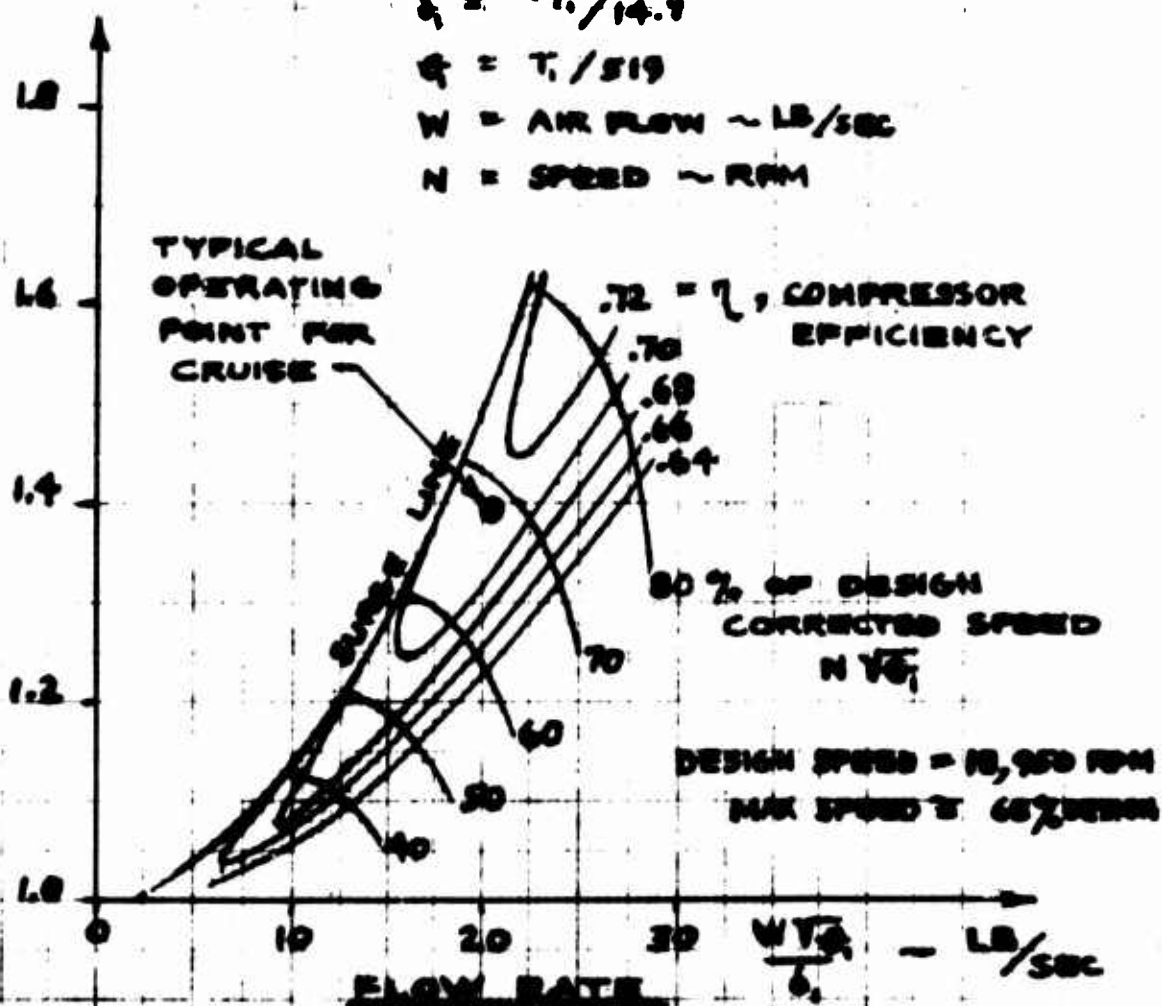


FIG 2.4 ATMC COMPRESSOR PERFORMANCE

ENGINEER	NORTHROP CORPORATION NORAIR DIVISION	PAGE
CHECKER		2.35
DATE	June 1967	REPORT NO. NOR 67-136
		MODEL X-21A

DATA : AIRSEARCH MODEL 6TMC

22.2 MDA THREE STAGE HIGH PRESSURE

PRESSURE

RATIO

$$\left(\frac{P_2}{P_1}\right)$$

P_1 = INLET TOTAL PRESSURE, PSIA

P_2 = DISCHARGE TOTAL PRESSURE, PSIA

T_1 = INLET TOTAL TEMP, °R

$$\delta_T = T_1 / 14.7$$

$$\delta_T = T_1 / 1519$$

W = AIRFLOW ~ LB/SEC

N = SPEED ~ RPM

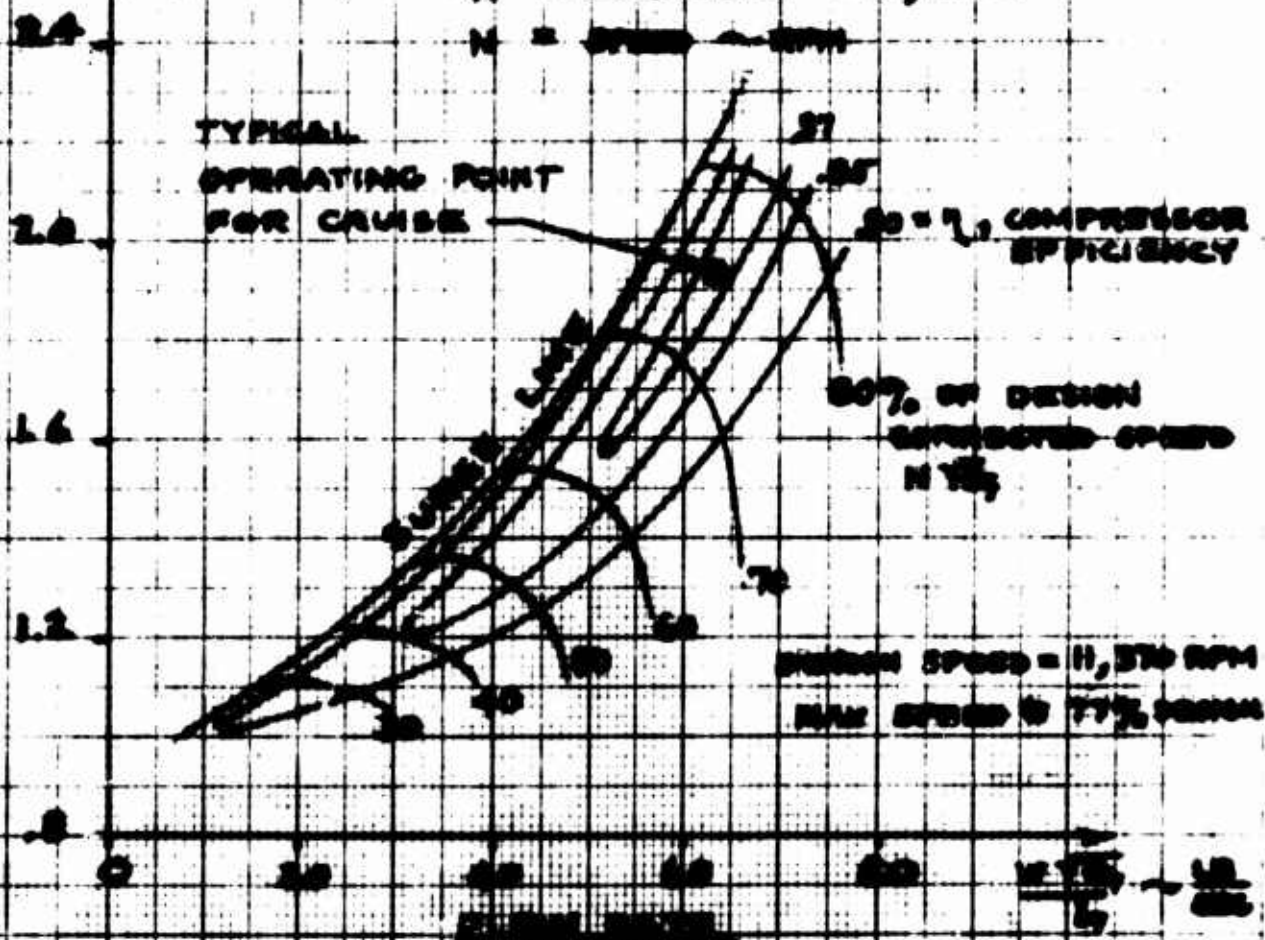


FIG. 2.5 6TMC AIRSEARCH MODEL 6TMC

ENGINEER	NORTHROP CORPORATION NORAIR DIVISION	PAGE 8.36
CHECKER		REPORT NO. NOR 67-136
DATE June 1967		MODEL X-21A

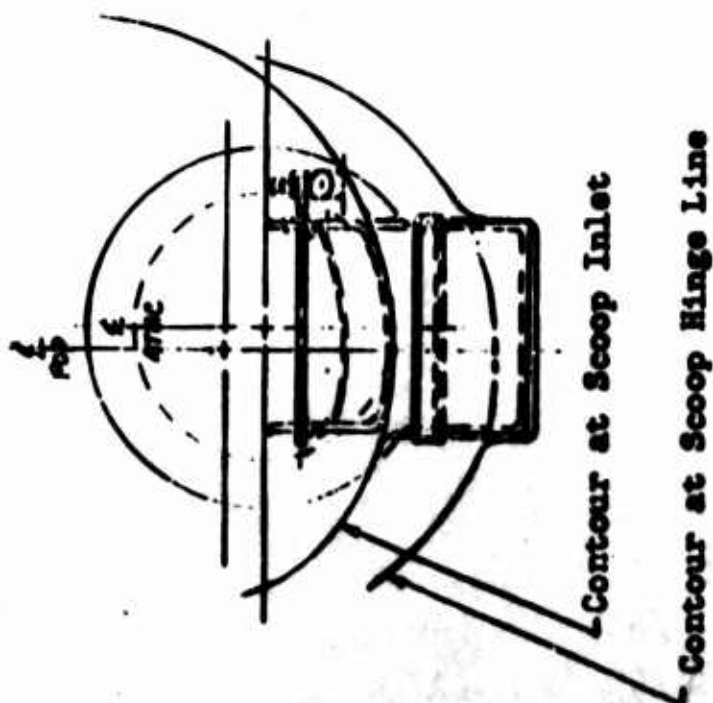
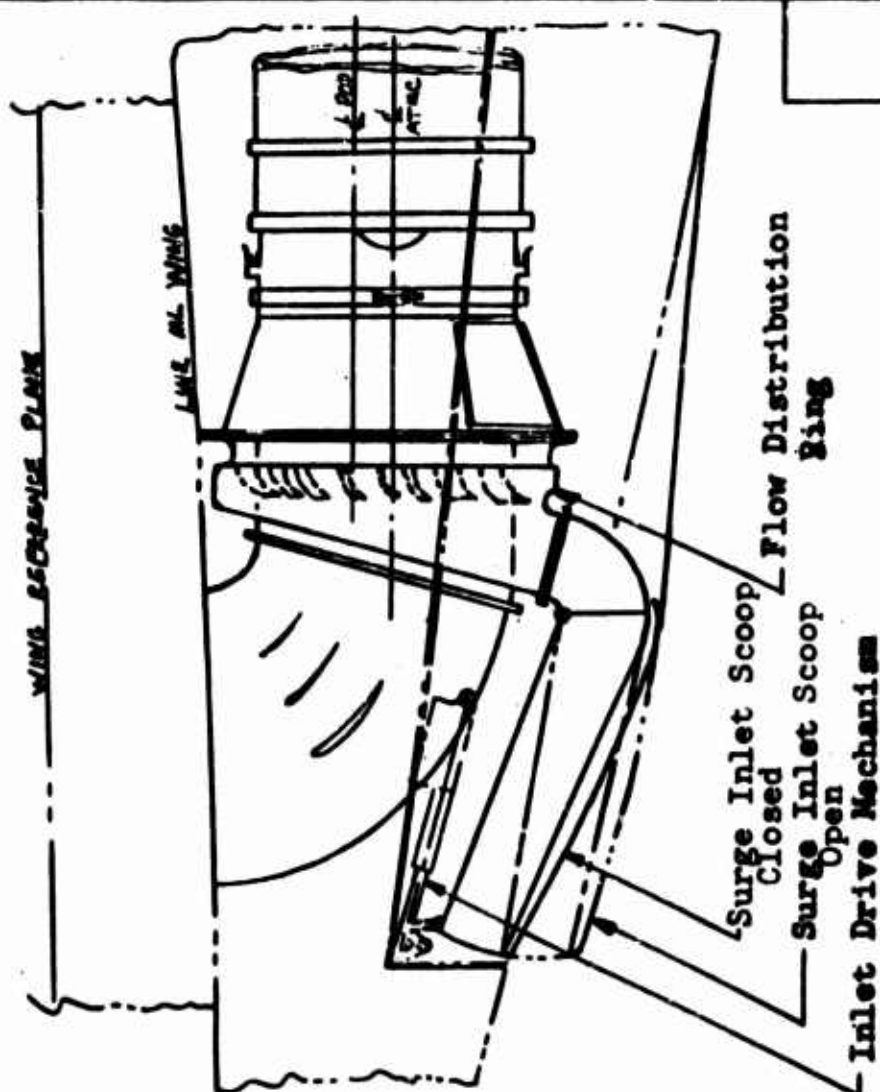
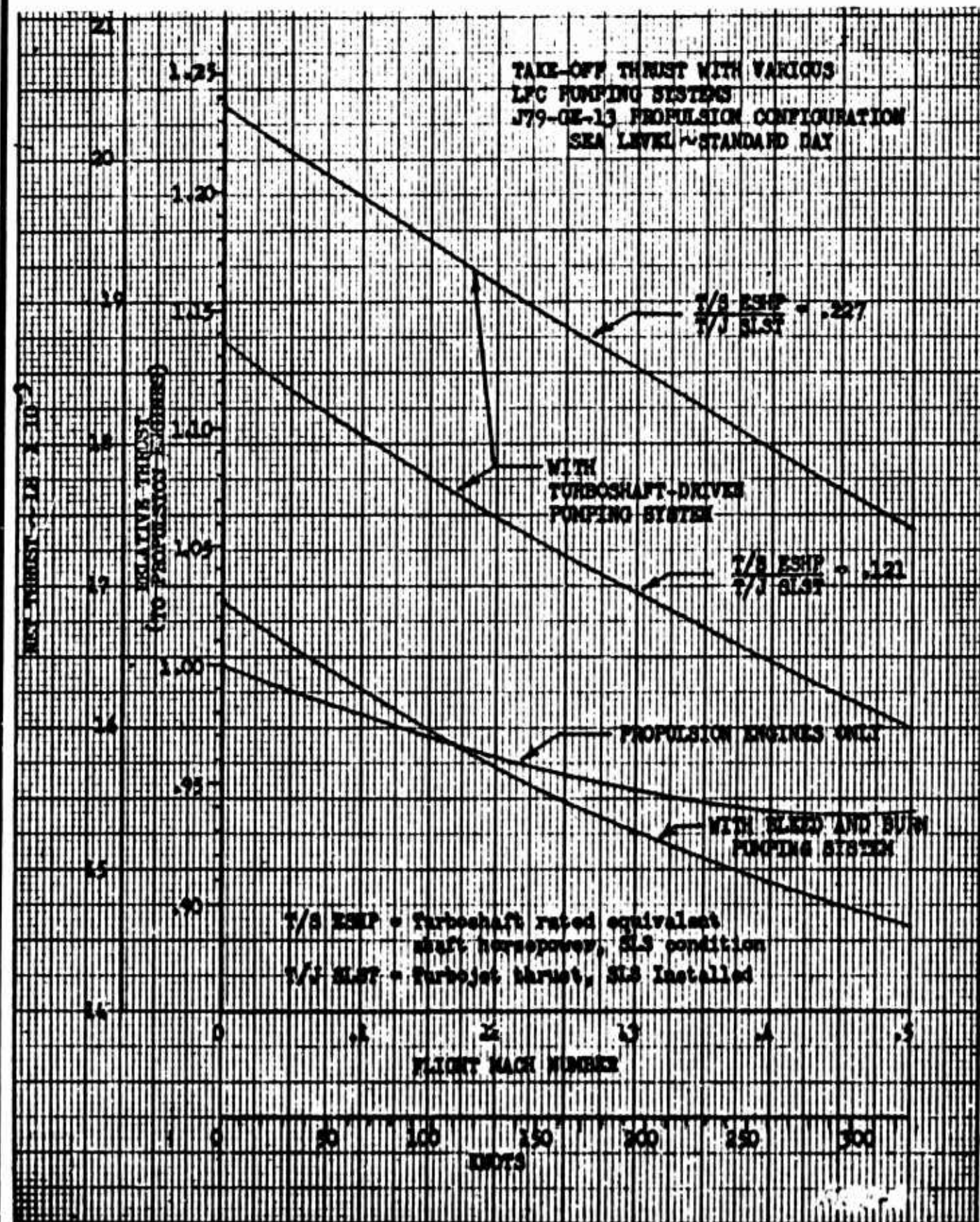


FIG 8.6 ANTI-SURGE INLET LAYOUT

ENGINEER	NORTHROP CORPORATION NORAIR DIVISION	PAGE 8.37
CHECKER		REPORT NO. NOR 67-136
DATE June 1967		MODEL X-21A

FIGURE 3.7



JUNE 1967

PAGE 8.39
REPORT NO. NOR 67-136
MODEL X-21A

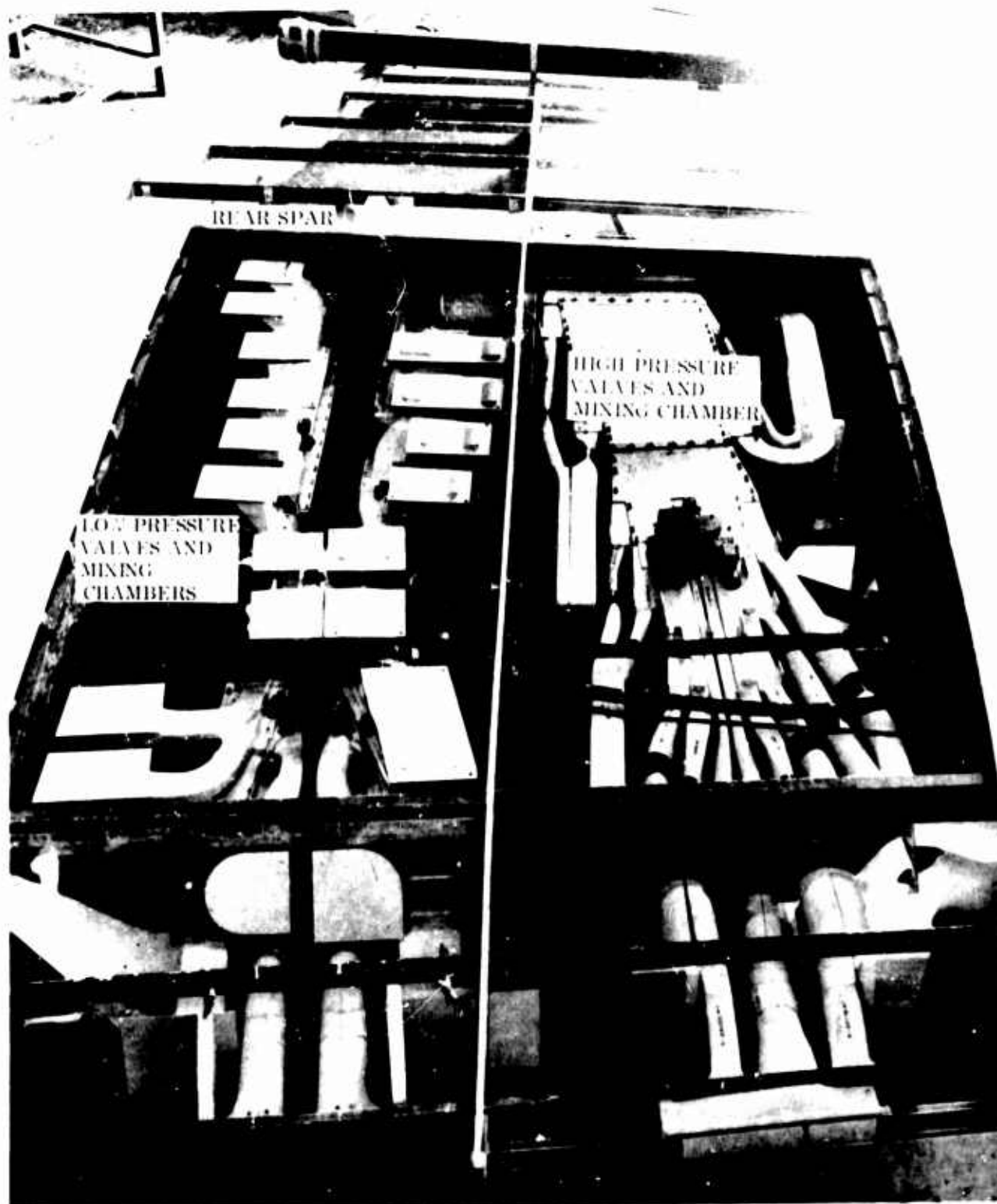


FIGURE 8.9 MOCK-UP WING SECTION AND PUMPING POD (L. H.)

JUNE 1967

PAGE 8.40
REPORT NO. NOR 67-136
MODEL X-21A



FIGURE 8.10 LOW PRESSURE BAY VALVES (L.H.)
View of Inboard Side

JUNE 1967

PAGE 8.41
REPORT NO. NOR 67-136
MODEL X-21A



FIGURE 8.11 HIGH PRESSURE BAY VALVES (R. H.)
View of Outboard Side

JUNE 1967

PAGE 8.42
REPORT NO. NOR 67-136
MODEL X-21A

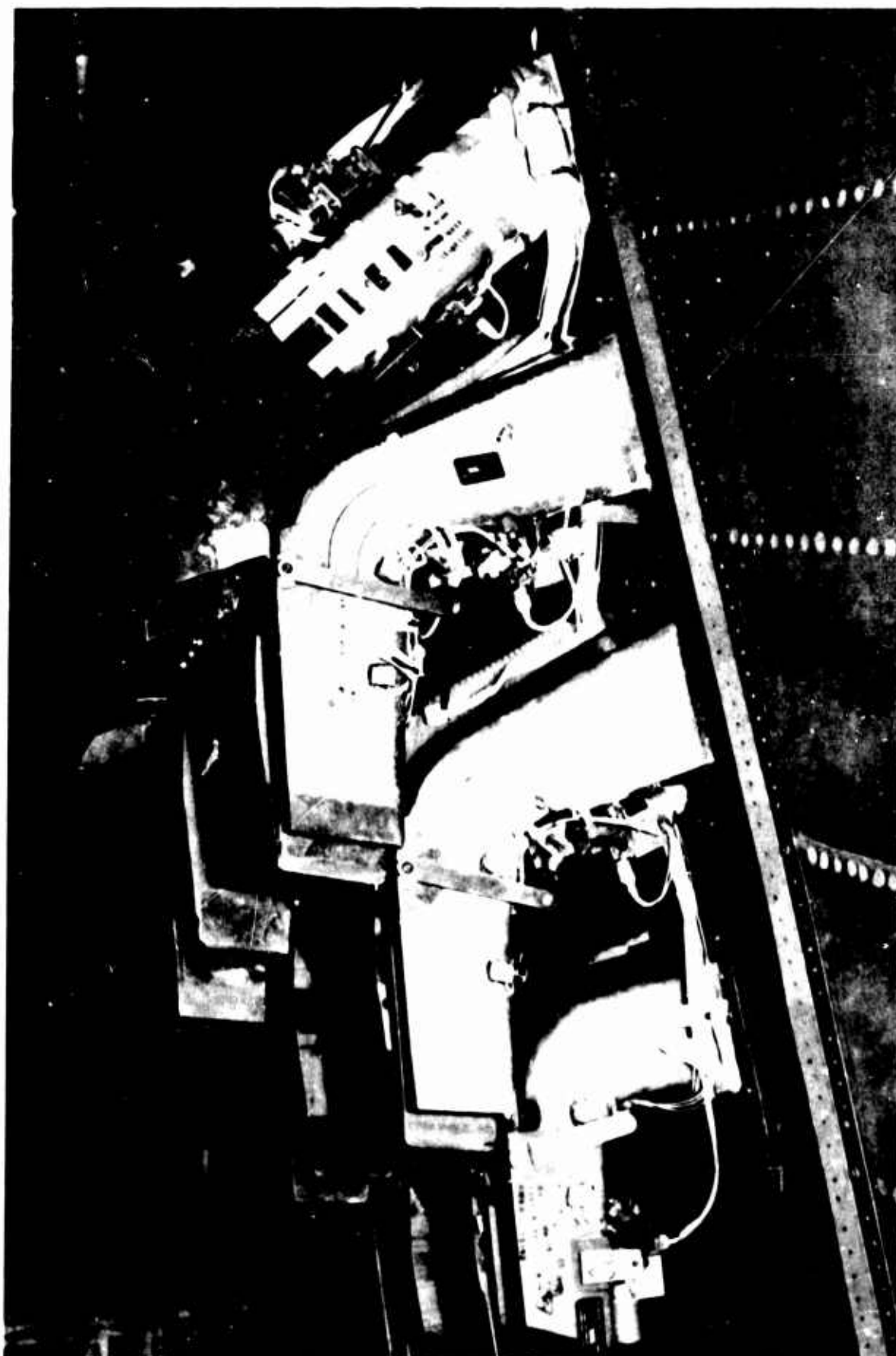


FIGURE 8.12 TRAILING EDGE VALVES

ENGINEER	NORTHROP CORPORATION NORAIR DIVISION	PAGE 8.43
CHECKER		REPORT NO. NOR 67-136
DATE June 1967		MODEL X-21A

Figure 8.13 a

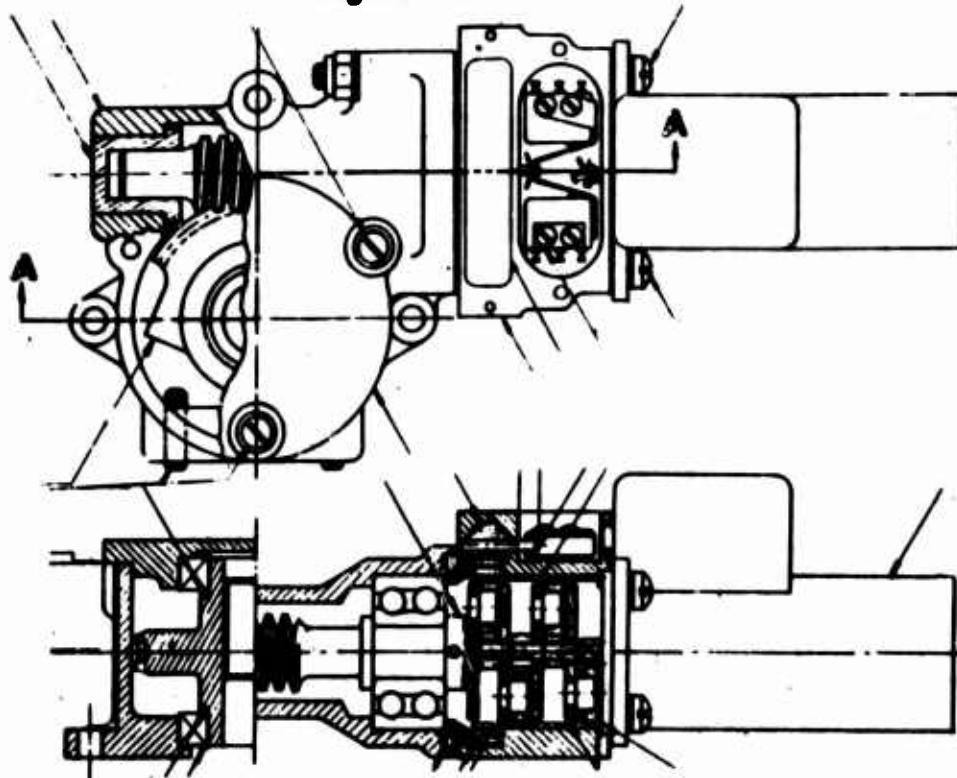


Figure 8.13 b

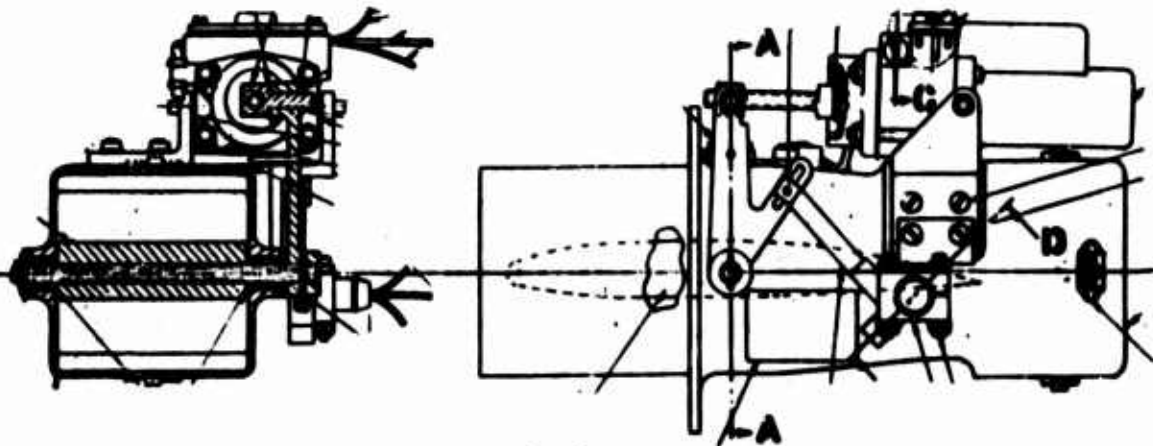
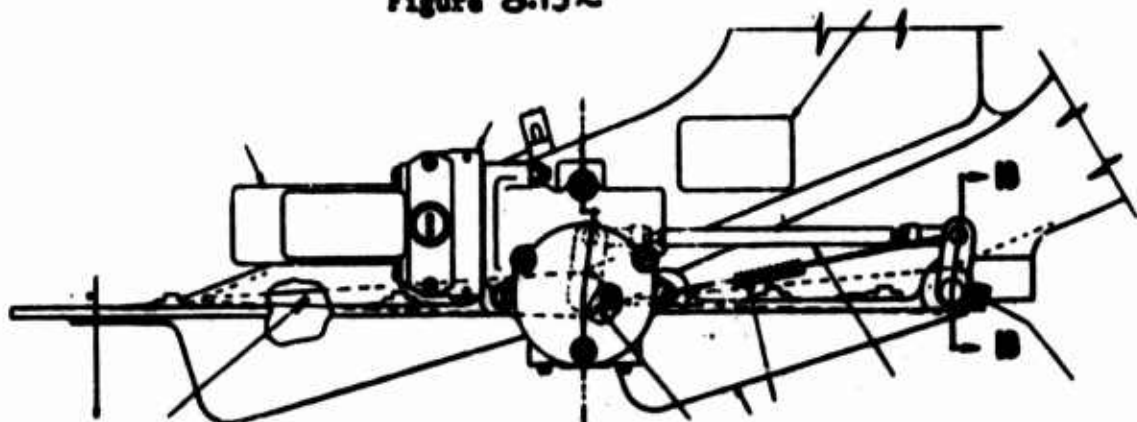
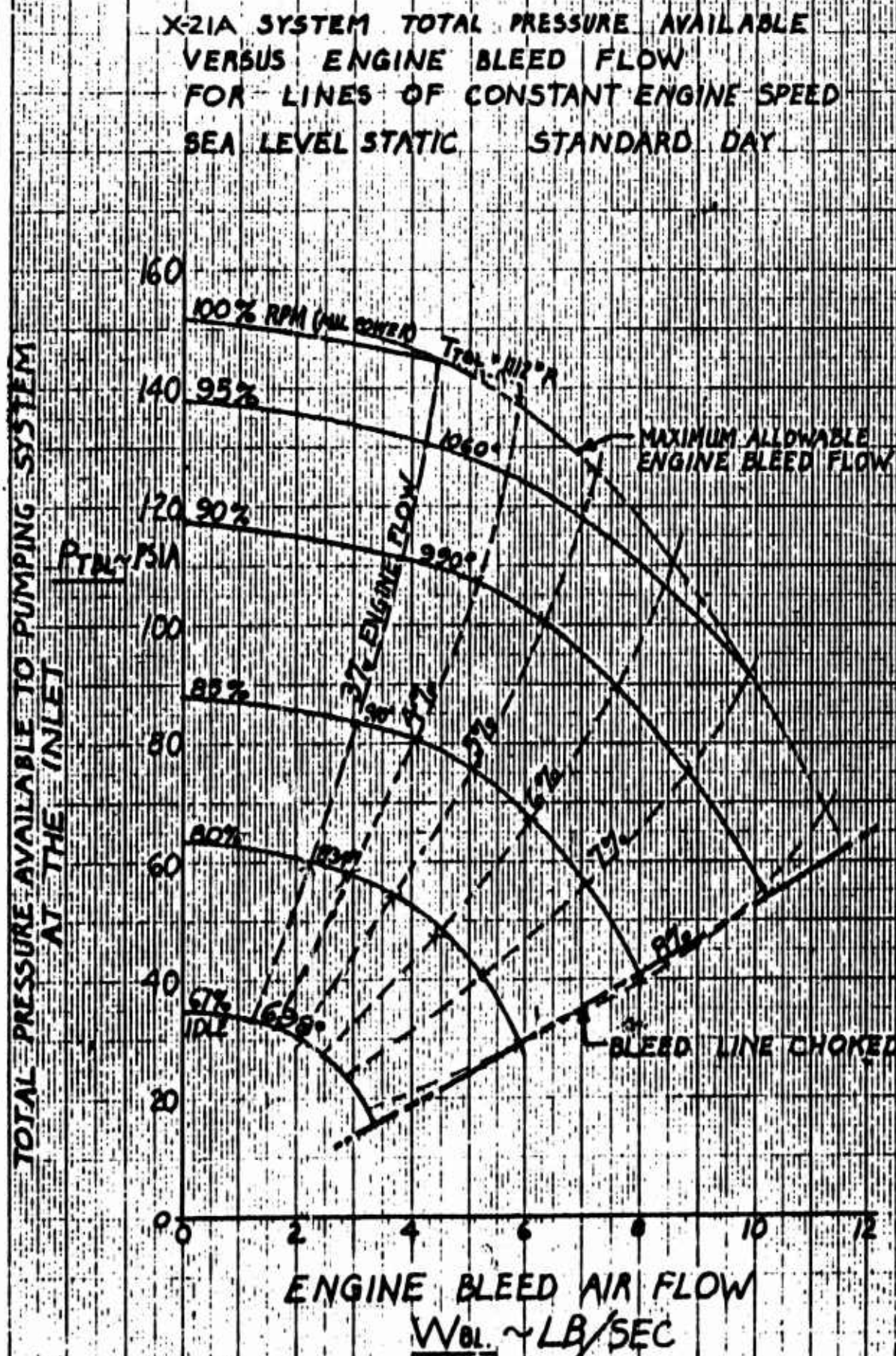


Figure 8.13 c

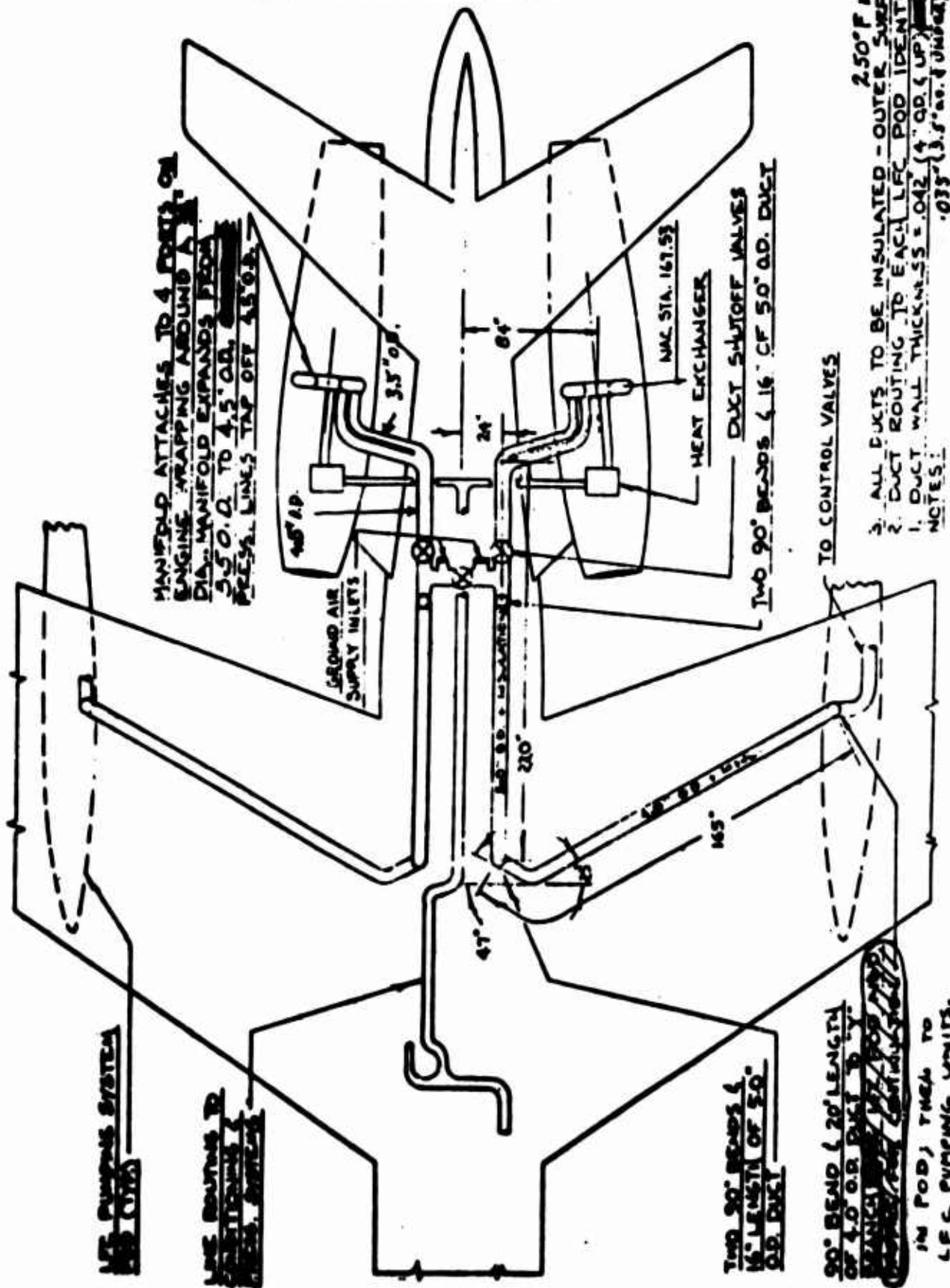


ENGINEER	NORTHROP CORPORATION NORAIR DIVISION	PAGE 8.44
CHECKER		REPORT NO. NOR 67-136
DATE June 1967	FIG 8.14	MODEL X-21A



ENGINEER	NORTHROP CORPORATION NORAIR DIVISION	PAGE 8.44
CHECKER		REPORT NO. NOR 67-136
DATE June 1967	FIG. 8.15	MODEL X-21A

SCHEMATIC - X-21A ENGINE COMPRESSOR
BLEED AIR DUCT AND VALVE SYSTEM



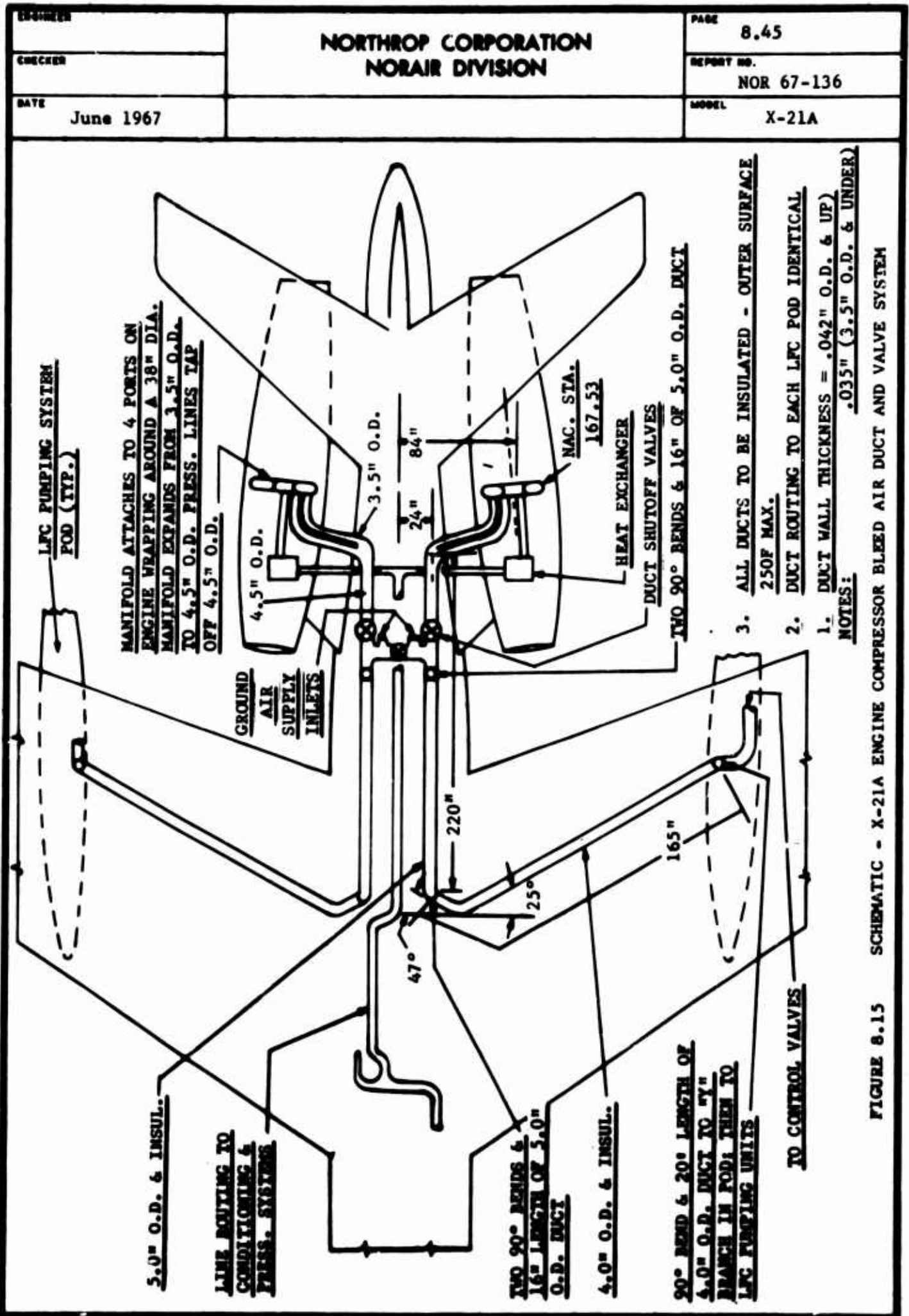


FIGURE 8.15

X-21A ENGINE COMPRESSOR BLEED AIR DUCT AND VALVE SYSTEM

DESIGNER	NORTHROP CORPORATION NORAIR DIVISION	PAGE 8,46
CHECKER		REPORT NO. NOR 67-136
DATE June 1967		MODEL X-21A

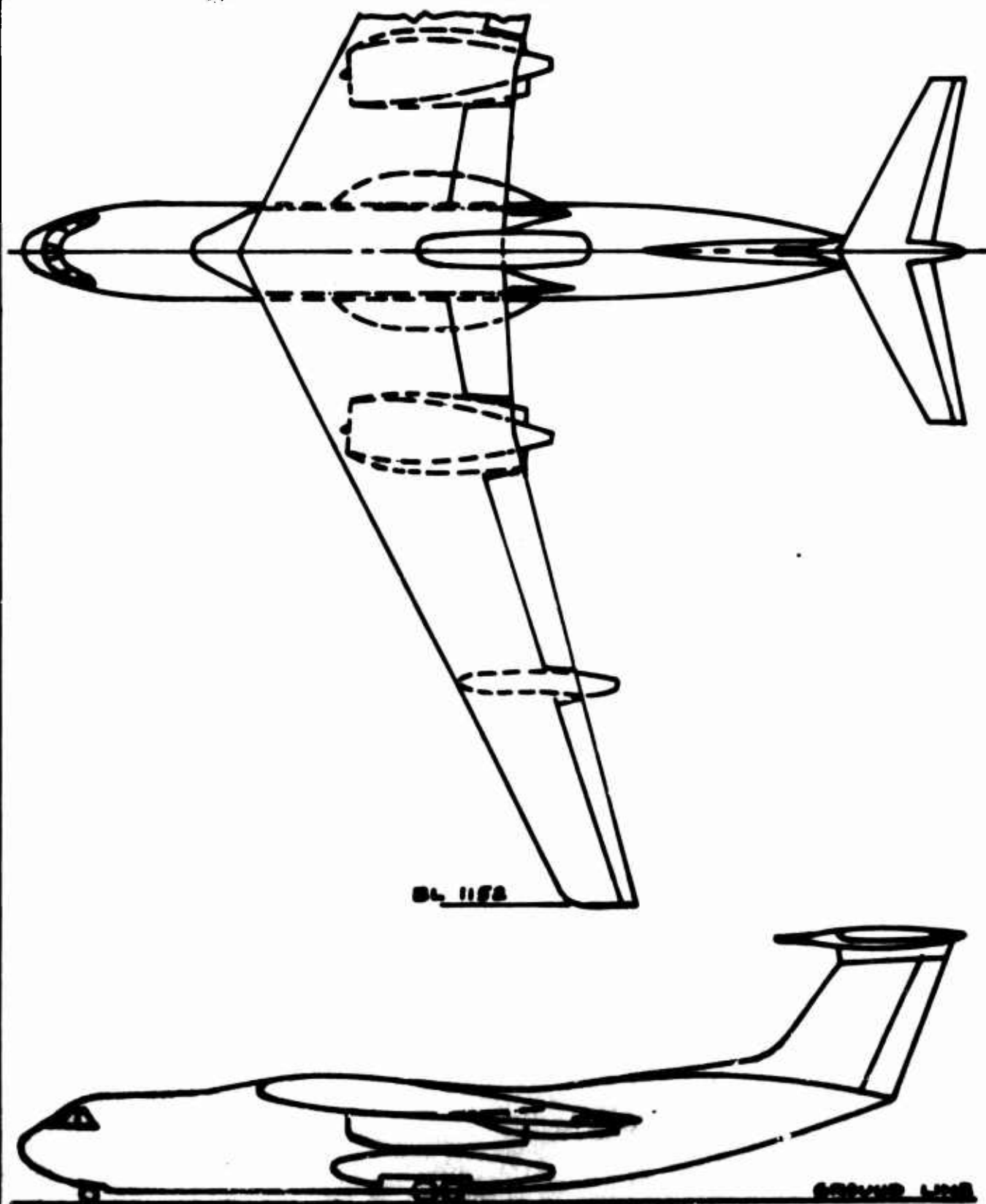
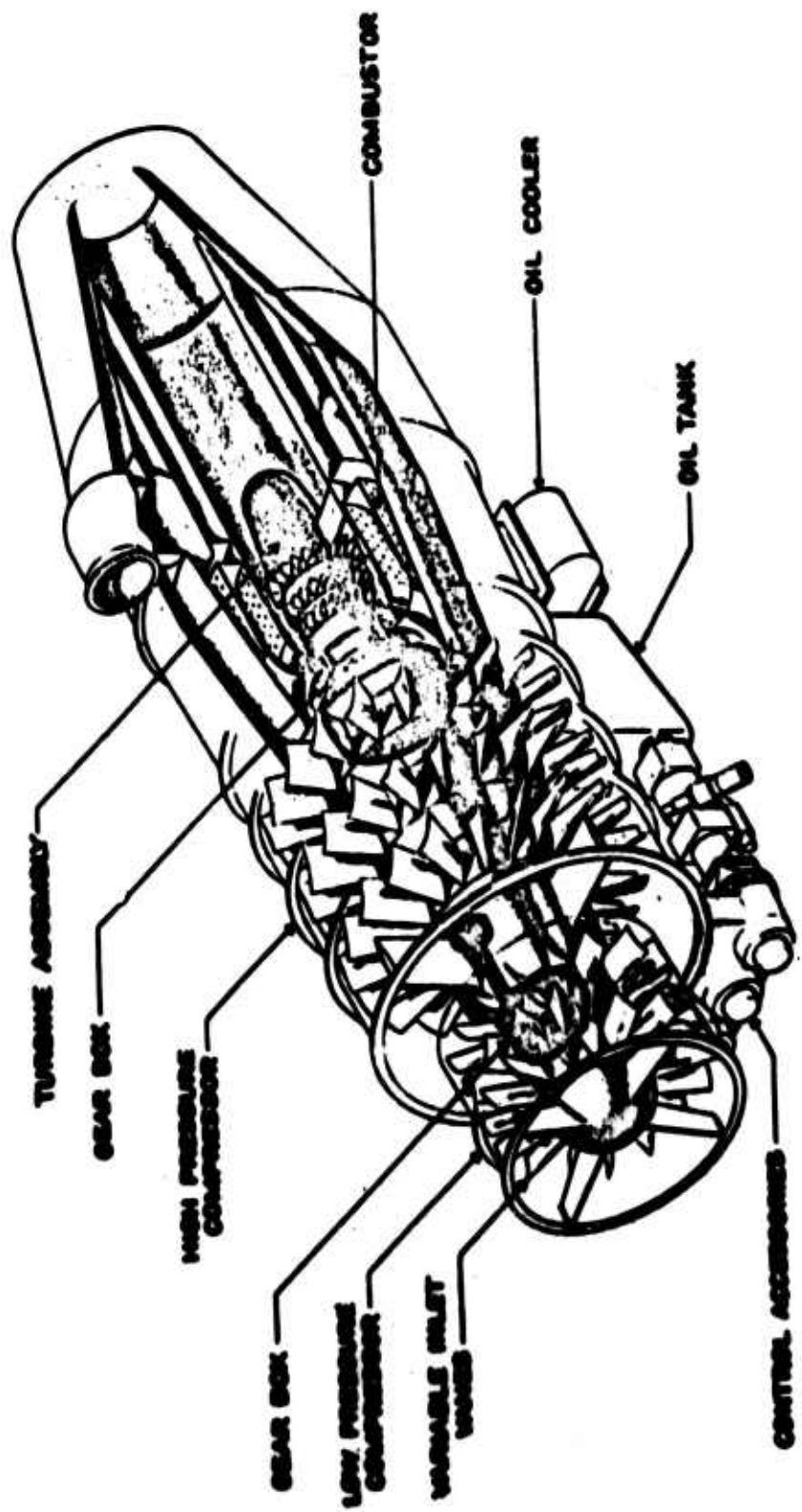


FIGURE 8.16 LAMINAR FLOW CONTROL -- LARGE
TRANSFORM AIRPLANE (LFC-15A)

ENGINEER	NORTHROP CORPORATION NORAIR DIVISION	PAGE 8.47
CHECKER		REPORT NO. NOR 67-136
DATE June 1967	FIGURE 8-1 ^a	MODEL X-21A

FIGURE 8.17 SUCTION COMPRESSOR
Low Pressure and High Pressure Compressors
Driven by a Common Bleed-and-Burn Gas Turbine



Courtesy of AResearch, Phoenix Div..

ENGINEER	NORTHROP CORPORATION NORAIR DIVISION	PAGE 9.00
CHECKER		REPORT NO. NOR 67-136
DATE June 1967		MODEL X-21A

SECTION 9

MAIN PROPULSION SYSTEM

BY:

W. A. Monahan, Jr.

March 1964

Revised May 1967

ENGINEER	NORTHROP CORPORATION NORAIR DIVISION	PAGE 9.00
CHECKER		REPORT NO. NOR 67-136
DATE June 1967		MODEL X-21A

SECTION 9

MAIN PROPULSION SYSTEM

BY:

W. A. Monahan, Jr.

March 1964

Revised May 1967

ENGINEER	NORTHROP CORPORATION NORAIR DIVISION	PAGE
CHECKER		9.01
DATE		REPORT NO.
June 1967		NOR 67-136
		MODEL
		X-21A

<u>SECTION</u>	<u>SECTION TITLE</u>	<u>PAGE NO.</u>
9.0	Propulsion System	9.02
9.1	System Requirements and Installation	9.02
9.1.1	Location and Configuration	9.02
9.1.1.1	Propulsion Engines	9.02
9.1.1.2	Pumping Pod Location	9.03
9.1.2	Engine Type Section	9.03
9.1.3	Inlet Design	9.04
9.1.3.1	Pressure Recovery	9.04
9.1.3.2	Sonic Inlet Considerations	9.04
9.2	System Performance Analysis	9.05
9.2.1	General Description of Method	9.05
9.2.2	Pumping System Performance	9.06
9.2.3	In-Flight Thrust Measurement	9.07
9.2.4	Minimum RPM for Laminar Flight (X-21A)	9.09
9.3	Description of X-21A System	9.10
9.3.1	Location and Configuration	9.11
9.3.2	Requirements of Engine	9.14
9.3.3	Inlet Design	9.16
9.4	Description of LFC-LTA System	9.18
9.4.1	Location and Configuration	9.18
9.4.2	Requirements for Engine for LFC-LTA	9.19

ENGINEER	NORTHROP CORPORATION NORAIR DIVISION	PAGE 9.02
CHECKER		REPORT NO. NOR 67-136
DATE June 1967		MODEL X-21A

9.0 PROPULSION SYSTEM

The determination of the optimum configuration for the propulsion system will be discussed in this section, treating such fundamental considerations as number of engines, location of engines and pylons. While not considered to be a part of the main propulsion system, the location of the pumping system is dictated by many of the usual criteria for locating a propulsion engine and by the need for a satisfactory overall configuration; hence, pumping system location also is discussed.

Propulsion and pumping system performance analysis utilizing installation-loss factors is treated, and the two systems are combined into an overall system for thrust specific fuel consumption determination. Flight test analysis methods are described. The optimization of pumping system power sources is also covered.

The features of the X-21A propulsion system that stem from its use in an LFC application are described.

Finally, the incorporation of all the design principles covered previously, and which were used in an LFC large transport airplane study, are briefly described.

9.1 System Requirements and Installation

9.1.1 Location and Configuration

9.1.1.1 Propulsion Engine

The determination of the "best" location of the propulsion engines entails much more study for a laminar aircraft than for a turbulent aircraft. Extensive configuration comparisons, treating all aspects of wing-mounted versus fuselage-mounted locations, are necessary. No "rules" have emerged from numerous design studies to provide a shortcut to configuring a vehicle, and optimum locations will vary: for the X-21A the best engine location was found to be on the aft fuselage in nacelles; but in the LFC-LTA study, two wing-mounted flush nacelles, each carrying two engines, were found to be optimum. The arguments leading to each selection are given in paragraphs 9.3.1 and 9.4.1, respectively.

Laminar flow control imposes only three constraints on propulsion engine and pumping system location in addition to the normal airplane design considerations.

- 1) Keep the laminar surfaces as free as possible of anything which will affect the pressure distribution and disturb the linearity of the isobars.

ENGINEER	NORTHROP CORPORATION NORAIR DIVISION	PAGE	9.03
CHECKER		REPORT NO.	NOR 67-136
DATE		MODEL	X-21A
June 1967			

- 2) Locate the pumping systems, including necessary ducts and valves, such as to minimize duct size and weight and to optimize flow paths for low loss and for control.
- 3) Provide an engine installation design that will cause as low as possible acoustic impact on laminar surfaces.

9.1.1.2 Pumping Pod Location and Shape

For a flush wing-mounted pod to create as small a turbulent area as possible, it is important that the front of the pod be small and that the major portion of its volume be located far aft on the chord (Section 7). Figure 9-1 shows the relative turbulent areas caused by the pumping pod and aileron actuator fairings on the X-21A. To minimize the disturbed area, pod nose shape undergoes a peculiar twist in this case.

The equipment "dry bays" within the wing will subtract from fuel volume. It will be necessary to consider the trade-off between using wing volume for good equipment accessibility or for fuel tankage.

A part pan location of pumping equipment permits the greatest flexibility in variation of suction airflow from the inner and outer wings and is also considered to be a very desirable factor with respect to minimizing duct losses.

9.1.2 Engine Type Selection

The engine type category having been selected by Mach number-altitude considerations, the general thrust class is dictated by both of the following: Thrust level of engines alone to meet take-off requirements, and thrust level of engines alone, when at cruise power, to meet approximately 90% of the cruise thrust required. Then a detailed comparative analysis of those engines meeting the type and class requirements can be made. The main selection factors are still the traditional trade-off comparisons involving weight, payload, range, fuel, take-off distance, wing area, aspect ratio, etc., but the requirements of providing for an LFC system enter into the competition for the first time. One of the trade-offs of primary concern is TSFC at cruise, including pumping system thrust and fuel flow.

ENGINEER	NORTHROP CORPORATION NORAIR DIVISION	PAGE 9.04
CHECKER		REPORT NO. NOR 67-136
DATE June 1967		MODEL X-21A

9.1.3 Inlet Design

Suppression of forward-propagating compressor noise can be achieved very efficiently by the use of an inlet duct centerbody which translates or expands to cause a normal shock wave to stand in the duct. Noise attenuation by this means is not selective as to frequency and can reach 25 to 30 db without appreciable pressure loss. (See Section 11 for noise attenuation discussion.) Suppressions of 3 to 5 db can be achieved by lining the inlet duct walls with sound absorbent materials. Attenuation by this means is tunable for reduction of specific frequencies and can be achieved with no more loss than the centerbody arrangement.

9.1.3.1 Pressure Recovery

For a normal inlet, pressure loss is made up of lip loss, expansion loss, and friction loss. For an inlet with a variable centerbody, friction loss will be higher, expansion loss will probably be higher but depends on expansion angle, and shock loss is added. From one-dimensional normal shock functions, the loss of total pressure downstream of a weak shock is less than 0.1% between 1.00 and 1.10 Mach number and is, therefore, of little significance.

9.1.3.2 Integration of "Sonic" Inlet with Usual Inlet Requirements

- (a) A choked flow condition should be maintained over the cruise power airflow demands.
- (b) The minimum duct area with centerbody retracted can be determined by corrected airflow demand at maximum attainable corrected speed. Maximum corrected speed usually occurs only at very low Mach numbers where LFC will probably not be required. Thus, an unchoked condition can be attained with a larger duct size and higher recovery, or a choked condition can be attained with a smaller duct size.
- (c) The minimum duct area with centerbody extended will be that LFC condition at which RPM, and hence corrected airflow, is least. For a cruise-only application, the area variation required will be least.
- (d) The length of duct necessary to minimize distortions is that length that will keep diffuser wall divergence under an equivalent 14° included angle for cruise or take-off.

ENGINEER	NORTHROP CORPORATION NORAIR DIVISION	PAGE
CHECKER		9.05
DATE		REPORT NO.
June 1967		NOR 67-136
		MODEL
		X-21A

- (e) Radial and circumferential distortions at the compressor face will not be materially increased over those of a similar duct without a "sonic" plug provided that the diffusion equivalent angle does not exceed the 14° limit. If the 14° limit is exceeded at low corrected flows, the increased distortions will have a smaller detrimental effect on blade fatigue.
- (f) The external lip shape and contours need not be different from those shapes that would otherwise be suitable without a "sonic" inlet.
- (g) The internal lip shape need not be different from those shapes that would otherwise be suitable without a variable centerbody.

9.2 System Performance Analysis

This part will discuss some propulsion system performance analysis problems and techniques peculiar to an LFC airplane. Included also are comments on the method of analyzing pumping system performance and combining it with that of the propulsion engine to arrive at the overall propulsion system performance.

9.2.1 General Description of Method

The effect of the pumping system on the propulsion engine is:

- 1) To reduce cruise thrust required from the propulsion engines. Cruise thrust is reduced because LFC reduces airplane drag and because the pumping system contributes to total thrust.
- 2) To increase engine power extraction requirements, either compressor air bleed or shaft horsepower.
- 3) To alter engine specific fuel consumption (SFC). The overall SFC of the LFC aircraft may or may not be reduced by the propulsion of the pumping system (depending upon selection of engine types, percentage of aircraft surface laminarized, exhaust velocity of the pumped LFC air, and other design variables of the LFC aircraft); but the product of SFC and the necessary power (i.e., the actual fuel flow in pounds per mile) is reduced in comparison with a turbulent airplane of comparable weight or size.

ENGINEER	NORTHROP CORPORATION NORAIR DIVISION	PAGE
CHECKER		9.06
DATE		REPORT NO.
June 1967		NOR 67-136
		MODEL
		X-21A

For any given flight condition, the performance of the propulsion engine is calculated over a range of powers to cover the range of expected drags, and over a range of extractions from minimum aircraft uses to full pumping system and aircraft requirements. Pumping system performance calculations must also cover a range of expected LFC flow variations at that same flight condition. The propulsion engine and the pumping system performance are then merged into one overall "propulsion system" analysis.

The X-21A program followed the above procedure. Calculations of engine performance manually were supplanted by EDP (electronic data processing) machine calculations which gave, in addition, secondary system outputs which previously were unobtainable because of the amount of calculation. The use of EDP also allows more frequent updating of inputs to keep abreast of model test results, revised specifications, configuration changes, flight test results, and other refinements as a design idea reaches its manifestation in hardware. Pumping system calculations were hand calculations throughout, in spite of the fact that they were quite tedious, because of frequent changing of LFC flow and lack of reliable compressor performance maps.

For an LFC application program, much the same procedure is recommended but with additional emphasis on machine calculations. For example, the engine and its installation can be programmed from the beginning and changed when necessary to update inputs. For proposal comparison, pumping machinery is likely to be so diverse that only hand calculations would be versatile enough to cover all cases, and a "one-shot" comparison is also required. In the early design phase also, combined performance may be done by hand until a suitable program using reliable inputs is checked out; from then on, EDP machine computing is preferable.

9.2.2 Pumping System Performance

Detailed analysis starts with the given flight point and LFC flow and pressure. Compressor "corrected airflow" is found and, with pressure ratio and appropriate Reynolds number correction, allows horsepower to be found. From horsepower, turbine torque, speed, fuel flow and airflow, both actual and "corrected", are found. From these values pumping system thrust is determined; and, subtracting from a given drag, propulsion engine thrust-required is solved for. The detailed steps must be appropriate to the actual hardware involved.

ENGINEER	NORTHROP CORPORATION NORAIR DIVISION	PAGE 9.07
CHECKER		REPORT NO. NOR 67-136
DATE June 1967		MODEL X-21A

Analysis of the X-21A pumping system followed a different scheme than that of the engine: engine performance was analyzed over a wide range of altitudes, Mach number and RPM; the pumping system was analyzed only at 11 specific altitude/Mach number flight conditions for which LFC airflow and pressure and laminar drag were given. For several of these conditions, LFC flow was perturbed in 5 steps from -15% to +30% of the nominal amount.

9.2.3 In-Flight Thrust Measurement

9.2.3.1 General

The measurement of in-flight thrust is one of three ways by which drag may be analyzed, the other two ways being measurement of pressure recovery in the wing wake and fuel flow reduction. (See Section 12 for discussion of these latter two methods.)

For steady-state flight, thrust is equal in magnitude to drag; thus for either turbulent or laminar flow the summation of all thrust terms yields the total drag. The paragraphs that follow identify the terms that contribute to thrust and drag. The engine analysis is handled in the usual manner.

9.2.3.2 Pumping System LFC Airflow

The low pressure compressor map, Figure 8.4, is entered with values of the ratio of diffuser static pressure (P_{S_3}) to inlet total (P_{T_1}), and corrected rotor speed ($N/\sqrt{\theta_1}$), to obtain the corrected airflow parameter ($W_{c_1} \sqrt{\theta_1}/\delta_1$). Compressor airflow becomes:

$$W_{c_1} = \frac{\text{Corrected Airflow} \times \delta_1}{\sqrt{\theta_1}} \quad \text{lbs/sec}$$

where the symbols are defined on the compressor map.

The effect of Reynolds number on reducing airflow, though small, is compensated by utilizing a speed correction curve and re-entering the compressor map with the newly-corrected rotor speed. High pressure airflow is the sum of the low pressure discharge and high pressure suction airflows and is located on the GTMC compressor map, Figure 8.5, by inlet total pressure (P_{T_7}) and temperature (T_7),

exit total pressure, and rotor speed. The calculation procedure for determining the GTMC airflow is the same as that described for the low pressure compressor.

ENGINEER	NORTHROP CORPORATION NORAIR DIVISION	PAGE 9.08
CHECKER		REPORT NO. NOR 67-136
DATE June 1967		MODEL X-21A

9.2.3.3 Pumping System Bleed Airflow

For the low pressure compressor, turbine exhaust discharge flow is subcritical in the duct for all cases, and flow coefficient is estimated to be 0.80. The steps required to calculate turbine exhaust flow are:

- a) Compute the ratio (P_T/P_S) and read the corrected flow rate parameter ($W\sqrt{T_T}/P_T A$) from a graph constructed specifically for the low pressure turbine exhaust duct. The symbols are:

P_T = total pressure, P_S = static pressure,

W = weight flow rate, T_T = total temperature,
and A = duct area.

- b) Compute the actual weight flow rate W as follows:

$$W = \frac{(\text{corrected flow rate parameter}) P_T A}{\sqrt{T_T}} \times .80$$

Total air bleed from each engine is measured by a boost venturi, and high pressure turbine airflow is total bleed flow minus low pressure turbine airflow.

9.2.3.4 Pumping System Thrust

The X-21 low pressure turbine exhausts to free stream through a 4.0 inch diameter duct slanted 30° downward from the horizontal. The velocity coefficient for turbulent flow is estimated at .83 which, in combination with the flow coefficient of .83 and the axial component of the thrust vector of .866, yields an estimated thrust coefficient of .60. Gross thrust was calculated in early flight tests and when it proved to be approximately zero (as analysis had previously indicated it would), it was thereafter neglected.

Thrust of the high pressure compressor nozzle is defined by a standard subcritical nozzle thrust curve using the ratio of specific heats $\gamma = 1.4$ and is based on the same equations as that of an engine nozzle working at a low pressure ratio and a constant nozzle area. The data inputs are measured values of compressor exit total pressure (P_T) and ambient static pressure (P_{am}). The only calculation required to obtain gross thrust is to multiply the curve value of F_g/δ_{am} by δ_{am} , where δ_{am} is the ratio of ambient static pressure to standard sea level pressure. F_g is the gross thrust.

ENGINEER	NORTHROP CORPORATION NORAIR DIVISION	PAGE 9.09
CHECKER		REPORT NO. NOR 67-136
DATE June 1967		MODEL X-21A

The thrust of the turbine exhaust nozzle is determined in the same way as that described in the preceding paragraph for the high pressure compressor nozzle, except that the ratio of specific heats incorporated in the nozzle performance curve is $\gamma = 1.33$ instead of 1.40.

Ram drag of the suction air must be subtracted from system gross thrust; its value is the product of mass flow rate and true airspeed (ram drag of bleed air is charged to the engine and, therefore, neglected here).

$$FRHPC = \frac{W_{c2}}{g} \times V_o \times 1.689$$

where: W_{c2} = GTMC compressor airflow lb/sec.

V_o = True airspeed, knots.

Thus the net thrust for the system is:

$$FNPS = FGLPT + FGHPT + FGHPC + FRHPC$$

Definition of terms:

HPC - High Pressure Compressor Unit
 LPC - Low Pressure Compressor Unit
 FNPS - Net Thrust of Pumping System
 FGLPT - Gross Thrust of LPC Turbine
 FGHPT - Gross Thrust of HPC Turbine
 FGHPC - Gross Thrust of HPC Compressor
 FRHPC - Ram Drag of HPC Compressor

An example of net thrust versus fuel flow for the X-21A airplane is shown in Figure 9.2.

9.2.4 Minimum RPM for Laminar Flight (X-21A)

Since noise may prove to be detrimental in the establishment and maintenance of laminar flow, it is apparent that a thorough investigation of the influence of noise must be made at the highest design Reynolds number of 40×10^6 . The "quiet limit" in such a test would be to establish a shallow dive, shut down engines entirely, and take measurements. Obviously, it is not possible to shut down engines and continue to operate the aircraft systems including the LPC pumping equipment in which engine compressor bleed air is required. A low engine RPM which simultaneously supplies (1) sufficient bleed, (2) sufficient thrust, and (3) sufficient airflow to choke the inlet, is the least noisy laminar condition.

ENGINEER	NORTHROP CORPORATION NORAIR DIVISION	PAGE
CHECKER		9.10
DATE		REPORT NO.
June 1967		NOR 67-136
		MODEL
		X-21A

Pumping system performance calculations at nominal LFC airflow rates were made along the 40×10^6 Reynolds number line at a weight of 80,000 pounds. These calculations indicated the pumping system task, and corresponding speed required to deliver sufficient pressure and flow of bleed air to do the pumping system task. The results are plotted on Figure 9-3. Thrust requirements to maintain level flight of the airplane along the same line are also plotted. The final calculations indicated the minimum engine corrected airflows, and hence engine speed required to just maintain choked inlet conditions along that line and are also plotted on Figure 9.3. As the figure shows, engine speed sufficient to maintain choked inlet conditions is higher than that required to operate the pumping system. If engine speed is allowed to drop below that causing choking airflow, nominal LFC airflow can still be maintained, but the inlets will be emitting compressor noise. Any inhibition to initiation or maintenance of laminar flow can then be measured. In fact, however, no loss of laminar flow due to compressor noise was observed in X-21A flight tests.

9.3 Description of X-21A System

The X-21A is powered by two non-afterburning YJ79-GE-13 engines redesignated from the J79-GE-3A after being modified by removal of afterburner and associated equipment. In addition to providing propulsion thrust, the engines also supply compressor bleed air for operation of the LFC pumping equipment. Mounted on each engine are two hydraulic pumps, a constant speed drive and alternator, and an auxiliary electrical generator for flight test instrumentation. Other accessory systems are a fire detection system and an ice detector system. These engines are mounted in nacelles on each side of the aft fuselage. The nacelle is of typical construction consisting of frames, longerons, intercostals and skins. The inlet contains a movable plug to create sonic velocity in the inlet duct, thus preventing the forward propagation of engine noise. The tailcone is removable. An access door on the bottom of the nacelle provides for servicing the engine and, together with the removable tailcone, allows for installation and removal of the engine. Engine bay cooling is provided by a ram air chin scoop and a tailpipe ejector.

Fuel can be supplied directly to the engines from the aft fuselage main tank or from the inboard wing main tanks. Any combination of fuel supply from the three main fuel tanks can be selected. During normal fuel system management, the wing tanks are maintained full while the fuselage fuel, by way of the aft fuselage main tank, feeds the engines. The wing main tanks continue to supply fuel to the engines after the fuselage fuel has been consumed. Sequence of fuel supply is only limited by airplane CG control and wing bending considerations.

ENGINEER	NORTHROP CORPORATION NORAIR DIVISION	PAGE 9.11
CHECKER		REPORT NO. NOR 67-136
DATE June 1967		MODEL X-21A

The determination of the optimum configuration for the propulsion and pumping systems will be discussed in this section treating such fundamental considerations as number of engines, location of engines, pylons, and pumping system location. Finally, detailed factors of design are described wherever the consideration of LFC necessitated some deviation from usual practices.

9.3.1 Location and Configuration - See Figure 9.4

It is shown on comparison charts, pages 9.12 to 9.13 inclusive, that the aft-fuselage-mounting arrangement is superior in the two considerations deemed to have most importance in this program: wing isobar linearity and low noise level. The weight penalty for this, a 10.5% reduction in useful load for ballast, did not compromise the design mission.

ENGINEER		NORTHROP CORPORATION NORAIR DIVISION	PAGE 9.12
CHECKER			REPORT NO. NOR 67-136
DATE June 1967		Comparison of Wing versus Aft-Mounted Engine Location	MODEL X-21A
Item of Consideration	Wing-Mounted	Aft-Mounted	
1. Isobar linearity and pressure patterns.	Turbofan engines (because of their size) mounted on the wing cause an increase in pressure coefficient in a local area. This amount of increase will limit the maximum lift coefficient attainable before the wing becomes turbulent. The smaller turbojet causes less disturbance.	Influence of aft-mounted engines, whether turbojet or turbofan, on the pressure patterns will be measurable but small.	
2. Noise Considerations.			
a. Estimated noise levels (laminar flight regime) over the wing throughout the LFC flight regime for straight jet engine without noise suppression devices.	a. See Section 11 for a discussion of the effects of engine noise on laminarized surfaces.	See Section 11 for a discussion of the effects of engine noise on laminarized surfaces.	
b. Same as (a) above with noise suppression devices.	b. Model tests of three-dimensional sonic inlet plug have shown that when choked, reductions in the overall SPL on the order of 20 db can be obtained (18 db in the plane of the inlet, 25 to 29 db a nozzle diameter ahead of the inlet plane). Although Norair has not conducted any tests on sonic exhaust treatment, General Electric data indicate that sound suppression mufflers for the J79 engine could reduce overall SPL near the wing 4 to 5 db.	Same	
c. Same as (a) above for turbofan engines.	c. No data are available on a sound suppression nozzle for a turbofan engine; however, the reduction is expected to be comparable. An ejector shroud on the straight jet and a mixing tailpipe on the turbofan would provide additional decrease but no quantitative test data are available.	Such noise suppression devices will probably not be required.	

ENGINEER	NORTHROP CORPORATION NORAIR DIVISION		PAGE 9.13
CHECKER			REPORT NO. NOR 67-136
DATE June 1967	Comparison of Wing versus Aft-Mounted Engine Location		MODEL X-21A
Item of Consideration	Wing-Mounted	Aft-Mounted	
3. Station Location	Located at Wing Station 180, approximately the maximum out-board location compatible with "one engine out" stability. The exhaust plane is 60 inches aft of the wing trailing edge. This minimizes impingement of noise on wing laminar surfaces.	The aft engine inlet, at Fuselage Station 608, is 60 inches aft of the wing trailing edge. The tailpipe is ended at the trailing edge of the horizontal tail so noise will not impinge on any airplane structure.	
4. Maximum Engine	Total suspended weight of engine, nacelle, and pylon is limited by wing flutter considerations. No engine considered exceeded weight which could be accommodated.	Any engine requires forward ballast. This puts premium on lightest engine. Strength of X-21A fuselage dictates the use of an engine in the weight class of the J79 or lighter.	
5. Operational Hazards			
a. FOD	More susceptible to vortex-lifted foreign objects due to low inlet. Can be minimized by "blow-away" jet.	More susceptible to tire-thrown foreign objects. Wheel fenders can be used to minimize.	
b. Inlet Distortion	No unusual problems associated with wing-mounted jet.	Distortions due to angle-of-attack are reduced. The location is selected to keep the inlet out of the wing wake.	
c. Flame-Out	No susceptibility to flame-out due to LFC airplane design.	Same as wing-mounted comment.	
d. Extreme Angle-of-Attack	No unusual problem.	No effects of normal large angles of attack, as engine inlet is below wing wake.	
e. Maneuver Effects	No problem expected.	No problem expected.	
f. One Engine Out	Can be accommodated at selected wing station. (See 3 above.)	No problem.	
6. <u>Pylon Position</u>			
The high pylon position allows the use of the existing speed brake with only a minor shortening of the upper aft corner to provide nacelle clearance when in the open position. An additional benefit is that the pylon-to-nacelle structure is above the nacelle centerline, thus allowing the maximum arc for an engine access door.			

ENGINEER	NORTHROP CORPORATION NORAIR DIVISION	PAGE
CHECKER		9.14
DATE		REPORT NO.
June 1967		NOR 67-136
		MODEL
		X-21A

7. Vertical Position and Tilt

The nacelle is positioned vertically to meet these three governing criteria: 1) the engine should be sufficiently high to prevent the entry of foreign objects thrown up by the wheels; 2) the engine should be not so high that it will be in the wing wake at any angle of attack, so as to prevent flame-out; 3) the thrust vector should pass approximately through the airplane C.G. The vertical position chosen places the upper inlet lip eleven inches below the extended wing chord. The engine is tilted two degrees nose down to align the inlet into the angle midway between zero angle of attack and stall angle.

8. Horizontal Position and Cant

The nacelle is positioned horizontally such that the inboard inlet lip is approximately one inlet diameter removed from the fuselage and is canted three degrees nose outboard. For least fuselage-to-nacelle interference drag it was desirable to increase this separation but pylon structural weight thereafter increased rapidly. The three degrees outboard cant of the engine positions the C.G. of the inlet parallel to the fuselage local slope to minimize interference drag.

9. Longitudinal Position

In the interest of reducing noise effects, it was desirable to place the engine as far aft as possible but this was limited by the fixed location of the main landing gear; the airplane center of gravity must obviously remain ahead of the main landing gear. The ejector should not terminate much, if any, ahead of the horizontal surface so as to eliminate interferences on the horizontal stabilizer from engine jet wake effects. To maintain safe landing and ground handling characteristics the selected location is considered to be a fair compromise between nose ballast capabilities, proximity of inlet to wing trailing edge, airplane stability, and minimum structural rework to the aft fuselage.

9.3.2 Requirement of Engine

In addition to requirements of the sort in paragraph 9.1.2, there were other requirements for the X-21A engines:

"Existing" Status - The basic engine shall have in-use or in-production status and shall have passed a 150-hour Qualification Test.

Modification - The basic engine may be modified, if required, to meet the requirements of these criteria using methods and material in compliance with ANA Bulletin No. 343.

Augmentation and Exhaust Nozzle - The engine shall not be equipped with thrust augmentation and shall be equipped with a fixed area tailpipe, the nominal area to be selected so as to achieve maximum sea level static thrust. Tabs shall be provided by which the area may be adjusted 4% larger and 7.5% smaller than nominal.

ENGINEER	NORTHROP CORPORATION NORAIR DIVISION		PAGE 9.15
CHECKER			REPORT NO. NOR 67-136
DATE June 1967		MODEL X-21A	
<p><u>Requirements List</u> - The engine shall have performance and configuration features compatible with the "Required" column of the following table.</p>			
ITEM	GENERAL REQUIREMENT	SPECIFIC REQUIREMENT	AVAILABLE FROM J79-13
Minimum Cruise Thrust	Sufficient to achieve $M_o = .80$ at 45,000 ft. (turbulent) ⁰	1695 lbs	1720 lbs. at MIL & 1% comp. bleed
Minimum T.O. Thrust	Sufficient to T.O. at S.L. from 5,000 ft. runway over 50' obstruction at 55,000 lbs. T.O. gross weight	8300 lbs. (Installed Thrust)	8940 lbs.
Compatibility with Sonic Inlet	Must be relatively insensitive to inlet distortion. Compressor stability and blade stresses considered	Compatible with inlet plug in any position	6% radial distortion; 12% circum. distortion
Compressor Bleed Air	For pumping equipment, cabin conditioning, and anti-icing uses	2.21 lbs/sec. approx. maximum	3.24 throughout cruise range
Weight	Low enough to utilize aft-mounting considering airplane balance	3,000 lbs. approx. maximum	2550 lbs.
Maximum Diameter	a. Nacelle size not so large as to cause excessive interference drag b. Nacelle and exhaust nozzle ground clearance considerations	Diameter small enough to meet conditions in preceding column	Maximum diameter = 44.00 in.
Specific Fuel Consumption	Low S.F.C. not essential. Although desirable to minimize, not of first importance since evaluation of LFC determined by other methods	S.F.C. low enough to provide sufficient range	Installed S.F.C. approx. 1.22 at cruise conditions of 45,000 ft. alt. & $M_o = 0.8$
Accessory Capability	Mechanical PTO's for: a. 2 hydraulic pumps b. 30 KVA CSD and Alt. c. 500 amp. D-C Generator	See General Requirements	a. 600 in. # cont. b. 450 in. # cont. c. 450 in. # cont.
Maximum Length	Not significant, as extended tail-pipe or aft-mounting used in all configurations	See General Requirement	Maximum length = 174 in.

ENGINEER	NORTHROP CORPORATION NORAIR DIVISION	PAGE 9.16
CHECKER		REPORT NO. NOR 67-136
DATE June 1967		MODEL X-21A

A USAF directive indicated that the engine should be selected from a list of engines in the USAF Inventory, of 10,000 pounds thrust category, considered to be in "long supply." The J79-GE-3A, several older models of the J57, and the J71-A-13 were offered as choices. Later engines which offered better fuel consumption were available only with a ten to eighteen-month lead time, and would mean procurement from project funds rather than as GFAE. In all cases, a non-afterburning engine was to be used, by removing the afterburner and associated components if so equipped originally. The best engine of those offered, determined by factor comparison, was the J79-GE-3A, and it was the only one below the maximum weight limit. The improved fuel economy of engines available eighteen months hence was not, in itself, sufficient reason to delay the program, and the money for their cost could be used more advantageously elsewhere in the program.

"Available" column of the previous table shows that the requirements of the X-21A are met with the non-afterburning J79-GE-3A, redesignated the J79-GE-13.

9.3.3 Inlet Design

The shape, proportion, and dimensions of the X-21A sound-suppressing inlet are shown in Figure 9.5 and 9.6. It has a manually-controlled translating centerbody for the purpose of causing a normal shock wave to stand in the duct. The efficient suppression of forward-propagating compressor noise that can be obtained with this scheme has previously been demonstrated in the Northrop Norair wind tunnels.

9.3.3.1 Flow Criteria

- a. The minimum duct area with centerbody in intermediate positions is to be determined by engine airflow demands at cruise and shall cause a choked flow condition to be optionally maintained over a wide regime of cruise power settings.
- b. The minimum duct area with centerbody retracted is to be determined by engine airflow demands at $108\% N/\sqrt{\theta}$, the maximum attainable corrected speed, without choking.
- c. The minimum duct area with centerbody extended is to be determined by the requirement that choked flow conditions must be obtained at a low altitude and a low free stream Mach number. The condition selected is 3,000 feet at $.42 M_0$.

ENGINEER	NORTHROP CORPORATION NORAIR DIVISION	PAGE 9.17
CHECKER		REPORT NO. NOR 67-136
DATE June 1967		MODEL X-21A

- d. The length of duct shall be determined by the length needed to keep diffuser wall divergence under an equivalent 14° included conical angle for cruise or take-off positions.
- e. Radial and circumferential distortions at the compressor face shall be minimized, possibly to the limits of engine Model Specification.
- f. The external lip shape and contour shall be of the NACA 1-series and shall have a critical Mach number above the design cruise Mach number.
- g. The internal lip shape and contour shall be elliptical and optimized for a satisfactory compromise between take-off and cruise performance.
- h. Inlet overall pressure ratios shall be designed to be as high as possible consistent with the above requirements. Minimum desirable ratios shall be .96 at choked flow with cruise corrected airflow demands, and .96 unchoked flow with maximum corrected airflow demands.
- i. Design, performance, and test data shall be organized in such a manner that the data can be presented in accordance with Specification MIL-S-17984A(ASG).

9.3.3.3 Inlet Performance Results

Total pressure ratio versus corrected airflow was measured in typical flight and is shown in Figure 9.7. Notice that recovery is some 1% to $1\frac{1}{2}\%$ higher than the estimated .96 used for design at the choke point. But if corrected flow is further increased without retracting the plug, recovery is severely reduced. This points up the necessity of having shock sensors of high sensitivity. The drop in recovery is attributed to shock losses and losses from separation and distortion.

During static tests, choking occurred at 100% corrected speed as compared to the design objective of 108% corrected speed. Data showed that corrected airflow at 100% speed was up from the specification amount of 161 lbs/sec to 163 lbs/sec and the inlet was manufactured to an area smaller than that used in sizing calculations.

ENGINEER	NORTHROP CORPORATION NORAIR DIVISION	PAGE 9.18
CHECKER		REPORT NO. NOR 67-136
DATE June 1967		MODEL X-21A

Minimum flow choke point was 111 lbs/sec for design and was measured to be 113 from model tests, 114 from flight tests, and 115.5 from static thrust stand tests. Using 114 as an average, an engine of specification airflow will choke at 85.8% RPM, up .8% from design, and a typical engine will choke at 86.8%, up 1.8% from design. Both RPM's are acceptable for the minimum cruise investigation.

Radial distortion versus corrected airflow is also shown on Figure 9.7 and shows that the target limit of 6% is always exceeded at choke. Radial distortions in static tests at choke varied from 10% with plug fully extended to 13% when fully retracted. The flight test data, Figure 9.7, show somewhat higher values of radial distortion at choke. If corrected flow is increased beyond the value causing choke, distortion increases rapidly. Early static tests had shown that radial distortions would exceed the manufacturer's limit and a series of tests was conducted imposing distortions of 24, 19, and 22% at plug extensions of 3.7 inches, 8.0 inches, and fully extended respectively, to establish where the distortion limit really existed. No detrimental performance effects on engine operation were noted, indicating that the J79-GE-13 engine is highly insensitive to radial distortion.

Circumferential distortion indices versus airflow are also shown in Figure 9.7 and do not define distinct trends similar to radial distortion. In general, maximum distortions occur when the inlet is choked and no appreciable increase in distortion results when the inlet is overchoked. Distortion indices are considerably less than engine manufacturer's limits.

For noise reduction discussions, see Section 11.

9.4 Description of LFC Large Transport Airplane (LFC-LTA) System

As stated previously in Section 8.4, the design principles and know-how acquired in the X-21A program were applied to a study for the application of LFC to a large transport airplane of the C-141 type. The application study was constrained by the assumption that the LFC design could be phased into the production of the non-LFC airplane on a minimum change basis.

9.4.1 Location and Configuration

Propulsion arrangement for the LFC-LTA resulted in two wing-mounted pods, each carrying two engines, as being superior when the restraint of limited redesign was imposed. The arrangement evolved as follows:

ENGINEER	NORTHROP CORPORATION NORAIR DIVISION	PAGE 9.19
CHECKER		REPORT NO. NOR 67-136
DATE June 1967		MODEL X-21A

Straightest isobars and least noise, hence best LFC, again occurred with an aft-fuselage mounted arrangement. The resulting aft shift of the CG could be counteracted by: 1) forward ballast of approximately 40% of payload; or 2) wing and landing gear relocation of a more aft position. The first solution was obviously too great a payload penalty and the second was ruled out because it necessitated scrapping of too much expensive tooling, especially fuselage-to-gear attach frame forging dies. The engines must, therefore, remain on the wing.

Noise levels of various LFC-LTA layouts are estimated to be as shown in Figure 9.8. The allowable noise level of the LFC-LTA wing is approximately the same as that of the X-21A wing, or 100 db SPL. It is obvious that some noise reduction scheme must be found. A co-axial extended tailpipe carrying separate fan and jet exhaust, terminating co-planar at the wing trailing edge, reduced noise below the maximum permissible value.

The general principles of nacelle location and configuration are discussed in Section 7.0; following those principles, the flush-mounted nacelle illustrated in Figure 8.16 was found to be superior for this study.

The dual-engine pod will not materially increase pre-flight or post-flight inspection time over a single-engine nacelle design because items normally checked are equally accessible in either configuration.

9.4.2 Requirements of Engine for LFC-LTA

Selection of an engine for the laminarized LTA was to be made from turbofan or bypass engines which were, or were soon to be, in production. Fan engines were more desirable than straight turbojets because of their better specific fuel consumption and lower exhaust noise characteristics. Selection was based on: 1) take-off thrust, and 2) cruise performance.

If the wing uses only those high-lift devices whose retracted smoothness will still result in full-chord laminar flow, then take-off thrust requirements are the highest. This occurs because maximum lift coefficient is smallest and, to realize sufficient actual lift for take-off, highest speed must be attained. To keep take-off distance within limits, acceleration derived from thrust must be the highest. By giving up full-chord laminar flow on parts of the wing and equipping those portions with high-lift devices, it is possible to reduce the take-off thrust requirement. In this case a higher lift coefficient is in use and sufficient actual lift is realized at a slower speed. For the same take-off distance, then, less acceleration, hence less thrust, is required. The trade-off exchanges less take-off thrust-required for a more complicated flap system. With simple flaps, an engine of 17,500 pounds rating is required.

ENGINEER	NORTHROP CORPORATION NORAIR DIVISION	PAGE 9.20
CHECKER		REPORT NO. NOR 67-136
DATE June 1967		MODEL X-21A

The laminarized airplane will require a cruise thrust rating of approximately 2,160 pounds and an SFC minimum at that thrust. The original engines must be reduced in power to a point below which minimum SFC occurs, thereby suffering a 2.0% penalty in SFC. A comparison based on cruise fuel consumption and weight showed no other engines having a lower installed SFC. When an airplane with high-lift devices and lighter, lower take-off thrust engines is at cruise, the partial loss of laminar flow adds enough drag to overcome the weight advantage. For engines having a large-enough saving in weight, a higher SFC may be accepted if range, considering overall weight, is greater.

Thus it seems the most desirable engine is one having high thrust at take-off and low thrust at cruise. This would indicate that a take-off thrust-augmented (afterburner, water-injection, or the like) engine should be chosen to realize the highest thrust-to-weight ratio during cruise. Unfortunately, augmentation also costs weight and lowers thrust-to-weight ratio. The ideal engine would have a high ratio of take-off thrust to cruise thrust, have 17,500 pounds of take-off thrust, lowest SFC at 2,160 pounds cruise thrust, and of course low weight. With engines of bypass ratios, $W_{fan}/W_{primary}$, in the order of 1 to 1.5, the size is set by take-off thrust requirements. When all their secondary effects were compared, the original engines used in the turbulent airplane were better than any other considered. In addition, little or no change was required in existing systems.

The LFC-LTA airplane powered with the original engine showed more-than-adequate take-off performance and, with its abundance of cruise thrust, suggested that its payload-range envelope could be greatly extended if airplane gross weight were allowed to increase. This was the subject of additional study and the results were even more favorable for LFC.

ENGINEER		NORTHROP CORPORATION NORAIR DIVISION		PAGE 9.21
CHECKER				REPORT NO. NOR 67-136
DATE June 1967				MODEL X-21A
ITEM	GENERAL REQUIREMENTS	SPECIFIC REQUIREMENTS PER ENGINE	AVAILABLE FROM EACH ENGINE	
1. Take-off thrust	Sufficient to meet take-off of 4,400 ft at 1.2V _s and critical field length of 6000 ft	17,500 lbs. rating. (95% recovery used)	21,000 lbs. rating. (95% recovery used)	
2. Cruise Thrust	Sufficient to achieve cruise Mach number	2,160 lbs. at lowest SFC	2,700 lbs. at lowest SFC. 2,160 lbs. at .02 SFC penalty	
3. S.F.C.	To achieve range of 4,200 N.M. with 70,000 lbs. P.L.	.75 desirable maximum (no-loss SFC at 2,160 lb. F _n)	.765 (no loss SFC at 2,160 lb. F _n)	
4. Attenuation of noise emitting from compressor inlet	Inlet duct was too short to permit variable geometry "sonic plug" inlet, so high distortion-tolerance not critical as on X-21A. See para. 9.1.3 for "tuned" acoustical duct wall treatment used.	Normal Mil. Spec. tolerance to inlet distortion was acceptable	Met Mil Spec. requirements	
5. Maximum Diameter	Small diameter to minimize nacelle parasite drag and turbulent area of wing	Small as feasible.	Twin mounting results in a smaller parasite drag and turbulent area than individual nacelles. See para. 9.1.1.1	
6. Compressor Bleed Air	LFC Pumping Equipment, cabin conditioning and anti-icing uses considered at cruise	2.2 lbs/sec (1.7 lbs/sec for LFC + .5 lbs/sec other uses)	5.5% of primary flow = 3.0 lbs/sec	
7. Weight	Highest engines possible, as moving them aft on wing required 0.13 lbs nose ballast per lb of engine weight. See Fig. 8.16	No maximum established but 3945 lbs desirable	4535 lbs.	
8. Accessory Drive Capability	Adequate electrical and hydraulic power for airplane uses	As exists on LTA except replace 90KVA alternators with 120KVA	Minor engine rework required to meet 120KVA torque requirements	

ENGINEER	NORTHROP CORPORATION NORAIR DIVISION	PAGE 9.22
CHECKER		REPORT NO. NOR 67-136
DATE June 1967		MODEL X-21A

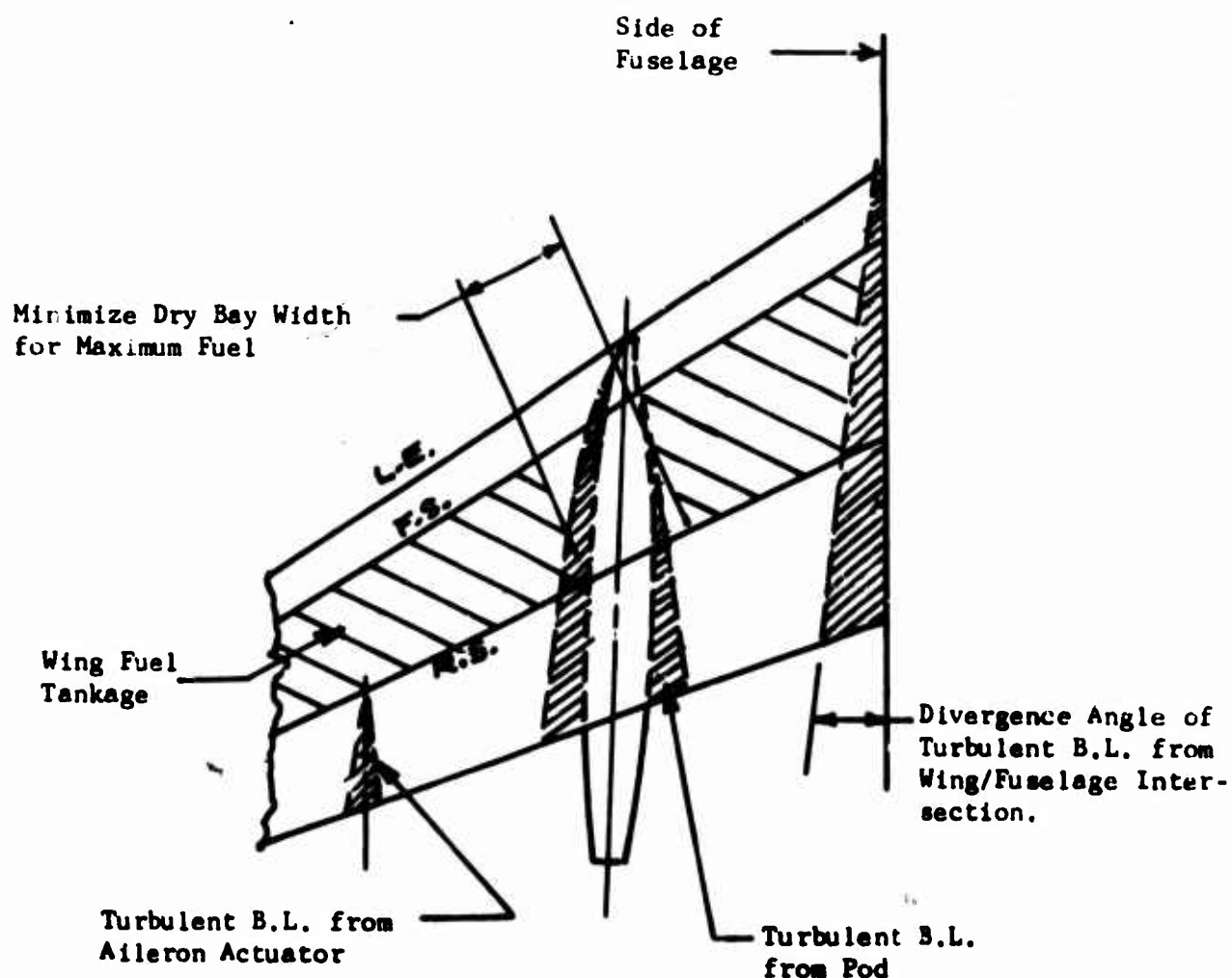


FIG. 9.1 TURBULENT AREAS FROM FUSELAGE AND POD

ENGINEER	NORTHROP CORPORATION NORAIR DIVISION	PAGE 9.23
CHECKER		REPORT NO. NOR 67-136
DATE June 1967		MODEL X-21A

DATA

XJ79-13 JET ENGINE

$h = 45,000$ FT

$M = .80$

25 HP EXTRACTED

ARDC STD DAY

NET THRUST

$F_N \sim \text{LB}$

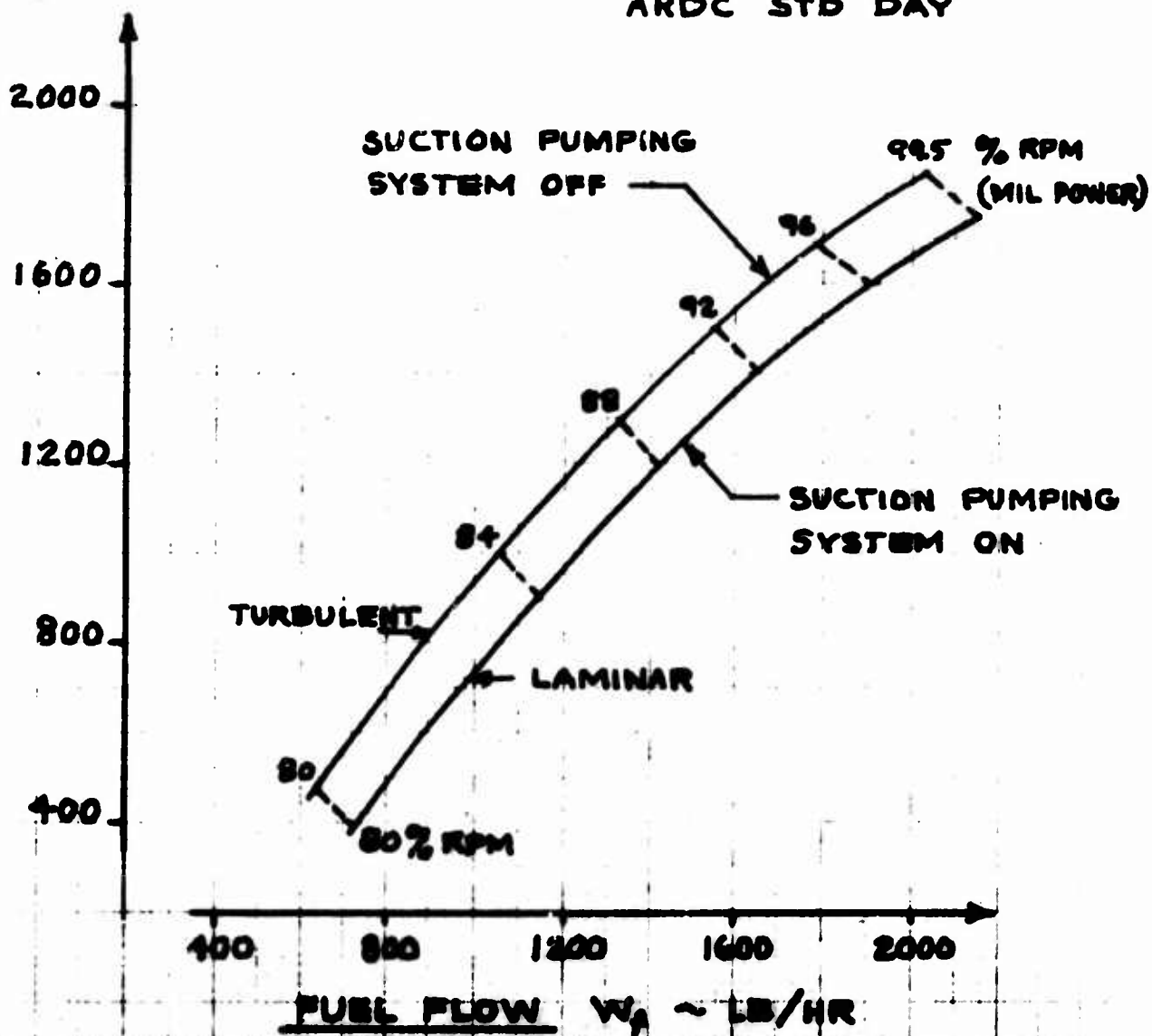
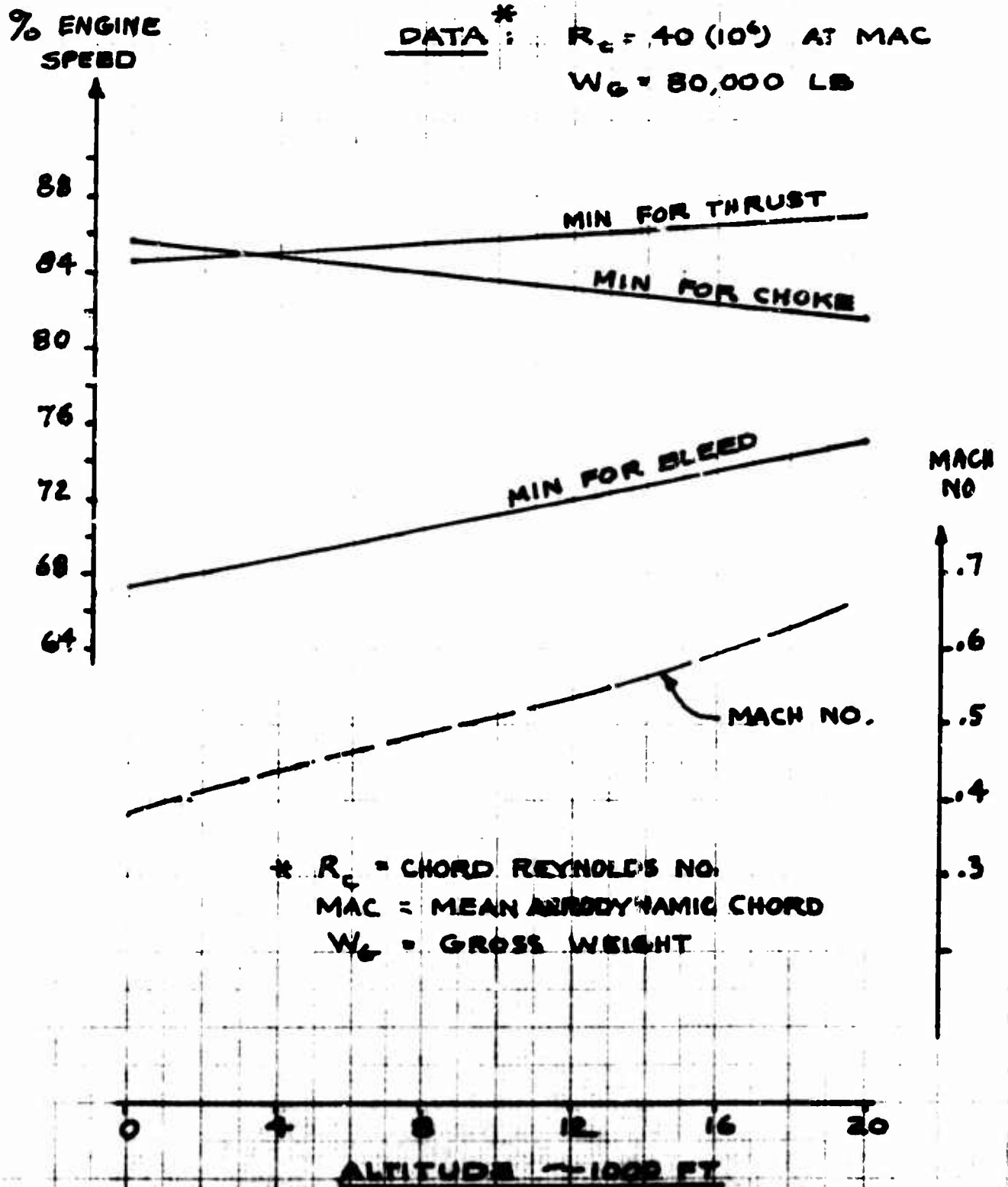


FIG 9.2 ENGINE THRUST VS FUEL FLOW
AT HIGH ALTITUDE

ENGINEER	NORTHROP CORPORATION NORAIR DIVISION	PAGE 9.24
CHECKER		REPORT NO. NOR 67-136
DATE June 1967		MODEL X-21A



**FIG 9.3 ENGINE SPEED REQUIRED VS ALTITUDE
AT HIGH REYNOLDS NUMBER**

JUNE 1967

PAGE 9.25
REPORT NO. NOR 67-136
MODEL X-21A



FIGURE 9.4 COMPRESSOR POD AND ENGINE NACELLE (R.H.)

JUNE 1967

PAGE 9.27
REPORT NO. NOR 67-136
MODEL X-21A



FIGURE 9.6 ENGINE NACELLE SHOWING TRANSLATING CENTER BODY
(SONIC PLUG) IN FORWARD POSITION (R. H.)

ENGINEER	NORTHROP CORPORATION NORAIR DIVISION	PAGE 9.28
CHECKER		REPORT NO. NOR 67-136
DATE June 1967		MODEL X-21A

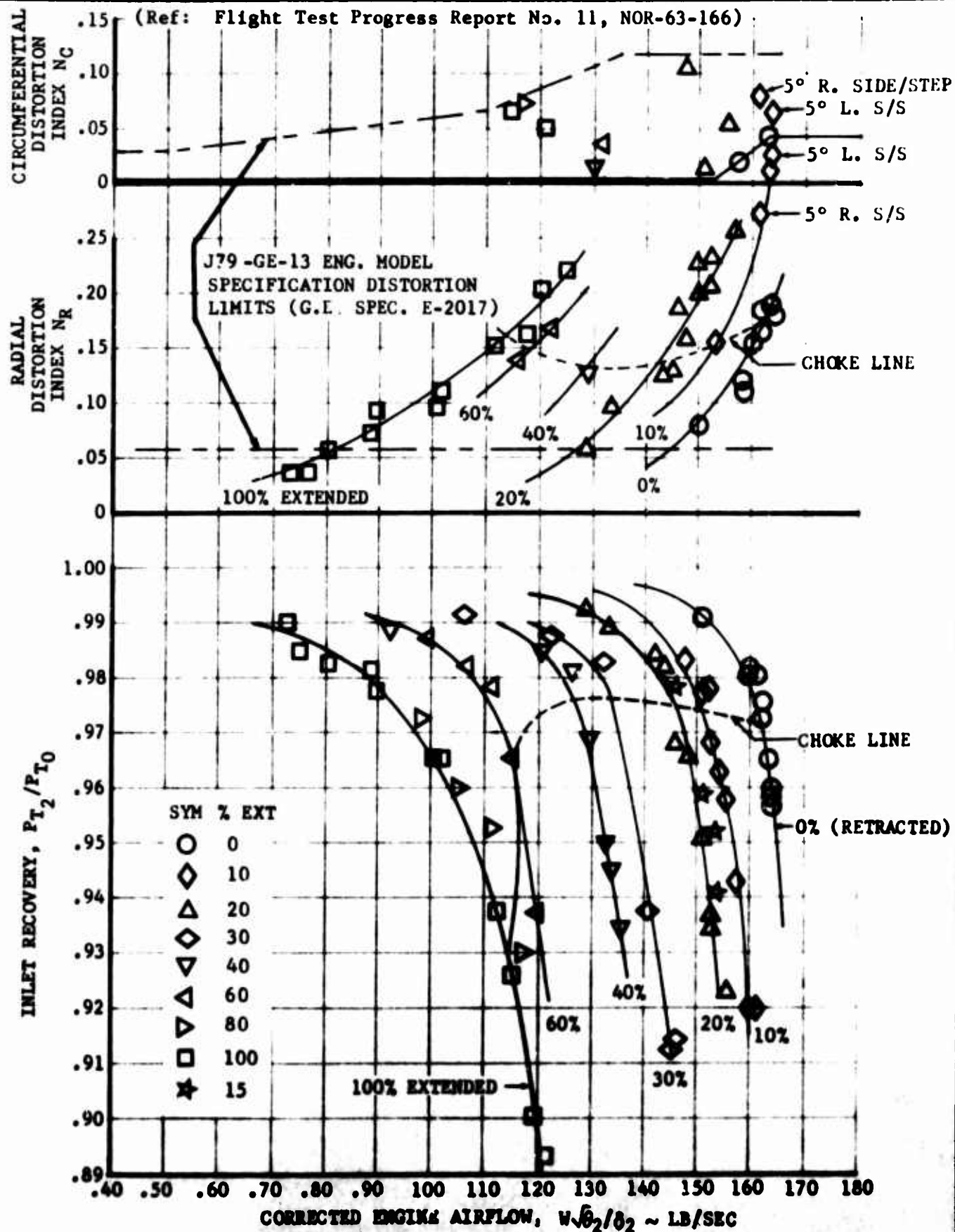


FIGURE 9.7 IN-FLIGHT ENGINE INLET PERFORMANCE X-21A,
J79-GE-13 ENGINE INSTALLATION L.H. NACELLE

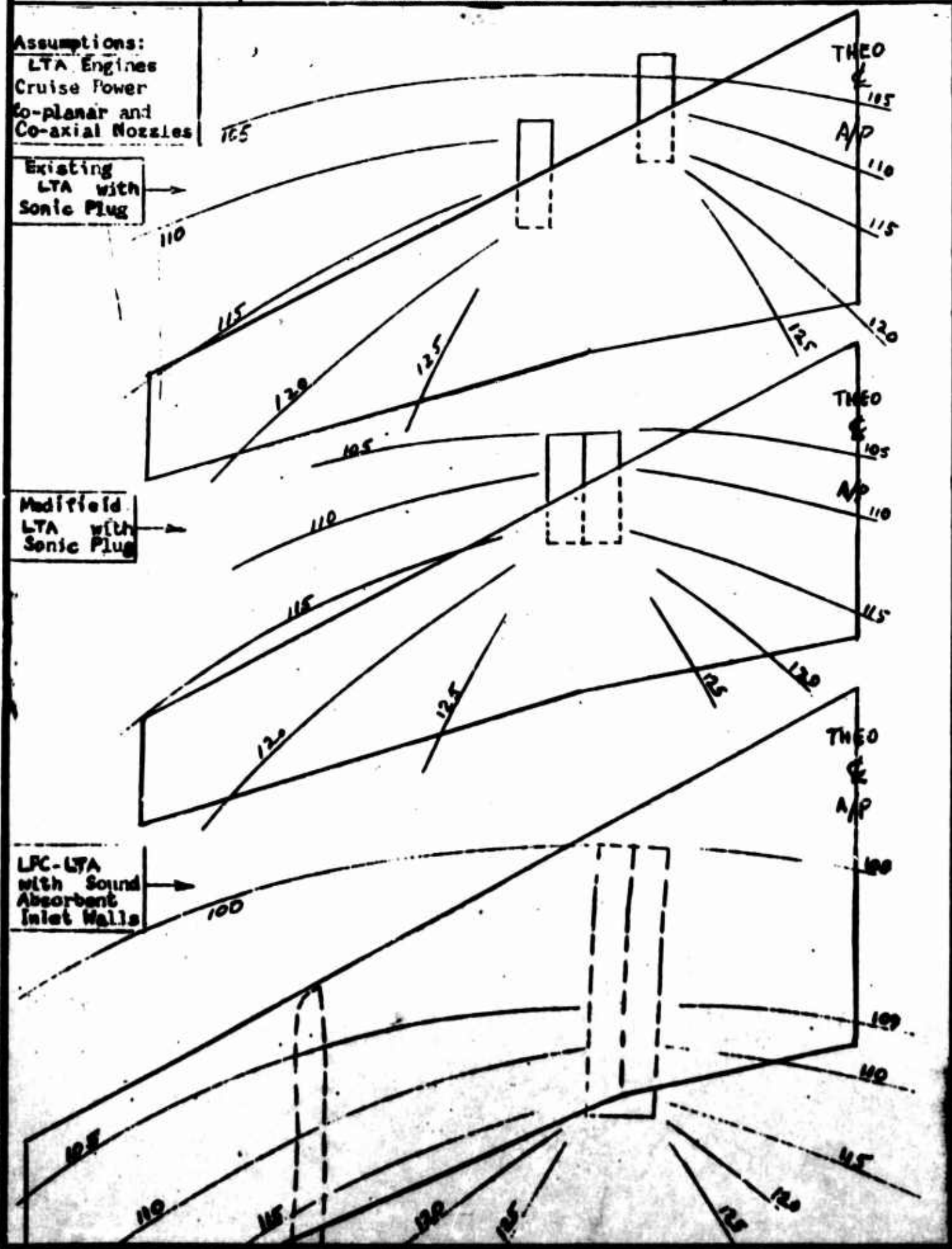
ENGINEER	NORTHROP CORPORATION NORAIR DIVISION	PAGE 9.29
CHECKER		REPORT NO. NOR 67-136
DATE June 1967	FIGURE 9.8 ESTIMATED SOUND PRESSURE LEVELS ON THE WINGS	MODEL X-21A

Assumptions:
LTA Engines
Cruise Power
Co-planar and
Co-axial Nozzles

Existing
LTA with
Sonic Plug

Modifield
LTA with
Sonic Plug

LPC-LTA
with Sound
Absorbent
Inlet Walls



ENGINEER	NORTHROP CORPORATION NORAIR DIVISION	PAGE 10.00
CHECKER		REPORT NO. NOR 67-136
DATE June 1967		MODEL X-21A

SECTION 10

WAVINESS AND SURFACE SMOOTHNESS CRITERIA

BY:

H. A. Gerhardt

March, 1964

Revised May, 1967

ENGINEER	NORTHROP CORPORATION NORAIR DIVISION	PAGE
CHECKER		10.01
DATE		REPORT NO.
June 1967		NOR 67-136
		MODEL
		X-21A

10.1 SUMMARY

The effect of surface imperfections such as roughness, gaps, steps, and waves on the laminar flow performance of an LFC wing are briefly discussed. Smoothness criteria for designing, manufacturing and maintenance purposes are presented. The techniques of waviness measurement are also presented.

The structural design and manufacturing approaches for attainment of surface smoothness on LFC wings are outlined with reference to the X-21A airplane.

10.2 INTRODUCTION

Attainment of laminar boundary layers requires aerodynamically smooth surfaces. The concept of aerodynamic smoothness here includes surface waviness. The maximum magnitude of the surface imperfections at the condition of aerodynamic smoothness is a function of the Reynolds number and to some extent of the Mach number.

As an LFC airplane proceeds from manufacturing stage to flight service the types of surface irregularities to be prevented or eliminated change. Appropriate design and manufacturing is required to ensure a relative freedom from waves, gaps and steps along joints. Once the airplane (free of waves and steps) enters flight status, roughness due to accumulation of dust and to contamination by insects during the flight becomes a maintenance matter.

10.3 MECHANISM OF BOUNDARY LAYER DISTURBANCE DUE TO SURFACE IMPERFECTIONS

10.3.1 ROUGHNESS, GAPS AND STEPS

The effect of roughness, gaps and steps on boundary layer behavior is the creation of vortex-like disturbances. These may be either damped or undamped (leading to boundary layer transition) depending on the ratio of protuberance height (depth) and boundary layer thickness, or more specifically, on the relation between the magnitude of the irregularity and the unit Reynolds number. Transition is usually (but not necessarily) observed immediately behind the irregularity. A point-like disturbance source such as an impacted insect creates a wedge-shaped zone of turbulence. The wedge half angle is approximately 7.5° ; an exception is when a disturbance exists at the stagnation line of a swept wing. For this case the inboard turbulent boundary of the wedge

ENGINEER	NORTHROP CORPORATION NORAIR DIVISION	PAGE 10.02
CHECKER		REPORT NO. NOR 67-136
DATE June 1967		MODEL X-21A

maintains its position as flight conditions change. But the outboard boundary is a function of the boundary layer thickness Reynolds number, encompassing a larger and larger turbulent area.

10.3.2 WAVINESS

Surface waviness causes boundary layer instability and can lead to transition to turbulent flow. For waves with crests and valleys oriented spanwise, the primary mechanism of disturbance probably is the generation of streamwise-axis vortices in the unstable, concave, region of the wave. Subsequent regions of convex flow appear to be relatively ineffective in damping the vortices, and the strength of the disturbance grows from wave to wave. The presence of wing sweep may aggravate the situation by adding crossflow pressure gradients that amplify the vortex system. Tollmien-Schlichting traveling wave fronts also may be present or even predominant if the surface waves are in resonance with the traveling waves. A similar description of boundary layer vortex formation applies to the waves oriented normal to the wing span of a swept wing. In the case of the X-21A wing, the former appears to be more critical.

Compressibility effects can cause a strong interaction between waviness and boundary layer stability, and thus may become the governing factor with respect to permissible waviness. First, a surface wave increases the local Mach number and induces a negative pressure peak which is magnified in the presence of compressible flow. At a sufficiently high local Mach number a shock may form at the wave. Second, the pressure difference between the surface and the suction chamber will be reduced to the point where outflow from the suction slots may even result. Either of these facts can lead to boundary layer transition.

For a given local Mach number these sonic effects are directly proportional to the ratio of wave amplitude to wave length.

10.4 SURVEY OF SMOOTHNESS CRITERIA

10.4.1 ROUGHNESS, GAPS AND STEPS

Criteria specifying wing surface condition: with respect to roughness have been determined primarily through wind tunnel testing on a flat plate. These studies are summarized in Reference 1. A special compilation is set up in Figure 10.1 which specifies tolerable particle dimensions as a function of unit Reynolds number.

ENGINEER	NORTHROP CORPORATION NORAIR DIVISION	PAGE 10.02
CHECKER		REPORT NO. NOR 67-136
DATE June 1967		MODEL X-21A

maintains its position as flight conditions change. But the outboard boundary is a function of the boundary layer thickness Reynolds number, encompassing a larger and larger turbulent area.

10.3.2 WAVINESS

Surface waviness causes boundary layer instability and can lead to transition to turbulent flow. For waves with crests and valleys oriented spanwise, the primary mechanism of disturbance probably is the generation of streamwise-axis vortices in the unstable, concave, region of the wave. Subsequent regions of convex flow appear to be relatively ineffective in damping the vortices, and the strength of the disturbance grows from wave to wave. The presence of wing sweep may aggravate the situation by adding crossflow pressure gradients that amplify the vortex system. Tollmien-Schlichting traveling wave fronts also may be present or even predominant if the surface waves are in resonance with the traveling waves. A similar description of boundary layer vortex formation applies to the waves oriented normal to the wing span of a swept wing. In the case of the X-21A wing, the former appears to be more critical.

Compressibility effects can cause a strong interaction between waviness and boundary layer stability, and thus may become the governing factor with respect to permissible waviness. First, a surface wave increases the local Mach number and induces a negative pressure peak which is magnified in the presence of compressible flow. At a sufficiently high local Mach number a shock may form at the wave. Second, the pressure difference between the surface and the suction chamber will be reduced to the point where outflow from the suction slots may even result. Either of these facts can lead to boundary layer transition.

For a given local Mach number these sonic effects are directly proportional to the ratio of wave amplitude to wave length.

10.4 SURVEY OF SMOOTHNESS CRITERIA

10.4.1 ROUGHNESS, GAPS AND STEPS

Criteria specifying wing surface condition with respect to roughness have been determined primarily through wind tunnel testing on a flat plate. These studies are summarized in Reference 1. A special compilation is set up in Figure 10.1 which specifies tolerable particle dimensions as a function of unit Reynolds number.

ENGINEER	NORTHROP CORPORATION NORAIR DIVISION	PAGE 10.03
CHECKER		REPORT NO. NOR 67-136
DATE June 1967		MODEL X-21A

Criteria for steps and gaps are also presented in Figure 10.1 in terms of critical Reynolds numbers based on the length of the exposed areas. The requirements for gaps and forward facing steps are similar to conventional aircraft. However, aft-facing step requirements are more severe. Some smoothness tolerance values applying to the flight condition of $M = .8$ and 45,000 ft. altitude are given to illustrate the requirements. Permissible step heights are 0.02 inches for a forward facing step, 0.009 inches for an aft facing step. The width of a spanwise running gap is not to exceed 0.25 inches.

10.4.2 WAVINESS

Waviness criteria are established from data resulting from flight test experiments on an unswept laminar suction wing and from several low turbulence wind tunnel tests on a 30° swept laminar suction wing. The results of these tests are summarized in Reference 2 and in a USAF document, listed here as Reference 3. The critical amplitude is found to be proportional to the square root of the wave length. A diagram containing the basic relations between critical waviness and Reynolds number appears in Reference 2 and is reproduced here as Figure 10.2. It is valid for single sine waves. If consecutive waves exist at one station, the values from Figure 10.2 must be reduced by a factor of 1/2 to 1/3 depending upon the number of waves. The data from Figure 10.2 apply to wave lengths taken at right angles to the local direction of sweep; however, it may be more convenient to consider waves in the streamwise direction to avoid complicating the instructions in taking measurements. In this case the error is small and conservative.

The compressibility constraints on waviness can be calculated in the following manner. The pressure increment due to waviness (sine waves) is, in incompressible flow (Reference 3):

$$\Delta p/q = -5.73h/\lambda'$$

with h = wave amplitude
 λ' = wave length measured perpendicular to local wing sweep
 q = local dynamic pressure

ENGINEER	NORTHROP CORPORATION NORAIR DIVISION	PAGE 10.04
CHECKER		REPORT NO. NOR 67-136
DATE June 1967		MODEL X-21A

The negative pressure peak on the wave is increased by $1/\sqrt{1-M^2}$ (M being local Mach number) or by a factor determined by a more sophisticated rule such as Spreiter's. Accompanying the decrease in pressure is an increase in local Mach number which can be determined by an inverse application of Spreiter's rule.

Critical values for the wave amplitude/length ratio will result from the conditions that:

- a. The induced pressure level on the surface has to remain sufficiently higher than the design suction pressure level inside the suction duct system to minimize the change in suction distribution or at least to avoid outflow.
- b. The local Mach number is limited to a value of 1.04 for the successful operation of a subsonic laminar suction wing.

There exists, of course, the possibility of restricting the maximum local Mach number level by appropriate aerodynamic design of the wing and by restricting the wing lift coefficient in order to gain satisfactory waviness tolerances.

For a given maximum Reynolds number a diagram like Figure 10.3 can be derived from Figure 10.2 as a basis for waviness tolerances to be applied to a particular airplane. The ratio of (total) wave amplitude/wave length is plotted versus the wave length. Applying to the X-21A airplane Figure 10.3 is valid for multiple waves (reduction factor 1/3) and a chord Reynolds number of 45×10^6 . This diagram also includes constraints due to transonic effects. These restrictions affect only short waves and they apply only to zones of high local Mach number.

As the diagram (Figure 10.3) applies for a maximum Reynolds number which, on a tapered wing, exists on the inboard wing at the station next to the fuselage, these tolerances may be gradually or successively relaxed as one proceeds outboard in a spanwise direction. Very short waves, say less than one inch of length, make a deviation from Figure 10.3 desirable to avoid difficulties in taking measurements. It is recommended that a constant maximum amplitude be specified for these short waves.

ENGINEER	NORTHROP CORPORATION NORAIR DIVISION	PAGE 10.05
CHECKER		REPORT NO. NOR 67-136
DATE June 1967		MODEL X-21A

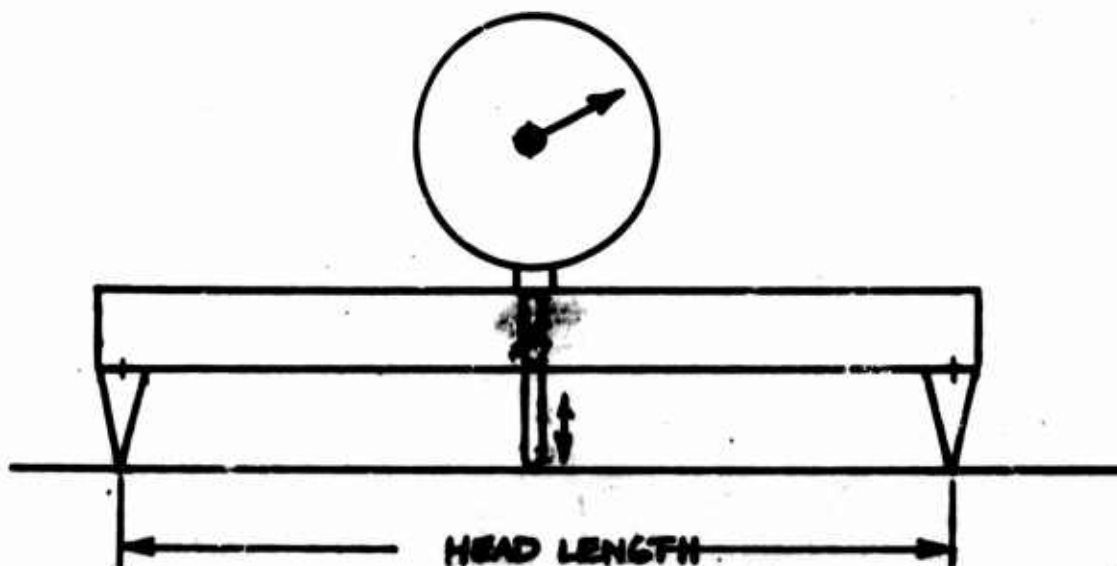
In Figure 10.3 the tolerances for waves normal to the wing span were set up rather arbitrarily to be twice the value applying to waves with crests running parallel to the span direction. Waviness measured spanwise along the leading edge, however, should satisfy closer tolerances because of the three-dimensional nature of the flow in that region.

10.5 MEASURING TECHNIQUES

Special techniques must be adopted to measure surface imperfections which are of the order of one-thousandth of an inch. The invisibility to the naked eye and random occurrence of waves necessitates a fast scanning and recording instrument in order to survey large wing areas in a reasonable period of time.

A technique which yields the true wave pattern of the airfoil surface is the taking of offset measurements from a straight reference line and subtracting the results from the theoretical contour. This method is successful in disclosing excessive waviness because the amplitude of the wave is of the same order of magnitude as the maximum ordinate of the difference-curve. However, it requires a separate computation to define the theoretical surface shape for each station at which a measurement is to be made. Moreover, difficulties may arise when basic contour errors of the manufactured wing occur over large distances which cannot be recognized as actual waves.

A more direct method is the use of a three-pronged measuring head which is moved across the surface. As sketched here, the head consists of a base beam with three equi-distant prongs extending down from it. The two outer prongs are fixed to the beam, whereas the middle prong is movable and actuates either a dial gauge or an induction type transducer for a paper tape recorder.



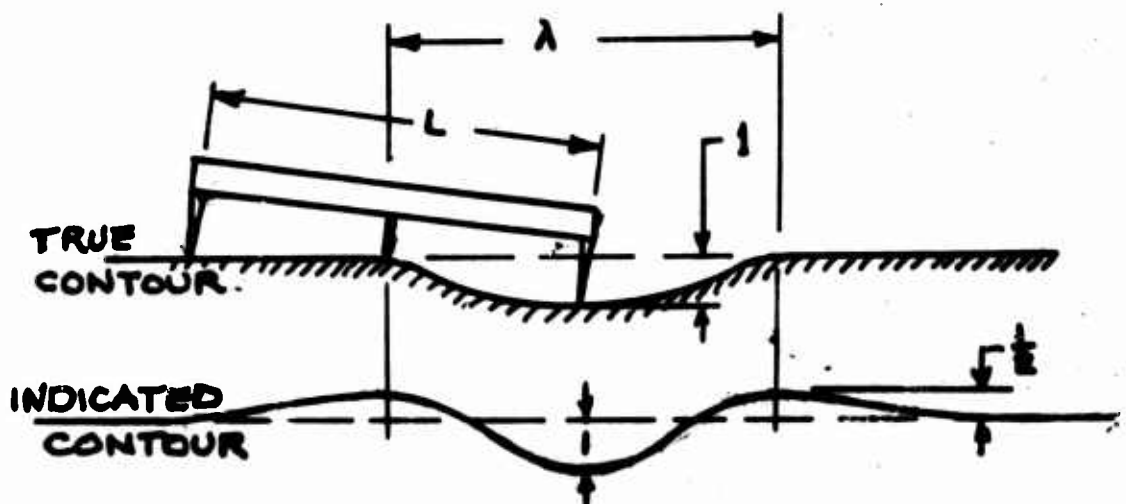
ENGINEER	NORTHROP CORPORATION NORAIR DIVISION	PAGE 10.06
CHECKER		REPORT NO. NOR 67-136
DATE June 1967		MODEL X-21A

The head does not indicate the true wave amplitude nor the true wave length.

In all practical cases the center prong is actuated successively as each of the three legs passes through a wave, and as the indication of the outer legs is inversely reflected by the center leg indication, the head actually yields magnified wave amplitudes.

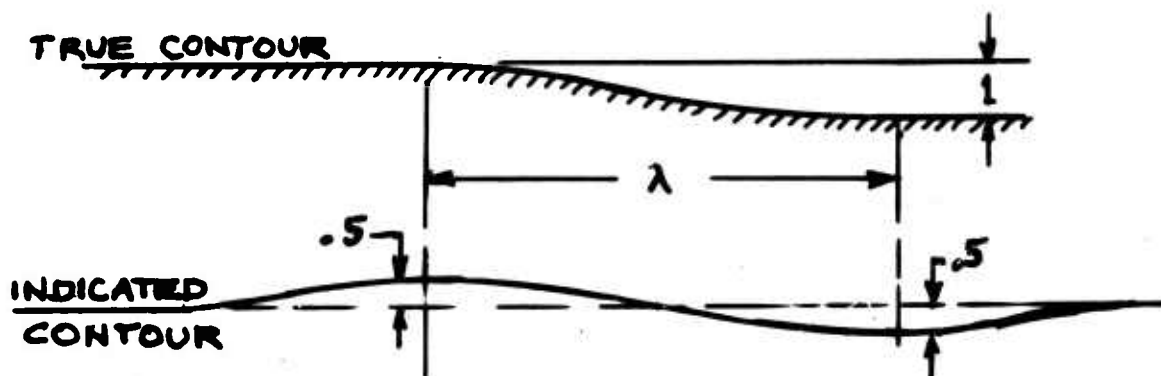
In the event that the head length is small relative to the wave length, the head output is proportional to the local radius of curvature of the surface, or, as the change in the first derivative is small, proportional to the second derivative. Thus the true surface contour can be derived by integrating twice. However, the separation of the wave pattern from the airfoil contour leads to the same difficulties as are encountered for taking offset measurements from a straight line.

Though the uncorrected head output does not yield the true wave dimensions, the measured curve reveals frequently the wave type such as trough, crest or step shape. Presuming that head-length and wave-length are equal the true shape of a trough compares with the indicated shape as follows:



The wave banks are indicated as crests in such a manner that, if $L = \lambda$, the total indicated wave amplitude is $1\frac{1}{2}$ times the true wave amplitude. A "smooth" step is sketched below (True amplitude and indicated amplitude are equal here):

ENGINEER	NORTHROP CORPORATION NORAIR DIVISION	PAGE 10.07
CHECKER		REPORT NO. NOR 67-136
DATE June 1967		MODEL X-21A



In the case that consecutive contour deviations of changing type are being encountered, the interpretation of the head output becomes difficult. The interpretation is aggravated by the fact that the indication is a function of the ratio of wave-length/head-length. Short waves are incompletely mapped by a long measuring head and vice versa.

Nevertheless, it is possible to judge waviness from the head readings with respect to amplitude/wave-length ratio tolerances. It requires that the criteria be applied to "indicated" waviness rather than to true waviness, and that several measurements with different head-lengths be carried out at each surface station in order to assure satisfaction of criteria for all wave lengths which may exist on that surface.

This procedure has also the advantage that no measurements of the wave lengths are required. Having set up the amplitude tolerances for the different head-lengths rather than for the wave-lengths (which can be done by a geometric analysis), the three-pronged head represents an easy-to-handle tool for surface measurement. It is also a valuable aid for direction of surface finishing operations.

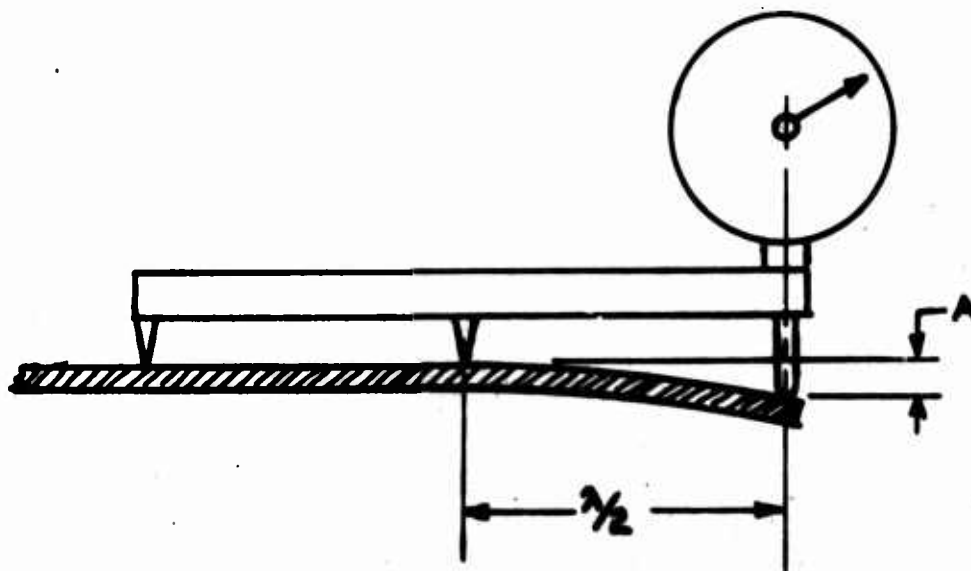
A typical trace recorded with the three-prong head is shown in Figure 10.4. As the head proceeds through the leading edge the rapidly changing airfoil curvature is reflected through a curve with increasing slope. The wave amplitudes must be measured with reference to a mean line. It is sufficient to define a mean line by visual estimation of an average curve and drawing it free-handed into the diagram. In the vicinity of the leading edge only heads with short prong distances can be used; in the X-21A program a measurement around the nose is made with a one-inch-head. Figure 10.4 also contains X-21A tolerance values of indicated waviness for different head-lengths which were established on the basis of the true-wave tolerances presented in Figure 10.3.

ENGINEER	NORTHROP CORPORATION NORAIR DIVISION	PAGE	10.08
CHECKER		REPORT NO.	NOK 67-136
DATE		MODEL	X-21A
June 1967			

Waviness measurements are not only required on the completed wing, but during manufacturing. In the X-21A program measurements were obtained on separate panels and on the assembled wing after the following stages:

- After third stage panel bonding
- After slotting
- After final installation
- During flight testing

Special attention must be paid to panel edges which, in X-21A experience, showed more deviation from the defined contour than the remainder of the panel. This will be improved by a manufacturing technique whereby the panel edges are machine cut after bonding. As the center prong of the previously described measuring head does not reach the end of the panel, only a part of the amplitude of a bent edge is indicated. Therefore, the use of a three-prong-head with recording stylus located at one end of the base beam is recommended for measuring edges of individual panels before assembly. Presuming that the panel is fairly smooth (with the exception of an imperfect edge) and the head-length is at least twice as long as the deflected length $\lambda/2$, the true amplitude A is as indicated in the sketch:



ENGINEER	NORTHROP CORPORATION NORAIR DIVISION	PAGE 10.09
CHECKER		REPORT NO. NOR-67-136
DATE June 1967		MODEL X-21A

10.6 CORRELATION OF CRITERIA AND FLIGHT TEST RESULTS

During the last few months of flight testing the second (-410) X-21A airplane, several different investigations were made to correlate surface smoothness criteria with laminar flow test results. In general, the correlation showed that the allowable deviations in surface smoothness, as shown in the charts of this section, could be exceeded somewhat in the X-21A outer wing panel without loss of LFC performance.

One of the investigations was to determine the effect of minimum maintenance. As reported in Program Progress Report for October 1965, only routine cleaning was performed on the upper outboard wing, beginning with Flight 122. Sixteen flights later, Flight 138 showed no deterioration in LFC performance over the test area, although numerous chips, pits, and other surface defects had developed in the mid-chord and aft regions. Flight 138 concluded the test of minimum maintenance.

Another investigation was made with a spanwise gap .125 inches wide in the chord direction and about .18 inches deep on the lower left outboard wing at 60% chord. The tests were made primarily at the cruise condition ($h=40,000$ ft at $M=.75$), where the value of $R'L$ for the gap was $1.8(10^5)$ as compared with an allowable value of $2.7(10^5)$, where R' is the unit Reynolds number of the free stream and L is the gap dimension in inches, as shown in Figure 10.1. The flight tests showed that the wing can tolerate the .125 gap plus .040 gaps at 44% chord and 32% chord without loss of laminar area or change in suction distribution. The addition of a .050 gap (in addition to the other three gaps) at 15% chord plus a .080 gap at 8% chord required a lowering of suction in the forward ducts in order to maintain laminarization.

Laminarization across the aileron seal provides a correlation for the rearward facing step. The allowable value of $R'L$, from Figure 10.1, is $1.0(10^4)$, but laminarization was achieved across the seal to the trailing edge at values of $R'L$ of about $2(10^4)$, by means of reducing suction ahead of the aileron either by reducing duct flow rates or by sealing several of the slots immediately ahead of the aileron.

Following the minimum maintenance test on the upper outer right wing, a test of waviness allowables was made in the same area. Filler material was stripped from the wing, creating spanwise surface waves in excess of the allowables shown in this report. The tests were made in two steps, first with a wave in the region of the aft spar; then with a wave added near the front spar. In both tests nearly all of the test area was laminarized. Prior to stripping the filler material all of the test area had been laminarized. Apparently the creation of a surface wave in excess of allowable values at the rear spar caused only a minor deterioration of laminarization, and the addition of a similar wave at the front spar did not worsen the situation. The results indicate that waves as far apart as the front and rear spars can be treated by single wave rather than multiple wave criteria.

ENGINEER	NORTHROP CORPORATION NORAIR DIVISION	PAGE 10.10
CHECKER		REPORT NO. NOR 67-136
DATE June 1967		MODEL X-21A

10.7 REFERENCES

1. Carmichael, B.H., "Prediction of Critical Reynolds Number for Single Three-Dimensional Roughness Elements." Norair Division, Northrop Corporation, Report NAI-58-412 (BLC-109), Unclass., dated May 1958.
2. Carmichael, B.H., "Surface Waviness Criteria for Swept and Unswept Laminar Suction Wings." Norair Report NOR 59-438 (BLC-123), Unclass., dated August 1959.
3. Norair Boundary Layer Research Group, "Summary of Laminar Boundary Layer Control Research" Wright Air Development Center Report WADC TR56-111, Unclass., dated December 1959.

ENGINEER	NORTHROP CORPORATION NORAIR DIVISION	PAGE 10.11
CHECKER		REPORT NO. NOR 67-136
DATE June 1967		MODEL X-21A



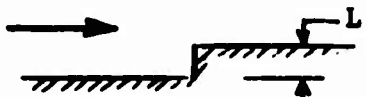

	CRITICAL REYNOLDS NUMBER $R_L = (\frac{U}{\nu})L = R' L$ (L ~ inches)	
One spanwise gap downstream of 0.25C 	2.7	10^5
	5.5	10^5
One up step downstream of 0.25C 	2.3	10^4
One down step downstream of 0.25C 	1.0	10^4
One gap normal to 30° swept wing	1.7	10^5
	At 2% Chord	At 30% Chord
Sandpaper Roughness	6.3 10^3	9.6 10^3
Single Sphere, Single Cube	1.3 10^4	2.0 10^4
Single Flat Disc	0.9 10^4	1.5 10^4

FIG. 10.1 SMOOTHNESS CRITERIA FOR GAPS, STEPS, AND ROUGHNESS

Fig. 10.2 -
CRITICAL ST
SINGLE WAVES C
SUCTION WIT

$\frac{h}{\lambda} = \frac{\text{WAVE HEIGHT}}{\text{WAVE LENGTH}}$

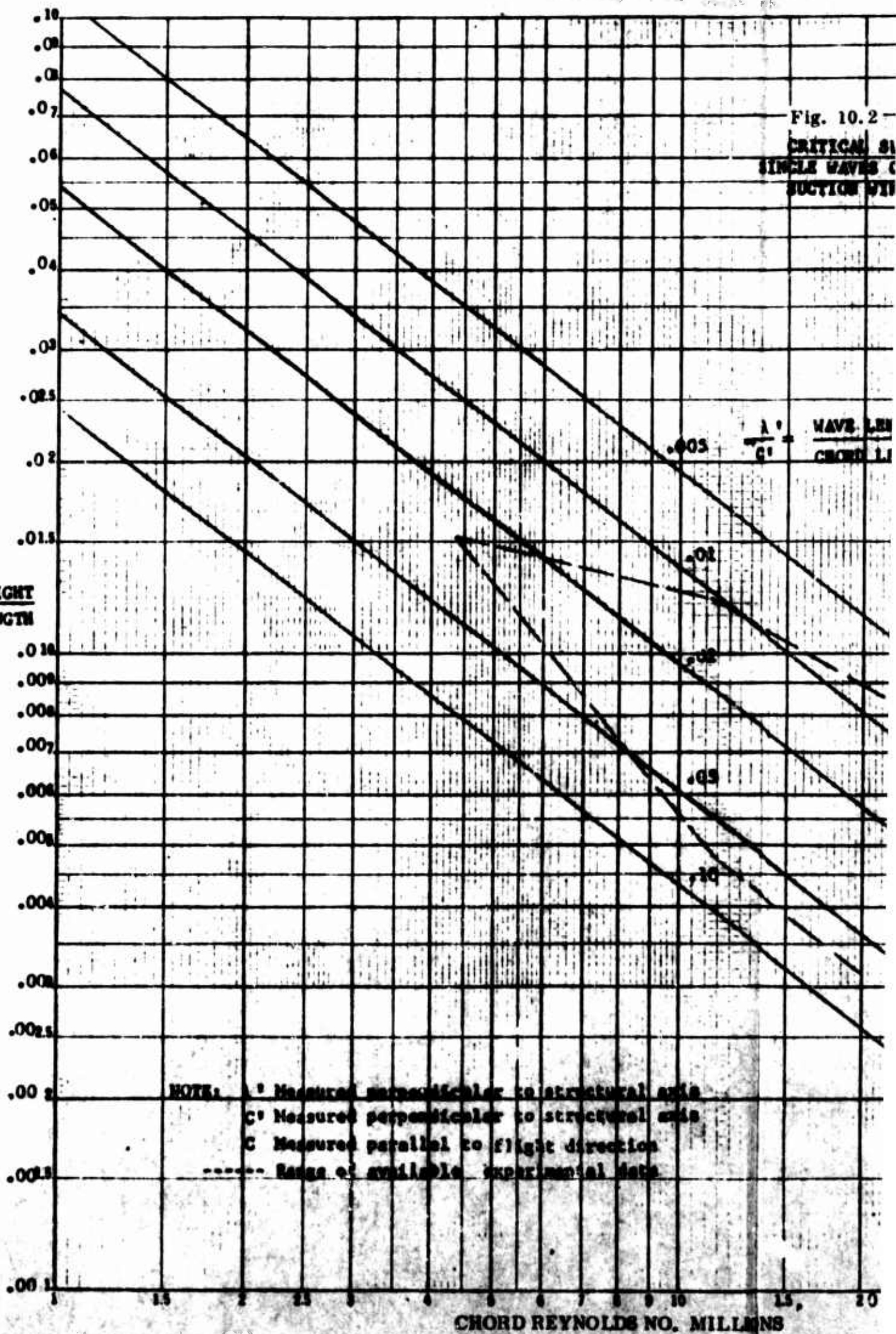
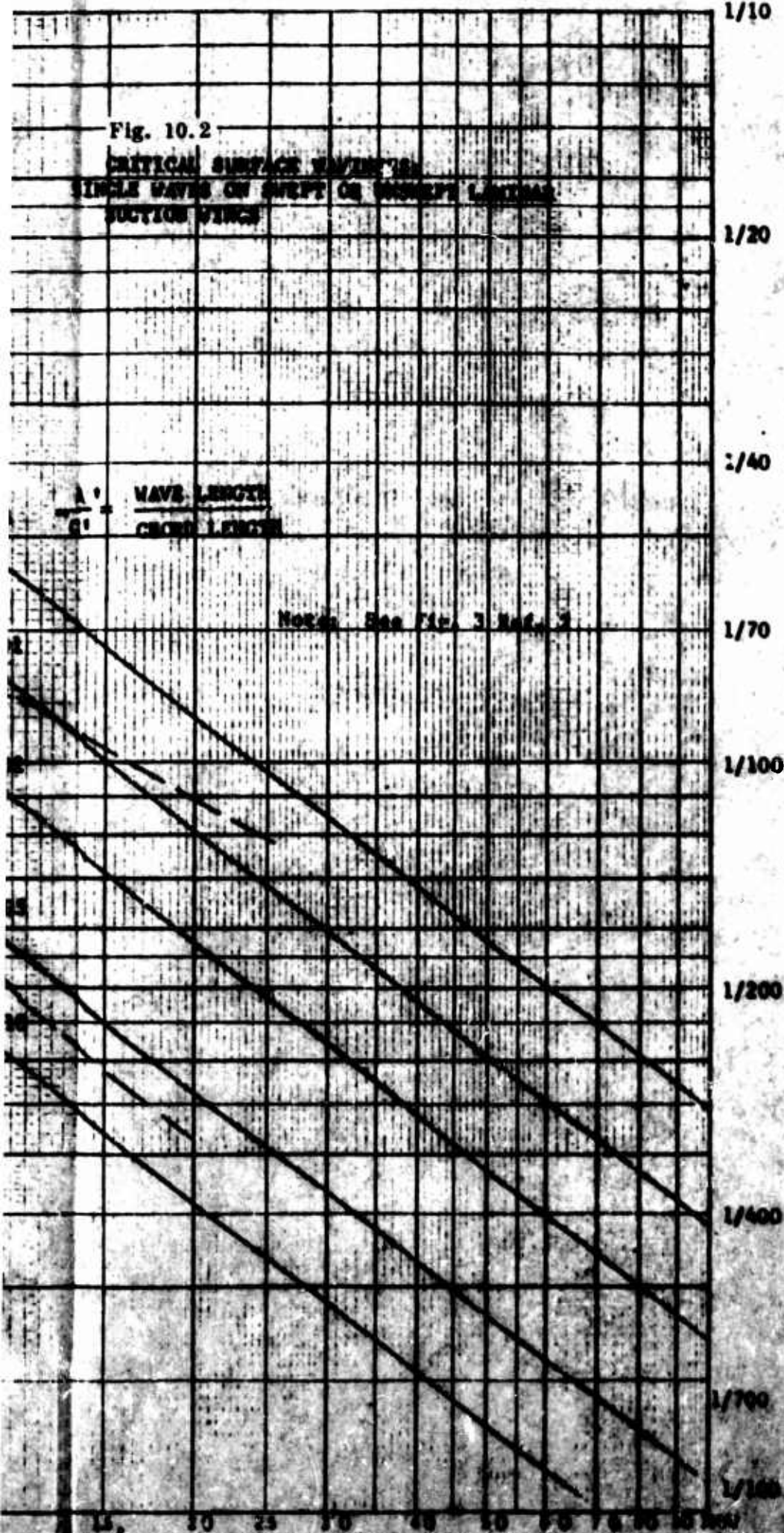


Fig. 10.2

CRITICAL SURFACE WAVES
SINGLE WAVES ON SWEPT OR CONCEPT LAMINAR
SECTION FINCH



$$\frac{h}{\lambda} = \frac{\text{WAVE HEIGHT}}{\text{WAVE LENGTH}}$$

ENGINEER	NORTHROP CORPORATION NORAIR DIVISION	PAGE 10.13
CHECKER		REPORT NO. NOR 67-136
DATE June 1967		MODEL X-21A

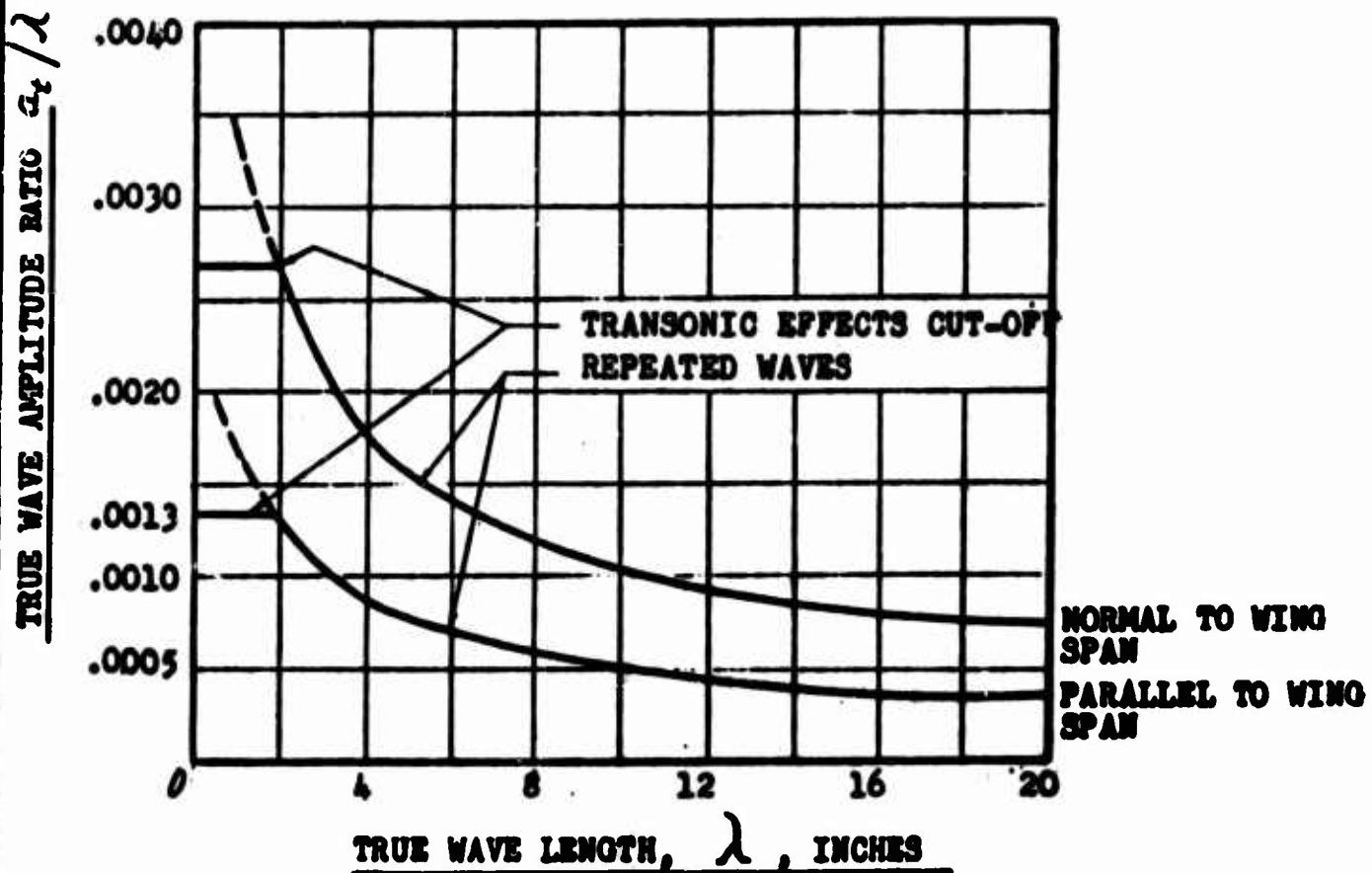


FIG 10.13 MAXIMUM TRUE WAVE AMPLITUDE RATIO VS. WAVE LENGTH

ENGINEER	NORTHROP CORPORATION NORAIR DIVISION	PAGE 10, 14
CHECKER		REPORT NO. NOR 67-136
DATE June 1967		MODEL X-21A

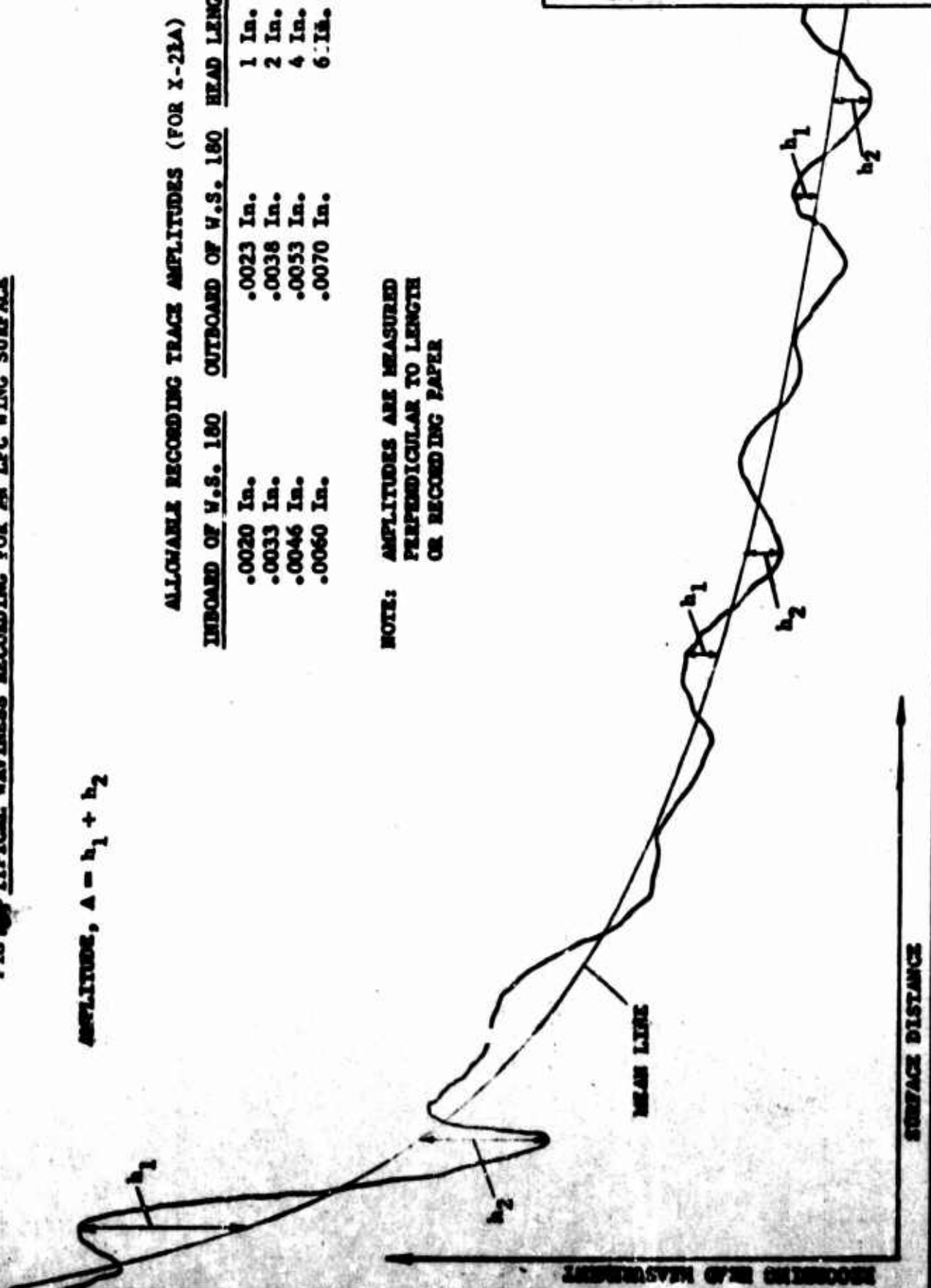
FIG 88 TYPICAL WAVINESS RECORDING FOR AN LFC WING SURFACE

AMPLITUDE, $A = h_1 + h_2$

ALLOWABLE RECORDING TRACE AMPLITUDES (FOR X-21A)

INBOARD OF V.S. 180	OUTBOARD OF V.S. 180	HEAD LENGTH
.0020 In.	.0023 In.	1 In.
.0033 In.	.0038 In.	2 In.
.0046 In.	.0053 In.	4 In.
.0060 In.	.0070 In.	6 In.

NOTE: AMPLITUDES ARE MEASURED
PERPENDICULAR TO LENGTH
OR RECORDING PAPER



11.00
NOR 67-136
X-21A

SECTION 11

EFFECT OF ACOUSTICAL AND VIBRATION ENVIRONMENT
ON THE MAINTENANCE OF LAMINAR FLOW

by R. F. Carmichael

March 1964

Revised May 1967

TABLE OF CONTENTS

11.0 Effect of the Acoustic and Vibration Environments On the Maintenance of Laminar Flow

11.1 Introduction

11.2 External Acoustics

- 11.21 Background
- 11.22 Acoustic Wind Tunnel Test Program
- 11.23 Acoustic Sensitivity Criteria
- 11.24 X-21A Flight Test Results
- 11.25 Summary

11.3 Internal Acoustics

- 11.31 Introduction
- 11.32 Wind Tunnel Tests
- 11.33 X-21A Flight Tests
- 11.34 Laboratory Duct Model Test
- 11.35 Hypothetical Explanation of Wind Tunnel Results
- 11.36 Summary

11.4 Vibration

- 11.41 Natural Environment
- 11.42 Forced Vibration
- 11.43 Summary

11.5 Conclusions

Table I Typical Internal Duct Sound Pressures

ENGINEER	NORTHROP CORPORATION NORAIR DIVISION	PAGE	11.02
CHECKER		REPORT NO.	NOR 67-136
DATE		MODEL	X-21A
June 1967			

LIST OF ILLUSTRATIONS

Figure

- 11.1 Acoustical Test Installation in Norair 7 by 10 Foot Wind Tunnel
- 11.2 Transition Resulting from Longitudinal Wave Fronts of Discrete Frequencies with Partial Suction on the 30° Swept Laminar Suction Model
- 11.3 Norair Acoustic Wind Tunnel Test Results - Transition Resulting from Acoustic Disturbances on a 30° Swept Laminar Suction Wing Model
- 11.4 Effect of Increased Suction on Acoustic Sensitivity of a 30° Swept Laminar Suction Wing Model
- 11.5 Chord Length Reynolds Number at Transition as a Function of the Disturbance Velocity Divided by the Freestream Velocity
- 11.6 Chord Length Reynolds Number vs. Disturbance Velocity Ratio Resulting from Normal X-21A Acoustic Environment
- 11.7 X-21A Flight Test Results - Chord Length Reynolds Number vs. Disturbance Velocity Ratio, $\Delta u/U_\infty$
- 11.8 Laboratory Duct Model Test Configuration
- 11.9 Laboratory Duct Model Test - Detail Suction System Configuration
- 11.10 Normalized Correlation Function, $\left(\frac{\Delta w}{P_D}\right)_N$
- 11.11 Exponent, x , for Mach Number Function, $f(M)$
- 11.12 Exponent, y , for Tributary Duct Nozzle Diameter Function, $(D_n/.088)$
- 11.13 Velocity Disturbance Ratio, $\Delta w/U_\infty$, Versus Frequency
- 11.14 Typical Panel Response During Forced Vibration Tests

ENGINEER	NORTHROP CORPORATION NORAIR DIVISION	PAGE 11.03
CHECKER		REPORT NO. NOR 67-136
DATE June 1967		MODEL X-21A

Figure

Page

- 11.15 Acoustic Power Spectral Density - Lower Wing Surface with Laminar and Turbulent Flow
- 11.16 Acoustic Power Spectral Density - Lower Wing Surface with Laminar Flow and Forced Vibration
- 11.17 Panel Vibration Test - Momentum Loss as Measured at Trailing Edge Probes

ENGINEER	NORTHROP CORPORATION NORAIR DIVISION	PAGE	11.04
CHECKER		REPORT NO.	NOR 67-136
DATE		MODEL	X-21A
June 1967			

11.0 Effect of the Acoustic and Vibration Environments on the Maintenance of Laminar Flow.

11.1 Introduction

It has been demonstrated in wind tunnel and flight tests with laminar flow control surfaces that acoustic disturbances, or noise of relatively high intensity, can cause transition of an otherwise stable laminar boundary layer. Thus, one of the primary requirements in the development of a laminar flow aircraft is to provide assurance that acoustic disturbances will not cause premature transition from laminar to turbulent flow.

This section discusses the development of the X-21A design criteria for external acoustic disturbances, the results of wind tunnel and X-21A tests concerning both internally and externally originating acoustic disturbances, and the results of X-21A flight tests in which wing panels were forcibly vibrated. The section is concluded with an interpretation of the impact of these test results on the design of a laminar flow aircraft plus suggested areas concerning acoustic disturbances in which further development is necessary.

11.2 Acoustic - External

11.21 Background

The boundary layer over a conventional lifting surface tends to remain laminar for a relatively short distance aft of the leading edge, the laminar distance being strongly influenced by sweep (crossflow) and other factors. As the layer grows in thickness with increasing distance, it becomes unstable and breaks down into turbulent flow. The transition point can be delayed to some extent by careful attention to surface smoothness. Early wind tunnel experiments on smooth flat plates indicated that the transition between laminar and turbulent flow occurred at chord length Reynolds number of the order of 3×10^5 . Reduction of the turbulence to velocity fluctuations to the order of 10^{-4} times free stream velocity, achieved laminar flow up to length Reynolds numbers of 3×10^6 , demonstrating the critical nature of the inter-relationship between stability of the boundary layer and external disturbances.

During these flat plate experiments it was observed that the remaining fluctuations in the wind tunnel, after installation of effective multiple damping screens, were not solely due to turbulence, but rather resulted from noise generated in the tunnel (Ref. 1).

ENGINEER	NORTHROP CORPORATION NORAIR DIVISION	PAGE
CHECKER		11:05
DATE		REPORT NO. NOR 67-136
June 1967		MODEL X-21A

Theoretically, the transition phenomena on airfoils, flat plates, and bodies of revolution result from two types of instability; viscous instability and inflectional instability. The Tollmien-Schlichting theory of amplification refers to viscous instability and indicates that for specified regions dependent on the thickness Reynolds number of the boundary layer and on the frequency and amplitude of the external disturbance, disturbances in the freestream flow are amplified within the boundary as they are convected past the surface. Amplification is followed by the generation of streamwise traveling vortices and localized turbulent spots and finally by the growth and spreading of these spots until the entire layer is turbulent. The second type, inflectional instability, occurs when the velocity profile of the boundary layer contains an inflection point. Such a condition exists on a swept wing due to spanwise flow or "crossflow." A spanwise pressure gradient exists on a swept wing and the relatively low velocity air in the boundary layer is deflected more by this pressure gradient than the air outside the boundary layer. The boundary layer, therefore, develops a "crossflow" component in a direction normal to the potential flow direction. Under certain flow conditions, the velocity profiles in the boundary layer "crossflow" have inflection points, and the flow is highly unstable. There exists a critical "crossflow" Reynolds number beyond which amplification of the disturbances occurs, streamwise vortices develop, and transition takes place. Inflectional instability predominates over viscous instability on a swept wing, although Tollmien-Schlichting type instabilities can occur under certain conditions.

Both theory and experiments have shown that boundary layer instability can be delayed considerably by applying suction to remove the low velocity flow immediately adjacent to the surface. The maximum Reynolds number achieved in these experiments, while encouraging, was still much lower than theoretical studies would indicate for an ideal suction surface. For some early suction configurations, the maximum Reynolds number attainable before transition to turbulent flow was clearly a function of the design of the configuration. However, the transition Reynolds numbers for later improved suction configurations were dependent upon the magnitude of the disturbances or fluctuations in the freestream (Ref. 2, 3, 4, 5).

ENGINEER	NORTHROP CORPORATION NORAIR DIVISION	PAGE
CHECKER		11.06
DATE		REPORT NO.
June 1967		NOR 67-136
		MODEL
		X-21A

11.22 Acoustic Wind Tunnel Test Program

While qualitative experimental observations had provided valuable insight into the problem of acoustically induced transition phenomena, quantitative data concerning the magnitude and frequency spectrum of critical disturbances were limited at the initiation of the X-21A program. To establish more definitive information, an experimental program was conducted to investigate the influence of sound on the behavior of a 30° swept laminar suction wing model. A brief description of the test setup, some significant observations and test results follow. A more complete description and evaluation of the test is presented in Ref. 6.

The 7 foot chord-30° swept wing laminar suction model was installed in the Norair 7 x 10 foot low turbulence wind tunnel.* Internal walls of the tunnel test section, the areas immediately upstream of the test section, and the turning vanes downstream of the test section were treated with an acoustic liner consisting of alternate layers of glass fiber insulation, fine mesh screen, and perforated metal sheet to absorb a major percentage of the reflected sound waves. This treatment permitted the introduction of a noise field approaching, as nearly as possible, the desired condition of plane wave fronts moving through the test section and over the model wing. Provisions were made for introducing both transverse sound waves, with wave fronts moving normal to the direction of flow, and longitudinal sound waves over the model. The sound source is transferred to a position in the ceiling of the test section, over the model wing, for the generation of transverse sound waves.

The acoustic environment existing over the surfaces of a jet aircraft in flight contains both discrete frequency noise components from the engine compressor and broad spectrum noise from the jet exhaust and turbulent boundary layers. To simulate these conditions, provisions were made to broadcast pure tone and continuous spectrum noise up to the maximum frequency of the sound source. The principal sound generator for both longitudinal and transverse sound was a Ling-Altec Electro-Pneumatic Transducer with a usable frequency range from 200 to 1500 cps. An alternate system was available for generating transverse sound, consisting of a bank of ten loudspeakers mounted in the test section over the model wing. The loudspeaker system extended the usable test frequency range up to 5,000 cps.

* See Figure 11.1.

ENGINEER	NORTHROP CORPORATION NORAIR DIVISION	PAGE
CHECKER		11.07
DATE		REPORT NO.
June 1967		NOR 67-136
		MODEL
		X-21A

In addition to frequency, amplitude and spectra of the acoustic disturbances, the following parameters were varied during the experiments: model chord Reynolds number, total suction quantity and chordwise suction distribution. The suction system on the model provided more than twice the suction quantity required to maintain full chord laminar flow, and a multiple valve system permitted wide latitude in chordwise suction distribution.

Sound pressure levels of the acoustic disturbance over the wing were monitored by a flush microphone positioned at a reference point near the model. The microphone was mounted in a streamlined housing similar to those used for the Northrop in-flight noise measurements (Ref. 7). The housing assures maintenance of laminar flow over the microphone diaphragm, thereby preventing distortion of the data by pressure fluctuations in the flow over the microphone. Hot wire anemometers were employed to measure disturbance particle velocities at the suction surface which compared closely to the particle velocities derived from microphone measurements. Flow stability over the suction surface was monitored by means of microphones connected to static pressure orifices located along the wing chord which, although not used for quantitative measurements, would sense the distinct difference between the perceived sound of laminar and turbulent flow, thus providing a useful indication of transition. In addition, a pressure rake was attached at the trailing edge to show the variation in wake profile.

During the first stage of the test program, transition often was experienced as a result of unexpected phenomena, emphasizing the extremely complex nature of such aerodynamic-acoustic testing. In particular, it was found that cavities on the surface, such as static pressure orifices or unused suction slots, would cause premature transition in the presence of high intensity sound over a wide frequency range. Without sound, full chord laminar flow was observed. Presumably, this premature transition resulted from periodic pulsations of air in and out of the cavities caused by fluctuating sound pressures. Highly unstable boundary layer profiles with inflection points and boundary layer oscillations can develop downstream of the open cavities, particularly when the frequency of the acoustic excitation coincides with the resonant frequency of the air column in the cavity. This difficulty was eliminated by sealing the orifices and unused slots with clay, resulting in an appreciable increase in the critical sound pressure levels.

ENGINEER	NORTHROP CORPORATION NORAIR DIVISION	PAGE
CHECKER		11.08
DATE		REPORT NO.
June 1967		NOR 67-136
		MODEL
		X-21A

Early tests were run with partial suction on the model. Full chord laminar flow could be maintained without sound when suction was stopped in the front portion of the wing forward of the 45% chord. When sound was introduced for these conditions, transition was definitely caused by amplified oscillations within the frequency range predicted by the Tollmien-Schlichting theory. Figure 11.2 shows the variation of critical sound pressure level with frequency for a partial suction test condition at a chord Reynolds number of 7×10^6 . When suction was applied in the front portion of the wing, Tollmien-Schlichting instabilities did not occur on the model, and subsequent transition resulted from crossflow or inflectional instability. References 6 and 8 present an explanation of this phenomenon.

Test results have shown that for a specific model, the major parameters controlling acoustic sensitivity were suction quantity and chordwise suction distribution. Suction quantity, in itself, did provide a solution to the problem of acoustic sensitivity, but an over-all increase in suction over the chord can reduce the thickness of the boundary layer to the point where surface roughness becomes critical and may cause the flow to be unstable. Variation in suction distribution provided a more valuable means of raising the sensitivity levels on the model. Increasing the suction quantity in local areas of the chord, where "weak" spots occurred, raised transition levels considerably with only moderate increases in the total suction quantity. For example, at a chord Reynolds number of 11.5×10^6 with the basic chordwise suction distribution, transition was triggered by transverse white noise in the octave band between 1200 and 2400 cps at a sound pressure level of 114.5 db. With an increase in suction on the slots forward of the 66% chord and a decrease in suction aft of the 66% chord so that the total suction quantity was increased approximately 20%, transition did not occur at the maximum attainable octave band sound pressure level of 123 db (Ref. 7). Shown on Figure 11.3 are representative data points from the acoustic wind tunnel program (Ref. 6). They are divided into areas of partial suction, where forward suction slots were sealed and Tollmien-Schlichting instabilities occurred; basic suction distribution, where minimum drag was achieved; and modified suction distributions, where suction was increased locally to stabilize the boundary layer. The disturbance velocities shown are those which occurred at the critical frequency or frequency bandwidth (i.e. lowest $\Delta u/U_\infty$). Also, the increase in $\Delta u/U_\infty$ with modified suction is that which occurred in the same frequency or frequency bandwidth at which the lowest sound pressure level caused

ENGINEER	NORTHROP CORPORATION NORAIR DIVISION	PAGE 11.09
CHECKER		REPORT NO. NOR 67-136
DATE June 1967		MODEL X-21A

transitions when the basic suction distribution was employed. It should be noted that in most cases when modified suction was applied, transition could not be triggered because of the power limitations of the acoustic generator and/or the increased stability of the boundary layer.

Figure 11.4 shows the incremental change in transition sound pressure level versus the percent increase in total suction quantity for conditions where the chordwise suction distribution was held constant and where the distribution was modified locally with either a small or insignificant increase in total suction quantity. Significant increases in acoustic sensitivity levels (up to 10 db) can be gained by local modifications to the suction distribution that increase the total suction quantity by no more than 20%; whereas, when the basic chordwise distribution is maintained, a similar increase in sensitivity levels requires an increase in total suction quantity of greater than 60%.

11.23 Acoustic Sensitivity Criteria

The fact that acoustic disturbances have significant effect on the stability of the boundary layer makes it mandatory to establish and employ acoustic design criteria in the design of a laminar flow control airplane. It should be realized that the acoustically originated disturbances are only one source of transition mechanisms and that there are many other parameters involved in the determination of any critical acoustic disturbance. Further, the critical acoustic disturbance magnitude will be established on a particular surface under a specific set of conditions by the most marginal portion of the laminar boundary layer. Since the theoretical state of the art has not been developed sufficiently to provide an analytical description of the phenomenon, it is necessary to rely on experimental data to establish these engineering design criteria.

Differentiation should be clearly established between the critical acoustic disturbance magnitude that causes transition and the design acoustic criteria. Obviously, a design would not be established at the critical level. Some margin of safety, dependent upon the knowledge of the phenomenon and the degree of conservatism desired, would establish the design criteria at some less severe level than the level causing transition.

ENGINEER	NORTHROP CORPORATION NORAIR DIVISION	PAGE
CHECKER		11.10
DATE		REPORT NO.
June 1967		NOR 67-136
		MODEL
		X-21A

Figure 11.5 presents data relating to the ratio of distance velocity to the freestream velocity at transition from laminar to turbulent flow as a function of the chord length Reynolds number. The National Bureau of Standards data were obtained on a flat plate with zero pressure gradient (Ref. 1). The disturbance velocity, A_u , for the NBS tests primarily represents total tunnel turbulence which contained continuous energy over a wide range of frequencies. The NASA Ames data also refer to a zero pressure gradient flat plate. However, the Ames disturbance velocities were computed from sound pressure levels measured at one point in the test section.

The preceding data were obtained from flat plates without suction. Examination of these data indicates that each experimental series behaves primarily as a continuous family of points. The emergence of such families can be reasonably expected because of the major differences between experiments. Note, however, that there is a significant similarity in the relationship between disturbance velocity ratio and chord length Reynolds number for each family.

The remaining data points on Figure 11.5 were obtained from surfaces with boundary layer control suction systems. The 30° swept model had a 12% thick airfoil with a 7 foot chord, the TDT model had a 15% thick airfoil with a 5 foot chord, the Zurich model had a 13% thick airfoil with a 7 foot chord. Although the surfaces have differing geometry, they are related by the fact that the suction quantities and chord-wise suction distributions approximated the conditions required for minimum drag. For the 30° swept model at Ames, the

A_u/U_∞ was calculated from noise measurements made in the tunnel. The data for the 30° swept model were obtained from analyses of the Northrop acoustic tunnel test results presented in Reference 6. Data for the other suction models were obtained from measured turbulence levels in the respective wind tunnels.

Early flight test data were obtained from flight tests conducted over a wide range of Reynolds numbers on an F-94 aircraft fitted with a seven foot laminar suction glove (Ref. 3 and 4). The test program demonstrated that the flow over the glove remained laminar up to an aircraft limit chord Reynolds number of 36×10^6 . Transition occurred at the beginning of an accelerated run at an altitude of 600 feet and a Mach number of 0.61. Utilizing the procedures of Ref. 9, estimates have been made of the noise levels existing over the mid-chord of the glove immediately before

ENGINEER	NORTHROP CORPORATION NORAIR DIVISION	PAGE
CHECKER		11.11
DATE		REPORT NO.
June 1967		NOR 67-136
		MODEL
		X-21A

and after transition. The sound sources considered in these estimates were the engine exhaust noise at military and afterburner power settings and the noise radiated from the turbulent boundary layer of the fuselage and tip tank.

The suction model data shown by Figure 11.5, covering a Reynolds number range between 2×10^6 and 30×10^6 , were obtained with suction quantities and distributions that resulted in minimum drag for each specific model. It has been shown that the suction distribution can be modified with a small increase in the total suction quantity and drag and yet raise the sound pressure level required for transition up to ten decibels. The X-21A design criteria for acoustic sensitivity, shown by Figure 11.5, were selected on the basis of these data, anticipating that modified suction distribution would provide an adequate margin of safety.

For those experimental cases where the magnitude of the disturbances was determined from measured sound pressure levels, the corresponding value of disturbance velocity ratio, $\Delta u/U_\infty$, was calculated by assuming the disturbance was in the form of a plane traveling wave front. While it is recognized that this condition does not exist in the normal wind tunnel test section, the correlation obtained between boundary layer suction models of dissimilar geometry tested under widely varying conditions lends reasonable confidence to this assumption. The relationship between the disturbance velocity ratio, $\Delta u/U_\infty$, and sound pressure level for the plane wave condition can be calculated from the following expression:

$$SPL = 20 \log \frac{\Delta P}{.0002}, \text{ in db re one microbar}$$

where ΔP = root mean square sound pressure
in dynes/cm²

$$\Delta P = \frac{\Delta u}{U_\infty} \gamma M_\infty P_\infty$$

where $\frac{\Delta u}{U_\infty}$ = Ratio of the root mean square
disturbance velocity to the
freestream velocity

M_∞ = Freestream Mach number

γ = Ratio of specific heats

ENGINEER	NORTHROP CORPORATION NORAIR DIVISION	PAGE 11.12
CHECKER		REPORT NO. NOR 67-136
DATE June 1967		MODEL X-21A

P_{∞} = Freestream static pressure in dynes/cm²

$$\text{or, } \frac{\Delta u}{U_{\infty}} = \frac{10^{(SPL/20-3.7)}}{\gamma M_{\infty} P_{\infty}}$$

This expression can be further related to the geometry of the vehicle by replacing the Mach number term with the equivalent expression in terms of length Reynolds number:

$$\Delta P = \frac{\Delta u}{U_{\infty}} \gamma P_{\infty} \frac{R_C v}{a l}$$

where R_C = Length Reynolds number

v = Kinematic viscosity in ft.²/sec.

a = Speed of sound in ft./sec.

l = Representative chord length in feet

and finally,

$$SPL = 20 \log \left[\frac{\Delta u}{U_{\infty}} \frac{\gamma P_{\infty} R_C v}{.0002 a l} \right]$$

11.24 X-21A Flight Test Results

Figure 11.6 presents envelopes of the chord length Reynolds numbers and the accompanying $\Delta u/U_{\infty}$ values for both surfaces as functions of wing station and three representative test Mach number and altitude conditions. The $\Delta u/U_{\infty}$ values were calculated from the sound pressure levels estimated to exist during laminar conditions at the 40% chord position at each wing station. These estimated sound pressure levels were based on measured data obtained with a turbulent wing (Ref. 9) and some measurements in a laminar condition during tests conducted on the inboard wing.

ENGINEER	NORTHROP CORPORATION NORAIR DIVISION	PAGE 11.13
CHECKER		REPORT NO. NOR-67-136
DATE June 1967		MODEL X-21A

Figure 11.6 shows that full chord laminar flow was obtained on the upper surface at all wing stations and flight conditions. However, full chord laminar flow on the lower surface was limited in these tests to positions outboard of the pumping pod at all altitudes below 40,000 feet. Figure 11.6 also shows that the X-21A acoustic sensitivity design criteria were exceeded by the sound pressure levels existing on both surfaces at all shown flight conditions at wing station 250 and inboard of wing station 250. Figure 11.7 shows some of the chord length Reynolds number conditions for both surfaces where full chord laminar flow was obtained. The maximum Reynolds number of 47.3×10^6 that was obtained was on the inboard upper surface at Mach number 0.464 and 10,060 feet. The maximum Reynolds number of 33.5×10^6 where full chord laminar flow (to the aileron hinge line) was obtained on the lower surfaces was on the outer wing (W.S. 270) at Mach number 0.488 and 10,170 feet. For the purposes of this discussion of acoustic sensitivity, it is assumed that transition resulted from the discontinuity of the aileron hinge and that without this discontinuity full chord laminar flow would have been achieved.

Figure 11.7 clearly shows that full chord laminar flow has been achieved on both surfaces of the X-21A at $\Delta u/U_\infty$ values resulting from sound pressure levels 8-10 decibels higher than the design criteria levels.

11.25 Summary

The remaining points shown by Figure 11.7 are the same data as shown by Figure 11.3 and are repeated here for comparison with the X-21A data points. It should be noted that the data from the X-21A and the wind tunnel tests are not all directly comparable. The X-21A data are based on an overall sound pressure level whereas the wind tunnel results are based on the sound pressure level of the critical frequency or critical octave band level. Also, the majority of the wind tunnel data resulted in transition with the basic suction quantity and chordwise distribution whereas the X-21A data points did not cause transition and were obtained with modified chordwise distributions.

There is no inconsistency between the X-21A and wind tunnel groups of data, especially when the X-21A data are compared with the wind tunnel data resulting from modified suction.

ENGINEER	NORTHROP CORPORATION NORAIR DIVISION	PAGE
CHECKER		11.14
DATE		REPORT NO. NOR 67-136
June 1967		MODEL X-21A

The data that are not available, and which would be truly comparable to the wind tunnel data, are the critical magnitudes and frequencies of the acoustic disturbances that cause transition on the X-21A. It may be that the external acoustic environment of the inboard wing was of such magnitude that to obtain laminar flow, suction quantities at or approaching those critical for surface roughness had to be employed as they were during the high Reynolds number wind tunnel tests. The last two sentences emphasize the need of determining the actual critical sound pressure levels and frequencies that cause transition on an actual laminar flow aircraft without the standing wave and other compromising effects that are inherent in wind tunnel-acoustic experiments. Without these data, there will always be some doubt regarding the validity of any acoustic sensitivity criteria and further, a lack of complete understanding regarding the basic transition mechanism originating with external acoustic disturbances.

11.3 Internal Acoustic Disturbances

11.31 Introduction

Investigations of the effect of internal sound upon the maintenance of laminar flow have been conducted in both wind tunnel and flight experiments. It should be noted that the internal sound in itself can have no effect upon the boundary layer except as the origin of a disturbance introduced into the boundary layer at the intersection of the suction slot and the wing surface. Supplementing the wind tunnel and flight tests, laboratory investigations were conducted to develop the relationship between the sound pressure in the spanwise duct and the perturbation velocity in the suction slot. This section discusses these tests, their results, and concludes with an interpretation of the probability of internal sound affecting the maintenance of laminar flow.

11.32 Wind Tunnel Tests

The wind tunnel experiments are discussed in References 11 and 12. For purposes of continuity in this discussion, the wind tunnel results that pertain to internal acoustics are summarized briefly as follows:

1. The internal sound pressure levels necessary for transition were dependent upon both the frequency of the sound and the suction rate of the affected ducts.

ENGINEER	NORTHROP CORPORATION NORAIR DIVISION	PAGE 11.15
CHECKER		REPORT NO. NOR 67-136
DATE June 1967		MODEL X-21A

2. At low chord Reynolds number conditions, transition due to internal sound could always be eliminated by increasing the suction flow. At high Reynolds number conditions, increasing suction to avoid transition from internal sound brought about transition due to surface roughness or from a disturbance originating with the suction flow itself.
3. The portion of the chord that appeared to be the most critical relative to internal sound is the constant pressure distribution portion or mid-chord region.
4. The transition mechanism appears to be related to tangential instability of the boundary layer.
5. The critical frequency can be approximated by the Tollmien-Schlichting theory of amplified oscillations.

11.33 X-21A Flight Tests

The X-21A flight tests were conducted in two phases. The objective of the first phase was to determine the normal sound pressure levels existing in representative spanwise ducts at suction system settings used to obtain maximum laminar flow at altitudes of 5,000, 25,000, and 40,000 feet. Table I shows the overall sound pressure levels that existed at these flight conditions.

The objective of the second phase of the X-21A flight tests was to introduce sound into selected spanwise ducts to determine the effect of the introduced sound on the laminar boundary layer. Sound generators were installed at the inboard ends of the upper surface duct No. 8 (8-15% chord) and the lower inboard surface duct No. 506 (5-8% chord). The tests consisted of introducing discrete sound at intervals of approximately one-third octave between 500 and 10,000 cps and at flight conditions of Mach 0.70, 0.75 at 40,000 feet, Mach 0.6 at 24,500 feet, and Mach 0.47 at 10,000 feet. Broad band noise between 1,000 and 10,000 cps in one-third octave bandwidths was also introduced into the same upper and lower surface ducts at Mach 0.75 and 40,000 feet.

The introduced sound was generally 6-15 db above the normal overall sound pressure level in the duct and 10-20 db above the corresponding normal noise spectrum level in the duct.

ENGINEER	NORTHROP CORPORATION NORAIR DIVISION	PAGE 11.16
CHECKER		REPORT NO. NOR 67-136
DATE June 1967		MODEL X-21A

There was no evidence of any deterioration of the laminar flow during any of the introduced internal sound tests.

11.34 Laboratory Duct Noise Test

This section discusses the laboratory duct model experiment from which an expression was developed that predicts the perturbation velocity in the suction slot resulting from an acoustic pressure in the main spanwise duct.

The detailed descriptions of the test configuration, procedures and results are presented in Reference 13. For continuity of this discussion, Figure 11.8 shows a sketch of the test configuration and the following brief description of the test is presented.

The central component was a slotted door from the lower inboard wing surface of X-21A aircraft. The door was approximately five feet long with eight spanwise slots, each .006 inch wide. The nozzles of the tributary ducts below the slots were mostly .088 inch in diameter. An acoustically treated chamber with a volume of approximately three cubic feet was located above the door in which a regulated pressure and airflow could be maintained. A simulated spanwise suction duct of 24 square inches cross sectional area, possessing a trapezoidal shape with no parallel sides was located below the door. A valve was placed at the upstream end of the duct, approximately three feet from the edge of the test panel, which controlled the amount of additional duct airflow. Devices such as throttling screens, felt, mufflers, and contoured air valves were employed wherever possible to reduce the ambient noise level. A sound generator located downstream of the test panel was capable of producing both sinusoidal and random noise sound pressure levels of 120 db (re: .0002 dy/cm²) between 600 and 8,000 cps at the test section. A variable sonic throat was located further downstream to eliminate the noise from the laboratory exhaust system.

The test procedure consisted of introducing both discrete and broad band sound into the main duct at a downstream distance of about three feet from the test panel. The pressure in the chamber above the test panel was varied to simulate pressure altitudes of 1,000, 25,000 and 36,000 feet. Airflow across the panel was varied to encompass the range of suction flow rates existing on the X-21A aircraft. Sound pressure levels were measured at several positions in the main suction duct and above the test panel. Slot perturbation velocities were measured at the top of the suction slot at both ends of the tributary duct as shown in Figure 11.9.

ENGINEER	NORTHROP CORPORATION NORAIR DIVISION	PAGE 11.17
CHECKER		REPORT NO. NOR 67-136
DATE June 1967		MODEL X-21A

One of the primary results of this test is the following "transfer function" relating the slot perturbation velocity to the sound pressure level in the main duct. The slot perturbation velocity, Δw , had been found to be proportional to:

$$\Delta w \sim (P_D), \frac{1}{\rho c}, \left[(1-M_n) (1-M_s) \right]^x, (D_n)^y$$

where x and y are frequency dependent.

The quantitative expression has been normalized to standard sea level conditions, $M_n = .268$, $M_s = .078$, $D_n = .088$ inch and is

$$\Delta w = (P_D) \left(\frac{\Delta w}{P_D} \right)_N \frac{\rho_o c_o}{\rho c} \left[\frac{(1-M_n)(1-M_s)}{.677} \right]^x \frac{D_n}{.088}^y$$

where

Δw = rms slot perturbation velocity (cm/sec).

P_D = rms sound pressure in main spanwise suction duct (dy/cm^2).

$\left(\frac{\Delta w}{P_D} \right)_N$ = normalized frequency and position dependent ratio of the rms values of the perturbation slot velocity to the main spanwise suction duct sound pressure at the normalising conditions $\left(\frac{cm/sec}{dy/cm^2} \right)$ shown by Figure 11.10

$\frac{\rho_o c_o}{\rho c}$ = ratio of the characteristic impedance of the air at standard sea level conditions to the ambient condition, (density x speed of sound in any compatible units)

M_n = Mach number in core of tributary duct nozzle

M_s = average Mach number in suction slot

D_n = tributary duct nozzle diameter (inches)

x = frequency dependent Mach number function exponent, shown by Figure 11.11

y = frequency and tributary nozzle diameter dependent exponent for nozzle diameter function, shown by Figure 11.12

ENGINEER	NORTHROP CORPORATION NORAIR DIVISION	PAGE 11.18
CHECKER		REPORT NO. NOR 67-136
DATE June 1967		MODEL X-21A

It should be noted that this expression applies only to a suction system configuration similar to that of the X-21A.

Perhaps the more important result of this experiment from a practical design viewpoint was the discovery of a disturbance originating with the suction system flow itself (Ref. 13). This disturbance is discussed in Ref. 14. The point to be made in this discussion is that with the suction system configuration of the X-21A and at slot Reynolds numbers above 120-140, the wake of the slot flow oscillates and creates a disturbance that propagates upstream to the wing surface and thus disturbs the laminar flow. Relative to the discussion of internal noise, the expression presented above is not applicable at high slot Reynolds numbers because the slot perturbation velocity resulting from the sound transmitted from the duct is masked by the suction system flow disturbance unless the duct sound is extremely intense.

Figure 11.13 shows the use of the slot perturbation velocity prediction method as it applied to one of the X-21A internal noise flight test conditions. Several statements can be made concerning the data shown by Figure 11.13.

- (a) The laminar boundary layer was not affected by the introduced sound which, on a spectral basis, was 10-15 decibels higher in intensity than the normal duct noise.
- (b) The disturbance at the wing surface, originating with the suction system flow completely dominated the disturbance originating with the normal duct sound pressure levels. Note also that the disturbance at the surface originating with the more intense introduced sound was not masked by the suction system flow disturbance.
- (c) The wake of the suction system flow as it exited the slot oscillated.

11.35 Hypothetical Explanation of Wind Tunnel Results

Figure 11.13 may also be employed to present a clearer understanding of the effects of internal sound in conjunction with the following hypothetical explanation of the wind tunnel test results.

ENGINEER	NORTHROP CORPORATION NORAIR DIVISION	PAGE 11.19
CHECKER		REPORT NO. NOR-67-136
DATE June 1967		MODEL X-21A

Assume that during the wind tunnel tests at a Reynolds number condition, the relative magnitudes of the disturbances at the wing surface originating with the normal duct noise, the introduced sound and the suction system flow were as shown by Figure 11.13. Assume further that transition occurred due to the surface disturbance originating with the introduced sound within the noted critical frequency bandwidth. It is known that increasing the suction system flow will: (1) increase the stability of the laminar flow; (2) decrease the disturbance at the wing surface due to duct noise; (3) increase the disturbance at the wing surface due to non-viscous suction system flow; and (4) approach the critical suction system flow relative to surface roughness. Figure 11.13 shows clearly the phenomena that are occurring, for as the suction flow is increased, the surface disturbance due to the introduced sound will decrease and laminar flow will be regained, but the surface disturbance due to the non-viscous suction system flow will increase. A point will eventually be reached where any further increase in the suction system flow will cause transition due to the disturbance at the surface originating with the suction system flow itself, or because the critical suction system flow relative to surface roughness has been reached.

11.36 Summary

The lack of any evidence of deterioration in the laminar flow during the X-21A internal noise tests may have been due to the following:

- (a) The introduced sound may not have been of sufficient intensity within the critical frequency bandwidth to cause transition at the suction system flow quantities employed on the X-21A.
- (b) It is possible that internal sound was not introduced at the most critical chordwise position. The ducts forward of the front spar; i.e., ahead of 15% chord, were selected for the duct noise test because of accessibility. It is possible that a duct noise test nearer mid-chord would have produced some effect on laminarisation.

ENGINEER	NORTHROP CORPORATION NORAIR DIVISION	PAGE 11.20
CHECKER		REPORT NO. NOR 67-136
DATE June 1967		MODEL X-21A

It is not currently possible to state that internal sound is a negligible factor in the design of a laminar flow wing. More information regarding the critical disturbance frequency and magnitude at the wing surface as a function of the relevant boundary layer stability parameters is required.

It does appear, however, that the lack of any evidence of deterioration in the laminar flow, with sound 10-15 decibels higher on a spectral basis than the normal duct sound pressure levels, provides reasonable assurance that internal sound is not a factor of primary concern in the maintenance of laminar flow. A factor of much more concern is the disturbance originating with the suction system flow itself. Recent work has been accomplished (Ref. 14) showing that improvements in the detail slot-plenum-control hole portion of the suction system will permit higher slot Reynolds numbers without propagation of oscillating disturbances from the plenum chamber through the slot to the boundary layer.

11.4 Vibration

11.41 Natural Environment - X-21A

Measurements of the natural vibration at several locations on the wing were obtained over a wide range of flight conditions and with the wing possessing both a laminar and turbulent flow (Ref. 10). The locations represented typical leading and trailing edge structure, the center structural box section and trailing edge access panels. The frequency range was 20-5,000 cps and the maximum measured overall root-mean-square acceleration was less than two g's_{rms}. This maximum value existed on trailing edge structure at the 75 percent chord line or well aft of the rear spar of the structural box section. Most overall accelerations were under one g_{rms}.

Measurements were also obtained on spanwise shear webs constructed of plain aluminum sheet and aluminum faced honeycomb. Again, the maximum overall root-mean-square acceleration was less than two g's_{rms}. The plain honeycomb sheet construction displayed sharp resonant responses whereas the honeycomb panels displayed relatively smooth band responses with no sharp resonant peaks.

ENGINEER	NORTHROP CORPORATION NORAIR DIVISION	PAGE
CHECKER		11.21
DATE		REPORT NO.
June 1967		NOR 67-136
		MODEL
		X-21A

One of the objectives of these measurements was to determine whether the duct wall motion could result in a pumping action which would induce high suction slot velocity at the wing surface. For the honeycomb panels, the broad band response precludes any significant web area being in phase so that the change in duct volume due to panel motion can be disregarded. For the plain sheet construction, which does possess a strong resonant response, the panel will be in phase over distances equal to a half wave length and there is a possibility that a local pumping action could result. However, conservative analyses showed that the induced slot velocity is negligible for the vibration amplitudes measured. Also, there was no discernible evidence that any deterioration in the maintenance of laminar flow could be related to this pumping action.

11.42 Forced Vibration - X-21A

The forced vibration tests were conducted to determine the critical frequency bandwidth and magnitude of vibration affecting the maintenance of laminar flow (Ref. 10). Two wing panels were selected to be forcibly vibrated; one forward and one aft of the wing structural box section on the lower outboard wing surface. The panels were selected because of their flexibility, accessibility for instrumentation, space requirements for the electrodynamic shakers and the ease with which laminar flow could be readily obtained.

The test frequency range was nominally between 200-2,000 cps, but due to shaker power limitations, the effective test range was between 400 and 1,800 cps. The test procedure was to establish laminar flow over the test area of the wing and then slowly vary the frequency of vibration between the frequency limits. Figure 11.14 shows the typical panel acceleration and velocity responses versus frequency for both leading and trailing edge panels.

The tests were conducted at Mach 0.7 to 0.8 at 40,000 feet, Mach 0.6 at 25,000 feet and Mach 0.44 at 5,000 feet. The disturbance velocity ratio, $\Delta w/U_\infty$, was generally between 1 and 6×10^{-4} for these tests, shown typically by Figure 11.14 and which is the actual velocity disturbance ratio for the leading edge panel forced vibration test at Mach 0.70 and 40,000 feet.

ENGINEER	NORTHROP CORPORATION NORAIR DIVISION	PAGE 11.22
CHECKER		REPORT NO. NOR-67-136
DATE June 1967		MODEL X-21A

The effects of forced vibration on the laminar boundary layer were recorded by two flush mounted microphones located immediately aft of each vibrated panel, one probe microphone located aft of the trailing edge test panel, and the trailing edge total pressure probes which measured the momentum loss of the boundary layer.

Figure 11.15 shows the acoustic power spectral density sensed by the flush mounted microphone located aft of the trailing edge panel at Mach 0.70 and 40,000 feet for both normal (no forced vibration) turbulent and laminar boundary layer flow. This plot graphically displays the difference in the energy content between laminar and fully developed turbulent flow. Figure 11.16 shows the same function as sensed by the microphone during the forced vibration test of the leading edge panel at the same flight condition. There is essentially no difference in the sensed excitation between the normal laminar flow condition and laminar flow with induced vibration except at the frequencies of the induced vibration.

Figure 11.17 shows the change in momentum loss indicated by the trailing edge total pressure probes during the forced vibration test of the leading edge panel at Mach 0.7 and 40,000 feet. The peaks at 280 cps and 460 cps were not repeatable in subsequent tests and are attributed to local atmospheric conditions or other transient effects not related to the panel vibration.

Figures 11.15 through 11.17 are shown to demonstrate the method of determining the effect of the panel vibration on the maintenance of laminar flow as well as the test results for this flight condition. Other flight conditions showed essentially the same results.

11.43 Summary

These tests have shown that for a laminar flow aircraft configuration, with the propulsion engines mounted aft of the wing and with the wing skin stiffness required by the smoothness and waviness criteria, the normal vibration environment will not affect the maintenance of laminar flow. These tests have also shown that vibration within frequencies between 400 and 1,800 cps, and at magnitudes far in excess of the normal vibration environment, did not affect the maintenance of laminar flow.

11.5 Conclusions

11.51 External Acoustics

It has been shown that transition from laminar to turbulent flow resulting from external acoustic disturbances is an

ENGINEER	NORTHROP CORPORATION NORAIR DIVISION	PAGE
CHECKER		11.23
DATE		REPORT NO.
June 1967		NOR 67-136
		MODEL
		X-21A

extremely complex phenomenon. The critical acoustic disturbance is a function of frequency, magnitude, and propagation direction, and is intimately related to the stability of the laminar boundary layer, suction quantity and chordwise distribution and surface roughness. The necessity of an acoustic sensitivity criteria and the factors that must be included in its development have been presented. Wind tunnel and X-21A flight test results have been shown as functions of the chord length Reynolds number and the ratio of the perturbation velocity to the freestream velocity. The ramifications of calculating the perturbation velocity based on the overall sound pressure level rather than the sound pressure level existing within the critical frequency bandwidth have been discussed. The necessity of developing methods of establishing the critical frequency bandwidth for acoustical disturbances as functions of the boundary layer stability parameters has been stated.

It has been shown that full chord laminar flow has been achieved at all wing stations on the upper surface of the X-21A wing at all primary acoustic flight test conditions. Also, full chord laminar flow was achieved on the upper inboard wing surface at a chord length Reynolds number of 47.3×10^6 in an area that was exposed to the highest noise level environment existing on the upper wing surface.

11.52 Internal Acoustics

A brief review of the internal noise tests conducted in the wind tunnel and on the X-21A has been presented. Also, a method of determining the common disturbance parameter, the perturbation velocity at the suction slot-wing surface intersection, which is required to compare the results of these internal noise tests, has been derived.

It has been shown that in the X-21A, with introduced sound 10-15 decibels higher than the normal duct sound environment, there was no evidence of deterioration of the laminar flow. This result is interpreted as providing reasonable assurance that internal sound is not a factor of primary concern in the maintenance of laminar flow.

Of far greater concern is the disturbance originating with the suction system flow itself. It has been shown that with the X-21A suction system configuration and at slot Reynolds numbers above 120-140, suction system flow created a disturbance at the slot-wing surface intersection that completely

ENGINEER	NORTHROP CORPORATION NORAIR DIVISION	PAGE 11.24
CHECKER		REPORT NO. NOR 67-136
DATE June 1967		MODEL X-21A

dominated the disturbance created by the normal internal duct sound pressures. Further investigation into the improvement of the slot-plenum-control hole configuration permitting higher slot Reynolds numbers without slot flow oscillations has been cited.

As with the external sound, there was no evidence during the X-21A tests that disturbances originating with internal sound had any deleterious effect on the maintenance of laminar flow. However, the fact that both external and internal sound caused transition on every wind tunnel test where the effect of sound was investigated, and the lack of complete understanding of the transition mechanism and relevant parameters involved with acoustically originated disturbances emphasize the requirement of a conservative approach until this lack of understanding can be overcome.

11.53 Vibration

It has been shown that for the X-21A laminar flow aircraft configuration, with the propulsion engines mounted aft of the wing and with the wing skin stiffness dictated by the smoothness and waviness criteria, the normal vibration environment did not affect the maintenance of laminar flow. Also, no deleterious effects on the maintenance of laminar flow were detected with forced vibration between 400 and 1,800 cps and at magnitudes far in excess of the normal vibration environment. Since this frequency bandwidth encompasses the range of amplified response for typical laminar flow aircraft wing skin panels, it is concluded that the normal wing panel vibration is not a factor of concern in the design of a laminar flow aircraft.

ENGINEER	NORTHROP CORPORATION NORAIR DIVISION	PAGE 11.25
CHECKER		REPORT NO. NOR-67-136
DATE June 1967		MODEL X-21A

11.6 References

1. G. B. Schubauer and H. K. Skramstad: "Laminar Boundary Layer Oscillations and Stability of Laminar Flow," NACA Report 909.
2. W. Pfenninger and J. W. Bacon, Jr.: "About the Development of Swept Laminar Suction Wings with Full Chord Laminar Flow," Northrop Norair Report NOR-60-299, September 1960.
3. W. Pfenninger, E. E. Groth, B. H. Carmichael and R. C. Whites: "Low Drag Boundary Layer Suction Experiments In Flight on the Wing Glove of an F-94 Airplane. Phase I - Suction through Twelve Slots," Northrop Norair Report NAI-55-458, April 1955.
4. W. Pfenninger, E. E. Groth, B. H. Carmichael and R. C. Whites: "Low Drag Boundary Layer Suction Experiments In Flight on the Wing Glove of an F-94 Airplane. Phase II - Suction through 69 Slots," Northrop Norair Report NAI-57-318, February 1957.
5. W. Pfenninger: "Experiments with a 15% - Thick Slotted Laminar Suction Wing Model in the NACA, Langley Field, Low Turbulence Wind Tunnel," AFTR 5982, April 1953.
6. J. W. Bacon, Jr., W. Pfenninger and C. Roger Moore: "Influence of Acoustical Disturbances on the Behavior of a Swept Laminar Suction Wing," Northrop Norair Report NOR-62-124 (BLC-141), October 1962.
7. R. F. Carmichael and D. E. Pelke: "In-Flight Noise Measurements Performed on the X-21A Laminar Flow Control Aircraft," Northrop Norair Report NOR-64-81, April 1964.
8. W. Pfenninger, L. Gross and J. W. Bacon, Jr.: "Experiments on a 30° Swept 12% Thick Symmetrical Laminar Suction Wing in the 5 by 7 Foot Michigan Tunnel," Northrop Norair Report NAI-57-317 (BLC-93), February 1957.
9. T. R. Rooney, R. F. Carmichael and K. E. Eldred: "Investigation of Noise with Respect to the LFC, NB-66 Aircraft," Northrop Norair Report NOR-61-10, April 1961.
10. Internal Northrop Norair Memorandum, 1936-65-6 dtd 18 May 1965; Subject: "X-21A PANEL VIBRATION TESTS"
11. J. C. Carlson and J. W. Bacon, Jr.: "Influence of Acoustical Disturbances in the Suction Ducting System on the Laminar Flow Control Characteristics of a 33° Swept Suction Wing," Northrop Norair Report NOR-65-232, August 1965.

ENGINEER	NORTHROP CORPORATION NORAIR DIVISION	PAGE 11.26
CHECKER		REPORT NO. NOR-67-136
DATE June 1967		MODEL X-21A

12. J. C. Carlson: "Investigation of the Laminar Flow Control Characteristics of a 33° Swept Suction Wing at High Reynolds Numbers in the NASA Ames 12-Foot Pressure Wind Tunnel in August 1965," Northrop Norair Report NOR-66-58, January 1966.

13. R. F. Carmichael, P. E. Finwall: "Analysis of the Results of the Laboratory Duct Model Test for the X-21A Laminar Flow Aircraft," Northrop Norair Report NOR-65-303, November 1965.

14. W. Pfenninger, J. Bacon, J. Goldsmith: "About Flow Disturbances Induced by Low Drag Boundary Layer Suction through Slots," Presented at the IUGG-IUTAM Symposium on Boundary Layers and Turbulence Including Geophysical Applications, September 1966, Kyoto, Japan.

ENGINEER	NORTHROP CORPORATION NORAIR DIVISION	PAGE
CHECKER		11.27
DATE		REPORT NO.
June 1967		NOR 67-136
		MODEL
		X-21A

TABLE I

TYPICAL INTERNAL DUCT SOUND PRESSURE LEVELS

Upper Surface

Duct No.	Percent Chord	Location	Sound Pressure Levels (db)*		
			Altitude (ft.)		
			5-10,000	23,000	40,000
8	7.7-15	Inboard	112	110	106
112	25-30	Inboard	114	111	---
143	55-60	Outboard	120	118	115
201	60-67	Outboard	109	111	103
281	81-87	Outboard	116	124	116
292	88-92	Inboard	126	128	121

Lower Surface

Duct No.	Percent Chord	Location	Sound Pressure Level (db)*		
			Altitude (ft.)		
			5-10,000	23,000	40,000
501	0-1.2	Outboard	119	117	113
502	0-1.2	Inboard	123	124	120
504	1.2-5	Inboard	120	119	118
505	5-8	Outboard	110	111	113
506	5-8	Inboard	115	122	114
632	44-50	Inboard	108	105	---
643	55-60	Outboard	113	112	105
701	81-87	Outboard	108	109	104

* Referenced to: 2×10^{-4} dy/cm²

ENGINEER R. F. Carmichael	NORTHROP CORPORATION NORAIR DIVISION	PAGE 11.28
CHECKER		REPORT NO. NOR 67-136
DATE March 1964		MODEL X-21A

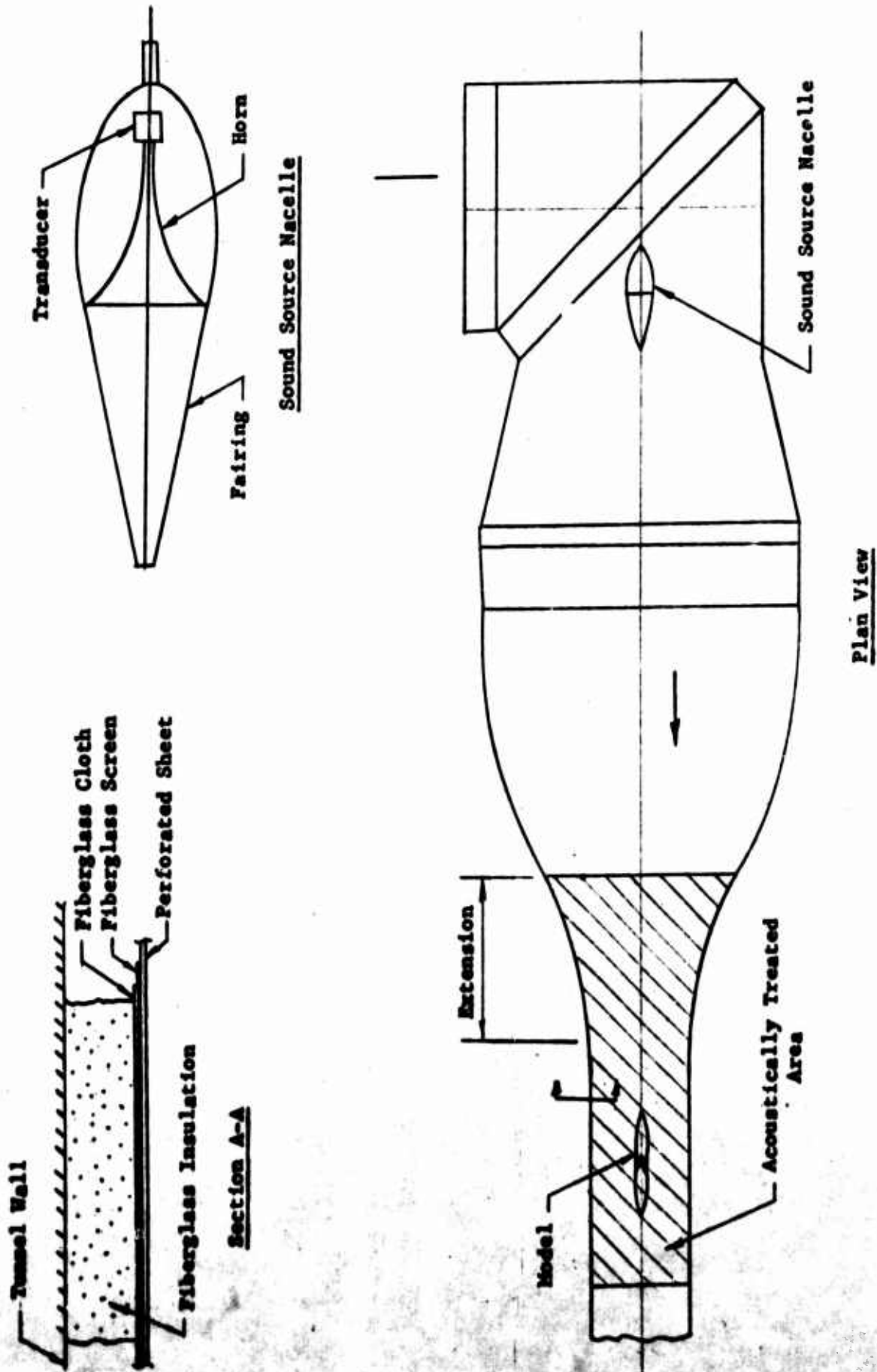


FIGURE 11.1 ACOUSTICAL TEST INSTALLATION IN NORAIR 7-BY 10-FOOT WIND TUNNEL

ENGINEER	NORTHROP CORPORATION NORAIR DIVISION	PAGE
CHECKER		11.29
DATE	June 1967	REPORT NO. NOR 67-136
		MODEL X-21A

Suction from 0.45c to 0.95c, front slots and static pressure orifices sealed, no suction upstream of 0.45c.

Chord Reynolds Number = 7×10^6

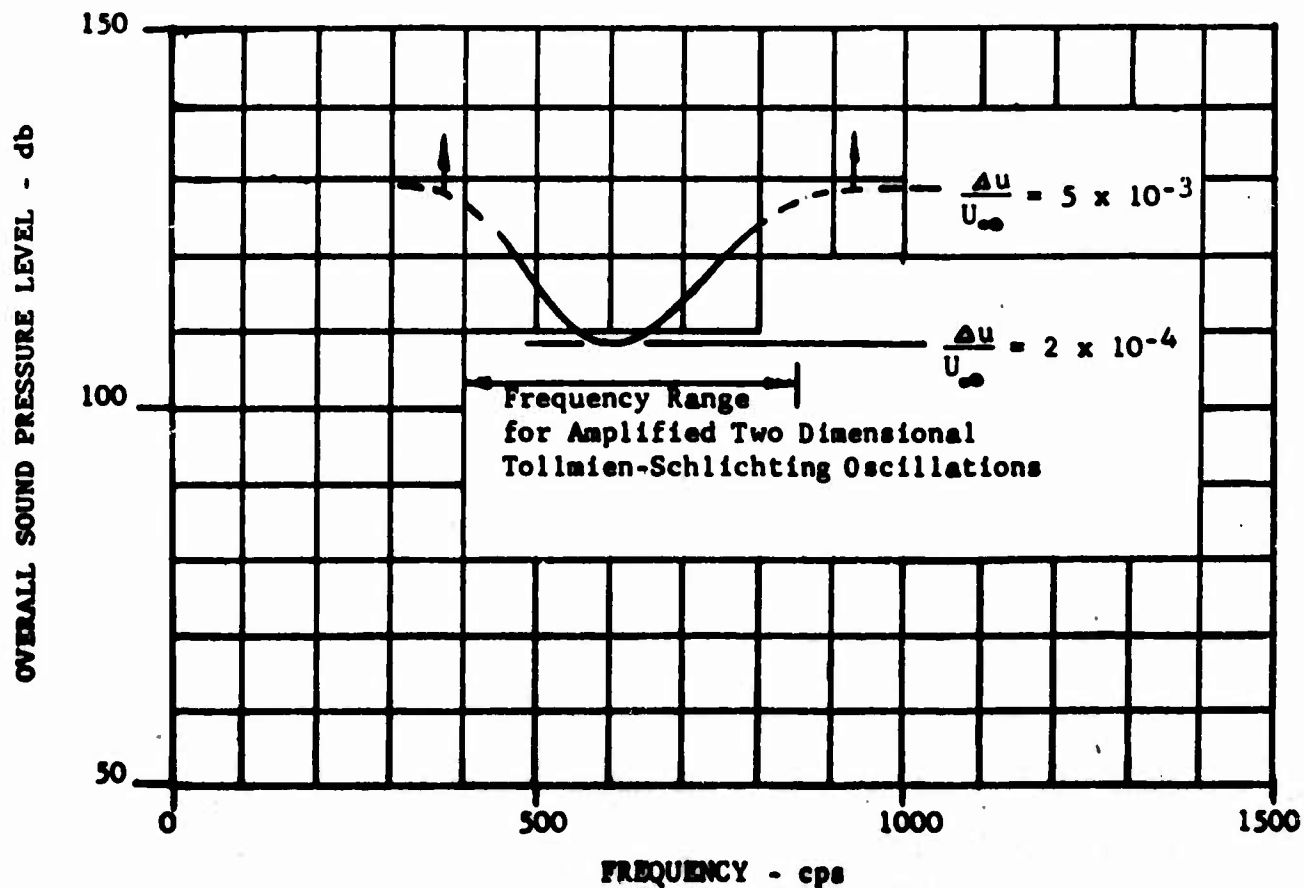


FIGURE 11.2 TRANSITION RESULTING FROM LONGITUDINAL WAVE FRONTS OF DISCRETE FREQUENCIES WITH PARTIAL SUCTION ON THE 30° SWEEP LAMINAR SUCTION MODEL

ENGINEER	NORTHROP CORPORATION NORAIR DIVISION	PAGE	11.30
CHECKER		REPORT NO.	NOR 67-136
DATE		MODEL	X-21A
June 1967			

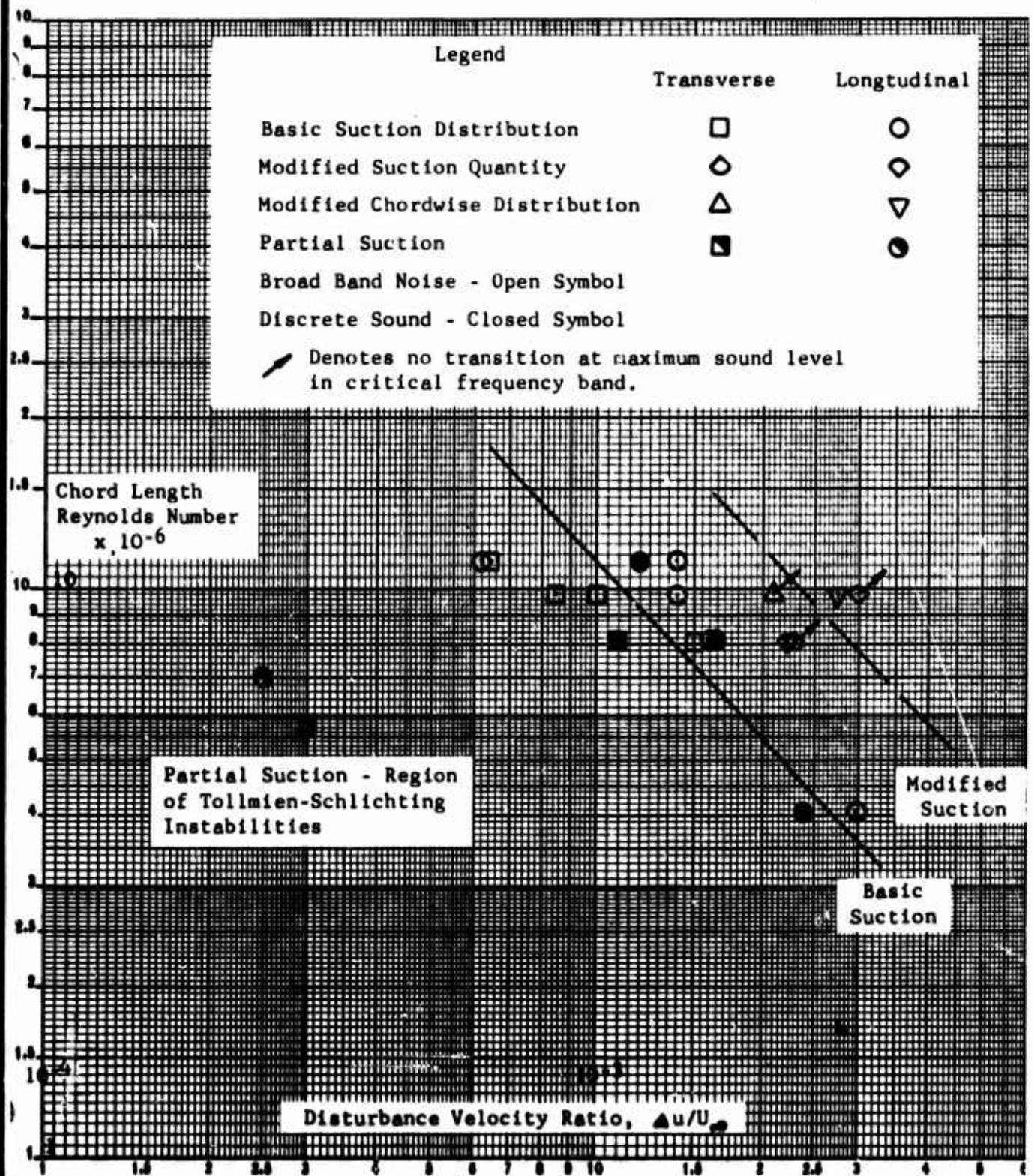


FIGURE 11.3 NORAIR ACOUSTIC WIND TUNNEL TEST RESULTS - TRANSITION RESULTING FROM ACOUSTIC DISTURBANCES ON A 30° SWEEP LAMINAR SUCTION WING MODEL

ENGINEER	NORTHROP CORPORATION NORAIR DIVISION	PAGE 11.31
CHECKER		REPORT NO. NOR 67-136
DATE June 1967		MODEL X-21A

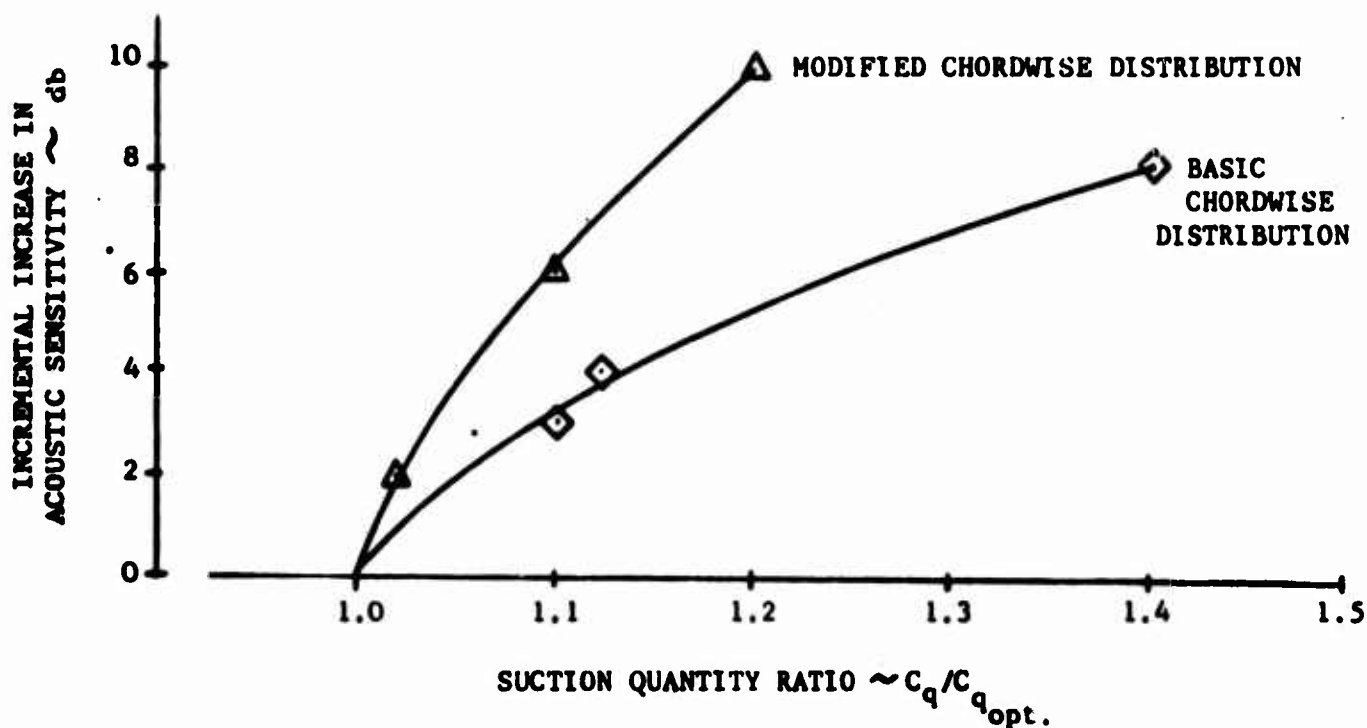


FIGURE 11.4 EFFECT OF INCREASED SUCTION ON ACOUSTIC SENSITIVITY OF A 30° SWEEP LAMINAR SUCTION WING MODEL

ENGINEER	NORTHROP CORPORATION NORAIR DIVISION	PAGE 11.32
CHECKER		REPORT NO. NOR 67-136
DATE June 1967		MODEL X-21A

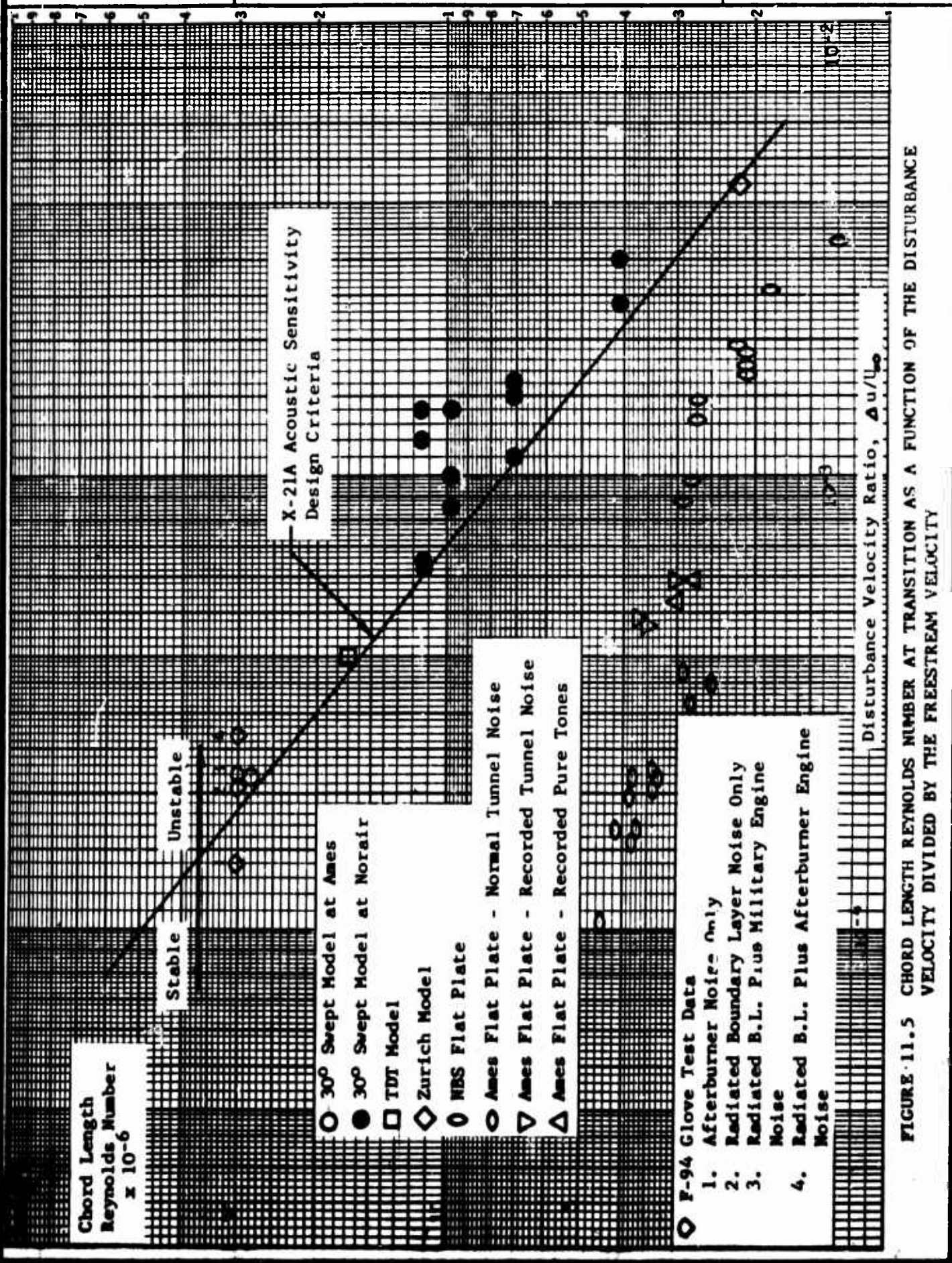


FIGURE 11.5 CHORD LENGTH REYNOLDS NUMBER AT TRANSITION AS A FUNCTION OF THE DISTURBANCE VELOCITY DIVIDED BY THE FREESTREAM VELOCITY

ENGINEER	NORTHROP CORPORATION NORAIR DIVISION	PAGE 11.33
CHECKER		REPORT NO. NOR 67-136
DATE June 1967		MODEL X-21A

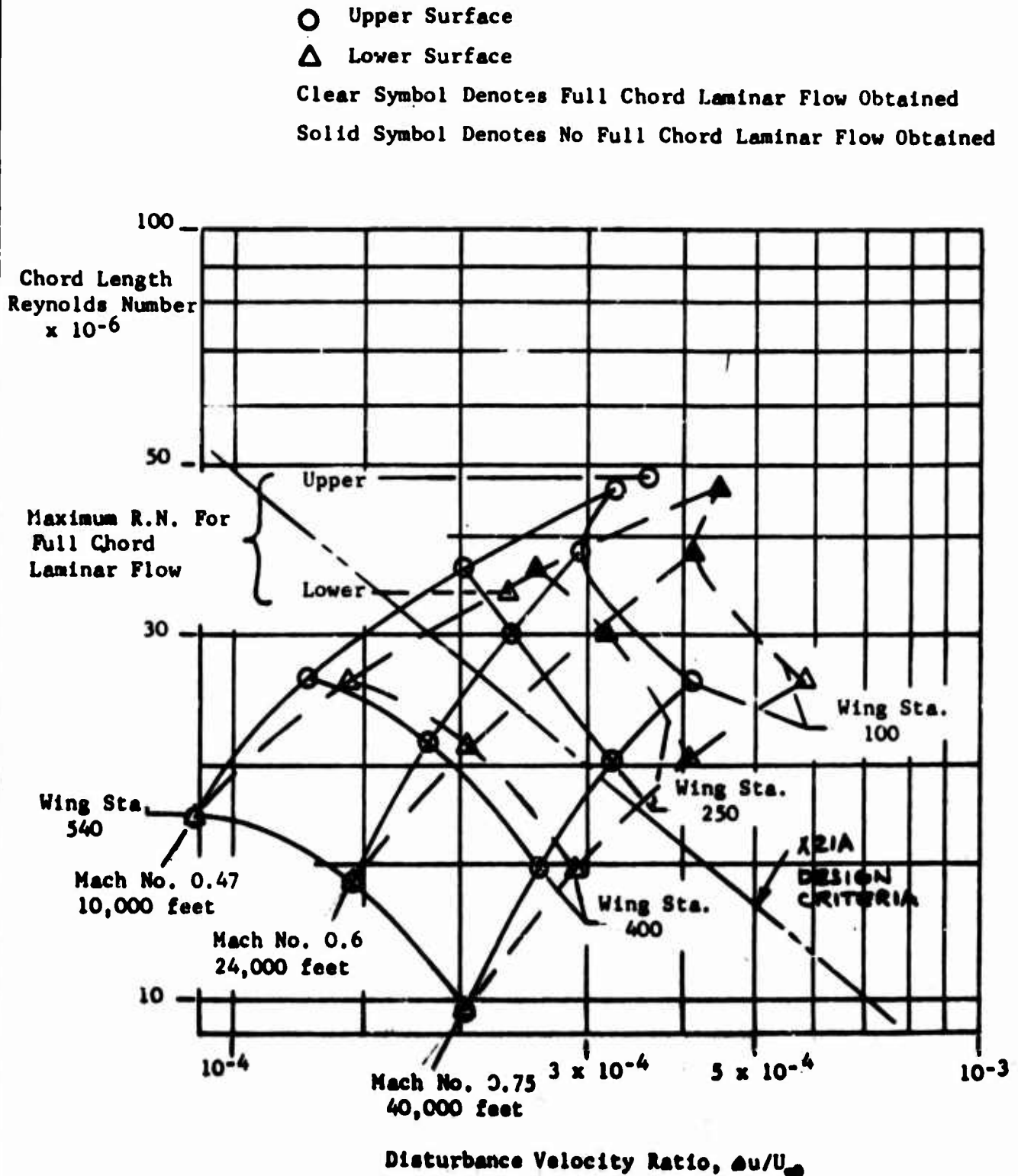
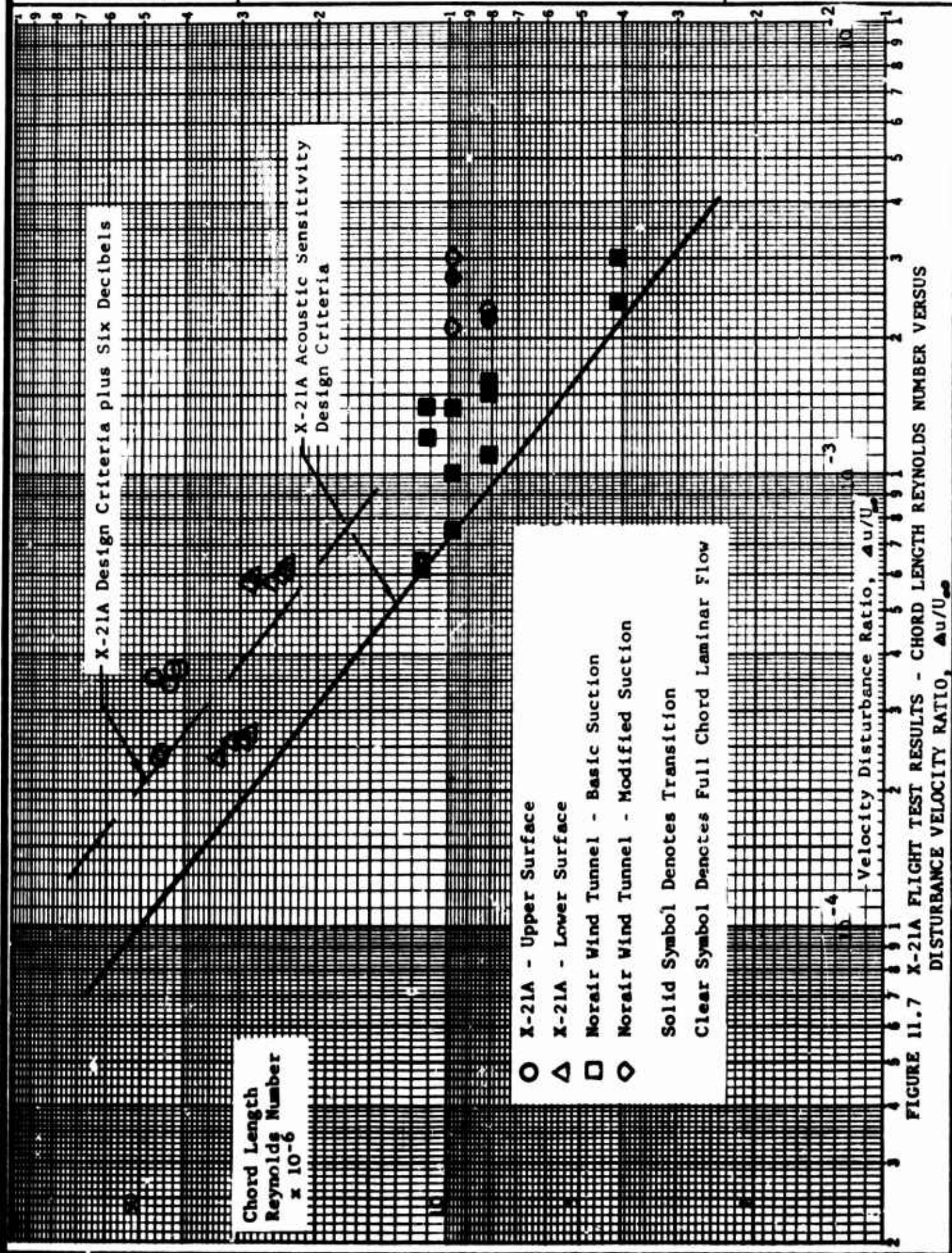


FIGURE 11.6 CHORD LENGTH REYNOLDS NUMBER vs. DISTURBANCE VELOCITY RATIO RESULTING FROM NORMAL X-21A ACOUSTIC ENVIRONMENT

ENGINEER	NORTHROP CORPORATION NORAIR DIVISION	PAGE
CHECKER		11.34
DATE		REPORT NO. NOR 67-136
June 1967		MODEL X-21A



ENGINEER	NORTHROP CORPORATION NORAIR DIVISION	PAGE 11.35
CHECKER		REPORT NO. NOR 67-136
DATE June 1967		MODEL X-21A

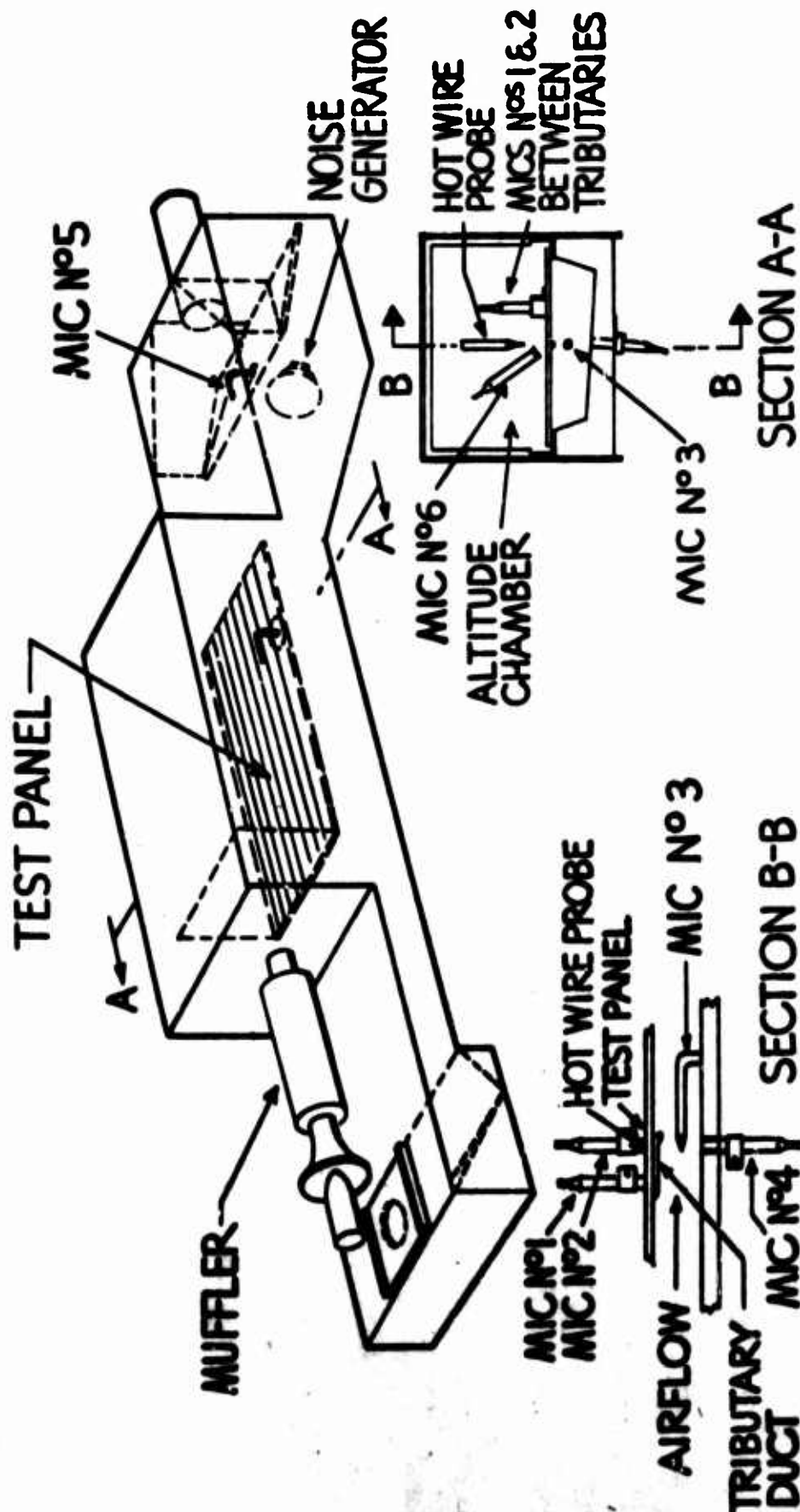


FIGURE 11.8 LABORATORY DUCT MODEL TEST CONFIGURATION

ENGINEER	NORTHROP CORPORATION NORAIR DIVISION	PAGE	11.36
CHECKER		REPORT NO.	NOR 67-136
DATE		MODEL	X-21A

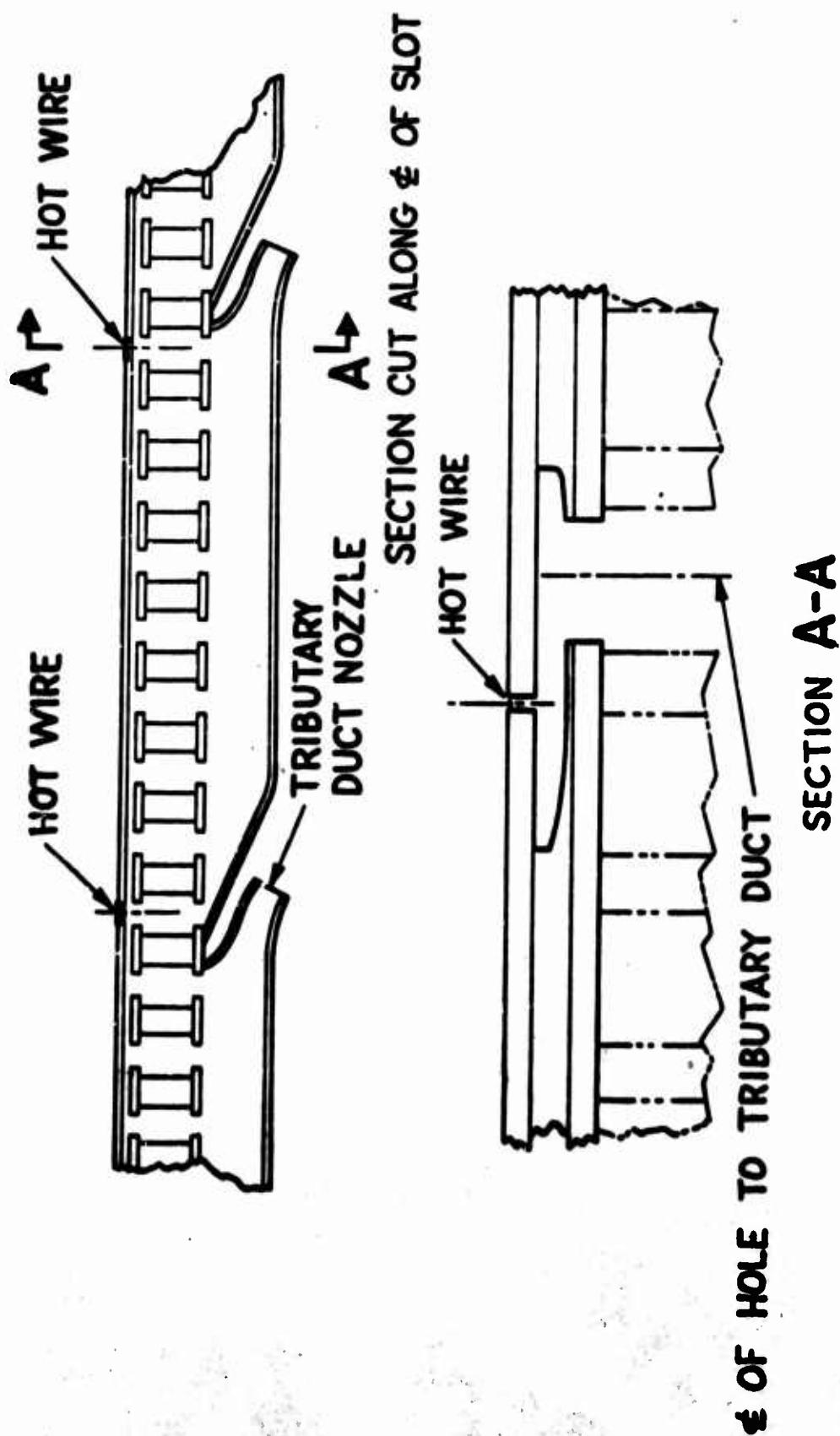


FIGURE 11.9 LABORATORY DUCT MODEL TEST - DETAIL SUCTION SYSTEM CONFIGURATION

ENGINEER	NORTHROP CORPORATION NORAIR DIVISION	PAGE 11.37
CHECKER		REPORT NO. NOR 67-136
DATE June 1967		MODEL X-21A

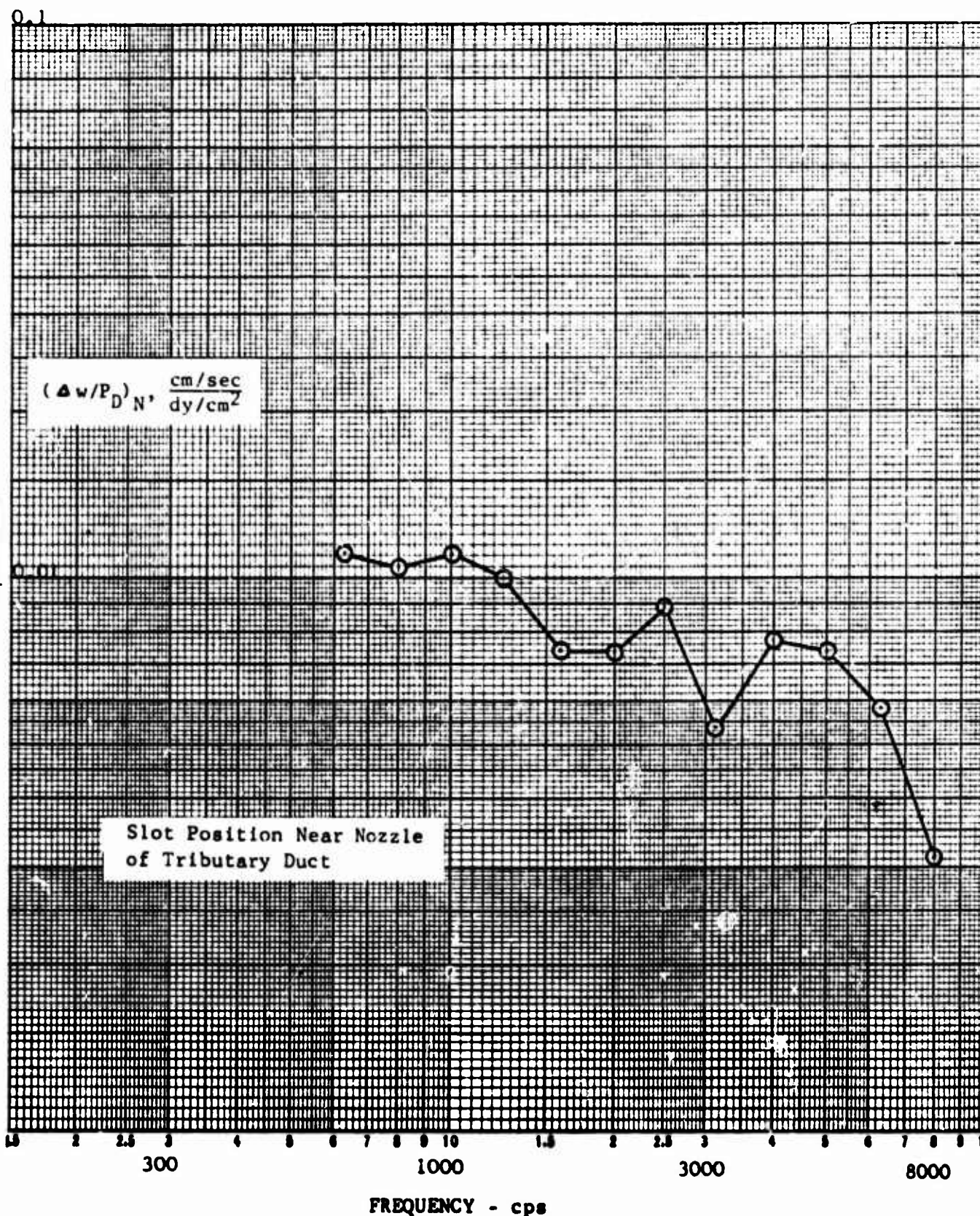


FIGURE 11.10 NORMALIZED CORRELATION FUNCTION, $(\frac{\Delta w}{P_D})_N$

ENGINEER	NORTHROP CORPORATION NORAIR DIVISION	PAGE 11.38
CHECKER		REPORT NO. NOR 67-136
DATE June 1967		MODEL X-21A

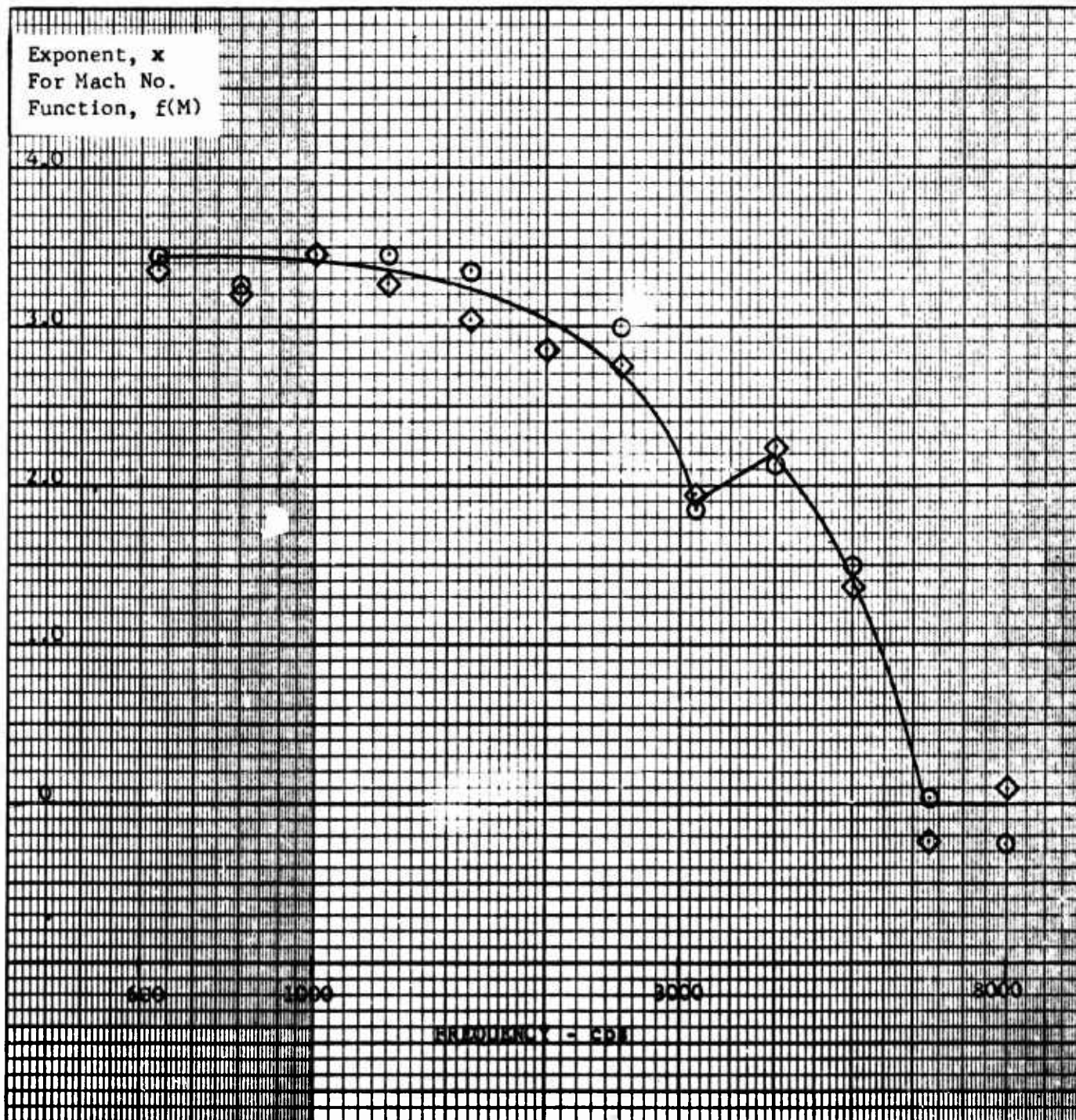


FIGURE 11.11 EXPONENT, x , FOR MACH NUMBER FUNCTION, $f(M)$

ENGINEER	NORTHROP CORPORATION NORAIR DIVISION	PAGE 11.39
CHECKER		REPORT NO. NOR 67-136
DATE June 1967		MODEL X-21A

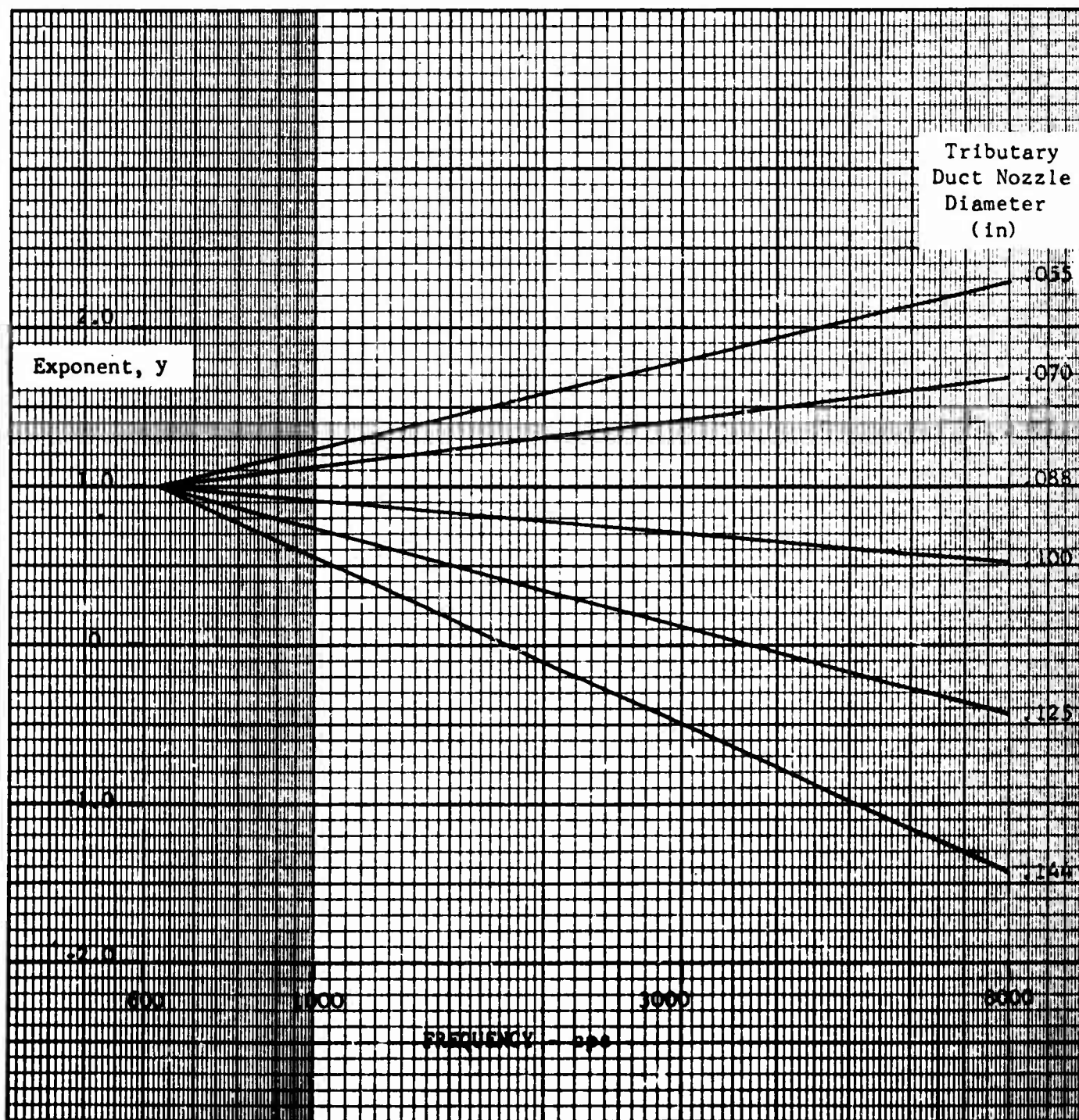


FIGURE 11.12. EXPONENT, y , FOR TRIBUTARY DUCT NOZZLE DIAMETER FUNCTION, $(D_n/.088)$

ENGINEER	NORTHROP CORPORATION NORAIR DIVISION	PAGE 11.40
CHECKER		REPORT NO. NOR 67-136
DATE June 1967		MODEL X-21A

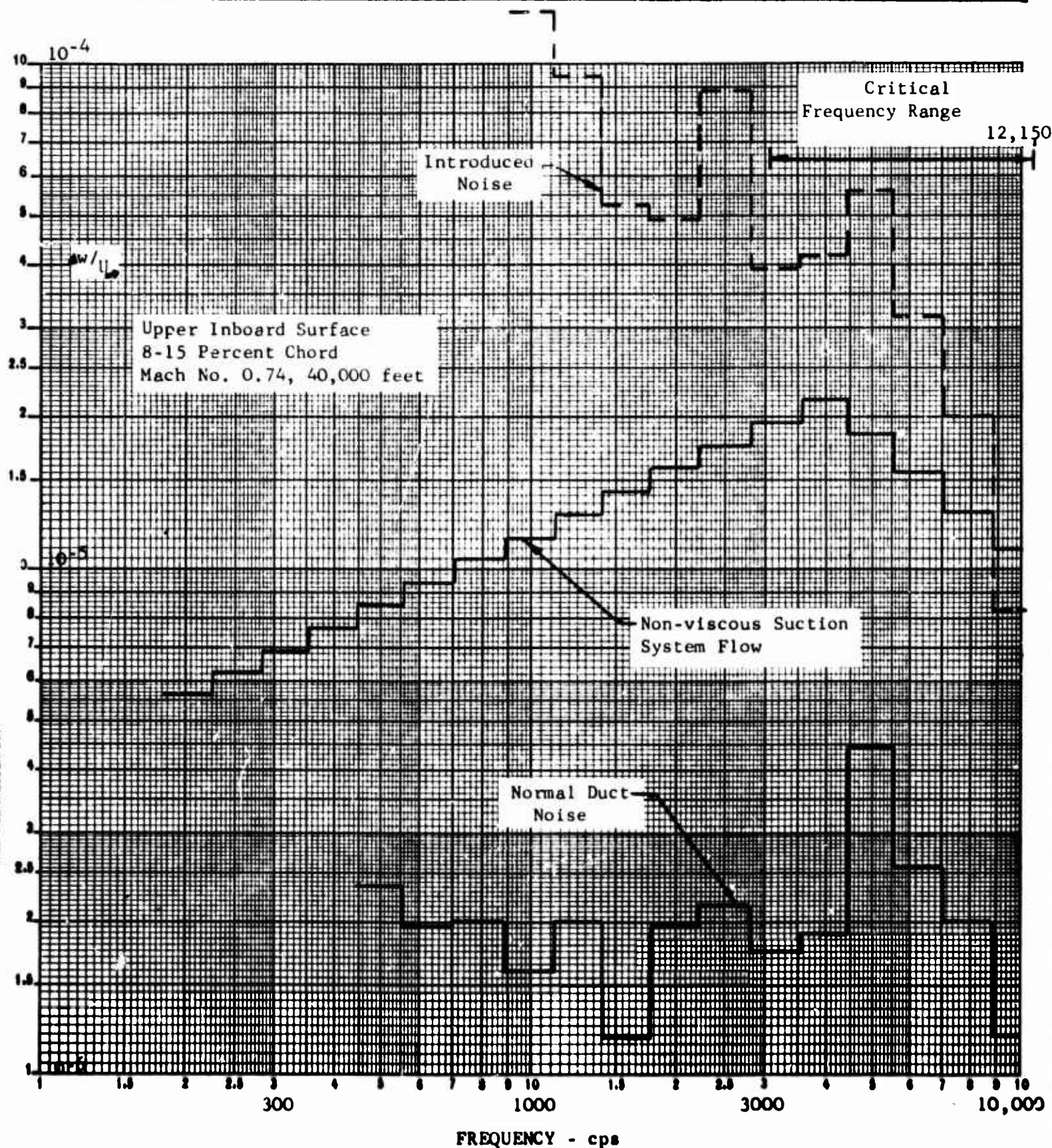


FIGURE 11.13 VELOCITY DISTURBANCE RATIO, $\Delta w/U_{\infty}$, VERSUS FREQUENCY

ENGINEER	NORTHROP CORPORATION NORAIR DIVISION	PAGE	11.41
CHECKER		REPORT NO.	NOR 67-136
DATE June 1967		MODEL	X-21A

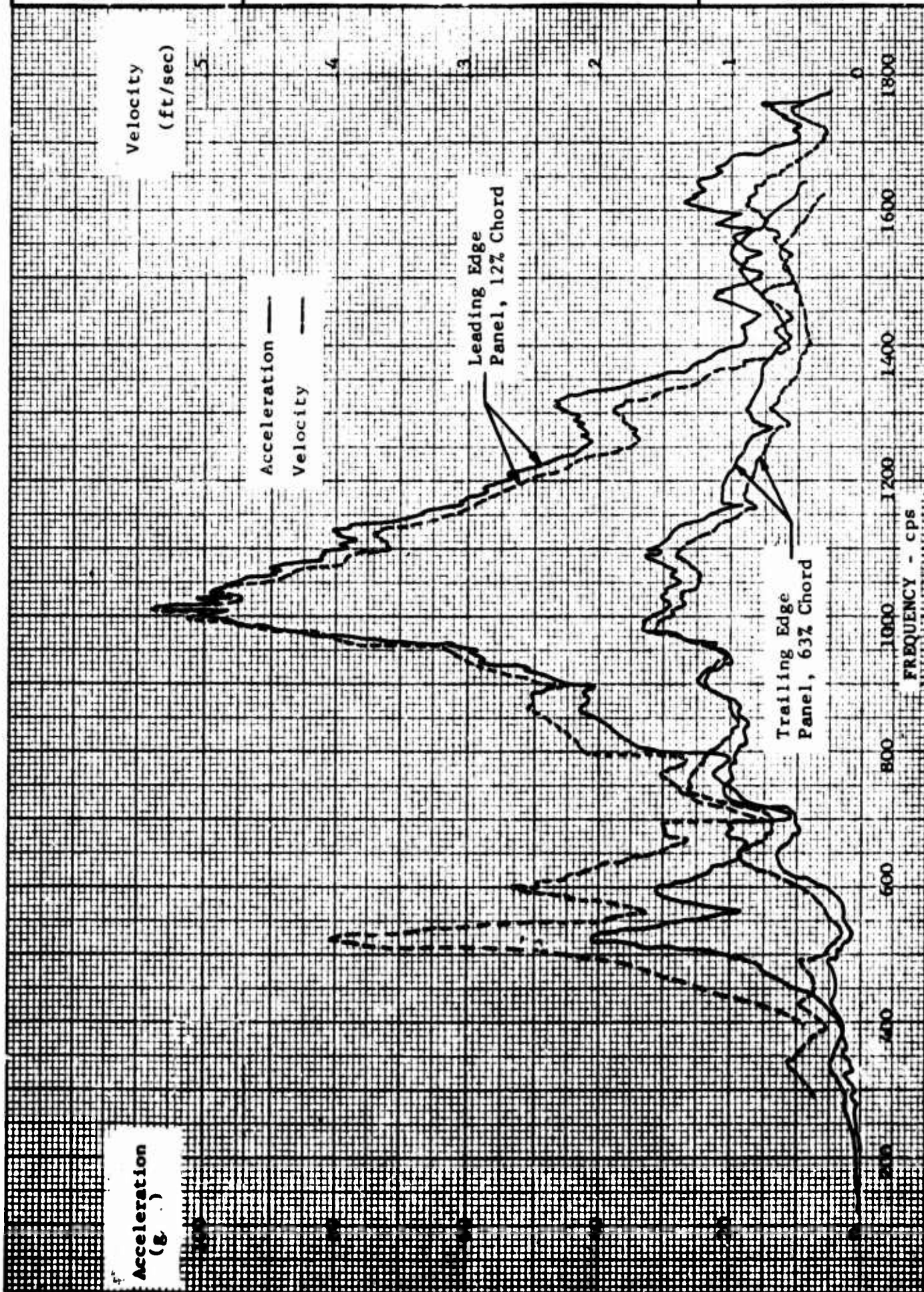
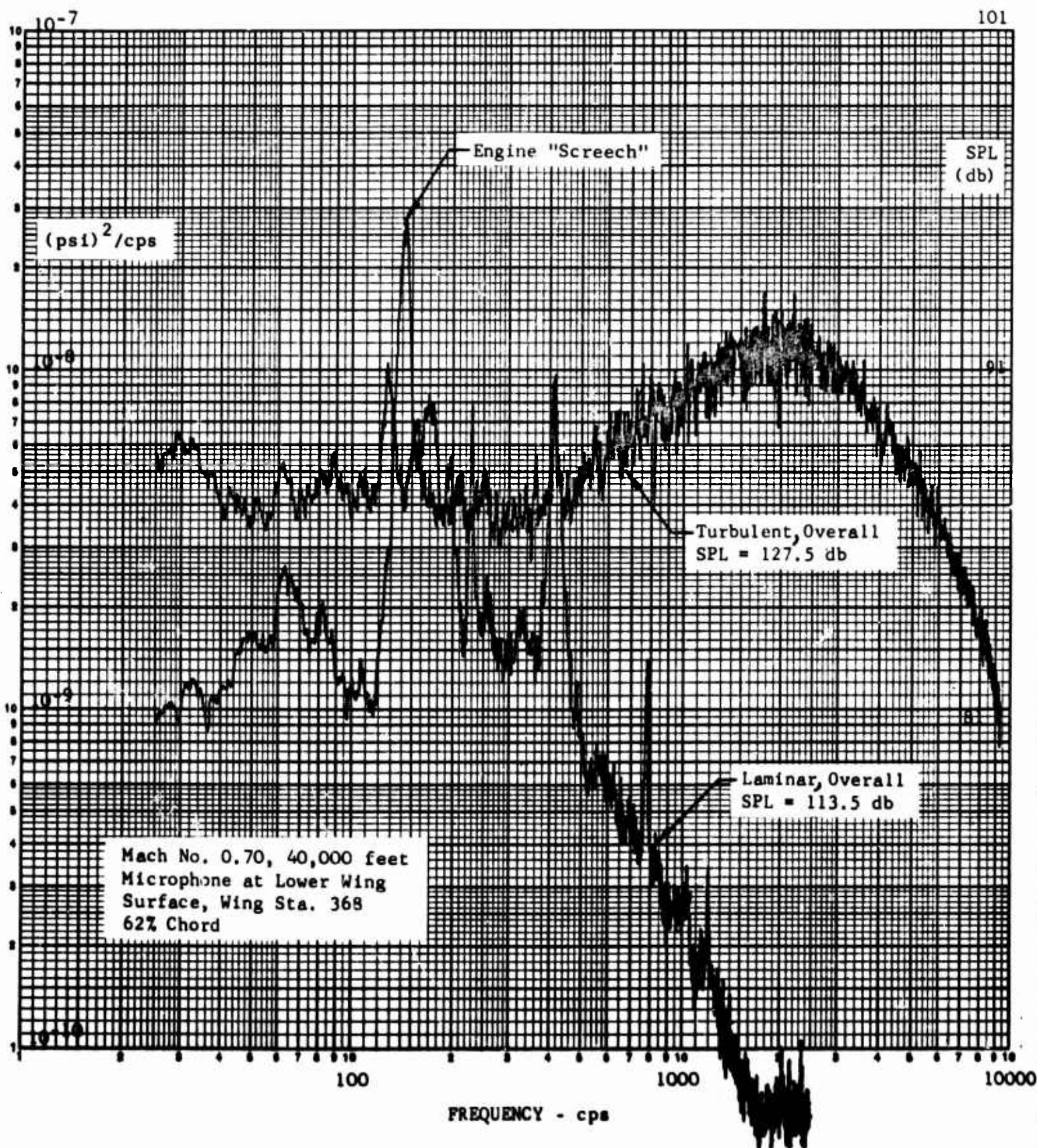


FIGURE 11.14 TYPICAL PANEL RESPONSE DURING FORCED VIBRATION TESTS

ENGINEER	NORTHROP CORPORATION NORAIR DIVISION	PAGE 11.42
CHECKER		REPORT NO. NOR 67-136
DATE June 1967		MODEL X-21A



K&E LOGARITHMIC
5 X 5 CYCLES
REPRODUCED BY K&E CO.

FIGURE 11.15 ACOUSTIC POWER SPECTRAL DENSITY - LOWER WING SURFACE
WITH LAMINAR AND TURBULENT FLOW

ENGINEER	NORTHROP CORPORATION NORAIR DIVISION	PAGE 11.43
CHECKER		REPORT NO. NOR 67-136
DATE June 1967		MODEL X-21A

KE LOGARITHMIC
 46 7403
 3 X 3 CYCLES
 KEUFFEL & ESSER CO.

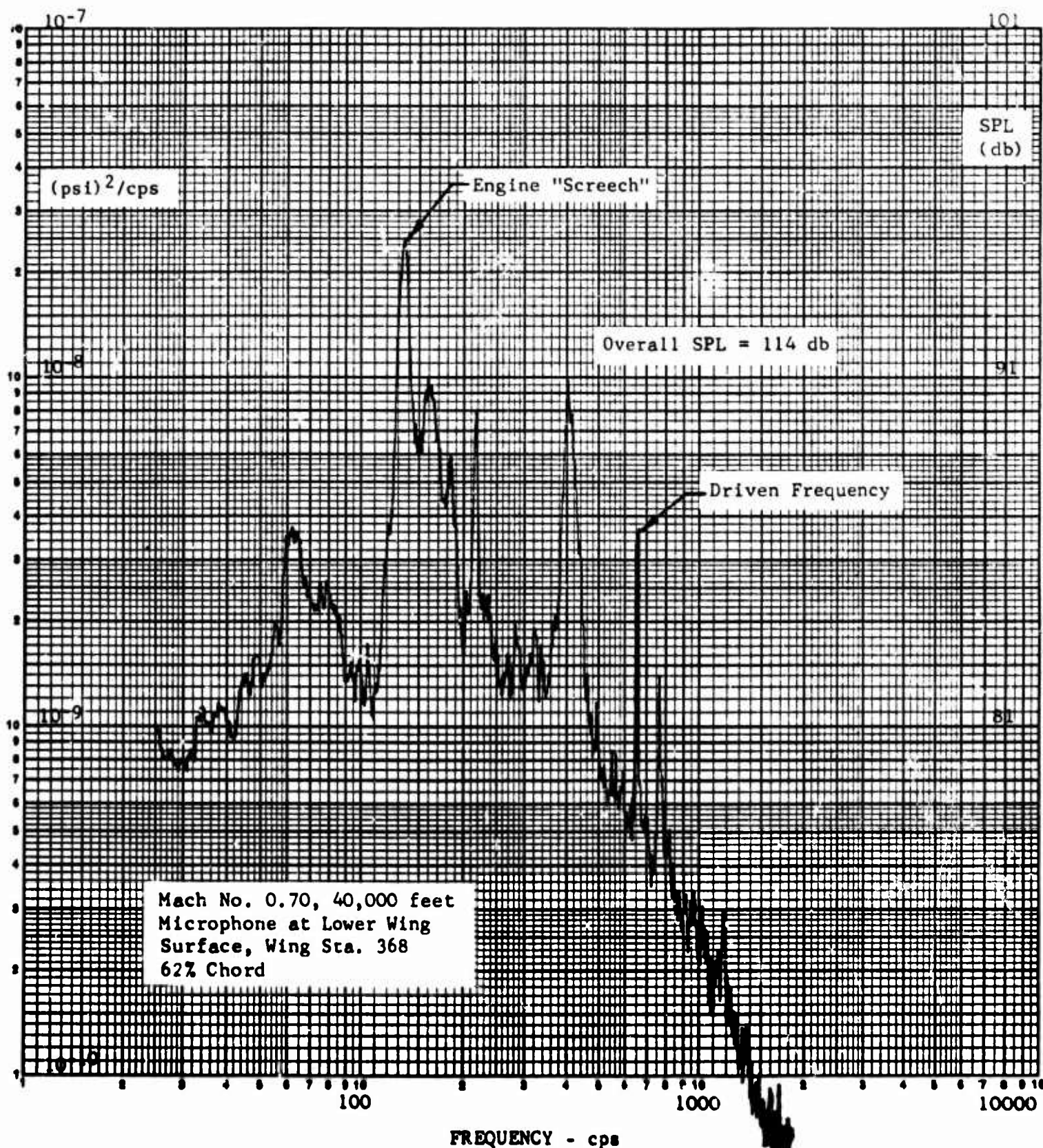


FIGURE 11.16 ACOUSTIC POWER SPECTRAL DENSITY - LOWER WING SURFACE WITH LAMINAR FLOW AND FORCED VIBRATION

ENGINEER	NORTHROP CORPORATION NORAIR DIVISION	PAGE	11.44
CHECKER		REPORT NO.	NOR 67-136
DATE June 1967		MODEL	X-21A

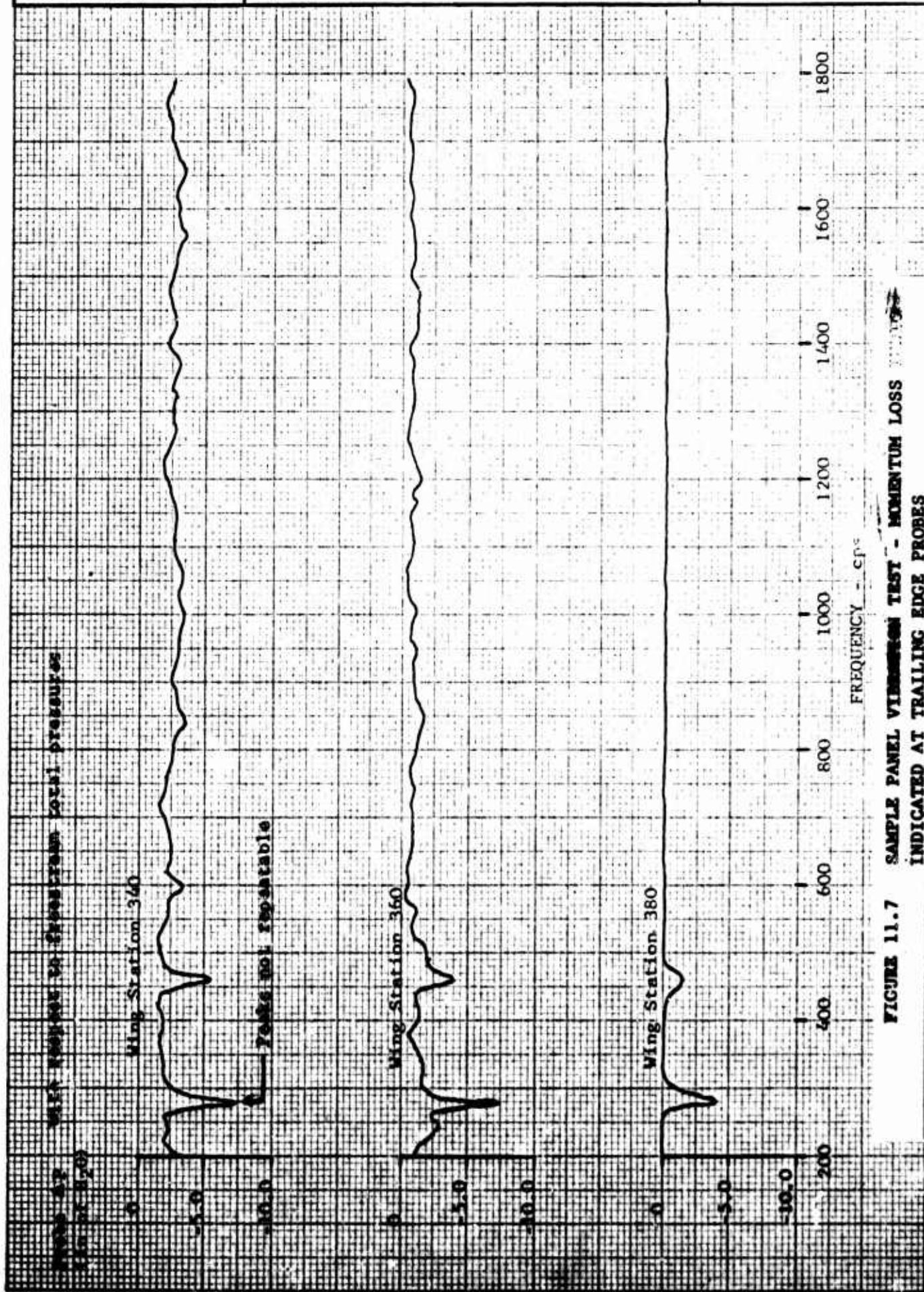


FIGURE 11.7 SAMPLE PANEL VIBRATION TEST - MOMENTUM LOSS INDICATED AT TRAILING EDGE PROBES

ENGINEER	NORTHROP CORPORATION NORAIR DIVISION	PAGE 12.00
CHECKER		REPORT NO. NOR 67-136
DATE June 1967		MODEL X-21A

SECTION 12

PERFORMANCE PREDICTION AND EFFECT OF LFC ON
PERFORMANCE PARAMETERS

By

L. K. Barker

March, 1964

~~March, 1964~~
Revised April, 1967

ENGINEER	NORTHROP CORPORATION NORAIR DIVISION	PAGE 12.01
CHECKER		REPORT NO. NOR 67-136
DATE June 1967		MODEL X-21A

12.1 INTRODUCTION

The application of laminar flow control to an aircraft results in a considerable improvement of flight performance, such as range and endurance, compared to an equivalent turbulent aircraft. The performance gains ensue from the inherent low friction drag of laminar boundary layers maintained on a maximum practicable proportion of airplane surfaces.

The drag reduction of a laminarized wing (and empennage, if applicable) is composed of a large decrease in minimum profile drag and a minor decrease in the drag-due-to-lift portion of the profile drag. The savings in thrust and therefore in fuel flow (due to the reduced wake drag) are reduced by the power (and therefore the fuel flow) necessary to operate the suction system.

If a wind tunnel test is conducted to obtain drag data, it need not be performed on a laminarized model. The data of a turbulent model are valid for a laminar airplane, if a proper correction is applied to account for the changes associated with laminarizing the suction surfaces. The procedure of establishing the drag-lift-polar of an LFC aircraft on the basis of turbulent model data is discussed in this section of this report.

12.2 SYMBOLS

A	Aspect ratio
C	Local streamwise chord, ft
C_D	Drag coefficient = Drag/ $q_0 S$
C_d	Local drag coefficient = (Drag/unit span)/ $q_0 C$
C_{D_F}	Drag coefficient of turbulent wedge wing areas = Drag/ $q_0 S$
$C_{D_{P_{min}}}$	Minimum parasite drag coefficient = Minimum Drag/ $q_0 S$
C_{D_S}	Equivalent suction drag coefficient = $\left[W_{s2} J C_{P_h} / q_0 S V_g \right] \left[T_2 (P_0 / P_2)^{\frac{\gamma-1}{\gamma}} - t_0 \right]$
C_{D_W}	Wing laminar profile drag coefficient = $C_{d_W} (S_{wetted})_{laminar} / S_{wing}$
C_{d_W}	Local wing laminar profile drag coefficient = (Profile drag/unit span)/ $q_0 C$

ENGINEER	NORTHROP CORPORATION NORAIR DIVISION	PAGE
CHECKER		12.02
DATE	June 1967	REPORT NO. NOR 67-136
		MODEL X-21A

- C_f Skin friction coefficient for a turbulent flat plate =

$$.44/(\log_{10} R_N)^{2.58}$$
- C_L Lift coefficient = $Lift/q_o S$
- $C_{L_{opt}}$ Lift coefficient at $C_{D_{p_{min}}}$
- C_{p_h} Specific heat at constant pressure = 0.25 Btu/lb $^{\circ}$ R
- C_Q Suction quantity coefficient, $\frac{Q_a}{V_o \rho S}$
- e_1 Factor to account for the deviation of the spanwise lift distribution from the ideal elliptical distribution
- e_2 Factor to account for the variation of profile drag coefficient with lift coefficient
- e_3 Factor to account for the deviation of the drag polar from the initial parabola at values of the lift coefficient greater than the laminar limit lift coefficient
- h Pressure altitude
- J Mechanical work equivalent of heat = 778 ft-lbs/Btu
- M Mach number
- MF Multiplying factor to correct turbulent flat plate friction drag for non-zero pressure gradient
- F_o Free stream static pressure, psf
- P_2 Total pressure at the compressor face, psf
- Q_s Suction air volume flow, ft 3 /sec
- q_o Free stream dynamic pressure, psf
- R_N Reynolds number
- S Wing area, ft 2
- T_2 Total temperature at the compressor face, $^{\circ}$ R
- t_o Free stream static temperature, $^{\circ}$ R
- V_o Free stream velocity, fps

ENGINEER	NORTHROP CORPORATION NORAIR DIVISION	PAGE 12.03
CHECKER		REPORT NO. NOR 67-136
DATE June 1967		MODEL X-21A

- W_{s2} Weight flow of suction air at the compressor face, lbs/sec
 α Angle of attack
 γ Ratio of specific heats = 1.40
 θ Boundary layer momentum thickness

12.3 DEFINITIONS AND EQUATIONS FOR THE COMPONENTS OF DRAG OF AN LFC AIRPLANE

The following equation is used to represent the drag polar of a subsonic LFC aircraft:

$$C_D = C_{D_{P_{min}}} + C_L^2 / (\pi A e_1) + (C_L - C_{L_{opt}})^2 (1 - e_2) / (\pi A e_2) \quad (\text{Eq. 1})$$

where:

- $C_{D_{P_{min}}}$ = Minimum parasite drag coefficient, including the effect of Mach number
 e_1 = Factor to account for the deviation of the spanwise lift distribution from the ideal elliptical distribution
 e_2 = Factor to account for the variation of profile drag coefficient with lift coefficient
 $C_{L_{opt}}$ = Lift coefficient at $C_{D_{P_{min}}}$

It is expedient to include in the drag equation the term

$$(C_L - C_{L_{opt}})^2 \cdot (1 - e_2) / (\pi A e_2)$$

isolated from the other two terms, so that corrections may be made to the drag-due-to-lift when operation of the airplane changes from turbulent to laminar. It is undesirable to mask this effect by combining it with the induced drag due to the wing trailing vortices, which is represented by the second term in the drag polar.

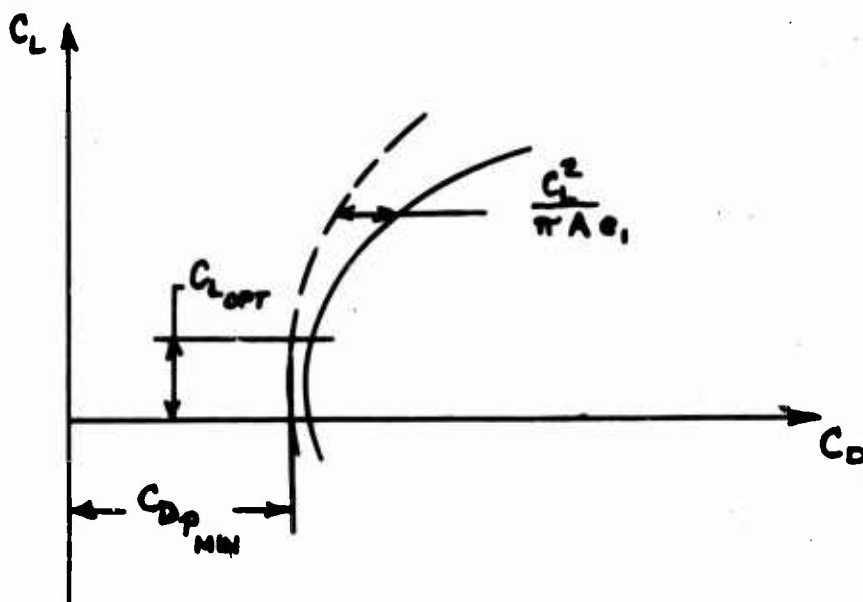
The procedure to determine the requisite turbulent drag coefficients and efficiency factors from wind tunnel data is the following: The drag coefficient for the wing alone is obtained by subtracting the body drag from wing-body drag at equal angles of attack.

Trimmed drag-lift polars are prepared in the usual manner by interpolating at equal angles of attack drag, lift and a horizontal stabilizer setting for the condition of zero pitching moment. Laminar flow control does not have an influence on the trim condition.

ENGINEER	NORTHROP CORPORATION NORAIR DIVISION	PAGE 12.04
CHECKER		REPORT NO. NOR 67-136
DATE June 1967		MODEL X-21A

The wing drag data obtained in the first step are then used to evaluate the efficiency factors. The efficiency factor e_1 relating the ideal induced drag to the actual induced drag of the wing is found from plotting C_{D_i} versus $C_L^2/\pi A$. The slope of the resulting line represents the magnitude of e_1 .

Next, the induced wing drag C_{D_i} is subtracted from the trimmed polar of the complete airplane. The difference represents a curve (dashed line in the sketch below) from which the values of $C_{D_{pmin}}$ and $C_{L_{opt}}$ are obtained.



Finally, the efficiency factor e_2 is determined as the slope of the line resulting from plotting the term $(C_D - C_{D_{pmin}} - C_L^2/\pi A e_1)$ against $(C_L - C_{L_{opt}})^2$.

12.4 DRAG REDUCTION DUE TO LAMINAR OPERATION

12.4.1 PARASITE DRAG

The parasite drag of an airplane operating under laminar flow conditions consists of:

ENGINEER	NORTHROP CORPORATION NORAIR DIVISION	PAGE 12.05
CHECKER		REPORT NO. NOR 67-136
DATE June 1967		MODEL X-21A

A. Wing drag, composed of:

1. Laminar wake drag (also referred to as laminar profile drag)
2. Turbulent drag of wedge shaped turbulent areas near wing-body and wing-nacelle intersections, and at the wing tip.

B. Turbulent drag of the fuselage, nacelles, etc. If the empennage is designed turbulent, it is included in item 12.4.1.2. If it is designed to incorporate laminar flow, it is included with the wing in item 12.4.1.1.

12.4.1.1 LAMINAR WAKE DRAG

This is defined, in the conventional manner, as the rate of decrease of the momentum of the air that passes over the wing.

$$C_{D_W} = C_{d_w} (S_{\text{wetted}})_{\text{laminar}} / S_{\text{wing}} \quad (\text{Eq. 2})$$

The section drag coefficient, C_{d_w} , is computed in connection with suction requirement calculations. This program is discussed elsewhere in this report. Figure 12.1 shows section drag coefficients as calculated by a computer program for the X-21A which are also suitable for use for other LFC aircraft.

12.4.1.2 TURBULENT WEDGE WING DRAG

There are certain areas of the wing where laminar flow is not expected. These areas are shown in Figure 12.2 and are noted below:

- a. Wing-fuselage intersection
- b. Wing-nacelle intersection
- c. Wing tip

The turbulent drag of these areas is determined from:

$$C_{D_T} = (MF) C_f (S_{\text{wetted}})_{\text{turbulent}} / S_{\text{wing}} \quad (\text{Eq. 3})$$

ENGINEER	NORTHROP CORPORATION NORAIR DIVISION	PAGE	12.06
CHECKER		REPORT NO.	NOR 67-136
DATE		MODEL	X-21A
June 1967			

where

C_f = skin friction coefficient for a turbulent flat plate

and

MF = factor to correct turbulent flat plate friction drag for non-zero pressure gradient

12.4.1.3 WAKE DRAG OF FUSELAGE, NACELLES, ETC.

The drag of the remaining aircraft components is determined in the conventional manner for fully turbulent flow.

The total minimum parasite drag is determined by the addition of the various components.

12.4.2 DRAG-DUE-TO-LIFT

Changing from turbulent to laminar flow conditions on the same wing changes not only the minimum profile drag but also the drag-due-to-lift. It was previously pointed out that the induced drag parabola is not affected since the span loading is unchanged. The efficiency factor e_2 used to express the variation of the profile drag with lift does change. It is established for a laminar airplane according to the following considerations:

For the range of angles of attack expected for laminar flow cruise, configuration trim drag changes; and the change in drag coefficient with angle of attack for fuselage, nacelles and empennage is negligible. The laminar wake drag of the wing is also virtually unaffected by a change of the angle of attack, α . However, the drag of the turbulent wedges does vary.

Thus, the efficiency factor e_2 for laminar flow conditions is derived by correcting the fully turbulent $CD_p / (C_L - C_{Lopt})^2$ by the ratio $S_{wadded\ turbulent} / S_{wadded\ total}$, following otherwise the procedure outlined in 12.3.

Finally, it should be pointed out that the drag-due-to-lift is subject to a change as the Reynolds number changes. If lift and drag coefficients vary with R_N , the efficiency factors also vary. Using this fact, the functional relationship between the e 's and Reynolds number can be established. Typical results for the X-21A are shown in Figure 12.3.

ENGINEER	NORTHROP CORPORATION NORAIR DIVISION	PAGE 12.07
CHECKER		REPORT NO. NOR 67-136
DATE June 1967		MODEL X-21A

12.5 EQUIVALENT SUCTION DRAG

If the external aerodynamic drag for a laminar airplane is computed as outlined in Section 12.4 and compared with the normal turbulent aircraft drag, an appreciable reduction is realized. This reduction is not obtained cost free because of the momentum losses of the suction air as it passes through the suction system. These losses must be restored in the process of pumping the air back to the free stream; but, depending upon the efficiency of the pumping process, varying amounts of energy can be used. To provide a numerical basis for computing pumping requirements and for comparing the "total" drag of an LFC system with an otherwise turbulent aircraft, the mathematical concept of "equivalent suction drag" has been adopted. Equivalent suction drag is defined as the hypothetical force equivalent of the power expenditure in restoring the boundary layer air from pumping compressor-face conditions of pressure, temperature and velocity to free stream pressure and velocity by an isentropic (frictionless) process. In the practical case, a process employing less than perfect efficiency is used, and the exhaust air may, by choice, be pumped to greater total energy than ambient. "Total LFC suction drag" is defined as the sum of laminar suction wake drag plus equivalent suction drag. Figure 12.4 shows the relative magnitudes of wake drag, equivalent suction drag and total drag, together with their variation with suction quantity coefficient, C_Q , for a 30° swept suction wind tunnel model.

In the calculations for aircraft performance, equivalent suction drag, as such, is not used. Rather, the conventional procedure is followed with fuel flow to the suction system added to the fuel flow of the propulsion system to obtain total aircraft fuel flow, and air bleed from the propulsion system to the suction system causing a change in main-engine propulsion system efficiency. This new fuel flow and efficiency are then used in the usual manner.

The equation for equivalent suction drag is:

$$C_{D_s} = \left[W_{s_2} J C_{P_h} / q_o S V_o \right] \left[T_2 (P_o / P_2)^{\frac{\gamma-1}{\gamma}} - t_o \right] \quad (\text{Eq. 4})$$

The variation of the equivalent suction drag with lift has been found to be very small for a symmetrical airfoil, and was negligible for the cambered airfoil used on the X-21A.

12.6 LIFT COEFFICIENT LIMITATIONS

There are limits to the wing lift coefficient above which laminar flow cannot be maintained through LFC without special regions of very high suction and without appreciable penalty to the suction system power required. Depending on the flight conditions, the limits are manifested in the following three criteria:

ENGINEER	NORTHROP CORPORATION NORAIR DIVISION	PAGE 12.08
CHECKER		REPORT NO. NOR 67-136
DATE June 1967		MODEL X-21A

1. $M_{local} > 1.04$ (component normal to wing element lines),
2. incipient laminar boundary layer separation,
3. surface pressures below minimum suction pressure.

The first and second criteria arise from the inability of the LFC system as designed to impede laminar boundary layer separation under strong adverse pressure gradients. The third criterion is associated with the limited suction pressure potential of the compressor system used.

The object of the local Mach number criterion is to exclude conditions of shock-induced boundary layer transition. The C_L versus M_{local} relationship, which can be determined from pressure distribution measurements, establishes upper lift coefficient limits as a function of free stream Mach number.

The second criterion, incipient laminar boundary layer separation, marks the low speed-low altitude limitation for laminar flow of the suction surface as designed. It is associated with relatively modest C_L -values and should not be confused with incipient wing stall. Turbulent boundary layers have the ability to pass through regions of much higher adverse pressure gradients and as such promote the attainment of high C_L -values essential for take-off and landing.

For conditions of turbulent flow at the higher C_L -values, the polar curve can be approximated by the equation:

$$C_D = C_{D(C_L \text{ limit})} + (C_L^2 - C_{L \text{ limit}}^2) / \pi A e_3 \quad (\text{Eq. 5})$$

where

e_3 = factor to account for the deviation of the drag polar from the initial parabola.

For the X-21A, the upper lift coefficient limit was initially estimated to be 0.4. Figure 12.5 shows the trimmed drag polar as estimated prior to flight test at $M = .70$, with the effect of lift coefficient limitation also shown. It was found during flight testing that the lift coefficient limit of 0.4 could be exceeded and full-chord laminar flow could be obtained on the outboard wing.

The suction drag values included in Figures 12.5 and 12.6 are computed from Equation 4, assuming a pressure drop of $.05 q_0$ through the outer skin and adding a constant $.0005$ to account for additional losses in the suction system, in accordance with Reference 2.

ENGINEER	NORTHROP CORPORATION NORAIR DIVISION	PAGE 12.09
CHECKER		REPORT NO. NOR 67-136
DATE June 1967		MODEL X-21A

The critical Mach number of 1.04 also is a conservative value and has been exceeded occasionally in flight testing. The initial limit lift coefficient of 1.4 and the critical Mach number of 1.0 used to establish it are considered reasonable values for the design of the laminar airplane.

12.7 AIRPLANE DRAG

The drag of a turbulent aircraft can be broken down into wing friction drag, drags of the fuselage, empennage and nacelles, and drag-due-to-lift. As was previously discussed, laminar flow control primarily reduces the wing friction drag, but it also yields a slight reduction of the section drag-due-to-lift. Both appear as reductions in the wake drag of the wing. There is an additional drag item, equivalent suction drag, which needs only be considered in computing certain comparative performance parameters, such as the lift/drag ratio.

Figure 12.6 is included to show the comparison of laminar and turbulent drag as estimated for the wing and the total airplane to illustrate the effect of full-chord laminar flow on the X-21A.

Figure 12.7 is a comparison of turbulent section drags for the X-21A as predicted by Eq. 3 and as determined from boundary layer rake flight test data by means of the compressible flow method (Reference 1). The good agreement evinces the reliability of the prediction method.

In order to verify the drag of an LFC wing by spanwise integration of measured suction drags, a method was developed to utilize the numerous single-tube boundary layer probes at the trailing edge of the X-21A as section drag indicators. Section drags at a few spanwise stations were determined (for various chordwise transition locations) from boundary layer rake data and correlated with the wake pressure at the height of 1/4 inch above the surface, which corresponded to the vertical position of the single-tube probes.

Figures 12.8 and 12.9 show spanwise pressure distributions for the left wing, upper and lower surfaces, of one particular flight, which were determined by the method described above.

12.8 REFERENCES

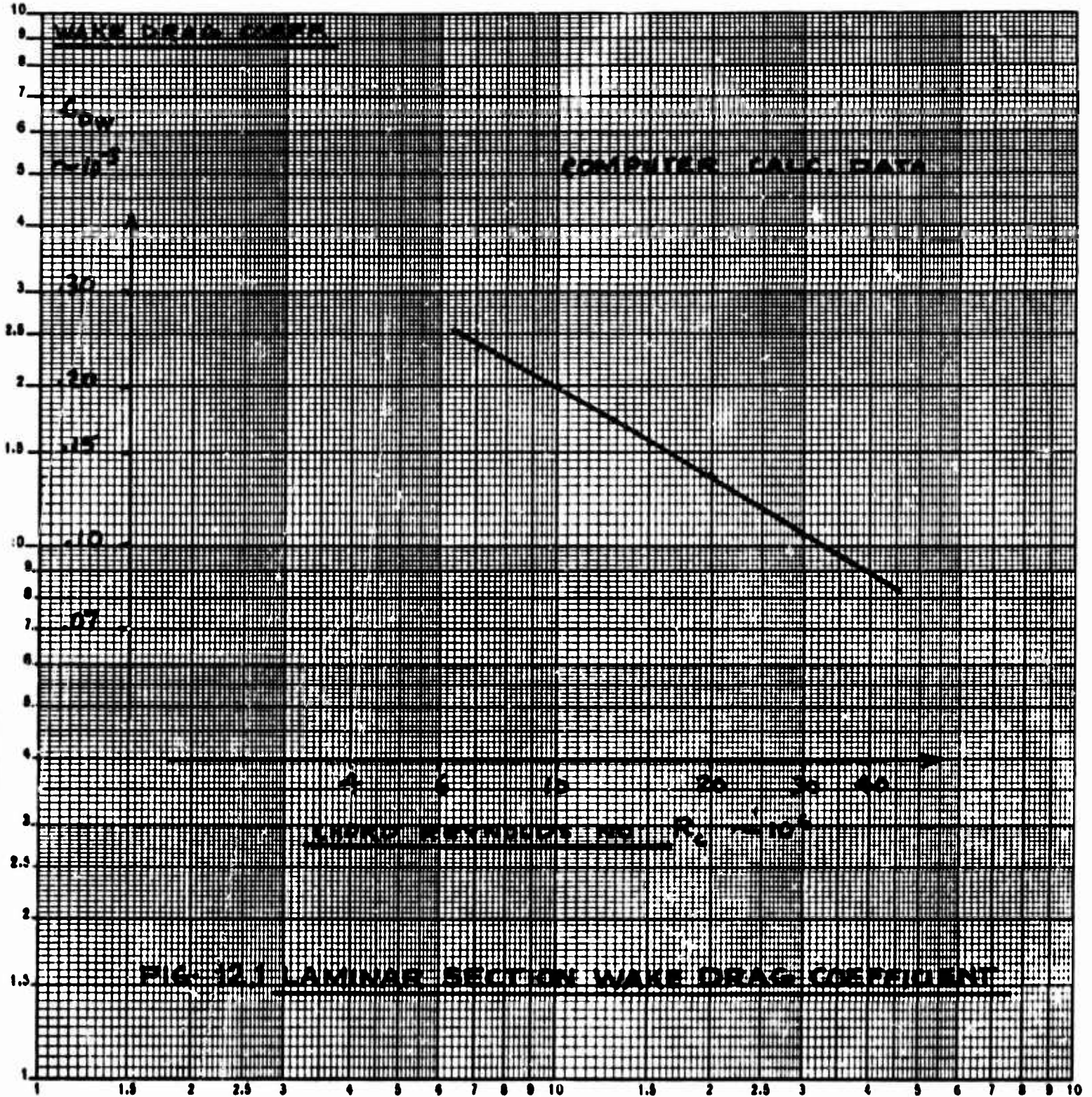
1. Chang, Chieh-Chien, "A Simplified Method of Obtaining Drag of a High Speed Body from Wake Surveys," Journal of the Aeronautical Sciences, February 1948.
2. Klabunde, W. A., "Aerodynamic Drag of NB-66 Aircraft," Report NOR 61-126, 1961.

12.10

NOR 67-136

X-21A

June 1967



ENGINEER	NORTHROP CORPORATION NORAIR DIVISION	PAGE 12.11
CHECKER		REPORT NO. NOR 67-136
DATE June 1967		MODEL X-21A

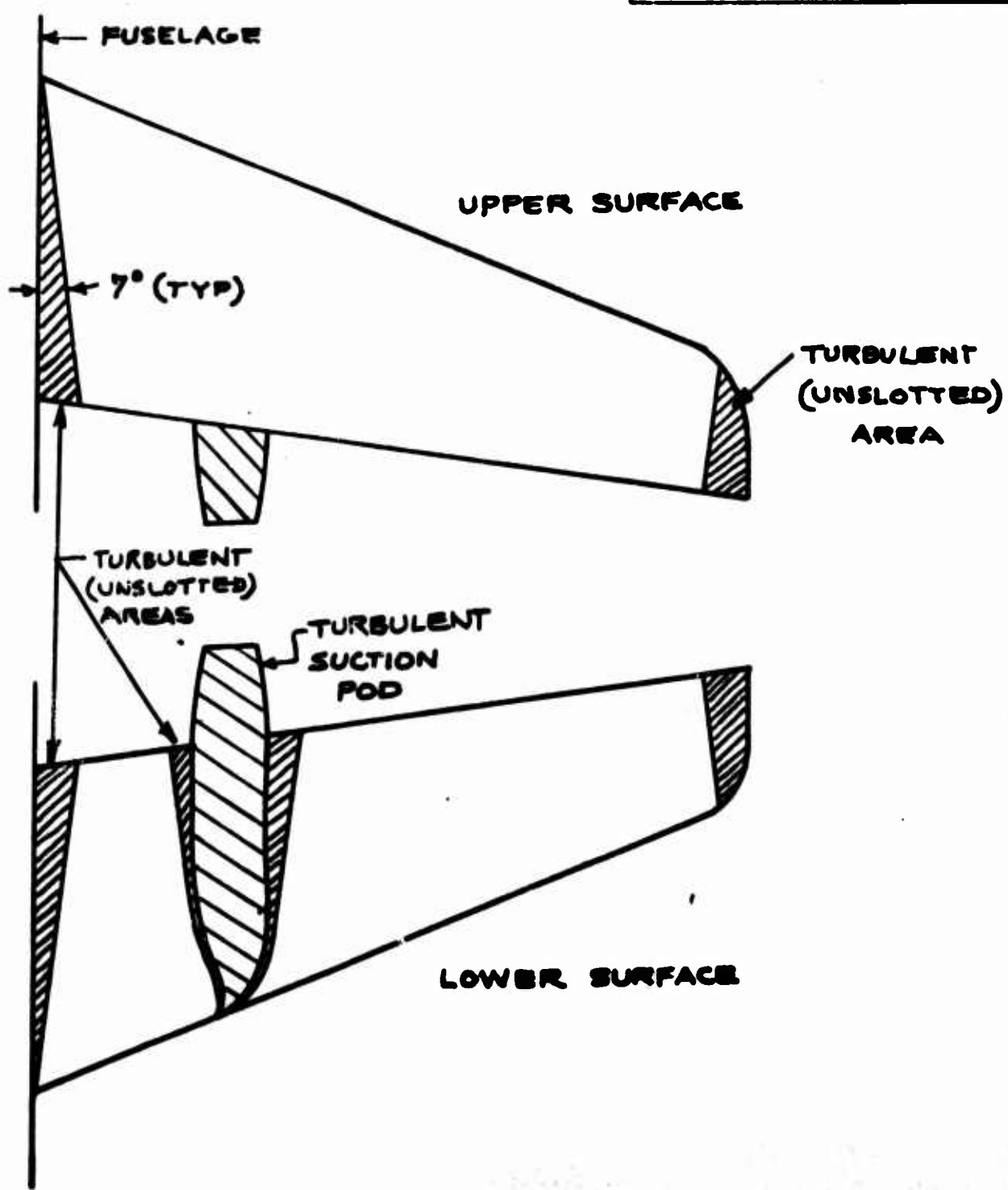


FIG 12.2 **WING NON-LAMINAR AREAS**

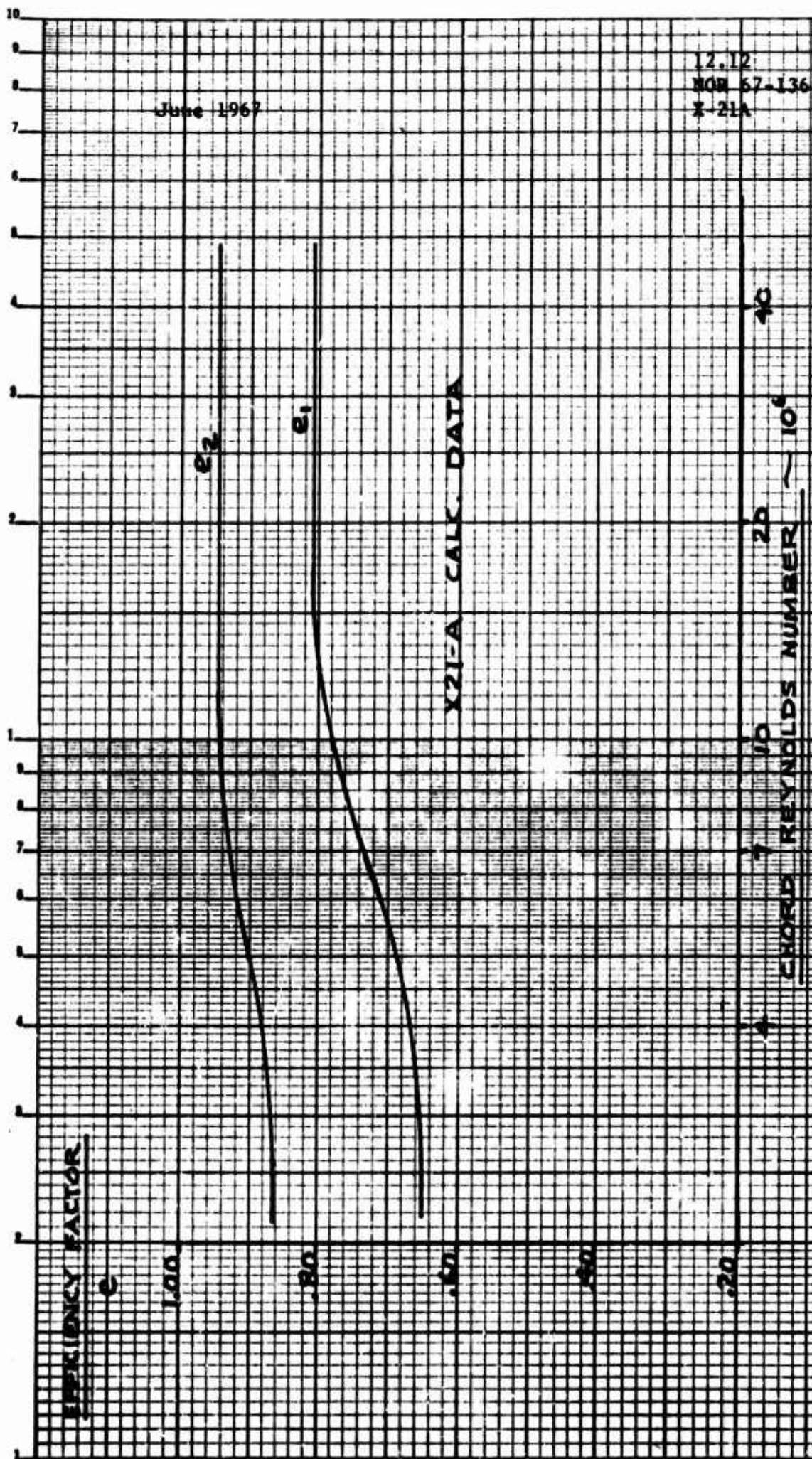


FIG 12.3 EFFICIENCY FACTORS e_1 AND e_2 VS REYNOLDS NO.

ENGINEER	NORTHROP CORPORATION NORAIR DIVISION	PAGE 12.13
CHECKER		REPORT NO. NOR 67-136
DATE June 1967		MODEL X-21A

DRAG COEFFICIENT

$C_D \sim 10^{-4}$

$R_e = 19.9 (10^6) = \text{CHORD REYNOLDS NO.}$
 $30^\circ \text{ SWEPT W.T. MODEL LFC WING}$

8

6

4

2

0

TOTAL

SUCTION

WAKE

3.2

3.6

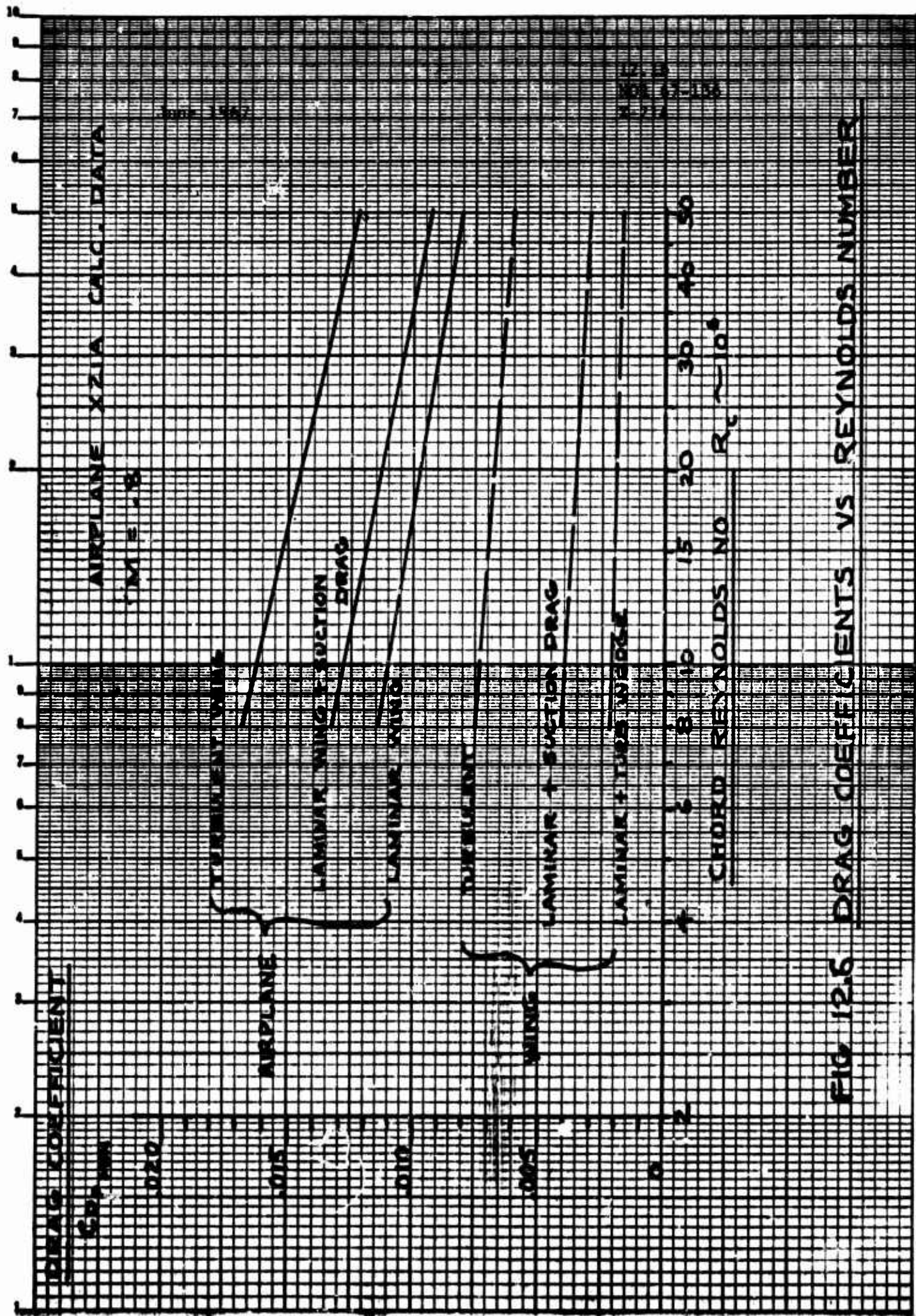
4.0

4.4

4.8

FLOW COEFFICIENT $C_Q \sim 10^{-4}$

FIG 12.4 DRAG COEFFICIENTS vs SUCTION



ENGINEER	NORTHROP CORPORATION NORAIR DIVISION	PAGE 12.16
CHECKER		REPORT NO. NOR 67-136
DATE June 1967		MODEL X-21A

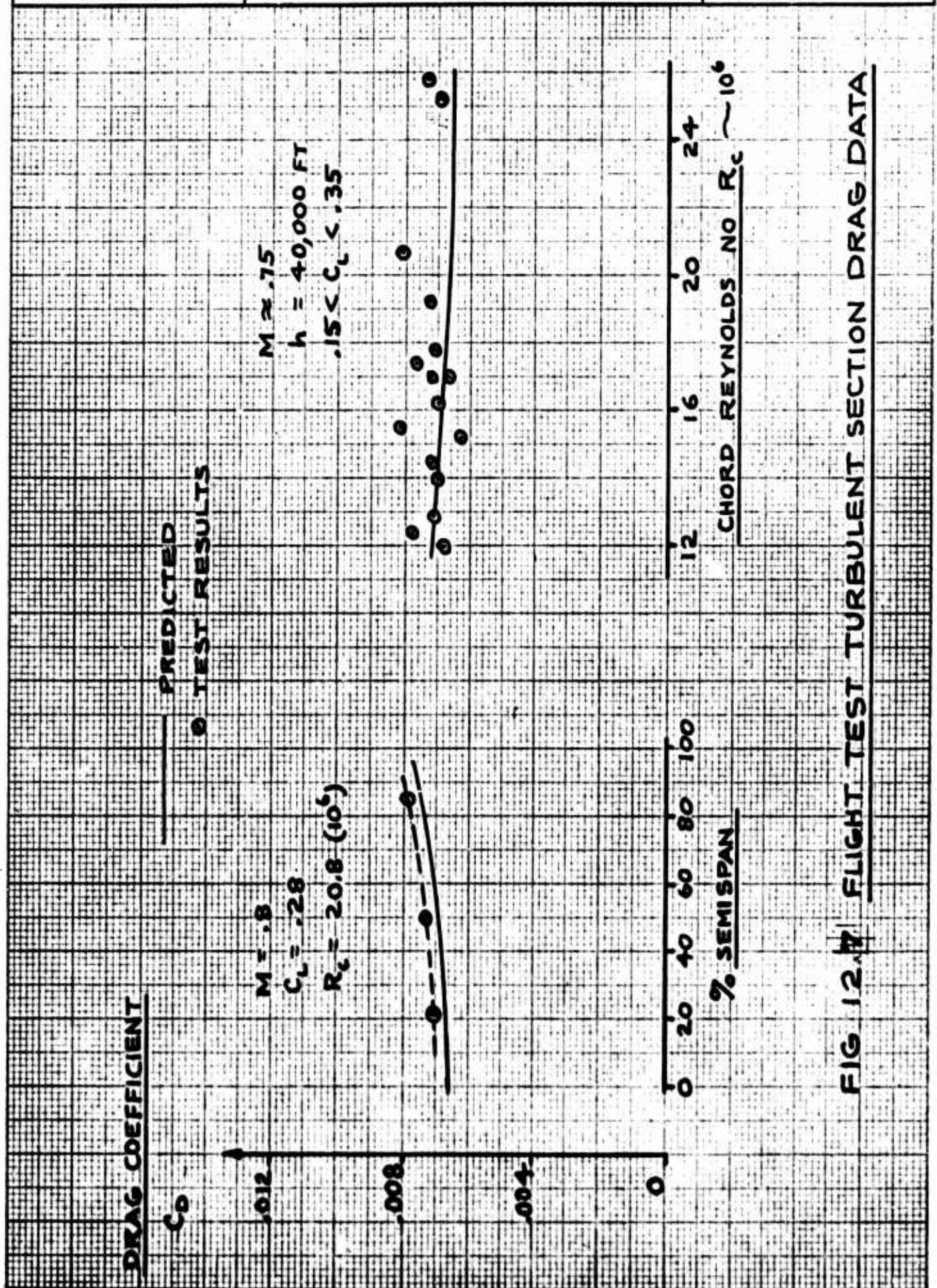


FIG 12.17 FLIGHT TEST TURBULENT SECTION DRAG DATA

ENGINEER	NORTHROP CORPORATION NORAIR DIVISION	PAGE 12.17
CHECKER		REPORT NO. NOR 67-136
DATE June 1967		MODEL X-21A

AIRPLANE AF 55-410
FLIGHT 120 RUN 3
UPPER SURFACE
L.H. WING
M = .75 h = 40,110 FT
PROBE HT = .25 IN AT T.E.

WAKE
DRAG
COEFFICIENT

$C_{D\text{ WAKE}}$

AVERAGE $C_{D\text{ WAKE}} = .0012$



FIG 12.3 WAKE DRAG COEFFICIENT VS SPAN
UPPER SURFACE

ENGINEER	NORTHROP CORPORATION NORAIR DIVISION	PAGE 12.18
CHECKER		REPORT NO. NOR 67-136
DATE June 1967		MODEL X-21A

AIRPLANE AF55-410
FLIGHT 120 RUN 3
LOWER SURFACE
L.H. WING
M = .75 h = 40,110 FT
PROBE HT = .25 IN AT L.E.

WAKE
DRAG
COEFFICIENT

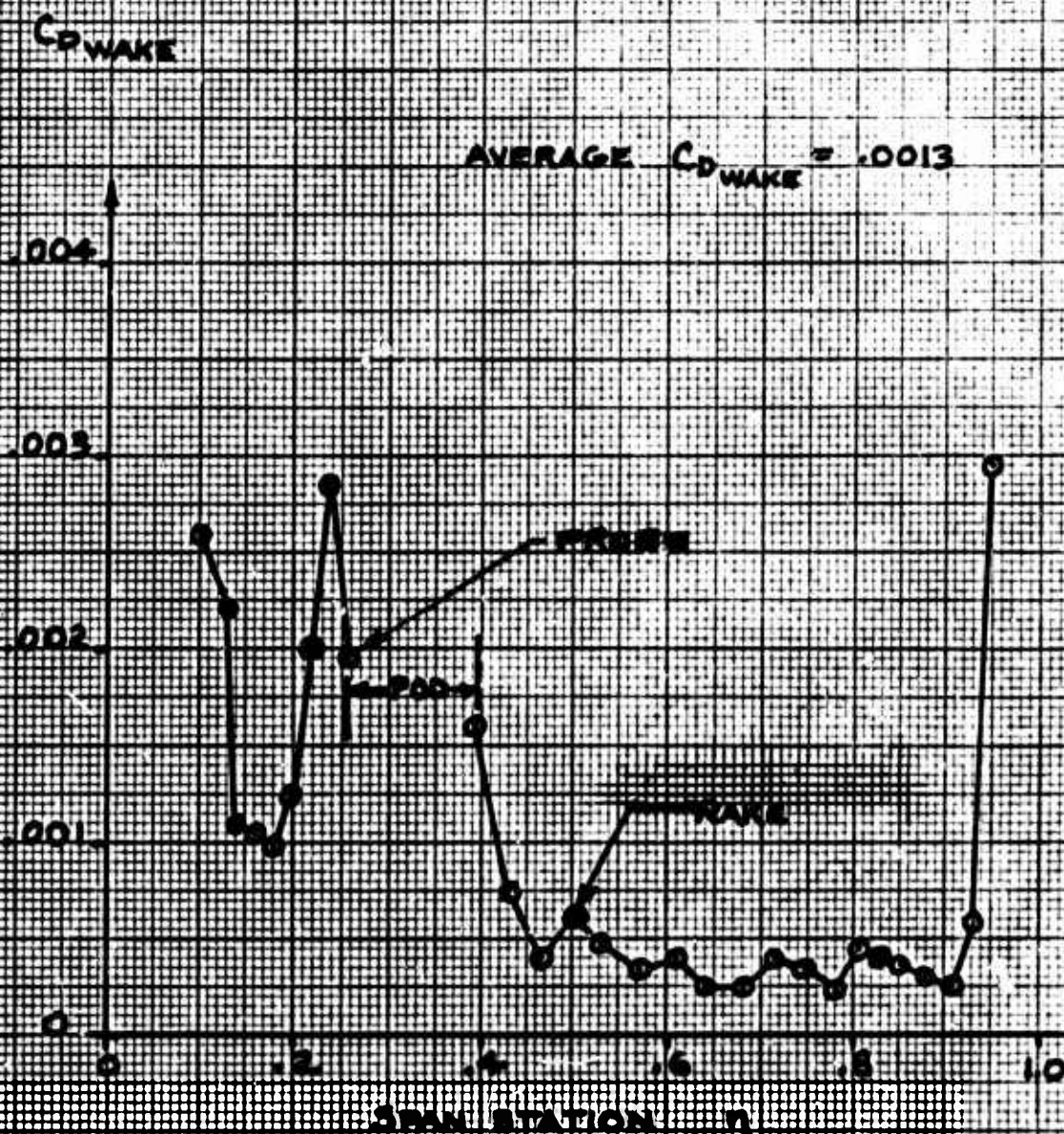


FIG 12.5 - WAKE DRAG COEFFICIENT VS SPAN
- LOWER SURFACE

ENGINEER	NORTHROP CORPORATION NORAIR DIVISION	PAGE 13.00
CHECKER		REPORT NO. NOR 67-136
DATE June 1967		MODEL X-21A

SECTION 13

DESIGNING FOR SATISFACTORY FLYING QUALITIES
ON AN LFC AIRCRAFT

By

J. C. Carlson

March, 1964
Revised April, 1967

ENGINEER	NORTHROP CORPORATION NORAIR DIVISION	PAGE 13.01
CHECKER		REPORT NO. NOR 67-136
DATE June 1967		MODEL X-21A

13.1 SUMMARY

Based on present day state-of-the-art design of laminar flow control systems, the LFC airplane is restricted to large and heavy aircraft and should be designed for satisfactory flying qualities accordingly. Since the LFC system design is based on wing surface pressures, retention of a laminar boundary layer associated with rapid changes in surface pressures during maneuvers is beyond the capability of the suction system, although laminar flow has been demonstrated during gradual steady turns, including entry and return to level flight, on the X-21A aircraft.

Specific areas of design which tend to be different from those of the typical turbulent high subsonic speed heavy jet aircraft are:

1. Larger design wing area - The reduction in friction drag results in an increase in wing span for the optimum wing configuration for the same take-off gross weight as the turbulent airplane.
2. Narrow chord ailerons - Although the ailerons may be slotted to obtain laminar flow for moderate deflections, the narrow chord results in a minimum of interference with laminar flow over the wing.
3. Avoidance of longitudinal instability region for swept-back wings at high angles of attack - Leading edge flaps and chordwise fences may be incompatible with LFC criteria due to leading edge smoothness. The laminar area requirements may necessitate the use of an angle of attack sensor connected to a suitable pilot warning system to avoid pitch-up.
4. Longitudinal and lateral-directional damping - It is anticipated that both longitudinal and lateral-directional artificial damping devices will be required to maintain the steady flight condition necessary for continuous laminar flow during cruise for swept wing design. Final airframe-autopilot compatibility with laminar flow should be determined by flight testing, as is normal new-airframe practice.

Analysis of wind tunnel and X-21A flight test data has shown the trim changes due to leading edge slot outflow and/or sudden loss of laminar flow to be small.

13.2 INTRODUCTION

In designing an LFC aircraft for satisfactory flying qualities, the question arises as to what influence laminar flow over the wing has on aircraft controllability. In addition the effect of sudden loss of laminar flow on either one or both wings raises questions concerning sudden pitching, yawing, and rolling moments associated with the thickening of the boundary layer when transition to turbulent flow occurs.

ENGINEER	NORTHROP CORPORATION NORAIR DIVISION	PAGE 13.02
CHECKER		REPORT NO. NOR 67-136
DATE June 1967		MODEL X-21A

Due to the many slots needed for laminar flow control, several slots have common internal ducts. With large pressure gradients existing on the wing surface near the leading edge, flow will occur from regions of high pressure to regions of low pressure when the suction system is inoperative, resulting in outflow near the wing leading edge.

This report presents the results of studies undertaken to determine the effects mentioned above on aircraft flying qualities as well as suggested solutions to problems not common to conventional turbulent aircraft. Results from the X-21A flight test program are presented where applicable.

13.3 SYMBOLS AND NOMENCLATURE

- a_{∞} Free stream speed of sound, ft/sec.
- b Wing span, ft.
- c Wing chord in the flight direction, ft.
- \bar{c} Wing mean aerodynamic chord in the flight direction, ft.
- $.25\bar{c}$ Quarter chord of wing mean aerodynamic chord, ft.
- L Airplane lift, lbs, $L = C_L q_{\infty} S$
- m Airplane pitching moment, ft-lbs.
- M_{∞} Free stream Mach number, $M_{\infty} = U_{\infty} / a_{\infty}$
- n Load factor, $n = L/W$
- p Static pressure, lb/ft²
- p_{∞} Free stream static pressure, lb/ft²
- q_{∞} Free stream dynamic pressure, lb/ft², $q_{\infty} = .7 p_{\infty} M_{\infty}^2$
- Re/ft Reynolds number per foot, $Re/ft = (U_{\infty} \rho / \mu)_{\infty}$
- S Wing area, ft²
- U_{∞} Free stream velocity, ft/sec
- W Airplane weight, lbs
- x Distance from the wing leading edge in the chord plane, ft.

ENGINEER	NORTHROP CORPORATION NORAIR DIVISION	PAGE 13.03
CHECKER		REPORT NO. NOR-67-136
DATE June 1967		MODEL X-21A

- C_L Lift coefficient, $C_L = L/q_\infty S$
- C_m Pitching moment coefficient, $C_m = m/q_\infty S \bar{c}$
- C_p Pressure coefficient, $C_p = (p - p_\infty)/q_\infty$
- C_{L_α} Change in lift coefficient per unit change in α , per degree
- C_{m_α} Change in pitching moment coefficient per unit change in α , per degree
- α Angle of attack of the zero lift line of the airplane, degrees
- α_{FRL} Angle of attack of the fuselage reference line, degrees
- ν_∞ Free stream kinematic viscosity, ft^2/sec

13.4 TEST REQUIREMENTS AND ANALYSIS OF RESULTS

In order to establish the aerodynamic data necessary for evaluating aircraft flying qualities, a conventional series of high and low speed wind tunnel tests employing a scale model is necessary covering the design Mach number and lift coefficient envelopes of the aircraft. The data to be obtained are identical to those for any conventional aircraft, i.e., longitudinal, lateral and directional characteristics and the effect of basic and auxiliary control surfaces. Conventional estimating techniques are adequate for determining the rotary derivatives from the static data.

As LFC wings in general will not employ standard NACA wing sections, high Reynolds number tests are required to establish airplane maximum lift coefficient and longitudinal stability characteristics at high lift. The longitudinal stability characteristics at high angles of attack for the case of a swept tapered wing are especially critical due to possible premature flow separation at the wing tip and subsequent airplane pitch-up as a result of the large center of pressure shift. Reference 1 has correlated combinations of wing sweep, aspect ratio and taper ratio to a longitudinal stability boundary. Large high subsonic speed aircraft wings tend to optimize for maximum range along this stability boundary and only high Reynolds number tests will adequately define these stability characteristics. Figure 13.1 shows the effect of Reynolds number on pitching moment and lift for an X-21A .06 scale model tested in Ames 12 foot pressure wind tunnel.

Utilizing a conventional atmospheric low speed wind tunnel at speeds greater than landing speeds in an attempt to increase the test Reynolds number can lead to erroneous results due to the large wing suction pressure peak encountered at high angles of attack. The large velocity associated with

ENGINEER	NORTHROP CORPORATION NORAIR DIVISION	PAGE 13.04
CHECKER		REPORT NO. NOR-67-136
DATE June 1967		MODEL X-21A

this negative pressure might exceed sonic velocity with a resultant shock as the flow decelerates back to a subsonic velocity, completely clouding the effects of the increased Reynolds number.

If the high Reynolds number tests indicate the airplane has an unstable pitching moment break at high angles of attack, the airplane must be equipped with a suitable device to warn the pilot, such as an angle of attack vane sensor connected to an audio warning or stick shaker. This device must provide an adequate margin of safety due to the inherent danger of encountering a gust during operation at high angles of attack. Figure 13.2 shows the programmed stall warning angle of attack versus Mach number for the X-21A airplane as well as the wind tunnel determined angle of attack for neutral stability at an airplane center of gravity of .25c. This system has been proven reliable during the flight test program of the X-21A.

The present surface smoothness requirements for manufacture of the wing leading edge make difficult the use of leading edge flaps which have been shown to alleviate the unstable pitching moment break. The use of chordwise fences to prevent the strong spanwise flow out towards the wing tips may not be desirable due to the added turbulent wetted area of the fence and the chordwise turbulent wedge.

Analog studies utilizing the X-21A aerodynamic characteristics at high angles of attack have indicated that once pitch acceleration attains a certain value, corrective longitudinal control inputs by the pilot are too late to prevent the airplane from attaining large pitch angles. Figure 13.3 shows some typical analog time histories of X-21A airplane flight characteristics during pitch-up for an initial velocity of 200 ft/sec. It can be seen that full down elevator could not prevent the airplane from rotating to $\alpha \approx 29^\circ$.

A slotted two-dimensional swept wing wind tunnel model was used to evaluate: (1) the effects of outflow through the leading edge slots on the wing stall characteristics and (2) the effect of complete loss of suction on the wing lift and moment. Figure 13.4 presents the results of the slot outflow study at high angles of attack and shows there is essentially no change in the wing pressure distribution indicating no lift or moment changes as a result of leading edge slot outflow.

Measurement of wing surface pressures was made for full chord laminar flow and for fully turbulent flow. The results presented in Figure 13.5 show that the change in boundary layer thickness does not affect the wing surface pressures appreciably. Therefore, no lift or pitching moment changes will occur during sudden loss of laminar flow. Since no lift change occurs, the wing downwash will remain constant and no change in effective tail angle of attack will result. The thickening of the boundary layer will cause a small reduction in effective dynamic pressure in the wake, which may be in

ENGINEER	NORTHROP CORPORATION NORAIR DIVISION	PAGE 13.05
CHECKER		REPORT NO. NOR 67-136
DATE June 1967		MODEL X-21A

the vicinity of the horizontal tail, but this is believed to be negligible as the wing is designed to be much smoother than a conventional turbulent wing and will, therefore, have a thinner turbulent boundary layer. Reference 2 presents the results of an Australian wind tunnel test evaluating blowing out of leading edge slots, and the results are consistent with Norair findings.

No steady state control nor trim problems are generated in the extreme (and hypothetical) case of complete loss of laminar flow on one wing. The unequal friction drag results in first a yawing and then a rolling moment. A calculated case for the X-21A at 0.80 Mach number, 40,000 ft. altitude, showed that the resulting yawing moment could be balanced by approximately 4.5° of rudder. A flight test record shows a maximum angle of roll of about 2 degrees following shutdown of the right wing suction system on the X-21A airplane.

Swept wing aircraft operating at high altitudes are very susceptible to lateral-directional oscillations so that these aircraft normally employ artificial damping devices to meet flying quality specifications. The yawing motion due to a disturbance will change the effective sweep angle of both the advancing and trailing wing which will change the crossflow component of the boundary layer. Since the suction quantity necessary for laminar flow is a function of the sweep angle, the possibility of losing laminar flow on the wing which trails exists particularly if the suction setting is the minimum required for a given sweep angle. The increased drag would tend to aggravate the yawing motion by decreasing the effective yaw damping.

The long period longitudinal mode requires close examination also. The dominant damping term is normally the airplane drag, but as this term becomes smaller for a laminar flow airplane, the motion can become divergent to the point where pilot fatigue becomes a problem. Furthermore, the constant variation of speed and altitude changes the flight Reynolds number which in turn influences the boundary layer.

Based on the above statements, artificial damping of both the Dutch-roll and the Phugoid modes is desirable for cruise operation of swept laminar flow control aircraft. It is expected that a flight test program will be necessary to uncover any problems which might exist between airplane dynamic characteristics and boundary layer stability.

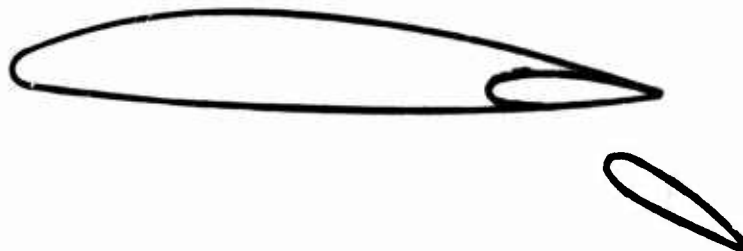
No problems are anticipated for aileron design for adequate roll control. The basic wing structure to house internal ducting is sufficiently rigid that aileron reversal speeds occur outside of the operating envelope of the airplane. The aileron hinge line should be close to the upper surface mold line, which will minimize the upper surface gap and surface discontinuity,

ENGINEER	NORTHROP CORPORATION NORAIR DIVISION	PAGE 13.06
CHECKER		REPORT NO. NOR-67-136
DATE June 1967		MODEL X-21A

even with ailerons deflected several degrees. Suction slots should be considered for the ailerons as laminar flow can be maintained across the ailerons for small deflections. Figure 15.6 shows the results of a specific flight of the X-21A airplane where laminar flow was maintained across the aileron hinge. Total pressure probes installed at the wing trailing edge were used to determine whether laminar or turbulent flow conditions existed.

To meet take-off and landing requirements, the LFC aircraft may require flaps. Plain flaps are desirable if the required maximum lift coefficient can be obtained since the flap hinge line can be designed similar to that for the ailerons insuring a smooth surface when the flaps are closed. Even more important are the internal duct design features necessary to provide for inflow through the flap surface when in the closed position for maintenance of laminar flow. For a plain flap, a bellows can be used to duct the flow from the flap area forward into the main wing structure. If take-off and/or landing requirements dictate a more sophisticated flap system, i.e., slotted, Fowler, etc., where actual slots appear between wing and flap when the flap is deflected, consideration should be given to not providing for laminar flow on the flap surfaces. Since flap complexity increases cost, careful analysis should be made comparing laminar area lost against reduced suction requirements and lower initial costs. Preliminary design studies made by Norair indicate each case must be evaluated separately depending upon mission requirements, type of engines available, etc. A factor of prime importance is that the drag of the turbulent area is greater than that computed by applying the turbulent wing friction drag coefficient to the flap area. This is due to two factors: (1) the friction drag coefficient must be based on the length Reynolds number on the flap and (2) the flap is in the adverse pressure gradient region of the wing where the turbulent boundary layer is thicker.

The application of suction or blowing near the leading edge of a plain flap offers a possible solution to obtaining design maximum lift coefficient without sacrificing possible wing laminar area. Since the compressor units would already be available, it appears that high lift boundary layer control could be obtained at little additional cost. Another solution is a flap similar to the one shown in the sketch. This allows essentially full-chord laminar flow on at least the upper surface with no intervening hinge line.



ENGINEER	NORTHROP CORPORATION NORAIR DIVISION	PAGE 13.07
CHECKER		REPORT NO. NOR 67-136
DATE June 1967		MODEL X-21A

It is expected that laminar flow control can be applied to the horizontal and vertical tail for use during the cruise portion of flight. There is no reason to assume that sudden loss of laminar flow over any portion of the empennage will result in more than a small out-of-trim condition.

13.5 CONCLUSIONS

Results of low speed wind tunnel tests utilizing a slotted two-dimensional swept wing model have shown that neither leading edge slot outflow or sudden loss of laminar flow will cause control problems on an LFC aircraft.

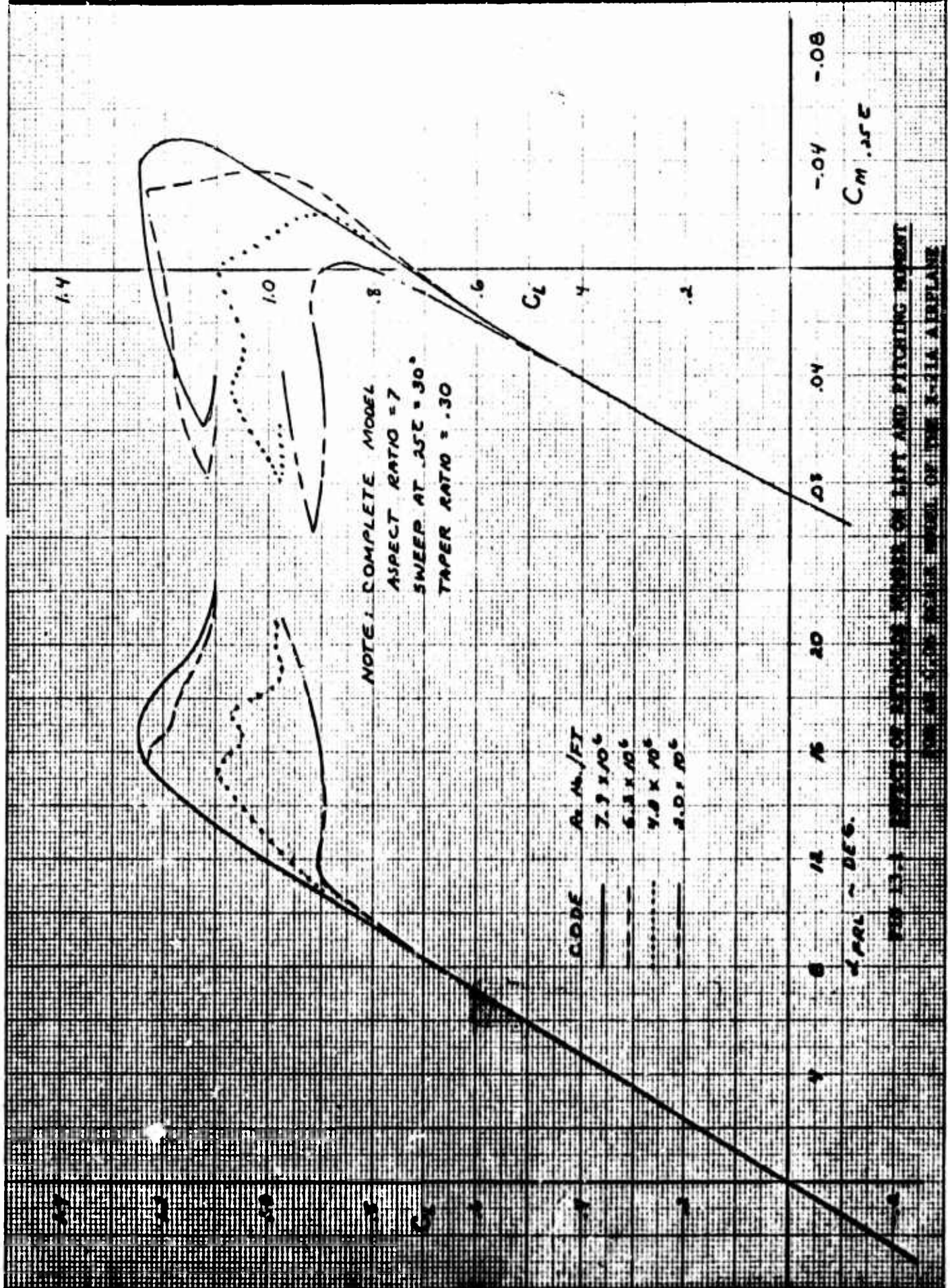
The unstable pitching moment associated with certain combinations of sweep, aspect ratio and taper ratio at high angles of attack possibly cannot be eliminated by conventional methods due to LFC requirements, necessitating visual indication and audio warning to the pilot of approach to the pitch up region. LFC aircraft will not be designed for large maneuvering load factors and in general will not be operated near the pitch-up region except in the landing condition.

It appears that the lateral-directional and long period longitudinal dynamic motions may require more stringent artificial damping than the minimum considered acceptable by pilots for turbulent heavy aircraft during cruise operation. This can only be determined during flight testing by flying typical missions. The period of both motions is of sufficient duration that pilot corrective action can be applied and, therefore, the airplane dynamics do not present a danger to flight safety.

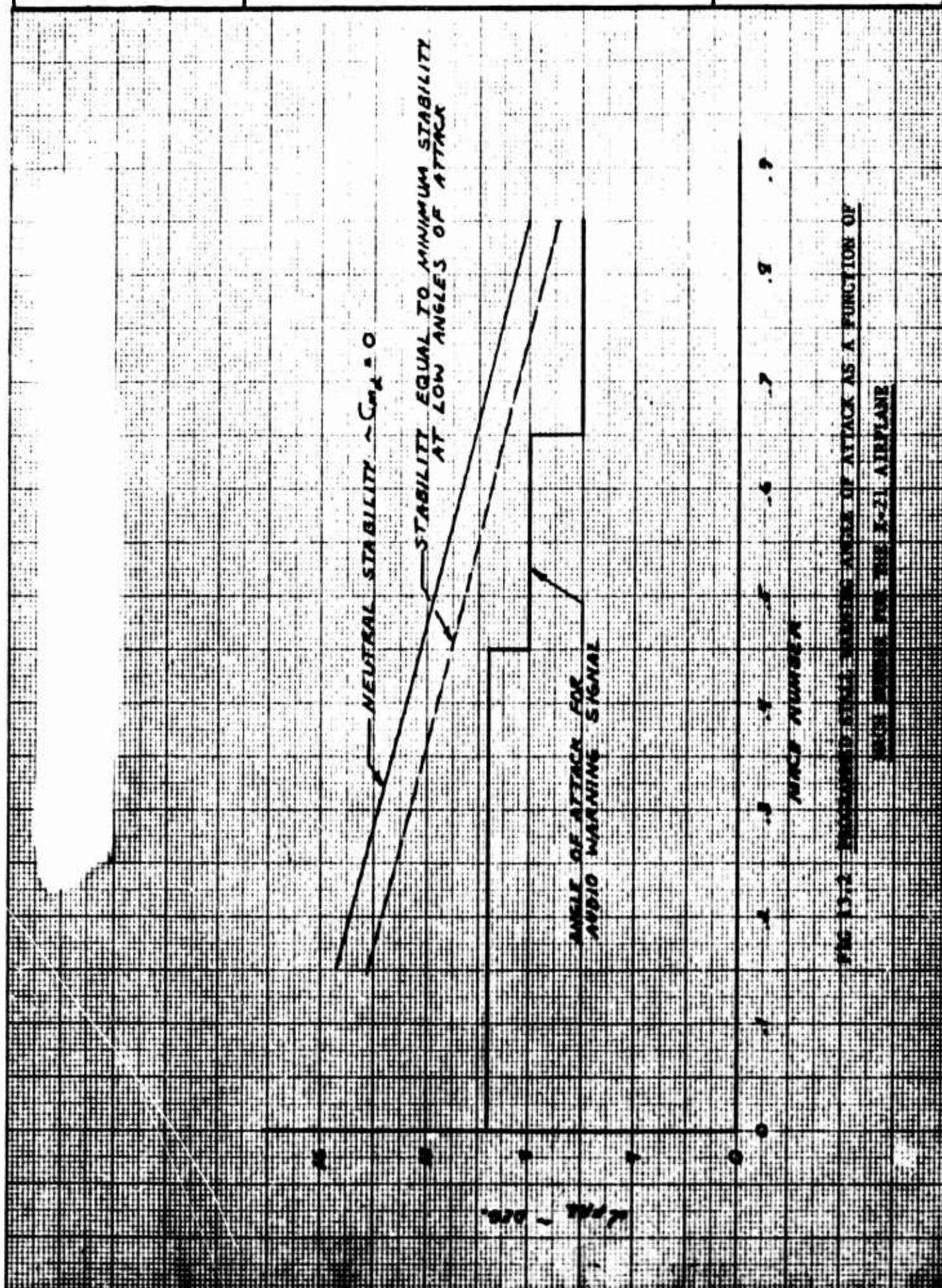
13.6 REFERENCES

1. NACA TR-1339, "A Summary and Analysis of the Low Speed Longitudinal Characteristics of Swept Wings at High Reynolds Number," by G. Furlong and J. McHugh, 1957.
2. The Australian Department of Supply, Research and Development Branch, Aeronautical Research Laboratories Note A.R.F./F25, "Low Speed Tests of an Airbrake Using Low Pressure Air Ejected through Spanwise Slots," by R. S. Trayford, August 1956.

ENGINEER	NORTHROP CORPORATION NORAIR DIVISION	PAGE 13.08
CHECKER		REPORT NO. NOR 67-136
DATE June 1967		MODEL X-21A



ENGINEER	NORTHROP CORPORATION NORAIR DIVISION	PAGE 13.09
CHECKER		REPORT NO. NOR 67-136
DATE June 1967		MODEL X-21A



ENGINEER	NORTHROP CORPORATION NORAIR DIVISION	PAGE 13.10
CHECKER		REPORT NO. NOR 67-136
DATE June 1967		MODEL X-21A

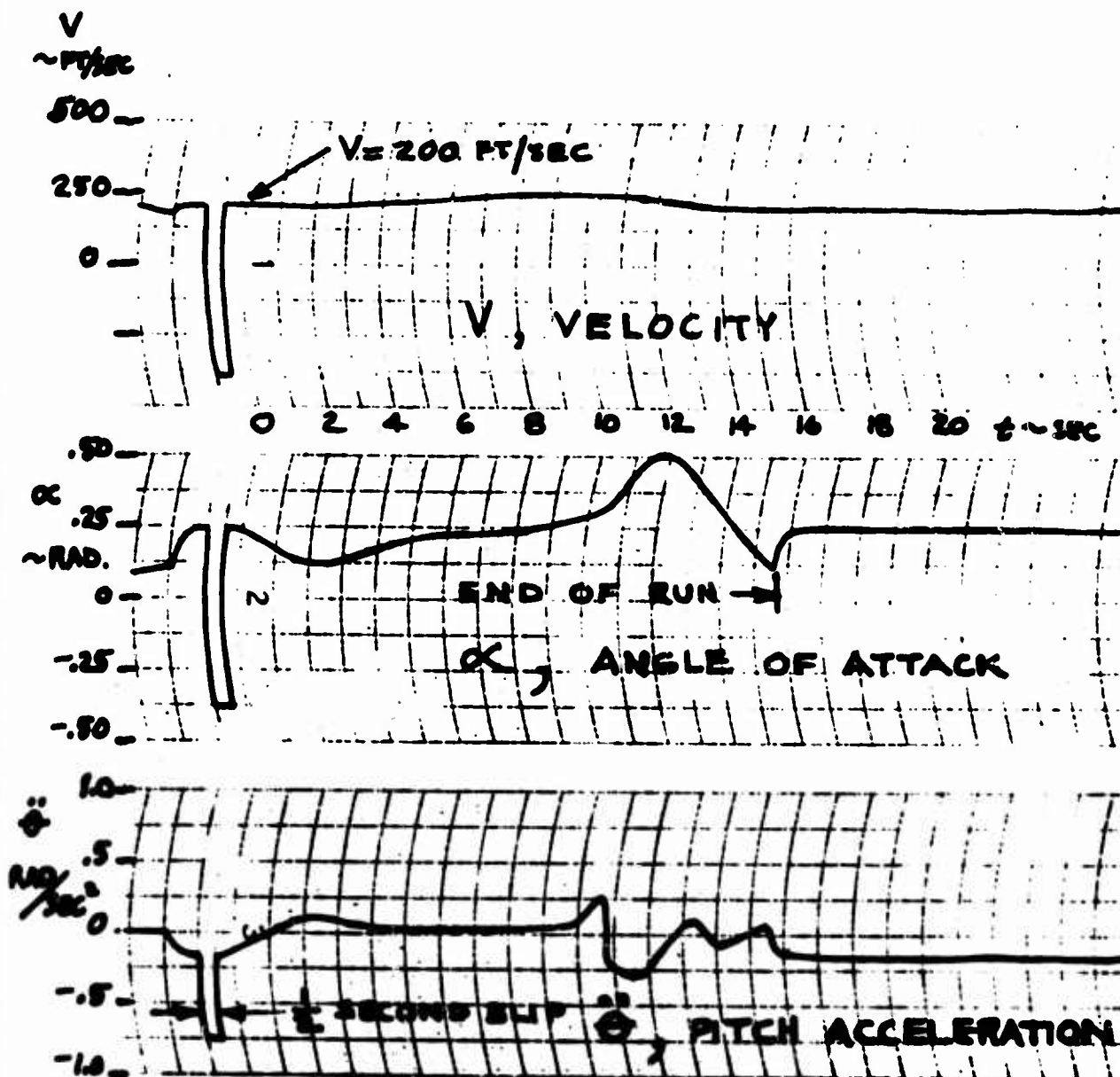


FIG 13.3A ANALOG TIME HISTORY OF X-21A PITCH-UP UTILIZING WIND TUNNEL DATA
— V, α , AND $\ddot{\theta}$ VS. TIME

ENGINEER	NORTHROP CORPORATION NORAIR DIVISION	PAGE 13.11
CHECKER		REPORT NO. NOR 67-136
DATE June 1967		MODEL X-21A

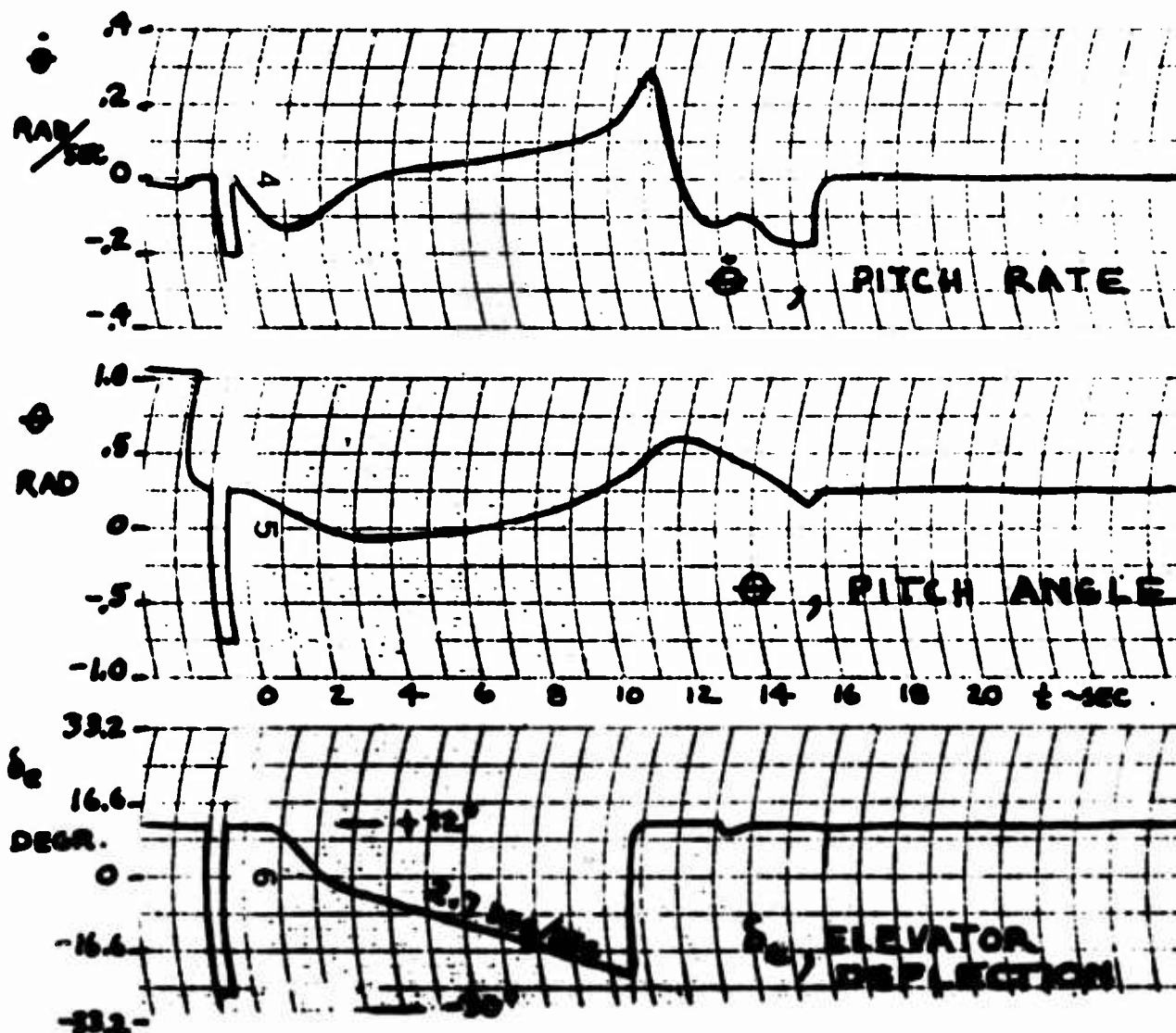


FIG 13.3B ANALOG TIME HISTORY OF X-21A PITCH-UP UTILIZING WIND TUNNEL DATA

— $\dot{\theta}$, θ , AND δ_e VS. TIME

ENGINEER	NORTHROP CORPORATION NORAIR DIVISION	PAGE 13.12
CHECKER		REPORT NO. NOR 67-136
DATE June 1967		MODEL X-21A

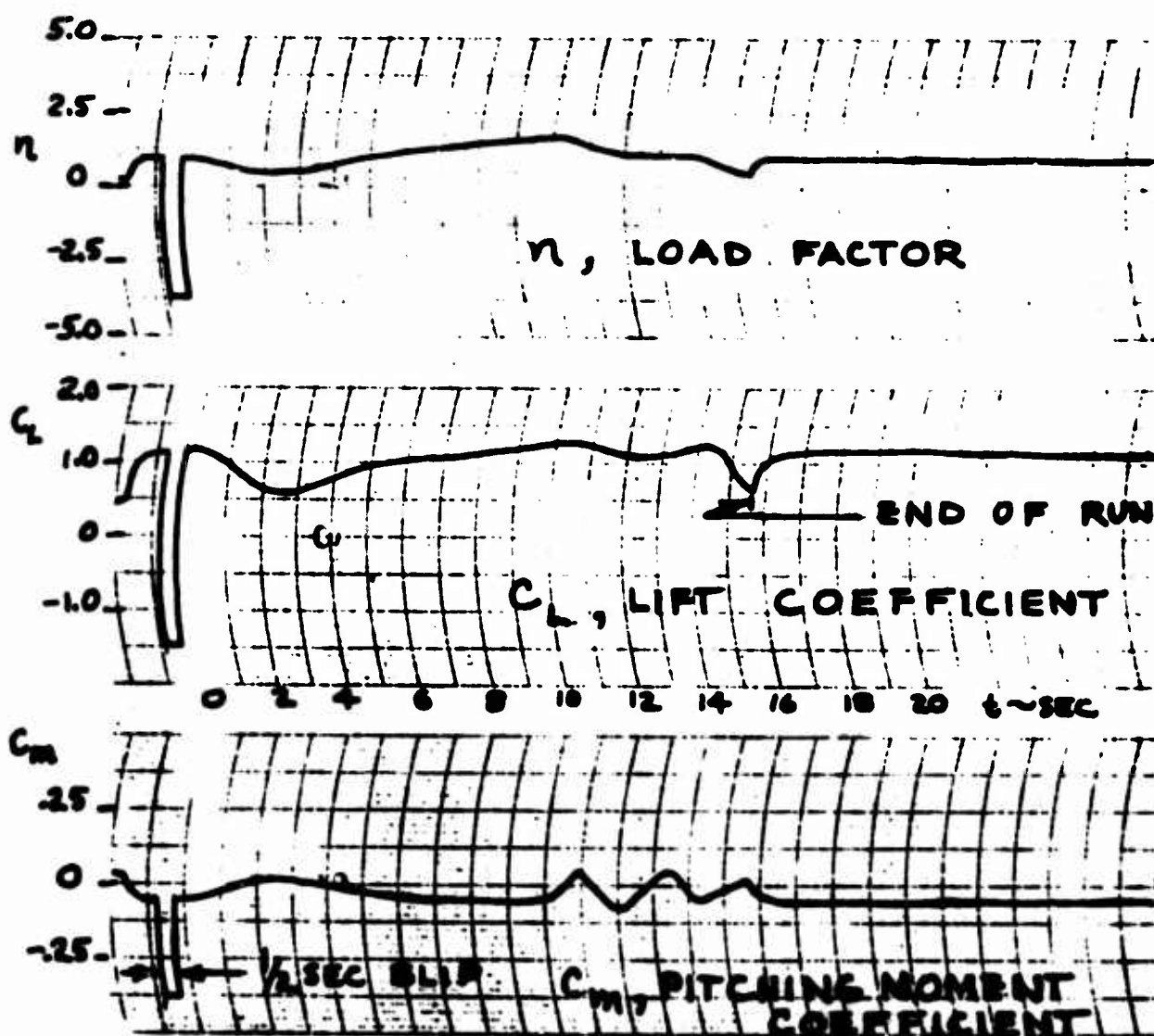
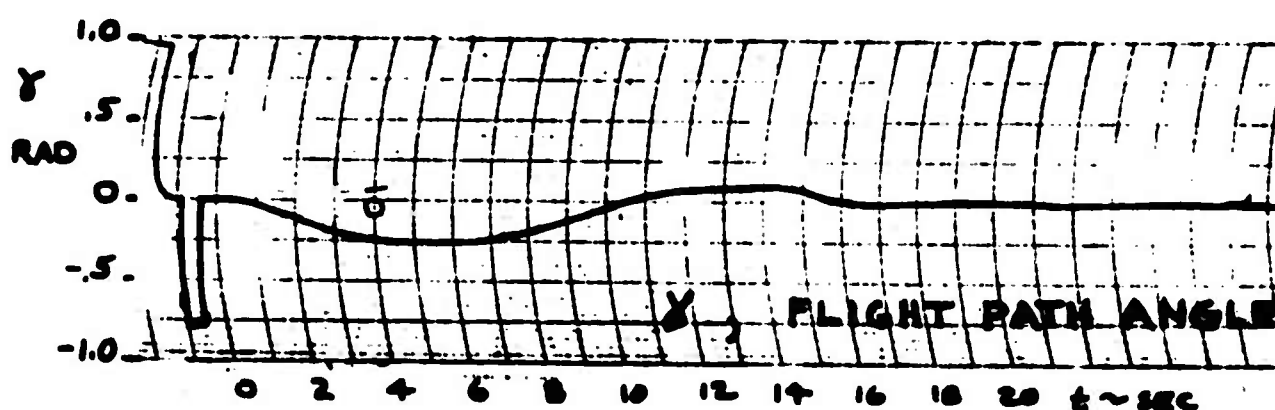


FIG 13.3C ANALOG TIME HISTORY OF X-21A PITCH-UP UTILIZING WIND TUNNEL DATA

n , C_L , AND C_m VS. TIME

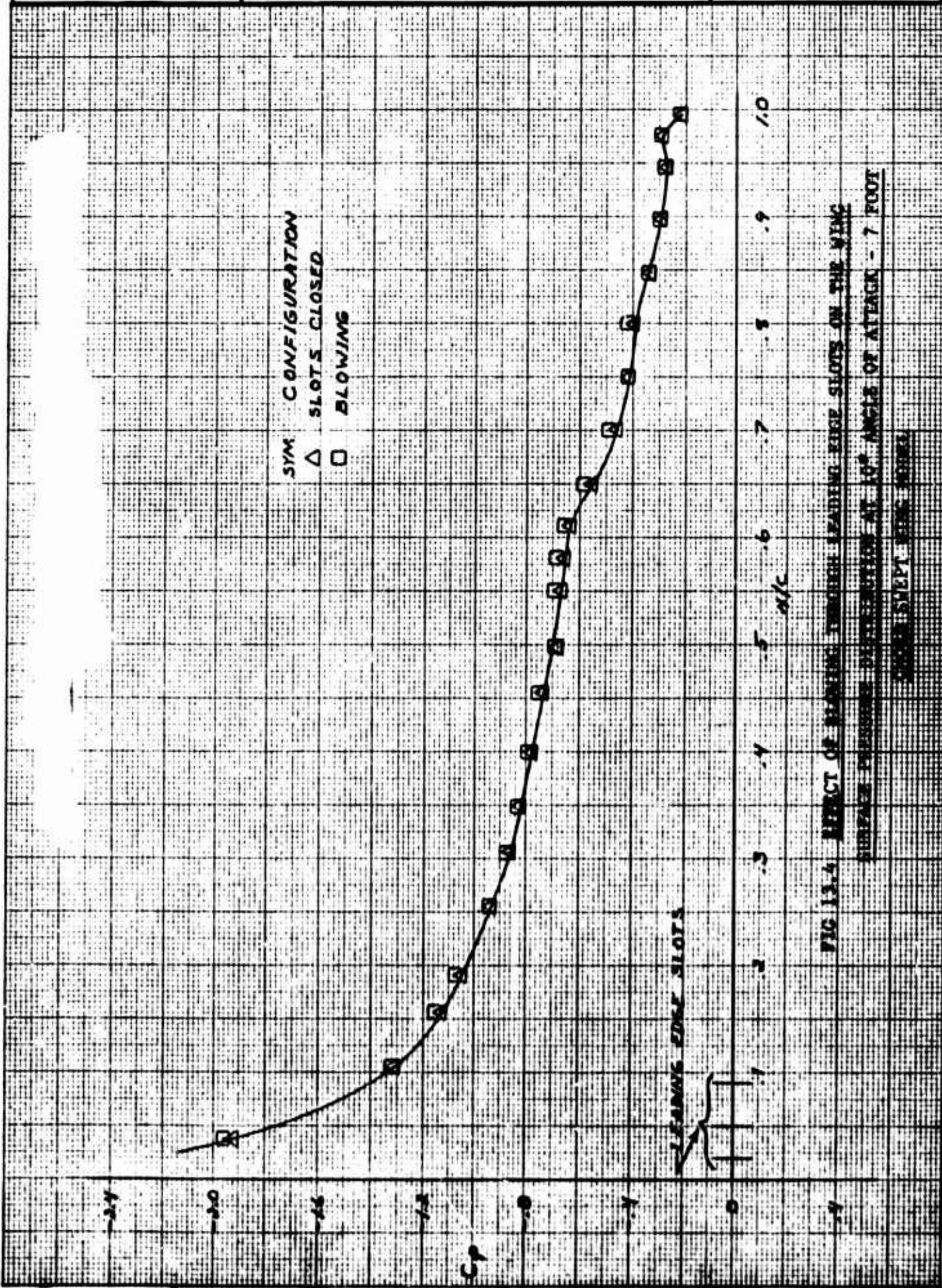
ENGINEER	NORTHROP CORPORATION NORAIR DIVISION	PAGE 13.13
CHECKER		REPORT NO. NOR 67-136
DATE June 1967		MODEL X-21A



	α	$\ddot{\theta}$	$\dot{\theta}$	n
	DEGR	RAD/SEC ²	RAD/SEC	g's
PEAK VALUES	28.6	.25	.29	1.7

FIG 13.3D ANALOG TIME HISTORY OF X-21A PITCH-UP UTILIZING WIND TUNNEL DATA
- γ VS TIME, AND SUMMARY OF PEAK VALUES

ENGINEER	NORTHROP CORPORATION NORAIR DIVISION	PAGE 13.14
CHECKER		REPORT NO. NOR 67-136
DATE June 1967		MODEL X-21A



ENGINEER	NORTHROP CORPORATION NORAIR DIVISION	PAGE 13.15
CHECKER		REPORT NO. NOR 67-136
DATE June 1967		MODEL X-21A

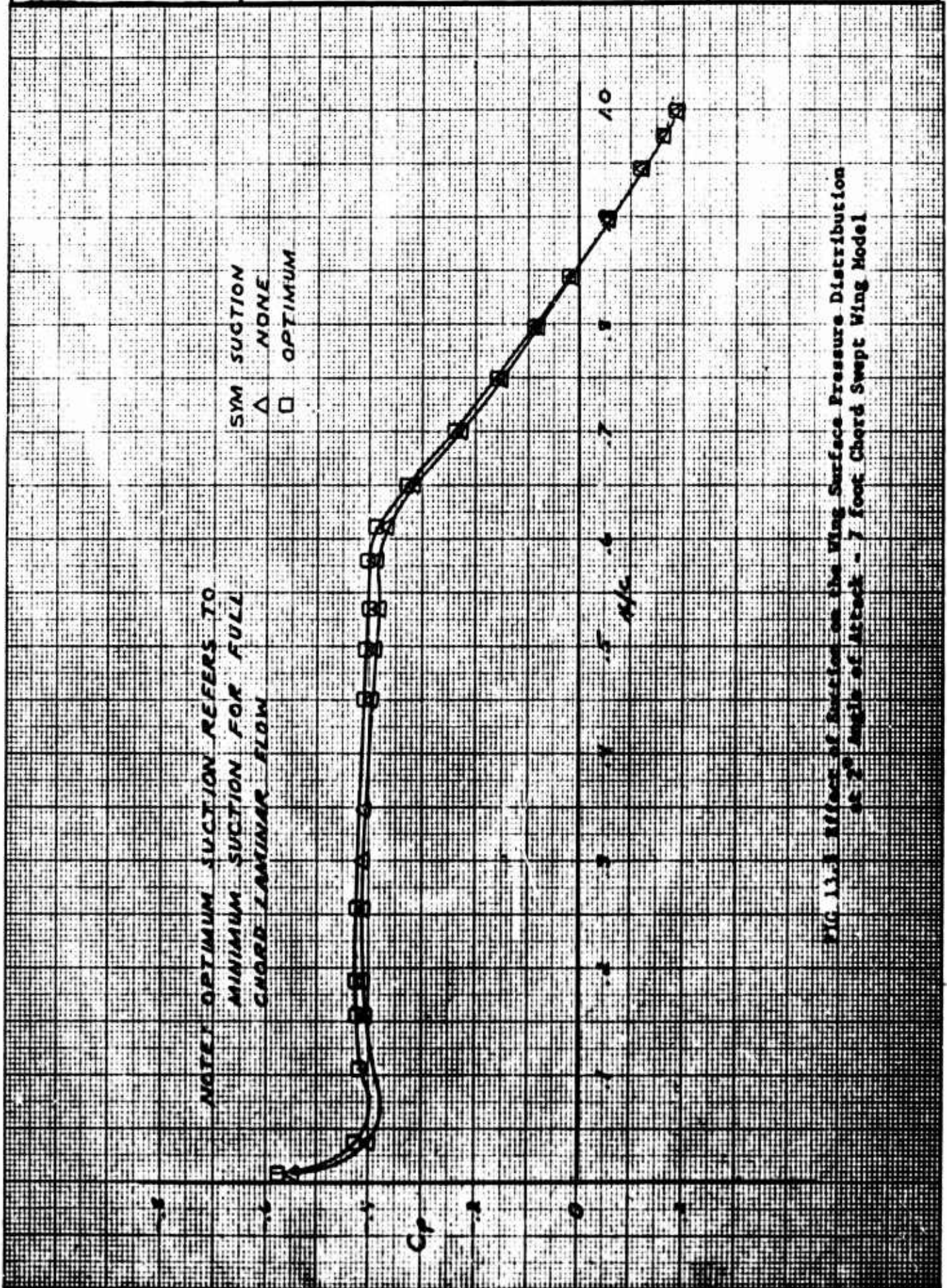


FIG 13.1 Effect of Suction on the Wing Surface Pressure Distribution at 2° Angle of Attack - 7 foot Chord Swept Wing Model

ENGINEER	NORTHROP CORPORATION NORAIR DIVISION	PAGE 13.16
CHECKER		REPORT NO. NOR 67-136
DATE June 1967		MODEL X-21A

X-21A LEFT WING UPPER
AIRPLANE AF 55-410A
FLIGHT 115 RUN 18
MACH NO. = .74
ALTITUDE = 41,300 FT
LIFT COEFF. $C_{L_A} = .32$

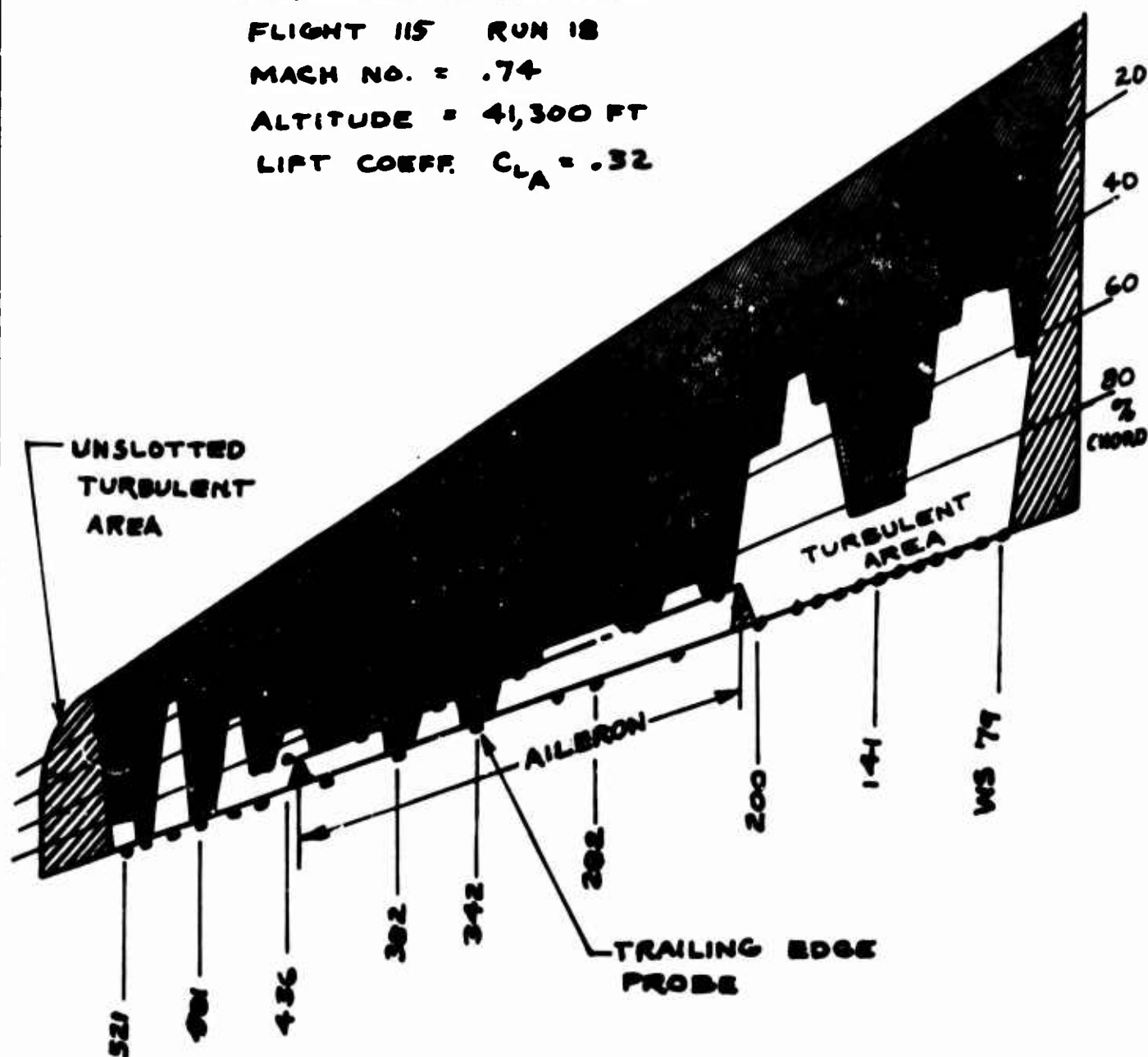


FIG. 13.6 LAMINAR FLOW OVER AILERON HINGE

ENGINEER	NORTHROP CORPORATION NORAIR DIVISION	PAGE 14.00
CHECKER		REPORT NO. NOR 67-136
DATE June 1967		MODEL X-21A

SECTION 14

ICE PROTECTION SYSTEMS

By

W. L. Eichelkraut

March, 1964
Revised April, 1967

ENGINEER	NORTHROP CORPORATION NORAIR DIVISION	PAGE 14.01
CHECKER		REPORT NO. NOR-67-136
DATE June 1967		MODEL X-21A

14.1 INTRODUCTION

Design of ice protection systems for slotted LFC wing surfaces presents design problems and considerations not associated with conventional airfoil surfaces. Icing characteristics of the airfoil with and without suction system operation, runback refreezing, and compromises to the internal air ducting of the LFC system must be considered. System concepts generally will be limited to large transport type aircraft.

A minimum amount of development work has been done to date regarding ice protection of laminarized wings; therefore, the discussion primarily is concerned with generalized design considerations and anticipated problem areas.

14.2 DISCUSSION

It does not appear possible to maintain LFC during an icing encounter because the impinging water droplets disrupt laminarization. Therefore, the de-icing design condition may not require operation of the suction system. The icing characteristics are similar to those of an airfoil without slots. The only added consideration for an LFC wing may be ice accumulations within the slots, which will be discussed later.

Present day ideas of design and fabrication of LFC wings do not lend themselves to the use of hot air ice protection systems. Not only are the bleed air requirements excessive for a transport type aircraft but the designs do not appear to be adaptable to the transfer of heat from the air to the outer skin. The ducting for the hot air system would have to be placed in areas used for ducting the LFC air. The double skin passage technique for heating the outer skin cannot be used because of the induction system of slots, plenum chambers and control holes.

The use of electrical power to provide ice protection eliminates most of the problems associated with hot air systems. The most important advantage is the relative ease with which heat may be applied to the outer surface. Figure 14.1 presents some of the basic configurations that could be used. An electrical ice protection system should be designed for cyclic de-icing to minimize the electrical power required, particularly on large transport-type aircraft.

Of course electrical de-icing systems are not without problems, especially when used for a laminarized wing. Because of wing smoothness requirements, runback refreezing is an important consideration. One possible design feature to eliminate this problem would be a small spanwise evaporating anti-icing strip located at the aft edge of the impingement area.

Another area of investigation is icing within the slot. If ice does form in the slot, a cyclic de-icing method possibly could damage the outer skin or slot when the pieces of ice leave the wing. Heat can be supplied to the slot

ENGINEER	NORTHROP CORPORATION NORAIR DIVISION	PAGE	14.02
CHECKER		REPORT NO.	NOR-67-136
DATE		June 1967	MODEL

edge by conduction with the installations shown in Figure 14.1; however, it would seem that the ice in the slot would have to be completely melted rather than loosened at the edges if the ice is to leave the slot without damaging the skins. An investigation and solution to the problem can best be accomplished on a model in an icing wind tunnel.

With reference to Figure 14.1, the heating blankets are between the outer, slotted skin and the inner, honeycomb panel. The heavy dashed lines represent the electrical heating elements imbedded in a dielectric material to form the heating blanket. Design A is a continuous blanket with void strips in the heating element pattern at each slot location. The plenums and holes are cut into the blanket at the voids or non-heated strips of the blanket. Design A is the one selected for the X-21A tests. Design B is a continuous blanket with continuous heating element patterns across the slot region, and the holes from plenum to duct must be drilled through the pattern of heating elements, perhaps rendering the heating elements ineffective in the plenum region. Design B has a disadvantage compared with Design A in that the heating elements are farther from the surface skin. In Design C the heating blanket is made of separate strips that are bonded-on between the plenum regions. Filler strips of adhesive or the like must be added between the blanket strips. Design A also was considered superior to Design C.

Figure 14.2 is a sketch made from a reproduction of an x-ray of a portion of the X-21A de-icing panel, approximately full size. The original x-ray, which was somewhat more revealing in detail and showed the .063 diameter holes spaced .25 apart along the slot lines, no longer is available. The sketch shows different wiring patterns for different strips to provide the required chordwise distribution of heat density. It also shows provisions for clearance of the fasteners at a spanwise splice in the wing nose panel structure. The diagram, Figure 14.2, corresponds to Design A. Typical power density of the wiring pattern is 18 watts per square inch. Such a design can be with slot spacing as narrow as .5 inches.

A design consideration for the heating blanket is the repair or replacement of damaged elements. Small local areas of repair may be accomplished by removing the outer skin adjacent to the heating blanket while for large areas of heating element damage, entire panels may have to be removed and rebuilt. Such a major repair can be minimized if considered early in the design of the wing structure and associated LFC components.

One of the X-21A airplanes (AF55-410A) has a de-iced leading edge test section approximately ten (10) feet long located near the outboard end of the left hand wing. The chordwise extent of de-icing is to the fifteen (15) percent chordline on the upper surface and the eight (8) percent chordline on the lower surface. The upper surface limit was selected to provide a heated area aft of the impingement zone to minimize runback re-freezing. The lower surface limit was chosen to be just ahead of the removable access doors.

ENGINEER	NORTHROP CORPORATION NORAIR DIVISION	PAGE 14.03
CHECKER		REPORT NO. NOR-67-136
DATE June 1967		MODEL X-21A

The X-21A system is a cyclic electrical de-icing heater blanket and associated controls. There are twelve (12) cycled elements with a two (2) minute complete cycle time. The heaters operate on 115V, 400 cycle, 3 phase power. There are three spanwise continuously heated parting strips located on the stagnation line and on the upper and lower surfaces. No chordwise parting strips are used.

Design of the de-iced test section was not optimized and is intended only to be a test of one design configuration for a slotted wing. Icing tests were planned behind a tanker airplane as well as in natural icing conditions but no tests were actually conducted. Tests were to have been made with the LFC suction system ON and OFF to see what effects, if any, there are on slot icing and impingement limits. Data recording on the X-21A was to consist of movie cameras to photograph the ice buildup and shedding, and the LFC probes located at the trailing edge of the wing behind the test section.

14.3 CONCLUSIONS

Ice protection of slotted laminarized wings is possible, although there are certain design considerations peculiar to LFC aircraft. To further investigate these added requirements and obtain the necessary design data, icing tunnel tests are required. Of the systems studied, the cyclic electrical de-icing systems appear to require the least number of design compromises when integrated with the LFC system.

ENGINEER	NORTHROP CORPORATION NORAIR DIVISION	PAGE 14.04
CHECKER		REPORT NO. NOR 67-136
DATE June 1967		MODEL X-21A

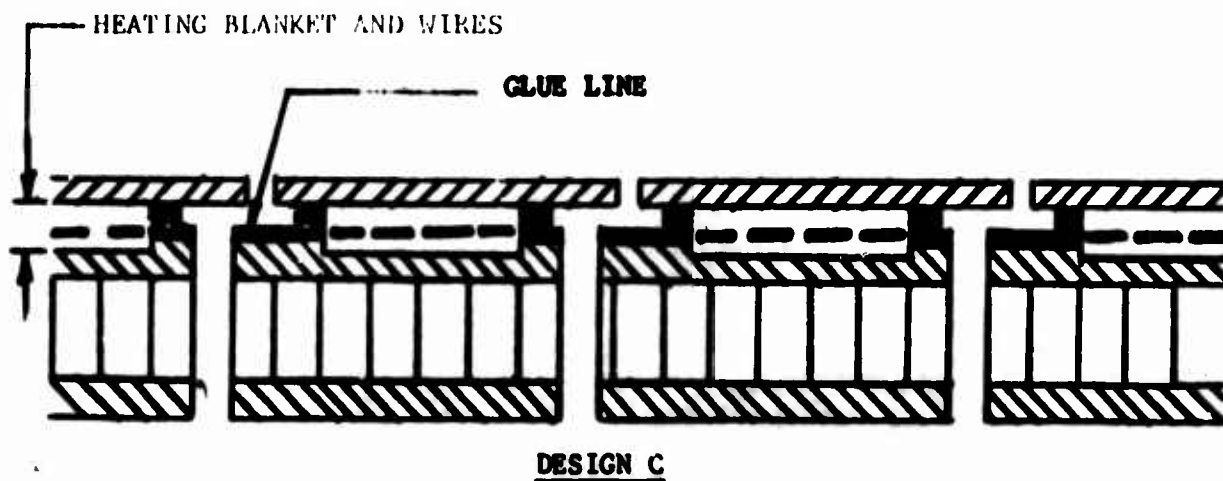
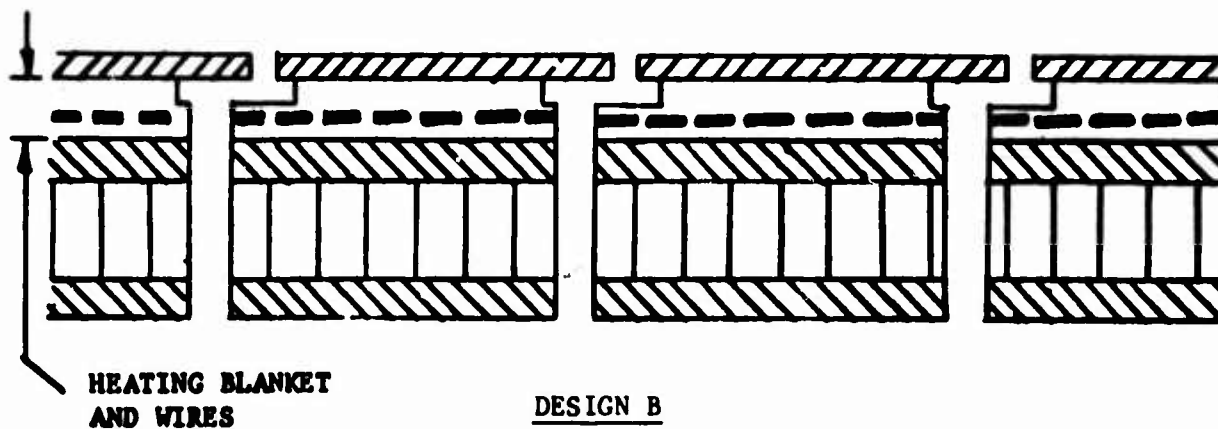
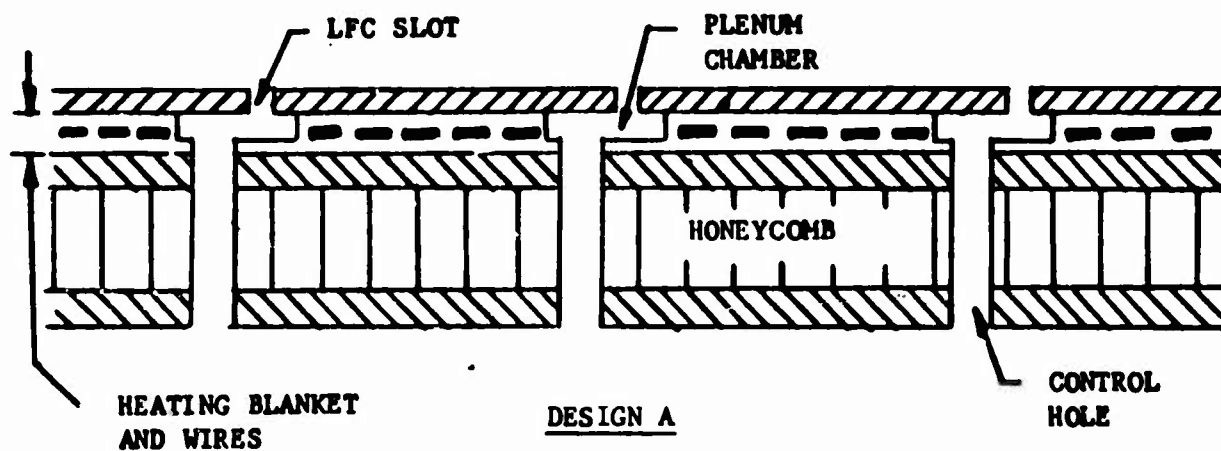


FIG 14.1 TYPICAL INSTALLATIONS

ENGINEER	NORTHROP CORPORATION NORAIR DIVISION	PAGE 14.05
CHECKER		REPORT NO. NOR 67-136
DATE June 1967		MODEL X-21A

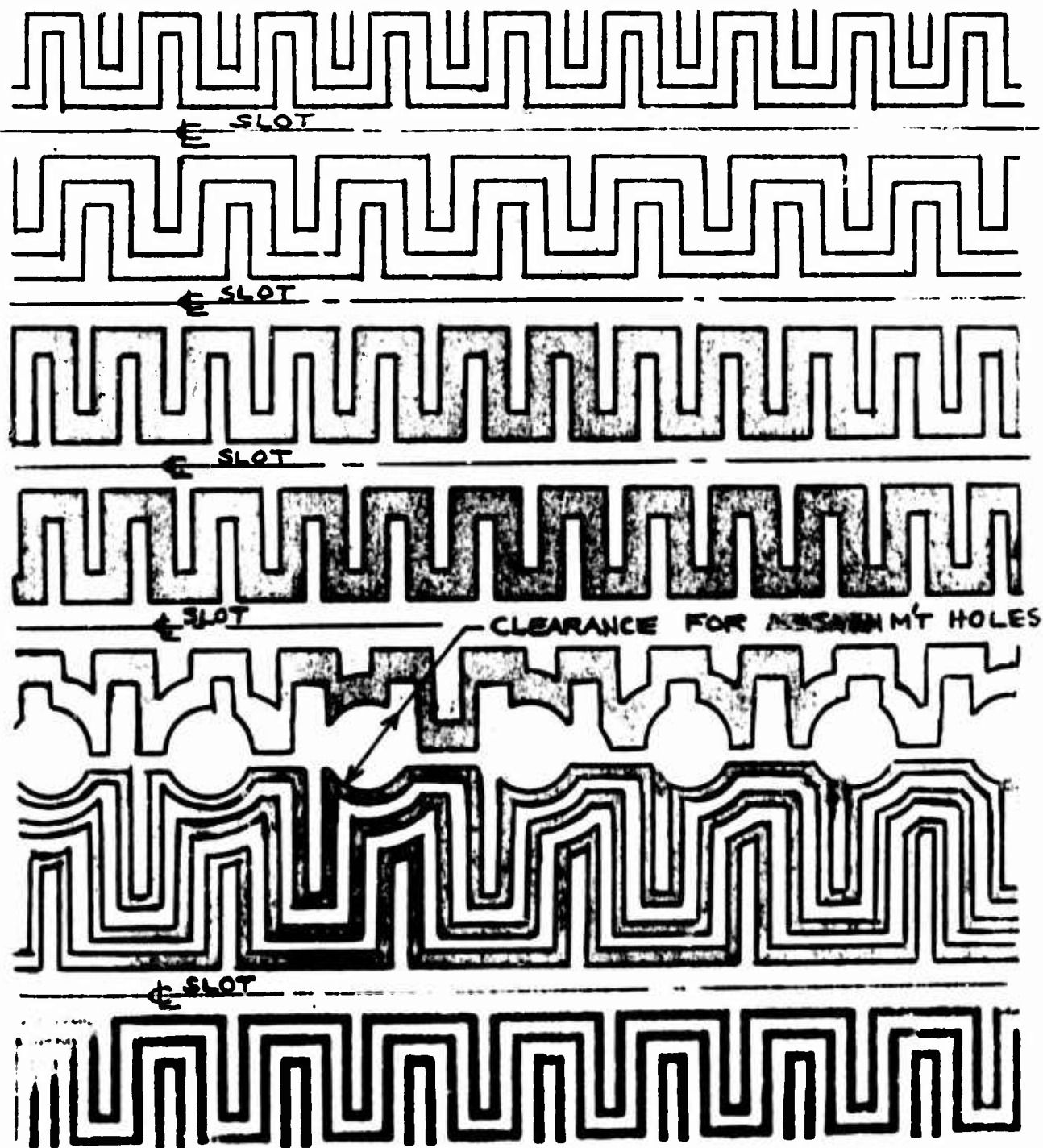


FIG 14.2 TYPICAL WIRE PATTERN -- DESIGN A

ENGINEER	NORTHROP CORPORATION NORAIR DIVISION	PAGE 15.00
CHECKER		REPORT NO. NOR-67-136
DATE June 1967		MODEL X-21A

SECTION 15

STRUCTURAL DESIGN AND STRESS ANALYSIS

- LFC WING

By: A. E. Arslan, G. O. Bezner, and E. A. Ellestad

April 1964

revised July 1967

ENGINEER	NORTHROP CORPORATION NORAIR DIVISION	PAGE 15.01
CHECKER		REPORT NO. NOR 67-136
DATE June 1967		MODEL X-21A

15.1 TABLE OF CONTENTS

<u>Section No.</u>	<u>Title</u>	<u>Page No.</u>
15.2	Summary	15.02
15.3	Introduction	15.03
15.4	Structural Design Requirements - X-21A	15.03
15.5	General Description of X-21A Wing Structure	15.03
15.6	Design Analysis - X-21A Wing	15.04
15.7	Specific Design Details of X-21A Wing and Suggested Revisions for Future LFC Wing Design - Development	15.07
15.7.1	Main Structural Box	15.07
15.7.2	Leading Edge Region (Forward of Front Spar)	15.08
15.7.3	Trailing Edge Region (Aft of Rear Spar)	15.12
15.7.4	Outer Skin Panel Splices and Access Panels	15.14
15.7.5	Compressor Pod and Dry Bay Area	15.17
15.7.6	Integral Fuel Tank Inspection	15.18
15.7.7	Inspection, Maintenance and Environmental Protection	15.19
15.8	Structural Tests	15.20
15.8.1	Wing Test Box	15.20
15.8.2	Inboard Wing Cover Assembly Beam Column Panel Tests	15.21
15.8.3	Inboard Wing Cover Assembly Beam Column Splice Tests	15.21
15.8.4	Main Box Inner Cover Compression Panels	15.21
15.8.5	Vee Stringer Tests	15.22
15.8.6	Trailing Edge Panel Compression Tests	15.23
15.8.7	Trailing Edge Panel Column Tests	15.23
15.8.8	Aileron Hinge Test	15.23
15.8.9	Coupon Fatigue Tests	15.23
15.9	References	15.24
	Figures	

ENGINEER	NORTHROP CORPORATION NORAIR DIVISION	PAGE 15.02
CHECKER		REPORT NO. NOR 67-136
DATE June 1967		MODEL X-21A

15.2 SUMMARY

The successful construction and operation of the X-21A wing demonstrates that an LFC wing can be made with only a relatively small sacrifice in structural weight. The LFC wing structural requirements were, primarily: a smooth external suction surface incorporating external slots and internal plenums, holes, and tributary ducts; spanwise suction ducts leading to mixing chambers at the pumping pod; and an integral fuel tank in the main box section. The unit weight of the X-21A wing is 9.2 pounds per square foot based on the planform area and the weight of both upper and lower surfaces, which is considered to be a reasonable value. The unit weight does not include the weight of removable valves, duct connections, and pumping equipment in the dry bay and pod region. These items are chargeable to the pumping system. The weight penalty for the wing structure of future LFC aircraft is estimated to be less than 8% of the wing weight.

Structural design concepts and methods have been developed for the solution of problems imposed by LFC requirements. The development of plenums in the adhesive bonding of the outer skin, LFC panel splices, LFC removable panels, tributary ducts and nozzles, transfer nozzle duct systems, an LFC aileron, and the use of wing load carrying structure for suction ducts are some of the examples.

In general, the design concepts, analytical methods, and manufacturing methods developed are considered applicable to future LFC wing designs. However, the operational life and usage of the X-21A have been too limited to adequately evaluate material protection techniques necessary to prevent corrosion in LFC structure of production aircraft. Additional research and development are desirable if not required in this area. Another development which may modify the present LFC wing structural concept is the possible use of a perforated or porous suction surface instead of slots in the wing nose region in order to reduce the strength of boundary layer vortices and thereby improve laminarization. This possible development is contingent upon additional experimental and theoretical LFC investigations of large wing nose sections. Improvements in panel splice designs and improvements in ducting configuration in the forward regions of the wing also appear possible.

ENGINEER	NORTHROP CORPORATION NORAIR DIVISION	PAGE 15.03
CHECKER		REPORT NO. NOR-67-136
DATE June 1967		MODEL X-21A

15.3 INTRODUCTION

The incorporation of laminar flow by suction imposes several unique requirements in structural design and analysis. This section of the report contains a presentation of these requirements, the Northrop approach used to fulfill them on the X-21A, and recommended design improvements and areas of investigation for the design of future laminar flow control aircraft.

It is noted that in the structural design of aircraft, consideration must be given to manufacturing problems, capabilities, and limitations. This is especially significant in an LFC airplane where smooth, substantially wave-free external surfaces are mandatory. Reference 1 contains a further discussion of the manufacturing problem.

15.4 STRUCTURAL DESIGN REQUIREMENTS - X-21A WING

The X-21A wing principal design requirements were: a very smooth, substantially wave-free external surface; suction slots in the external skin leading to plenum chambers beneath, with holes in the inner skin to conduct the suction air to the suction ducts; spanwise suction ducts, a part of the wing load carrying structure, to lead the air to the mixing chambers at the suction pod; and integral fuel tanks in the wing box region except at the dry bay region of the pumping pod. Another criterion was to laminarize as much of the wing as appeared to be practical, including the aileron, panel splices, and removable access panels. Originally, all suction slots were specified to be spanwise, but the test programs showed better laminarization with short chordwise slots along the leading edge flow attachment zone, requiring design modifications in that area of the inboard wing.

It should be mentioned that the X-21A was designed to a load factor 25% greater than normal because no static test was to be made. The airplane would then be flown to only 80% of the design limit load factor, the usual practice for an airplane prior to static test. The design ultimate load factor was 5.1.

15.5 GENERAL DESCRIPTION OF X-21A WING STRUCTURE

The wing is the only part of the airplane utilizing structure peculiar to the LFC concept. The wing outboard of the side of the fuselage consists of a main structural box (Fig. 15.1), the original leading edge section forward of the front spar (Fig. 15.2), and a trailing edge section aft of the rear spar (Fig. 15.3). The main structural box, which also functions as an integral fuel cell, is composed of two spars, chordwise ribs,

ENGINEER	NORTHROP CORPORATION NORAIR DIVISION	PAGE 15.04
CHECKER		REPORT NO. NOR 67-136
DATE June 1967		MODEL X-21A

15.5 GENERAL DESCRIPTION OF X-21A WING STRUCTURE (Cont'd.)

and upper and lower covers. Each cover consists of an inner and outer honeycomb sandwich structure separated by I-shaped and V-shaped stringers 1.5 to 2.0 inches in depth. The ducts formed in this manner are used as a flow path for the suction air. The external air is sucked through nominally .006-inch wide slots cut along spanwise lines in an outer skin which is .020 to .025 inch thick. The outer skin is bonded to the outer face of the outer honeycomb sandwich panel. The adhesive used for this bond is the Minnesota Mining and Manufacturing Company's AF-32, as described in Norair Process Specification MA-76F. An .023-inch tape is bonded to the sandwich panel, plenum chambers are machined into the adhesive, an .003-inch tape is applied, and the outer skin is bonded on. The final glue line thickness varies from .020 to .024 inch with the plenums machined into it being .188 inch wide and .0135 to .0165 inch deep. To provide for suction of the air from these small plenum chambers into the main ducts, holes .062 inch in diameter at .25 inch spacing are drilled through the outer sandwich panel (see Figure 15.4). Tributary ducts, bonded to the panels, serve to regulate the inflow of suction air into the duct and direct it downstream in the duct.

The leading and trailing edge sections (forward and aft of the front and rear spars respectively) incorporate honeycomb sandwich skins which are slotted and drilled in a manner similar to that of the main box. Full depth, canted, spanwise shear webs of honeycomb sandwich construction function as spanwise duct walls and as continuous chordwise rib trusses. In the outer bonded panels, non-perforated honeycomb core is required to prevent crossflow between adjacent suction holes and ducts. This necessitates the use of an adhesive with extremely low volatile content. The adhesive used for this bond is the Bloomingdale Rubber Company's FM-61, as described in Norair Process Specification MA-76F.

15.6 DESIGN ANALYSIS - X-21A WING

The external smoothness requirements were met by the extensive use of honeycomb sandwich structure, which is non-buckling to ultimate load and has relatively low deflections under external pressure loads, and by the development of manufacturing techniques to keep manufacturing tolerances to a minimum (see Reference 1).

Early in the program it was planned to machine the plenum chambers in the outer sheet of the honeycomb sandwich panels. In the thicker gauges, no material would have been added to the inside of this sheet. In the thinner gauges such as those used in the leading edge and trailing edge structure, additional material would have been left under the plenum chambers by starting with thicker skin and machining it down between these plenum chambers. Requirements for more closely spaced slots made machining between the

ENGINEER	NORTHROP CORPORATION NORAIR DIVISION	PAGE 15.05
CHECKER		REPORT NO. NOR-67-136
DATE June 1967		MODEL X-21A

15.6 DESIGN ANALYSIS - X-21A WING (Cont'd.)

plenum chambers impractical. This resulted in a condition wherein excess metal was provided between the plenum chambers, and an undesirable stress concentration occurred at the plenum chambers, where the skin was thinner. A row of holes further reduced the net area. A design where the plenum chambers were machined in a thicker glueline, leaving a constant thickness of face skin, was investigated, and it was found that, with the use of a thermal setting adhesive such a design resulted in a practical structure. The external smoothness was even better than had previously been obtained, since the thick glueline could compensate for minor variations in smoothness of the honeycomb sandwich.

Tests conducted under a USAF boundary layer control research contract to determine the efficiency and torsional stiffness of a structural box with inner and outer skin separated by I-shaped stiffeners, with internal ribs only between the inner skins, showed that such structures can transfer torsional shear between inner and outer skins. In these tests, I-shaped stiffeners were used at approximately 3.0 inch spacing to stabilize the compression covers and to act as ribs (by Vierendeel truss action) to distribute shear stresses to both the inner and outer covers. In the X-21A, a combination of I- and V-shaped stiffeners was used at 6.0 to 10.0 inch spacings, but the use of heavier stiffeners and the ability of a V-shape to transfer shear as a truss instead of only by bending provided a positive load path between outer and inner covers and eliminated any Vierendeel truss type bending.

Once it had been established that the internal structure could satisfactorily redistribute local airloads and inertia loads, and the usual assumptions that plane sections remained plane in bending and the entire section rotated as a unit were valid, conventional methods of internal load distribution were followed.

The primary shear flow and bending stress distributions were determined using the standard Northrop tapered beam "Mc/I" flexure formula programmed on the 7090 computer, handling the effects of sweep and shear lag in the conventional manner of applying effectivity factors to the various bending item areas. Since the inboard wing sections actually contain 31 cells and since this program was set up for a maximum of 29 cells, some lumping of the smaller cells was necessary. Although the accuracy lost in this process is undoubtedly small, the unlumping process of adjusting the shear flows for all of the numerous sections and conditions was troublesome and time consuming. The 29 cell limit was imposed by the limitation of the 704 computer for which the program was originally made. The 7090 does not have this same limitation, so the program should be revised for future aircraft.

ENGINEER	NORTHROP CORPORATION NORAIR DIVISION	PAGE 15.06
CHECKER		REPORT NO. NOR-67-136
DATE June 1967		MODEL X-21A

15.6 DESIGN ANALYSIS - X-21A WING (Cont'd.)

The main box cover assemblies are subjected to secondary bending and shear as a result of their being supported intermittently at the discrete ribs. On the X-21A wing, these secondary bending effects were calculated for each stringer and adjacent cover skin using beam column formulas for a single fixed ended bay symmetrically loaded. The effects of bending curvature, initial curvature and normal running loads are included. For future designs it would be desirable to establish procedures and programs for solution on electronic computers. Some thought might also be given to combining the primary and secondary bending loads calculations into one computer run. At present, the entering of the primary bending results into the secondary bending calculations is a tedious and time consuming task.

For the analysis of the honeycomb cover panels, direct reading allowable curves for (1) edgewise compression, (2) edgewise shear, and (3) edgewise bending, have been prepared. The curves for panel buckling due to edgewise compression and edgewise shear were developed directly from the information presented in the preliminary issue of Part III of MIL-HDBK-23. They show the allowable facing stress as a function of two parameters, A_1 and A_2 . These parameters are a function of panel geometry, facing thicknesses, core height and core shear modulus. By presenting the design curves in this form, the iterative procedure that is required to use the general curves presented in Part III of MIL-HDBK-23 is eliminated. Curves have been prepared for various aspect ratios, and two ratios of spanwise to chordwise bending have been developed from the information presented in a Forest Products Laboratory report, and are in the same form as those for edgewise compression and edgewise shear.

The inner upper cover panels on the X-21A wing are subjected to fuel pressure loads as well as axial compression resulting from wing bending. For the loads and panel proportions used on the X-21A wing, these panels are not critical for buckling but will fail due to beam column type loads which result in facing or core stress which exceeds the material allowables. In this case, the addition of edgewise load to the panel, subjected to normal pressure, results in a magnification of the stresses due to normal pressure. From Forest Product Laboratory reports and other references, this magnification factor can be determined. The net stresses are then the sum of the magnified stresses and the edgewise compression stress. Since there appears to be little or no theoretical work backed by test information available

ENGINEER	NORTHROP CORPORATION NORAIR DIVISION	PAGE
CHECKER		15.07
DATE		REPORT NO.
June 1967		NOR 67-136
		MODEL
		X-21A

15.6 DESIGN ANALYSIS - X-21A WING (Cont'd.)

for this type of combined loading, it is believed that this is an area where some fairly extensive investigations are warranted.

Another interesting problem in the X-21A analysis was the interaction between the compressor pod and the wing structure. Since the compressor pod is constructed as an integral part of the wing structure, the result is a structure of multiple redundancy. The primary mass of the GTMC (high pressure or main pumping unit) is located very near to the wing trailing edge. During a dynamic gust type of condition, this mass in the pod is subjected to a 13 g down load. In addition to this type of loading, another type of loading develops as a result of the large cutouts in the lower cover and the canted webs directly above the pod. Since the shear stiffness of these members is so drastically reduced, it is assumed that the sides of the pod and some effective trailing edge width, directly over the side of the pod, act as ribs to unload all of the shears carried in the trailing edge forward into the main box. This problem was solved on the 7090 computer using a Northrop Matrix Deflection Method.

15.7 SPECIFIC DESIGN DETAILS OF X-21A WING AND SUGGESTED REVISIONS FOR FUTURE LFC WING DESIGN - DEVELOPMENT

15.7.1 Main Structural Box (Refer to Figures 15.1 and 15.5, Typical Cross Sections)

The dual requirements of spanwise suction ducts and integral fuel tanks clearly lead to the design choice of double skin panel cover assemblies. The outer and inner panels form duct boundaries and the inside surface of the inner panels forms a fuel tank boundary. The front and rear spars form the fore and aft boundaries of the main box and the fuel tanks, with the spar caps acting also as air duct boundaries.

Stringers are required in order to stabilize the outer and inner skin panels as well as to partition the suction ducts, which must be sealed relative to each other. Since suction air must be transferred spanwise via these stringer ducts to the compressor pods, the use of full depth ribs is not practical. Thus, the stringers are also used to transfer torsional shear loads between the outer and inner panels. Conventional stringers with single webs normal to the wing contour, such as "I," "C," and "Z" sections, are not capable of providing the required torsional shear continuity between ribs and outer panels except by Vierendeel truss action which necessitates either close stringer spacing or thick webbed stringers. Close

ENGINEER	NORTHROP CORPORATION NORAIR DIVISION	PAGE 15.08
CHECKER		REPORT NO. NOR 67-136
DATE June 1967		MODEL X-21A

15.7.1 Main Structural Box (Cont'd.)

stringer spacing has the disadvantage of inefficient location of wing primary bending material along with introducing local moments into the outer panel. Wide stringer spacing (with thick webs) has the drawback of introducing higher local moments into the outer skin panels yielding undesirable stress concentrations with attendant reduction in fatigue life. In order to circumvent these problems, "V" stringers which permit shear transfer from the ribs to the outer skin panels with essentially pure shear load at the outer skin panel were utilized on the X-21A (see Figure 15.6). A secondary function of two of these stringers was their use as fuel vents.

The cover assemblies are stabilized by conventional means of chordwise ribs, which have stiffeners backing up the "V" stringers to minimize rib cap secondary bending and have cutouts for fuel transfer.

The inner skin panels, which serve as fuel tank boundaries as well as duct boundaries, must withstand high normal pressure loads in addition to the axial and transverse loads imposed by wing bending and torsion. On the X-21A the inner skins were designed as honeycomb sandwich panels with aluminum alloy facings and with the core crushed in the area of stringer attachments. The non-buckling panel design was chosen in order to prevent possible vibration disturbances that might feed through to the boundary layer and affect laminarization adversely. The precaution may have been unnecessary. Subsequent flight tests of the X-21A airplane showed no loss in laminarization due to mechanically forced vibration of panels. Consequently, an alternate design using thin inner panels might have been equally satisfactory.

The alternate design for the inner panels consists of thin buckling skins which carry fuel pressure loads in diaphragm action. Pads are required in this version of the design to satisfy fastener bearing and net section requirements. The panels may be milled chemically or mechanically, or have bonded-on doublers (see Figure 15.7).

15.7.2 Leading Edge Region (Forward of Front Spar)

15.7.2.1 Structural Configuration in Leading Edge Region - General

The leading edge structure on the X-21A is unique in that it consists of outer skin panels and inner diagonal webs arranged to form a chordwise truss

ENGINEER	NORTHROP CORPORATION NORAIR DIVISION	PAGE 15.09
CHECKER		REPORT NO. NOR 67-136
DATE June 1967		MODEL X-21A

15.7.2.1 Structural Configuration in Leading Edge Region - General (Cont'd.)

cantilevered off the main structural box (see Figure 15.2). This concept was chosen because it allowed maximum utilization of the cross sectional area for ducting by eliminating the requirement for ribs.

The internal diagonal members were designed as non-buckling honeycomb panels in order to withstand truss compression loads combined with normal loads due to differential pressures. A secondary consideration was to minimize panel vibration. As mentioned in the preceding part 15.7.1, subsequent flight tests of the X-21A airplane showed no loss in laminarization due to mechanically forced vibration of panels.

Several problems were experienced with this type of truss structure.

1. The surface-to-surface web structure was difficult to build to the limits required to hold exterior surface smoothness.
2. The combined loading on the webs, normal loads from duct pressure and axial loads from rib loading, resulted in heavier webs than anticipated.
3. The routing of the air from a forward duct back through all of the webs and ducts aft of it resulted in a congested area at the suction pod and one which was difficult to seal properly.
4. Leaks in the ducts were found to be difficult to seal after final assembly.
5. Access to all but the aft duct is limited after final assembly.
6. Inspection of the ducts for corrosion and/or fatigue cracks, a requirement on production aircraft, would be difficult with this structural arrangement.

ENGINEER	NORTHROP CORPORATION NORAIR DIVISION	PAGE 15.10
CHECKER		REPORT NO. NOR 67-136
DATE June 1967		MODEL X-21A

15.7.2.1 Structural Configuration in Leading Edge Region - General (Cont'd.)

These problems might be lessened in a future design by the use of a double-skinned structure instead of a diagonal truss configuration. The double-skinned design is shown in Figure 15.8. The double-skinned design would provide better control of the surface contour; suction air from the forward ducts would not be ducted through the other leading edge ducts in the dry bay region; and better access to ducts would be provided for inspection and sealing. The wing nose suction surface may be either slotted or perforated, but in either case the flow attachment zone leads to a single nose duct rather than to a split nose duct arrangement as in the original X-21A design. As shown in Figure 15.8, the wing nose is slotted, with chordwise slots along the stagnation or flow attachment zone. The plenums beneath the chordwise slots lead to the spanwise plenums and tributary ducts of the first spanwise slots. A further discussion of chordwise slots is presented in Section 3.3.

Disadvantages of the double-skinned design are the shear ties between the outer and inner panels, and the two layers of doors required for access to the inner portion of the structure after assembly. A comprehensive analysis and comparison of the truss and the double-skinned designs are required for determining the better choice for future LFC aircraft.

15.7.2.2 Slot Spacing in Leading Edge Region

The steep pressure gradients in the nose section lead to the dual requirements of close slot spacing and narrow ducts. Nose splitter flange widths had to be held to a minimum to keep from exceeding slot spacing requirements. In certain areas, it was necessary to have slots closer together than the width of a tributary duct (.50 inch). In these cases special double tributary ducts were fabricated by cutting and splicing standard tributary ducts, as shown in the nose area of Figure 15.2. In order to achieve an additional pressure drop in certain areas, a second plenum chamber with metering holes was located between panel and tributary ducts as shown on the same illustration.

ENGINEER	NORTHROP CORPORATION NORAIR DIVISION	PAGE
CHECKER		15.11
DATE		REPORT NO.
June 1967		NOR 67-136
		MODEL
		X-21A

15.7.2.2 Slot Spacing in Leading Edge Region (Cont'd.)

The minimum slot spacing which can be allowed structurally is determined by the following considerations:

1. There must be sufficient land remaining between the plenum chambers to adequately bond the strip of slotted skin between the slots.
2. There must be sufficient space within the slot pattern (but not necessarily between two adjacent slots) to adequately splice the skin panels.
3. On highly curved panels such as the nose panel, the slot spacing must be determined by clearance between tributary ducts on the inner surface of the panel because that distance becomes appreciably less than the slot spacing on the outer surface.

15.7.2.3 Scab-On Revision to Leading Edge - X-21A Airplane

During the flight test program of the X-21A airplane, a "scab-on" revision to the flow attachment zone of the inboard leading edge region of the second airplane (AF 55-410A) resulted in much improved laminarization. The scab-on section included a smaller leading edge radius and chordwise slots spaced .75 inches apart. The revision is described in detail in Section 3.3, and a sketch of a typical cross-section of the revision is shown in Figure 15.9.

15.7.2.4 Finely Perforated or Porous Suction Surfaces in the Wing Nose Region

Because much of the boundary layer disturbance on the X-21A airplane appears to originate in the wing nose region, it has been suggested that additional improvements in laminarization might be made by the use of finely perforated or porous suction surfaces in the wing nose region. The finely perforated surface would more nearly approach the ideal condition of distributed suction and presumably would decrease the strength of boundary layer vortices that occur on swept LFC wing nose sections with slotted suction surfaces. The aerodynamic analysis and structural design of the perforated or porous wing nose may be the subject of future research and development.

ENGINEER	NORTHROP CORPORATION NORAIR DIVISION	PAGE 15.12
CHECKER		REPORT NO. NOR 67-136
DATE June 1967		MODEL X-21A

15.7.3 Trailing Edge Region (Aft of Rear Spar)

15.7.3.1 Structural Configuration in Trailing Edge Region - General

The problems encountered in the design of the trailing edge of the X-21A airplane were for the most part the same as those already discussed in the section on the leading edge. The structure was the same as that of the leading edge, trussed honeycomb sandwich webs with honeycomb sandwich skins, cantilevered off the main box (see Figure 15.3).

Although the allowable waviness on the trailing edge was greater than that on the leading edge, more deviations from tolerances were experienced. This was due partly to the greater size and flatter panels, partly to design, and partly to tooling.

A wave occurred near the trailing edge where the honeycomb core was dropped off because there was not enough depth between upper and lower surfaces to allow its continuation, resulting in a reduction in panel stiffness. In a new design, the core could be feathered, rather than stopping short, or the area could be supported by a web between the two skins.

15.7.3.2 Transfer Ducting

The geometry of the trailing edge and aileron necessitates the transfer of air from the aft low volume ducts and non-continuous ducts (in the aileron and outboard of the aileron) into the larger, more forward ducts. On the X-21A, this transfer is accomplished through nozzles, the most complex of which are shown in Figure 15.10.

15.7.3.3 Movable Surfaces

One of the objectives of the X-21A program was to demonstrate the attainment of laminar flow across a movable surface such as an aileron or flap in a range of low deflections. In order to accomplish this, the aileron hinge area had to be designed so that it would remain fair and sealed to the adjacent trailing structure. Any leakage of air from lower to upper surface through the hinge would upset the boundary layer and cause turbulence

ENGINEER	NORTHROP CORPORATION NORAIR DIVISION	PAGE 15.13
CHECKER		REPORT NO. NOR 67-136
DATE June 1967		MODEL X-21A

15.7.3.3 Movable Surfaces (Cont'd.)

from there aft. The design of the hinge area is shown in Figure 15.11.

The aileron hinge is of the continuous type and is on the upper surface. A continuous hinge was chosen over individually-spaced hinge points to prevent differential deflections between aileron and trailing structure which would result in steps in the surface. The hinge and its attachment to the trailing structure were designed to be flexible so that the hinge could roll and still remain relatively fair with the surface whenever the aileron is deflected while the wing is bent by flight loads. The hinge is sealed against air leaks by a flap of rubber attached to the trailing structure, and wiping the aileron spar so that any pressure difference which tends to cause outflow through the hinge will force the seal up tight and prevent the outflow. Laminar flow was achieved over part, but not all, of the span of the aileron upper surface.

The lower surface of the original design was faired and sealed by a thin steel wiper overhung from the trailing structure and riding on the leading edge radius of the aileron. The trailing edge of the thin steel wiper was wavy rather than straight and thus unsatisfactory. During the flight test program, the thin steel wiper was replaced with a thicker aluminum strip, which was in effect an extension of the aluminum skin farther forward. The aft edge of the aluminum strip was beveled to minimize the step height at contact with the aileron. The aluminum strip was much straighter than the steel wiper, resulting in laminar flow across the lower surface of the aileron in the revised area. The original rather than the revised wiper strip is shown in Figure 15.11. The revised aileron wiping seal and an example of the laminarization across the revised strip are shown in Figure 15.12.

The aileron actuator is mounted externally because burying it within the trailing structure would have meant considerable compromise of the internal ducting. In future designs, it may be possible to put the actuators inside without compromising the ducts if the trailing edge structure is of a type similar to that of the X-21A main box. This placement would make maintenance on the actuator considerably more difficult, however, since access would be through two levels of doors (airfoil surface and inner duct walls).

ENGINEER	NORTHROP CORPORATION NORAIR DIVISION	PAGE 15.14
CHECKER		REPORT NO. NOR 67-136
DATE June 1967		MODEL X-21A

15.7.3.3 Movable Surfaces (Cont'd.)

The incorporation of flaps on a future design may be accomplished in a manner similar to the X-21A aileron if the flaps used are the simple drooped trailing edge type.

The aileron structure is of conventional type consisting of upper and lower skins, a front spar, ribs and two auxiliary spars (one full span and one partial span). The ribs are used to break the aileron up into suction areas, each area having its own take-off duct and transfer nozzle. The upper and lower surfaces are not isolated from each other but are sucked directly into the same duct. The air sucked off the aileron surfaces is ducted forward through the aileron front spar, through bellows ducts into a transfer nozzle which exhausts into the trailing suction duct immediately forward of the aileron. Access to these ducts is provided by making the lower wiper seal removable.

15.7.4 Outer Skin Panel Splices and Access Panels

15.7.4.1 Chordwise Splices - Original X-21A Design

In addition to normal design requirements for outer skin panel splices, the addition of LFC also imposes the design criteria of continuity of slots, suction holes and plenum chambers (i.e., suction system continuity) across joints.

A typical double shear type splice is shown in Figure 15.13 with attachments flush in the outer splice plate. Plenum chambers are milled in the outer splice plate, suction holes are drilled through the splice plates and panels, and slots are sawed in the light cover skin which is cold-bonded to the outer splice plate subsequent to assembly of the joints.

An alternate version, used primarily for door panel attachments, has fasteners installed after bonding of the cover skin and subsequently filled and smoothed with a suitable putty-like sealant.

ENGINEER	NORTHROP CORPORATION NORAIR DIVISION	PAGE 15.15
CHECKER		REPORT NO. NOR 67-136
DATE June 1967		MODEL X-21A

15.7.4.1 Chordwise Splices - Original X-21A Design (Cont'd.)

Interference fit fasteners are used for fixed splices to keep joint deflection to a minimum and to ensure maximum fatigue life. From a manufacturing standpoint, it is not practical to join the panels with no gap at the outer skins. Therefore, filled gaps must be provided. These gaps are filled and slots are sawed through the filler material. In order to provide for joint deflections under load, and to maintain slot continuity and surface smoothness, thin "slits" are provided at the joint. "Slits" are provided by installing shim stock coated with the proper parting agent into the gaps prior to injecting an epoxy-type putty and removing the shims after curing of the putty. The filler material is sanded to the proper surface smoothness and slots are sawed through the gap filler material.

The maximum permissible width of filler gaps is governed by the maximum allowable length of a plenum chamber which is only as wide as the slot and as deep as the normal plenum chamber. Consideration must be given to the fact that installation of putty-consistency filler material will block the plenum chamber in the panel for approximately .10 inch (when slit is oriented on splice plate side of gap as shown in Figure 15.13). The minimum width of gap to be filled is governed by the practical considerations of filling the gap and providing the slit.

Suction slot location and spacing design requirements are closely related to the structural design requirements at the outer skin panel chordwise splices. The location of slots immediately adjacent to stringers and spar caps is governed by fastener and flange width requirements at the stringer and spar cap splices. The minimum slot-spacing between stringers is governed by the fastener diameters and types required for the skin panel and the tributary duct configuration adopted.

15.7.4.2 Suggested Revision to Chordwise Splices

The flight test program showed that the chordwise splices as originally designed are a source of boundary layer disturbance and are not entirely satisfactory for the LFC airplane. As a result,

ENGINEER	NORTHROP CORPORATION NORAJR DIVISION	PAGE 15.16
CHECKER		REPORT NO. NOR-67-136
DATE June 1967		MODEL X-21A

15.7.4.2 Suggested Revision to Chordwise Splices (Cont'd.)

a relatively simple improvement to the chordwise splice was designed and was flight tested on the X-21A airplane and found to be structurally satisfactory. The improvement is a spanwise overlap of the outer skin of the splice strip, with the overlap portion bonded onto the mating panels. The outer skin of the splice strip then takes part of the loads and deflections of the joint and reduces the size and deflections of the surface gap between the panel and the chordwise splice strip. A sketch of the improved joint is shown in Figure 15.14. Additional research and development of the improved splice, including fatigue testing, are recommended before it is applied to a new LFC wing design.

Another, obvious, way to reduce the problem of chordwise splices in a new LFC wing design is to make the panels as long as possible, thereby minimizing the number of chordwise splices.

15.7.4.3 Spanwise Splices

Surface waves of appreciable magnitude were created at the spanwise splices of the surface panels at the front and rear spars of the X-21A airplane because of difficulty in matching the contour and surface height of the edges of the mating panels. Recommendations for improved spanwise splice joints include making the panels oversize and then cutting off the flat edge region, thereby providing the proper surface curvature at the edge of the panel. Another improvement is machining the mating overlap portion after bonding instead of before bonding. A third improvement is the application and curing of plastic or liquid shims on final assembly while the panels are held in place against contour boards. The last improvement described is shown in the sketch of a panel joint in the front spar region in Figure 15.15.

The deflections of the surface gap of the spanwise splice are believed to be no problem to laminarization because, in contrast to the chordwise splices, no suction slots cross the spanwise splices.

ENGINEER	NORTHROP CORPORATION NORAIR DIVISION	PAGE 15.17
CHECKER		REPORT NO. NOR 67-136
DATE June 1967		MODEL X-21A

15.7.4.4 Access Panels

The general LFC requirements for access panels on the suction surfaces are the same as those of the fixed chordwise and spanwise splice joints. Therefore, the suggestions of the preceding paragraphs should be incorporated in the design of access panels, as far as possible. The removable panels on the X-21A wing lower surface, as shown in Figures 15.2 and 15.3, usually appeared to be satisfactory; but they may be subject to improvement, as were the fixed panel joints.

15.7.5 Compressor Pod and Dry Bay Area

In the region of the compressor pods, dry bays are required in which air from the stringer suction ducts must be transferred to the low pressure and high pressure mixing chambers. On the X-21A this was achieved by means of transfer ducts which attach to "duct outlet" panels. The "duct outlet" panels are removable inner panels which have cutouts between each stringer permitting the required air transfer.

"Deflectors" and "splitters" were required to direct the airflow into the transfer ducts and also to separate the flow between the outboard stringer ducts and inboard stringer ducts. The deflectors and splitters are notched around tributary ducts and tributary duct ramps, and are cold-bonded to the outer skin panel. Gaps around the periphery of the stringer ducts are sealed to withstand a pressure differential approximately 2 psi in order to prevent spanwise flow between stringer ducts. Tributary duct ramps are provided locally in the area of the splitters to direct the airflow into the transfer ducts. Local fairing strips are cold-bonded to the duct outlet panels and stringer inner flanges to prevent flow disturbances in the duct transfer areas caused by sharp edges or nutplates and bolt protrusions into the ducts. Rigid polyurethane blocks, notched to clear obstructions, were used for this purpose on the X-21A (refer to Figure 15.16).

Large cutouts are provided in both the front and rear spar webs to allow transfer of the suction air aft to the compressor. Shear continuity for the spars was maintained by normal methods of local web reinforcement, thick plate design, or local truss work.

ENGINEER	NORTHROP CORPORATION NORAIR DIVISION	PAGE 15.18
CHECKER		REPORT NO. NOR 67-136
DATE June 1967		MODEL X-21A

15.7.5 Compressor Pod and Dry Bay Area (Cont'd.)

For assembly and installation requirements, the transfer ducts are split at the spar webs to simplify installation.

The basic design concepts used in the compressor pod and dry bay areas of the X-21A, as described above, are considered adequate for further applications. Minor revisions, however, are in order to improve accessibility to valves and other equipment stored in this area.

15.7.6 Integral Fuel Tank Inspection

The requirement of an LFC wing to have spanwise suction ducts immediately beneath the outer skin panels causes the upper and lower boundaries of a wing integral fuel tank to be some distance from the outer mold lines and, therefore, not externally visible. The normal fuel tank check-out methods (i.e., internal pressurization of the fuel tank, along with the use of bubble solution to obtain a visual inspection) cannot be used to inspect the upper and lower boundaries of an LFC wing.

It is necessary, therefore, to employ some other method of inspection to check the sealing integrity of an LFC wing integral fuel tank. One such method, which was used on the X-21A wing, is a no pressure drop test over some selected period of time. The first step is to pressurize the tank to a pressure within the safe limits of the structure and visually inspect the periphery of the tank (spars and end ribs) with bubble solution. This procedure is repeated until all leaks on the periphery of the tank have been located and repaired. The tank is then pressurized to a pressure compatible with the fuel system operating pressure and held for the previously selected period of time. If the tank shows a pressure drop indicating a leak, it is necessary to inspect the upper and lower boundaries. This is done by covering the slots on the outer surface of the wing and pressurizing the spanwise suction ducts to a pressure within the safe limits of the structure. Using bubble solution visually inspect the interior of the tank to locate and repair all leaks. The no pressure drop stand test can then be repeated to verify that all leaks have been found and repaired.

A valuable aid to inspection in checking out an LFC wing fuel tank is a "sniffing" device capable of detecting the presence of carbon tetrachloride or similar vapors. By introducing such a compound into the fuel tank under pressure, and "sniffing" along the slots on the exterior surface, leak indications can be localized. A similar device capable of

ENGINEER	NORTHROP CORPORATION NORAIR DIVISION	PAGE 15.19
CHECKER		REPORT NO. NOR-67-136
DATE June 1967		MODEL X-21A

15.7.6 Integral Fuel Tank Inspection (Cont'd.)

detecting a combustible gas or vapor is useful to find fuel tank leaks after the airplane has reached operational status.

Based on the results of the X-21A program, it is concluded that similar inspection techniques would be adequate for operational aircraft.

15.7.7 Inspection, Maintenance and Environmental Protection

A part of the X-21A program was an investigation to determine the internal accessibility, inspection and maintenance requirements for an LFC type aircraft. Among the things learned on this investigation was the problem being encountered by users of jet transport aircraft in regard to the deterioration of honeycomb assemblies after reaching a service life approaching 10,000 hours. The deterioration of these assemblies consists of core-to-skin delaminations and corrosion of the aluminum core, resulting from a collection of water and moisture within the honeycomb.

Since aluminum honeycomb assemblies were used extensively on the X-21A airplane wing, it is necessary to afford corrosion protection for the assemblies. The decision was reached that chromic acid anodization of the completed assemblies would provide the necessary protection for the time span of this program. It should be noted that the anticipated flight test life of the two modified RB-66 airplanes used on this program was 500 hours and that the flight test program of these airplanes has been Edwards Air Force Base; a dry, low humidity area which is, therefore, not representative of a wide range of operational conditions.

It is necessary to be cognizant of the fact that there are areas, relative to the use of aluminum honeycomb, which require continuing investigation when talking in terms of an operational aircraft. Additional research is required to determine the most reliable means of protection of aluminum core from corrosion. The reliability of current and new adhesive systems and sealants in preventing inter-cell passage of moisture when subjected to an operational environment also requires further investigation.

ENGINEER	NORTHROP CORPORATION NORAIR DIVISION	PAGE 15.20
CHECKER		REPORT NO. NOR 67-136
DATE June 1967		MODEL X-21A

15.8 STRUCTURAL TESTS

Following is a description of the structural component tests which were made to substantiate analytical data used in the design and analysis of the structure of the X-21A airplane. The philosophy and scope of the test program took into consideration the fact that the airplanes were to be used only as test vehicles, with limitations on service life and operational use. It is recognized that the structural component tests on a production airplane would be considerably more extensive. The test program consisted of the following types of tests.

15.8.1 Wing Test Box

A wing test box, typical of the actual wing main box structure in the vicinity of the pumping pod, was fabricated. It consisted of upper and lower cover assemblies, spars and ribs. The cover assemblies consisted of outer and inner covers separated into three main bays by ribs. Two bays were fuel bays, and one end bay was a dry bay. The lower cover assemblies contained access doors, and both cover assemblies, including the stringers and spars, contained chordwise splices in the dry bay. The upper cover assembly contained a spanwise splice along a stringer and the lower cover assembly contained spanwise splices along the access door edges. The ends of the box were heavily reinforced to allow the introduction of a concentrated bending moment and torsion.

Prior to the ultimate strength test, a surface smoothness test and several fuel tank leakage tests were made. The ultimate strength test resulted in a failure at 86% of the ultimate bending moment. The failure was a buckle across the entire width of the outer compression cover just outboard of the splice along the transition line of honeycomb to solid material. It was concluded that this failure was a result of the splice eccentricity causing an overloading of the inner facing. As a result, design changes were made to reduce eccentricities at the splice, to add doublers to the inner face at this local critical area, and to change the geometry along the edge member to provide a scalloped contour along the edge member to honeycomb core intersection rather than the original straight line. Subsequent tests of panels with and without the design change showed that the design change was adequate.

ENGINEER	NORTHROP CORPORATION NORAIR DIVISION	PAGE 15.21
CHECKER		REPORT NO. NOR 67-136
DATE June 1967		MODEL X-21A

15.8.2 Inboard Wing Cover Assembly Beam Column Panel Tests

Panels typical of the inboard wing main box upper cover assembly were tested as beam columns. These panels consisted of an outer and inner cover separated by stringers. Each panel contained three stringers dividing the panels into two spanwise bays. In the actual wing the cover assembly is subjected to beam column type loading resulting from the effect of wing curvature and intermittent support provided by ribs. This type of loading was simulated in the panel tests by inducing curvature into the panel during the application of axial load. The curvature was induced by applying loads normal to the panel at simulated rib cap locations and reacting this load at the panel ends through a loading fixture, which provided simple support at each end of the panel. The curvature was calculated to provide a secondary bending moment which, when combined with the primary axial stress, would cause failure midway between the simulated rib supports. The first panel was loaded to 100% of the ultimate test load without failure. At this point the test was stopped to make an adjustment to the supporting jig. Upon retesting, the panel failed by buckling of the cover at 87% of the ultimate test load. The failing load is not particularly significant because the panel already had carried 100% design load without failure. The second panel failed in the same manner at 107% of the ultimate test load.

15.8.3 Inboard Wing Cover Assembly Beam Column Splice Tests

These panels were similar to the panels described above except that the outer cover contained a chordwise splice. Four panels were tested, two of which incorporated the splice design utilized on the previously mentioned test box and two of which utilized the redesigned splice. These panels were tested as beam columns in the manner described above. The failures in the panels with the test box splice duplicated closely the test box failure. The panels with the redesigned splice failed in the basic panel away from the splice. The redesigned panels carried more than 100% ultimate load without failure.

15.8.4 Main Box Inner Cover Compression Panels

These panels were typical of the inboard wing inner main box cover. In the actual wing these covers are subjected to fairly high normal pressure resulting from fuel and air pressure, as well as axial load resulting from wing bending. To simulate this loading, these panels were tested under

ENGINEER	NORTHROP CORPORATION NORAIR DIVISION	PAGE 15.22
CHECKER		REPORT NO. NOR 67-136
DATE June 1967		MODEL X-21A

15.8.4 Main Box Inner Cover Compression Panels (Cont'd.)

combined normal pressure and axial load. The panels were simply supported by knife edge fixtures at the loaded ends and by vee groove blocks along the unloaded sides. One of the matters of interest in conducting these tests was to determine how well the facing stresses could be predicted using a method involving a so-called "magnification factor" developed in several different texts.

$$m = \frac{1}{1 - \frac{f_c}{F}} \text{ and } f'_{x,y,xz, \text{ or } yz} = m f_{x,y,xz, \text{ or } yz}$$

Where: m = magnification factor

f_c = applied compression stress

F = allowable buckling stress

f_x = stress due to normal load only

f'_x = stress due to normal load with axial load present

Two panels were tested and both failed at well over the predicted failure load. As a result of these two tests, it was concluded that the use of the magnification factor for panels of aspect ratio three or above is quite conservative.

15.8.5 Vee Stringer Tests

Vee stringers were used to provide shear continuity between the rib caps and the outer cover. To determine the ability of the vee stringers to make this shear transfer, tests were run on several four-inch lengths of stringer attached to a short length of inner cover and rib cap. As a result of these tests, it was determined that yielding of the Jo-bolt collars, which attach the stringer flanges to rib caps, was the critical item in the design and that the design was more than adequate to ensure that the entire section worked as a continuous structure.

ENGINEER	NORTHROP CORPORATION NORAIR DIVISION	PAGE
CHECKER		15.23
DATE		REPORT NO. NOR 67-136
June 1967		MODEL X-21A

15.8.6 Trailing Edge Panel Compression Tests

Two compression panels, typical of the trailing edge cover in the outboard wing region, were tested. These tests were made to substantiate the method of analysis for lighter gauge panels. The panels had an aspect ratio of four and were clamped along the loaded (short) edges and simply supported by vee groove blocks along the unloaded (long) edges. The panels failed by buckling slightly below the predicted value, but above the required value.

Two panels containing a typical trailing edge chordwise splice were tested. These panels were similar to the trailing edge compression panels described previously and were loaded in the same manner. Both panels failed by buckling of the basic panel away from the splice.

15.8.7 Trailing Edge Panel Column Tests

Column tests were made on three-inch wide chordwise strips taken from a panel having the same configuration as the compression panels mentioned above. Since the trailing edge structure acts as a continuous rib, the cover panels under some conditions are subjected to chordwise compression loads. These tests were run to determine the effect of the slotted skin for chordwise column type loading. The result of these column tests showed that neglecting the slotted skin completely in computing the column section properties is only slightly conservative.

15.8.8 Aileron Hinge Test

A test of the continuous aileron piano hinge fitting was made to determine the interaction effects between the deflected aileron and the wing trailing section. This test was made using a production aileron mounted on a steel beam having provisions for inducing a controlled curvature. With a curvature corresponding to an actual limit flight condition, the aileron was deflected to the full up and down positions. The hinge loads determined by measuring hinge deflection were slightly less than the predicted values. Aileron hinge moments due to friction at maximum load and deflection were low.

15.8.9 Coupon Fatigue Tests

A series of fatigue test coupons of typical cover panels, incorporating holes and slots, were tested and results showed that the stress concentration factors were less than 4.0, which is comparable to conventional structure. It is, therefore, concluded that there would be no penalty for LFC type structure due to fatigue considerations.

ENGINEER	NORTHROP CORPORATION NORAIR DIVISION	PAGE 15.24
CHECKER		REPORT NO. NOR 67-136
DATE June 1967		MODEL X-21A

15.9 REFERENCES

1. Northrop Norair Report NOR 61-142, LFC Manufacturing Techniques, March 1964, by LFC Manufacturing Engineering, J. W. Quick, Director.

FRONT SPAR
REF. PLANE

MAIN STRUCTURAL BOX

SPANWISE SUCTION DUCTS

UPPER
WING

LOWER
WING

INTEGRAL FUEL TANK

FUEL TANK
ACCESS PANEL

PAGE	15.25
REPORT NO.	NOR 67-136
MODEL	X-21A

TYPICAL CROSS-SECTION-WING MAIN BOX

FIGURE 15.1

NOTE THE WING NOSE STRUCTURE SHOWN APPLIES TO THE OUTBOARD WING. A "SCAB-ON" SECTION WITH CHORDWISE SLOTS IN THE FLOW-ATTACHMENT ZONE WAS ADDED TO THE INBD WING NOSE OF AF 55-410A AS SHOWN IN FIG. 15.9 A REVISED LEADING EDGE STRUCTURAL ARRANGEMENT IS SHOWN IN FIG 15.8

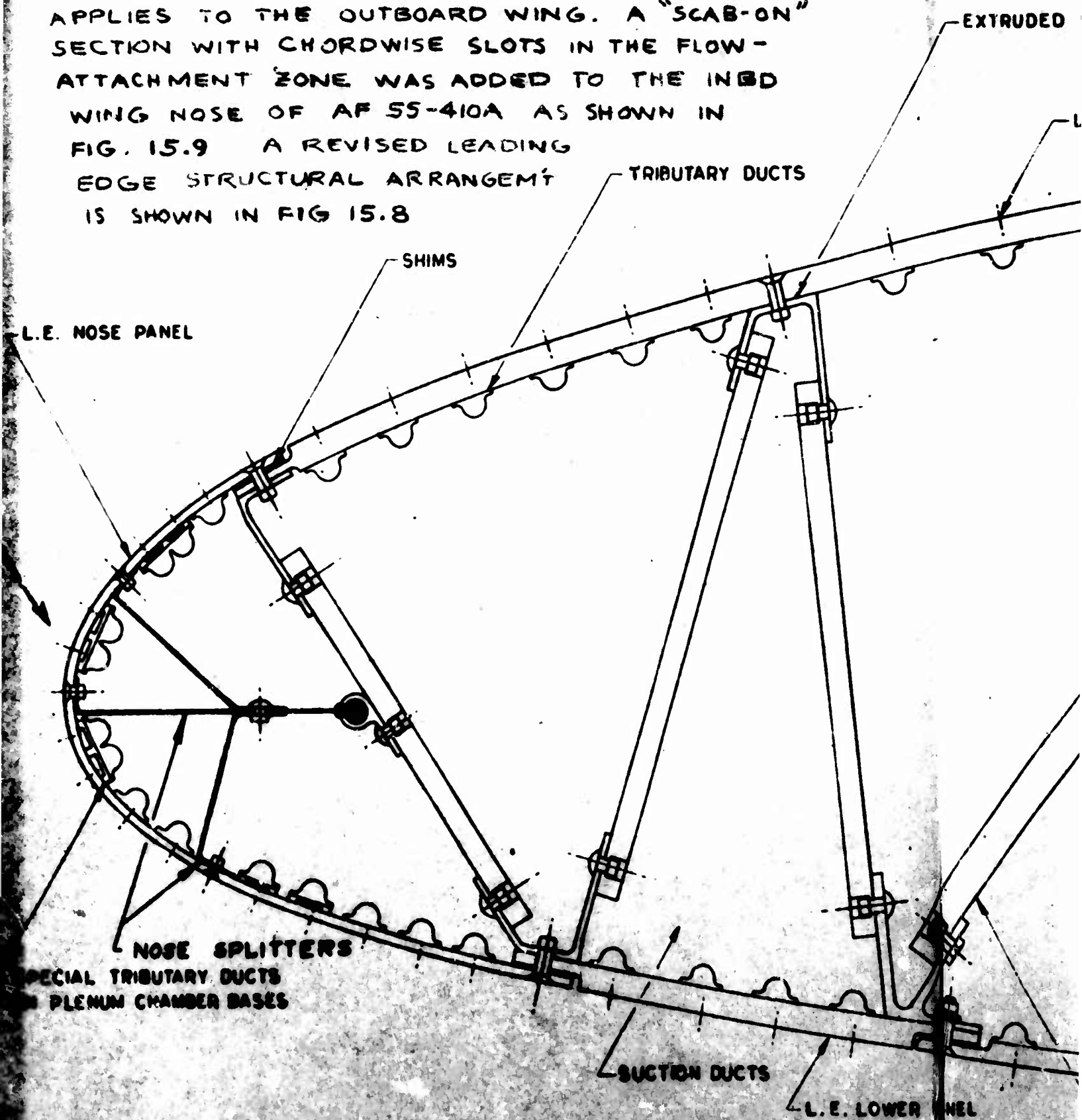
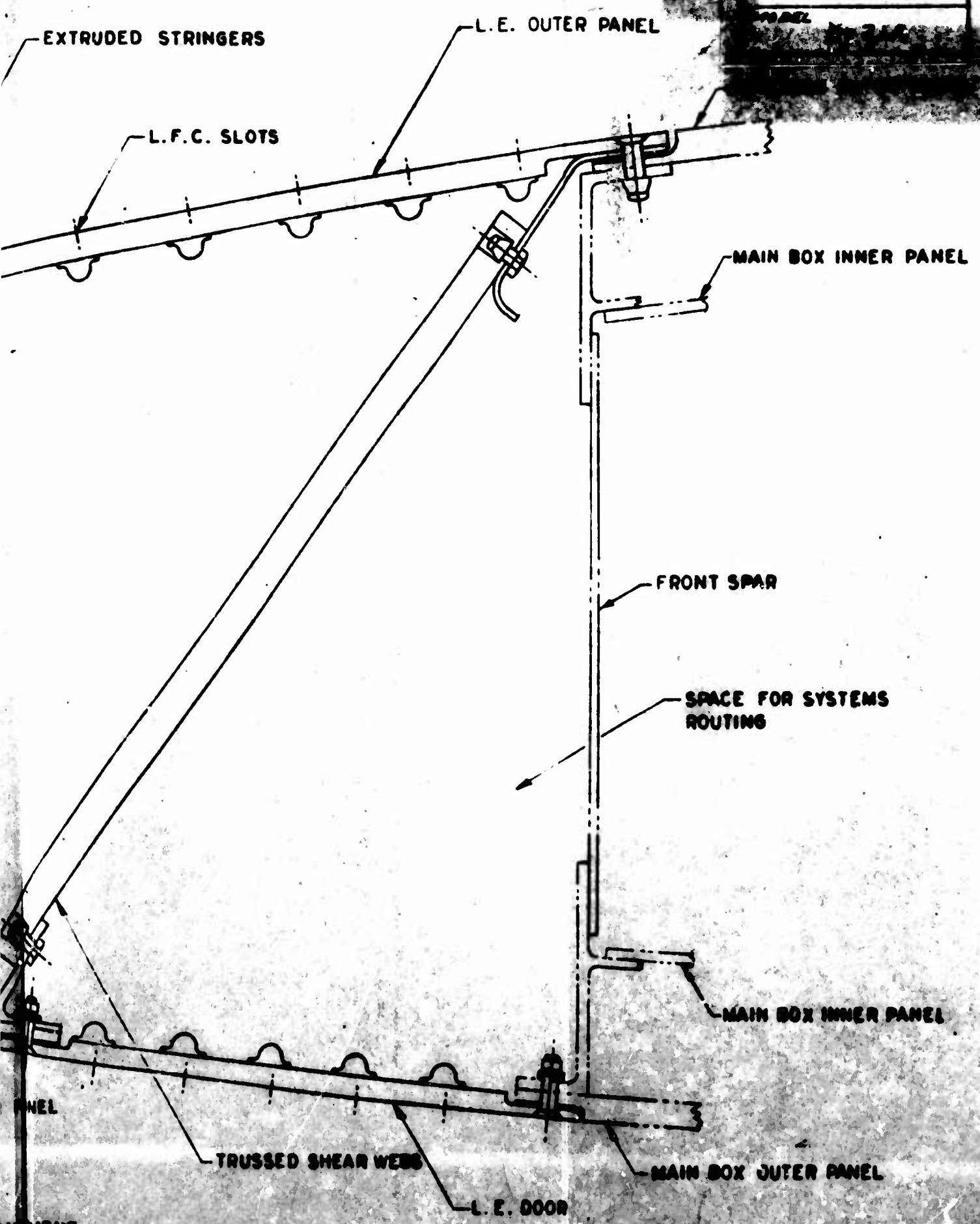


FIGURE 15.2
GENERAL STRUCTURAL ARRANGEMENT
OF THE X-21A LEADING EDGE

15.26
NDR 67-136



2

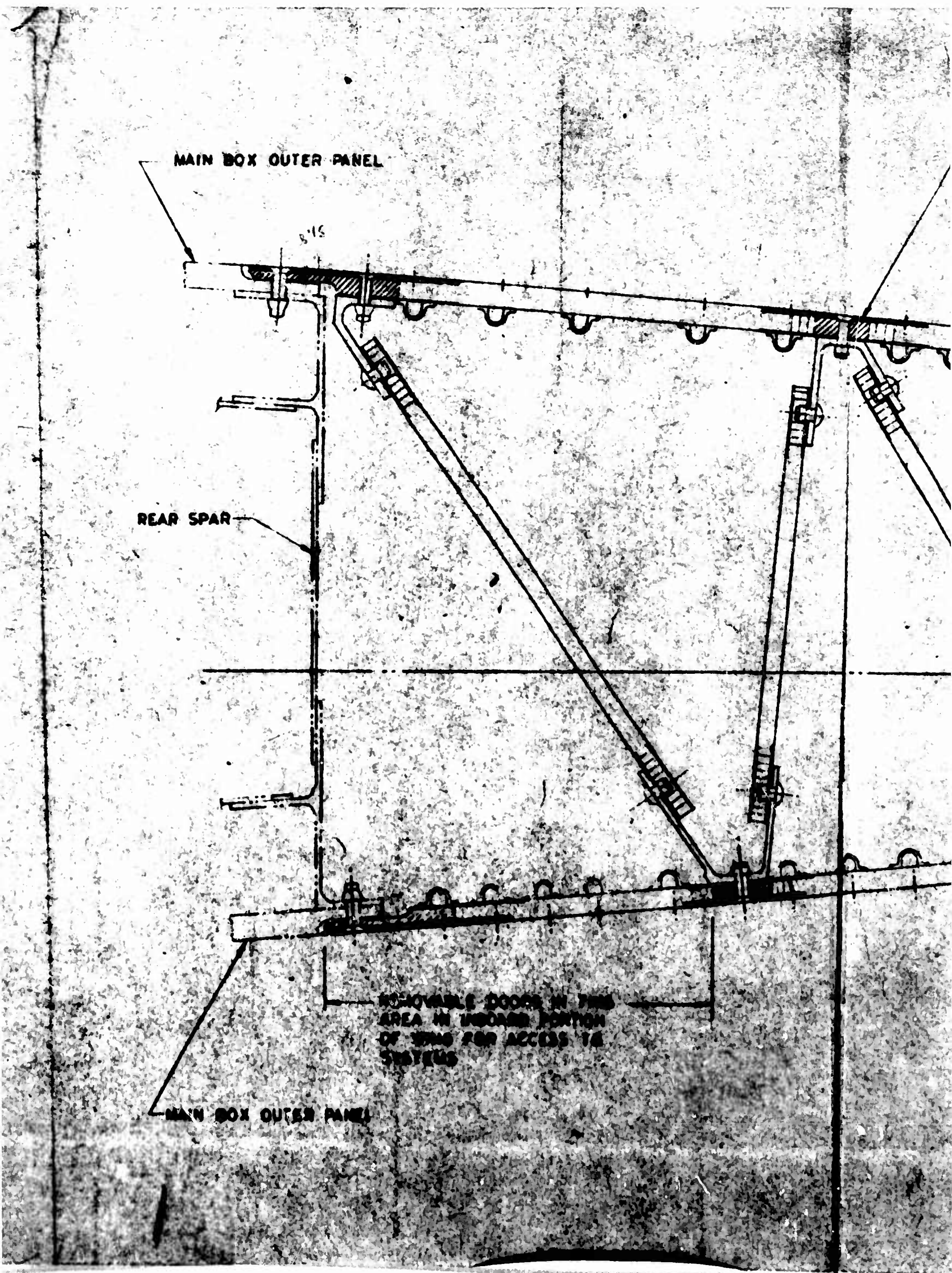
MAIN BOX OUTER PANEL

8.15

REAR SPAR

REMOVABLE DOORS IN THIS
AREA IN INSIDE PORTION
OF WING FOR ACCESS TO
SYSTEMS

MAIN BOX OUTER PANEL



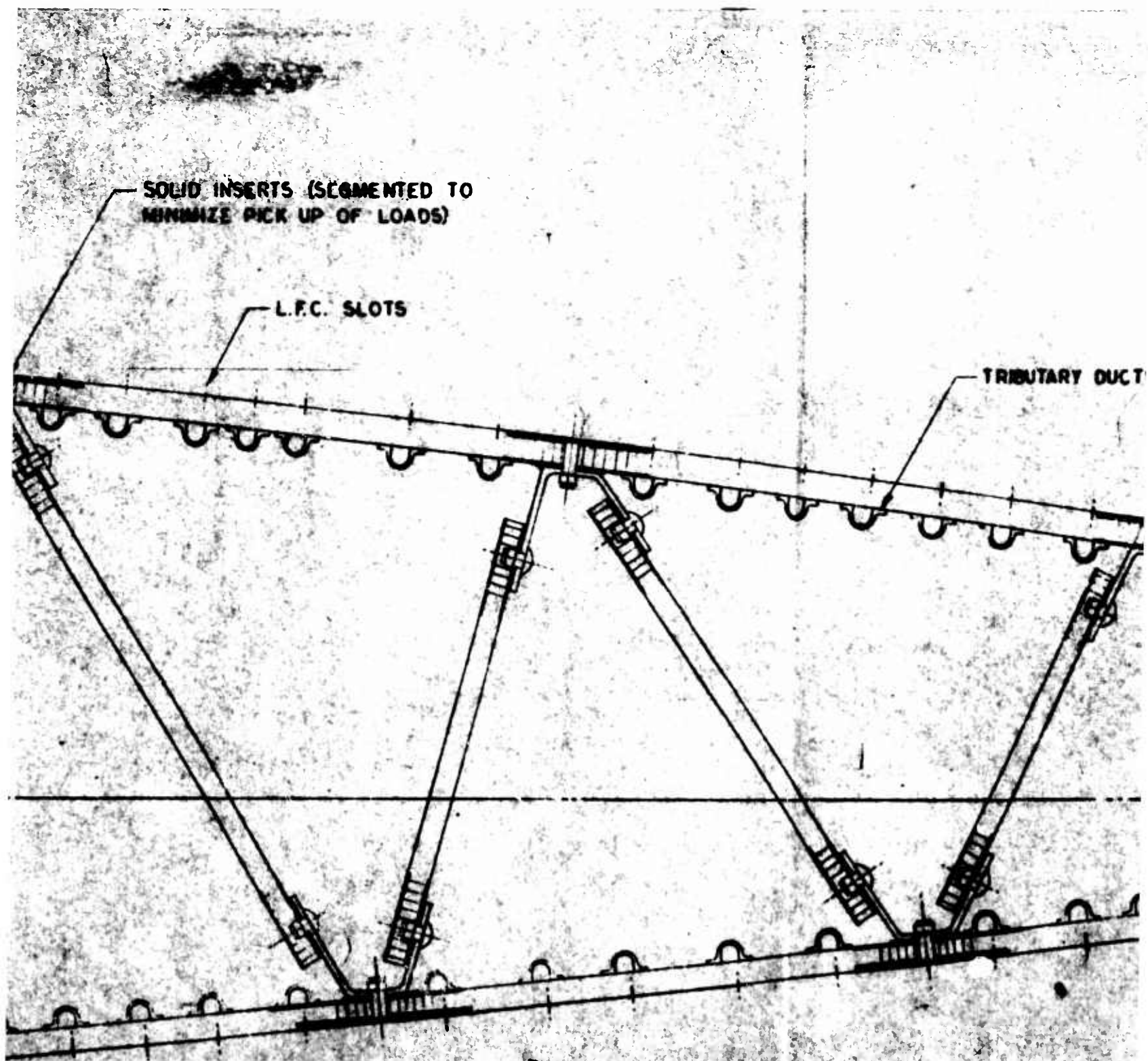
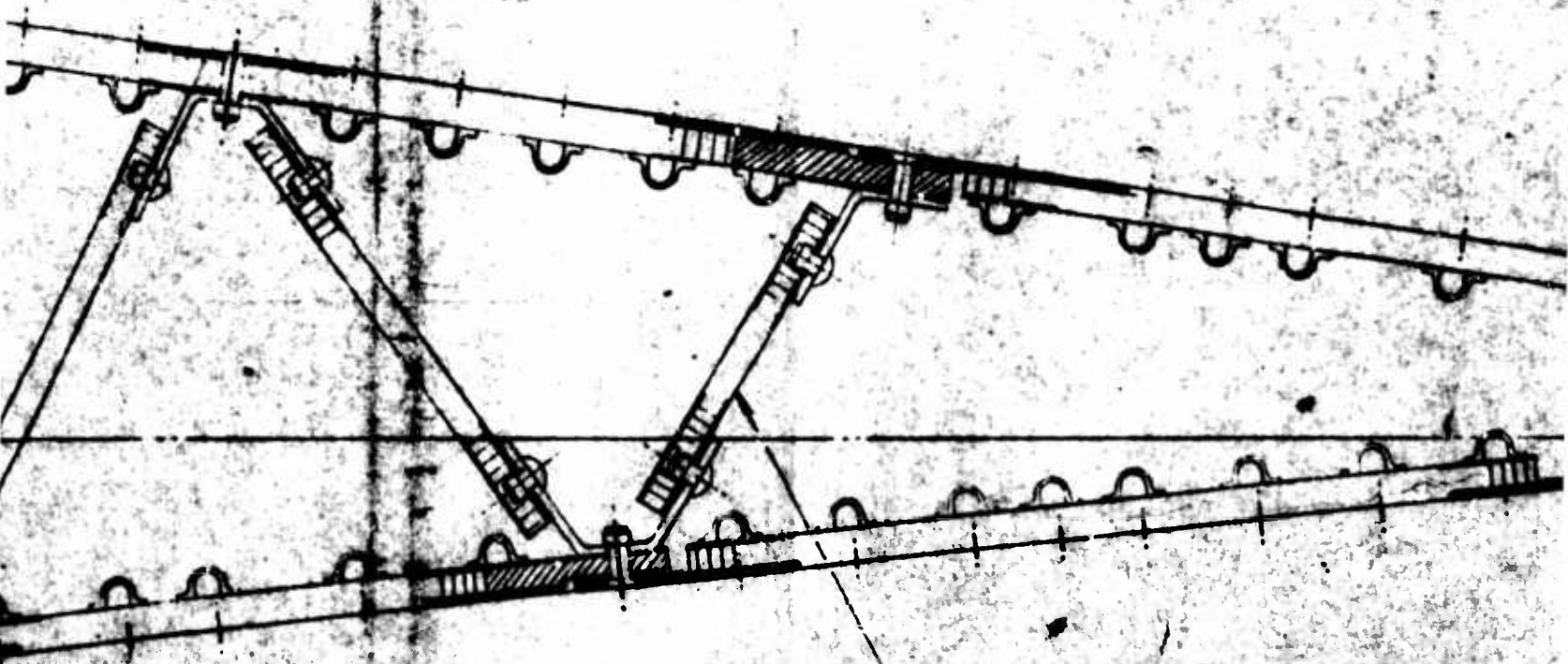


FIGURE 15.3

GENERAL STRUCTURAL ARRANGEMENT
OF THE A-BA TRAILING EDGE

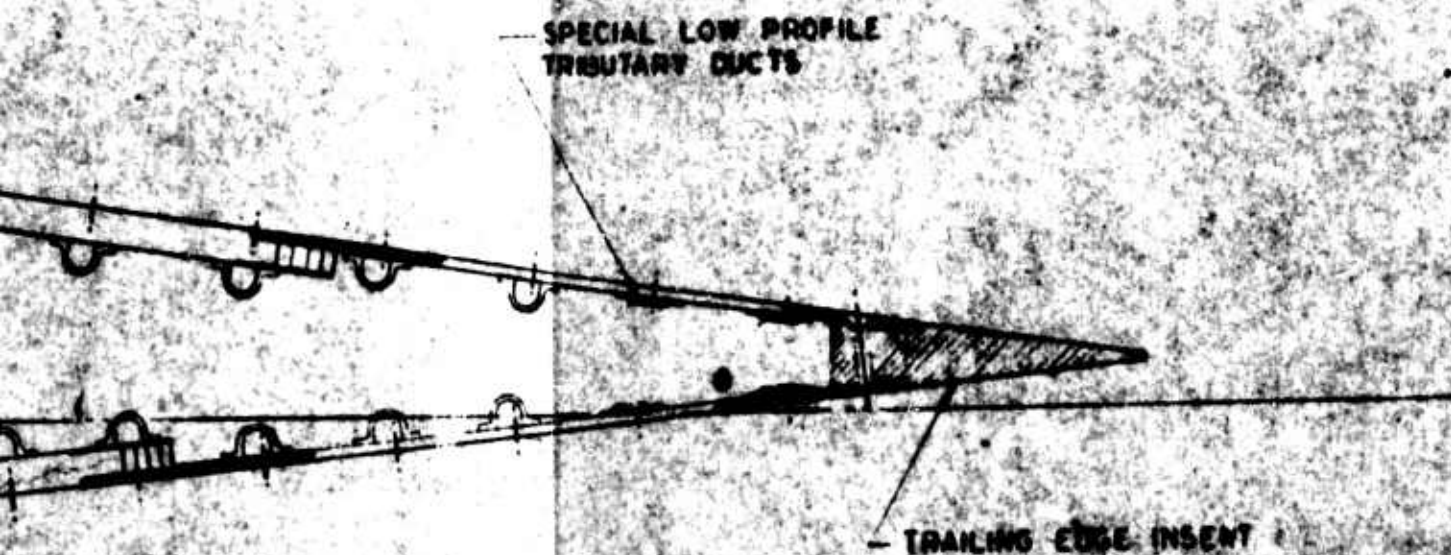
TRIBUTARY DUCTS

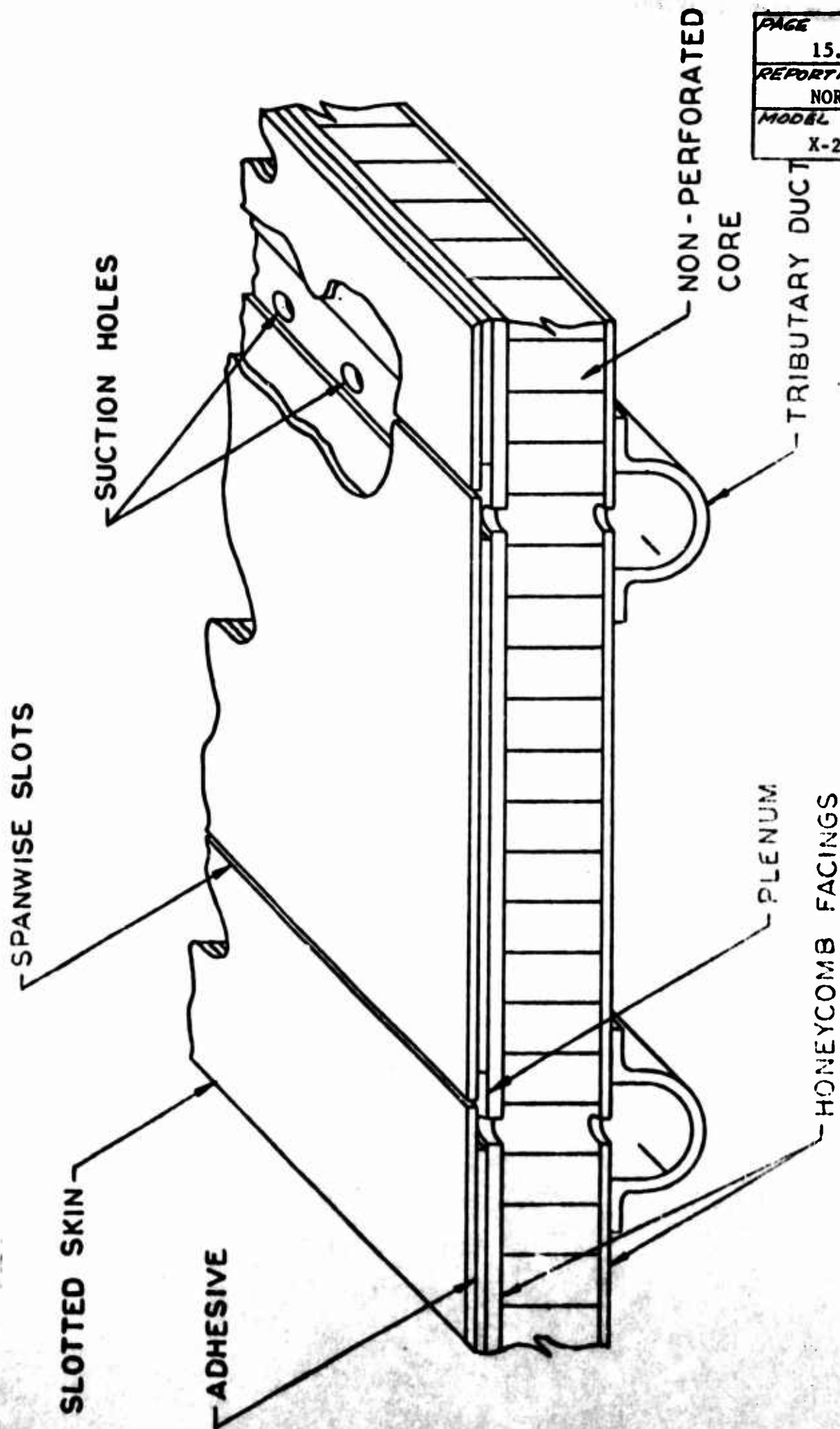


TRUSSED SHEAR WEBS

15.27
NDA 67-136
X-21A

FIG 15.3

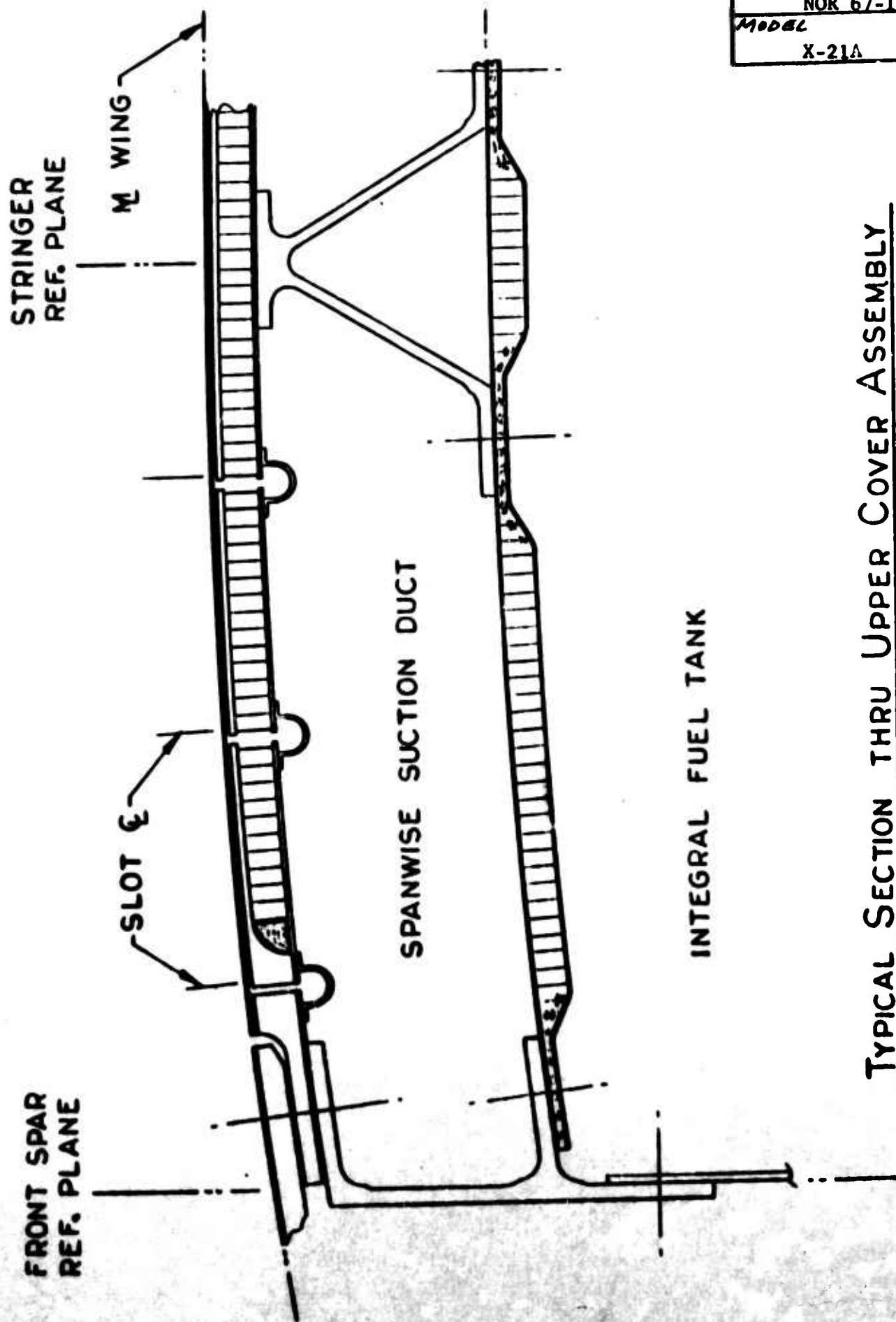




PAGE	15.28
REPORT NO.	NOR 67-136
MODEL	X-21A

TYPICAL OUTER SKIN PANEL CONSTRUCTION

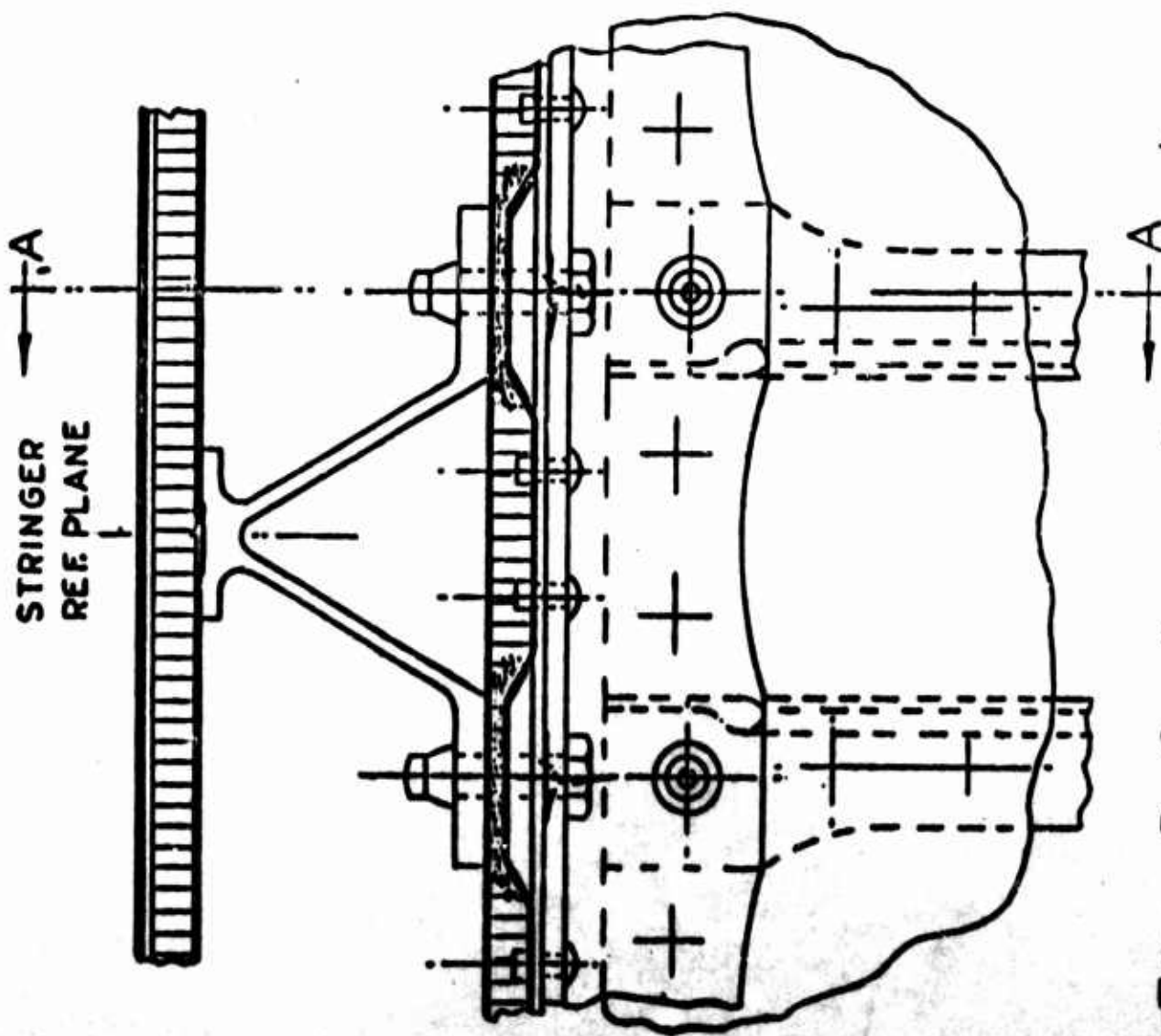
FIGURE 15.4



PAGE	15.29
REPORT NO	NOR 67-136
MODEL	X-21A

TYPICAL SECTION THRU UPPER COVER ASSEMBLY

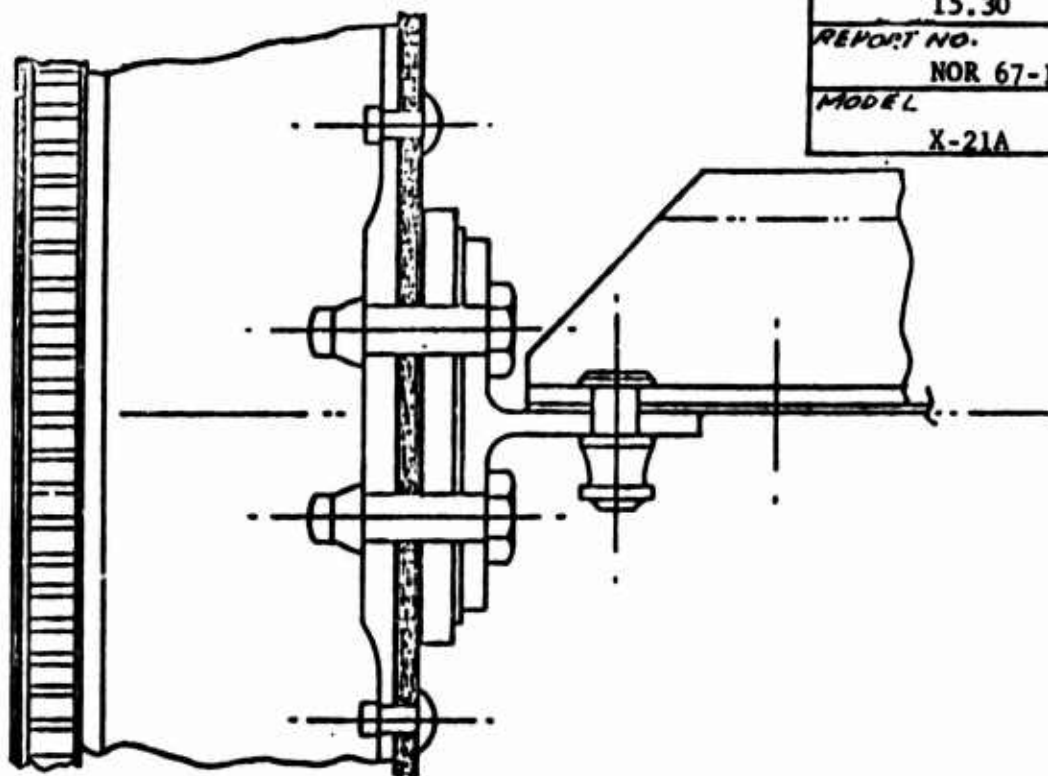
FIGURE 15.5



TYPICAL RIB CAP-STRINGER CONNECTION

(INDICATES TORSIONAL SHEAR TRANSFER)

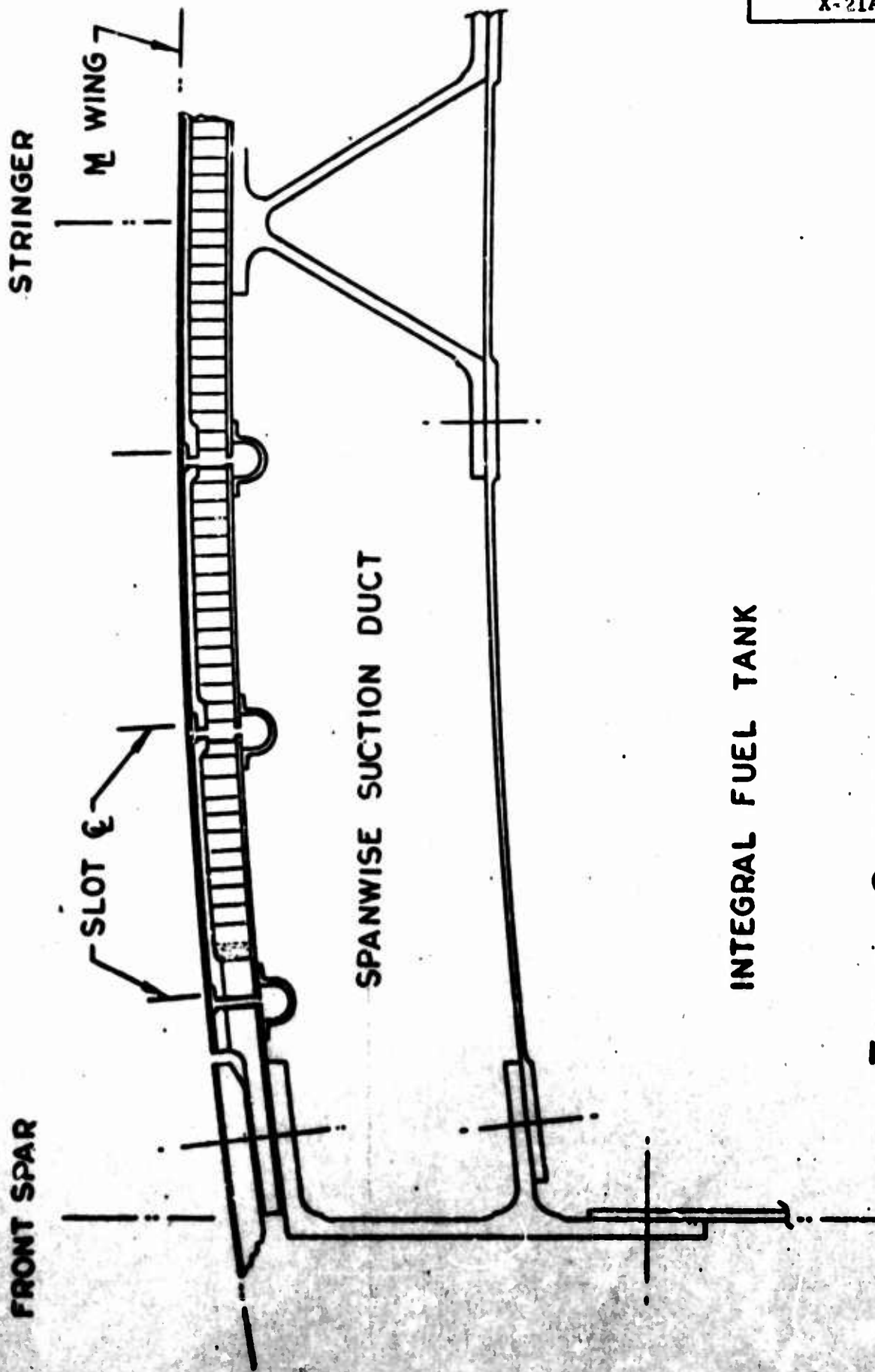
RIB REF.
PLANE



SECTION A-A

PAGE	15.30
REPORT NO.	NOR 67-136
MODEL	X-21A

FIGURE 15.6 VEE STRINGER DETAILS



PAGE	15.31
REPORT NO.	NOR 67-136
MODEL	X-21A

TYPICAL SECTION THRU UPPER COVER ASSEMBLY
(ALTERNATE DESIGN OF SKIN PANELS)

FIGURE 15.7

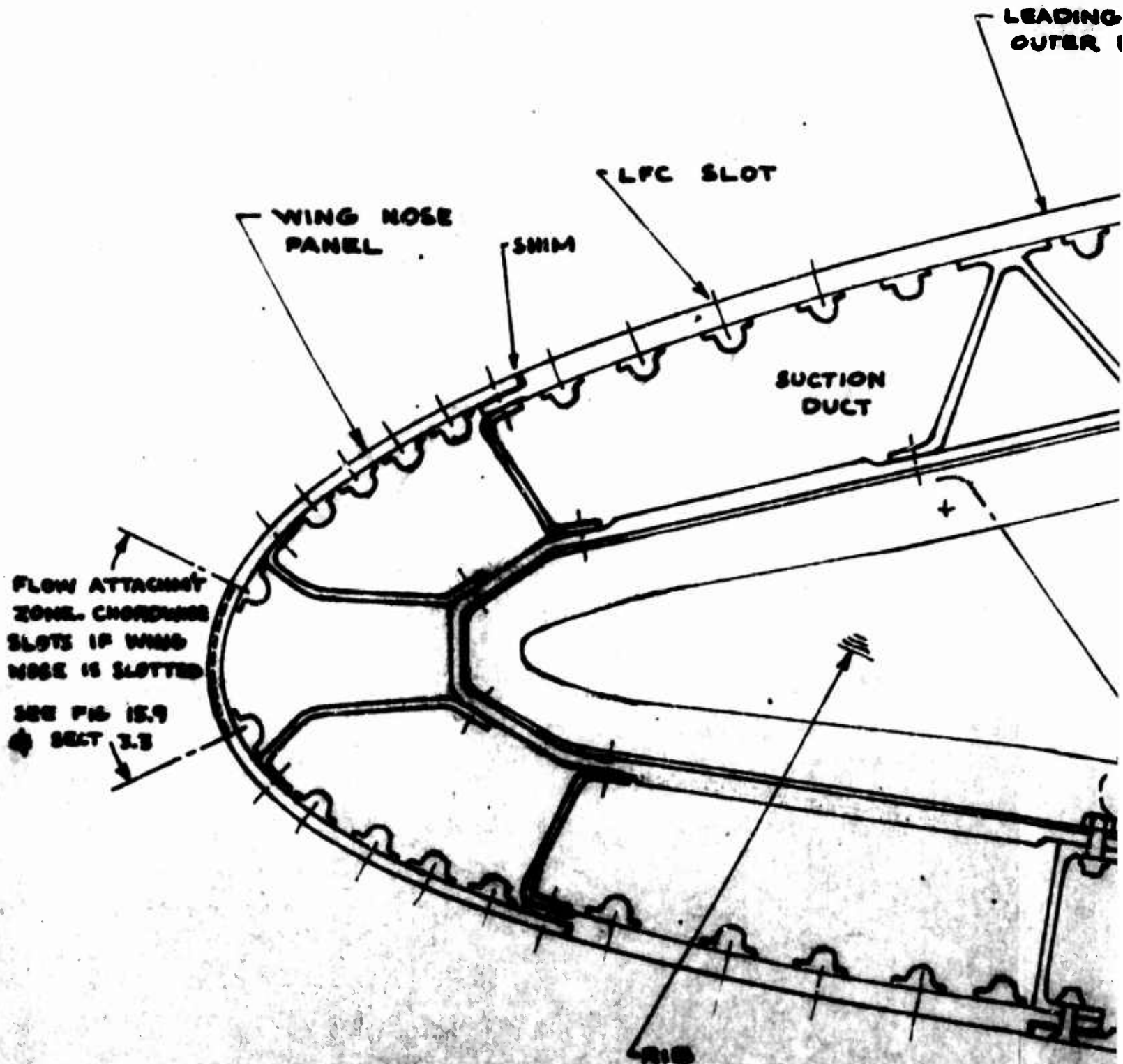
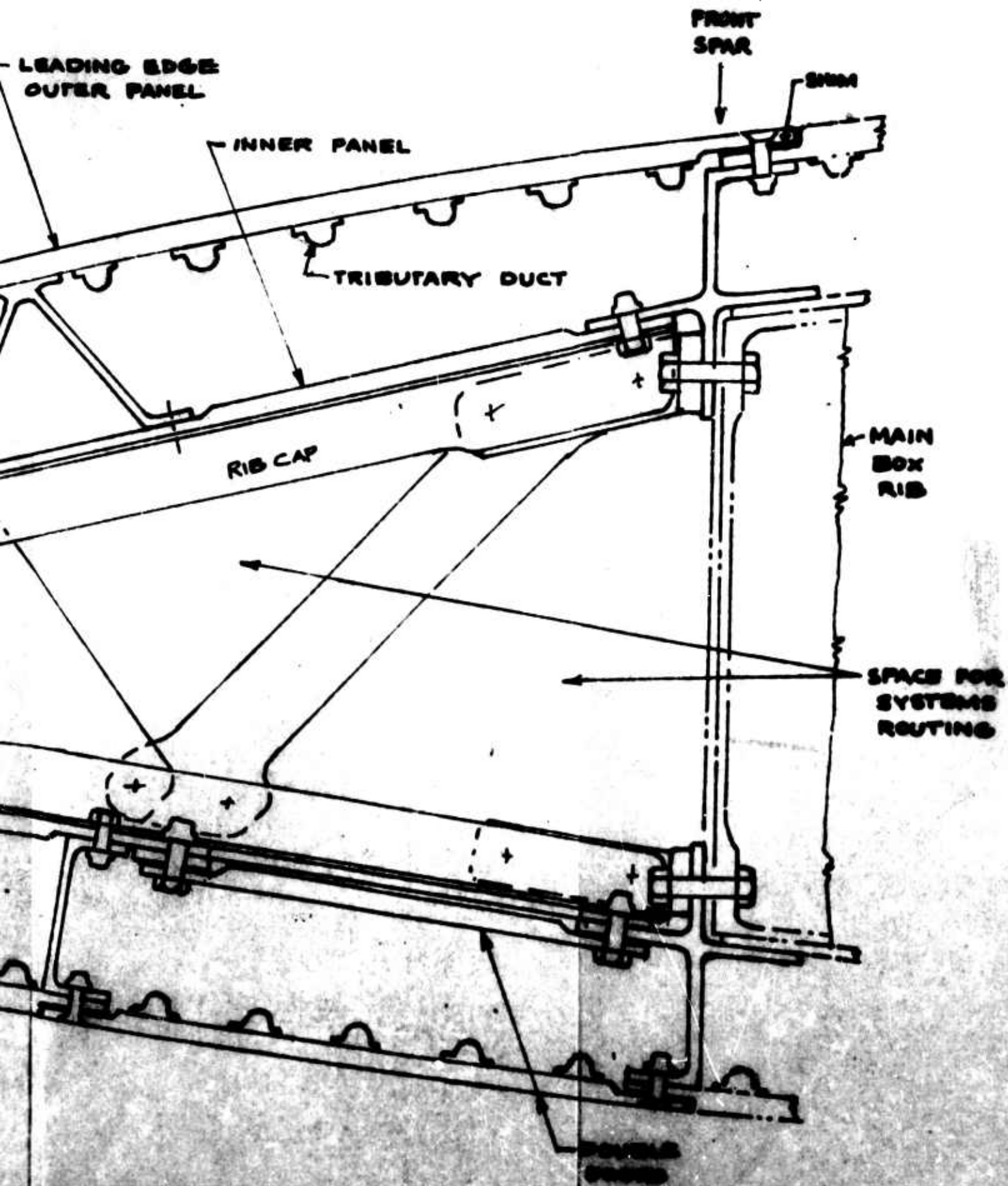
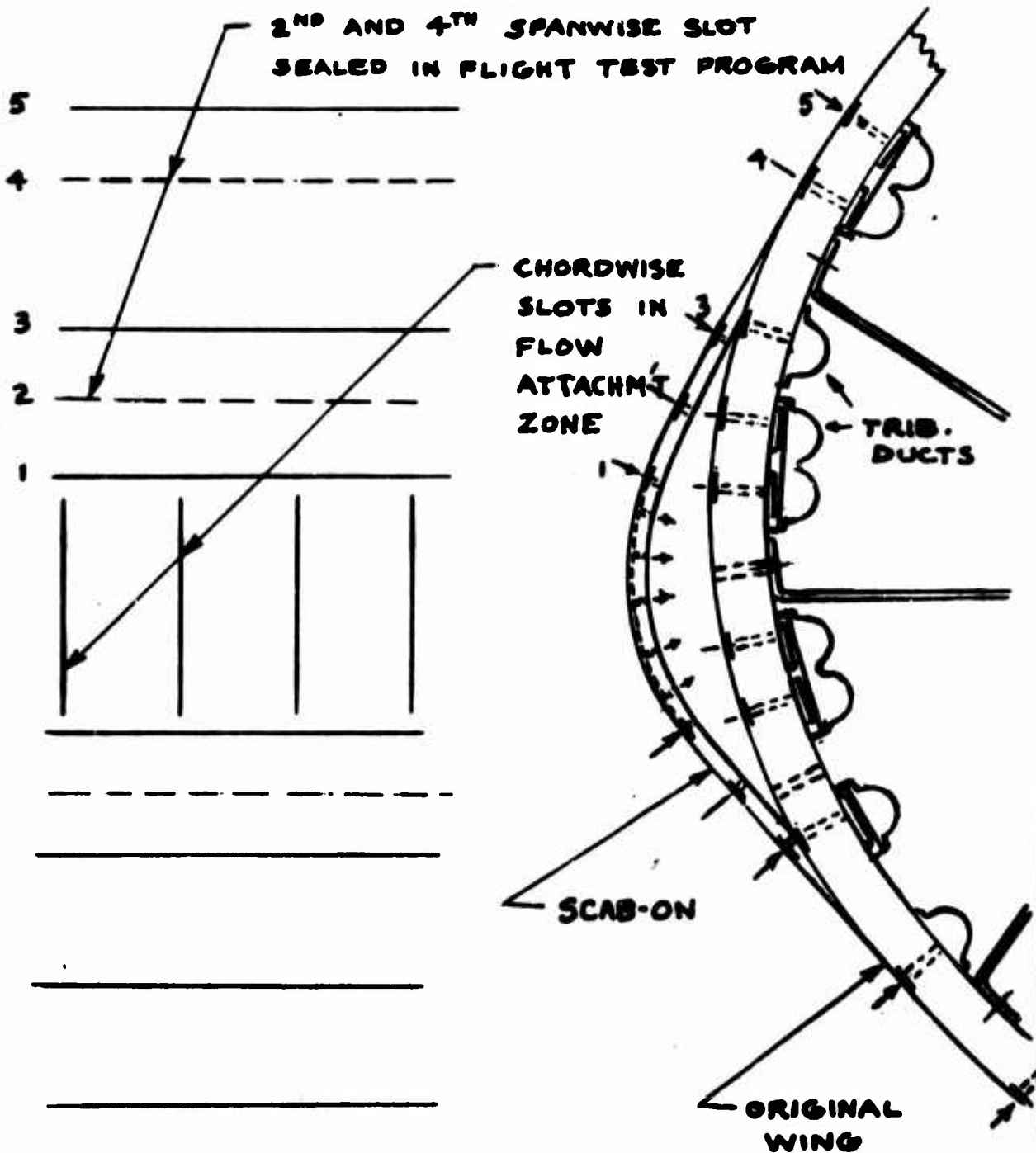


FIG. 15.8 PROPOSED STRUCTURAL AIR
LEADING EDGE REGION

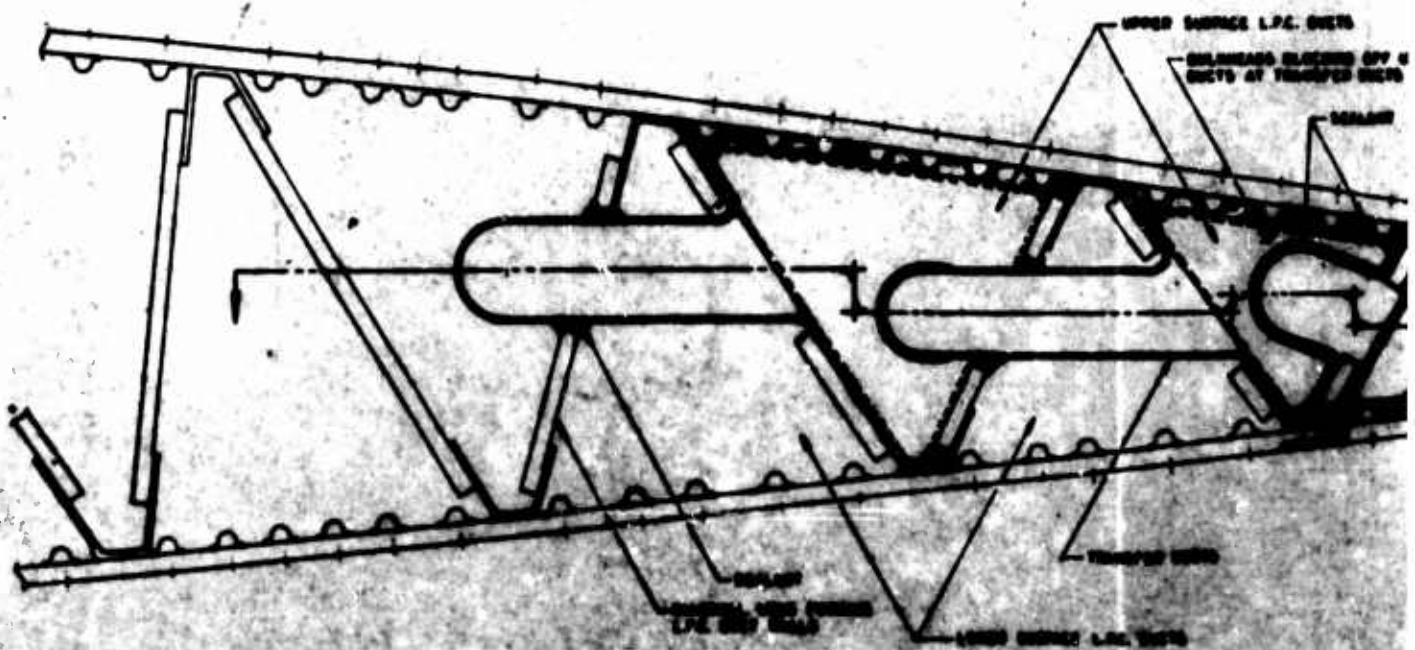
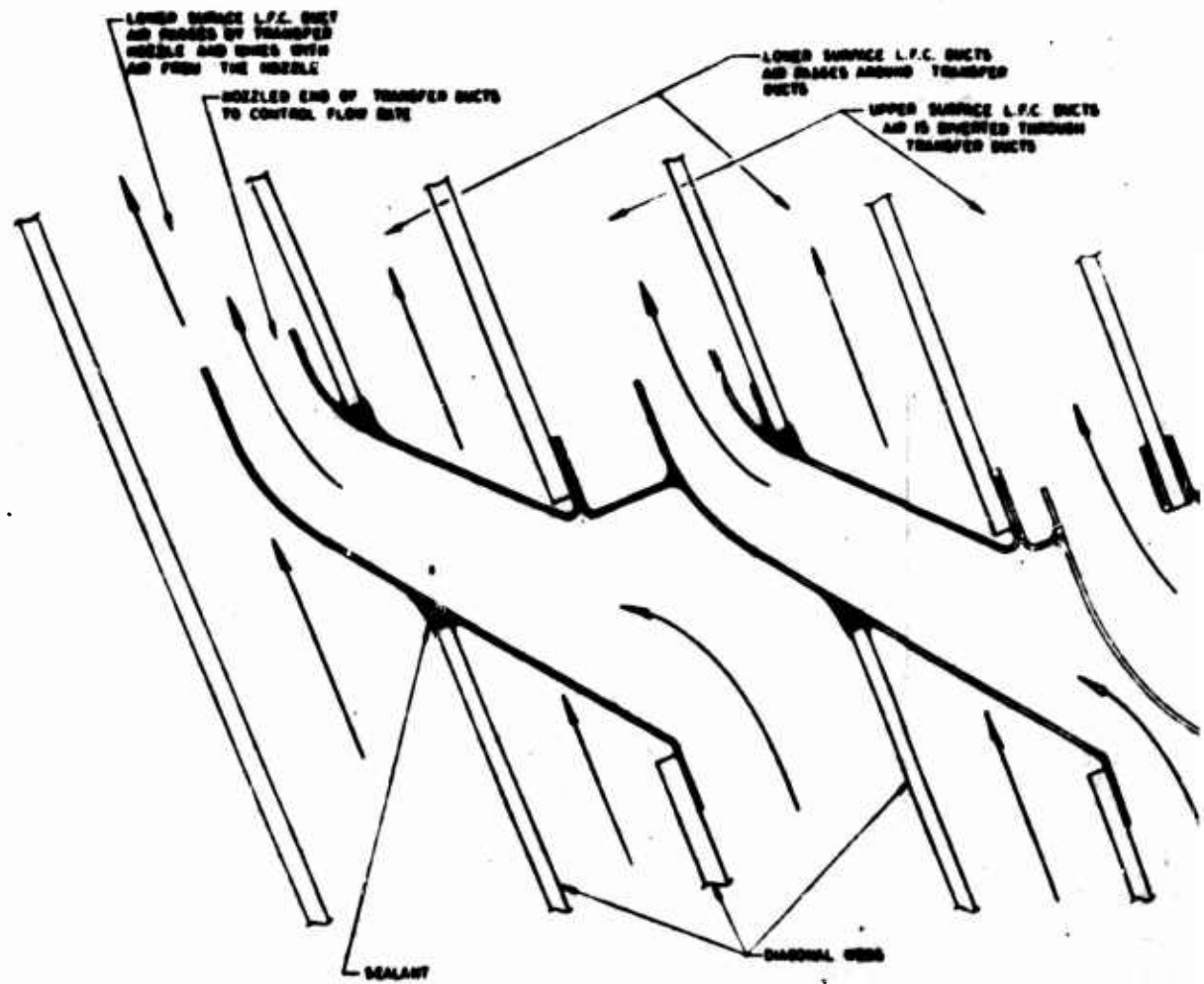


INTERNAL ARRANGEMENT OF
SECTION

ENGINEER	NORTHROP CORPORATION NORAIR DIVISION	PAGE 15.33
CHECKER		REPORT NO. NOR 67-136
DATE June 1967		MODEL X-21A



**FIG 15.9 SCAB-ON WING NOSE SECTION
AT FSS 40 (WS 90)**



SECTION THROUGH TRANSFER DUCTS AT ENDS OF TRANSFER DUCTS

FIG 15.40

GENERAL VIEW
IN THE X-Y

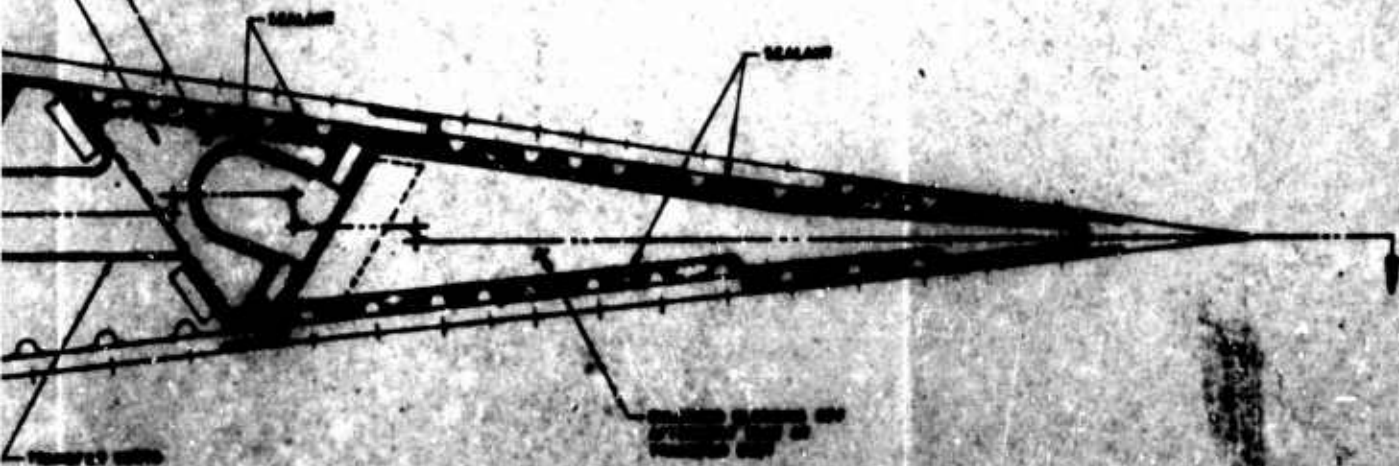
PAGE	15-34
REPORT NO.	NOR 67-136
MODEL	X-21A

ICE L.P.C. DUCTS
 MOUND TRANSFER

UPPER SURFACE L.P.C. DUCTS
 AIR IS EXHAUSTED THROUGH
 TRANSFER DUCTS



UPPER SURFACE L.P.C. DUCTS
 BALANCING BLASTING FOR UPPER
 DUCTS AT TRANSFER DUCTS



ICE L.P.C. DUCTS

**GENERAL ARRANGEMENT OF TRANSFER DUCTING
 IN THE ICE-MA TRAILER EDGE REGION**

2

PAGE	15.35
REPORT NO.	NOR 67-136
MODEL	X-21A

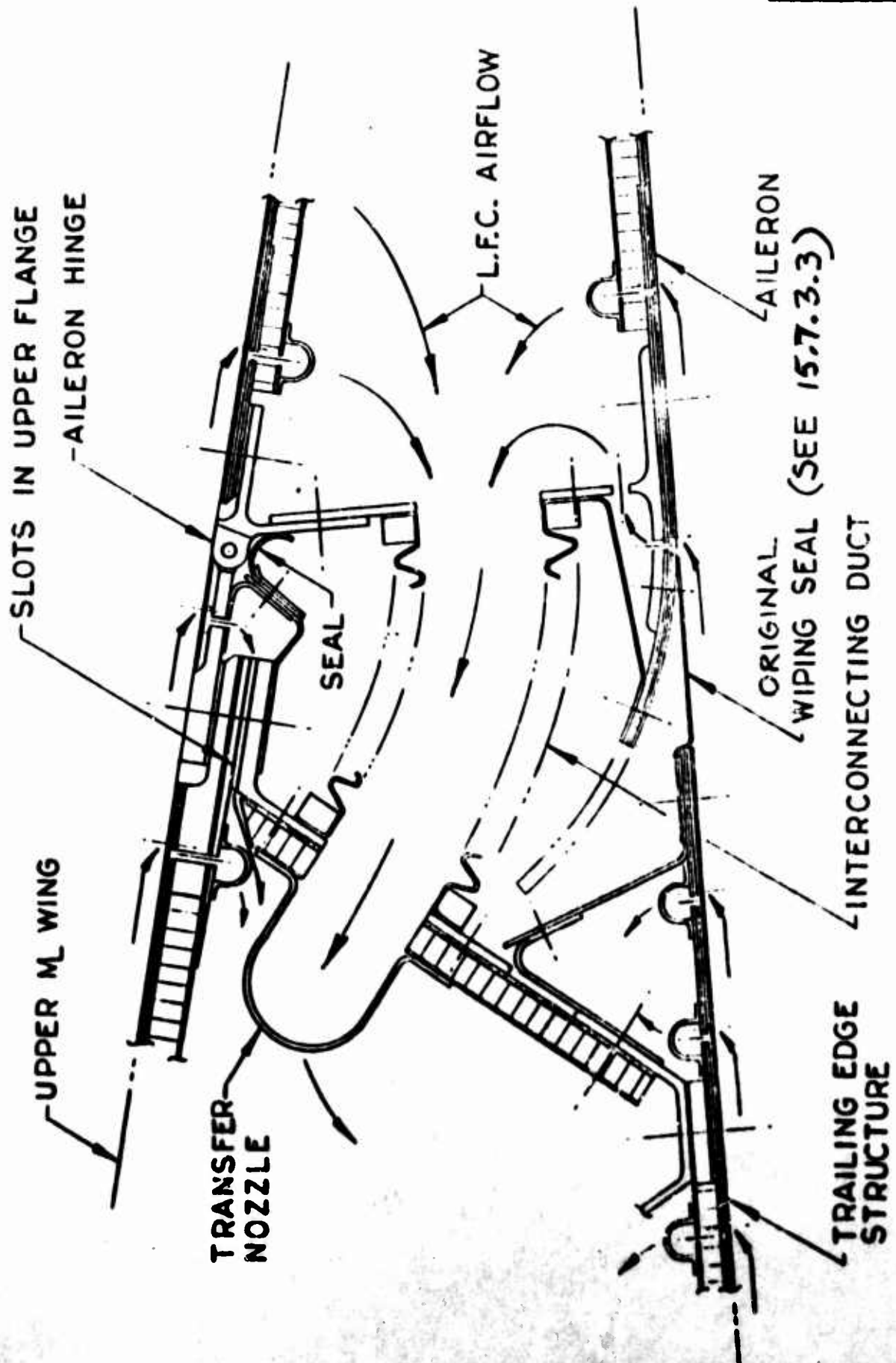


FIGURE 15.11
GENERAL ARRANGEMENT
AILERON HINGE AREA

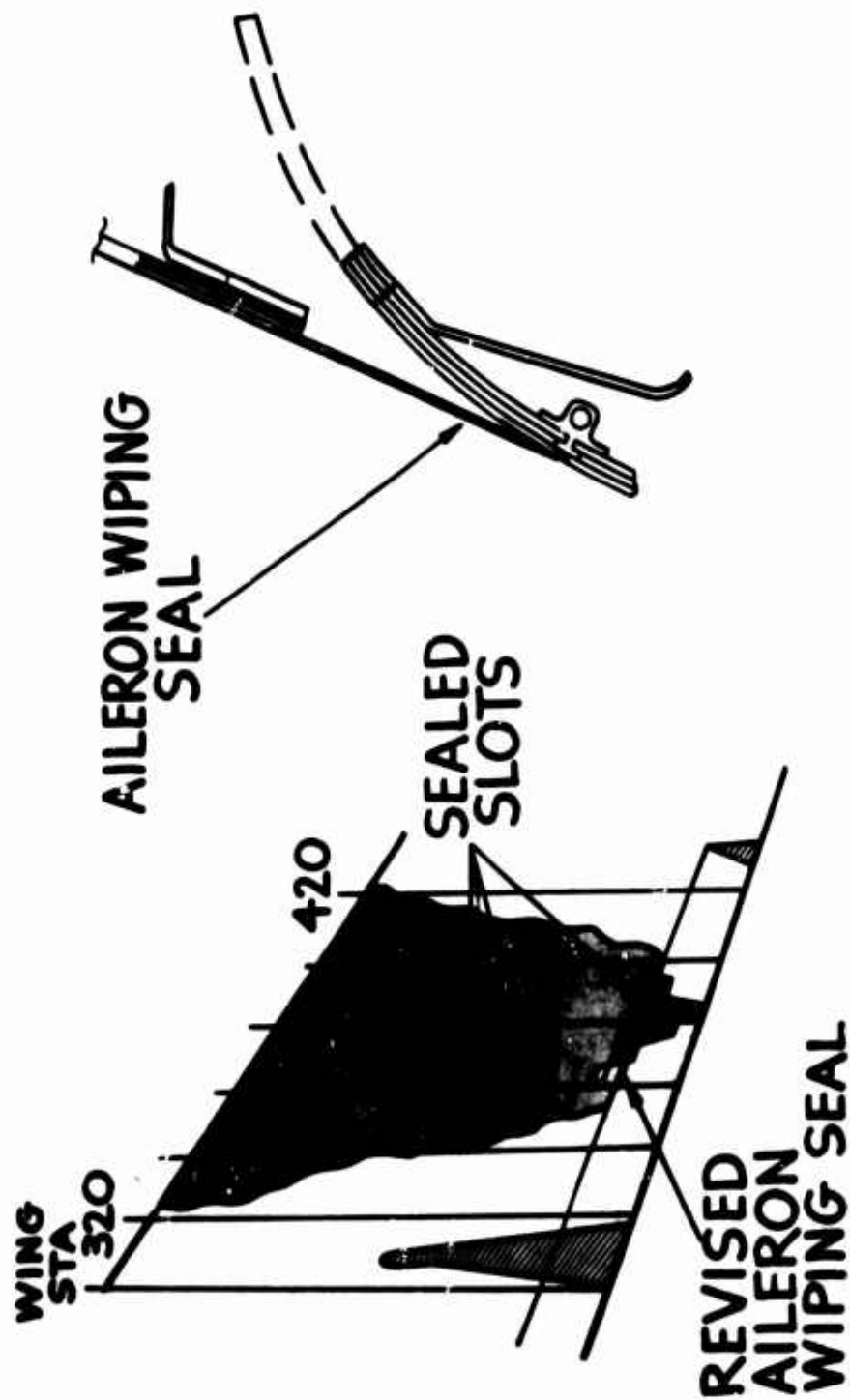
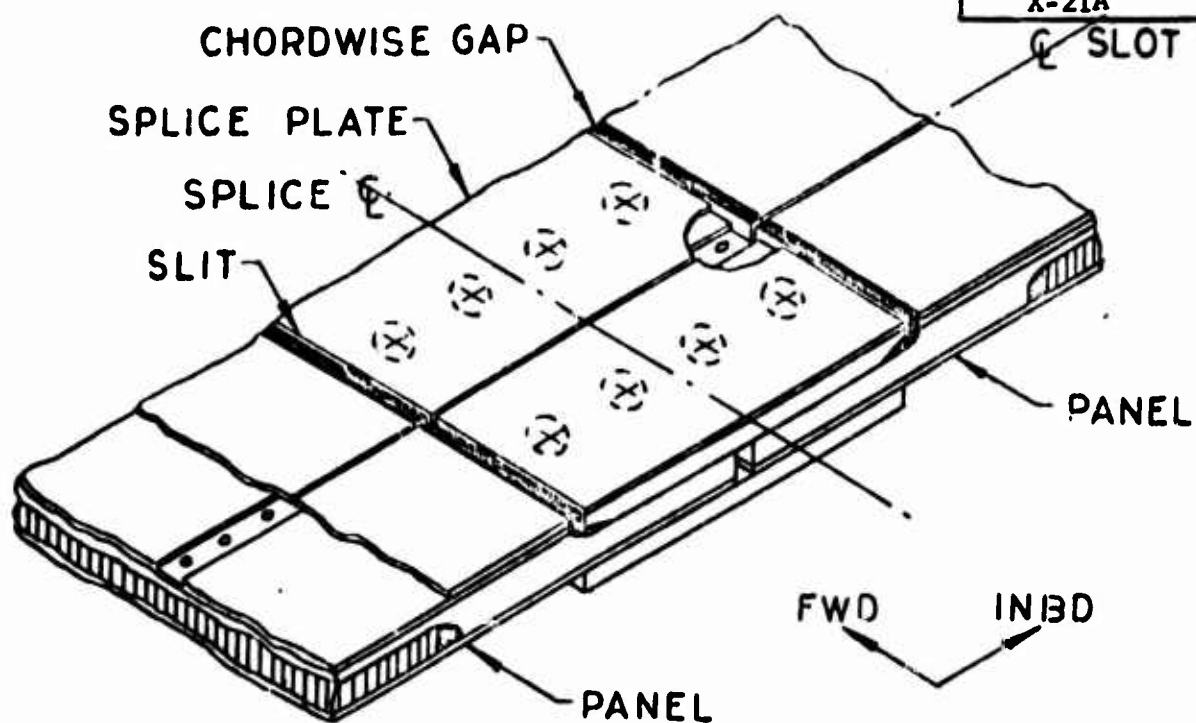
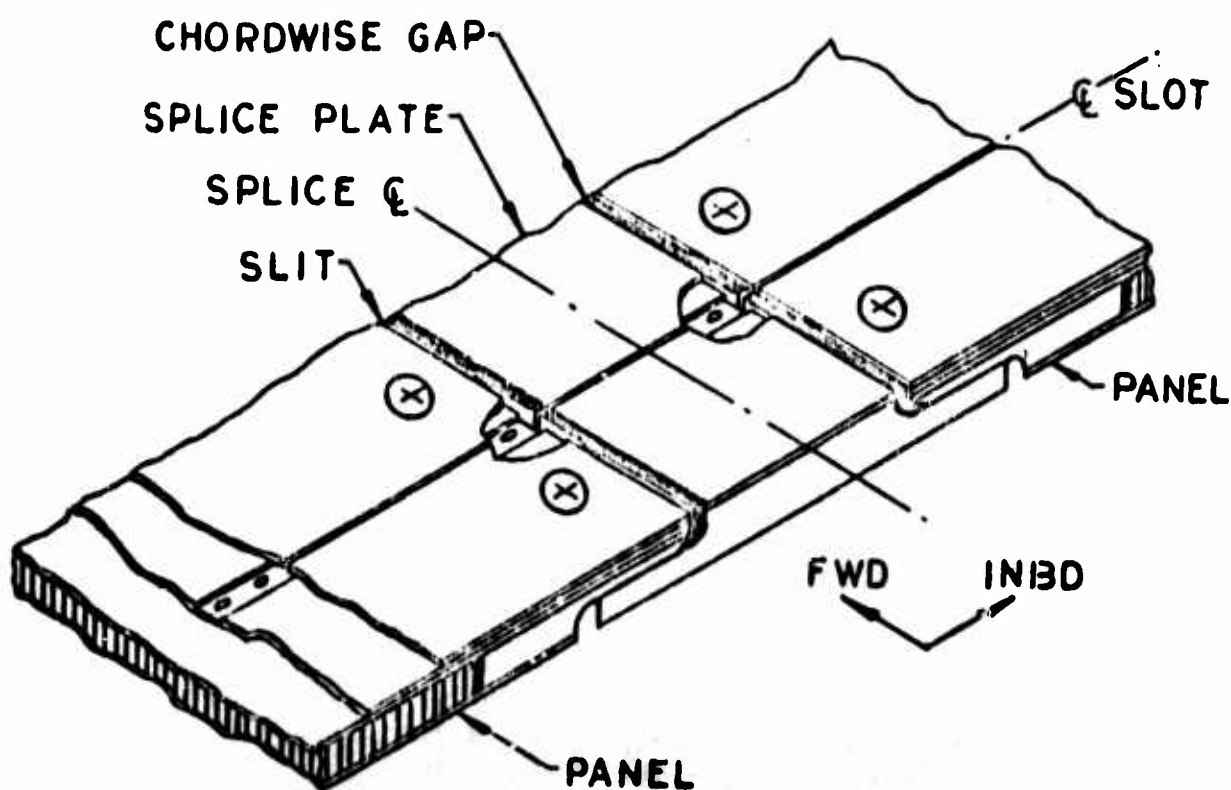


FIGURE 15.12 REVISED AILERON WIPING SEAL AND
LAMINARIZATION OF REVISED STRIP

FIG 15.13
TYPICAL CHORDWISE PANEL SPLICES*



DOUBLE SHEAR (FIXED)



SINGLE SHEAR (REMOVABLE)

* AS ORIGINALLY USED ON X-21A AIRPLANE

ENGINEER	NORTHROP CORPORATION NORAIR DIVISION	PAGE 15.38
CHECKER		REPORT NO. NOR 67-136
DATE June 1967		MODEL X-21A

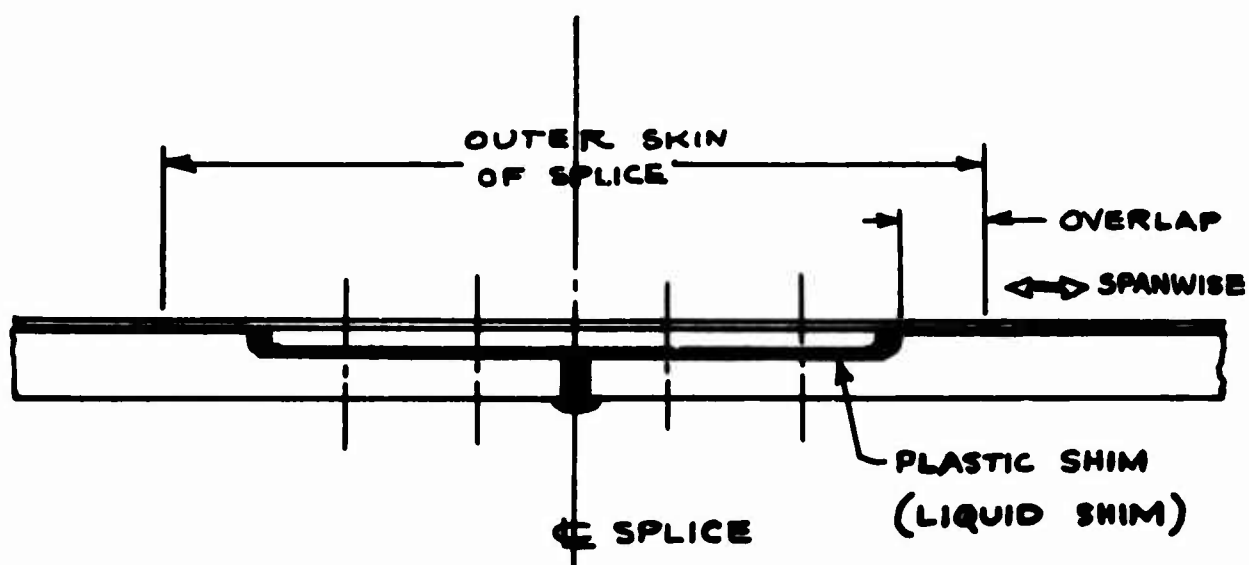


FIG. 15.14. IMPROVED CHORDWISE SPLICE

ENGINEER	NORTHROP CORPORATION NORAIR DIVISION	PAGE 15.39
CHECKER		REPORT NO. NOR 67-136
DATE June 1967		MODEL X-21A

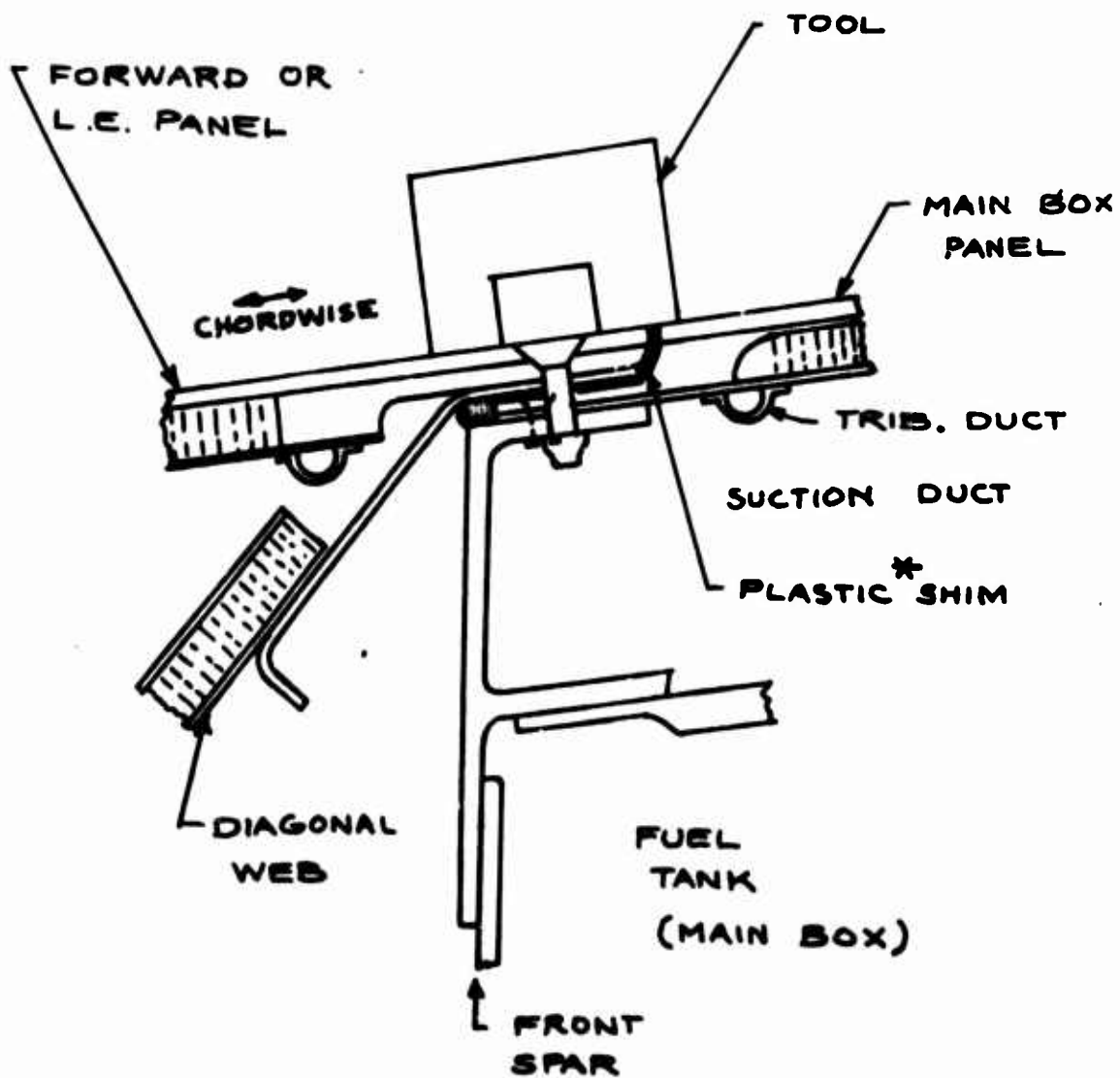


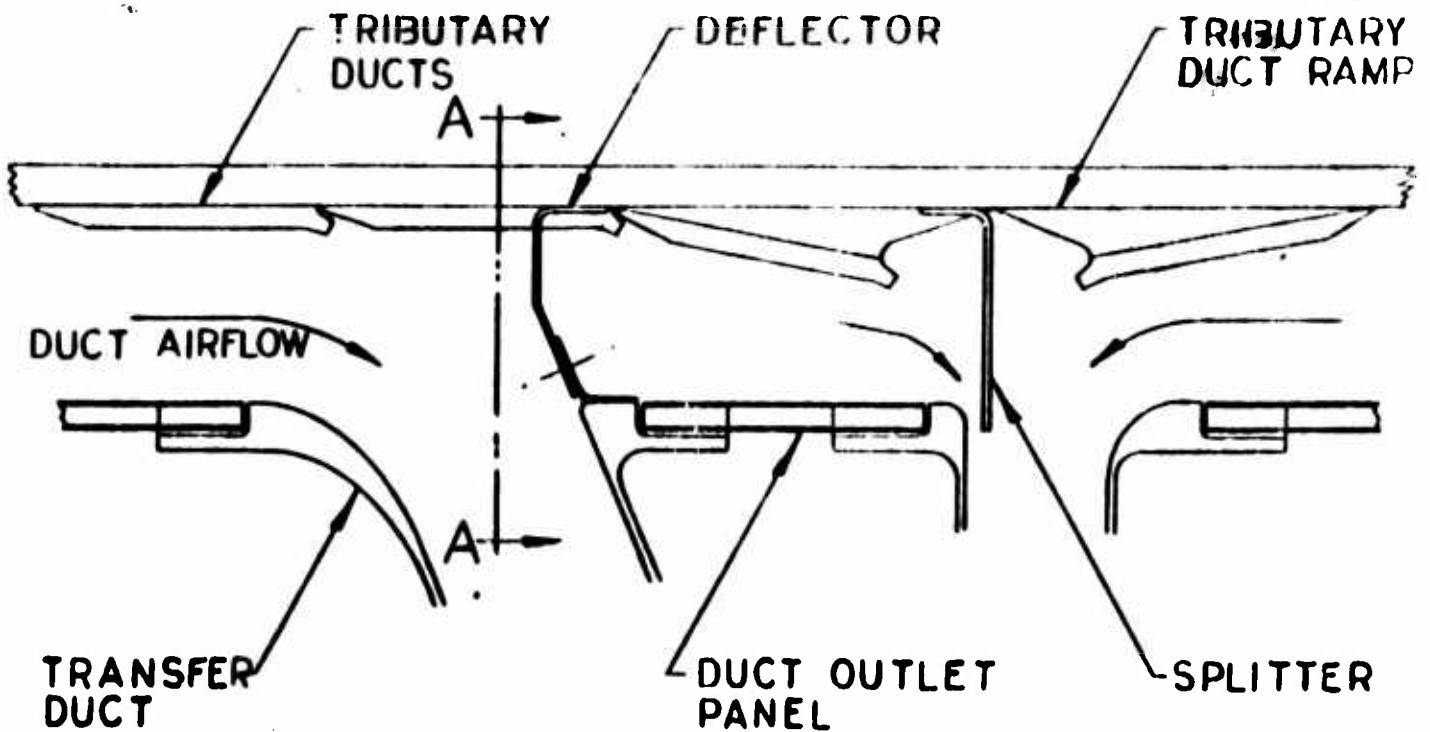
FIG 15.15 SPANWISE SPLICE WITH PLASTIC* SHIM ALONG FRONT SPAR

* ALSO CALLED LIQUID SHIM

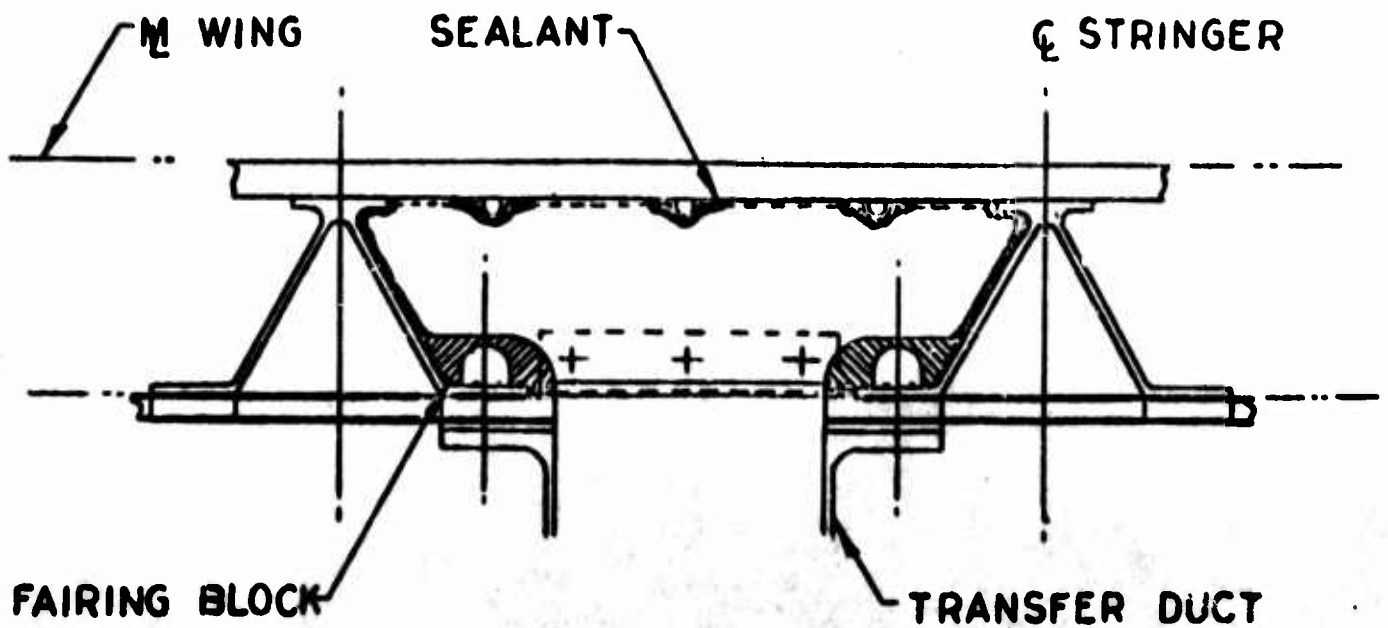
FIG 15.16

DUCT SECTIONS IN DRY BAY AREA

PAGE	15.40
REPORT NO.	NOR 67-136
MODEL	X-21A



SECTION THRU DUCT OUTLET PANEL



SECTION A-A